

UCLA

UCLA Electronic Theses and Dissertations

Title

Studies Pertaining to the Chemistry of Strained Cyclic Allenes

Permalink

<https://escholarship.org/uc/item/2f49s9g7>

Author

McVeigh, Matthew Scott

Publication Date

2024

Peer reviewed|Thesis/dissertation

UNIVERSITY OF CALIFORNIA

Los Angeles

Studies Pertaining to the Chemistry of Strained Cyclic Allenes

A dissertation submitted in partial satisfaction of the
requirements for the degree Doctor of Philosophy
in Chemistry

by

Matthew S. McVeigh

2024

© Copyright by

Matthew S. McVeigh

2024

ABSTRACT OF THE DISSERTATION

Studies Pertaining to the Chemistry of Strained Cyclic Allenes

by

Matthew S. McVeigh

Doctor of Philosophy in Chemistry

University of California, Los Angeles, 2024

Professor Neil Kamal Garg, Chair

This dissertation describes the development of methodologies that engage strained cyclic allene intermediates in complexity-generating reactions. One major effort involves palladium-catalyzed interception of strained cyclic allenes for the synthesis of saturated polycyclic products. Additionally, a novel mode of reactivity of cyclic allenes is reported involving the interception of 1,2-cyclohexadiene with a nitroxyl radical. The ability of strained cyclic allenes to engage with exocyclic alkenes in [2+2] cycloadditions is also described, pushing the limits of complexity in products formed from cyclic allene reactivity. Finally, the development of silyl tosylates as strained intermediate precursors is reported.

Chapter one offers a current perspective on the field of strained cyclic alkynes and allenes. Despite being validated over fifty years ago, strained cyclic alkynes and allenes have become valuable building blocks for the synthesis of complex small molecules. This chapter highlights recent methodologies and syntheses using strained alkynes, allenes, and alkynes to generate complex products bearing stereodefined quaternary centers or generate enantioenriched products with multiple fused rings.

Chapters two and three are related to the development of palladium-catalyzed reactions of strained cyclic allenes. Chapter two describes the development of a modular annulation reaction of strained allenes. This methodology employs aryl halides and cyclic allene precursors to generate fused heterocyclic products via the formation of two new bonds and a new stereocenter; moreover, an asymmetric variant of the transformation is employed. Chapter three details the engagement of strained cyclic allenes with π -allylpalladium species to afford complex polycyclic products. Through judicious choice of the ligand used in the transformation, either of two isomeric products can be accessed with high selectivity. The development of these metal-catalyzed reactions demonstrates that despite their high reactivity and short lifetimes, strained cyclic intermediates can be efficiently engaged in catalysis, to access complex products with control of absolute stereochemistry.

Chapter four details the study of a novel mode of monoradical reactivity with strained cyclic allenes. Use of the nitroxyl radical TEMPO allows for the interception of 1,2-cyclohexadiene, affording a ketone product. The transformation demonstrates the viability of engaging cyclic allenes in one electron chemistry.

Chapter five describes the investigation of [2+2] cycloadditions between strained cyclic allenes and exocyclic alkenes to afford highly substituted cyclobutanes, providing an alternative

strategy to photochemical methods. Under mild reaction conditions, scope studies demonstrate that a variety of alkene trapping partners can engage with cyclic allenes with a high degree of selectivity. Furthermore, the cyclobutanes accessed via this methodology contain many features indicative of structural complexity such as spiro centers, multiple contiguous stereocenters, and vicinal quaternary centers. The strained alkylidene cyclobutanes that are accessed can undergo thermal isomerization. Cycloadducts are also further elaborated, demonstrating the utility of the transformation in providing rapid access to structurally complex scaffolds.

Chapter six illustrates the development of an alternative precursor toward strained cyclic allenes and alkynes. Our studies of strained cyclic allenes revealed that, in some cases, silyl triflate precursors were inaccessible. This study shows that silyl tosylates can serve as alternative precursors to strained cyclic allenes and alkynes.

The dissertation of Matthew S. McVeigh is approved.

Kendall N. Houk

Miguel A. García-Garibay

Yi Tang

Neil Kamal Garg, Committee Chair

University of California, Los Angeles

2024

“And now that you don’t have to be perfect, you can be good.”

– John Steinbeck

For my parents, Bryan and Kenda

TABLE OF CONTENTS

ABSTRACT OF THE DISSERTATION	ii
COMMITTEE PAGE.....	v
DEDICATION PAGE.....	vi
TABLE OF CONTENTS	vii
LIST OF FIGURES.....	xiv
LIST OF SCHEMES	xxxii
LIST OF TABLES	xxxiii
LIST OF ABBREVIATIONS	xxxv
ACKNOWLEDGEMENTS	xxxix
BIOGRAPHICAL SKETCH.....	xlix
CHAPTER ONE: Leveraging Fleeting Strained Intermediates to Access Complex Scaffolds.....	1
1.1 Abstract	1
1.2 Introduction	1
1.3 Use of Heterocyclic Alkynes in the Synthesis of Medicinal and Materials Scaffolds..	5
1.4 Use of Arynes and Cyclic Alkynes to Access Quaternary Stereocenters (Non-Catalytic)	
.....	13
1.5 Arynes in Asymmetric Catalysis.....	19
1.6 Use of Strained Cyclic Allenes to Access Polycyclic Scaffolds.....	22

1.7 Strained Cyclic Allenes in Enantioselective and Stereospecific Reactions	28
1.8 Outlook and Future Directions	32
1.9 Notes and References	34
CHAPTER TWO: Palladium-Catalyzed Annulations of Strained Cyclic Allenes	61
2.1 Abstract	61
2.2 Introduction	61
2.3 Reaction Design	63
2.4 Reaction Optimization.....	64
2.5 Scope of the Annulation Reaction.....	65
2.6 Development of Stereoselective Variants	68
2.7 Conclusion.....	71
2.8 Experimental Section	71
2.8.1 Materials and Methods	71
2.8.2 Experimental Procedures.....	74
2.8.2.1 Syntheses of Annulation Partners	74
2.8.2.1.1 Syntheses of <i>N</i> -Tosyl-Arylamines.....	74
2.8.2.1.2 Synthesis of Alcohol 2.43	81
2.8.2.2 Synthesis of Silyl Triflate 2.46	82
2.8.2.3 Optimization of the Racemic Annulation.....	85
2.8.2.4 Scope of the Racemic Annulation.....	88

2.8.2.5 Diastereoselective Annulation.....	103
2.8.2.6 Optimization of the Asymmetric Annulation.....	104
2.8.2.7 Synthesis of (-)- 2.47 via Asymmetric Annulation.....	111
2.8.2.8 Elaboration of Annulation Product of (-)- 2.47	112
2.9 Spectra Relevant to Chapter Two.....	118
2.10 Notes and References	162
CHAPTER THREE: Catalyst-Controlled Annulations of Strained Cyclic Allenes with π -	
Allylpalladium Complexes.....	172
3.1 Abstract	172
3.2 Introduction	172
3.3 Reaction Optimization.....	175
3.4 Scope of Annulation Reactions	176
3.5 Reaction Mechanism	180
3.6 Investigating the Feasibility of an Enantioselective Variant.....	181
3.7 Conclusion.....	184
3.8 Experimental Section	184
3.8.1 Materials and Methods	184
3.8.2 Experimental Procedures.....	186
3.8.2.1 Synthesis of <i>N</i> -Tosyl-vinyl Benzoxazinones	186

3.8.2.2 Optimization of the Racemic Annulation.....	196
3.8.2.3 Scope of the Racemic Annulation.....	201
3.8.2.4 Representative Asymmetric Annulations.....	228
3.8.2.5 Extended Evaluation of Chiral Ferrocenyl Phosphine Ligands ..	232
3.8.2.6 Assignment of Absolute Stereochemical Configuration.....	236
3.9 Spectra Relevant to Chapter Three.....	246
3.10 Notes and References	290
CHAPTER FOUR: Interception of 1,2-Cyclohexadiene with TEMPO Radical	301
4.1 Abstract	301
4.2 Introduction	301
4.3 Reactivity of 1,2-Cyclohexadiene with TEMPO Radical	303
4.4 Reaction Mechanism	303
4.5 Isotopic Labeling Study	304
4.6 Conclusion.....	305
4.7 Experimental Section	305
4.7.1 Materials and Methods	305
4.7.2 Experimental Procedures.....	306
4.7.2.1 1,2-Cyclohexadiene trapping with TEMPO (4.15)	306
4.7.2.2 Isotope labeling study with ¹⁸ O-enriched 4.15	307
4.8 Spectra Relevant to Chapter Four	308
4.9 Notes and References	312

CHAPTER FIVE: Access to Complex Scaffolds Through [2+2] Cycloadditions of Strained Cyclic

Allenes.....	317
5.1 Abstract	317
5.2 Introduction	317
5.3 Surveying Exocyclic Alkenes in [2+2] Cycloaddition.....	320
5.4 Scope of [2+2] Cycloadditions with Dienamine Partners.....	322
5.5 Scope of [2+2] Cycloadditions with Styrenyl Partners.....	325
5.6 [2+2] Cycloadditions with Carbocyclic Allenes	326
5.7 Thermal Isomerization of Cycloadducts	327
5.8 Synthetic Elaborations of Cycloadducts	329
5.9 Conclusion.....	331
5.10 Experimental Section	332
5.10.1 Materials and Methods	332
5.10.2 Experimental Procedures.....	335
5.10.2.1 Syntheses of Trapping Partners.....	335
5.10.2.2 Synthesis of Silyl Triflate 5.68	349
5.10.2.3 Survey of [2+2] Cycloadditions with Exocyclic Alkenes.....	351
5.10.2.4 Optimization of [2+2] Cycloadditions with Exocyclic Alkenes.....	356
5.10.2.5 Scope of [2+2] Cycloadditions with Dienamines	359
5.10.2.6 Scope of [2+2] Cycloadditions with (Het)aryl-Substituted Alkenes	367
5.10.2.7 [2+2] Cycloadditions of 1,2-Cyclohexadiene (5.63) and 1,2- Cycloheptadiene (5.66)	379

5.10.2.8 Thermal Isomerizations of [2+2] Cycloadducts.....	381
5.10.2.9 Elaborations of [2+2] Cycloadducts.....	384
5.11 Spectra Relevant to Chapter Five.....	393
5.12 Computational Section	475
5.12.1 Computational Methods	475
5.12.2 Calculated Energies for Thermal Isomerization Products.....	475
5.12.3 Cartesian Coordinates and Energies of Optimized Structures	475
5.13 Notes and References	481
CHAPTER SIX: Silyl Tosylate Precursors to Cyclohexyne, 1,2-Cyclohexadiene, and 1,2-Cycloheptadiene.....	498
6.1 Abstract	498
6.2 Introduction	498
6.3 Synthesis of Silyl Tosylate Precursors to Cyclohexyne and 1,2-Cyclohexadiene....	500
6.4 Comparing Silyl Tosylates and Silyl Triflates as Precursors to Cyclohexyne.....	501
6.5 Comparing Silyl Tosylates and Silyl Triflates as Precursors to 1,2-Cyclohexadiene	502
6.6 Preparation of a Precursor to 1,2-Cycloheptadiene and its Subsequent Trapping....	503
6.7 Competition Experiments Between Silyl Triflates and Silyl Tosylates.....	504
6.8 Conclusion.....	505
6.9 Experimental Section	506
6.9.1 Materials and Methods	506
6.9.2 Experimental Procedures.....	507
6.9.2.1 Syntheses of Silyl Tosylates 6.9 and 6.11	507

6.9.2.2 Cyclohexyne Trapping Experiments.....	509
6.9.2.3 1,2-Cyclohexadiene Trapping Experiments.....	511
6.9.2.4 Synthesis of Silyl Tosylate 6.28	513
6.9.2.5 1,2-Cycloheptadiene Trapping Experiment	515
6.9.2.6 Silyl Tosylate and Silyl Triflate Competition Experiments.....	516
6.10 Spectra Relevant to Chapter Six.....	518
6.11 Notes and References	527

LIST OF FIGURES

CHAPTER ONE

Figure 1.1	Historical perspective, growth of “aryne” or “benzyne” chemistry, and select synthetic applications	4
Figure 1.2	Representative natural products and pharmaceuticals containing heterocycles and representative nitrogen- and oxygen-containing strained cyclic alkynes	6
Figure 1.3	Selected trapping experiments involving piperidyne 1.19	7
Figure 1.4	Selected trapping experiments of heterocyclic alkynes using silyl triflate precursors	8
Figure 1.5	Regioselectivity of piperidyne 1.14 and oxacyclohexyne 1.15 trappings...	9
Figure 1.6	Notable polycyclic aromatic hydrocarbons	10
Figure 1.7	Modular strategy to access 9,10-diphenylanthracene derivatives and representative products 1.48–1.50	11
Figure 1.8	Utilizing arynes to access 9,10-diphenylanthracene derivatives	12
Figure 1.9	Intercepting arynes and cyclic alkynes for the installation of stereodefined quaternary stereocenters	14
Figure 1.10	Selected substrate scope of α -arylation methodology	15
Figure 1.11	α -Arylation reaction demonstrated in one-pot	15
Figure 1.12	The tubingensin alkaloids and natural products with quaternary stereocenters introduced using aryne chemistry	17
Figure 1.13	Overview of (–)-tubingensin B total synthesis	19

Figure 1.14	Enantioselective synthesis of helicenes using arynes and asymmetric catalysis	20
Figure 1.15	Enantioselective synthesis of triple helicenes via the catalytic asymmetric trapping of arynes.....	21
Figure 1.16	Catalytic enantioselective α -arylation of 1,3-dicarbonyls	22
Figure 1.17	Strained cyclic allenes and representative trapping reactions	23
Figure 1.18	Intramolecular Diels–Alder reactions afford tetracyclic products	24
Figure 1.19	Representative azacyclic and oxacyclic allene trapping experiments.....	26
Figure 1.20	Regioselectivity investigation of substituted azacyclic allenes.....	28
Figure 1.21	Transfer of stereochemical information in allene cycloadditions	29
Figure 1.22	Stereospecific cycloadditions of heterocyclic allenes using enantioenriched silyl triflates.....	30
Figure 1.23	Cyclic allene racemization	31
Figure 1.24	Catalytic asymmetric reactions of cyclic allenes	32

CHAPTER TWO

Figure 2.1	Selected in-situ-generated strained cyclic intermediates and overview of strained cyclic allene reactivity	63
Figure 2.2	Scope of the annulation reaction with iodoaniline derivatives 2.20	67
Figure 2.3	Variation of the pronucleophile to furnish structurally diverse products..	68
Figure 2.4	Stereocontrolled annulations and synthetic elaboration of an annulation product.....	70
Figure 2.5	Ligand families evaluated during asymmetric reaction development.....	107
Figure 2.6	ORTEP representation of X-ray crystallographic structure (+)- 2.50	115

Figure 2.7	SFC trace for (\pm)- 2.47	117
Figure 2.8	SFC trace for ($-$)- 2.47	117
Figure 2.9	^1H NMR (400 MHz, CDCl_3) of compound 2.56	119
Figure 2.10	^{13}C NMR (100 MHz, CDCl_3) of compound 2.56	119
Figure 2.11	^1H NMR (500 MHz, CDCl_3) of compound 2.58	120
Figure 2.12	^{13}C NMR (125 MHz, CDCl_3) of compound 2.58	120
Figure 2.13	^1H NMR (400 MHz, CDCl_3) of compound 2.60	121
Figure 2.14	^{13}C NMR (125 MHz, CDCl_3) of compound 2.60	121
Figure 2.15	^{19}F NMR (376 MHz, CDCl_3) of compound 2.60	122
Figure 2.16	^1H NMR (500 MHz, CD_3OD) of compound 2.62	123
Figure 2.17	^{13}C NMR (125 MHz, CD_3OD) of compound 2.62	123
Figure 2.18	^1H NMR (500 MHz, CDCl_3) of compound 2.64	124
Figure 2.19	^{13}C NMR (125 MHz, CDCl_3) of compound 2.64	124
Figure 2.20	^1H NMR (500 MHz, CD_3OD) of compound 2.66	125
Figure 2.21	^{13}C NMR (125 MHz, CD_3OD) of compound 2.66	125
Figure 2.22	^1H NMR (500 MHz, CDCl_3) of compound 2.45	126
Figure 2.23	^{13}C NMR (125 MHz, CDCl_3) of compound 2.45	126
Figure 2.24	^1H NMR (500 MHz, CDCl_3) of compound 2.69	127
Figure 2.25	^{13}C NMR (125 MHz, CDCl_3) of compound 2.69	127
Figure 2.26	^1H NMR (500 MHz, CDCl_3) of compound 2.71	128
Figure 2.27	^{13}C NMR (125 MHz, CDCl_3) of compound 2.71	128
Figure 2.28	^1H NMR (500 MHz, CDCl_3) of compound 2.73	129
Figure 2.29	^{13}C NMR (125 MHz, CDCl_3) of compound 2.73	129

Figure 2.30	^1H NMR (500 MHz, CDCl_3) of compound 2.43	130
Figure 2.31	^{13}C NMR (125 MHz, CDCl_3) of compound 2.43	130
Figure 2.32	^1H NMR (400 MHz, CDCl_3) of compound 2.75	131
Figure 2.33	^{13}C NMR (100 MHz, CDCl_3) of compound 2.75	131
Figure 2.34	^1H NMR (400 MHz, CDCl_3) of compound 2.76	132
Figure 2.35	^{13}C NMR (100 MHz, CDCl_3) of compound 2.76	132
Figure 2.36	^1H NMR (500 MHz, CDCl_3) of compound 2.46	133
Figure 2.37	^{13}C NMR (125 MHz, CDCl_3) of compound 2.46	133
Figure 2.38	^1H NMR (500 MHz, CDCl_3) of compound 2.19a	134
Figure 2.39	^1H NMR (500 MHz, DMSO-d_6) of compound 2.19b	135
Figure 2.40	^{13}C NMR (100 MHz, DMSO-d_6) of compound 2.19b	135
Figure 2.41	^1H NMR (500 MHz, DMSO-d_6) of compound 2.19c	136
Figure 2.42	^{13}C NMR (125 MHz, DMSO-d_6) of compound 2.19c	136
Figure 2.43	^1H NMR (400 MHz, CDCl_3) of compound 2.22	137
Figure 2.44	^{13}C NMR (100 MHz, CDCl_3) of compound 2.22	137
Figure 2.45	^1H NMR (500 MHz, CDCl_3) of compound 2.23	138
Figure 2.46	^{13}C NMR (125 MHz, CDCl_3) of compound 2.23	138
Figure 2.47	^1H NMR (600 MHz, CDCl_3) of compound 2.24	139
Figure 2.48	^{13}C NMR (125 MHz, CDCl_3) of compound 2.24	139
Figure 2.49	^{19}F NMR (376 MHz, CDCl_3) of compound 2.24	140
Figure 2.50	^1H NMR (500 MHz, CDCl_3) of compound 2.25	141
Figure 2.51	^{13}C NMR (125 MHz, CDCl_3) of compound 2.25	141
Figure 2.52	^1H NMR (400 MHz, CDCl_3) of compound 2.26	142

Figure 2.53	^{13}C NMR (100 MHz, CDCl_3) of compound 2.26	142
Figure 2.54	^1H NMR (500 MHz, CDCl_3) of compound 2.27	143
Figure 2.55	^{13}C NMR (125 MHz, CDCl_3) of compound 2.27	143
Figure 2.56	^1H NMR (500 MHz, CDCl_3) of compound 2.28	144
Figure 2.57	^{13}C NMR (125 MHz, CDCl_3) of compound 2.28	144
Figure 2.58	^1H NMR (500 MHz, CDCl_3) of compound 2.29	145
Figure 2.59	^{13}C NMR (125 MHz, CDCl_3) of compound 2.29	145
Figure 2.60	^1H NMR (500 MHz, CDCl_3) of compound 2.30	146
Figure 2.61	^{13}C NMR (125 MHz, CDCl_3) of compound 2.30	146
Figure 2.62	^{19}F NMR (376 MHz, CDCl_3) of compound 2.30	147
Figure 2.63	^1H NMR (500 MHz, CDCl_3) of compound 2.31	148
Figure 2.64	^{13}C NMR (125 MHz, CDCl_3) of compound 2.31	148
Figure 2.65	^1H NMR (500 MHz, CDCl_3) of compound 2.32	149
Figure 2.66	^{13}C NMR (100 MHz, CDCl_3) of compound 2.26	149
Figure 2.67	^1H NMR (600 MHz, CDCl_3) of compound 2.33	150
Figure 2.68	^{13}C NMR (125 MHz, CDCl_3) of compound 2.33	150
Figure 2.69	^1H NMR (500 MHz, CDCl_3) of compound 2.34	151
Figure 2.70	^{13}C NMR (125 MHz, CDCl_3) of compound 2.34	151
Figure 2.71	^1H NMR (500 MHz, CDCl_3) of compound 2.36	152
Figure 2.72	^{13}C NMR (100 MHz, CDCl_3) of compound 2.36	152
Figure 2.73	^1H NMR (500 MHz, CDCl_3) of compound 2.38	153
Figure 2.74	^{13}C NMR (100 MHz, CDCl_3) of compound 2.38	153
Figure 2.75	^1H NMR (500 MHz, CDCl_3) of compound 2.40	154

Figure 2.76	¹ H NMR (600 MHz, CDCl ₃) of compound 2.42	155
Figure 2.77	¹³ C NMR (100 MHz, CDCl ₃) of compound 2.42	155
Figure 2.78	¹ H NMR (500 MHz, CDCl ₃) of compound 2.44	156
Figure 2.79	¹³ C NMR (125 MHz, CDCl ₃) of compound 2.44	156
Figure 2.80	¹ H NMR (500 MHz, CDCl ₃) of compound 2.86	157
Figure 2.81	¹³ C NMR (125 MHz, CDCl ₃) of compound 2.86	157
Figure 2.82	NOESY (500 MHz, CDCl ₃) of compound 2.86	158
Figure 2.83	¹ H NMR (500 MHz, CDCl ₃) of compound (–)- 2.47	159
Figure 2.84	¹³ C NMR (125 MHz, CDCl ₃) of compound (–)- 2.47	159
Figure 2.85	¹ H NMR (500 MHz, CDCl ₃) of compound (+)- 2.49	160
Figure 2.86	¹³ C NMR (125 MHz, CDCl ₃) of compound (+)- 2.49	160
Figure 2.87	¹ H NMR (500 MHz, CDCl ₃) of compound (+)- 2.50	161
Figure 2.88	¹³ C NMR (125 MHz, CDCl ₃) of compound (+)- 2.50	161

CHAPTER THREE

Figure 3.1A	Strained cyclic intermediates 3.1–3.4	174
Figure 3.1B	Approaches for metal-catalyzed reactions of strained cyclic allenes.....	174
Figure 3.1C	Overview of current study.....	174
Figure 3.2	Scope of the annulation reaction using PPh ₃ as the ligand.....	178
Figure 3.3	Scope of the annulation reaction using dppf as the ligand.....	179
Figure 3.4	Proposed catalytic cycle.....	181
Figure 3.5	Unsuccessful and low yielding substrates evaluated during scope studies	227
Figure 3.6	Ligand families evaluated during asymmetric reaction development.....	234

Figure 3.7	ORTEP representation of X-ray crystallographic structure (–)- 3.43	238
Figure 3.8	SFC trace of (±)- 3.43	241
Figure 3.9	SFC trace of (–)- 3.43 (from reaction mixture).....	241
Figure 3.10	SFC trace of (–)- 3.43 (Crystals used for X-ray analysis).....	242
Figure 3.11	SFC trace of (±)- 3.52	243
Figure 3.12	SFC trace of (–)- 3.52	243
Figure 3.13	SFC trace of (±)- 3.51	244
Figure 3.14	SFC trace of 3.51	244
Figure 3.15	SFC trace of (±)- 3.91	245
Figure 3.16	SFC trace of 3.91	245
Figure 3.17	¹ H NMR (500 MHz, CDCl ₃) of compound 3.54	247
Figure 3.18	¹³ C NMR (125 MHz, CDCl ₃) of compound 3.54	247
Figure 3.19	¹ H NMR (500 MHz, CDCl ₃) of compound 3.56	248
Figure 3.20	¹³ C NMR (125 MHz, CDCl ₃) of compound 3.56	248
Figure 3.21	¹ H NMR (500 MHz, CDCl ₃) of compound 3.49	249
Figure 3.22	¹³ C NMR (125 MHz, CDCl ₃) of compound 3.49	249
Figure 3.23	¹ H NMR (600 MHz, CDCl ₃) of compound 3.58	250
Figure 3.24	¹³ C NMR (125 MHz, CDCl ₃) of compound 3.58	250
Figure 3.25	¹ H NMR (500 MHz, CDCl ₃) of compound 3.60	251
Figure 3.26	¹³ C NMR (125 MHz, CDCl ₃) of compound 3.60	251
Figure 3.27	¹ H NMR (500 MHz, CDCl ₃) of compound 3.61	252
Figure 3.28	¹³ C NMR (125 MHz, CDCl ₃) of compound 3.61	252
Figure 3.29	¹ H NMR (500 MHz, CDCl ₃) of compound 3.63	253

Figure 3.30	^{13}C NMR (125 MHz, CDCl_3) of compound 3.63	253
Figure 3.31	^1H NMR (600 MHz, CDCl_3) of compound 3.65	254
Figure 3.32	^{13}C NMR (125 MHz, CDCl_3) of compound 3.65	254
Figure 3.33	^1H NMR (500 MHz, CDCl_3) of compound 3.66	255
Figure 3.34	^{13}C NMR (125 MHz, CDCl_3) of compound 3.66	255
Figure 3.35	^1H NMR (600 MHz, CDCl_3) of compound 3.67	256
Figure 3.36	^{13}C NMR (150 MHz, CDCl_3) of compound 3.67	256
Figure 3.37	^1H NMR (500 MHz, CDCl_3) of compounds 3.17 and 3.68	257
Figure 3.38	^{13}C NMR (125 MHz, CDCl_3) of compounds 3.17 and 3.68	257
Figure 3.39	NOESY (500 MHz, CDCl_3) of compound 3.17	258
Figure 3.40	^1H NMR (500 MHz, CDCl_3) of compound 3.22	259
Figure 3.41	^{13}C NMR (125 MHz, CDCl_3) of compound 3.22	259
Figure 3.42	^1H NMR (500 MHz, CDCl_3) of compound 3.23	260
Figure 3.43	^{13}C NMR (125 MHz, CDCl_3) of compound 3.23	260
Figure 3.44	^1H NMR (600 MHz, CDCl_3) of compounds 3.24 and 3.72	261
Figure 3.45	^{13}C NMR (150 MHz, CDCl_3) of compounds 3.24 and 3.72	261
Figure 3.46	^1H NMR (500 MHz, CDCl_3) of compound 3.25	262
Figure 3.47	^{13}C NMR (125 MHz, CDCl_3) of compound 3.25	262
Figure 3.48	^{19}F NMR (282 MHz, CDCl_3) of compound 3.25	263
Figure 3.49	^1H NMR (500 MHz, CDCl_3) of compounds 3.26 , 3.75 , and 3.39	264
Figure 3.50	^{13}C NMR (125 MHz, CDCl_3) of compounds 3.26 , 3.75 , and 3.39	264
Figure 3.51	^{19}F NMR (282 MHz, CDCl_3) of compounds 3.26 , 3.75 , and 3.39	265
Figure 3.52	^1H NMR (500 MHz, CDCl_3) of compounds 3.27 and 3.77	266

Figure 3.53	¹³ C NMR (125 MHz, CDCl ₃) of compounds 3.27 and 3.77	266
Figure 3.54	¹ H NMR (500 MHz, CDCl ₃) of compounds 3.28 and 3.78	267
Figure 3.55	¹³ C NMR (125 MHz, CDCl ₃) of compounds 3.28 and 3.78	267
Figure 3.56	¹ H NMR (500 MHz, CDCl ₃) of compounds 3.29 and 3.79	268
Figure 3.57	¹³ C NMR (125 MHz, CDCl ₃) of compounds 3.29 and 3.79	268
Figure 3.58	¹ H NMR (500 MHz, CDCl ₃) of compounds 3.30 and 3.80	269
Figure 3.59	¹³ C NMR (125 MHz, CDCl ₃) of compounds 3.30 and 3.80	269
Figure 3.60	¹ H NMR (500 MHz, CDCl ₃) of compounds 3.31 and 3.82	270
Figure 3.61	¹³ C NMR (125 MHz, CDCl ₃) of compounds 3.31 and 3.82	270
Figure 3.62	NOESY (600 MHz, CDCl ₃) of compound 3.31	271
Figure 3.63	¹ H NMR (500 MHz, CDCl ₃) of compounds 3.32 and 3.83	272
Figure 3.64	¹³ C NMR (125 MHz, CDCl ₃) of compounds 3.32 and 3.83	272
Figure 3.65	¹ H NMR (500 MHz, CDCl ₃) of compounds 3.33 and 3.85	273
Figure 3.66	¹³ C NMR (125 MHz, CDCl ₃) of compounds 3.33 and 3.85	273
Figure 3.67	NOESY (500 MHz, CDCl ₃) of compound 3.85	274
Figure 3.68	¹ H NMR (500 MHz, CDCl ₃) of compounds 3.18 and 3.17	275
Figure 3.69	¹³ C NMR (125 MHz, CDCl ₃) of compounds 3.18 and 3.17	275
Figure 3.70	¹ H NMR (500 MHz, CDCl ₃) of compound 3.35	276
Figure 3.71	¹³ C NMR (125 MHz, CDCl ₃) of compound 3.35	276
Figure 3.72	¹ H NMR (500 MHz, CDCl ₃) of compounds 3.36 and 3.23	277
Figure 3.73	¹³ C NMR (125 MHz, CDCl ₃) of compound 3.36 and 3.23	277
Figure 3.74	¹ H NMR (500 MHz, CDCl ₃) of compounds 3.37 and 3.24	278
Figure 3.75	¹³ C NMR (125 MHz, CDCl ₃) of compound 3.37 and 3.24	278

Figure 3.76	¹ H NMR (500 MHz, CDCl ₃) of compounds 3.38 and 3.25	279
Figure 3.77	¹³ C NMR (125 MHz, CDCl ₃) of compound 3.38 and 3.25	279
Figure 3.78	¹⁹ F NMR (282 MHz, CDCl ₃) of compound 3.38 and 3.25	280
Figure 3.79	¹ H NMR (500 MHz, CDCl ₃) of compounds 3.39 and 3.26	281
Figure 3.80	¹³ C NMR (125 MHz, CDCl ₃) of compound 3.39 and 3.26	281
Figure 3.81	¹⁹ F NMR (282 MHz, CDCl ₃) of compound 3.39 and 3.26	282
Figure 3.82	¹ H NMR (600 MHz, CDCl ₃) of compounds 3.40 and 3.27	283
Figure 3.83	¹³ C NMR (150 MHz, CDCl ₃) of compound 3.40 and 3.27	283
Figure 3.84	¹ H NMR (500 MHz, CDCl ₃) of compounds 3.41 , 3.28 , and 3.78	284
Figure 3.85	¹³ C NMR (125 MHz, CDCl ₃) of compounds 3.41 , 3.28 , and 3.78	284
Figure 3.86	¹ H NMR (500 MHz, CDCl ₃) of compound 3.42	285
Figure 3.87	¹³ C NMR (125 MHz, CDCl ₃) of compound 3.42	285
Figure 3.88	¹ H NMR (500 MHz, CDCl ₃) of compound 3.43	286
Figure 3.89	¹³ C NMR (125 MHz, CDCl ₃) of compound 3.43	286
Figure 3.90	¹ H NMR (600 MHz, CDCl ₃) of compound 3.44	287
Figure 3.91	¹³ C NMR (125 MHz, CDCl ₃) of compound 3.44	287
Figure 3.92	¹ H NMR (500 MHz, CDCl ₃) of compound 3.52	288
Figure 3.93	¹³ C NMR (125 MHz, CDCl ₃) of compound 3.52	288
Figure 3.94	¹ H NMR (500 MHz, CDCl ₃) of compounds 3.51 and 3.91	289
Figure 3.95	¹³ C NMR (125 MHz, CDCl ₃) of compounds 3.51 and 3.91	289

CHAPTER FOUR

Figure 4.1	Selected <i>in situ</i> generated strained intermediates and the reactivity of 1,2-cyclohexadiene (4.5) in cycloaddition reactions	302
------------	---	-----

Figure 4.2	The reaction of <i>in situ</i> generated 1,2-cyclohexadiene and 4.15 to afford ketone 4.16	303
Figure 4.3	Potential mechanism for the formation of ketone 4.16	304
Figure 4.4	Isotope labeling study leveraging ¹⁸ O enriched TEMPO (4.15).....	305
Figure 4.5	HRMS spectrum of compound 4.15	309
Figure 4.6	HRMS spectrum of compound 4.16	310
Figure 4.7	¹ H NMR (600 MHz, CDCl ₃) of compound 4.16	311
 CHAPTER FIVE		
Figure 5.1A	Cyclobutane-containing, biologically relevant molecules 5.1–5.6	320
Figure 5.1B	Strained cyclic intermediates 5.7a–d and 5.8	320
Figure 5.1C	Overview of the current study.....	320
Figure 5.2	Survey of olefin partners 5.14 in [2+2] cycloaddition of oxacyclic allene 5.13	322
Figure 5.3	Scope of [2+2] cycloadditions with dienamine trapping partners 5.28 ...	324
Figure 5.4	Scope of [2+2] cycloadditions with (het)aryl-substituted alkenes 5.42 and 5.43	326
Figure 5.5	[2+2] cycloadditions of carbocyclic allenes 5.63 and 5.66 with dienamine 5.24	327
Figure 5.6	Thermal isomerization of cycloadducts 5.25 , 5.41 , and 5.61	329
Figure 5.7	Synthetic elaborations of cycloadducts 5.70 , 5.77 , and 5.80 to access complex products 5.73 , 5.78 , and 5.82 , respectively.....	331
Figure 5.8	SFC trace for mixture of 5.34 and <i>Z</i> - 5.34	339
Figure 5.9	SFC trace for 5.34	340

Figure 5.10	ORTEP representation of X-ray crystallographic structure 5.61	377
Figure 5.11	Unsuccessful and low yielding trapping partners evaluated during scope studies.....	379
Figure 5.12	¹ H NMR (500 MHz, CDCl ₃) of compound 5.24	394
Figure 5.13	¹³ C NMR (150 MHz, CDCl ₃) of compound 5.24	394
Figure 5.14	¹ H NMR (600 MHz, CDCl ₃) of compound 5.85	395
Figure 5.15	¹³ C NMR (150 MHz, CDCl ₃) of compound 5.85	395
Figure 5.16	¹ H NMR (600 MHz, CDCl ₃) of compound 5.32	396
Figure 5.17	¹³ C NMR (150 MHz, CDCl ₃) of compound 5.32	396
Figure 5.18	¹ H NMR (600 MHz, CDCl ₃) of compound 5.34	397
Figure 5.19	¹³ C NMR (150 MHz, CDCl ₃) of compound 5.34	397
Figure 5.20	NOESY (400 MHz, CDCl ₃) of compound 5.34	398
Figure 5.21	¹ H NMR (600 MHz, CDCl ₃) of compound 5.36	399
Figure 5.22	¹³ C NMR (150 MHz, CDCl ₃) of compound 5.36	399
Figure 5.23	¹⁹ F NMR (565 MHz, CDCl ₃) of compound 5.36	400
Figure 5.24	¹ H NMR (500 MHz, CDCl ₃) of compound 5.88	401
Figure 5.25	¹³ C NMR (125 MHz, CDCl ₃) of compound 5.88	401
Figure 5.26	¹ H NMR (500 MHz, CDCl ₃) of compound 5.38	402
Figure 5.27	¹³ C NMR (150 MHz, CDCl ₃) of compound 5.38	402
Figure 5.28	¹ H NMR (600 MHz, CDCl ₃) of compound 5.89	403
Figure 5.29	¹³ C NMR (150 MHz, CDCl ₃) of compound 5.89	403
Figure 5.30	¹ H NMR (500 MHz, CDCl ₃) of compound 5.40	404
Figure 5.31	¹³ C NMR (125 MHz, CDCl ₃) of compound 5.40	404

Figure 5.32	¹ H NMR (600 MHz, CDCl ₃) of compound 5.48	405
Figure 5.33	¹³ C NMR (150 MHz, CDCl ₃) of compound 5.48	405
Figure 5.34	¹ H NMR (600 MHz, CDCl ₃) of compound 5.56	406
Figure 5.35	¹³ C NMR (150 MHz, CDCl ₃) of compound 5.56	406
Figure 5.36	¹ H NMR (600 MHz, CDCl ₃) of compound 5.60	407
Figure 5.37	¹³ C NMR (150 MHz, CDCl ₃) of compound 5.60	407
Figure 5.38	¹ H NMR (600 MHz, CDCl ₃) of compound 5.79	408
Figure 5.39	¹³ C NMR (150 MHz, CDCl ₃) of compound 5.79	408
Figure 5.40	NOESY (400 MHz, CDCl ₃) of compound 5.79	409
Figure 5.41	¹ H NMR (500 MHz, CDCl ₃) of compound 5.96	410
Figure 5.42	¹³ C NMR (125 MHz, CDCl ₃) of compound 5.96	410
Figure 5.43	¹ H NMR (500 MHz, CDCl ₃) of compound 5.68	411
Figure 5.44	¹³ C NMR (125 MHz, CDCl ₃) of compound 5.68	411
Figure 5.45	¹⁹ F NMR (282 MHz, CDCl ₃) of compound 5.68	412
Figure 5.46	¹ H NMR (500 MHz, CDCl ₃) of compound 5.17	413
Figure 5.47	¹³ C NMR (125 MHz, CDCl ₃) of compound 5.17	413
Figure 5.48	¹ H NMR (500 MHz, CDCl ₃) of compound 5.19	414
Figure 5.49	¹³ C NMR (125 MHz, CDCl ₃) of compound 5.19	414
Figure 5.50	NOESY (600 MHz, CDCl ₃) of compound 5.19	415
Figure 5.51	¹ H NMR (500 MHz, CDCl ₃) of compounds 5.21 and <i>epi</i> - 5.21	416
Figure 5.52	¹³ C NMR (125 MHz, CDCl ₃) of compounds 5.21 and <i>epi</i> - 5.21	416
Figure 5.53	¹ H NMR (600 MHz, CDCl ₃) of compound 5.21	417
Figure 5.54	NOESY (600 MHz, CDCl ₃) of compound 5.21	417

Figure 5.55	^1H NMR (500 MHz, CDCl_3) of compound 5.23	418
Figure 5.56	^{13}C NMR (150 MHz, CDCl_3) of compound 5.23	418
Figure 5.57	^1H NMR (500 MHz, CDCl_3) of compound <i>epi</i> - 5.23	419
Figure 5.58	^{13}C NMR (150 MHz, CDCl_3) of compound <i>epi</i> - 5.23	419
Figure 5.59	NOESY (600 MHz, CDCl_3) of compound <i>epi</i> - 5.23	420
Figure 5.60	^1H NMR (600 MHz, CDCl_3) of compound 5.25	421
Figure 5.61	^{13}C NMR (150 MHz, CDCl_3) of compound 5.25	421
Figure 5.62	NOESY (600 MHz, CDCl_3) of compound 5.25	422
Figure 5.63	^1H NMR (600 MHz, CDCl_3) of compound 5.31	423
Figure 5.64	^{13}C NMR (125 MHz, CDCl_3) of compound 5.31	423
Figure 5.65	NOESY (500 MHz, CDCl_3) of compound 5.31	424
Figure 5.66	^1H NMR (600 MHz, CDCl_3) of compound 5.33	425
Figure 5.67	^{13}C NMR (125 MHz, CDCl_3) of compound 5.33	425
Figure 5.68	NOESY (600 MHz, CDCl_3) of compound 5.33	426
Figure 5.69	^1H NMR (500 MHz, CDCl_3) of compound 5.35	427
Figure 5.70	^{13}C NMR (150 MHz, CDCl_3) of compound 5.35	427
Figure 5.71	NOESY (400 MHz, CDCl_3) of compound 5.35	428
Figure 5.72	^1H NMR (600 MHz, CDCl_3) of compound 5.37	429
Figure 5.73	^{13}C NMR (150 MHz, CDCl_3) of compound 5.37	429
Figure 5.74	^{19}F NMR (565 MHz, CDCl_3) of compound 5.37	430
Figure 5.75	NOESY (400 MHz, CDCl_3) of compound 5.37	430
Figure 5.76	^1H NMR (500 MHz, CDCl_3) of compound 5.39	431
Figure 5.77	^{13}C NMR (125 MHz, CDCl_3) of compound 5.39	431

Figure 5.78	NOESY (500 MHz, CDCl ₃) of compound 5.39	432
Figure 5.79	¹ H NMR (600 MHz, CDCl ₃) of compounds 5.41 and <i>epi-5.41</i>	433
Figure 5.80	¹³ C NMR (150 MHz, CDCl ₃) of compounds 5.41 and <i>epi-5.41</i>	433
Figure 5.81	NOESY (400 MHz, toluene-d ₈) of compound 5.41	434
Figure 5.82	¹ H NMR (500 MHz, CDCl ₃) of compound <i>epi-5.41</i>	435
Figure 5.83	¹³ C NMR (125 MHz, CDCl ₃) of compound <i>epi-5.41</i>	435
Figure 5.84	¹ H NMR (600 MHz, CDCl ₃) of compound 5.27	436
Figure 5.85	¹³ C NMR (150 MHz, CDCl ₃) of compound 5.27	436
Figure 5.86	NOESY (400 MHz, CDCl ₃) of compound 5.27	437
Figure 5.87	¹ H NMR (600 MHz, CDCl ₃) of compound 5.47	438
Figure 5.88	¹³ C NMR (150 MHz, CDCl ₃) of compound 5.47	438
Figure 5.89	NOESY (400 MHz, CDCl ₃) of compound 5.47	439
Figure 5.90	¹ H NMR (600 MHz, CDCl ₃) of compound 5.49	440
Figure 5.91	¹³ C NMR (150 MHz, CDCl ₃) of compound 5.49	440
Figure 5.92	NOESY (600 MHz, CDCl ₃) of compound 5.49	441
Figure 5.93	¹ H NMR (600 MHz, C ₆ D ₆) of compound 5.51	442
Figure 5.94	¹³ C NMR (125 MHz, CDCl ₃) of compound 5.51	442
Figure 5.95	NOESY (600 MHz, C ₆ D ₆) of compound 5.51	443
Figure 5.96	¹ H NMR (500 MHz, CDCl ₃) of compound 5.53	444
Figure 5.97	¹³ C NMR (150 MHz, CDCl ₃) of compound 5.53	444
Figure 5.98	NOESY (600 MHz, CDCl ₃) of compound 5.53	445
Figure 5.99	¹ H NMR (600 MHz, CDCl ₃) of compound 5.55	446
Figure 5.100	¹³ C NMR (150 MHz, CDCl ₃) of compound 5.55	446

Figure 5.101	^{19}F NMR (565 MHz, CDCl_3) of compound 5.55	447
Figure 5.102	NOESY (400 MHz, CDCl_3) of compound 5.55	447
Figure 5.103	^1H NMR (600 MHz, CDCl_3) of compound <i>epi</i> - 5.55	448
Figure 5.104	^{13}C NMR (150 MHz, CDCl_3) of compound <i>epi</i> - 5.55	448
Figure 5.105	^{19}F NMR (565 MHz, CDCl_3) of compound <i>epi</i> - 5.55	449
Figure 5.106	^1H NMR (500 MHz, CDCl_3) of compound 5.57	450
Figure 5.107	^{13}C NMR (150 MHz, CDCl_3) of compound 5.57	450
Figure 5.108	NOESY (400 MHz, CDCl_3) of compound 5.57	451
Figure 5.109	^1H NMR (500 MHz, CDCl_3) of compound <i>epi</i> - 5.57	452
Figure 5.110	^{13}C NMR (125 MHz, CDCl_3) of compound <i>epi</i> - 5.57	452
Figure 5.111	^1H NMR (600 MHz, CDCl_3) of compound 5.59	453
Figure 5.112	^{13}C NMR (150 MHz, CDCl_3) of compound 5.59	453
Figure 5.113	^1H NMR (500 MHz, CDCl_3) of compound <i>epi</i> - 5.59	454
Figure 5.114	^{13}C NMR (125 MHz, CDCl_3) of compound <i>epi</i> - 5.59	454
Figure 5.115	NOESY (600 MHz, CDCl_3) of compound <i>epi</i> - 5.59	455
Figure 5.116	^1H NMR (600 MHz, CDCl_3) of compound 5.61	456
Figure 5.117	^{13}C NMR (150 MHz, CDCl_3) of compound 5.61	456
Figure 5.118	^1H NMR (500 MHz, CDCl_3) of compound 5.64	457
Figure 5.119	^{13}C NMR (125 MHz, CDCl_3) of compound 5.64	457
Figure 5.120	NOESY (400 MHz, CDCl_3) of compound 5.64	458
Figure 5.121	^1H NMR (600 MHz, CDCl_3) of compound 5.67	459
Figure 5.122	^{13}C NMR (150 MHz, CDCl_3) of compound 5.67	459
Figure 5.123	NOESY (600 MHz, CDCl_3) of compound 5.67	460

Figure 5.124	¹ H NMR (500 MHz, CDCl ₃) of compounds <i>epi</i> - 5.25 and 5.25	461
Figure 5.125	¹³ C NMR (125 MHz, CDCl ₃) of compounds <i>epi</i> - 5.25 and 5.25	461
Figure 5.126	¹ H NMR (500 MHz, CDCl ₃) of compound <i>epi</i> - 5.61	462
Figure 5.127	¹³ C NMR (125 MHz, CDCl ₃) of compound <i>epi</i> - 5.61	462
Figure 5.128	¹ H NMR (600 MHz, CDCl ₃) of compound 5.70	463
Figure 5.129	¹³ C NMR (150 MHz, CDCl ₃) of compound 5.70	463
Figure 5.130	NOESY (400 MHz, CDCl ₃) of compound 5.70	464
Figure 5.131	¹ H NMR (600 MHz, CDCl ₃) of compound 5.71	465
Figure 5.132	¹³ C NMR (150 MHz, CDCl ₃) of compound 5.71	465
Figure 5.133	NOESY (400 MHz, CDCl ₃) of compound 5.71	466
Figure 5.134	¹ H NMR (500 MHz, CDCl ₃) of compound 5.73	467
Figure 5.135	¹³ C NMR (125 MHz, CDCl ₃) of compound 5.73	467
Figure 5.136	¹ H NMR (600 MHz, CDCl ₃) of compound 5.77	468
Figure 5.137	¹³ C NMR (150 MHz, CDCl ₃) of compound 5.77	468
Figure 5.138	¹ H NMR (600 MHz, CDCl ₃) of compound 5.78	469
Figure 5.139	¹³ C NMR (150 MHz, CDCl ₃) of compound 5.78	469
Figure 5.140	NOESY (600 MHz, CDCl ₃) of compound 5.78	470
Figure 5.141	¹ H NMR (500 MHz, CDCl ₃) of compound 5.80	471
Figure 5.142	¹³ C NMR (125 MHz, CDCl ₃) of compound 5.80	471
Figure 5.143	NOESY (600 MHz, CDCl ₃) of compound 5.80	472
Figure 5.144	¹ H NMR (600 MHz, CDCl ₃) of compound 5.82	473
Figure 5.145	¹³ C NMR (125 MHz, CDCl ₃) of compound 5.82	473
Figure 5.146	NOESY (400 MHz, CDCl ₃) of compound 5.82	474

CHAPTER SIX

Figure 6.1	Strained cyclic intermediates and selected synthetic applications	499
Figure 6.2	Silyl triflate (previous) and silyl tosylate (current) precursors to 6.2 and 6.3	500
Figure 6.3	Syntheses of silyl tosylates 6.9 and 6.11	501
Figure 6.4	Silyl tosylate 6.28 to access 1,2-cycloheptadiene (6.29).....	504
Figure 6.5	Competition experiments between silyl triflate and silyl tosylate strained intermediate precursors	505
Figure 6.6	¹ H NMR (500 MHz, CDCl ₃) of compound 6.9	519
Figure 6.7	¹³ C NMR (125 MHz, CDCl ₃) of compound 6.9	519
Figure 6.8	¹ H NMR (500 MHz, CDCl ₃) of compound 6.11	520
Figure 6.9	¹³ C NMR (125 MHz, CDCl ₃) of compound 6.11	520
Figure 6.10	¹ H NMR (600 MHz, CDCl ₃) of compound 6.17	521
Figure 6.11	¹ H NMR (500 MHz, CDCl ₃) of compound 6.19	521
Figure 6.12	¹ H NMR (500 MHz, CDCl ₃) of compound 6.21	522
Figure 6.13	¹ H NMR (600 MHz, CDCl ₃) of compound 6.23	522
Figure 6.14	¹ H NMR (500 MHz, CDCl ₃) of compound 6.24	523
Figure 6.15	¹ H NMR (500 MHz, CDCl ₃) of compounds 6.26 and 6.34	523
Figure 6.16	¹ H NMR (500 MHz, CDCl ₃) of compounds 6.32	524
Figure 6.17	¹³ C NMR (125 MHz, CDCl ₃) of compound 6.32	524
Figure 6.18	¹ H NMR (600 MHz, CDCl ₃) of compounds 6.28	525
Figure 6.19	¹³ C NMR (125 MHz, CDCl ₃) of compound 6.28	525
Figure 6.20	¹ H NMR (500 MHz, CDCl ₃) of compounds 6.30	526

LIST OF SCHEMES

CHAPTER TWO

Scheme 2.1	Envisioned reaction design.....	64
------------	---------------------------------	----

LIST OF TABLES

CHAPTER TWO

Table 2.1	Reaction Optimization.....	65
Table 2.2	Temperature Screening Results.....	86
Table 2.3	Base Screening Results	86
Table 2.4	CsF Loading Screening Results	86
Table 2.5	Ligand Screening Results.....	87
Table 2.6	Chiral Ligand Screening Results.....	107
Table 2.7	Solvent Screening Results.....	108
Table 2.8	Fluoride Source Screening Results	109
Table 2.9	Palladium Source Screening Results.....	109
Table 2.10	Base Screening Results	110
Table 2.11	Crystal Data and Structure Refinement for Epoxide (+)- 2.50	115
Table 2.12	SFC Conditions and Data.....	116

CHAPTER THREE

Table 3.1	Select Results from Optimization Studies.....	176
Table 3.2	Evaluation of Select Chiral Ligands in the Annulation Reaction	183
Table 3.3	Evaluation of Vinyl Benzoxazinone Equivalents.....	199
Table 3.4	Evaluation of Temperature.....	199
Table 3.5	Evaluation of H ₂ O Loading.....	200
Table 3.6	Evaluation of Catalyst Loading.....	200
Table 3.7	Evaluation of Concentration.....	200
Table 3.8	Evaluation of Ligands	201

Table 3.9	Ligand Evaluation Results.	235
Table 3.10	Crystal Data and Structure Refinement for Compound (–)- 3.43	238
Table 3.11	SFC Conditions and Data.	239
CHAPTER FIVE		
Table 5.1	SFC Data for 5.34	340
Table 5.2	Evaluation of Equivalents of Trapping Partner 5.58	357
Table 5.3	Evaluation of Solvent and Equivalents of Additive.	358
Table 5.4	Evaluation of Equivalents of Trapping Partner 5.24	358
Table 5.5	Evaluation of Solvent and Additive.	359
Table 5.6	Crystal Data and Structure Refinement for Compound 5.61	378
Table 5.7	Computed Energies of Thermal Isomerization Products at 25 °C Using DFT (B3LYP/6-31G(d))	475
CHAPTER SIX		
Table 6.1	Silyl Tosylate 6.9 as a Precursor to Cyclohexyne (6.2)	502
Table 6.2	Silyl Tosylate 6.11 as a Precursor to 1,2-Cyclohexadiene (6.3)	503

LIST OF ABBREVIATIONS

α	alpha
β	beta
σ	sigma
μ	micro
λ	wavelength
π	pi
δ	chemical shift
Δ	heat or difference
(Het)	hetero
Ac	acetyl
acac	acetylacetonate
anth	anthracenyl
app.	apparent
aq.	aqueous
Ar	aryl
BINAP	([1,1'-binaphthalene]-2,2'-diyl)bis(diphenylphosphane)
B3LYP	Becke, 3-parameter, Lee–Yang–Parr (functional)
Bn	benzyl
Boc	<i>tert</i> -butyloxy carbonyl
BOX	bis(oxazoline)
br	broad
Bu	butyl
<i>n</i> -Bu	butyl (linear)
<i>t</i> -Bu	<i>tert</i> -butyl
<i>c</i>	concentration for specific rotation measurements
°C	degrees Celsius
calcd	calculated
Cbz	carboxybenzyl
CCDC	Cambridge Crystallographic Data Centre
cm	centimeter
cod	1,5-cyclooctadiene
conc.	concentration
Cp	cyclopentadienyl

Cy	cyclohexyl
DABCO	1,4-diazabicyclo[2.2.2]octane
DART-MS	Direct Analysis in Real Time – Mass Spectroscopy
dba	dibenzylideneacetone
DBU	1,8-diazabicyclo(5.4.0)undec-7-ene
DCE	1,2-dichloroethane
d	doublet
dd	doublet of doublets
ddd	doublet of doublet of doublets
ddt	doublet of doublet of triplets
δ	chemical shift
DFT	density functional theorem
DMAP	4-dimethylaminopyridine
DME	1,2-dimethoxyethane
DMF	<i>N,N</i> -dimethylformamide
DMSO	dimethyl sulfoxide
dppf	1,1'-bis(diphenylphosphino)ferrocene
dq	doublet of quartets
dr	diastereomeric ratio
dt	doublet of triplets
E	entropy
ee	enantiomeric excess
<i>epi</i>	epimer
equiv	equivalent
ESI	electrospray ionization
Et	ethyl
EtOAc	ethyl acetate
η	eta
FT	Fourier transform
g	gram(s)
G	Gibb's free energy
<i>gem</i>	geminal
h	hour(s)
H	enthalpy

Het	heterocycle
HMPA	hexamethylphosphoramide
HRMS	high resolution mass spectroscopy
Hz	hertz
IR	infrared (spectroscopy)
<i>i</i> -Pr	iso-propyl
<i>J</i>	coupling constant
kcal/mol	kilocalories to mole ratio
KHMDS	potassium hexamethyldisilazide
L	liter or ligand
LDA	lithium diisopropylamide
m	multiplet or milli
<i>m</i>	meta
M	molar
<i>m/z</i>	mass to charge ratio
<i>m</i> CPBA	<i>meta</i> -chloroperoxybenzoic acid
Me	methyl
MHz	megahertz
min	minute(s)
mm	millimeter
mol	mole(s)
MOM	Methoxymethyl ether
mp	melting point
Ms	mesyl
NaHMDS	sodium hexamethyldisilazide
NMR	nuclear magnetic resonance
NOESY	Nuclear Overhauser Enhancement Spectroscopy
<i>o</i>	ortho
OLED	organic light-emitting diode
ORTEP	Oak Ridge Thermal-Ellipsoid Plot Program
<i>p</i>	para
Ph	phenyl
PHOX	phosphinooxazoline
ppm	parts per million

q	quartet
quant	quantitative
QUINAP	1-(2-diphenylphosphino-1-naphthyl)isoquinoline
quint	quintet
rac	racemic
R _f	retention factor
s	singlet
sat.	saturated
SFC	supercritical fluid chromatography
t	triplet
temp	temperature
TASF	tris(dimethylamino)sulfonium difluorotrimethylsilicate
TBAF	tetrabutylammonium fluoride
TBAI	tetrabutylammonium iodide
TBAT	tetrabutylammonium difluorotriphenylsilicate
TEMPO	(2,2,6,6-tetramethylpiperidin-1-yl)oxyl
TES	triethylsilyl
Tf	trifluoromethanesulfonyl
THF	tetrahydrofuran
TIPS	triisopropylsilyl
TLC	thin layer chromatography
tol	tolyl
Ts	<i>p</i> -toluenesulfonyl (tosyl)
UV	ultraviolet
w/w	weight by weight
wt%	percentage by mass
ZPE	zero-point energy

ACKNOWLEDGEMENTS

Academia is a team sport, and through my own career I have had so many inspiring, motivating, and thoughtful figures that have helped me reach the finish line. During my time in high school, there were numerous teachers at The Woodlands High School that were pivotal to my development. To name a few, Dr. Elvira de Pieri (AKA “Doc”) sparked my passion for chemistry, James Rowland pushed me to be the best version of myself, and Andrew Salmon taught me the value of a good work ethic. I am forever indebted to their mentorship in my early years of school.

As an undergraduate at UT-Austin, my passion for research flourished. My undergraduate thesis advisor, Professor Eric Anslyn, was the main contributor to this, as he allowed me to perform research in his laboratory. I still remember the first time I walked into his lab and felt as though I had been transported to a whole new world full of things to discover. His love and passion for chemistry was contagious, and he was always open to discuss ideas or make time for my academic development. He also had a slew of amazing graduate students in his lab that helped me develop my early research techniques. Drs. Sarah Moor, Samuel Daulhauser, James Howard, Logan Bachman (more on him later), Jaime Coronado, Stephanie Valenzuela, and Igor Kolesnichenko were all so patient with me during my time in Eric’s lab, and I am grateful for their willingness to help me. Drs. Rogelio Escamilla and Brenden Herrera were excellent research mentors that taught me many valuable laboratory skills that I still use to this day. I also want to acknowledge Dr. Christopher Wight, for his endearing nature and reminder to approach research with humility and grace. Lastly, Dr. James Brewster has continued to be an amazing mentor and friend. Without his guidance and support in my academic career, I would not be where I am today.

Coming to UCLA for graduate school was the best decision I have ever made, and much of that is thanks to my thesis advisor, Professor Neil Garg. His dedication to my academic and

professional development puts him above and beyond the mentorship capabilities of most advisors. Whether it is being an advocate for us during the job hunt or celebrating our successes through “epic” parties, Neil has been such a supportive and encouraging mentor. His emphasis on our education through the many thought exercises he provided was very much appreciated, as he is also an excellent teacher. As such, he has successfully cultivated a collaborative environment in the laboratory where we can truly develop as outstanding scientists. Neil has always made time for me when I need it, and I have appreciated all the honest advice and guidance he has given me during my time here. I will forever be grateful for him, and I hope we can continue to have a great relationship through the next stages of my career.

I would also like to thank the rest of my doctoral thesis committee: Professors Ken Houk, Yi Tang, and Dean Miguel García-Garibay. They are an inspiring and accomplished group of professors, and have I appreciated their support and mentorship throughout my graduate studies.

Next, I would like to thank all the amazing and talented individuals in the Garg lab that I have had the privilege to work with. Starting with the postdoctoral scholars, I had the pleasure of briefly overlapping with Dr. Evan Darzi, whose enthusiasm about chemistry and overall encouragement provided for a warm welcome to the lab when I started. Following me from Texas, Dr. Logan Bachman (a.k.a. Logie) was the perfect friend to start my experience in the Garg lab with. His patient and calming nature quickly made him a lab favorite, and I am very appreciative of his advice and guidance. Whether it was a late-night rock-climbing session or just grabbing some Lone Stars at the end of the week, Logan made the transition into graduate school an easier experience, and I know that he impacted many people positively during his time here. Dr. Veronica Tona also joined the laboratory around the same time, and I had the privilege of working in MSB

5229 with her. She is sharp and hilariously blunt, and I valued her vast wisdom, as well as our conversations about the interesting vocabulary of the Italian language.

The next group of postdoctoral scholars to join the lab included Drs. Nathan Adamson and Daniel Nasrallah. Nathan is an extremely skilled chemist, whose immense chemical knowledge and intuition was very helpful to many of us in the lab during his time here. Luckily, I was able to work next to Dan for most of my graduate career. I can say without a doubt that he is one of the nicest and most thoughtful individuals. Not only is he a talented chemist, but he taught many of us the value of being a well-rounded scientist. I am proud that I was able to expand his “youth” vocabulary with words such as “slaps” and “banger”. I am excited that he has found a home at Roanoke College, and I know he will have a fantastic career as a professor that will shape the lives of many students.

Next, Drs. Lukas Wein and Jacob Sorrentino joined the lab during my fourth year of graduate school. Lukas is an incredibly bright chemist, who has an impressive knowledge of most named reactions. I enjoyed working on denksports with him, and his endearing nature and quick sense of humor made him a fast friend despite his short tenure in the lab. Jacob was an excellent project partner who provided a different outlook that complemented my conventional ways of solving problems, overall expanding my critical thinking abilities. His enthusiasm and encouragement kept me grounded and provided much needed support during our mutual job searches. I know he has a great career ahead of him.

To round out the postdoctoral scholars, the most recent additions to the lab include Drs. Jiaming Ding and Sarah French. I have had the pleasure of working in MSB 5229 with Jiaming, and his intellect and humor have made my last year of graduate school quite enjoyable. I know he will develop many important research areas in the lab during his time here. Sarah is a very driven

and motivated chemist with excellent laboratory skills. Additionally, her kindness and out-going nature has made her fit right into the lab culture.

Moving on to the graduate students, the group that had the biggest impact on me during my first year was the class of 2020, consisting of Drs. Michael Yamano, Jacob Dander, Robert Susick, and Jordan Dotson. Michael is a very adept and gifted chemist, who made for a great mentor to me as a “young pup”. I appreciated his wisdom and guidance during my first year, and I found our discussions on important concepts such as whether “a pop-tart is a sandwich” (it’s not) a great distraction. Jacob is one of the most eloquent scientists I have met, and I valued his insight during my first year. I had the privilege of working next to Rob, and I enjoyed our rock-climbing sessions together, as well as our trips to Pepe’s for post-climb burritos. Jordan has an immense knowledge of physical organic chemistry yet approached answering my many questions with kindness and patience.

The next group included Drs. Timothy Boit, Melissa Ramirez, and Sarah Anthony, making up the class of 2021. Tim is extremely detailed and sharp, providing as an excellent resource during my early years of graduate school. Melissa is incredibly kind and thoughtful. Despite COVID interrupting our experiences in MSB 5229 together, I am very thankful for her calm and encouraging nature, and I know she will be an awesome professor at the University of Minnesota. Sarah was one of the first people I met in the lab during recruitment weekend, and she was instrumental in my decision to attend UCLA. Her enthusiasm and quick-witted humor made her a great lab mate and friend. I look forward to her being close by in San Diego.

I was fortunate to overlap with the class of 2022, consisting of Drs. Rachel Knapp, Francesca Ippoliti, and Jason Chari. Rachel was a dependable friend and mentor during my early years of graduate school. She always gave the soundest advice, and I knew I could rely on her to

help me during times of “crisis”. I still remember her taking calming walks with me when my candidacy proposal was not cooperating or helping me outline important talks. I appreciated her patience and support. I enjoyed getting to know Fran during our time together in MSB 5234. Her consistent positivity and optimism made for an encouraging environment in the lab, and I felt as though I could come to her for anything I needed. I also enjoyed spending time with her and Josh outside of the lab, whether if it was playing board games or enjoying some delicious pizza at the Doughroom. Jason was another consistent source of positivity during my early years of graduate school, and I am thankful that we were able to work in the same room. He was always willing to drop whatever he was doing to help me, and I am so grateful for our friendship. I enjoyed our thoughtful discussions of chemistry, as well as many important life topics. He inspired me daily to strive for excellence but to remember the importance of helping others, and I know he had a massive impact in the current lab culture.

I was lucky to spend a majority of my graduate career with the class of 2023, consisting of Drs. Katie Spence, Milauni Mehta, and Andrew Kelleghan. Katie is one of the most out-going and motivated people I know. Not only is she skilled in the laboratory, but she also is an excellent advocator. She taught me the importance of believing in myself and my capabilities, and I am forever grateful for that. Milauni (a.k.a Mildred) was an excellent roommate and friend. I had the pleasure of sharing an apartment in Los Leones (a Garg lab staple) with her, where we survived a slew of interesting roommates during our time there. She is a very thoughtful person, and I always appreciate her useful insight about chemistry or life in general. Whether it was parties at Los Leones or watching The Great British Bakeoff after a long day in the lab, I have enjoyed our time together (especially with Saketh too) and look forward to our continued friendship. Lastly, I was fortunate to be mentored by Andrew. He is one of most intelligent people I have ever met, and his

vast chemical knowledge is awe-inspiring. Furthermore, he has always been so approachable and easy to talk to, making him an instant friend when I started in the program. I still look back fondly on Thanksgiving dinners at his place, as well as those six months where we were gym buddies every morning (sorry I did not keep it up). I have learned so much from him, and I am thankful for his kindness and patience with me during my early (and later) years of graduate school.

Moving on to my favorite class, I could not have imagined going through the trials and tribulations of graduate school with anyone else but Ana Bulger and Laura Wonilowicz. I still remember our first quarter together as first year graduate students, where despite all the stress and anxiety of our new life, we were always there to lift each other up and support one another. Ana is such a thoughtful and caring person, who is also an extremely skilled chemist. She is always there to listen and provide useful advice, and I am impressed by her ability to easily break down big problems with actionable solutions. Spending time with her and Nathaniel over the last five years has been one of the highlights of graduate school, as we have been able to commiserate and enjoy each other's company. Laura is also a great acquaintance and lab mate (see page xlvii for more).

At some point in my graduate career, I transitioned to one of the "older students" in laboratory, which is something I still have not gotten used to. As such, the class directly below me consists of Dominick Witkowski, Arismel Tena-Meza, and Luca McDermott. Dominick is a gifted experimentalist who approaches research with a methodical nature that is impressive and something I strive for. I know he will find success in his future career. Ari is an extremely motivated scientist. Her ability to balance so many different tasks is impressive, as she is heavily involved with many important DEI initiatives in our department. She is also hilariously "savage", and I am fortunate to have gotten to work near her over the last year. Luca (a.k.a. Big Luc) has become an amazing friend. His passion for chemistry is unrivaled, and I have always appreciated

the enthusiasm and excitement he brings to the lab every day. I feel more energized about my research after talking with him, and he has played a huge role in propagating this feeling throughout the lab. I will miss going to EDM concerts together and jamming to Madvillainy, but I look forward to visiting the McDermott lab in the coming years.

The class of 2026 is comprised of Georgia Scherer and Jordan Gonzalez, two of the nicest and most considerate people I have ever met. Georgia is incredibly talented, both in the lab and along the marathon route. I am impressed by her tenacity and work ethic, and I know she will continue to be a great leader and mentor to others in the lab. Jordan (a.k.a. Jdog) has been a wonderful project partner and friend. He is unbelievably polite and a very capable bench chemist. Working with him during this last year has been so enjoyable, as we have been able to explore some exciting chemistry together. It has been a pleasure to watch him grow as a scientist and mentor in the lab, and I know his last few years here will be full of success.

Zach Walters, Allison Hands, and Dani Turner make up the class of 2027. I have enjoyed getting to know Zach more over the past year, as we work next to each other in MSB 5229. He is a remarkable chemist, with a vast knowledge of organic synthesis. He is also a kindhearted individual, who is willing to help anyone when they need it. I am excited to see what his future holds. I had the distinct pleasure of mentoring Allison. She made mentoring enjoyable and easy for me, as she is such a thoughtful and competent individual. I am happy to see her find her groove in the lab, and I know she will be a great leader that many will rely on as she progresses through her graduate career. Dani has been a great source of positivity in the lab, and he always brightens any room that he enters. He has also grown into a talented scientist and has tackled some challenging chemistry in his early years of graduate school with vigor and tenacity, which has been very impressive.

Next, we have the class of 2028 consisting of Giulianna Miseo, Benjamin Janda, Allison Clark, and Christina Rivera. Although we were not able to overlap for long, it is evident they have already made a positive impact, and their excitement and engagement in research is awesome to see. I have particularly enjoyed working near Christina in MSB 5299 over the last year, as she is such a kind and thoughtful person. Additionally, I look forward to all their collective successes as they progress through graduate school.

To round out the Garg lab members, we have had a new undergraduate researcher join the lab, Lauren Van Auken. I had the pleasure of working with her virtually a few summers ago, and she is such an intelligent and polite individual. I hope that we continue to see more undergraduate researchers join the lab, as my own undergraduate research experience was so important to my development. Additionally, we had an amazing visiting student from Germany, Lisa Kamecke, who I worked near in MSB 5229 during her tenure in the lab. She is a very astute and hard-working person, and I will always remember her hilarious quips and out-going nature.

Outside of lab, I would like to acknowledge my parents, Kenda and Bryan. They have been so encouraging of my endeavors throughout my life and have instilled important values in me that have been pivotal to my success. My mom is the epitome of a kind and thoughtful person and has shown me the significance of caring for others. My dad has the biggest heart of anyone I know, and his generosity continues to amaze me. They both have so many traits that I aspire to incorporate in my life, and they are my role models. Through this journey, they have been there every step of the way to help, and I am so thankful for their unwavering love and support.

My sister and brother-in-law, Jacqueline and Nasir, have also been so important to me over my graduate career and in my life. Even though I am many miles away, they have continued to show so much support and care for me. I am thankful that I have such a loving sibling in Jacqueline

and that she was able to find such a thoughtful husband. I appreciate the check-in phone calls and texts that I have gotten from them when they know I am stressed or have a big deadline coming up. They have both been an anchor for me during this busy time.

Lastly, I would like to acknowledge the love of my life, Laura Wonilowicz. Not many couples get to experience all the big hurdles of this program together, but I believe they only made our relationship stronger. Over the last four years together, she has been a constant for me during the flurry of graduate school and unprecedented global events. Despite the world falling apart around us, we found joy in each other, and I consider myself the luckiest man in the world because of this. She is my rock, and I cannot wait to see what the future holds for us. Sisi and I love you so much.

Chapter 1 is a version of Anthony, S. M.; Wonilowicz, L. G.; McVeigh, M. S.; Garg, N. K. Leveraging Fleeting Strained Intermediates to Access Complex Scaffolds. *JACS Au* **2021**, *1*, 897–912. Anthony, Wonilowicz, McVeigh, and Garg were responsible for preparing the manuscript.

Chapter 2 is a version of Kelleghan, A. V.; Witkowski, D. C.; McVeigh, M. S.; Garg, N. K. Palladium-Catalyzed Annulations of Strained Cyclic Allenes. *J. Am. Chem. Soc.* **2021**, *143*, 9338–9342. Kelleghan, Witkowski, and McVeigh were responsible for experimental studies.

Chapter 3 is a version of Witkowski, D. C.; McVeigh, M. S.; Scherer, G. M.; Anthony, S. M.; Garg, N. K. Catalyst-Controlled Annulations of Strained Cyclic Allenes with π -Allylpalladium Complexes. *J. Am. Chem. Soc.* **2023**, *145*, 10491–10496. Witkowski, McVeigh, Scherer, and Anthony were responsible for experimental studies.

Chapter 4 is a version of McVeigh, M. S.; Garg, N. K. Interception of 1,2-Cyclohexadiene with TEMPO Radical. *Tetrahedron Lett.* **2021**, *87*, 153539–153543. McVeigh was responsible for experimental studies.

Chapter 5 is a version of McVeigh, M. S.; Sorrentino, J. P.; Hands, A. T.; Garg, N. K. Access to Complex Scaffolds Through [2+2] Cycloadditions of Strained Cyclic Allenes. *J. Am. Chem. Soc.* **2024**, *In Press*, doi.org/10.1021/jacs.4c03369. McVeigh, Sorrentino, and Hands were responsible for experimental studies.

Chapter 6 is a version of McVeigh, M. S.; Kelleghan, A. V.; Yamano, M. M.; Knapp, R. R.; Garg, N. K. *Org. Lett.* **2020**, *22*, 4500–4504. McVeigh, Kelleghan, Yamano, and Knapp were responsible for experimental studies.

BIOGRAPHICAL SKETCH

Education:

University of California, Los Angeles, CA

- Ph.D. in Organic Chemistry, anticipated Spring 2024
- Current GPA: 3.98/4.00; NIH Chemistry–Biology Interface Trainee, 2020–2023

The University of Texas, Austin, TX

- B.S. in Chemistry, 2019
- Cumulative GPA: 3.62/4.00; Graduated with Departmental Research Honors

Professional and Academic Experience:

Graduate Research Assistant: University of California, Los Angeles, CA

- Advisor: Prof. Neil K. Garg; July 2019 – present
 - Explored an approach toward the total synthesis of (–)-kermaphidin B, involving a Diels–Alder cycloaddition of a strained cyclic allene and nitrogen atom insertion.
 - Discerned the reactivity of strained cyclic allenes in [2+2] cycloaddition reactions.
 - Established a catalyst-controlled annulation of strained cyclic allenes and π -allylpalladium complexes.
 - Investigated the scope of a modular palladium-catalyzed annulation of strained cyclic allenes and metal complexes generated from aryl halides.
 - Developed a scalable synthetic route to silyl tosylates and established these compounds as alternative precursors to strained cyclic intermediates.
 - Achieved the first transformation between a monoradical and strained cyclic allene through the reaction of 1,2-cyclohexadiene with TEMPO radical.

Medicinal Chemistry Research Intern: Vertex Pharmaceuticals, San Diego, CA

- Manager: Dr. Carl Vogel; May 2022 – August 2022
 - Provided insight into the structure activity relationship of small molecule inhibitors of sodium ion channels.

Graduate Teaching Assistant: University of California, Los Angeles, CA

- Undergraduate organic chemistry laboratory sections (September 2019 – June 2020)
 - Taught students safe laboratory practices, fundamental organic chemistry lab techniques, and the underlying chemical concepts.

Undergraduate Research Assistant: The University of Texas, Austin, TX

- Advisor: Prof. Eric V. Anslyn; January 2016 – May 2019
 - Studied the mechanism of aniline-catalyzed hydrazone formation through UV/Vis kinetic isotope effect analysis.
 - Collaborated with Prof. Jonathan Sessler on the synthesis of oligoheterocycles and a 5,5-unsubstituted terpyrrole.
 - Synthesized *N*-methyl lysine for peptide synthesis and enantiopure standards for asymmetric reaction screening.

Undergraduate Teaching Assistant: The University of Texas, Austin, TX

- Undergraduate organic chemistry laboratory sections (January 2018 – June 2018)
 - Taught students safe laboratory practices, fundamental organic chemistry lab techniques, and the underlying chemical concepts.

Honors and Awards:

- Dr. Yuh Guo Pan Dissertation Award, UCLA, 2024
- Evelyn Pan Excellence in Research Award, UCLA, 2023
- Ralph and Charlene Bauer Award, UCLA, 2022
- Christopher S. Foote Fellowship, UCLA, 2022
- Horizon Prize for Education (team award), Royal Society of Chemistry, 2021

- Michael E. Jung Excellence in Teaching Award, UCLA, 2020
- Chemistry–Biology Interface Trainee, NIH, 2020–2023
- GRFP Honorable Mention, NSF, 2020
- Christopher S. Foote Fellowship, UCLA, 2019
- University Fellowship, UCLA, 2019
- Freshman Research Initiative Summer Fellow, The University of Texas at Austin, 2016

Publications:

Graduate Studies:

1. **Access to Complex Scaffolds Through [2+2] Cycloadditions of Strained Cyclic Allenes.** Matthew S. McVeigh,[†] Jacob P. Sorrentino,[†] Allison T. Hands, and Neil K. Garg. *J. Am. Chem. Soc.* **2024**, *In Press*, doi.org/10.1021/jacs.4c03369.
2. **Catalyst-Controlled Annulations of Strained Cyclic Allenes with π -Allylpalladium Complexes.** Dominick C. Witkowski, Matthew S. McVeigh, Georgia S. Scherer, Sarah M. Anthony, Neil K. Garg. *J. Am. Chem. Soc.* **2023**, *145*, 10491–10496.
3. **Interception of 1,2-Cyclohexadiene with TEMPO Radical.** Matthew S. McVeigh and Neil K. Garg. *Tetrahedron Lett.* **2021**, *87*, 153539 (special issue in honor of Professor Stephen F. Martin).
4. **Leveraging Fleeting Strained Intermediates to Access Complex Scaffolds.** Sarah M. Anthony, Laura G. Wonilowicz,[†] Matthew S. McVeigh,[†] and Neil K. Garg. *JACS Au* **2021**, *1*, 897–912.
5. **Palladium-Catalyzed Annulations of Strained Cyclic Allenes.** Andrew V. Kelleghan, Dominick C. Witkowski, Matthew S. McVeigh, and Neil K. Garg. *J. Am. Chem. Soc.* **2021**, *143*, 9338–9342.
6. **Silyl Tosylate Precursors to Cyclohexyne, 1,2-Cyclohexadiene, and 1,2-Cycloheptadiene.** Matthew S. McVeigh, Andrew V. Kelleghan, Michael M. Yamano, Rachel R. Knapp, and Neil K. Garg. *Org. Lett.* **2020**, *22*, 4500–4504.

Undergraduate Studies:

1. **Determination of Enantiomeric Excess and Diastereomeric Excess via Optical Methods. Application to α -methyl- β -hydroxy-carboxylic acids.** Sarah R. Moor, James R. Howard, Brenden T. Herrera, Matthew S. McVeigh, Federico Marini, Adrian T. Keatinge-Clay, and Eric V. Anslyn. *Org. Chem. Front.* **2023**, *10*, 1386–1392.
2. **Rapid Optical Determination of Enantiomeric Excess, Diastereomeric Excess, and Total Concentration Using Dynamic-Covalent Assemblies: A Demonstration Using 2-Aminocyclohexanol and Chemometrics.** Brenden T. Herrera, Sarah R. Moor, Matthew McVeigh, Emily K. Roesner, Federico Marini, and Eric V. Anslyn. *J. Am. Chem. Soc.* **2019**, *141*, 11151–11160.
3. **Synthesis of α,α' -linked Penta- and Septaheterocycles by Tandem Suzuki Coupling.** Hadiqa Zafar, James T. Brewster, Christopher D. Wight, Matthew McVeigh, Axel Steinbrück, Vincent M. Lynch, and Jonathan L. Sessler. *J. Porphyrins Phthalocyanines* **2019**, *23*, 28–33 (special issue devoted to women in porphyrin science).
4. **Gram-Scale Synthesis of a Bench-Stable 5,5''-Unsubstituted Terpyrrole.** James T. Brewster II, Hadiqa Zafar, Matthew McVeigh, Christopher D. Wight, Gonzalo Anguera, Axel Steinbrück, Vincent M. Lynch, and Jonathan L. Sessler. *J. Org. Chem.* **2018**, *83*, 9568–9570.
5. **2,2'-Bipyridine and Hydrazone Containing Peptides for Cyclization and Complex Quaternary Structural Control.** Erik T. Hernandez, P. Rogelio Escamilla, Sang-Yop Kwon, Jonathan Partridge, Matthew McVeigh, Sebastian Rivera, James F. Reuther, and Eric V. Anslyn. *New J. Chem.* **2018**, *42*, 8577–8582.

[†]These authors contributed equally

Outreach Activities:

- Los Angeles County Science Fair (volunteer) – Spring 2023 and 2024
- The O-Chem (re)-Activity Book (author) – Spring 2020
- QR Chem: Molecule of the Day (author) – Fall 2019 and Spring 2020
- UCLA Explore Your Universe (volunteer) – Fall 2019
- Warner Elementary Science Day (volunteer) – Fall 2019 and Spring 2023

CHAPTER ONE

Leveraging Fleeting Strained Intermediates to Access Complex Scaffolds

Sarah M. Anthony, Laura G. Wonilowicz,[†] Matthew S. McVeigh,[†] and Neil K. Garg*.

JACS Au **2021**, *1*, 897–912.

1.1 Abstract

Arynes, strained cyclic alkynes, and strained cyclic allenes were validated as plausible intermediates in the 1950s and 1960s. Despite initially being considered mere scientific curiosities, these transient and highly reactive species have now become valuable synthetic building blocks. This Chapter highlights recent advances in the field that have allowed access to structural and stereochemical complexity, including recent breakthroughs in asymmetric catalysis.

1.2 Introduction

In 1902, a provocative proposal was put forth by Stoermer and Kahlert, who contemplated the intermediacy of benzofuranyne **1.1** (Figure 1.1).¹ Although the existence of **1.1** would ultimately be called into question,^{2,3,4} the proposal led chemists to consider if triple bonds could exist in small rings. Roughly fifty years later, benzyne (**1.2**) and cyclohexyne (**1.3**) were validated experimentally, thanks to pioneering efforts by Roberts,^{5,6} Wittig,⁷ and Huisgen,⁸ in particular. Soon thereafter, in 1966, Wittig showed that 1,2-cyclohexadiene (**1.4**), an unusual-looking counterpart to benzyne (**1.2**) and cyclohexyne (**1.3**), could be generated and intercepted in cycloaddition processes.⁹ These results were striking at the time, as **1.2–1.4** possess functional groups (i.e., alkynes and allenes) that would ordinarily be linear. The bent nature of these species renders them transient and highly reactive intermediates that initially received little use in chemical

synthesis. However, over the past few decades, the field of arynes and related strained intermediates has undergone a substantial period of growth, as shown in Figure 1.1.¹⁰

The synthetic utility of arynes and related strained intermediates is often underappreciated, perhaps owing to common misconceptions regarding safety or high reactivity (and consequently, misconceptions regarding low selectivity in aryne reactions). Conversely, we highlight the impact of arynes and related intermediates in the syntheses of **1.5–1.9**. Popular ligands, such as XPhos (**1.5**), are made using aryne chemistry.¹¹ The medicinal chemistry route toward Chantix[®] (**1.6**) was enabled by an aryne cyclization.¹² Syngenta has prepared isopyrazam (**1.7**), an important fungicide, using an aryne Diels–Alder reaction on multikilogram scale.¹³ Lastly, there are numerous examples of arynes and related intermediates in total synthesis,^{14,15,16} such as the use of an aryne insertion in Sarpong’s synthesis of cossonidine (**1.8**) and a cyclohexyne insertion in Carreira’s synthesis of guanacastepene N (**1.9**).^{17,18} As these examples highlight, arynes and related intermediates can be used to build two new bonds in a single transformation. Moreover, it should be noted that arynes can be generated under exceedingly mild, safe, and operationally simple fluoride-based reaction conditions, thanks to the advent of Kobayashi silyl triflates.^{19,20,21,22} In turn, chemists have sought to leverage the synthetic utility of these once controversial species, in addition to deepening our fundamental understanding through electrophilicity studies²³ and regioselectivity studies.^{24,25,26}

Rather than providing a comprehensive overview of the field, several of which are available elsewhere,^{14,15,16,20,27,28 29,30,31,32,33,34,35,36,37} this Chapter examines some of the quickly emerging areas of aryne chemistry and related strained intermediates. We assess the following recent advances: a) the use of heterocyclic strained alkynes to construct scaffolds of value to medicinal and materials chemistry, b) access to quaternary stereocenters using non-catalytic

reactions of arynes and cyclic alkynes, c) catalytic asymmetric reactions of arynes, d) the assembly of intricate heterocyclic scaffolds via strained cyclic allene intermediates, and e) stereospecific and catalytic asymmetric transformations of strained cyclic allenes. We hope this discussion underscores the current excitement in the field and, moreover, helps to draw researchers into an area that continues to rapidly evolve with opportunities for discovery.

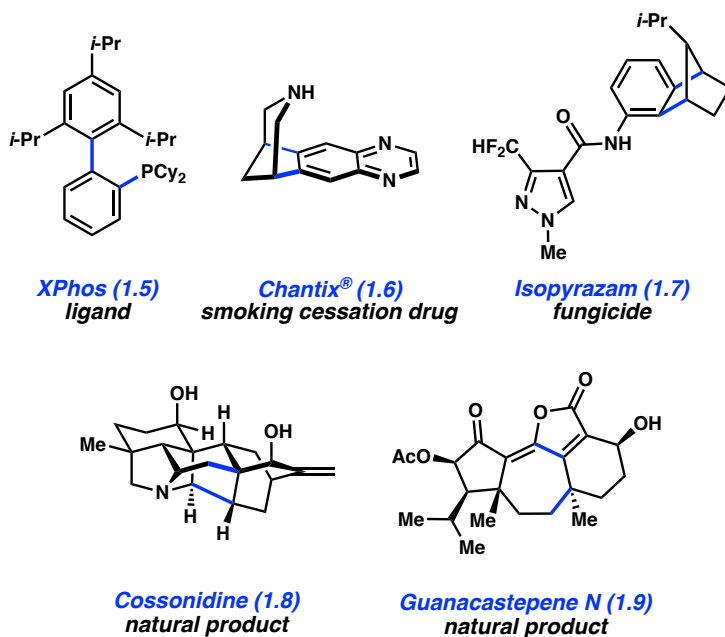
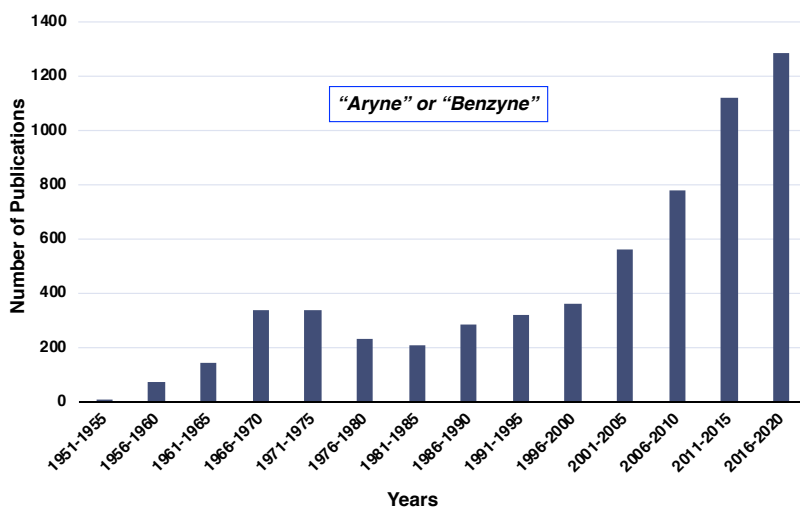
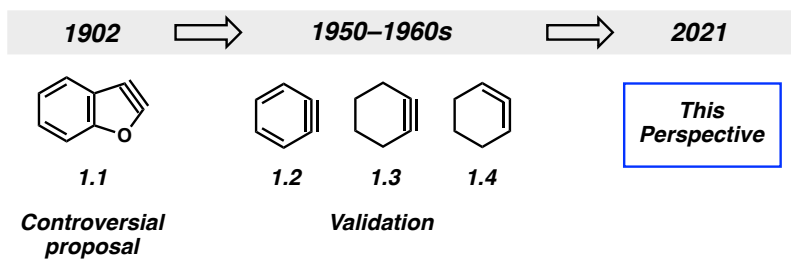


Figure 1.1. Historical perspective, growth of “aryne” or “benzyne” chemistry, and select synthetic applications.

1.3 Use of Heterocyclic Alkynes in the Synthesis of Medicinal and Materials Scaffolds

New strategies to access heterocyclic compounds, especially those with a high degree of sp^3 -rich character, remain highly sought after due to the numerous applications of heterocycles in drugs, agrochemicals, natural products, and materials.^{38,39,40,41,42,43} Just within the pharmaceutical industry, the vast majority of small-molecule drugs approved by the U.S. Food and Drug Administration contain a nitrogen or oxygen-containing heterocycle.^{44,45} A few examples are Plavix[®] (**1.10**), an antiplatelet, roeoadine (**1.11**), a sedative and antitussive, and the antimalarial drug artemisinin (**1.12**) (Figure 1.2).

Strained cyclic alkynes have emerged as valuable building blocks to access sp^3 -rich³⁸ medicinally relevant heterocycles (Figure 1.2).^{46,47,48,49} Heteroatom-containing cyclohexyne derivatives, such as 2,3-piperidynes **1.13**, 3,4-piperidynes **1.14**, and oxacyclohexyne **1.15** have been far less studied than related aryne counterparts, (e.g., 3,4-pyridyne (**1.16**)).^{50,51,52,53} For comparison, the 3,4-pyridyne (**1.16**) was first disclosed in 1955,⁵⁴ but studies involving 3,4-piperidynes were only reported recently. Specifically, the Danheiser group reported access to **1.13** in 2014⁴⁷ and our group described generation and interception of **1.14** and **1.15** in 2014 and 2016, respectively.^{48,49} These studies demonstrate the synthetic value of transient intermediates **1.13**–**1.16**.

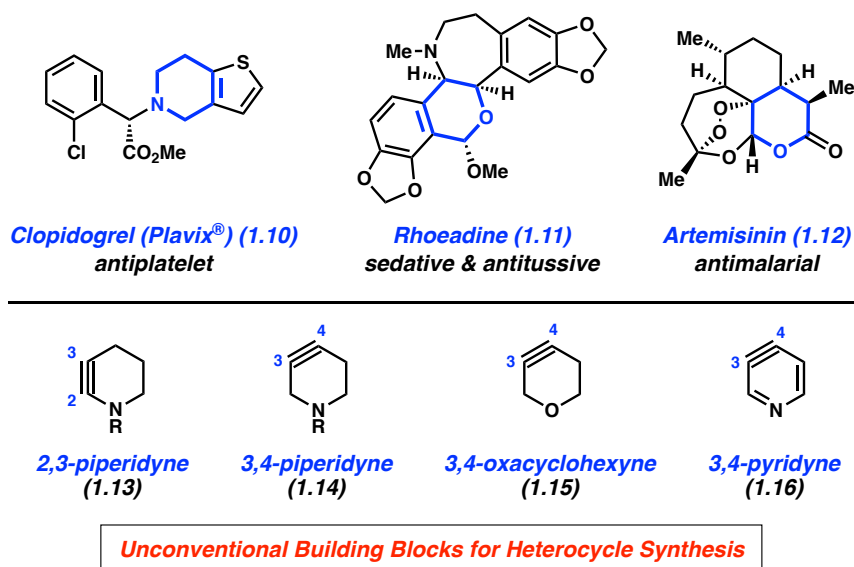


Figure 1.2. Representative natural products and pharmaceuticals containing heterocycles and representative nitrogen- and oxygen-containing strained cyclic alkynes.

The initial breakthrough in this area by Danheiser and coworkers involved piperidyne precursor **1.17** (Figure 1.3). Upon treatment of **1.17** with CsF or KF, in the presence of a cycloaddition partner, a variety of (3+2) and (2+2) cycloadducts **1.20** were obtained. Presumably, these reactions proceed via the regioselective trapping of cyclic alkyne **1.19**. Three examples are shown to highlight the diverse products (i.e., **1.22**, **1.24**, and **1.26**) that can be obtained using this methodology. Moreover, each of the cycloadducts shown were isolated as one major constitutional isomer, with the significant regioselectivity of the reaction being attributed to the electronic effect of the nitrogen atom.

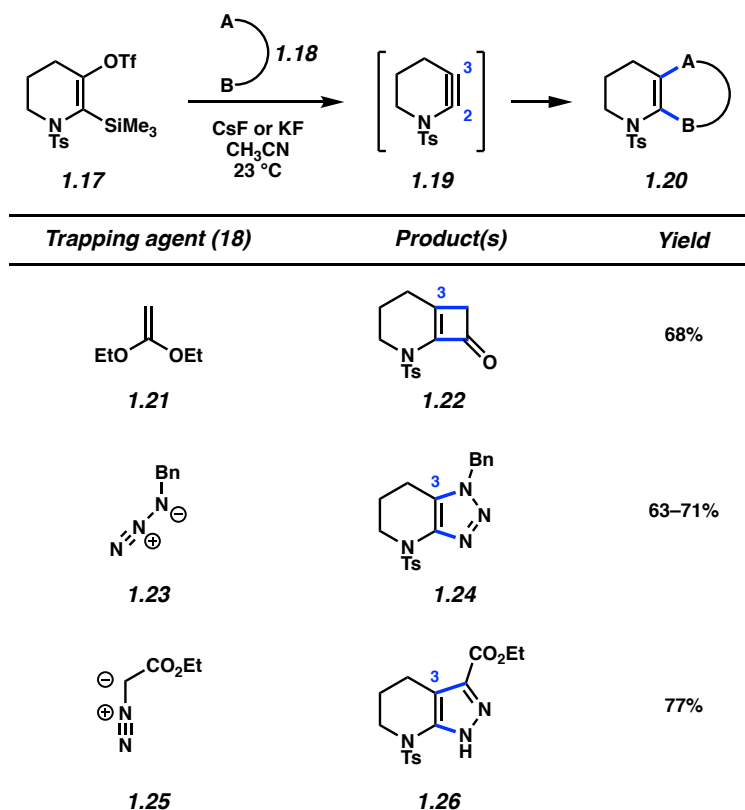


Figure 1.3. Selected trapping experiments involving piperidyne **1.19**.

Our laboratory had simultaneously engaged in complementary studies, which were geared toward accessing cyclic alkynes **1.28** (Figure 1.4). After developing synthetic routes to the requisite silyl triflates **1.27**, we performed experiments to generate and trap the corresponding heterocyclic alkynes. As summarized, strained intermediate trapping via (4+2) and (3+2) cycloadditions led to an array of interesting heterocyclic products, such as aza- and oxa-bicycles **1.30** and **1.32**, respectively, isooxazolines **1.34** and **1.35**, pyrazole **1.36**, and triazole **1.37**. Where applicable, reactions occurred regioselectively, indicative of initial bond formation occurring at C4 of the reactive strained intermediate. It should be emphasized that by strategically varying the trapping partner, one can utilize common silyl triflate precursors (i.e., **1.27**) to rapidly arrive at a variety of diverse heterocyclic scaffolds, including previously unknown scaffolds and analogs of medically relevant compounds.^{55,56,57,58}

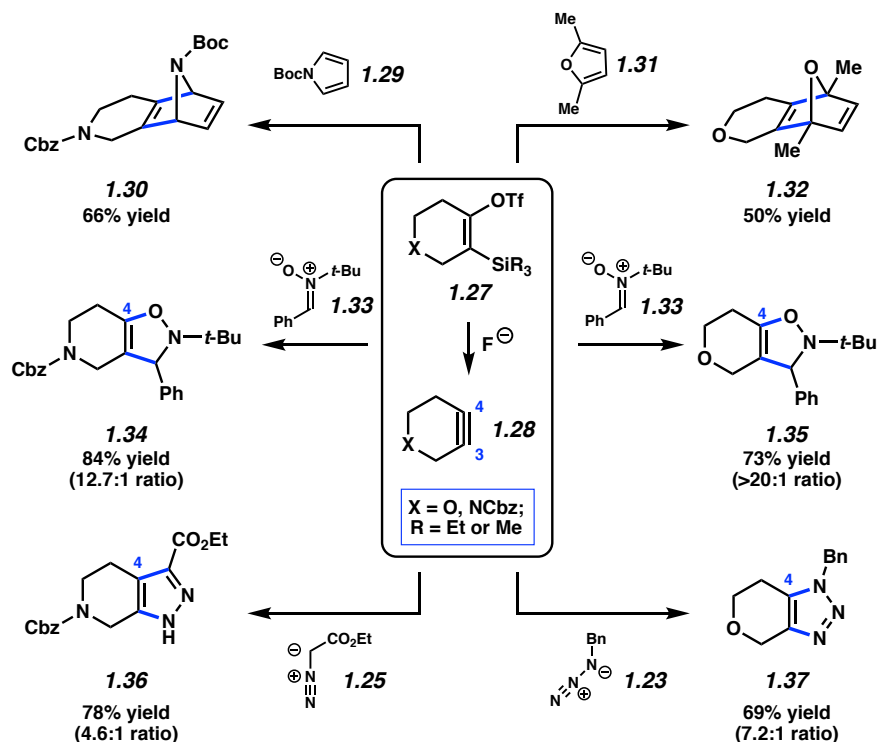


Figure 1.4. Selected trapping experiments of heterocyclic alkynes using silyl triflate precursors.

An attractive feature related to strained cyclic alkyne methodologies is the ability to make reliable predictions regarding regioselectivities using the aryne distortion model. This model, proposed by Houk and coworkers via our earlier collaborative studies,³³ shows that non-symmetrical cyclic alkynes are geometrically distorted in their ground state. Nucleophilic addition occurs more favorably at the alkyne terminus with a larger internal angle (i.e., more distorted toward linearity), which correlates to a lower calculated distortion energy seen in the corresponding transition state. Moreover, larger differences between the internal angles typically correlates with regioselectivities in trapping experiments. Thus, by analyzing the ground state structure of a strained cyclic alkyne, one can typically make meaningful regioselectivity predictions. In the cases of piperidyne **1.14** and oxacyclohexyne **1.15**, both react with a preference for C4 addition (Figure 1.5). Consistent with the distortion model, the ground state geometries of **1.14** and **1.15** shown by DFT calculations demonstrate that the C4 alkyne terminus is more

distorted toward linearity. Furthermore, the difference between the internal angles of **1.14** and **1.15** are 12° and 15° , respectively. The greater angle difference of 15° seen in **1.15** is consistent with observed regioselectivities. For example, as shown in Figure 1.4 the nitron trapping proceeds with higher selectivity when using **1.15** compared to **1.14**.

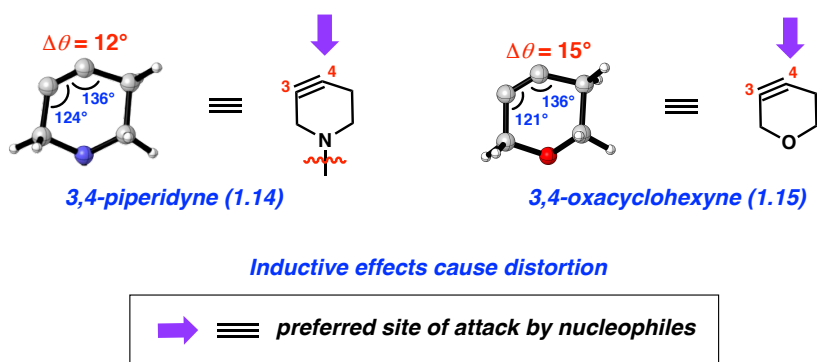


Figure 1.5. Regioselectivity of piperidyne **1.14** and oxacyclohexyne **1.15** trappings.

These methods demonstrate the value of strained heterocyclic alkynes for the synthesis of medicinally relevant scaffolds. Using common building blocks, rapid structural diversification can be achieved, with regioselectivity being predicted using simple calculations. Moreover, this chemistry provides a new and unusual strategy for accessing decorated heterocycles (i.e., using new strained intermediates). We expect these reports to influence future retrosynthetic analyses for the synthesis of heterocycles seen commonly in pharmaceuticals.

In addition to their value for the synthesis of medicinally relevant scaffolds, strained heterocyclic alkynes have seen recent utility in the synthesis of aromatic structures relevant to materials chemistry. Highly conjugated small molecules and polycyclic hydrocarbon frameworks have many potential applications in the field of organic electronics and material science.^{59,60} For example, these conjugated small molecules have been widely used in light-emitting diodes (OLEDs),^{61,62,63,64} field-effect transistors (OFETs),^{65,66,67,68} and photovoltaics (OPVs).^{69,70,71} Two common conjugated small molecules are 9,10-diphenylanthracene (**1.38**) and triphenylene (**1.41**)

(Figure 1.6).^{72,73,74,75} Heteroatom containing-derivatives of these compounds, such as **1.39**, **1.40**, **1.42**, and **1.43**, have been gaining interest as the presence of heteroatoms can modulate electronic properties.^{76,77,78} New synthetic methods to access novel heterocyclic conjugated materials are highly desirable. As such, in 2017, our laboratory synthesized heterohelicene⁷⁹ **1.43** (and derivatives) using an indolyne cyclotrimerization reaction.^{80,81} Indole trimers have been used in various materials applications.^{76,82,83,84,85,86,87} Building on these studies, we sought to access heteroatom-containing 9,10-diarylanthracene scaffolds using arynes and strained alkyne building blocks.

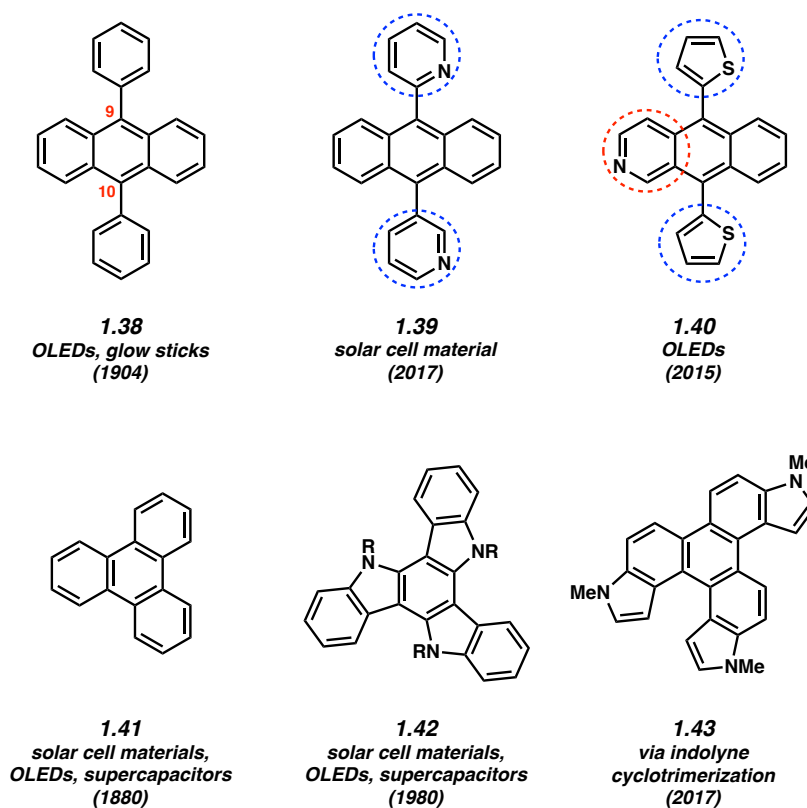


Figure 1.6. Notable polycyclic aromatic hydrocarbons.

In 2019, we disclosed a modular strategy toward *N*-containing 9,10-diphenylanthracene derivatives, wherein all four aryl rings could be easily modified.⁸⁸ The sequence was inspired by the collective seminal studies by Steglich, Nuckolls, and Wudl pertaining to double-aryne

annulations of oxadiazinones.^{89,90,91} As shown in Figure 1.7, our approach involved two steps. First, 3,4-piperidyne (**1.14**), generated in situ from the corresponding silyl triflate, undergoes reaction with oxadiazinones **1.44** to give pyrones **1.45** through a Diels–Alder/retro-Diels–Alder sequence.⁹² The oxadiazinones are easily prepared with two different aryl substituents from readily available starting materials.⁹³ In a second Diels–Alder/retro-Diels–Alder sequence, pyrones **1.45**, which are bench stable and isolable, react with an aryne or non-aromatic strained cyclic alkyne (i.e., **1.46**) to deliver polycyclic hydrocarbon frameworks **1.47**. **1.48–1.50** are representative products. As needed, subsequent oxidation can be performed to access more highly conjugated derivatives.

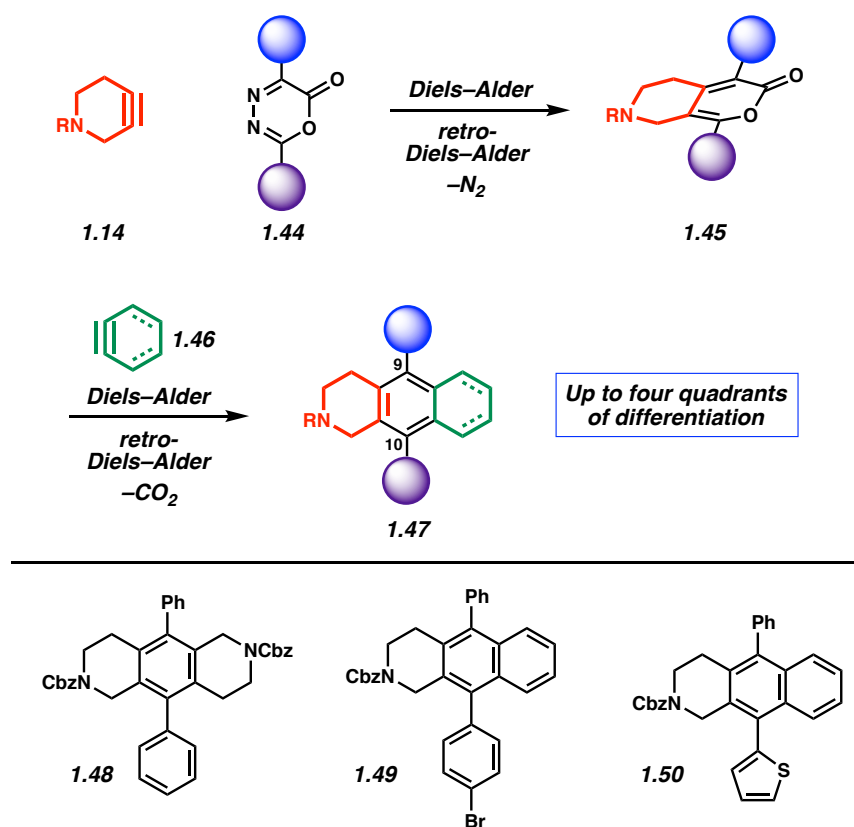


Figure 1.7. Modular strategy to access 9,10-diphenylanthracene derivatives and representative products **1.48–1.50**.

Figure 1.8 highlights two additional aspects of this chemistry. In the first, **1.51**, **1.52**, and **1.53** were shown to react at room temperature in the presence of CsF. This three-component coupling obviates the need to isolate a pyrone intermediate and delivers **1.54** in 56% yield. Additionally, the methodology could be used to access **1.55**, a novel heterocyclic PAH scaffold that fluoresces, displaying a blue emission. In the presence of acid, pyridinium salt **1.56** forms, which displays an orange emission. Stimuli responsive materials are useful in a host of applications such as pH fluorescence sensors^{94,95} and solid-state fluorescent switches.⁹⁶

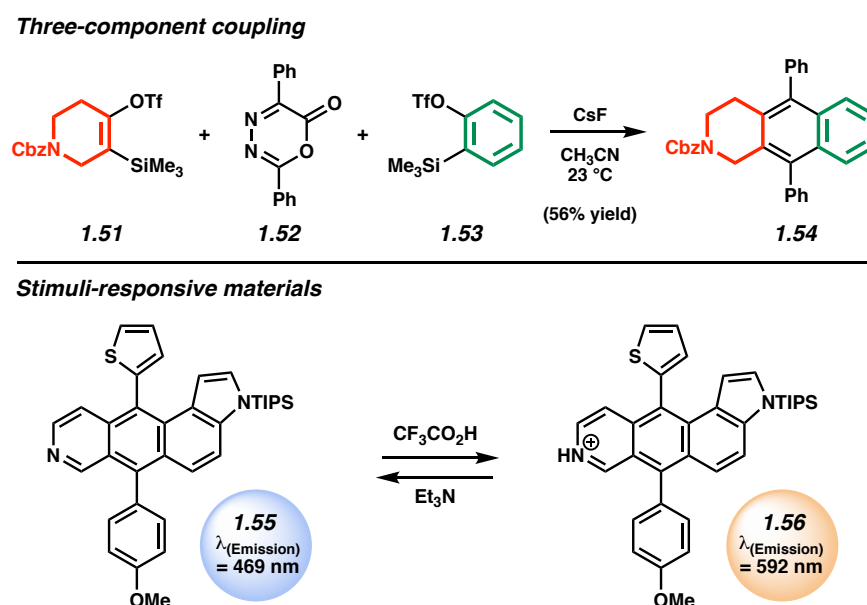


Figure 1.8. Utilizing arynes to access 9,10-diphenylanthracene derivatives.

The chemistry described above pertaining to PAHs showcases an exciting new direction of modern strained intermediate chemistry. Notably, Hosoya and coworkers published a complementary method in 2019 that utilizes a variety of strained intermediates, including thienobenzynes, to access PAH skeletons.⁹⁷ Our group has published a follow-up study as well, which provides additional experimental results, as well as a computational mechanistic investigation.⁹⁸ More specifically, heterocyclic strained intermediates can be strategically leveraged through a cycloaddition cascade sequence to rapidly generate PAH scaffolds. The

transformation enables access to structurally diverse products through the formation of four carbon–carbon bonds. It is expected that this chemistry and variants thereof will prompt the development of related methods that rely on strained intermediates to access compounds of value to materials chemistry.

1.4 Use of Arynes and Cyclic Alkynes to Access Quaternary Stereocenters (Non-Catalytic)

The majority of reported methodologies and synthetic applications that utilize strained cyclic alkynes are intermolecular reactions that generate achiral or racemic products. However, efforts have been put forth to generate enantioenriched products, including those that rely on the use of chiral auxiliaries or reagents. For example, reports by Lautens^{99,100} and Barrett^{101,102} demonstrate stereocontrolled intermolecular reactions of arynes for the introduction of tertiary stereocenters using Oppolzer or Schöllkopf reagents, respectively. As accessing quaternary stereocenters is especially valuable,^{103,104,105,106} we were interested in utilizing arynes and strained cyclic alkynes to access stereodefined quaternary centers in an intermolecular fashion.

Our efforts, which were reported in 2018,¹⁰⁷ concerned the reaction between β -ketoester **1.57** and strained cyclic alkyne **1.46** to yield α -substituted product **1.58**, as shown in Figure 1.9. Prior efforts to achieve this transformation in a racemic sense were accompanied by concomitant C–C bond fragmentation,¹⁰⁸ so we considered an alternative, two-step approach. First, β -ketoester **1.57** would be treated with amine **1.59** to afford the corresponding enamine **1.60**. Enamine **1.60** could then be used to trap aryne **1.46**, affording α -substituted product **1.58** after hydrolysis. We envisioned that employing a chiral amine (i.e., **1.59**) would render the reaction diastereoselective and yield **1.58** in enantioenriched form. It should be noted that enantioselective α -arylation of β -

ketoesters, one of the net transformations we hoped to develop, had remained a challenging synthetic problem.^{109,110,111,112,113,114,115,116}

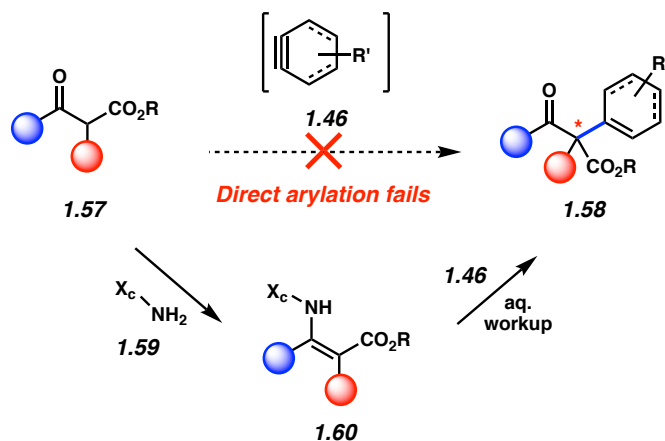


Figure 1.9. Intercepting arynes and cyclic alkynes for the installation of stereodefined quaternary stereocenters.

At the time of our study, the use of enamines and strained cyclic alkynes to construct quaternary stereocenters was unknown; thus, the racemic arylation^{117,118,119} was first developed (Figure 1.10). Benzylamine was condensed onto ketoester **1.61** to afford enamine **1.62** ($R = Bn$). Next, enamine **1.62** was used to trap benzyne, which was generated in situ from silyl triflate **1.53** using CsF in DME. Following hydrolysis with 1 M HCl, α -arylated product **1.63** was obtained in 92% yield. To effect the desired stereoselective variant, we ultimately arrived at the use of an anthracenyl derivative (i.e., $R = \mathbf{1.67}$). Several products that were obtained are shown in Figure 1.10 (i.e., **1.64–1.66**), which highlight the use of heterocyclic arynes and cyclic alkynes as trapping agents, as well as a 7-membered β -ketoester.

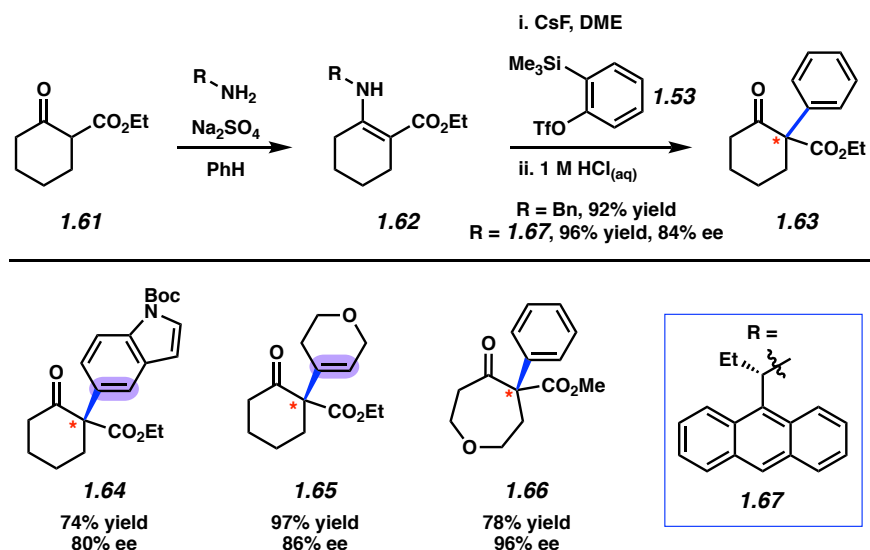


Figure 1.10. Selected substrate scope of α -arylation methodology.

Another attractive aspect of this reaction methodology is the one-pot variant shown in Figure 1.11. Treatment of ketoester **1.68** with chiral amine **1.67** yielded the corresponding enamine, which was not isolated. This intermediate was then subjected to silyl triflate **1.53** and CsF, followed by the addition of aqueous 1 M HCl. The product, ketoester **1.69**, was isolated in 68% yield and 92% ee. Of note, amine **1.67** was recovered in 67% yield. Overall, this methodology provided a means to access stereodefined quaternary stereocenters by the interception of strained intermediates in intermolecular processes. As will be discussed later in this review, an elegant catalytic asymmetric variant of this methodology has subsequently been developed.¹²⁰

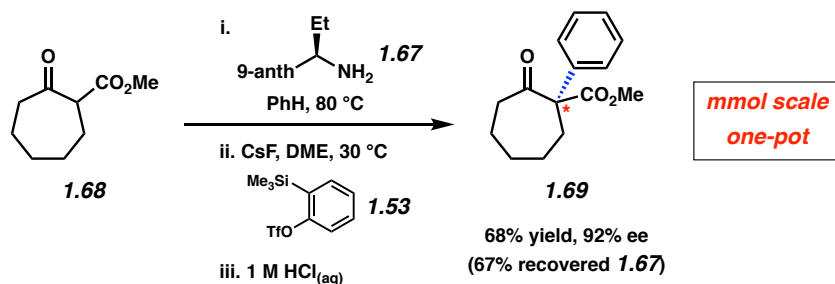
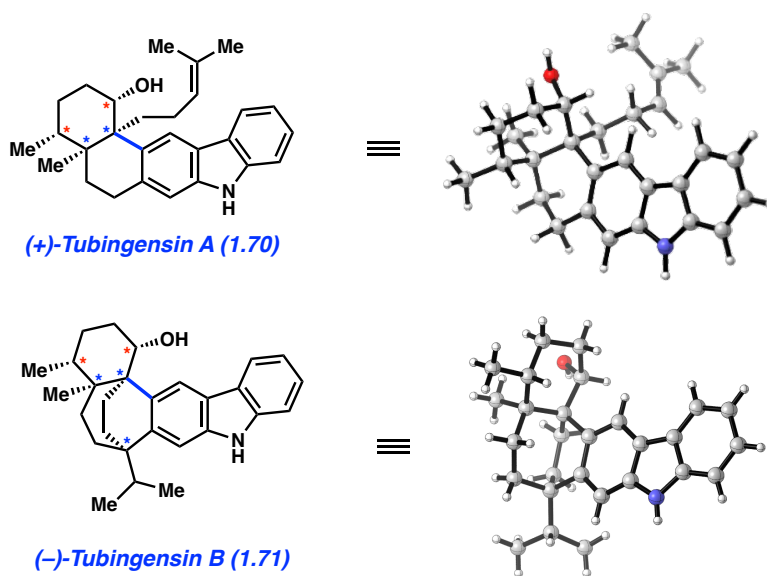


Figure 1.11. α -Arylation reaction demonstrated in one-pot.

The synthesis of natural products and their derivatives also provides an opportunity to use arynes in complex settings, as has been well demonstrated in the literature.^{14,16,32,33} With regard to several recent efforts, the Hoye group has used arynes generated from hexadehydro-Diels–Alder reactions with readily abundant natural products to access complex derivatives.¹²¹ Additionally, our laboratory has performed late-stage intermolecular aryne cycloadditions to access derivatives of strictosidine, the last common biosynthetic precursor to all monoterpene indole alkaloids.¹²² More commonly, natural products have been accessed through diastereoselective intramolecular aryne trappings of enantioenriched substrates. Early on, our laboratory used an “indolyne” cyclization to build the complex bridged bicyclic core of coveted welwitindolinone natural products.^{123,124,125,126,127} Subsequently, we targeted the tubingensin alkaloids, wherein we envisioned using an aryne cyclization to access a quaternary center.

Tubingensins A and B (**1.70** and **1.71**, respectively) are complex indole diterpenoids first isolated from *Aspergillus tubingensis* in 1989 (Figure 1.12).^{128,129} Both natural products feature disubstituted carbazole moieties. In tubingensin A (**1.70**), the carbazole is fused to a *cis*-decalin containing four contiguous stereocenters, two of which are vicinal quaternary stereocenters. Tubingensin B (**1.71**), however, contains a carbazole fused to a [3.2.2]-bridged bicycle containing five stereocenters, four of which are contiguous. As an additional layer of complexity, three of the stereocenters are quaternary, two of which are vicinal. Moreover, tubingensins A and B (**1.70** and **1.71**, respectively) possess antiviral activity against herpes simplex virus type 1 (HSV-1) along with pesticidal activity.^{128,129} At the time we began our efforts, there were no total syntheses of tubingensins A or B, although Li and Nicolaou reported an elegant route to (±)-**1.70** in 2012.¹³⁰



Quaternary centers accessed through aryne cyclizations

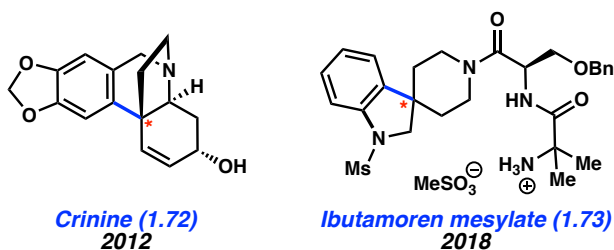


Figure 1.12. The tubingensin alkaloids and natural products with quaternary stereocenters introduced using aryne chemistry.

Given the intriguing structural features of tubingensins A and B, our group proposed synthetic routes to these compounds during a ‘Molecule of the Month’ (MOM) exercise in a 2009 group meeting. Several routes that would employ aryne intermediates were proposed, some of which were tested in the laboratory. Although our initial strategies proved unsuccessful in the laboratory, they helped us appreciate the challenge of establishing quaternary stereocenters in complex frameworks using arynes. Prior studies had largely focused on the use of arynes to access tertiary stereocenters.^{123,131,132,133,134} With regard to setting quaternary centers of natural products and drug candidates using arynes, notable precedent was available in the synthesis of crinine (**1.72**)¹³⁵ and ibutamoren mesylate (**1.73**)¹³⁶ (Figure 1.12). There were no such examples where

scaffolds bearing vicinal quaternary stereocenters, like those seen in the tubingsin alkaloids, were accessed using aryne cyclizations.

Following our initial total synthesis of (+)-tubingsin A (**1.70**),¹³⁷ we were well-poised to address the more complex family member, (-)-tubingsin B (**1.71**). As summarized in Figure 1.13, (+)-dihydrocarvone (**1.74**), an abundant chiral terpene building block, and 2-hydroxycarbazole (**1.75**) were used as starting materials and elaborated to give carbazolyne precursor **1.76**. Of note, **1.76** possesses all of the carbons that would be needed to complete the total synthesis. This key intermediate was subjected to sodium amide and *tert*-butanol in THF^{138,139} at 23 °C to effect carbazolyne cyclization. Although we were expecting to form a single C–C bond, we instead observed the formation of two new C–C bonds as evident by product cyclobutenol **1.78**. Although this outcome was undesired, the formation of **1.78** highlights the structural complexity accessible using aryne chemistry. The reaction likely proceeds via a formal [2+2] cycloaddition (e.g., **1.77**) and occurs with excellent diastereoselectivity. Nonetheless, this transformation served to establish the necessary vicinal quaternary stereocenter framework, construct the natural product's seven-membered ring, and preserve the phenylselenide moiety necessary for a late-stage radical cyclization. To complete the synthesis, cyclobutenol **1.78** was subjected to Murakami's Rh-catalyzed fragmentation conditions,¹⁴⁰ which delivered the ketone **1.79** in 53% yield via fragmentation of the cyclobutenol ring. In turn, ketone **1.79** could be elaborated to (-)-tubingsin B (**1.71**).¹⁴¹ This effort demonstrates the utility of highly reactive aryne intermediates for the assembly of sterically congested carbon–carbon bonds in natural products.

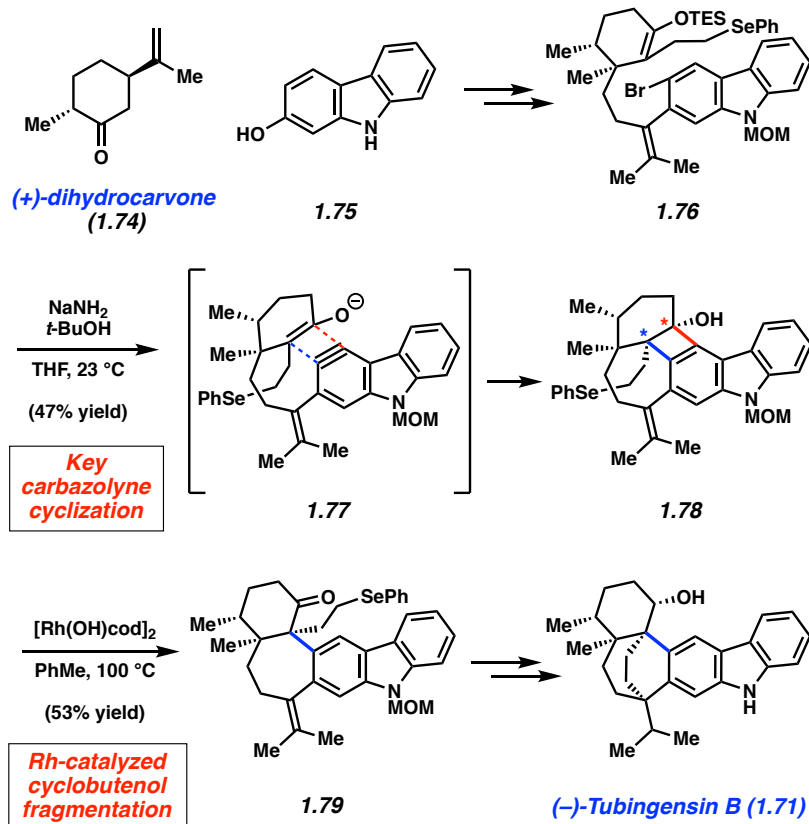


Figure 1.13. Overview of (-)-tubingensin B total synthesis.

1.5 Arynes in Asymmetric Catalysis

The aforementioned section highlights two key tactics for accessing enantioenriched products using aryne intermediates. More specifically, the use of chiral auxiliaries, chiral reagents, or enantioenriched substrates have been most common and successfully used to build intricate scaffolds and quaternary stereocenters. In turn, chemists have questioned: is it possible to leverage asymmetric catalysis in aryne trapping experiments? Such processes may be very challenging, as they could require two transiently generated intermediates,^{29,32} including a highly reactive aryne, to come together and undergo a productive reaction with stereocontrol. In addition to the fundamental scientific interest of using a fleeting aryne intermediate in a catalytic reaction, there are also practical advantages of asymmetric catalysis.^{142,143,144} We highlight three key studies in

this emerging field involving the synthesis of helicenes (axial chirality)^{145,146} and the introduction of quaternary stereocenters (point chirality).¹²⁰

A breakthrough involving the use of aryne in asymmetric catalysis was reported by Guitián and coworkers in 2006.¹⁴⁵ More specifically, the authors studied [2+2+2] cycloadditions of aryne and alkynes to access enantioenriched helicenes. Accessing helicenes in an enantioselective manner has remained an important area of research^{79,147,148} and prior aryne-based approaches had given rise to racemic products.^{149,150} As shown in Figure 1.14, silyl triflate **1.80** was treated with CsF, alkyne **1.81**, catalytic Pd₂(dba)₃, and BINAP to afford helicene **1.82**. The reaction likely proceeds through a palladium-catalyzed cyclotrimerization of two in situ-generated aryne intermediates (from silyl triflate **1.80**) and alkyne **1.81**. Although the yield was modest, helicene **1.82** was obtained in 67% ee. This study demonstrated an important proof-of-concept with regard to aryne and their use in asymmetric catalysis.

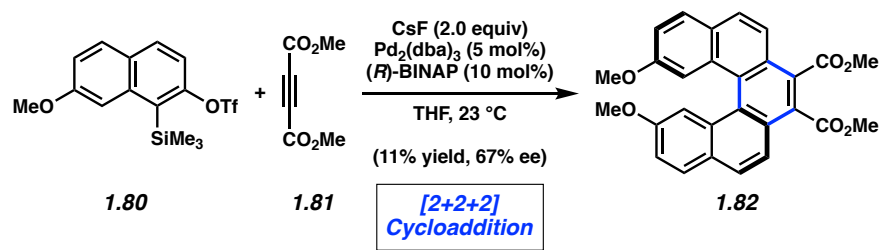


Figure 1.14. Enantioselective synthesis of helicenes using aryne and asymmetric catalysis.

Building upon this pioneering study and their own prior work in this area,¹⁵¹ the Kamikawa group published an enantioselective synthesis of helicenes in 2020.¹⁴⁶ For example, as shown in Figure 1.15, a cyclotrimerization was effected between aryne precursor **1.83** and alkyne **1.84** using Pd₂dba₃•CHCl₃, CsF, and (*S*)-QUINAP (**1.86**).¹⁵² This transformation features a design similar to the aforementioned example by Guitián and coworkers, and affords triple helicene (*M,P,M*)-**1.85** in 49% yield and 96% ee. Notably, despite using racemic aryne precursor **1.83**, both terminal helicenes exclusively formed the (*M*)-[5]-helicenyl moiety, which suggests a kinetic resolution or

dynamic kinetic resolution occurs in the reaction. Overall, this study achieved the first enantioselective synthesis of a triple helicene, while also providing the first practical catalytic asymmetric aryne trapping reaction.

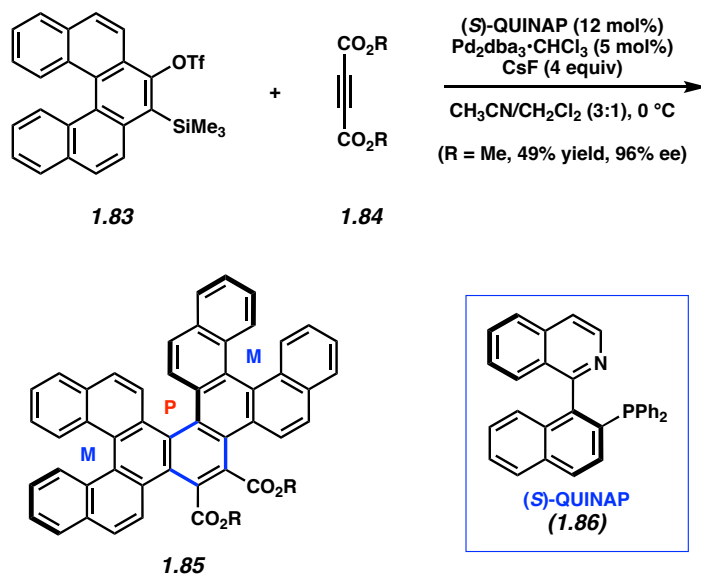


Figure 1.15. Enantioselective synthesis of triple helicenes via the catalytic asymmetric trapping of arynes.

Also in 2020, the Luo group reported a pioneering study in the catalytic asymmetric trapping of arynes and related strained intermediates.¹²⁰ Their methodology strategically blends organocatalysis and electrochemistry to achieve the α -functionalization of 1,3-dicarbonyl substrates and establish point chiral stereochemistry. For example, treatment of ketoester **1.61** with 1-aminobenzotriazole (**1.87**) and amine catalyst **1.88**, under their optimal electrochemical oxidation conditions, afforded α -arylated ketoester **1.63** in 71% yield and 94% ee (Figure 1.16). Mechanistically, the reaction is thought to proceed by way of an intermediate enamine species, which reacts with the aryne generated by electrochemical oxidation of **1.87**. The cobalt catalyst is proposed to bind the aryne triple bond and stabilize excess benzyne intermediate that is generated.^{153,154,155} Products **1.89–1.92** provide further examples of the products that were generated using this methodology. These studies demonstrate an electrochemical oxidation

approach to access benzyne and related strained intermediates, which nicely complements prior studies involving the use of non-electrochemical oxidation conditions for aryne generation.^{156,157,158,159,160} Moreover, this study demonstrates that arynes can be engaged in asymmetric catalysis to provide access to point chiral products in synthetically useful enantioselectivities. The ability to access stereodefined quaternary stereocenters is especially notable.

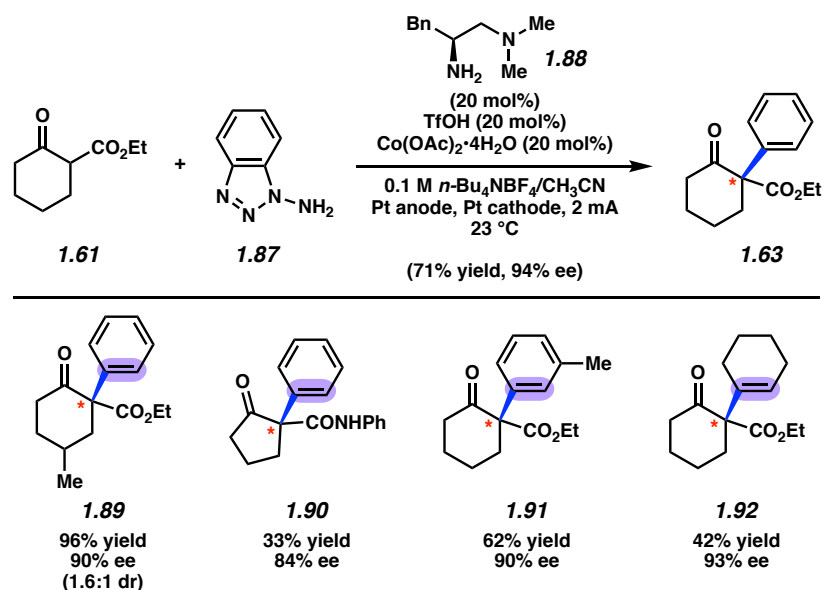


Figure 1.16. Catalytic enantioselective α -arylation of 1,3-dicarbonyls.

1.6 Use of Strained Cyclic Allenes to Access Polycyclic Scaffolds

Whereas arynes and strained cyclic alkynes have been studied extensively, a related counterpart, strained cyclic allenes (i.e., **1.4**, **1.93**, **1.94**, Figure 1.17), have received significantly less attention. Of note, the discovery of 1,2-cyclohexadiene (**1.4**) by Wittig was reported in 1966,⁹ only nine years after the validation of cyclohexyne (and thirteen years after the validation of benzyne in 1953).^{27,31,14} Theoretical investigations of these species have been reported,^{161,162,163,164,165,166,167,168,169} as well as synthetic advances, most notably by Christl.^{170,171,172,173,174,175,176} In a key finding, Guitián and coworkers developed Kobayashi

precursors to strained cyclic allenes and demonstrated their utility in several transformations, such as [4+2] cycloadditions.^{177,178} Subsequently, our laboratory and West's expanded the synthetic utility of Kobayashi cyclic allene precursors to encompass other intermolecular cycloadditions, especially [3+2] cycloadditions.^{179,180,181,182}

Here, we feature selected recent efforts aimed at harnessing strained cyclic allenes to build complex polycyclic scaffolds bearing heteroatoms and sp^3 centers. Generally speaking, these reactions proceed by treating silyl triflate precursors **1.95** with a fluoride source to generate cyclic allenes **1.96**. In situ trapping with cycloaddition partners **1.18** provides adducts **1.97** (Figure 1.17). As will be discussed in the remaining sections of this Chapter, strained cyclic allene chemistry provides exciting opportunities for study related to regiochemistry, pertaining to which olefin of the allene undergoes reaction, and stereochemistry, due to the inherent chirality of cyclic allenes and generation of a new sp^3 center.

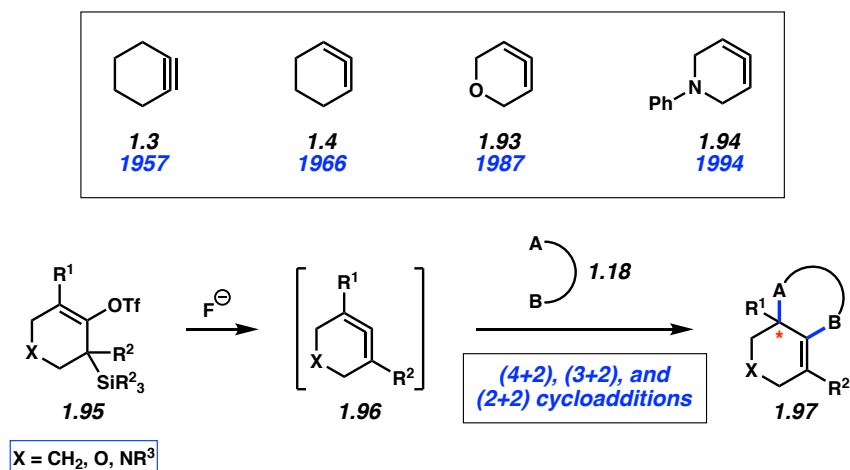


Figure 1.17. Strained cyclic allenes and representative trapping reactions.

A striking example of cyclic allene chemistry was reported by West and co-workers in 2019, where in situ-generated 1,2-cyclohexadienes underwent (4+2) cycloaddition with tethered furans to access complex tetracyclic products (Figure 1.18).¹⁸³ Substrates **1.98** were subjected to

TBAF to afford cycloadducts **1.100**, presumably by way of cyclic allene intermediate **1.99**. The products contain three stereocenters, set in a relative sense, including a quaternary center. Representative products **1.101** and **1.102** highlight that the linker length could be varied ($n = 1$ or 2). In addition, heteroatoms were tolerated in the linker, as shown by cycloadducts **1.103** and **1.104**. Of note, the transformations proceeded diastereoselectively in favor of the *endo* product and regioselectively, with the latter being governed by the tether. This methodology provides the first examples of an intramolecular cycloaddition with a six-membered cyclic allene and showcases the structural complexity that is accessible using cyclic allene chemistry.

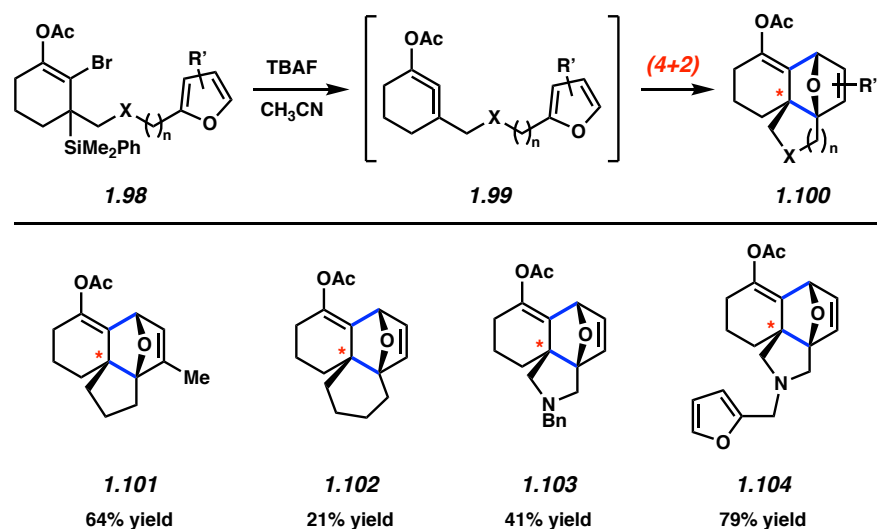
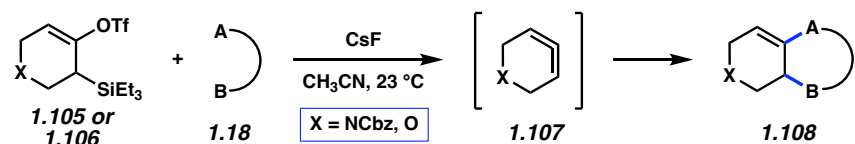


Figure 1.18. Intramolecular Diels–Alder reactions afford tetracyclic products.

Our laboratory was particularly interested in heterocyclic allenes and the possibility of accessing them using Kobayashi-type precursors. Many heterocyclic allenes had been accessed previously, but never using a silyl triflate as the precursor.^{184,185,186,187,188,189,190} After developing syntheses of the appropriate precursors to azacyclic and oxacyclic allenes (i.e. **1.105** and **1.106**, respectively), we demonstrated their use in cycloaddition reactions, with select results shown in Figure 1.19.^{191,192} Operationally, reactions are performed by treating the appropriate silyl triflate precursor (**1.105**, $X = \text{NCbz}$; or **1.106**, $X = \text{O}$) with a trapping agent **1.18** in the presence of CsF at

23 °C, ultimately leading to cycloadducts **1.108**. Three cycloadducts arising from azacyclic allene precursor **1.105** are shown reflective of (4+2), (3+2), and (2+2) cycloadditions (entries 1–3). The cycloadducts, **1.109**, **1.111**, and **1.112**, are formed in good yield and useful diastereoselectivities (when applicable). Similarly, oxacyclic allene precursor **1.106** could be employed in (4+2), (3+2), and (2+2) cycloadditions, thus giving rise to cycloadducts **1.114**, **1.116**, and **1.118**, respectively (entries 4–6). Overall, by varying the heterocyclic allene precursor and the trapping agent, one can now use strained cyclic allene chemistry as a strategy to synthesize structurally complex heterocyclic compounds.



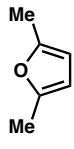
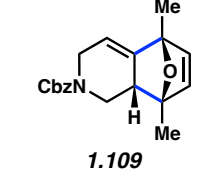
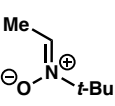
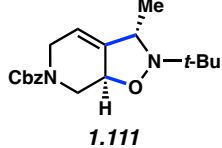
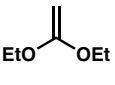
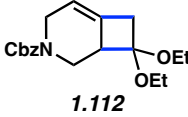
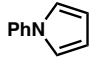
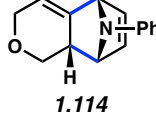
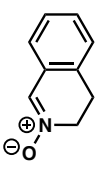
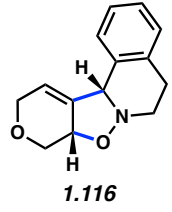
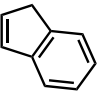
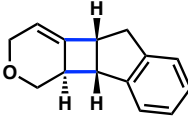
Entry	Substrate	Trapping agent	Product(s)	Yield (dr)
1	1.105 (X = NCbz)	 1.31	 1.109	82% (13.7:1)
2	1.105 (X = NCbz)	 1.110	 1.111	88% (>20:1)
3	1.105 (X = NCbz)	 1.21	 1.112	78%
4	1.106 (X = O)	 1.113	 1.114	91% (3.8:1)
5	1.106 (X = O)	 1.115	 1.116	94% (5.3:1)
6	1.106 (X = O)	 1.117	 1.118	96% (5.2:1)

Figure 1.19. Representative azacyclic and oxacyclic allene trapping experiments.

Whereas the results shown in Figure 1.19 showcase reactions of unsubstituted strained cyclic allenes, another important facet of these compounds is observing and understanding what happens when substituents are present on the allene carbons in intermolecular trapping

experiments. Our laboratory has probed this issue in the context of azacyclic allenes,¹⁹¹ with key results provided in Figure 1.20. Silyl triflate **1.119**, **1.122**, and **1.125** were accessed as precursors to the corresponding cyclic allenes **1.120**, **1.123**, and **1.126**, in order to probe the influence of electron-donating and electron-withdrawing substituents (i.e., alkyl and ester groups, respectively). As shown by the formation of **1.121**, cycloaddition occurs on the olefin of **1.120** distal to the methyl group, whereas the cycloaddition takes place on the olefin proximal to the ester of **1.123**. When both methyl and ester substituents were present, cycloaddition occurs proximal to the ester and distal to the methyl of cyclic allene **1.126**, as one might expect in this matched scenario (**1.125** + **1.113** → **1.127**). All three reactions proceeded in good yields and excellent diastereoselectivities to give structurally complex products, including two with quaternary centers (i.e., **1.124** and **1.127**), further highlighting the synthetic utility of this methodology. In a collaboration with the Houk group at UCLA, a distortion-interaction analysis demonstrated that interaction energies, related to electron-factors, likely govern regioselectivity.¹⁹¹ With regard to diastereoselectivity, reactions proceed with *endo* selectivity with respect to the unreactive cyclic allene double bond.^{191,193} Given the synthetic utility of this methodology and the ability to understand the regiochemical and stereochemical outcomes, we expect this methodology will see increased usage in chemical synthesis. For example, Schreiber and coworkers have recently harnessed heterocyclic allene chemistry for the synthesis of DNA-encoded libraries.¹⁹⁴

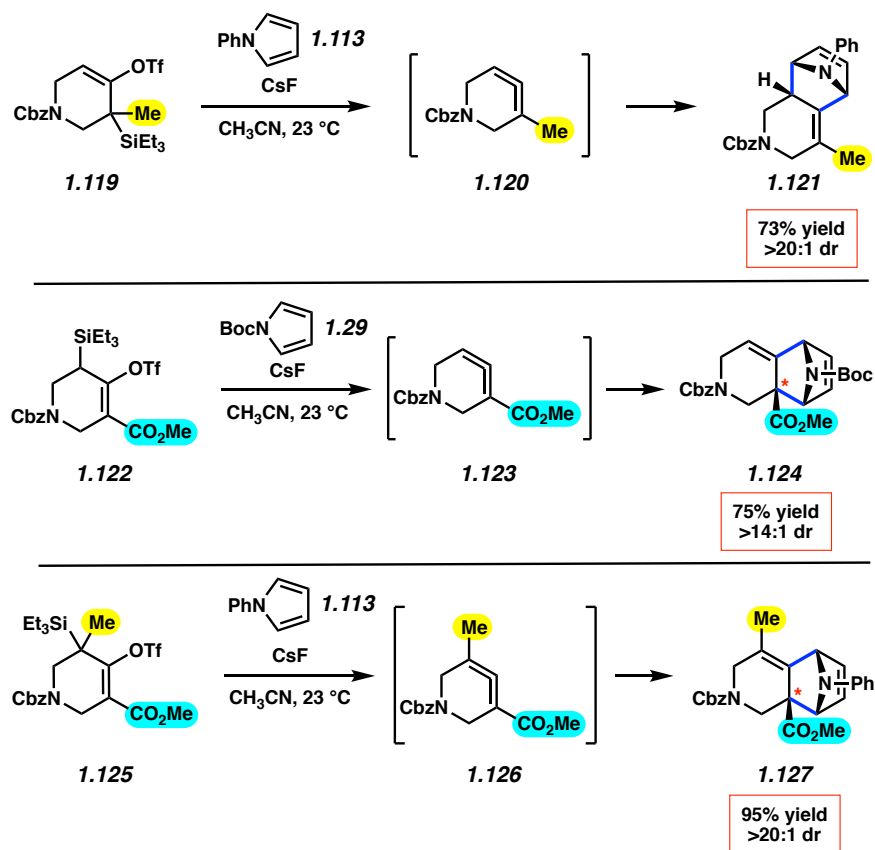


Figure 1.20. Regioselectivity investigation of substituted azacyclic allenes.

1.7 Strained Cyclic Allenes in Enantioselective and Stereospecific Reactions

The aforementioned studies demonstrate that cyclic allenes can undergo regio- and diastereoselective trapping to give polycyclic heterocyclic products. In an emerging area, efforts have also been put forth to control absolute stereochemistry in reactions of strained cyclic allenes. Seminal studies performed by Christl and coworkers demonstrated that enantioenriched cyclic allenes can be generated and intercepted using the Skattebøl rearrangement.^{171,172} Our laboratory devised the alternative approach shown in Figure 1.21.^{191,192} Silyl triflates **1.128** would be prepared with control of absolute stereochemistry and subjected to mild fluoride-based conditions. This could lead to the transmission of stereochemical information to cyclic allenes **1.129**, which in turn, could undergo stereospecific trapping with **1.18** to yield cycloadducts **1.130**. Of note, this overall

process would proceed with the transfer of point chirality from **1.128** to **1.130**, via the intermediacy of axially chiral intermediates (i.e., **1.129**), with potential ablation of the sole stereocenter present in the substrate. This approach involving enantioenriched silyl triflate precursors had not been examined previously.

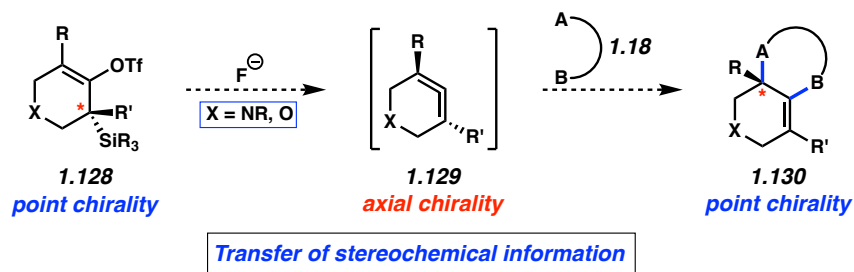


Figure 1.21. Transfer of stereochemical information in allene cycloadditions.

As shown in Figure 1.22, the success of the aforementioned approach was validated in the context of both aza- and oxacyclic allenes. In the first example, silyl triflate (+)-**1.119** was accessed in >99% ee by performing preparative chiral supercritical fluid chromatography (SFC) on a synthetic precursor. Under standard cyclic allene generation and trapping conditions, with diene **1.31** as the trapping agent, Diels–Alder adduct (+)-**1.131** was obtained in 98% ee (98% stereoretention).¹⁹¹ In the second example, silyl triflate (–)-**1.132** was obtained in 81% ee. The absolute stereochemistry was introduced by performing asymmetric allylic alkylation^{195,196,197,198,199} of a ketone precursor in collaboration with Stoltz and coworkers, thus obviating the need for preparative chiral chromatography. Nonetheless, cyclic allene generation and trapping provided (+)-**1.134** in 81% ee, reflective of >99% stereoretention.¹⁹² Collectively, these results demonstrate the feasibility of transferring stereochemical information from the silyl triflate to the cycloadduct through an axially chiral cyclic allene, while providing access to enantioenriched polycyclic products.

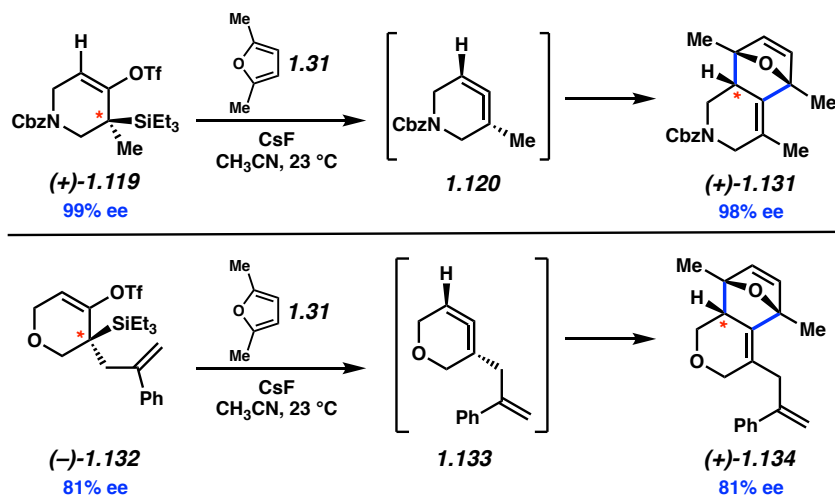


Figure 1.22. Stereospecific cycloadditions of heterocyclic allenes using enantioenriched silyl triflates.

An exciting new approach to control the absolute stereochemistry in reactions of cyclic allenes was recently demonstrated. This strategy was motivated by an interest in cyclic allene racemization, in contrast to the aforementioned approach involving transfer of stereochemical information. A key result that prompted this study is shown in Figure 1.23. Silyl triflate **1.122**, accessible in 87% ee (via chiral separation of a precursor), was subjected to cyclic allene generation and trapping.¹⁹¹ However, cycloadduct **1.135** was obtained racemically. This result suggested the importance of substituent effects and that racemization could plausibly outcompete cyclic allene trapping. Interestingly, computational studies suggest that ester-substituted cyclic allene **1.122** undergoes racemization readily, with an estimated barrier of only 14.1 kcal/mol.¹⁹¹ Thus, efforts were put forth toward developing an asymmetric trapping of cyclic allene intermediates using transition metal catalysis.

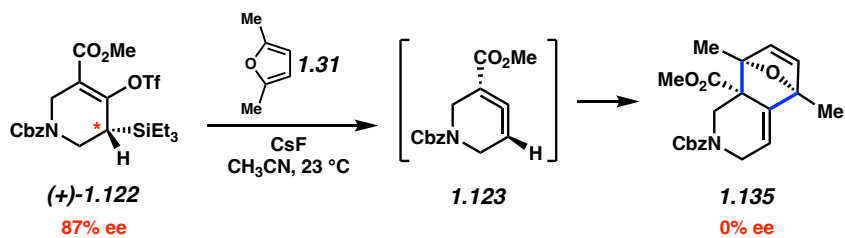


Figure 1.23. Cyclic allene racemization.

Only one prior example of a transition metal-mediated strained cyclic allene reaction was known in the literature, which involved a cyclotrimerization process.¹⁷⁷ Our laboratory has since developed two variants of asymmetric transition metal-catalyzed annulations of cyclic allenes, as shown in Figure 1.24. It was found that under nickel-catalyzed annulation conditions,²⁰⁰ cyclic allene precursor **1.136** and benzotriazinone **1.137** afforded tricycle **1.139** in 85% yield and 94% ee.²⁰¹ More recently, we demonstrated that reaction of silyl triflate **1.140** and iodopyridine **1.141** under palladium-catalyzed annulation conditions afforded tricycle **1.143** in 64% yield and 90% ee.²⁰² These transformations are thought to proceed via the reaction of an in situ-generated, racemic cyclic allene and a transient metallocycle formed by oxidative addition. Mechanistic details, including how absolute stereochemistry is introduced, have been proposed for the nickel-catalyzed annulation based on computations.²⁰¹ As such, these methodologies not only provide an advance in strained cyclic allene chemistry, but are also some of the few catalytic asymmetric reactions across the larger family of transiently-generated cyclic intermediates (e.g., arynes, cyclic alkynes, cyclic allenes).

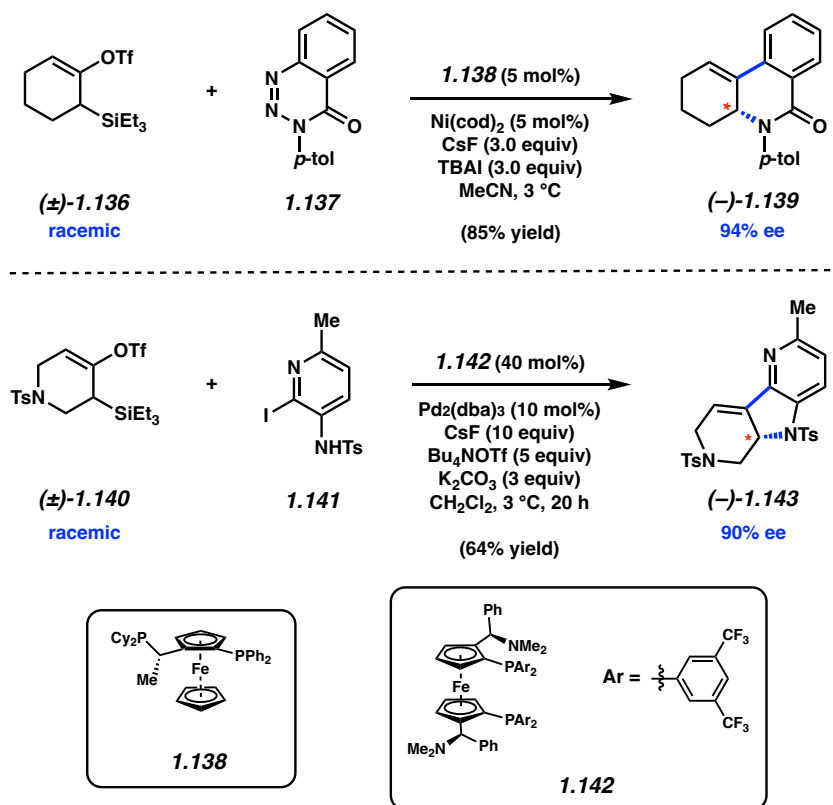


Figure 1.24. Catalytic asymmetric reactions of cyclic allenes.

1.8 Outlook and Future Directions

The study of arynes, strained cyclic alkynes, and strained cyclic allenes has seen tremendous growth in recent years. As highlighted in this Chapter, such strained intermediates were contemplated as early as 1902, and validated 50+ years later. In the modern era, these species can be strategically employed in a host of impressive synthetic applications. The increase in practical use can be attributed to a combination of factors, including the mild conditions used for their generation, the commercial availability of silyl triflate precursors,²⁰³ and advances in our ability to understand and predict how strained cyclic intermediates will react in complexity-generating transformations.^{24,25,26}

What does the future hold for arynes, cyclic alkynes, and cyclic allenes? We have shown in this Chapter how these transient species can be strategically leveraged to build complexity in

the form of polycyclic scaffolds. Notably, many of newly developed methods discussed herein have potential applications in drug discovery and materials, as well as in the synthesis of heterocycles, natural products, and sp^3 -rich compounds. Moreover, key advances to control absolute stereochemistry using asymmetric catalysis recently emerged and represent a particularly exciting area for future reaction development. As such, we curiously and enthusiastically await further advances from the synthetic community in the chemistry of arynes, strained cyclic alkynes, and strained cyclic allenes.

1.9 Notes and References

- (1) Stoermer, R.; Kahlert, B. Ueber das 1- und 2-Brom-cumaron. *Ber. Dtsch. Chem. Ges.* **1902**, *35*, 1633–1640.
- (2) Reinecke, M. G. Hetarynes. *Tetrahedron* **1982**, *38*, 427–498.
- (3) Kauffmann, T. The Hetarynes. *Angew. Chem., Int. Ed.* **1965**, *4*, 543–557.
- (4) Kauffmann, T.; Wirthwein, R. Progress in the Hetaryne Field. *Angew. Chem., Int. Ed.* **1971**, *10*, 20–33.
- (5) Roberts, J. D.; Simmons, H. E.; Carlsmith, L. A.; Vaughan, C. W. Rearrangement in the Reaction of Chlorobenzene-1-C¹⁴ with Potassium Amide. *J. Am. Chem. Soc.* **1953**, *75*, 3290–3291.
- (6) Scardiglia, F.; Roberts, J. D. Evidence for *Cyclohexyne* as an Intermediate in the Coupling of Phenyllithium with 1-Chlorocyclohexene. *Tetrahedron* **1957**, *1*, 343–344.
- (7) Wittig, G. Fortschritte auf dem Gebiet der Organischen Aniono-Chemie. *Angew. Chem.* **1954**, *1*, 10–17.
- (8) Huisgen, R.; Knorr, R. Sind Die Benz-ine Verschiedener Provenienz Identischi? *Tetrahedron Lett.* **1963**, *4*, 1017–1021.
- (9) Wittig, G.; Fritze, P. On the Intermediate Occurrence of 1,2-Cyclohexadiene. *Angew. Chem., Int. Ed.* **1966**, *5*, 846.
- (10) The graph in Figure 1.1 is based on a SciFinder search for the research topics “benzyne” or “aryne” (accessed October 20, 2020).

- (11) Mauger, C. C.; Mignani, G. A. An Efficient and Safe Procedure for the Large-Scale Pd-Catalyzed Hydrazonation of Aromatic Chlorides Using Buchwald Technology. *Org. Proc. Res. Dev.* **2004**, *8*, 1065–1071.
- (12) Coe, J. W.; Brooks, P. R.; Wirtz, M. C.; Bashore, C. G.; Bianco, K. E.; Vetelino, M. G.; Arnold, E. P.; Lebel, L. A.; Fox, C. B.; Tingley, F. D.; Schulz, D. W.; Davis, T. I.; Sands, S. B.; Mansbach, R. S.; Rollema, H.; O'Neill, B. T. 3,5-Bicyclic Aryl Piperidines: A Novel Class of $\alpha 4\beta 2$ Neuronal Receptor Partial Agonist for Smoking Cessation. *Bioorg. Med. Chem. Lett.* **2005**, *15*, 4889–4897.
- (13) Schleth, F.; Vettiger, T.; Rommel, M.; Tobler, H. Process for the Preparation of Pyrazole Carboxylic Acid Amides. International patent WO2011131544 A1, 2011.
- (14) Tadross, P. M.; Stoltz, B. M. A Comprehensive History of Arynes in Natural Product Total Synthesis. *Chem. Rev.* **2012**, *112*, 3550–3577.
- (15) Gampe, C. M.; Carreira, E. M. Arynes and Cyclohexyne in Natural Product Synthesis. *Angew. Chem., Int. Ed.* **2012**, *51*, 3766–3778.
- (16) Takikawa, H.; Nishii, A.; Sakai, T.; Suzuki, K. Aryne-Based Strategy in the Total Synthesis of Naturally Occurring Polycyclic Compounds. *Chem. Soc. Rev.* **2018**, *47*, 8030–8056.
- (17) Kou, K. G.; Pflueger, J. J.; Kiho, L. C.; Morrill, L. C.; Fischer, E. L.; Clagg, K.; Lebold, T. P.; Kisunzu, J. K.; Sarpong, R. A Benzyne Insertion Approach to Hetsisine-Type Diterpenoid Alkaloids: Synthesis of Cossonidine (Davisine). *J. Am. Chem. Soc.* **2018**, *140*, 8105–8109.

- (18) Gampe, C. M.; Carreira, E. M. Total Syntheses of Guanacastepenes N and O. *Angew. Chem., Int. Ed.* **2011**, *50*, 2962–2965.
- (19) Himeshima, Y.; Sonoda, T.; Kobayashi, H. Fluoride-Induced 1,2-Elimination of *O*-Trimethylsilylphenyl Triflate to Benzyne Under Mild Conditions. *Chem. Lett.* **1983**, *12*, 1211–1214.
- (20) Shi, J.; Li, L.; Li, Y. *o*-Silylaryl Triflates: A Journey of Kobayashi Aryne Precursors. *Chem. Rev.* **2021**, *121*, 3892–4044.
- (21) Kelleghan, A. V.; Busacca, C. A.; Sarvestani, M.; Volchkov, I.; Medina, J. M.; Garg, N. K. Safety Assessment of Benzyne Generation from a Silyl Triflate Precursor. *Org. Lett.* **2020**, *22*, 1665–1669.
- (22) For the use of silyl tosylates as strained intermediate precursors, see the following and references therein: McVeigh, M. S.; Kelleghan, A. V.; Yamano, M. M.; Knapp, R. R.; Garg, N. K. Silyl Tosylate Precursors to Cyclohexyne, 1,2-Cyclohexadiene, and 1,2-Cycloheptadiene. *Org. Lett.* **2020**, *22*, 4500–4504.
- (23) Fine Nathel, N. F.; Morrill, L. A.; Mayr, H.; Garg, N. K. Quantification of the Electrophilicity of Benzyne and Related Intermediates. *J. Am. Chem. Soc.* **2016**, *138*, 10402–10405.
- (24) Medina, J. M.; Mackey, J. L.; Garg, N. K.; Houk, K. N. The Role of Aryne Distortions, Steric Effects, and Charges in Regioselectivities of Aryne Reactions. *J. Am. Chem. Soc.* **2014**, *136*, 15798–15805.

- (25) Cheong, P. H.-Y.; Paton, R. S.; Bronner, S. M.; Im, G.-Y. J.; Garg, N. K.; Houk, K. N. Indolyne and Aryne Distortions and Nucleophilic Regioselectivities. *J. Am. Chem. Soc.* **2010**, *132*, 1267–1269.
- (26) Im, G.-Y. J.; Bronner, S. M.; Goetz, A. E.; Paton, R. S.; Cheong, P. H.-Y.; Houk, K. N.; Garg, N. K. Indolyne Experimental and Computational Studies: Synthetic Applications and Origins of Selectivities of Nucleophilic Additions. *J. Am. Chem. Soc.* **2010**, *132*, 17933–17944.
- (27) Wittig, G. 1,2-Dehydrobenzene. *Angew. Chem., Int. Ed. Engl.* **1965**, *4*, 731–737.
- (28) Wenk, H. H.; Winkler, M.; Sander, W. One Century of Aryne Chemistry. *Angew. Chem., Int. Ed.* **2003**, *42*, 502–528.
- (29) Dhokale, R. A.; Mhaske, S. B. Transition-Metal-Catalyzed Reactions Involving Arynes. *Synthesis* **2018**, *50*, 1–16.
- (30) Bhunia, A.; Yetra, S. R.; Biju, A. T. Recent Advances in Transition-Metal-Free Carbon–Carbon and Carbon–Heteroatom Bond-Forming Reactions Using Arynes. *Chem. Soc. Rev.* **2012**, *41*, 3140–3152.
- (31) Dubrovskiy, A. V.; Markina, N. A.; Larock, R. C. Use of Benzyne for the Synthesis of Heterocycles. *Org. Biol. Chem.* **2013**, *11*, 191–218.
- (32) Guitián, E.; Pérez, D.; Peña, D. Palladium-Catalyzed Cycloaddition Reactions of Arynes. *Top. Organomet. Chem.* **2005**, *14*, 109–146.
- (33) Bronner, S. M.; Goetz, A. E.; Garg, N. K. Understanding and Modulating Indolyne Regioselectivities. *Synlett* **2011**, *18*, 2599–2604.

- (34) Goetz, A. E.; Garg, N. K. Enabling the Use of Heterocyclic Arynes in Chemical Synthesis. *J. Org. Chem.* **2014**, *79*, 846–851.
- (35) Goetz, A. E.; Shah, T. K.; Garg, N. K. Pyridynes and Indolynes as Building Blocks for Functionalized Heterocycles and Natural Products. *Chem. Commun.* **2015**, *51*, 34–45.
- (36) Although outside of the scope of this chapter, an important area of modern aryne chemistry is the hexadehydro-Diels–Alder (HDDA) reaction. For a review, see: Diamond, O. J.; Marder, T. B. Methodology and Applications of the Hexadehydro-Diels–Alder (HDDA) reaction. *Org. Chem. Front.* **2017**, *4*, 891–910.
- (37) Another important field outside of the scope of this chapter involves biorthogonal reactions of cyclic alkynes in medium sized rings. For a pertinent review, see: Chupakhin, E. G.; Krasavin, M. Y. Achievements in the Synthesis of Cyclooctynes for Ring Strain-Promoted [3+2] Azide-Alkyne Cycloaddition. *Chem. Heterocycl. Compd.* **2018**, *54*, 483–501.
- (38) Gilchrist, T. L. Synthesis of Aromatic Heterocycles. *J. Chem. Soc., Perkin Trans. 1* **1999**, 2849–2866.
- (39) Lovering, F.; Bikker, J.; Humblet, C. Escape from Flatland: Increasing Saturation as an Approach to Improving Clinical Success. *J. Med. Chem.* **2009**, *52*, 6752–6756.
- (40) McGrath, N. A.; Brichacek, M.; Njardarson, J. T. A Graphical Journey of Innovative Organic Architectures That Have Improved Our Lives. *J. Chem. Educ.* **2010**, *87*, 1348–1349.

- (41) Ritchie, T. J.; Macdonald, S. J. F. The Impact of Aromatic Ring Count on Compound Developability – Are Too Many Aromatic Rings a Liability in Drug Design? *Drug Discov. Today* **2009**, *14*, 1011–1020.
- (42) Dinges, J.; Lamberth, C. *Bioactive Heterocyclic Compounds Classes: Agrochemicals*; Wiley-VCH: Weinheim, Germany, 2012.
- (43) Lovering, F. Escape from Flatland 2: Complexity and Promiscuity. *Med. Chem. Commun.* **2013**, *4*, 515–519.
- (44) Vitaku, E.; Smith, D. T.; Njardarson, J. T. Analysis of the Structural Diversity, Substitution Patterns, and Frequency of Nitrogen Heterocycles among U.S. FDA Approved Pharmaceuticals. *J. Med. Chem.* **2014**, *57*, 10257–10274.
- (45) Delost, D. M.; Smith, D. T.; Anderson, B. J.; Njardarson, J. T. From Oxiranes to Oligomers: Architectures of U.S. FDA Approved Pharmaceuticals Containing Oxygen Heterocycles. *J. Med. Chem.* **2018**, *61*, 10996–11020.
- (46) Medina, J. M.; McMahon, T. C.; Jiménez-Oses, G.; Houk, K. N.; Garg, N. K. Cycloadditions of Cyclohexynes and Cyclopentyne. *J. Am. Chem. Soc.* **2014**, *136*, 14706–14709.
- (47) Tlais, S. F.; Danheiser, R. L. *N*-Tosyl-3-azacyclohexyne. Synthesis and Chemistry of a Strained Cyclic Ynamide. *J. Am. Chem. Soc.* **2014**, *136*, 15489–15492.
- (48) McMahon, T. C.; Medina, J. M.; Yang, Y.-F.; Simmons, B. J.; Houk, K. N.; Garg, N. K. Generation and Regioselective Trapping of a 3,4-Piperidyne for the Synthesis of Functionalized Heterocycles. *J. Am. Chem. Soc.* **2015**, *137*, 4082–4085.

- (49) Shah, T. K.; Medina, J. M.; Garg, N. K. Expanding the Strained Alkyne Toolbox: Generation and Utility of Oxygen-Containing Strained Alkynes. *J. Am. Chem. Soc.* **2016**, *138*, 4948–4954.
- (50) Goetz, A. E.; Garg, N. K. Regioselective Reactions of 3,4-Pyridynes Enabled by the Aryne Distortion Model. *Nat. Chem.* **2013**, *5*, 54–60.
- (51) Enamorado, M. F.; Ondachi, P. W.; Comins, D. L. A Five-Step Synthesis of (*S*)-Macrostomine from (*S*)-Nicotine. *Org. Lett.* **2010**, *12*, 4513–4515.
- (52) Saito, N.; Nakamura, K.-i.; Shibano, S.; Ide, S.; Minami, M.; Sato, Y. Addition of Cyclic Ureas and 1-Methyl-2-oxazolidone to Pyridynes: A New Approach to Pyridodiazepines, Pyridodiazocines, and Pyridooxazepines. *Org. Lett.* **2013**, *15*, 386–389.
- (53) Saito, N.; Nakamura, K.-i.; Sato, Y. 1,3-Dipolar Cycloaddition of Pyridynes and Azides: Concise Synthesis of Triazolopyridines. *Heterocycles* **2014**, *88*, 929–937.
- (54) Levine, R.; Leake, W. W. Rearrangement in the Reaction of 3-Bromopyridine with Sodium Amide and Sodioacetophenone. *Science* **1955**, *121*, 780.
- (55) Vaca, M. J. A.; Gil, J. I. A.; Chrovian, C. C.; Coate, H. R.; Angelis, M. D.; Dvorak, C. A.; Gelin, C. F.; Letavic, M. A.; Savall, B. M.; Soyode-Johnson, A.; Stenne, B. M.; Swanson, D. M. P2X7 Modulators. US 20140275015, Sept 18, 2014.
- (56) Ashton, W. T.; Caldwell, C. G.; Mathvink, R. J.; Ok, H. O.; Reigle, L. B.; Weber, A. E. 3-Amino-4-phenylbutanoic Acid Derivatives as Dipeptidyl Peptidase Inhibitors for the Treatment or Prevention of Diabetes. WO 2004064778, Aug 05, 2004.

- (57) Thompson, F.; Maillet, P.; Damiano, T.; Cherrier, M. P.; Clerc, F. New Tetrahydropyrazolo(3,4-c)pyridine Derivatives are Kinase Modulators Used Especially for Treating Cancer. FR 2857362, Jan 14, 2005.
- (58) Blatt, L. M.; Seiwert, S.; Beigelman, L.; Kercher, T.; Kennedy, A. L.; Andrews, S. W. Novel Inhibitors of Hepatitis C Virus Replication. WO 2008005511, Jan 10, 2008.
- (59) Facchetti, A. π -Conjugated Polymers for Organic Electronics and Photovoltaic Cell Applications. *Chem. Mater.* **2011**, *23*, 733–758.
- (60) Forrest, S. R. The Path to Ubiquitous and Low-Cost Organic Electronic Appliances on Plastic. *Nature* **2004**, *428*, 911–918.
- (61) Kulkarni, A. P.; Tonzola, C. J.; Babel A.; Jenekhe, S. A. Electron Transport Materials for Organic Light-Emitting Diodes. *Chem. Mater.* **2004**, *16*, 4556–4573.
- (62) Duan, L.; Hou, L.; Lee, T.-W.; Qiao, J.; Zhang, D.; Dong, G.; Wang, L.; Qiu, Y. Solution Processable Small Molecules for Organic Light-Emitting Diodes. *J. Mater. Chem.* **2010**, *20*, 6392–6407.
- (63) Tao, Y.; Yang, C.; Qin, J. Organic Host Materials for Phosphorescent Organic Light-Emitting Diodes. *Chem. Soc. Rev.* **2011**, *40*, 2943–2970.
- (64) Yu, T.; Liu, L; Xie, Z; Ma, Y. Progress in Small-Molecule Luminescent Materials for Organic Light-Emitting Diodes. *Sci. China Chem.* **2015**, *58*, 907–915.
- (65) Mas-Torrent, M.; Rovira, C. Novel Small Molecules for Organic Field-Effect Transistors: Towards Processability and High Performance. *Chem. Soc. Rev.* **2008**, *37*, 827–838.

- (66) Allard, S.; Forster, M.; Souharce, B.; Thiem, H.; Scherf, U. Organic Semiconductors for Solution-Processable Field-Effect Transistors (OFETs). *Angew. Chem., Int. Ed.* **2008**, *47*, 4070–4098.
- (67) Sirringhaus, H. 25th Anniversary Article: Organic Field-Effect Transistors: The Path Beyond Amorphous Silicon. *Adv. Mater.* **2014**, *26*, 1319–1335.
- (68) Back, J. Y.; Kim, Y.; An, T. K.; Kang, M. S.; Kwon, S.-K.; Park, C. E.; Kim, Y.-H. Synthesis and Electrical Properties of Novel Oligomer Semiconductors for Organic Field-Effect Transistors (OFETs): Asymmetrically End-Capped Acene-heteroacene Conjugated Oligomers. *Dyes Pig.* **2015**, *112*, 220–226.
- (69) Mishra, A.; Bäuerle, P. Small Molecule Organic Semiconductors on the Move: Promises for Future Solar Energy Technology. *Angew. Chem., Int. Ed.* **2012**, *51*, 2020–2067.
- (70) Lin, Y.; Li, Y.; Zhan, X. Small Molecule Semiconductors for High-Efficiency Organic Photovoltaics. *Chem. Soc. Rev.* **2012**, *41*, 4245–4272.
- (71) Roncali, J.; Leriche, P.; Blanchard, P. Molecular Materials for Organic Photovoltaics: Small is Beautiful. *Adv. Mater.* **2014**, *26*, 3821–3838.
- (72) Haller, A.; Guyot, A. Sur le γ -diphenylanthracene et le Dihydrure de γ -Diphenylanthracene Symetriques. *C. R. Acad. Sci.* **1904**, *138*, 1251–1254.
- (73) Carmel, J. H.; Ward, J. S.; Cooper, M. M. A Glowing Recommendation: A Project-Based Cooperative Laboratory Activity to Promote Use of the Scientific and Engineering Practices. *J. Chem. Educ.* **2017**, *94*, 626–631.

- (74) Jo, W. J.; Kim, K.-H.; No, H. C.; Shin, D.-Y.; Oh, S.-J.; Son, J.-H.; Kim, Y.-H.; Cho, Y.-K.; Zhao, Q.-H.; Lee, K.-H.; Oh, H.-Y.; Kwon, S.-K. High Efficient Organic Light Emitting Diodes Using New 9,10-Diphenylanthracene Derivatives Containing Bulky Substituents on 2,6-Position. *Synth. Met.* **2009**, *159*, 1359–1364.
- (75) Schmidt, H.; Schultz, G. II. Ueber Diphenylbenzole. *Justus Liebigs Ann. Chem.* **1880**, *203*, 118–137.
- (76) Markiewicz, J. T.; Wudl, F. Perylene, Oligorylenes, and Aza-Analogs. *ACS Appl. Mater. Interfaces* **2015**, *7*, 28063–28085.
- (77) Anthony, J. E. Functionalized Acenes and Heteroacenes for Organic Electronics. *Chem. Rev.* **2006**, *106*, 5028–5048.
- (78) Stępień, M.; Gońka, E.; Żyła, M.; Sprutta, N. Heterocyclic Nanographenes and Other Polycyclic Heteroaromatic Compounds: Synthetic Routes, Properties, and Applications. *Chem. Rev.* **2017**, *117*, 3479–3716.
- (79) Shen, Y.; Chen, C. F. Helicenes: Synthesis and Applications. *Chem. Rev.* **2012**, *112*, 1463–1535.
- (80) Lin, J. B.; Shah, T. K.; Goetz, A. E.; Garg, N. K.; Houk, K. N. Conjugated Trimeric Scaffolds Accessible from Indolyne Cyclotrimerizations: Synthesis, Structures, and Electronic Properties. *J. Am. Chem. Soc.* **2017**, *139*, 10447–10455.
- (81) Peña, D.; Escudero, S.; Pérez, D.; Guitián, E.; Castedo, L. Efficient Palladium-Catalyzed Cyclotrimerization of Arynes: Synthesis of Triphenylenes. *Angew. Chem., Int. Ed.* **1998**, *37*, 2659–2661.

- (82) Ji, L.; Fang, Q.; Yuan, M.-S.; Liu, Z.-Q.; Shen, Y.-X.; Chen, H.-F. Switching High Two-Photon Efficiency: From 3,8,13-Substituted Triindole Derivatives to Their 2,7,12-Isomers. *Org. Lett.* **2010**, *12*, 5192–5195.
- (83) Gómez-Lor, B.; Alonso, B.; Omenat, A.; Serrano, J. L. Electroactive C_3 Symmetric Discotic Liquid-Crystalline Triindoles. *Chem. Commun.* **2006**, 5012–5014.
- (84) Talarico, M.; Termine, R.; García-Frutos, E. M.; Omenat, A.; Serrano, J. L.; Gómez-Lor, B.; Golemme, A. New Electrode-Friendly Triindole Columnar Phases with High Hole Mobility. *Chem. Mater.* **2008**, *20*, 6589–6591.
- (85) Su, P.-Y.; Huang, L.-B.; Liu, J.-M.; Chen, Y.-F.; Xiao, L.-M.; Kuang, D.-B.; Mayor, M.; Su, C.-Y. A Multifunctional Poly-*N*-vinylcarbazole Interlayer in Perovskite Solar Cells for High Stability and Efficiency: A Test with New Triazatruxene-based Hole Transporting Materials. *J. Mater. Chem. A* **2017**, *5*, 1913–1918.
- (86) Bajpai, M.; Yadav, N.; Kumar, S.; Srivastava, R.; Dhar, R. Incorporation of Liquid Crystalline Triphenylene Derivative in Bulk Heterojunction Solar Cell with Molybdenum Oxide as Buffer Layer for Improved Efficiency. *Liq. Cryst.* **2016**, *43*, 928–936.
- (87) Ramos, F. J.; Rakstys, K.; Kazim, S.; Graätzel, M.; Nazeeruddin, M. K.; Ahmad, S. Rational Design of Triazatruxene-based Hole Conductors for Perovskite Solar Cells. *RSC Adv.* **2015**, *5*, 53426–53432.
- (88) Darzi, E. R.; Barber, J. S.; Garg, N. K. Cyclic Alkyne Approach to Heteroatom-Containing Polycyclic Aromatic Hydrocarbon Scaffolds. *Angew. Chem., Int. Ed.* **2019**, *58*, 9419–9424.

- (89) Steglich, W.; Buschmann, E.; Gansen, G.; Wilschowitz, L. Herstellung und Reaktionen von 2,5-Diphenyl-6-oxo-1,3,4-oxadiazin. *Synthesis* **1977**, 252–253.
- (90) Miao, Q.; Chi, X.; Xiao, S.; Zeis, R.; Lefenfeld, M.; Siegrist, T.; Steigerwald, M. L.; Nuckolls, C. Organization of Acenes with a Cruciform Assembly Motif. *J. Am. Chem. Soc.* **2006**, *128*, 1340–1345.
- (91) Chun, D.; Cheng, Y.; Wudl, F. The Most Stable and Fully Characterized Functionalized Heptacene. *Angew. Chem., Int. Ed.* **2008**, *47*, 8380–8385.
- (92) Rickborn, B. The Retro-Diels–Alder Reaction Part II. Dienophiles with One or More Heteroatom. *Org. React.* **1998**, *53*, 223–629.
- (93) Tintas, M. L.; Diac, A. P.; Soran, A.; Terec, A.; Grosu, I.; Bogdan, E. Structural Characterization of New 2-Aryl-5-Phenyl-1,3,4-Oxadiazin-6-ones and their *N*-Aroylhydrazone Precursors. *J. Mol. Struct.* **2014**, *1058*, 106–113.
- (94) Liu, X.; Liu, J.; Zheng, B.; Yan, L.; Dai, J.; Zhuang, Z.; Du, J.; Guo, Y.; Xiao, D. *N*-Doped Carbon Dots: Green and Efficient Synthesis on a Large-Scale and Their Application in Fluorescent pH Sensing. *New J. Chem.* **2017**, *41*, 10607–10612.
- (95) Ma, Q.-J.; Li, H.-P.; Yang, F.; Zhang, J.; Wu, X.-F.; Bai, Y.; Li, X.-F. A Fluorescent Sensor for Low pH Values Based on a Covalently Immobilized Rhodamine–Naphthalimide Conjugate. *Sens. Actuators, B* **2012**, *166*, 68–74.
- (96) Tan, L.; Mo, S.; Fang, B.; Cheng, W.; Yin, M. Dual Fluorescence Switching of a Rhodamine 6G-Naphthalimide Conjugate with High Contrast in the Solid State. *J. Mater. Chem. C* **2018**, *6*, 10270–10275.

- (97) Meguro, T.; Chen, S.; Kanemoto, K.; Yoshida, S.; Hosoya, T. Modular Synthesis of Unsymmetrical Doubly-Ring-Fused Benzene Derivatives Based on a Sequential Ring Construction Strategy Using Oxadiazinones as a Platform Molecule. *Chem. Lett.* **2019**, *48*, 582–585.
- (98) Ramirez, M.; Darzi, E. R.; Donaldson, J. S.; Houk, K. N.; Garg, N. K. Cycloaddition Cascades of Strained Alkynes and Oxadiazinones. *Angew. Chem., Int. Ed.* **2021**, *60*, 18201–18208.
- (99) Dockendorff, C.; Sahli, S.; Olsen, M.; Milhau, L.; Lautens, M. Synthesis of Dihydronaphthalenes via Aryne Diels–Alder Reactions: Scope and Diastereoselectivity. *J. Am. Chem. Soc.* **2005**, *127*, 15028–15029.
- (100) Webster, R.; Lautens, M. Conformational Effects in Diastereoselective Aryne Diels–Alder Reactions: Synthesis of Benzo-Fused [2.2.1] Heterobicycles. *Org. Lett.* **2009**, *11*, 4688–4691.
- (101) Jones, E. P.; Jones, P.; Barrett, A. G. M. Asymmetric Synthesis of α -Aryl Amino Acids; Aryne-Mediated Diastereoselective Arylation. *Org. Lett.* **2011**, *13*, 1012–1015.
- (102) Jones, E. P.; Jones, P.; White, A. J. P.; Barrett, A. G. M. Asymmetric Synthesis of Quaternary Aryl Amino Acid Derivatives via a Three-Component Aryne Coupling Reaction. *Beilstein J. Org. Chem.* **2011**, *7*, 1570–1576.
- (103) Quasdorf, K. W.; Overman, L. E. Catalytic Enantioselective Synthesis of Quaternary Carbon Stereocentres. *Nature* **2014**, *516*, 181–191.

- (104) Liu, Y.; Han, S.-J.; Liu, W.-B.; Stoltz, B. M. Catalytic Enantioselective Construction of Quaternary Stereocenters: Assembly of Key Building Blocks for the Synthesis of Biologically Active Molecules. *Acc. Chem. Res.* **2015**, *48*, 740–751.
- (105) Shockley, S. E.; Holder, J. C.; Stoltz, B. M. Palladium-Catalyzed Asymmetric Conjugate Addition of Arylboronic Acids to α,β -Unsaturated Cyclic Electrophiles. *Org. Process Res. Dev.* **2015**, *19*, 974–981.
- (106) Zeng, X.-P.; Cao, Z.-Y.; Wang, Y.-H.; Zhou, F.; Zhou, J. Catalytic Enantioselective Desymmetrization Reactions to All-Carbon Quaternary Stereocenters. *Chem. Rev.* **2016**, *116*, 7330–7396.
- (107) Picazo, E.; Anthony, S. M.; Giroud, M.; Simon, A.; Miller, M. A.; Houk, K. N.; Garg, N. K. Arynes and Cyclic Alkynes as Synthetic Building Blocks for Stereodefined Quaternary Centers. *J. Am. Chem. Soc.* **2018**, *140*, 7605–7610.
- (108) Tambar, U. K.; Stoltz, B. M. The Direct Acyl-Alkylation of Arynes. *J. Am. Chem. Soc.* **2005**, *127*, 5340–5341.
- (109) Altman, R. A.; Hyde, A. M.; Huang, X.; Buchwald, S. L. Orthogonal Pd- and Cu-Based Catalyst Systems for C- and N-Arylation of Oxindoles. *J. Am. Chem. Soc.* **2008**, *130*, 9613–9620.
- (110) Taylor, A. M.; Altman, R. A.; Buchwald, S. L. Palladium-Catalyzed Enantioselective α -Arylation and α -Vinylolation of Oxindoles Facilitated by an Axially Chiral P-Stereogenic Ligand. *J. Am. Chem. Soc.* **2009**, *131*, 9900–9901.

- (111) Li, P.-F.; Buchwald, S. L. Continuous-Flow Synthesis of 3,3-Disubstituted Oxindoles by a Palladium-Catalyzed α -Arylation/Alkylation Sequence. *Angew. Chem., Int. Ed.* **2011**, *50*, 6396–6400.
- (112) Beringer, F. M.; Forgione, P. S.; Yudis, M. D. Diaryliodonium Salts—XII: The Phenylation of Dimedone, Dibenzoylmethane and Tribenzoylmethane. *Tetrahedron* **1960**, *8*, 49–63.
- (113) Ochiai, M.; Kitagawa, Y.; Takayama, N.; Takaoka, Y.; Shiro, M. Synthesis of Chiral Diaryliodonium Salts, 1,1'-Binaphthyl-2-yl(phenyl)iodonium Tetrafluoroborates: Asymmetric α -Phenylation of β -Keto Ester Enolates. *J. Am. Chem. Soc.* **1999**, *121*, 9233–9234.
- (114) Oh, C. H.; Kim, J. S.; Jung, H. H. Highly Efficient Arylation of Malonates with Diaryliodonium Salts. *J. Org. Chem.* **1999**, *64*, 1338–1340.
- (115) Xie, X.; Chen, Y.; Ma, D. Enantioselective Arylation of 2-Methylacetoacetates Catalyzed by CuI/*trans*-4-Hydroxy-L-proline at Low Reaction Temperatures. *J. Am. Chem. Soc.* **2006**, *128*, 16050–16051.
- (116) Beare, M. A.; Hartwig, J. F. Palladium-Catalyzed Arylation of Malonates and Cyanoesters Using Sterically Hindered Trialkyl- and Ferrocenyldialkylphosphine Ligands. *J. Org. Chem.* **2002**, *67*, 541–555.
- (117) For pioneering studies of racemic enamine arylations, see: Kuehne, M. E. The Arylation of Enamines. *J. Am. Chem. Soc.* **1962**, *84*, 837–847.

- (118) For the α -arylation of enamines with arynes to give functionalized achiral enamines, see reference 119 and the following: Ramtohul, Y. K.; Chartrand, A. Direct C-Arylation of β -Enamino Esters and Ketones with Arynes. *Org. Lett.* **2007**, *9*, 1029–1032.
- (119) Li, R.; Wang, X.; Wei, Z.; Wu, C.; Shi, F. Reaction of Arynes with Vinylogous Amides: Nucleophilic Addition to the *ortho*-Quinodimethide Intermediate. *Org. Lett.* **2013**, *15*, 4366–4369.
- (120) Li, L.; Li, Y.; Fu, N.; Zhang, L.; Luo, S. Catalytic Asymmetric Electrochemical α -Arylation of Cyclic β -Ketocarboxyls with Anodic Benzyne Intermediates. *Angew. Chem., Int. Ed.* **2020**, *59*, 14347–14351.
- (121) Ross, S. P.; Hoye, T. R. Reactions of Hexahydro-Diels–Alder Benzyne with Structurally Complex Multifunctional Natural Products. *Nat. Chem.* **2017**, *9*, 523–530.
- (122) Anthony, S. M.; Tona, V.; Zou, Y.; Morrill, L. A.; Billingsley, J. M.; Lim, M.; Tang, Y.; Houk, K. N.; Garg, N. K. Total Synthesis of (–)-Strictosidine and Interception of Aryne Natural Product Derivatives “Strictosidyne” and “Strictosamidyne”. *J. Am. Chem. Soc.* **2021**, *143*, 7471–7479.
- (123) Hutters, A. D.; Styduhar, E. D.; Garg, N. K. Total Syntheses of the Elusive Welwitindolinones with Bicyclo[4.3.1] Cores. *Angew. Chem., Int. Ed.* **2012**, *51*, 3758–3765.
- (124) Hutters, A. D.; Quasdorf, K. W.; Styduhar, E. D.; Garg, N. K. Total Synthesis of (–)-*N*-Methylwelwitindolinone C Isothiocyanate. *J. Am. Chem. Soc.* **2011**, *133*, 15797–15799.

- (125) Quasdorf, K. W.; Hutters, A. D.; Lodewyk, M. K.; Tantillo, D. J.; Garg, N. K. Total Synthesis of Oxidized Welwitindolinones and (–)-*N*-Methylwelwitindolinone C Isonitrile. *J. Am. Chem. Soc.* **2012**, *134*, 1396–1399.
- (126) Styduhar, E. D.; Hutters, A. D.; Weires, N. A.; Garg, N. K. Enantiospecific Total Synthesis of *N*-Methylwelwitindolinone D Isonitrile. *Angew. Chem., Int. Ed.* **2013**, *52*, 12422–12425.
- (127) Weires, N. A.; Styduhar, E. D.; Baker, E. L.; Garg, N. K. Total Synthesis of (–)-*N*-Methylwelwitindolinone B Isothiocyanate via a Chlorinative Oxabicyclic Ring-Opening Strategy. *J. Am. Chem. Soc.* **2014**, *136*, 14710–14713.
- (128) TePaske, M. R.; Gloer, J. B.; Wicklow, D. T.; Dowd, P. F. Tubingensin A: An Antiviral Carbazole Alkaloid from the Sclerotia of *Aspergillus Tubingensis*. *J. Org. Chem.* **1989**, *54*, 4743–4746.
- (129) TePaske, M. R.; Gloer, J. B.; Wicklow, D. T.; Dowd, P. F. The Structure of Tubingensin B: A Cytotoxic Carbazole Alkaloid from the Sclerotia of *Aspergillus tubingensis*. *Tetrahedron Lett.* **1989**, *30*, 5965–5968.
- (130) Bian, M.; Wang, Z.; Xiong, X.; Sun, Y.; Matera, C.; Nicolaou, K. C.; Li, A. Total Synthesis of Anominine and Tubingensin A. *J. Am. Chem. Soc.* **2012**, *134*, 8078–8081.
- (131) Buszek, K. R.; Brown, N.; Luo, D. Concise Total Synthesis of (±)-*cis*-Triketrin A and (±)-Herbindole A via Intermolecular Indole Aryne Cycloaddition. *Org. Lett.* **2009**, *11*, 201–204.
- (132) Matsumoto, T.; Yamaguchi, H.; Tanabe, M.; Yasui, Y.; Suzuki, K. Synthetic Study of Aquayamycin. Part 3: First Total Synthesis. *Tetrahedron Lett.* **2000**, *41*, 8393–8396.

- (133) Sato, S.; Sakata, K.; Hashimoto, Y.; Takikawa, H.; Suzuki, K. First Total Syntheses of Tetracenomyces C and X. *Angew. Chem., Int. Ed.* **2017**, *56*, 12608–12613.
- (134) Torres-Ochoa, R. O.; Buyck, T.; Wang, Q.; Zhu, J. Heteroannulation of Aryne with α -Amino Imides: Synthesis of 2,2-Disubstituted Indolin-3-ones and Application to the Enantioselective Total Synthesis of (+)-Hinkdentine A. *Angew. Chem., Int. Ed.* **2018**, *57*, 5679–5683.
- (135) Candito, D. A.; Dobrovolsky, D.; Lautens, M. Development of an Intramolecular Aryne Ene Reaction and Application to the Formal Synthesis of (\pm)-Crinine. *J. Am. Chem. Soc.* **2012**, *134*, 15572–15580.
- (136) Xu, H.; He, J.; Shi, J.; Tan, L.; Qiu, D.; Luo, X.; Li, Y. Domino Aryne Annulation via a Nucleophilic–Ene Process. *J. Am. Chem. Soc.* **2018**, *140*, 3555–3559.
- (137) Goetz, A. E.; Silberstein, A. L.; Corsello, M. A.; Garg, N. K. Concise Enantiospecific Total Synthesis of Tubingensin A. *J. Am. Chem. Soc.* **2014**, *136*, 3036–3039.
- (138) Caubere, P. Applications of Sodamide-Containing Complex Bases in Organic Synthesis. *Acc. Chem. Res.* **1974**, *7*, 301–308.
- (139) Gregoire, B.; Carre, M.-C.; Caubere, P. Arynic Condensation of Ketone Enolates. 17. New General Access to Benzocyclobutene Derivatives. *J. Org. Chem.* **1986**, *51*, 1419–1427.
- (140) Ishida, N.; Sawano, S.; Masuda, Y.; Murakami, M. Rhodium-Catalyzed Ring Opening of Benzocyclobutenols with Site-Selectivity Complementary to Thermal Ring Opening. *J. Am. Chem. Soc.* **2012**, *134*, 17502–17504.

- (141) Corsello, M. A.; Kim, J.; Garg, N. K. Total Synthesis of (–)-Tubingensin B Enabled by the Strategic Use of an Aryne Cyclization. *Nat. Chem.* **2017**, *9*, 944–949.
- (142) Mahatthananchai, J.; Dumas, A. M.; Bode, J. W. Catalytic Selective Synthesis. *Angew. Chem., Int. Ed.* **2012**, *51*, 10954–10990.
- (143) Trost, B. M. Asymmetric Catalysis: An Enabling Science. *Proc. Natl. Acad. Sci. U.S.A.* **2004**, *101*, 5348–5355.
- (144) Douglas, C. J.; Overman, L. E. Catalytic Asymmetric Synthesis of All-Carbon Quaternary Stereocenters. *Proc. Natl. Acad. Sci. U.S.A.* **2004**, *101*, 5363–5367.
- (145) Caeiro, J.; Peña, D.; Cobas, A.; Pérez, D.; Guitián, E. Asymmetric Catalysis in the [2+2+2] Cycloaddition of Arynes and Alkynes: Enantioselective Synthesis of a Pentahelicene. *Adv. Synth. Catal.* **2006**, *348*, 2466–2474.
- (146) Yubuta, A.; Hosokawa, T.; Gon, M.; Tanaka, K.; Chujo, Y.; Tsurusaki, A.; Kamikawa, K. Enantioselective Synthesis of Triple Helicenes by Cross-Cyclotrimerization of a Helicenyl Aryne and Alkynes via Dynamic Kinetic Resolution. *J. Am. Chem. Soc.* **2020**, *142*, 10025–10033.
- (147) Stará, I. G.; Starý, I. Helically Chiral Aromatics: The Synthesis of Helicenes by [2 + 2 + 2] Cycloisomerization of π -Electron Systems. *Acc. Chem. Res.* **2020**, *53*, 144–158.
- (148) Gingras, M.; Félix, G.; Peresutti, R. One Hundred Years of Helicene Chemistry. Part 2: Stereoselective Syntheses and Chiral Separations of Carbohelicenes. *Chem. Soc. Rev.* **2013**, *42*, 1007–1050.

- (149) Peña, D.; Pérez, D.; Guitián, E.; Castedo, L. Synthesis of Hexabenzotriphenylene and Other Strained Polycyclic Aromatic Hydrocarbons by Palladium-Catalyzed Cyclotrimerization of Arynes. *Org. Lett.* **1999**, *1*, 1555–1557.
- (150) Peña, D.; Cobas, A.; Pérez, D.; Guitián, E.; Castedo, L. Dibenzo[*a,o*]phenanthro[3,4-*s*]pycene, a Configurationally Stable Double Helicene: Synthesis and Determination of Its Conformation by NMR and GIAO Calculations. *Org. Lett.* **2003**, *5*, 1863–1866.
- (151) Hosokawa, T.; Takahashi, Y.; Matsushima, T.; Watanabe, S.; Kikkawa, S.; Azumaya, I.; Tsurusaki, A.; Kamikawa, K. Synthesis, Structures, and Properties of Hexapole Helicenes: Assembling Six [5]Helicene Substructures into Highly Twisted Aromatic Systems. *J. Am. Chem. Soc.* **2017**, *139*, 18512–18521.
- (152) QUINAP has been used previously to access enantioenriched helicenes. For a recent example, see: Karras, M.; Holec, J.; Bednárová, L.; Pohl, R.; Schmidt, B.; Stará, I. G.; Starý, I. Asymmetric Synthesis of Nonracemic 2-Amino[6]helicenes and Their Self-Assembly into Langmuir Films. *J. Org. Chem.* **2018**, *83*, 5523–5538.
- (153) Gandeepan, P.; Cheng, C.-H. Cobalt Catalysis Involving π Components in Organic Synthesis. *Acc. Chem. Res.* **2015**, *48*, 1194–1206.
- (154) Zheng, T.; Sun, H.; Chen, Y.; Li, X.; Dürr, S.; Radius, U.; Harms, K. Synergistic Effect of a Low-Valent Cobalt Complex and a Trimethylphosphine Ligand on Selective C–F Bond Activation of Perfluorinated Toluene. *Organometallics* **2009**, *28*, 5771–5776.
- (155) Gandon, V.; Aubert, C.; Malacria, M. Recent Progress in Cobalt-Mediated [2 + 2 + 2] Cycloaddition Reactions. *Chem. Commun.* **2006**, 2209–2217.

- (156) Campbell, C. D.; Rees, C. W. Reactive Intermediates. Part I. Synthesis and Oxidation of 1- and 2-Aminobenzotriazole. *J. Chem. Soc. C* **1969**, 5, 742–747.
- (157) Kato, H.; Nakazawa, S.; Kiyosawa, T.; Hirakawa, K. Heterocycles by Cycloaddition. Part II. Cycloaddition-Extrusion Reactions of Five-Membered Mesoionic Compounds with Benzyne: Preparation of Benz[*c*]azole and Benzo[*c*]thiophen Derivatives. *J. Chem. Soc., Perkin Trans. 1* **1976**, 672–675.
- (158) Rigby, J. H.; Holsworth, D. D.; James, K. Vinyl Isocyanates in Synthesis. [4 + 2] Cycloaddition Reactions with Benzyne Addends. *J. Org. Chem.* **1989**, 54, 4019–4020.
- (159) Sakurai, H.; Sakaba, H.; Nakadaira, Y. Facile Preparation of 2,3-Benzo-1,4-diphenyl-7-silanorbornadiene Derivatives and the First Clear Evidence of Silylene to Disilene Thermal Rearrangement. *J. Am. Chem. Soc.* **1982**, 104, 6156–6158.
- (160) Cresp, T. M.; Wege, D. The Addition of Benzyne to Azulene. *Tetrahedron* **1986**, 42, 6713–6718.
- (161) Engels, B.; Schöneboom, J. C.; Münster, A. F.; Groetsch, S.; Christl, M. Computational Assessment of the Electronic Structures of Cyclohexa-1,2,4-triene, 1-Oxacyclohexa-2,3,5-triene (3 δ^2 -Pyran), Their Benzo Derivatives, and Cyclohexa-1,2-diene. An Experimental Approach to 3 δ^2 -Pyran. *J. Am. Chem. Soc.* **2002**, 124, 287–297.
- (162) Hänninen, M. M.; Peuronen, A.; Tuononen, H. M. Do Extremely Bent Allenes Exist? *Chem. Eur. J.* **2009**, 15, 7287–7291.
- (163) Schmidt, M. W.; Angus, R. O.; Johnson, R. P. Small Ring Cyclic Allenes: An ab Initio Study of the Structure of 1,2-Cyclohexadiene. *J. Am. Chem. Soc.* **1982**, 104, 6838–6839.

- (164) Taskesenligil, Y.; Kashyap, R. P. Watson, W. H.; Balci, M. Is the Intermediate in the Reaction of 3-Bromo-6,7-benzobicyclo[3.2.1]octa-2,6-diene with Potassium *tert*-Butoxide an Allene or an Alkyne? *J. Org. Chem.* **1993**, *58*, 3216–3218.
- (165) Daoust, K. J. Hernandez, S. M.; Konrad, K. M.; Mackie, I. D.; Winstanley, J.; Johnson, R. P. Strain Estimates for Small-Ring Cyclic Allenes and Butatrienes. *J. Org. Chem.* **2006**, *71*, 5708–5714.
- (166) Dillon, P. W.; Underwood, G. R. Cyclic Allenes. I. The Electronic Structure and Probable Deformation of the Allene Linkage When Included in a Ring. An INDO–MO Study. *J. Am. Chem. Soc.* **1974**, *96*, 779–787.
- (167) Angus, R. O.; Schmidt, M. W.; Johnson, R. P. Small-Ring Cyclic Cumulenes: Theoretical Studies of the Structure and Barrier to Inversion in Cyclic Allenes. *J. Am. Chem. Soc.* **1985**, *107*, 532–537.
- (168) Johnson, R. P. Strained Cyclic Cumulenes. *Chem. Rev.* **1989**, *89*, 1111–1124.
- (169) Nendel, M.; Tolbert, L. M.; Herring, L. E.; Islam, M. N.; Houk, K. N. Strained Allenes as Dienophiles in the Diels–Alder Reaction: An Experimental and Computational Study. *J. Org. Chem.* **1999**, *64*, 976–983.
- (170) Christl, M. Cyclic Allenes Up to Seven-Membered Rings. *Mod. Allene Chem*, 1; Wiley-VCH Verlag GmbH & Co. **2004**, *1*, 243–357.

- (171) Christl, M.; Braun, M.; Fischer, H.; Groetsch, S.; Müller, G.; Leusser, D.; Deuerlein, S.; Stalke, D.; Arnone, M.; Engels, B. The Stereochemical Course of the Generation and Interception of a Six-Membered Cyclic Allene: 3 δ^2 -1*H*-Naphthalene (2,3-Didehydro-1,2-dihydronaphthalene). *Eur. J. Org. Chem.* **2006**, 5045–5058.
- (172) Christl, M.; Fischer, H.; Arnone, M.; Engels, B. 1-Phenyl-1,2-cyclohexadiene: Astoundingly High Enantioselectivities on Generation in a Doering–Moore–Skattebøl Reaction and Interception by Activated Olefins. *Chem. Eur. J.* **2009**, *15*, 11266–11272.
- (173) Christl, M.; Schreck, M.; Fischer, T.; Rudolph, M.; Moigno, D.; Fischer, H.; Deuerlein, S.; Stalke, D. 1-Phenyl-1,2-cyclohexadiene: Generation, Interception by Activated Olefins, Dimerisation and Trimerisation. *Chem. Eur. J.* **2009**, *15*, 11256–11265.
- (174) Christl, M.; Schreck, M. 7-Arylbicyclo[4.2.0]oct-1-ene – Synthese durch [2+2]-Cycloadditionen von 1,2-Cyclohexadien Sowie 1-Methyl-1,2-cyclohexadien und Thermische Äquilibrierung der *Exo/Endo*-Isomeren. *Chem. Ber.* **1987**, *120*, 915–920.
- (175) Hioki, Y.; Mori, A.; Okano, K. Steric Effects on Deprotonative Generation of Cyclohexynes and 1,2-Cyclohexadienes from Cyclohexenyl Triflates by Magnesium Amides. *Tetrahedron* **2020**, *76*, 131103.
- (176) Inoue, K.; Nakura, R.; Okano, K.; Mori, A. One-Pot Synthesis of Silylated Enol Triflates from Silyl Enol Ethers for Cyclohexynes and 1,2-Cyclohexadienes. *Eur. J. Org. Chem.* **2018**, *2018*, 3343–3347.
- (177) Quintana, I.; Peña, D.; Pérez, D.; Guitián, E. Generation and Reactivity of 1,2-Cyclohexadiene under Mild Reaction Conditions. *Eur. J. Org. Chem.* **2009**, 5519–5524.

- (178) Peña, D.; Iglesias, B.; Quintana, I.; Pérez, D.; Guitián, E.; Castedo, L. Synthesis and Reactivity of New Strained Cyclic Allene and Alkyne Precursors. *Pure Appl. Chem.* **2006**, *78*, 451–455.
- (179) Barber, J. S.; Styduhar, E. D.; Pham, H. V.; McMahon, T. C.; Houk, K. N.; Garg, N. K. Nitron Cycloadditions of 1,2-Cyclohexadiene. *J. Am. Chem. Soc.* **2016**, *138*, 2512–2515.
- (180) Lofstrand, V. A.; West, F. G. Efficient Trapping of 1,2-Cyclohexadienes with 1,3-Dipoles. *Chem. Eur. J.* **2016**, *22*, 10763–10767.
- (181) For recent studies of substituted allenes, see: Wang, B.; Constantin, M.-G.; Singh, S.; Zhou, Y.; Davis, R. L.; F. G. West. Generation and Trapping of Electron-Deficient 1,2-Cyclohexadienes. Unexpected Hetero-Diels–Alder Reactivity. *Org. Biomol. Chem.* **2021**, *19*, 399–405.
- (182) Almealmadi, Y. A.; West, F. G. A Mild Method for the Generation and Interception of 1,2-Cycloheptadienes with 1,3-Dipoles. *Org. Lett.* **2020**, *22*, 6091–6095.
- (183) Lofstrand, V. A.; McIntosh, K. C.; Almealmadi, Y. A.; West, F. G. Strain-Activated Diels–Alder Trapping of 1,2-Cyclohexadienes: Intramolecular Capture by Pendent Furans. *Org. Lett.* **2019**, *21*, 6231–6234.
- (184) Uyegaki, M.; Ito, S.; Sugihara, Y.; Murata, I. 1-Benzoxepin and its Valence Isomers, 4,5-Benz-3-oxatricyclo[4.1.0.0^{2,7}]heptene and 3,4-Benz-2-oxabicyclo[3.2.0]hepta-3,6-diene. *Tetrahedron Lett.* **1976**, *49*, 4473–4476.
- (185) Schreck, M.; Christl, M. Generation and Interception of 1-Oxo-3,4-cyclohexadiene. *Angew. Chem., Int. Ed.* **1987**, *26*, 690–692.

- (186) Christl, M.; Braun, M. Friesetzung und Abfangreaktionen von 1-Oxa-2,3-cyclohexadien. *Chem. Ber.* **1989**, *122*, 1939–1946.
- (187) Ruzziconi, R.; Naruse, Y.; Schlosser, M. 1-Oxa-2,3-cyclohexadiene ("2H-Isopyran"): A Strained Heterocyclic Allene Undergoing Cycloaddition Reactions with Characteristic Typo-, Regio-, and Stereoselectivities. *Tetrahedron* **1991**, *47*, 4603–4610.
- (188) Jamart-Grégoire, B.; Mercier-Girardot, S.; Ianelli, S.; Nardelli, M.; Caubère, P. Aggregative Activation and Heterocyclic Chemistry II Nucleophilic Condensation of Ketone Enolates on Dehydrodihydropyran Generated by Complex Bases. *Tetrahedron* **1995**, *51*, 1973–1984.
- (189) Christl, M.; Braun, M.; Wolz, E.; Wagner, W. Cycloallene, 9. 1-Phenyl-1-aza-3,4-cyclohexadien, das Erste Isodihydropyridin: Erzeugung und Abfangreaktionen. *Chem. Ber.* **1994**, *127*, 1137–1142.
- (190) Drinkuth, S.; Groetsch, S.; Peters, E.-M.; Peters, K.; Christl, M. 1-Methyl-1-azacyclohexa-2,3-diene(*N-B*)borane - Generation and Interception of an Unsymmetrical Isodihydropyridine. *Eur. J. Org. Chem.* **2001**, *14*, 2665–2670.
- (191) Barber, J. S.; Yamano, M. M.; Ramirez, M.; Darzi, E. R.; Knapp, R. R.; Liu, F.; Houk, K. N.; Garg, N. K. Diels–Alder Cycloadditions of Strained Azacyclic Allenes. *Nat. Chem.* **2018**, *10*, 953–960.
- (192) Yamano, M. M.; Knapp, R. R.; Ngamnithiporn, A.; Ramirez, M.; Houk, K. N.; Stoltz, B. M.; Garg, N. K. Cycloadditions of Oxacyclic Allenes and a Catalytic Asymmetric Entryway to Enantioenriched Cyclic Allenes. *Angew. Chem., Int. Ed.* **2019**, *58*, 5653–5657.

- (193) Ramirez, M.; Svatunek, D.; Liu, F.; Garg, N. K.; Houk, K. N. Origins of *Endo* Selectivity in Diels–Alder Reactions of Cyclic Allene Dienophiles. *Angew. Chem., Int. Ed.* **2021**, *60*, 14989–14997.
- (194) Westphal, M. V.; Hudson, L.; Mason, J. W.; Pradeilles, J. A.; Zécéri, F. J.; Briner, K.; Schreiber, S. L. Water-Compatible Cycloadditions of Oligonucleotide-Conjugated Strained Allenes for DNA-Encoded Library Synthesis. *J. Am. Chem. Soc.* **2020**, *142*, 7776–7782.
- (195) Behenna, D. C.; Mohr, J. T.; Sherden, N. H.; Marinescu, S. C.; Harned, A. M.; Tani, K.; Seto, M.; Ma, S.; Novák, Z.; Krout, M. R.; McFadden, R. M.; Roizen, J. L.; Enquist, J. A.; White, D. E.; Levine, S. R.; Petrova, K. V.; Iwashita, A.; Virgil S. C.; Stoltz, B. M. Enantioselective Decarboxylative Alkylation Reactions: Catalyst Development, Substrate Scope, and Mechanistic Studies. *Chem. Eur. J.* **2011**, *17*, 14199–14223.
- (196) Hong, A. Y.; Stoltz, B. M. The Construction of All-Carbon Quaternary Stereocenters by Use of Pd-Catalyzed Asymmetric Allylic Alkylation Reactions in Total Synthesis. *Eur. J. Org. Chem.* **2013**, 2745–2759.
- (197) Tunge, J. A.; Burger, E. C. Transition Metal Catalyzed Decarboxylative Additions of Enolates. *Eur. J. Org. Chem.* **2005**, 1715–1726.
- (198) Weaver, J. D.; Recio, A.; Grenning, A. J.; Tunge, J. A. Transition Metal-Catalyzed Decarboxylative Allylation and Benzylolation Reactions. *Chem. Rev.* **2011**, *111*, 1846–1913.
- (199) Trost, B. M. Metal Catalyzed Allylic Alkylation: Its Development in the Trost Laboratories. *Tetrahedron* **2015**, *71*, 5708–5733.

- (200) Thorat, V. H.; Upadhyay, N. S.; Murakami, M.; Cheng, C.-H. Nickel-Catalyzed Denitrogenative Annulation of 1,2,3-benzotriazin-4-(3*H*)-ones with Benzyne for Construction of Phenanthridinone Scaffolds. *Adv. Synth. Catal.* **2018**, *360*, 284–289.
- (201) Yamano, M. M.; Kelleghan, A. V.; Shao, Q.; Giroud, M.; Simmons, B. J.; Li, B.; Chen, S.; Houk, K. N.; Garg, N. K. Intercepting Fleeting Cyclic Allenes with Asymmetric Nickel Catalysis. *Nature* **2020**, *586*, 242–247.
- (202) Kelleghan, A. V.; Witkowski, D. C.; McVeigh, M. S.; Garg, N. K. Palladium-Catalyzed Annulations of Strained Cyclic Allenes. *J. Am. Chem. Soc.* **2021**, *143*, 9338–9342.
- (203) Many of the silyl triflate precursors discussed herein (or close derivatives thereof) are currently commercially available. Benzyne precursor (**1.53**): CAS # 88284-48-4; 2-chlorobenzyne precursor: CAS # 1449472-59-6; 3,4-pyridyne precursor: CAS # 1211583-40-2; 2,3-pyridyne precursor: CAS # 134391-76-7; 2-bromobenzyne precursor: CAS # 1092542-31-8; 5-bromo-3,4-pyridyne precursor: CAS # 1413439-82-3; 4,5-indolyne precursor: CAS # 1259448-37-7; 4-methylbenzyne precursor: CAS # 262373-15-9; 4-methoxybenzyne precursor: CAS # 556812-41-0; 3-methoxybenzyne precursor: CAS # 217813-03-1; 2-methylbenzyne precursor: CAS # 556812-44-3; 4,5-dimethoxybenzyne precursor: CAS # 866252-52-0; 3-morpholinobenzyne precursor: CAS # 2047348-50-3; naphthalene precursor: CAS # 780820-43-1; azacyclohexyne precursor (**1.51**): Sigma–Aldrich product number 803928.

CHAPTER TWO

Palladium-Catalyzed Annulations of Strained Cyclic Allenes

Andrew V. Kelleghan, Dominick C. Witkowski, Matthew S. McVeigh, and Neil K. Garg

J. Am. Chem. Soc. **2021**, *143*, 9338–9342.

2.1 Abstract

We report Pd-catalyzed annulations of in-situ-generated strained cyclic allenes. This methodology employs aryl halides and cyclic allene precursors as the reaction partners in order to generate fused heterocyclic products. The annulation proceeds via the formation of two new bonds and a sp³ center. Moreover, both diastereo- and enantioselective variants of this methodology are validated, with the latter ultimately enabling the rapid enantioselective synthesis of a complex hexacyclic product. Studies leveraging transition metal catalysis to intercept cyclic allenes represent a departure from the more common, historical modes of cyclic allene trapping which rely on nucleophiles or cycloaddition partners. As such, this study is expected to fuel the development of reactions that strategically merge transition metal catalysis and transient strained intermediate chemistry for the synthesis of complex scaffolds.

2.2 Introduction

Since the early 1900s, transient strained cyclic intermediates, exemplified by benzyne (**2.1**, Figure 2.1A), have stimulated interest in the chemical community.¹ Although the proposal of benzyne (**2.1**) as a reactive intermediate led to significant controversy in the early 20th century, pioneering experiments by Roberts² and Wittig^{3,4} in the 1950s validated its existence, despite the

high degree of ring strain. Indeed, this ring strain gives rise to unique and synthetically useful reactivity, which in turn has motivated the development of heterocyclic arynes, such as **2.2**⁵ and **2.3**,⁶ and more highly saturated analogs of benzyne (**2.1**), such as cyclohexyne (**2.4**).^{7,8} These in-situ-generated intermediates have become increasingly prominent in the modern synthetic toolbox, finding applications in the construction of heterocycles,⁹ ligands for catalysis,¹⁰ natural products,^{11,12,13} agrochemicals,¹⁴ and organic materials.¹⁵

Whereas strained cyclic alkynes have received significant attention from the synthetic community, reactions of a related class of fleeting intermediates, strained cyclic allenes (e.g., 1,2-cyclohexadiene (**2.5**)), are relatively less developed.^{16,17} This is notable as cyclic allenes and alkynes were both discovered around the same time and share similar strain-promoted reactivity.¹⁸ Moreover, cyclic allenes are advantageous for the synthesis of sp³-rich and stereochemically complex targets, which are becoming increasingly more valuable.¹⁹ However, to date, only three major intermolecular reaction classes have been reported for these intermediates (Figure 2.1B), the most frequently studied being nucleophilic trappings (e.g., **2.7** + KO*t*-Bu → **2.6**) and cycloadditions (e.g., **2.7** + **2.8** → **2.9**).¹⁶ More than fifty studies detailing such reactions have been reported, including more recent studies by Guitián,^{20,21} West,^{22,23,24,25} Okano and Mori,^{26,27} Schreiber,²⁸ and our laboratory.^{29,30,31,32} A complementary, albeit rarely studied, approach utilizes transition metal catalysis to intercept the cyclic allene (e.g., **2.7** + **2.10** → **2.11**).^{20,33} However, this strategy poses an inherent kinetic challenge due to the requirement for reaction between a catalytically generated intermediate and an in-situ-generated fleeting cyclic allene, both of which are present in low concentration.

Previous efforts to intercept strained cyclic allenes with transition metal catalysis have been limited, with only two examples known in the literature. The first was a single example wherein

an in-situ-generated cyclic allene was intercepted in a Pd-catalyzed [2+2+2] reaction to generate a mixture of tetralin products, as demonstrated by Guitián and coworkers in 2009.²⁰ Subsequently, our laboratory developed a Ni-catalyzed annulation of cyclic allenes with benzotriazinones, including an asymmetric variant.³³ These studies demonstrate that the combination of transition metal catalysis and cyclic allenes provides an exciting new avenue in strained intermediate chemistry.

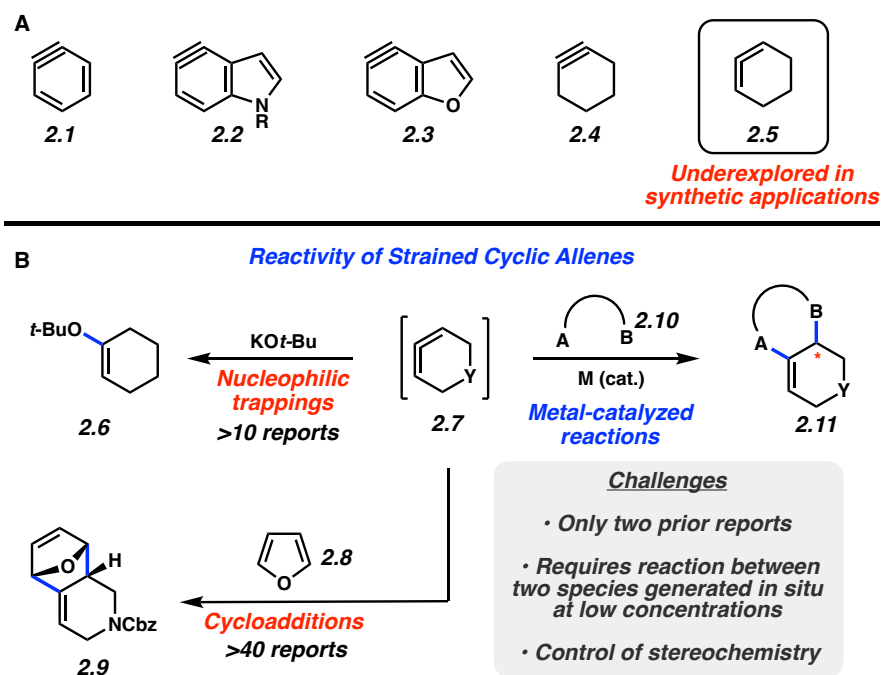
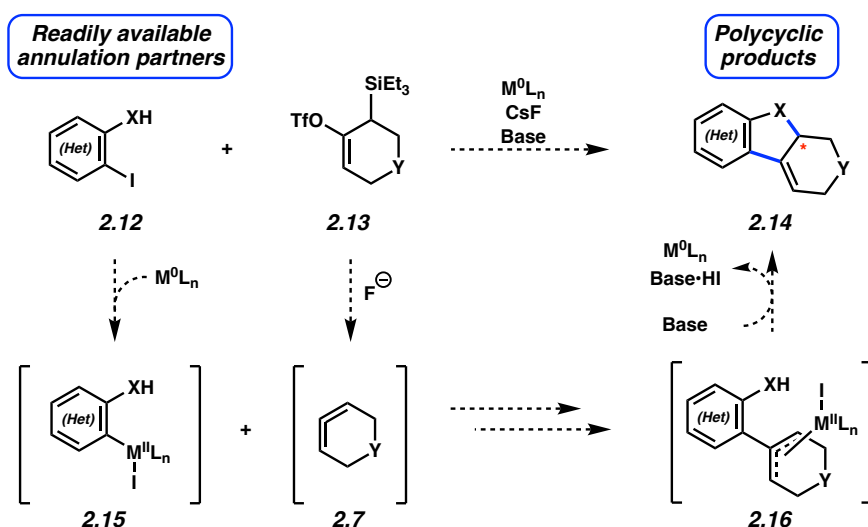


Figure 2.1. Selected in-situ-generated strained cyclic intermediates and overview of strained cyclic allene reactivity.

2.3 Reaction Design

With the aim of developing a modular new method for the metal-catalyzed interception of strained cyclic allenes, we designed the transformation depicted in Scheme 2.1.³⁴ We envisioned that bifunctional annulation partners **2.12** containing an aryl iodide and a pendant pronucleophile (XH) would first react with a transition metal catalyst, generating oxidative addition intermediate **2.15**. Concurrently, silyl triflate **2.13** would be converted to strained cyclic allene **2.7** via fluoride-

mediated desilylation. Cyclic allene **2.7** would then undergo migratory insertion into the Ar–M bond of **2.15**, ultimately giving rise to η^3 -coordinated complex **2.16**. Cyclization of the pendant pronucleophile would deliver tricycle **2.14** with regeneration of the catalyst. Herein, we demonstrate the successful implementation of this approach to annulate in-situ-generated cyclic allenes using Pd catalysis. An array of fused polycyclic products are obtained in synthetically useful yields by varying the cyclic allene precursor and the aryl halide substrate. Stereoselective examples are also demonstrated. These results highlight the value of merging transition metal catalysis with strained cyclic allene chemistry and should enable future reaction development in this emerging area.



Scheme 2.1. Envisioned reaction design.

2.4 Reaction Optimization

To validate our proposed reaction design, we studied the reaction of *o*-iodoaniline derivative **2.17** with silyl triflate **2.18** using fluoride-based conditions (Table 2.1). The conditions we had identified previously for the aforementioned Ni-catalyzed reaction of benzotriazinones with cyclic allenes³³ were deemed a suitable starting point for reaction discovery. Unfortunately, no desired product was observed with a $\text{Ni}(\text{cod})_2/\text{dppf}$ catalyst system, even at increased

temperature (entries 1 and 2). Given the widespread use of palladium in academic and industrial settings, along with its well-established competency in heteroannulation reactions,³⁴ we turned to Pd catalysis. We were gratified to observe that the use of a Pd catalyst enabled the desired reactivity, leading to tetrahydrocarbazole **2.19a**, albeit only in 8% yield (entry 3). Because unreacted silyl triflate **2.18** was observed under these conditions, we increased the loading of CsF. This led to a significant improvement in the yield, as shown in entry 4.³⁵ After evaluating other ligands (see Section 2.8.2.3 for details), we found that employing the bulky monophosphine Davephos was most effective,³⁶ generating **2.19a** in 71% yield (entry 5). Further optimization led to the use of DMF as solvent, Bu₄NOTf³⁷ as an additive, and a slight excess of silyl triflate **2.18**. Employing these conditions delivered **2.19a** in nearly quantitative yield after 1 h at 80 °C (entry 6).

Table 2.1. Reaction optimization.

Entry	Catalyst/Ligand	Solvent	Equiv. CsF	Temperature	Yield ^b
1 ^c	Ni(cod) ₂ /dppf	MeCN	2.5	35 °C	0%
2	Ni(cod) ₂ /dppf	MeCN	2.5	80 °C	0%
3	Pd(OAc) ₂ /dppf	MeCN	2.5	80 °C	8%
4	Pd(OAc) ₂ /dppf	MeCN	10	80 °C	51%
5	Pd(OAc) ₂ /Davephos	MeCN	10	80 °C	71%
6 ^d	Pd(OAc) ₂ /Davephos	DMF	10	80 °C	97%

^a Reaction conditions: **2.17** (1.0 equiv), **2.18** (1.0 equiv), catalyst (10 mol%), ligand (20 mol%), CsF (as shown), Na₂CO₃ (3 equiv), solvent (0.1 M), 3 h. ^b Yield determined by ¹H NMR analysis using 1,3,5-trimethoxybenzene as an external standard. ^c 24 h. ^d **2.18** (1.5 equiv), Bu₄NOTf (5.0 equiv), 1 h.

2.5 Scope of the Annulation Reaction

To assess the generality of this reaction, we tested a range of *o*-iodoaniline derivatives **2.20** and silyl triflates **2.13** (Figure 2.2). Although our conditions shown in Table 2.1, entry 6 were

generally useful, some modifications were made to obtain optimal yields based on empirical observations. Three different *N*-substituents were examined, namely tosyl (Ts), *t*-butyloxycarbonyl (Boc), and acetyl (Ac), with Ts providing the highest yield (90% of **2.19a**). Electronic and steric perturbations of the annulation partner were also tolerated, as evidenced by the formation of tetrahydrocarbazoles **2.22–2.30**. Of note, the annulation exhibits good functional group compatibility, leading to products bearing nitriles or esters (**2.26** and **2.27**), as well as aryl bromides, chlorides, or fluorides (**2.28–2.30**).³⁸ Given the importance of heterocycles in medicinal chemistry, we also assessed the compatibility of the reaction with heterocyclic annulation partners and heterocyclic allenes. Gratifyingly, an iodopyridyl annulation partner underwent the desired reaction to afford product **2.31** in excellent yield. The corresponding bromopyridine substrate could also be employed to give **2.31**, albeit in slightly diminished yield (78%).³⁹ Lastly, we varied silyl triflate **2.13** to enable further modulation of the product structure. Oxa- and aza-derivatives of **2.13**, readily available through known routes,^{30,31} were employed to furnish heterocycles **2.32** and **2.33**, respectively. This highlights the value of heterocyclic allenes in our methodology for the modular assembly of more complex heterocyclic products. Likewise, substituting a 7-membered cyclic allene precursor in place of a 6-membered cyclic allene precursor gave straightforward access to the 6-5-7 ring system seen in **2.34**.

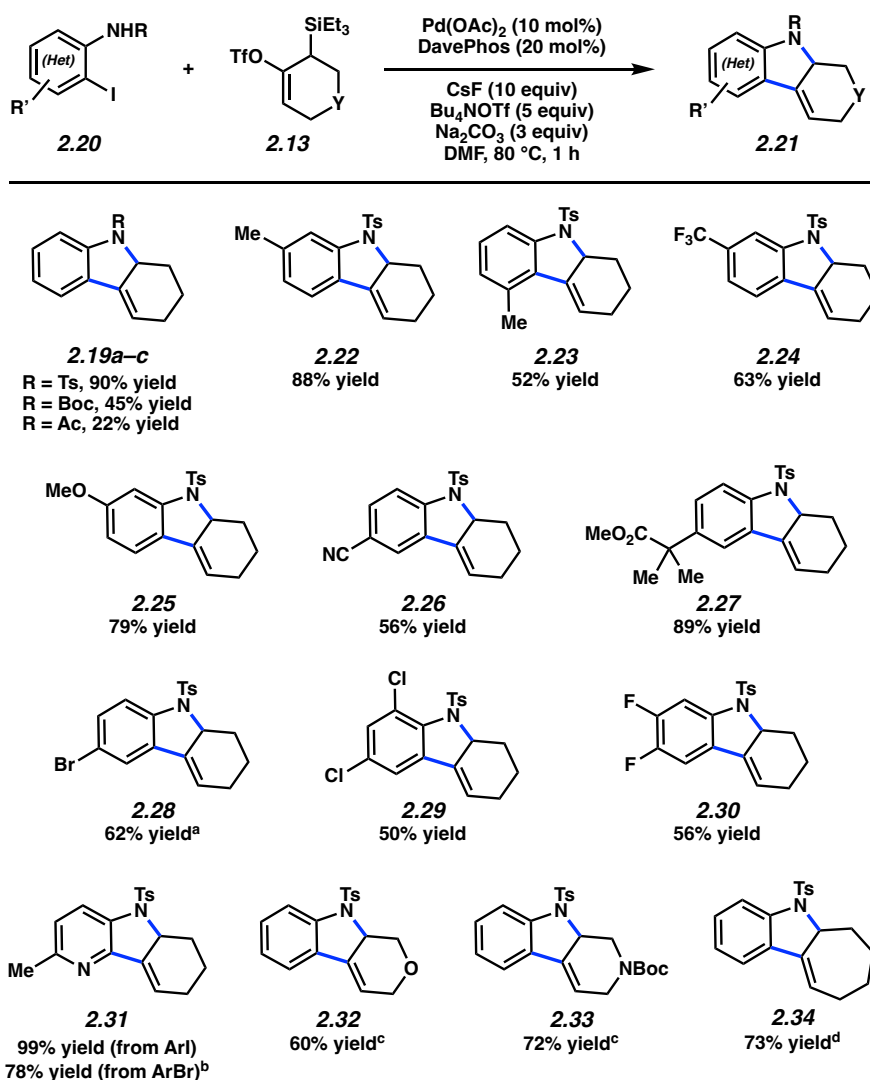


Figure 2.2. Scope of the annulation reaction with iodoaniline derivatives **2.20**. Reactions performed with **2.20** (1.0 equiv) and **2.13** (1.5 equiv). ^a Reaction was performed using 2-(*N,N*-dimethylaminomethyl)-1-diphenylphosphanylferrocene as ligand in MeCN at 60 °C for 3 h. ^b

ArX = 2-halo-6-methyl-3-*N*-tosylaminopyridine. ^c Reaction was performed using 2-(*N,N*-dimethylaminomethyl)-1-diphenylphosphanylferrocene as ligand with CsF (2.5 equiv) in MeCN at 60 °C for 24 h; performed in the absence of Bu₄NOTf. ^d A silyl tosylate was used as the allene precursor (see ref. 40).

We also questioned whether other pronucleophiles, beyond iodoaniline derivatives, could be employed in Pd-catalyzed reactions of strained cyclic allenes (Figure 2.3). With regard to oxygen nucleophiles, we found that benzyl alcohol **2.35** and benzoic acid **2.37** were successful in

delivering **2.36** and **2.38**, respectively, under our standard reaction conditions. Using modified conditions with Xantphos as the ligand, we found that amide **2.39** was a suitable *N*-pronucleophile, delivering **2.40** in 71% yield. Lastly, we tested the viability of a C-based pronucleophile by employing diester **2.41**. Using our standard reaction conditions, we obtained tetrahydrofluorene **2.42**, which bears a newly formed quaternary carbon. These examples underscore that the union of strained cyclic allenes and Pd catalysis provides a rapid entryway to the synthesis of structurally diverse polycyclic products, including 6-6-6 and 6-5-6 ring systems bearing ethers, lactones, amides, or all-carbon frameworks.

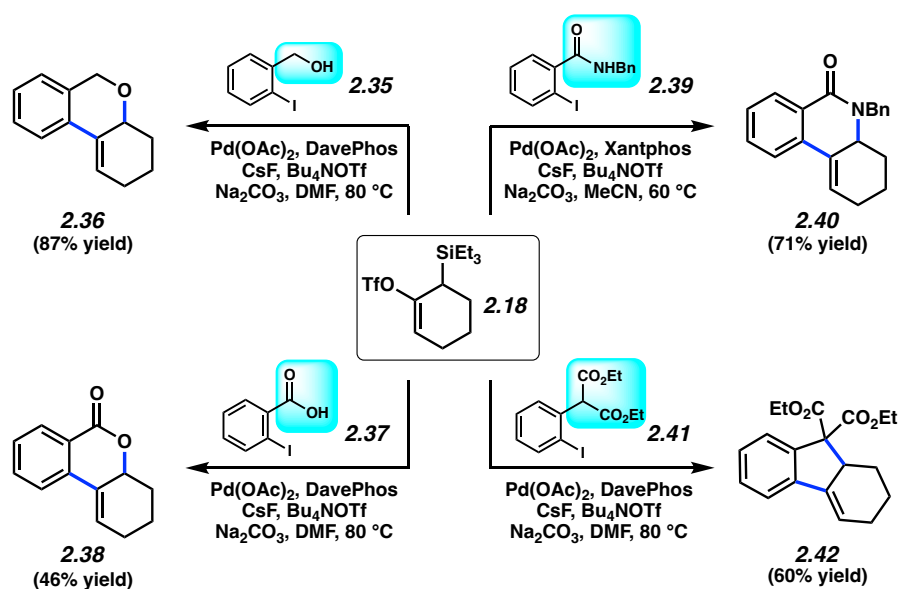


Figure 2.3. Variation of the pronucleophile to furnish structurally diverse products.

2.6 Development of Stereoselective Variants

The feasibility of diastereo- and enantioselective variants of the methodology was established as shown in Figure 2.4. In both cases, heterocyclic substrates were utilized to evaluate the strengths and limitations of the methodology, while providing access to polycyclic scaffolds.

Regarding the diastereoselective annulation, it should be noted that diastereoselective reactions of strained cyclic allenes have been reported in the context of cycloadditions,¹⁶ but there are no prior examples involving transition metal catalysis. Given our success in employing a benzylic alcohol (i.e., **2.35**, Figure 2.3), we prepared tertiary benzylic alcohol **2.43**. This substrate, rapidly accessed from a commercially available isatin precursor, was treated with 1,2-cyclohexadiene precursor **2.18** under standard annulation conditions. Tetracycle **2.44** was obtained as the major product, with d.r. = 5.6:1, thus providing the first example of substrate-guided stereocontrol in a metal-catalyzed reaction of cyclic allenes.⁴¹

To probe the feasibility of an enantioselective variant, we tested the reaction of iodopyridine **2.45** with silyl triflate **2.46** (Figure 2.4). Evaluation of chiral ligands led to the identification of Pd₂(dba)₃/Mandyphos as the optimal catalyst system. Moreover, with CH₂Cl₂ as solvent at decreased temperature (3 °C) (see Section 2.8.2.6 for extended optimization details), tricycle (–)-**2.47** was generated in 90% ee.⁴² As catalytic asymmetric reactions of in-situ-generated strained cyclic intermediates (i.e., arynes, cyclohexynes, cyclic allenes, etc.) are rare, we hope this result will promote further efforts in this area.

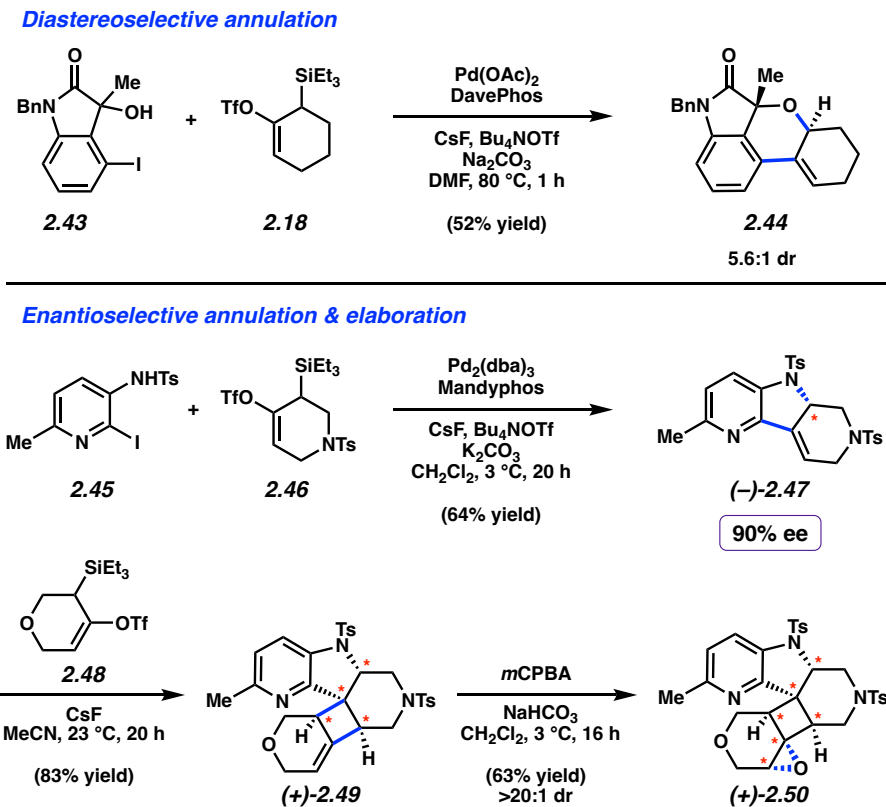


Figure 2.4. Stereocontrolled annulations and synthetic elaboration of an annulation product.

Finally, with unique polyheterocyclic product (–)-**2.47** in hand, we questioned if the styrenyl olefin present in the annulation products could be leveraged as a handle for further elaboration. (–)-**2.47** was subjected to oxacyclic allene precursor **2.48** in the presence of CsF to furnish (+)-**2.49** via a highly diastereoselective [2+2] cycloaddition. The olefin in (+)-**2.49**, newly introduced in the cyclic allene [2+2] reaction, then underwent diastereoselective epoxidation to furnish (+)-**2.50**. This short sequence leverages the asymmetric Pd-catalyzed annulation of an azacyclic allene to ultimately generate an enantioenriched hexacyclic compound (i.e., (+)-**2.50**) bearing five different fused heterocycles, a highly substituted cyclobutane, and six contiguous stereocenters, one of which is quaternary.

2.7 Conclusion

In summary, we have developed Pd-catalyzed annulations of in-situ-generated strained cyclic allenes. The methodology employs aryl halides and cyclic allene precursors as the reaction partners, ultimately forming two new bonds and generating an array of fused heterocyclic products. Moreover, through the syntheses of **2.44** and (–)-**2.47** (see Figure 2.4), we demonstrate stereoselective variants of this methodology. The catalytic asymmetric annulation and resulting swift access to hexacycle (+)-**2.50** highlight some of the opportunities afforded by the combination of strained intermediates and Pd catalysis. As this strategy represents a departure from the more common, historical modes of cyclic allene trapping using nucleophiles or cycloaddition partners, we hope this study will stimulate the future development of reactions that strategically merge transition metal catalysis and transient strained intermediate chemistry for the synthesis of complex scaffolds.

2.8 Experimental Section

2.8.1 Materials and Methods

Unless stated otherwise, reactions were conducted in flame-dried glassware under an atmosphere of nitrogen, and commercially obtained reagents were used as received unless otherwise specified. Anhydrous solvents were either freshly distilled or passed through activated alumina columns, unless otherwise stated. Non-commercially available substrates were synthesized according to known preparations or following protocols specified in the Experimental Procedures. Prior to use, acetonitrile, dimethylformamide (DMF), 1,2-dichloroethane (DCE), 1,2-dimethoxyethane (DME), and dichloromethane were passed through activated alumina columns and degassed by five freeze-pump-thaw cycles. *n*-Butyllithium (*n*-BuLi), *N*-(5-chloro-2-

pyridyl)bis(trifluoromethanesulfonamide) (Comins' Reagent), potassium *tert*-butoxide, potassium fluoride, tetrabutylammonium difluorotriphenylsilicate (TBAT), tetrabutylammonium fluoride monohydrate (TBAF•H₂O), sodium hydride (60 wt% in oil), 4-iodoindoline-2,3-dione (**2.72**), 2'-(dicyclohexylphosphino)-*N,N*-dimethyl-[1,1'-biphenyl]-2-amine (Davephos), sodium bicarbonate, *meta*-chloroperoxybenzoic acid (*m*CPBA), sodium *tert*-butoxide, allylpalladium chloride dimer ([Pd(allyl)Cl]₂), sodium acetate trihydrate, sodium bis(trimethylsilyl)amide (NaHMDS), methylmagnesium bromide (3.0 M in diethyl ether), benzyl bromide, and tris(dimethylamino)sulfonium difluorotrimethylsilicate (TASF) were obtained from Sigma-Aldrich. 1,4-diazabicyclo[2.2.2]octane (DABCO) and pyridine were obtained from Acros Organics. Triethylsilyl chloride, 4-toluenesulfonyl chloride (TsCl), 2-iodobenzyl alcohol (**2.35**), and 2-iodobenzoic acid (**2.37**) were obtained from Oakwood Chemical. 1,4,7,10,13,16-Hexaoxacyclooctadecane (18-crown-6) was obtained from Chem-Impex. Diisopropylamine was obtained from Alfa Aesar. Bis(1,5-cyclooctadiene)nickel(0) (Ni(cod)₂), 1,1'-bis(diphenylphosphino)ferrocene (dppf), cesium fluoride, palladium(II) acetate, bis(dibenzylideneacetone)palladium(0) (Pd(dba)₂), tris(dibenzylideneacetone)dipalladium(0) (Pd₂(dba)₃), palladium(II) chloride, and palladium(II) acetylacetonate (Pd(acac)₂) were obtained from Strem Chemicals. Tetrabutylammonium trifluoromethanesulfonate was obtained from TCI America. Potassium phosphate dibasic and potassium carbonate were obtained from Fisher Scientific. All ligands used for reaction optimization (Sections 2.8.2.3 and 2.8.2.6) were obtained from Strem Chemicals, TCI America, Sigma-Aldrich, or Solvias. All commercially available *o*-iodoanilines were obtained from Sigma-Aldrich, Enamine, or Combi-Blocks. Triethylsilyl chloride, pyridine, and diisopropylamine were distilled over CaH₂ prior to use. Na₂CO₃ and K₂CO₃ were dried in an oven heated to 120 °C for 48 h prior to use. Reaction temperatures at or above 23

°C were controlled using an IKA Mag temperature modulator, and unless stated otherwise, performed at room temperature (approximately 23 °C). Reactions conducted at 3 °C were performed in a refrigerator set to 3 °C and equipped with a stir plate. Thin-layer chromatography (TLC) was conducted with EMD gel 60 F₂₅₄ pre-coated plates (0.25 mm for analytical chromatography and 0.50 mm for preparative chromatography) and visualized using a combination of UV and potassium permanganate staining techniques. Silicycle Siliaflash P60 (particle size 40–63 μm) was used for flash column chromatography. ¹H-NMR and 2D-NOESY spectra were recorded on Bruker spectrometers (at 400, 500, and 600 MHz) and are reported relative to the residual solvent signal. Data for ¹H-NMR spectra are reported as follows: chemical shift (δ ppm), multiplicity, coupling constant (Hz) and integration. ¹³C-NMR spectra were recorded on Bruker spectrometers (at 100 and 125 MHz) and are reported relative to the residual solvent signal. Data for ¹³C-NMR spectra are reported in terms of chemical shift (δ ppm) and, when necessary, multiplicity, and coupling constant (Hz). ¹⁹F NMR spectra were recorded on Bruker spectrometers (at 376 MHz) and are reported in terms of chemical shift (δ ppm), multiplicity, coupling constant (Hz) and integration. IR spectra were recorded on a Perkin-Elmer UATR Two FT-IR spectrometer and are reported in terms of frequency absorption (cm⁻¹). DART-MS spectra were collected on a Thermo Exactive Plus MSD (Thermo Scientific) equipped with an ID-CUBE ion source and a Vapor Interface (IonSense Inc.). Both the source and MSD were controlled by Excalibur software version 3.0. The analyte was spotted onto OpenSpot sampling cards (IonSense Inc.) using CDCl₃ or CH₂Cl₂ as the solvent. Ionization was accomplished using UHP He plasma with no additional ionization agents. The mass calibration was carried out using Pierce LTQ Velos ESI (+) and (-) Ion calibration solutions (Thermo Fisher Scientific). Optical rotations were measured with a Rudolf Autopol III Automatic Polarimeter. Determination of

enantiopurity was carried out on a Mettler Toledo SFC (supercritical fluid chromatography) using a Daicel ChiralPak AD-H column. Data for SFC chromatograms are reported in enantiomeric excess (ee).

Aniline derivatives **2.17**⁴³, **2.57**⁴⁴, **2.79**⁴⁵, **2.80**⁴⁶, **2.81**⁴⁷, **2.82**⁴⁸, and **2.83**⁴⁹, benzamide **2.39**⁵⁰, diester **2.41**⁵¹, bromoketone **2.74**⁵², ferrocenyl ligands **2.78**⁵³ and **2.87**⁵⁴, and allene precursors **2.18**²⁹, **2.48**³¹, **2.84**³³, and **2.85**³² are all known compounds. The ¹H NMR spectral data matched those reported in literature.

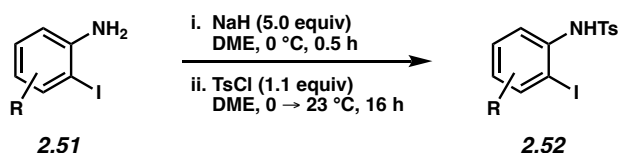
2.8.2 Experimental Procedures

2.8.2.1 Syntheses of Annulation Partners

2.8.2.1.1 Syntheses of *N*-Tosyl-Arylamines

Annulation partners **2.45**, **2.56**, **2.58**, **2.60**, **2.62**, **2.64**, **2.66**, **2.69**, and **2.71** were synthesized from the corresponding amines using the general procedures shown below.

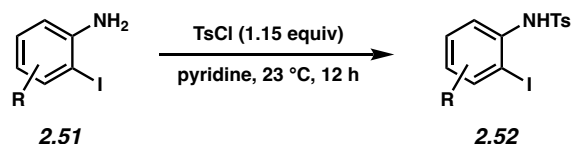
General Procedure 2.1 for the synthesis of *N*-tosyl-iodoanilines:



***N*-tosyl-iodoanilines 2.52.** To a solution of NaH (60 wt%, 5.0 equiv) in DME (5.8 M) at 0 °C was added iodoaniline **2.51** (1.0 equiv) in DME (1.2 M) dropwise over 2 min. The mixture was stirred at this temperature for 30 min prior to the rapid dropwise addition of TsCl (1.1 equiv) in DME (1.3 M) over 2 min. The resulting mixture was gradually warmed to 23 °C over 16 h then quenched by the addition of 1 M HCl (10 mL). The resulting mixture was extracted with EtOAc (3 x 15 mL).

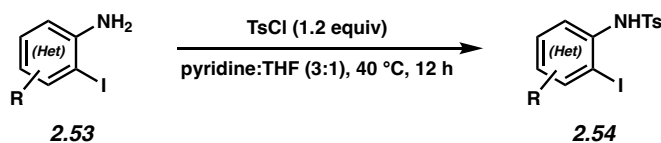
The combined organic layers were dried with Na₂SO₄, filtered, and concentrated under reduced pressure. The crude material was purified by flash column chromatography to provide *N*-tosyl-iodoaniline **2.52**.

General Procedure 2.2 for the synthesis of *N*-tosyl-iodoanilines:



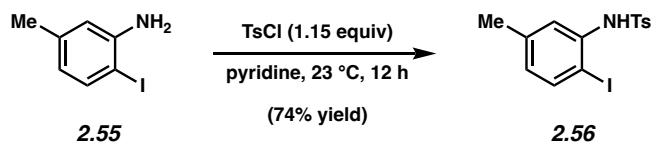
***N*-tosyl-iodoanilines 2.52.** Iodoaniline **2.51** (1.0 equiv) and TsCl (1.15 equiv) were dissolved in pyridine (0.4 M) at 23 °C, and the resulting mixture was stirred at this temperature for 12 h. The reaction was quenched by the addition of 1 M HCl (20 mL). The resulting mixture was extracted with EtOAc (3 x 20 mL), and the combined organic layers were then washed with water (2 x 20 mL) and saturated aqueous NaHCO₃ (20 mL). The combined organic layers were dried with Na₂SO₄, filtered, and concentrated under reduced pressure. The crude material was purified by flash column chromatography to provide *N*-tosyl-iodoaniline **2.52**.

General Procedure 2.3 for the synthesis of *N*-tosyl-arylamines:

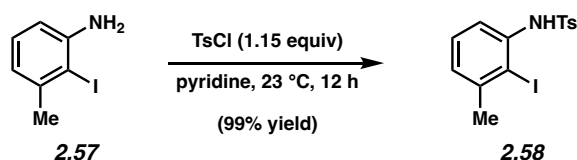


***N*-tosyl-arylamines 2.54.** Iodoamine **2.53** (1.0 equiv) and TsCl (1.2 equiv) were dissolved in a mixture of pyridine and THF (3:1, 0.41 M), and the resulting mixture was stirred at 40 °C in a sealed vial for 12 h, leading to the formation of a white precipitate. After 12 h, the solvent was removed under reduced pressure, and the crude residue was redissolved in EtOAc (10 mL) then washed with water (2 x 10 mL). The organic layer was dried with Na₂SO₄, filtered, and

concentrated under reduced pressure. The crude material was purified by flash column chromatography to provide *N*-tosyl-arylamine **2.54**.

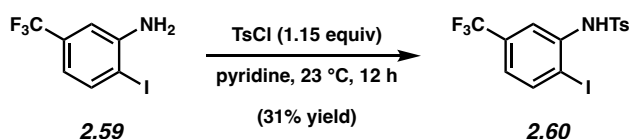


***N*-tosyl-iodoaniline 2.56.** Followed General Procedure 2.2 using **2.55** (250 mg, 1.07 mmol). Purification by flash column chromatography (9:1 hexanes:EtOAc) provided *N*-tosyl-iodoaniline **2.56** (317 mg, 74% yield) as a white solid. ***N*-tosyl-iodoaniline 2.56:** Mp: 120 °C; R_f 0.27 (9:1 hexanes:EtOAc); ^1H NMR (400 MHz, CDCl_3): δ 7.62 (d, $J = 8.3$, 2H), 7.49 (d, $J = 1.8$, 1H), 7.48 (d, $J = 8.2$, 1H), 7.21 (d, $J = 8.0$, 2H), 6.71 (br s, 1H), 6.65 (ddd, $J = 8.1$, 2.0, 0.6, 1H), 2.38 (s, 3H), 2.30 (s, 3H); ^{13}C NMR (100 MHz, CDCl_3): δ 144.2, 140.0, 138.6, 137.2, 136.0, 129.6, 128.0, 127.5, 123.4, 88.4, 21.6, 21.2; IR (film): 3244, 2917, 1475, 1336, 1161 cm^{-1} ; HRMS-APCI (m/z) [$M + H$] $^+$ calcd for $\text{C}_{14}\text{H}_{15}\text{INO}_2\text{S}^+$, 387.98627; found 387.98386.

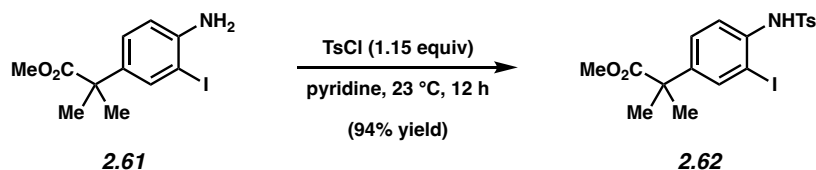


***N*-tosyl-iodoaniline 2.58.** Followed General Procedure 2.2 using **2.57** (532 mg, 2.28 mmol). Purification by flash column chromatography (2:1 benzene:hexanes) provided *N*-tosyl-iodoaniline **2.58** (883 mg, 99% yield) as a white solid. ***N*-tosyl-iodoaniline 2.58:** Mp: 95–96 °C; R_f 0.61 (9:1 benzene:Et₂O); ^1H NMR (500 MHz, CDCl_3): δ 7.65 (d, $J = 8.3$, 2H), 7.45 (d, $J = 8.4$, 1H), 7.19 (d, $J = 8.4$, 2H), 7.15 (t, $J = 8.0$, 1H), 7.04 (br s, 1H), 6.96 (d, $J = 8.0$, 1H), 2.36 (s, 3H), 2.35 (s,

3H); ^{13}C NMR (100 MHz, CDCl_3): δ 144.1, 142.9, 137.7, 136.0, 129.6, 128.7, 127.5, 126.5, 119.1, 99.5, 29.7, 21.6; IR (film): 3302, 2949, 1459, 1374, 1159 cm^{-1} ; HRMS-APCI (m/z) $[\text{M} - \text{H}]^-$ calcd for $\text{C}_{14}\text{H}_{13}\text{INO}_2\text{S}^-$, 385.97062; found 385.97246.

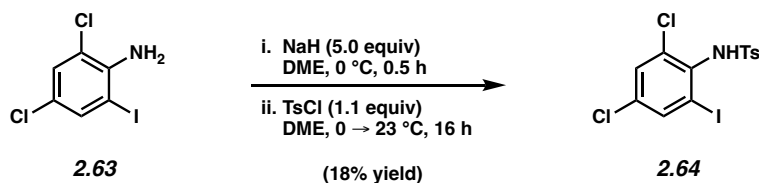


***N*-tosyl-iodoaniline 2.60.** Followed General Procedure 2.2 using **2.59** (300 mg, 1.05 mmol). Purification by flash column chromatography (9:1 hexanes:EtOAc) provided *N*-tosyl-iodoaniline **2.60** (48 mg, 31% yield) as an off-white solid. ***N*-tosyl-iodoaniline 2.60:** Mp: 171 °C; R_f 0.11 (9:1 hexanes:EtOAc); ^1H NMR (400 MHz, CDCl_3): δ 7.88 (d, $J = 1.8$, 1H), 7.78 (d, $J = 8.2$, 1H), 7.66 (d, $J = 8.3$, 2H), 7.24 (d, $J = 8.1$, 2H), 7.05 (ddd, $J = 8.3$, 2.1, 0.6, 1H), 6.94 (br s, 1H), 2.39 (s, 3H); ^{13}C NMR (125 MHz, CDCl_3): δ 144.8, 139.7, 138.4, 135.5, 132.1 (q, $J = 33.3$), 129.9, 127.5, 123.3 (q, $J = 272.6$), 122.8 (q, $J = 3.8$), 118.2 (q, $J = 3.8$), 95.7 (q, $J = 1.4$), 21.6; ^{19}F NMR (376 MHz, CDCl_3) δ -63.11 (s, 3F); IR (film): 3247, 1388, 1325, 1169, 1118 cm^{-1} ; HRMS-APCI (m/z) $[\text{M} + \text{H}]^+$ calcd for $\text{C}_{14}\text{H}_{12}\text{F}_3\text{INO}_2\text{S}^+$, 441.95800; found 441.95871.

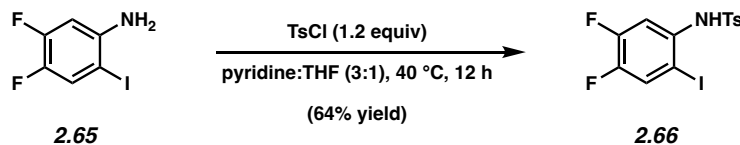


***N*-tosyl-iodoaniline 2.62.** Followed General Procedure 2.2 using **2.61** (100 mg, 0.313 mmol). Purification by flash column chromatography (5:1 hexanes:EtOAc) afforded *N*-tosyl-iodoaniline **2.62** (140 mg, 94% yield) as an off-white solid. ***N*-tosyl-iodoaniline 2.62:** Mp: 85–86 °C; R_f 0.42 (9:1 benzene:Et₂O); ^1H NMR (500 MHz, MeOD): δ 6.11 (d, $J = 2.0$, 1H), 6.04 (d, $J = 8.3$, 2H),

5.76–5.72 (m, 4H), 2.07 (s, 3H), 1.74 (br s, 1H), 0.83 (s, 3H), 0.07 (s, 6H); ^{13}C NMR (125 MHz, MeOD): δ 176.6, 144.6, 143.9, 137.4, 137.0, 136.7, 129.3, 127.2, 126.3, 126.0, 95.2, 51.5, 45.7, 25.4, 20.1; IR (film): 3267, 2950, 1728, 1336, 1161 cm^{-1} ; HRMS-APCI (m/z) $[\text{M} - \text{H}]^-$ calcd for $\text{C}_{18}\text{H}_{19}\text{INO}_4\text{S}^-$, 472.00740; found 472.00946.

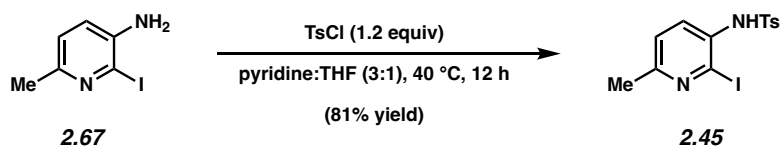


***N*-tosyl-iodoaniline 2.64.** Followed General Procedure 2.1 using **2.63** (100 mg, 0.347 mmol). Purification by flash column chromatography (benzene) provided *N*-tosyl-iodoaniline **2.64** (28 mg, 18% yield) as an off-white solid. ***N*-tosyl-iodoaniline 2.64:** Mp: 181 °C; R_f 0.24 (5:1 hexanes:EtOAc); ^1H NMR (500 MHz, CDCl_3): δ 7.78 (d, $J = 2.4$, 1H), 7.68 (d, $J = 8.3$, 2H), 7.39 (d, $J = 2.4$, 1H), 7.29 (d, $J = 8.3$, 2H), 6.28 (s, 1H), 2.44 (s, 3H); ^{13}C NMR (125 MHz, CDCl_3): δ 144.4, 138.3, 137.6, 134.7, 134.5, 133.9, 130.4, 129.7, 127.8, 101.2, 21.7; IR (film): 3252, 2923, 1436, 1336, 1162 cm^{-1} ; HRMS-APCI (m/z) $[\text{M} - \text{H}]^-$ calcd for $\text{C}_{13}\text{H}_9\text{Cl}_2\text{INO}_2\text{S}^-$, 439.87702; found 439.87871.



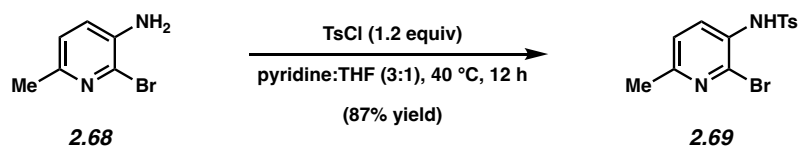
***N*-tosyl-iodoaniline 2.66.** Followed General Procedure 2.3 using **2.65** (100 mg, 0.392 mmol). Purification by flash column chromatography (9:1 hexanes:EtOAc \rightarrow 5:1 hexanes:EtOAc) provided *N*-tosyl-iodoaniline **2.66** (102 mg, 64% yield) as a white solid. ***N*-tosyl-iodoaniline 2.66:**

Mp: 131–133 °C; R_f 0.56 (9:1 benzene:Et₂O); ¹H NMR (500 MHz, MeOD): δ 6.11 (dd, J = 9.5, 8.7, 1H), 6.03 (d, J = 8.5, 2H), 5.78–5.73 (m, 3H), 0.84 (s, 3H); ¹³C NMR (125 MHz, MeOD): δ 149.8 (dd, J = 248.5, 13.2), 147.1 (dd, J = 251.7, 13.1), 144.1, 137.0, 135.6 (dd, J = 8.5, 3.8), 129.4, 127.2, 127.1 (d, J = 19.6), 115.4 (d, J = 20.2), 88.0 (dd, J = 6.2, 4.1), 20.1; IR (film): 3268, 3063, 1598, 1493, 1340 cm⁻¹; HRMS-APCI (m/z) [$M - H$]⁻ calcd for C₁₃H₉F₂INO₂S⁻, 407.93613; found 407.93727.



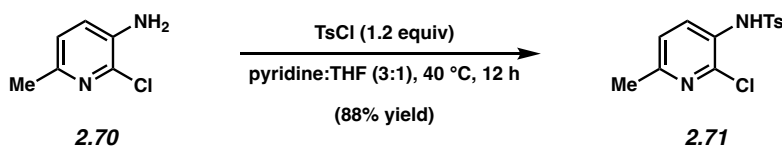
***N*-tosyl-aminopyridine 2.45.** Followed General Procedure 2.3 using **2.67** (175 mg, 0.748 mmol). Purification by flash column chromatography (98:2 benzene:Et₃N → 80:20:2 benzene:acetone:Et₃N) provided *N*-tosyl-aminopyridine **2.45** (235 mg, 81% yield) as a white solid.

***N*-tosyl-aminopyridine 2.45:** Mp: 121–123 °C; R_f 0.68 (1:1 CHCl₃:Et₂O); ¹H NMR (500 MHz, CDCl₃): δ 7.77 (d, J = 8.2, 1H), 7.60 (d, J = 8.3, 2H), 7.23 (d, J = 8.4, 2H), 7.06 (d, J = 8.2, 1H), 6.71 (br s, 1H), 2.46 (s, 3H), 2.39 (s, 3H); ¹³C NMR (125 MHz, CDCl₃): δ 157.2, 144.7, 135.5, 133.3, 130.1, 129.9, 127.4, 123.3, 116.4, 23.5, 21.6; IR (film): 3269, 2970, 1739, 1454, 1315 cm⁻¹; HRMS-APCI (m/z) [$M + H$]⁺ calcd for C₁₃H₁₄IN₂O₂S⁺, 388.98152; found 388.98140.



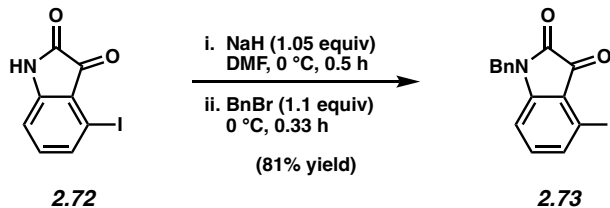
***N*-tosyl-aminopyridine 2.69.** Followed General Procedure 2.3 using **2.68** (200 mg, 1.07 mmol). Purification by flash column chromatography (98:2 benzene:Et₃N → 80:20:2

benzene:acetone:Et₃N) provided *N*-tosyl-aminopyridine **2.69** (316 mg, 87% yield) as a white solid. *N*-tosyl-aminopyridine **2.69**: Mp: 127 °C; R_f 0.68 (1:1 CHCl₃:Et₂O); ¹H NMR (500 MHz, CDCl₃): δ 7.85 (d, *J* = 8.9, 1H), 7.63–7.59 (m, 2H), 7.22 (d, *J* = 8.5, 2H), 7.08 (d, *J* = 8.4, 1H), 6.88 (br s, 1H), 2.45 (s, 3H), 2.37 (s, 3H); ¹³C NMR (125 MHz, CDCl₃): δ 156.1, 144.7, 135.5, 135.0, 131.1, 129.91, 129.88, 127.3, 123.3, 23.5, 21.6; IR (film): 3259, 2924, 1458, 1317, 1161 cm⁻¹; HRMS-APCI (*m/z*) [M + H]⁺ calcd for C₁₃H₁₄BrN₂O₂S⁺, 340.99539; found 340.99548.

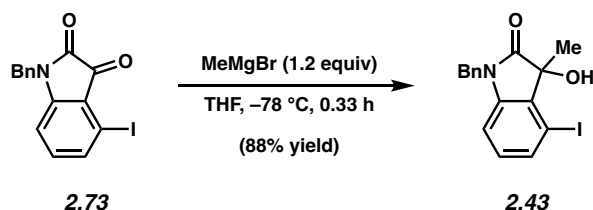


N-tosyl-aminopyridine **2.71**. Followed General Procedure 2.3 using **2.70** (200 mg, 1.40 mmol). Purification by flash column chromatography (98:2 benzene:Et₃N → 80:20:2 benzene:acetone:Et₃N) provided *N*-tosyl-aminopyridine **2.71** (368 mg, 88% yield) as a beige solid. *N*-tosyl-aminopyridine **2.71**: Mp: 125–128 °C; R_f 0.62 (1:1 CHCl₃:Et₂O); ¹H NMR (500 MHz, CDCl₃): δ 7.88 (d, *J* = 8.1, 1H), 7.62 (d, *J* = 8.3, 2H), 7.22 (d, *J* = 8.3, 2H), 7.06 (d, *J* = 8.2, 1H), 6.93 (br s, 1H), 2.43 (s, 3H), 2.36 (s, 3H); ¹³C NMR (125 MHz, CDCl₃): δ 155.5, 144.6, 141.7, 135.6, 131.5, 129.9, 128.0, 127.2, 123.0, 23.5, 21.6; IR (film): 3257, 1739, 1597, 1463, 1320 cm⁻¹; HRMS-APCI (*m/z*) [M + H]⁺ calcd for C₁₃H₁₄ClN₂O₂S⁺, 297.04590; found 297.04601.

2.8.2.1.2 Synthesis of Alcohol 2.43

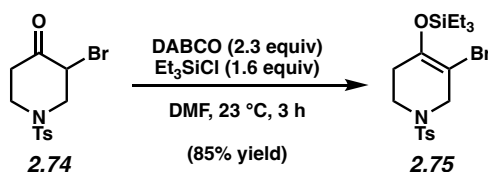


Isatin 2.73. To a solution of NaH (washed with hexanes, 46.1 mg, 1.92 mmol, 1.05 equiv) in DMF (2.5 mL) at 0 °C was added isatin **2.72** (500 mg, 1.83 mmol, 1.00 equiv) in DMF (2.5 mL) dropwise over 2 min, giving a deep purple solution. The reaction was stirred at 0 °C for 30 min followed by the dropwise addition of BnBr (240 μ L, 2.01 mmol, 1.10 equiv) over 2 min. The reaction was stirred for an additional 20 min at this temperature, then water (10 mL) was added in a single portion to precipitate the product. The resulting suspension was filtered, and the solid was washed with water (3 x 10 mL) then collected. The slightly wet solid was then dissolved in benzene (10 mL) and concentrated under reduced pressure. This process of dissolution and concentration was repeated twice more to provide isatin **2.73** (536 mg, 81% yield) as an orange solid. **Isatin 2.73:** Mp: 161 °C; R_f 0.43 (2:1 Hexanes:EtOAc); $^1\text{H NMR}$ (500 MHz, CDCl_3): δ 7.52 (dd, $J = 8.0, 0.5$, 1H), 7.36–7.28 (m, 5H), 7.10 (t, $J = 8.0$, 1H), 6.75 (dd, $J = 8.0, 0.5$, 1H), 4.93 (s, 2H); $^{13}\text{C NMR}$ (125 MHz, CDCl_3): δ 181.5, 157.4, 152.6, 138.0, 135.1, 134.2, 129.1, 128.3, 127.4, 119.3, 110.5, 92.9, 43.8; IR (film): 3063, 1735, 1594, 1445, 1328 cm^{-1} ; HRMS-APCI (m/z) $[\text{M} + \text{H}]^+$ calcd for $\text{C}_{15}\text{H}_{11}\text{INO}_2^+$, 363.98290; found 363.98161.



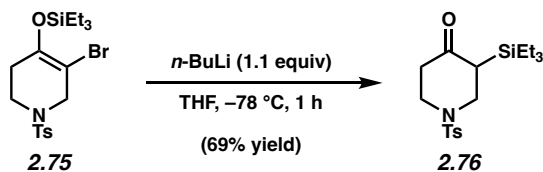
Alcohol 2.43. A solution of isatin **2.73** (250 mg, 0.688 mmol, 1.0 equiv) in THF (3.44 mL, 0.20 M) was cooled to $-78\text{ }^\circ\text{C}$. MeMgBr (299 μL , 2.76 M in THF, 0.826 mmol, 1.2 equiv) was added dropwise over 2 min, and the solution was stirred at $-78\text{ }^\circ\text{C}$ for 20 min. The reaction mixture was then quenched with a saturated aqueous solution of NH_4Cl (10 mL) and extracted with EtOAc (3 x 10 mL). The organic layers were combined, dried over Na_2SO_4 , filtered, and concentrated to afford the crude residue. Purification by flash column chromatography (9:1 benzene:Et₂O) afforded alcohol **2.43** (231 mg, 88% yield) as a light yellow solid. **Alcohol 2.43:** Mp: $148\text{ }^\circ\text{C}$; R_f 0.10 (9:1 benzene:Et₂O); ¹H NMR (500 MHz, CDCl₃): δ 7.44 (d, $J = 8.0$, 1H), 7.34–7.23 (m, 5H), 6.89 (t, $J = 8.0$, 1H), 6.68 (d, $J = 8.0$, 1H), 4.96 (d, $J = 15.6$, 1H), 4.80 (d, $J = 15.6$, 1H), 2.85 (s, 1H), 1.81 (s, 3H); ¹³C NMR (125 MHz, CDCl₃): δ 177.7, 143.7, 135.0, 133.6, 132.3, 130.8, 129.0, 127.9, 127.1, 109.4, 90.3, 75.6, 43.6, 22.7; IR (film): 3394, 2925, 1710, 1600, 1577 cm^{-1} ; HRMS-APCI (m/z) [$M - \text{HI} + \text{OH}$]⁻ calcd for C₁₆H₁₄NO₃⁻, 268.09682; found 268.09778.

2.8.2.2 Synthesis of Silyl Triflate 2.46



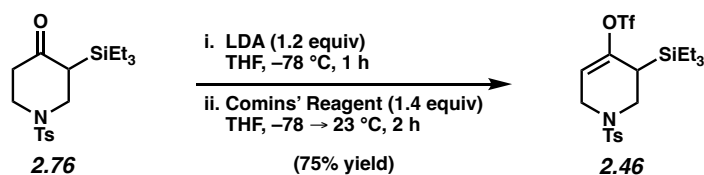
Silyl enol ether 2.75. To a solution of bromoketone **2.74** (1.40 g, 4.21 mmol, 1.0 equiv) in DMF (3.80 mL, 1.10 M) was added Et₃SiCl (1.14 mL, 6.74 mmol, 1.6 equiv) and DABCO (1.09 g, 9.69 mmol, 2.3 equiv) sequentially, and the resulting heterogeneous mixture was allowed to stir at $23\text{ }^\circ\text{C}$

for 3 h. The reaction was then quenched with saturated aqueous NaHCO₃ (20 mL) and diluted with water (20 mL). The resulting mixture was extracted with EtOAc (3 x 10 mL). The combined organic layers were washed sequentially with water (2 x 15 mL) and brine (1 x 15 mL), dried with Na₂SO₄, filtered, and concentrated under reduced pressure to provide the crude silyl enol ether as a colorless oil. The crude product was purified by flash column chromatography (19:1 hexanes:EtOAc) to provide silyl enol ether **2.75** (1.60 g, 85% yield) as a colorless oil. **Silyl enol ether 2.75**: R_f 0.23 (9:1 hexanes:EtOAc); ¹H NMR (400 MHz, CDCl₃): δ 7.67 (d, *J* = 8.4, 2H), 7.33 (d, *J* = 8.0, 2H), 3.81 (t, *J* = 2.1, 2H), 3.30 (t, *J* = 5.8, 2H), 2.43 (s, 3H), 2.30–2.26 (m, 2H), 0.96 (t, *J* = 8.5, 9H), 0.65 (q, *J* = 7.5, 6H); ¹³C NMR (100 MHz, CDCl₃): δ 145.4, 143.9, 133.7, 129.9, 127.6, 95.1, 50.1, 43.3, 31.3, 21.6, 6.6, 5.5; IR (film): 2955, 2876, 1972, 1340, 1163 cm⁻¹; HRMS-APCI (*m/z*) [M + H]⁺ calcd for C₁₈H₂₉BrNO₃SSi⁺, 446.08153; found 446.08015.



Silyl ketone 2.76. To a solution of silyl enol ether **2.75** (1.60 g, 3.57 mmol, 1.0 equiv) in THF (42 mL, 0.085 M) at -78 °C was added *n*-BuLi (2.63 M in hexanes, 1.50 mL, 3.93 mmol, 1.1 equiv) dropwise over 5 min. After stirring for 1 h at -78 °C, the reaction was quenched with saturated aqueous NaHCO₃ (25 mL) and allowed to warm to 23 °C. The mixture was extracted with EtOAc (3 x 25 mL). The combined organic layers were then dried over Na₂SO₄, filtered, and concentrated under reduced pressure. The resulting crude oil was purified by flash column chromatography (9:1 hexanes:EtOAc) to afford silyl ketone **2.76** (0.91 g, 69% yield) as a colorless oil. **Silyl Ketone 2.76**: R_f 0.28 (4:1 hexanes:EtOAc); ¹H NMR (400 MHz, CDCl₃): δ 7.63 (d, *J* = 8.2, 2H), 7.32 (d,

$J = 8.2, 2\text{H}$), 3.87–3.82 (m, 1H), 3.79 (dt, $J = 11.6, 2.7, 1\text{H}$), 2.90 (dd, $J = 11.8, 5.1, 1\text{H}$), 2.68 (td, 11.5, 4.1, 1H), 2.59–2.50 (m, 1H), 2.41 (s, 3H), 2.40–2.35 (m, 2H), 0.97 (t, $J = 8.1, 9\text{H}$), 0.72 (qd, $J = 7.4, 2.1, 6\text{H}$); ^{13}C NMR (100 MHz, CDCl_3): δ 206.6, 144.0, 132.7, 129.8, 127.7, 46.4, 45.4, 42.4, 40.1, 21.5, 7.3, 2.9; IR (film): 2954, 2876, 1688, 1361, 1163 cm^{-1} ; HRMS-APCI (m/z) [$\text{M} + \text{H}$] $^+$ calcd for $\text{C}_{18}\text{H}_{30}\text{NO}_3\text{SSi}^+$, 368.17102; found 368.16943.



Silyl triflate 2.46. To a solution of diisopropylamine (0.40 mL, 2.80 mmol, 1.25 equiv) in THF (4.0 mL) at $-78\text{ }^\circ\text{C}$ was added *n*-BuLi (2.63 M in hexanes, 1.02 mL, 2.69 mmol, 1.20 equiv) dropwise over 2 min. The reaction was stirred at $-78\text{ }^\circ\text{C}$ for 30 min, warmed to $23\text{ }^\circ\text{C}$ over 15 min, then re-cooled to $-78\text{ }^\circ\text{C}$ over 15 min. A solution of silyl ketone **2.76** (824 mg, 2.24 mmol, 1.00 equiv) in THF (4.0 mL) was then added dropwise over 3 min. The mixture was stirred at $-78\text{ }^\circ\text{C}$ for 1 h followed by the dropwise addition of Comins' Reagent (1.23 g, 3.14 mmol, 1.40 equiv) in THF (4.0 mL) over 3 min. The resulting mixture was stirred for 10 min at $-78\text{ }^\circ\text{C}$ before being warmed to $23\text{ }^\circ\text{C}$. After stirring for an additional 2 h at this temperature, the reaction mixture was quenched by the addition of saturated aqueous NaHCO_3 (20 mL), and the layers were separated. The aqueous layer was extracted with Et_2O (3 x 20 mL), and the combined organic layers were dried over Na_2SO_4 , filtered, and concentrated under reduced pressure. The resulting crude oil was purified by flash column chromatography (3:1 hexanes:benzene \rightarrow 1:1 hexanes:benzene) to give silyl triflate **2.46** (531 mg, 75% yield) as a colorless oil which solidified on standing at $-20\text{ }^\circ\text{C}$.

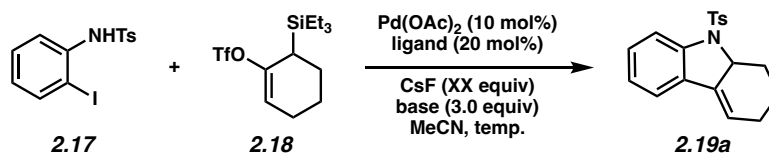
Silyl triflate 2.46: Mp: $36\text{ }^\circ\text{C}$; R_f 0.82 (9:1 benzene: Et_2O); ^1H NMR (500 MHz, CDCl_3): δ 7.68–

7.63 (m, 2H), 7.36–7.32 (m, 2H), 5.56–5.52 (m, 1H), 3.94 (ddd, $J = 16.4, 3.6, 2.3$, 1H), 3.67 (dd, $J = 11.8, 3.6$, 1H), 3.41 (dt, $J = 16.4, 3.1$, 1H), 2.99 (dd, $J = 11.8, 4.5$, 1H), 2.44 (s, 3H), 2.08–2.03 (m, 1H), 0.99 (t, $J = 8.1$, 9H), 0.78–0.72 (m, 6H); ^{13}C NMR (125 MHz, CDCl_3): δ 150.4, 144.2, 132.4, 129.9, 127.7, 118.4 (q, $J = 320.7$), 110.0, 45.2, 43.7, 28.0, 21.6, 7.2, 2.7; IR (film): 2957, 2914, 1419, 1210, 1168 cm^{-1} ; HRMS-APCI (m/z) $[\text{M} + \text{H}]^+$ calcd for $\text{C}_{19}\text{H}_{29}\text{F}_3\text{NO}_5\text{S}_2\text{Si}^+$, 533.09573; found 533.09737.

2.8.2.3 Optimization of the Racemic Annulation

Results from the optimization of the reaction between **2.17** and **2.18** appear below. Temperature, base, CsF loading, and ligand were varied using General Procedure 2.4, and results appear below in Tables 2.2, 2.3, 2.4, and 2.5 respectively.

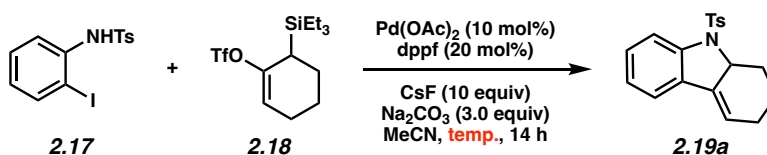
General Procedure 2.4 for the optimization of the racemic annulation:



Annulation Product 2.19a. A 1-dram vial containing a magnetic stir bar was charged with iodoaniline **2.17** (11.3 mg, 0.03 mmol, 1.0 equiv). A separate 1-dram vial was charged with silyl triflate **2.18** (10.3 mg, 0.03 mmol, 1.0 equiv). A third 1-dram vial was charged with Pd(OAc)₂ (0.674 mg, 0.003 mmol, 10 mol%). All three vials were taken into a glovebox where the ligand (0.006 mmol, 20 mol%), the base (0.09 mmol, 3.0 equiv), and CsF were added to the vial containing iodoaniline **2.17**. The vial containing the Pd(OAc)₂ and the vial containing silyl triflate **2.18** were then each treated with an aliquot of solvent (0.20 mL each) and agitated vigorously to ensure full dissolution. The solution of Pd(OAc)₂ and the solution of silyl triflate were then

transferred sequentially to the reaction vial containing iodoaniline **2.17**, and the vial was sealed with a Teflon-lined cap, removed from the glovebox, and stirred for 3 h at the desired reaction temperature. The mixture was then filtered through a pad of silica gel, eluting with EtOAc (10 mL). The eluate was concentrated to provide a crude residue, which was analyzed by ¹H NMR using 1,3,5-trimethoxybenzene an external standard.

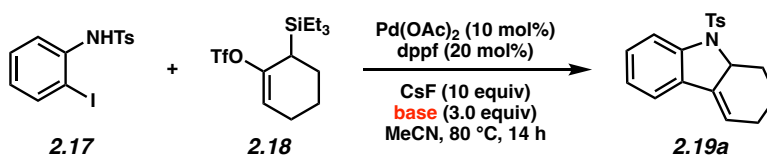
Table 2.2. Temperature screening results.



Entry	Temperature (°C)	¹ H NMR Yield ^a
1	35	35%
2	50	49%
3	65	49%
4	80	53%

^a ¹H NMR yield determined using 1,3,5-trimethoxybenzene as an external standard.

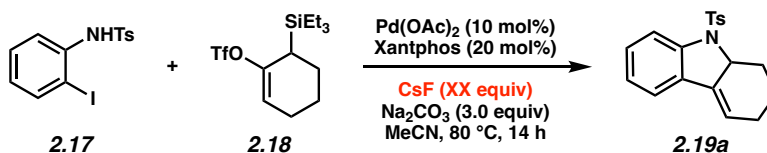
Table 2.3. Base screening results.



Entry	Base	¹ H NMR Yield ^a
1	Na ₂ CO ₃	53%
2	Et ₃ N	46%
3	NaOtBu	0%

^a ¹H NMR yield determined using 1,3,5-trimethoxybenzene as an external standard.

Table 2.4. CsF loading screening results.

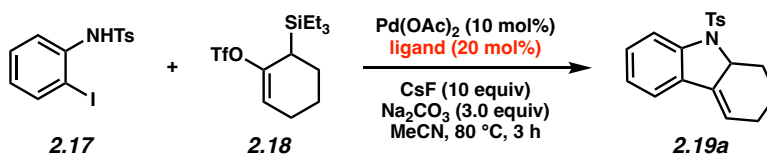


Entry	Equiv. CsF	¹ H NMR Yield ^a
-------	------------	---------------------------------------

1	2.5	11%
2	5	39%
3	7.5	45%
4	10	56%

^a ¹H NMR yield determined using 1,3,5-trimethoxybenzene as an external standard.

Table 2.5. Ligand screening results.



Entry	Ligand	¹ H NMR Yield ^a
1	PCy ₃	20%
2	dppe	22%
3	rac. BINAP	19%
4	dtbpf	29%
5	Xantphos	56%
6	dppf	53%
7	dppf Gen. 3 (10 mol%) ^b	42%
8	RuPhos Gen. 3 (10 mol%) ^b	44%
9	SPhos Gen. 4 (10 mol%) ^b	55%
10	Johnphos	37%
11	Xphos	54%
12	DPEphos	55%
13	2-(<i>N,N</i> -dimethylaminomethyl)-1-diphenylphosphinoferrocene (78) ^c	74%
14	Davephos	72%

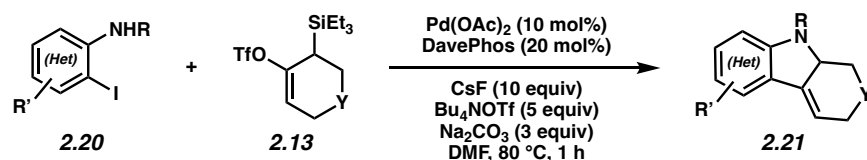
^a ¹H NMR yield determined using 1,3,5-trimethoxybenzene as an external standard.

^b Pd(OAc)₂ omitted from the reaction.

^c Reaction carried out at 60 °C.

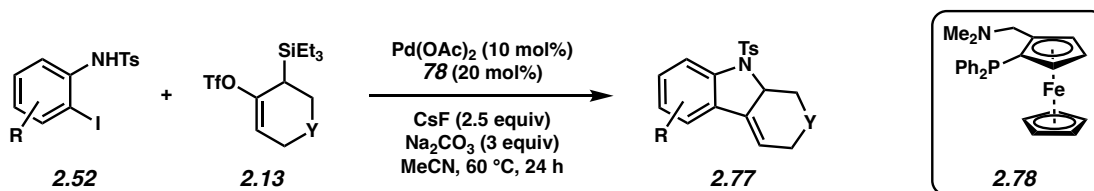
2.8.2.4 Scope of the Racemic Annulation

General Procedure 2.5 for the scope of the racemic annulation:



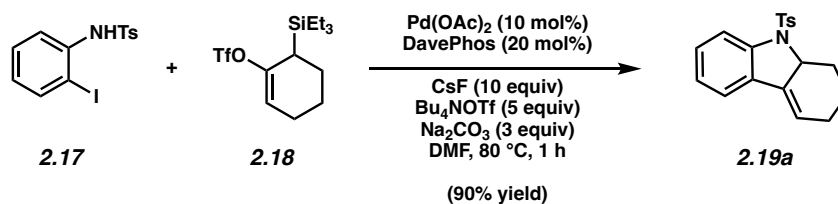
Annulation Products 2.21. A 1-dram vial containing a magnetic stir bar was charged with iodoaniline **2.20** (0.05 mmol, 1.0 equiv) and Bu₄NOTf (98.7 mg, 0.25 mmol, 5.0 equiv). A separate 1-dram vial was charged with silyl triflate **2.13** (0.075 mmol, 1.5 equiv). A third 1-dram vial was charged with Pd(OAc)₂ (1.12 mg, 0.005 mmol, 10 mol%). All three vials were taken into a glovebox where Na₂CO₃ (15.9 mg, 0.15 mmol, 3.0 equiv) and CsF (76.0 mg, 0.50 mmol, 10 equiv) were added to the vial containing iodoaniline **2.20**. Davephos (3.94 mg, 0.010 mmol, 20 mol%) was then added to the vial containing Pd(OAc)₂. The vial containing the Pd(OAc)₂/Davephos and the vial containing silyl triflate **2.13** were then each treated with an aliquot of DMF (0.25 mL each) and agitated vigorously to ensure full dissolution. The solution of Pd(OAc)₂/Davephos and the solution of silyl triflate were then transferred sequentially to the reaction vial containing iodoaniline **2.20**, and the vial was sealed with a Teflon-lined cap, removed from the glovebox, and stirred for 1 h at 80 °C. The mixture was then filtered through a pad of silica gel, eluting with EtOAc (10 mL). The eluate was concentrated by iteratively azeotroping with *n*-heptane (4 x 5 mL). The crude residue was redissolved in CH₂Cl₂ (1 mL) and filtered through a pad of silica gel eluting with CH₂Cl₂ (20 mL) to remove excess Bu₄NOTf. The eluate was concentrated and purified by preparative thin layer chromatography to provide annulation products **2.21**.

General Procedure 2.6 for the scope of the racemic annulation:

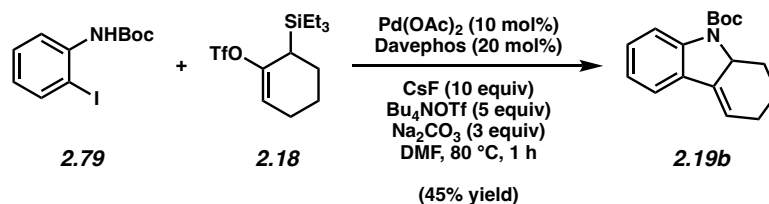


Annulation Products 2.77. A 1-dram vial containing a magnetic stir bar was charged with iodoaniline **2.52** (0.05 mmol, 1.0 equiv). A separate 1-dram vial was charged with silyl triflate **2.13** (0.075 mmol, 1.5 equiv). A third 1-dram vial was charged with Pd(OAc)₂ (1.12 mg, 0.005 mmol, 10 mol%). All three vials were taken into a glovebox where Na₂CO₃ (15.9 mg, 0.15 mmol, 3.0 equiv) and CsF (19.0 mg, 0.125 mmol, 2.5 equiv) were added to the vial containing iodoaniline **2.52**. Ligand **2.78** (4.27 mg, 0.010 mmol, 20 mol%) was then added to the vial containing Pd(OAc)₂. The vial containing the Pd(OAc)₂/ligand and the vial containing silyl triflate **2.13** were then each treated with an aliquot of MeCN (0.25 mL each) and agitated vigorously to ensure full dissolution. The solution of Pd(OAc)₂/ligand and the solution of silyl triflate were then transferred sequentially to the reaction vial containing iodoaniline **2.52**, and the vial was sealed with a Teflon-lined cap, removed from the glovebox, and stirred for 24 h at 60 °C. The mixture was then filtered through a pad of silica gel, eluting with EtOAc (10 mL). The eluate was concentrated and purified by preparative thin layer chromatography to provide annulation products **2.77**.

Any modification of the conditions shown in the general procedure above are specified in the following schemes.

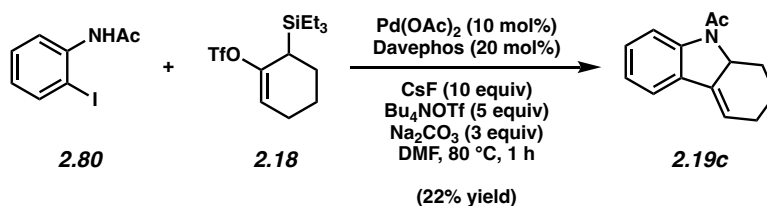


2.19a. Followed General Procedure 2.5. Purification by preparative thin layer chromatography (4:1 hexanes:acetone) generated annulation product **2.19a** (90% yield, average of two experiments) as a white solid. **Annulation product 2.19a:** Spectral data matched those reported in the literature.⁵⁵



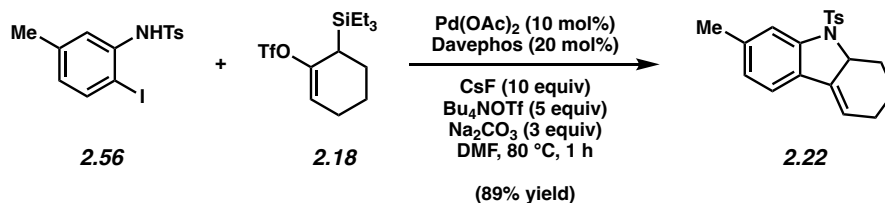
2.19b. Followed General Procedure 2.5. Purification by preparative thin layer chromatography (2:1 hexanes:CH₂Cl₂, eluted three times) generated annulation product **2.19b** (45% yield, average of two experiments) as a colorless oil. **Annulation product 2.19b:** R_f 0.32 (3:1 benzene:hexanes); ¹H NMR (500 MHz, DMSO-d₆): δ 7.75–7.59 (m, 1H), 7.39 (d, J = 7.6, 1H), 7.14 (t, J = 7.8, 1H), 6.93 (t, J = 7.7, 1H), 5.95 (q, J = 3.4, 1H), 4.46–4.36 (m, 1H), 2.70–2.61 (m, 1H), 2.29–2.16 (m, 2H), 1.87–1.78 (m, 1H), 1.69–1.59 (m, 1H), 1.48 (s, 9H), 1.29–1.16 (m, 1H); ¹³C NMR (100 MHz, DMSO-d₆): δ 152.6, 144.0, 136.8, 129.1, 128.9, 123.1, 120.3, 117.7, 115.2, 81.2, 61.8, 28.4, 28.1, 24.4, 19.9; IR (film): 2975, 2932, 1704, 1384, 1158 cm⁻¹; HRMS-APCI (m/z) [$M + H$]⁺ calcd for C₁₇H₂₂NO₂⁺, 272.16451; found 272.16508.

Note: 2.19b was obtained as a mixture of rotamers. These data represent empirically observed chemical shifts from the ¹H and ¹³C-NMR spectra.



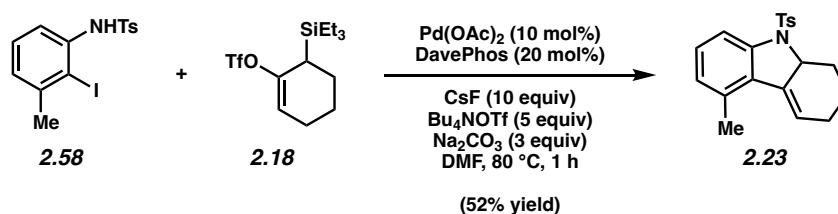
2.19c. Followed General Procedure 2.5. Purification by preparative thin layer chromatography (4:1 hexanes:acetone) generated annulation product **2.19c** (22% yield, average of two experiments) as an off-white solid. **Annulation product 2.19c:** Mp: 105–107 °C; R_f 0.29 (4:1 hexanes:acetone); ¹H NMR (500 MHz, DMSO-*d*₆): δ 8.04 (br s, 1H), 7.44 (d, J = 7.6, 1H), 7.14 (t, J = 7.6, 1H), 6.99 (t, J = 7.6, 1H), 6.00 (q, J = 3.6, 1H), 4.64 (br s, 1H), 2.67–2.49 (m, 1H), 2.31–2.18 (m, 5H), 1.84–1.76 (m, 1H), 1.75–1.62 (m, 1H), 1.32–1.21 (m, 1H); ¹³C NMR (125 MHz, DMSO-*d*₆): δ 170.2, 144.3, 137.4, 129.2, 129.0, 123.9, 120.2, 117.5, 116.8, 61.8, 28.8, 24.9, 24.1, 19.5; IR (film): 2933, 1662, 1461, 1383, 1319 cm⁻¹; HRMS-APCI (m/z) [$M + H$]⁺ calcd for C₁₄H₁₆NO⁺, 214.12264; found 214.12264.

Note: 2.19c was obtained as a mixture of rotamers. These data represent empirically observed chemical shifts from the ¹H and ¹³C-NMR spectra.

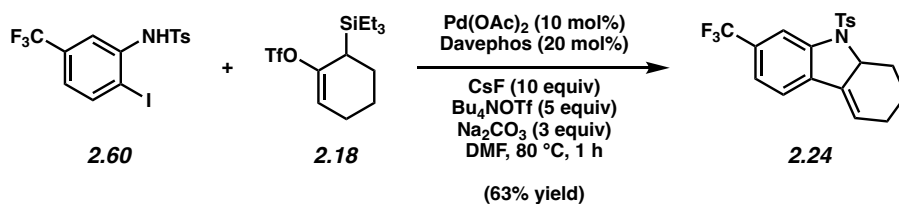


2.22. Followed General Procedure 2.5. Purification by preparative thin layer chromatography (9:1 hexanes:EtOAc) generated annulation product **2.22** (89% yield, average of two experiments) as an off-white solid. **Annulation product 2.22:** Mp: 148–150 °C; R_f 0.32 (9:1 hexanes:EtOAc); ¹H

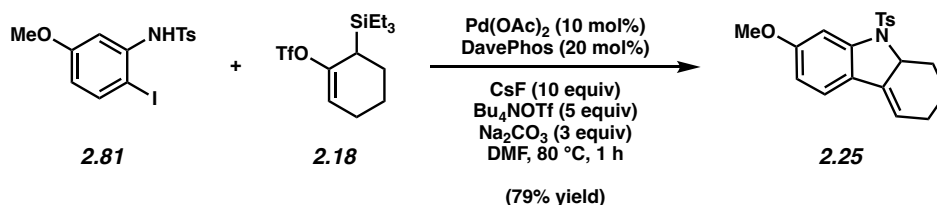
NMR (400 MHz, C₆D₆): δ 8.03–8.00 (m, 1H), 7.72 (d, J = 8.3, 2H), 6.90 (d, J = 7.9, 1H), 6.58–6.55 (m, 1H), 6.55–6.52 (m, 2H), 5.36 (q, J = 3.6, 1H), 4.27–4.16 (m, 1H), 2.95 (dq, J = 12.1, 3.8, 1H), 2.07 (s, 3H), 1.84–1.71 (m, 2H), 1.66 (s, 3H), 1.63–1.57 (m, 1H), 1.55–1.45 (m, 1H), 1.36–1.23 (m, 1H); ¹³C NMR (100 MHz, C₆D₆): δ 144.4, 143.4, 139.1, 135.7, 134.2, 129.3, 128.2, 127.1, 124.7, 119.8, 116.39, 116.35, 64.4, 29.2, 24.2, 21.5, 20.7, 20.1; IR (film): 2934, 1599, 1356, 1169, 665 cm⁻¹; HRMS-APCI (m/z) [M + H]⁺ calcd for C₂₀H₂₂NO₂S⁺, 340.13658; found 340.13751.



2.23. Followed General Procedure 2.5. Purification by preparative thin layer chromatography (9:1 hexanes:acetone, eluted twice) generated annulation product **2.23** (52% yield, average of two experiments) as a white solid. **Annulation product 2.23:** Mp: 99–101 °C; R_f 0.68 (9:1 benzene:Et₂O); ¹H NMR (500 MHz, CDCl₃): δ 7.68 (d, J = 8.5, 2H), 7.65 (d, J = 8.3, 1H), 7.21 (d, J = 8.5, 2H), 7.07 (t, J = 7.7, 1H), 6.78 (d, J = 7.7, 1H), 5.90 (q, J = 3.6, 1H), 4.20–4.11 (m, 1H), 2.88–2.81 (m, 1H), 2.35 (s, 3H), 2.32 (s, 3H), 2.32–2.27 (m, 2H), 1.96–1.89 (m, 1H), 1.76–1.64 (m, 2H); ¹³C NMR (100 MHz, CDCl₃): δ 144.1, 143.7, 136.3, 133.7, 133.4, 129.6, 128.0, 127.8, 127.3, 126.1, 120.7, 112.8, 63.9, 29.3, 25.1, 21.5, 20.6, 19.8; IR (film): 2942, 1585, 1458, 1356, 1168 cm⁻¹; HRMS-APCI (m/z) [M + H]⁺ calcd for C₂₀H₂₂NO₂S⁺, 340.13658; found 340.13733.

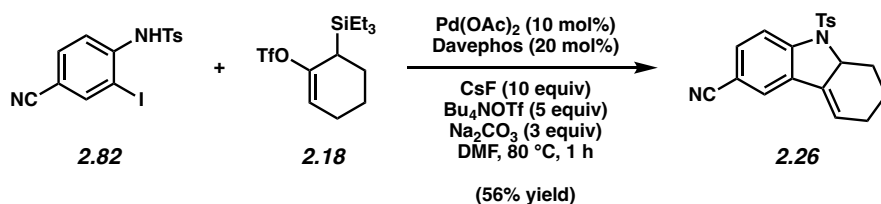


2.24. Followed General Procedure 2.5. Purification by preparative thin layer chromatography (9:1 hexanes:EtOAc) generated annulation product **2.24** (63% yield, average of two experiments) as an off-white solid. **Annulation product 2.24:** Mp: 128–130 °C; *R_f* 0.22 (9:1 hexanes:EtOAc); ¹H NMR (400 MHz, CDCl₃): δ 7.99 (s, 1H), 7.69 (d, *J* = 8.3, 2H), 7.29 (d, *J* = 7.9, 1H), 7.26 (d, *J* = 8.2, 2H), 7.22 (d, *J* = 8.0, 1H), 5.98 (q, *J* = 3.6, 1H), 4.26–4.23 (m, 1H), 2.83–2.80 (m, 1H), 2.37 (s, 3H), 2.30–2.29 (m, 2H), 2.00–1.97 (m, 1H), 1.71–1.67 (m, 2H); ¹³C NMR (125 MHz, CDCl₃): δ 144.7, 143.7, 134.7, 133.1, 132.7, 130.8 (q, *J* = 32.4), 129.8, 127.7, 124.0 (q, *J* = 272.4), 121.1, 120.9 (q, *J* = 4.0), 120.1, 112.3 (q, *J* = 4.0), 64.5, 29.0, 24.6, 21.6, 20.0; ¹⁹F NMR (376 MHz, CDCl₃) δ –62.25 (s, 3F); IR (film): 2935, 1430, 1324, 1167, 1124 cm⁻¹; HRMS-APCI (*m/z*) [M + H]⁺ calcd for C₂₀H₁₉F₃NO₂S⁺, 394.10868; found 394.10831.

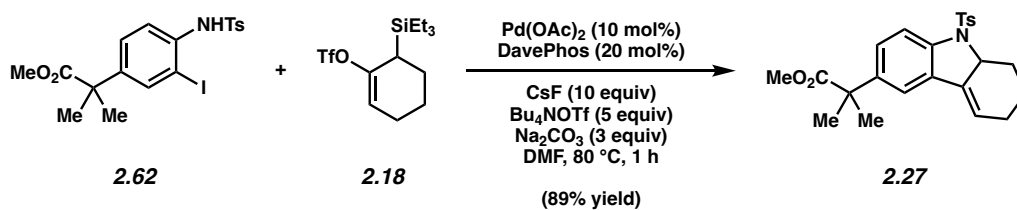


2.25. Followed General Procedure 2.5. Purification by preparative thin layer chromatography (4:1 hexanes:acetone, eluted twice) generated annulation product **2.25** (79% yield, average of two experiments) as a white solid. **Annulation product 2.25:** Mp: 104–107 °C; *R_f* 0.58 (9:1 benzene:Et₂O); ¹H NMR (500 MHz, CDCl₃): δ 7.70 (d, *J* = 8.2, 2H), 7.38 (d, *J* = 2.4, 1H), 7.24 (d, *J* = 8.2, 2H), 7.13 (d, *J* = 8.2, 1H), 6.54 (dd, *J* = 8.2, 2,4, 1H), 5.67 (q, *J* = 3.6, 1H), 4.20–4.10

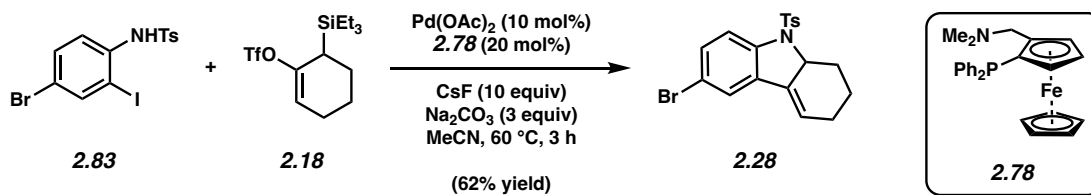
(m, 1H), 3.84 (s, 3H), 2.81–2.74 (m, 1H), 2.37 (s, 3H), 2.29–2.17 (m, 2H), 1.98–1.90 (m, 1H), 1.75–1.59 (m, 2H); ^{13}C NMR (100 MHz, CDCl_3): δ 160.8, 144.8, 144.2, 135.1, 133.4, 129.7, 127.7, 122.4, 120.6, 115.4, 110.4, 101.2, 64.8, 55.7, 29.2, 24.4, 21.6, 20.2; IR (film): 2938, 1738, 1607, 1489, 1355 cm^{-1} ; HRMS-APCI (m/z) $[\text{M} + \text{H}]^+$ calcd for $\text{C}_{20}\text{H}_{22}\text{NO}_3\text{S}^+$, 356.13149; found 356.13121.



2.26. Followed General Procedure 2.5. Purification by preparative thin layer chromatography (4:1 hexanes:EtOAc) generated annulation product **2.26** (56% yield, average of two experiments) as a yellow solid. **Annulation product 2.26:** Mp: 187 °C; R_f 0.11 (9:1 hexanes:EtOAc); ^1H NMR (400 MHz, CDCl_3): δ 7.79 (d, $J = 8.9$, 1H), 7.72–7.67 (m, 2H), 7.49–7.43 (m, 2H), 7.30–7.26 (m, 2H), 5.96 (q, $J = 3.6$, 1H), 4.31–4.21 (m, 1H), 2.86–2.74 (m, 1H), 2.39 (s, 3H), 2.34–2.22 (m, 2H), 2.05–1.93 (m, 1H), 1.75–1.59 (m, 2H); ^{13}C NMR (100 MHz, CDCl_3): δ 146.9, 145.0, 133.7, 133.4, 133.1, 130.4, 130.0, 127.5, 123.7, 121.3, 118.9, 115.4, 107.0, 64.7, 28.9, 24.6, 21.6, 19.9; IR (film): 2937, 2225, 1608, 1469, 1365 cm^{-1} ; HRMS-APCI (m/z) $[\text{M} + \text{H}]^+$ calcd for $\text{C}_{20}\text{H}_{19}\text{N}_2\text{O}_2\text{S}^+$, 351.11618; found 351.11690.

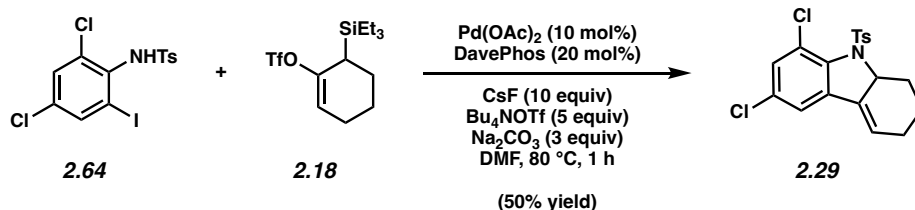


2.27. Followed General Procedure 2.5. Purification by preparative thin layer chromatography (4:1 hexanes:acetone, eluted three times) afforded annulation product **2.27** (89% yield, average of two experiments) as a white solid. **Annulation product 2.27:** Mp: 123–125; R_f 0.30 (4:1 hexanes:acetone); $^1\text{H NMR}$ (500 MHz, CDCl_3): δ 7.60 (d, $J = 8.2$, 2H), 7.57 (d, $J = 8.6$, 1H), 7.16–7.10 (m, 3H), 7.05 (dd, $J = 9.0$, 1.9, 1H), 5.76 (q, $J = 3.5$, 1H), 4.12–4.04 (m, 1H), 3.53 (s, 3H), 2.73–2.64 (m, 1H), 2.27 (s, 3H), 2.21–2.10 (m, 2H), 1.90–1.81 (m, 1H), 1.61–1.53 (m, 2H), 1.43 (s, 6H); $^{13}\text{C NMR}$ (125 MHz, CDCl_3): δ 177.1, 144.2, 142.2, 140.3, 135.6, 133.6, 129.7, 129.4, 127.7, 126.5, 118.2, 117.2, 115.0, 64.4, 52.3, 46.1, 29.0, 26.7, 26.5, 24.5, 21.6, 20.2; IR (film): 2947, 1730, 1478, 1361, 1167 cm^{-1} ; HRMS-APCI (m/z) $[\text{M} + \text{H}]^+$ calcd for $\text{C}_{24}\text{H}_{28}\text{NO}_4\text{S}^+$, 426.17336; found 426.17297.

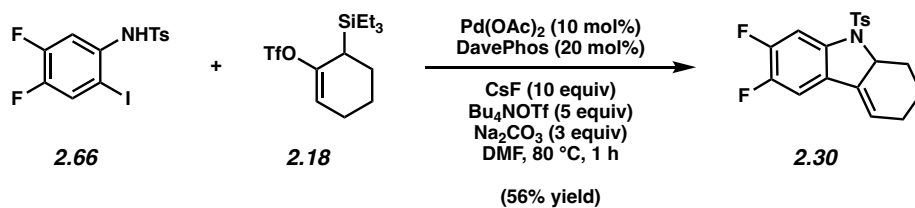


2.28. Followed a modified version of General Procedure 2.6 by altering the amount of silyl triflate **18** (17.2 mg, 0.05 mmol, 1.0 equiv), CsF (76.0 mg, 0.500 mmol, 10.0 equiv), and MeCN (0.66 mL in total, 0.075 M) used and by decreasing the reaction time to 3 h. Purification by preparative thin layer chromatography (9:1 hexanes:EtOAc) afforded annulation product **2.28** (62% yield, average of two experiments) as a white solid. **Annulation product 2.28:** Mp: 165–166 °C; R_f 0.4 (9:1 hexanes:EtOAc); $^1\text{H NMR}$ (500 MHz, C_6D_6): δ 7.82 (d, $J = 8.7$, 1H), 7.63 (d, $J = 8.3$, 2H), 7.11–

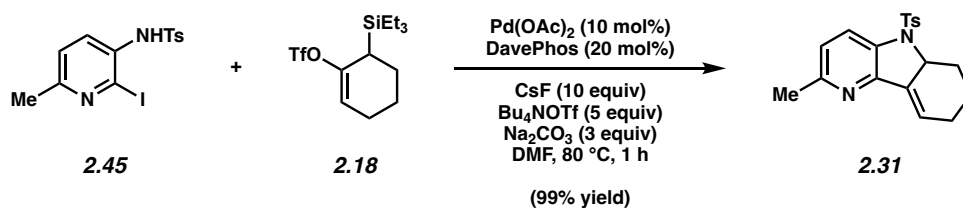
7.07 (m, 2H), 6.57 (d, $J = 8.2$, 2H), 5.12 (q, $J = 3.7$, 1H), 4.15–4.07 (m, 1H), 2.91–2.85 (dq, $J = 12.0$, 4.19, 1H), 1.71 (s, 3H), 1.69–1.63 (m, 2H), 1.52–1.42 (m, 2H), 1.27–1.18 (m, 1H); ^{13}C NMR (125 MHz, CDCl_3): δ 144.5, 142.5, 134.5, 133.0, 131.6, 131.5, 129.8, 127.7, 123.1, 119.8, 116.9, 116.8, 64.4, 29.0, 24.6, 21.6, 20.1; IR (film): 2935, 1458, 1361, 1166, 665 cm^{-1} ; HRMS-APCI (m/z) $[\text{M} + \text{H}]^+$ calcd for $\text{C}_{19}\text{H}_{19}\text{BrNO}_2\text{S}^+$, 404.03144; found 404.03104.



2.29. Followed General Procedure 2.5. Purification by preparative thin layer chromatography (4:1 hexanes:acetone, eluted twice) generated annulation product **2.29** (50% yield, average of two experiments) as a white solid. **Annulation product 2.29:** Mp: 119–121 °C; R_f 0.41 (4:1 hexanes:acetone); ^1H NMR (500 MHz, CDCl_3): δ 7.76 (d, $J = 8.3$, 2H), 6.93 (d, $J = 1.8$, 1H), 6.84 (d, $J = 1.8$, 1H), 6.71 (d, $J = 8.3$, 2H), 5.15 (q, $J = 3.5$, 1H), 5.01–4.93 (m, 1H), 2.64–2.54 (m, 1H), 1.81 (s, 3H), 1.76–1.67 (m, 2H), 1.44–1.36 (m, 1H), 1.35–1.17 (m, 2H); ^{13}C NMR (125 MHz, CDCl_3): δ 143.6, 139.9, 138.1, 134.9, 134.4, 130.2, 130.1, 129.3, 127.0, 122.7, 120.5, 118.4, 65.1, 28.9, 24.6, 21.6, 19.8; IR (film): 2933, 1563, 1443, 1341, 1162 cm^{-1} ; HRMS-APCI (m/z) $[\text{M} + \text{H}]^+$ calcd for $\text{C}_{19}\text{H}_{18}\text{Cl}_2\text{NO}_2\text{S}^+$, 394.04298; found 394.04342.

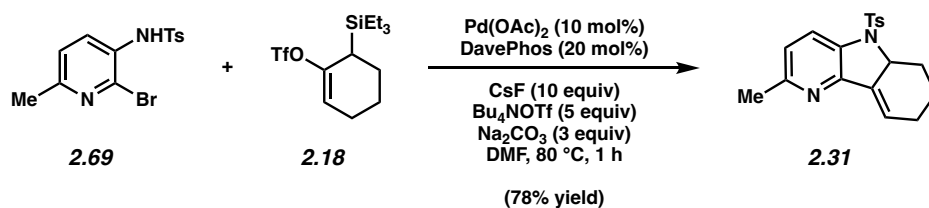


2.30. Followed General Procedure 2.5. Purification by preparative thin layer chromatography (4:1 hexanes:acetone, eluted twice) generated annulation product **2.30** (56% yield, average of two experiments) as a colorless crystalline solid. **Annulation product 2.30:** Mp: 169–171 °C; R_f 0.39 (4:1 hexanes:acetone); $^1\text{H NMR}$ (500 MHz, C_6D_6): δ 7.97 (dd, $J = 11.4, 7.0$, 1H), 7.59 (d, $J = 8.3$, 2H), 6.59 (d, $J = 8.3$, 2H), 6.51 (dd, $J = 9.1, 8.3$, 1H), 5.08 (q, $J = 3.7$, 1H), 4.17–4.04 (m, 1H), 2.89 (dq, $J = 11.1, 3.3$, 1H), 1.77–1.67 (m, 2H), 1.73 (s, 3H), 1.58–1.45 (m, 2H), 1.30–1.17 (m, 1H); $^{13}\text{C NMR}$ (100 MHz, CDCl_3): δ 150.4 (dd, $J = 247.7, 14.3$), 147.6 (dd, $J = 245.0, 14.3$), 144.7, 139.3 (dd, $J = 9.1, 1.6$), 134.2 (app. t, $J = 2.1$), 132.8, 129.9, 127.7, 125.5 (dd, $J = 6.3, 3.4$), 118.9 (d, $J = 1.8$), 108.3 (d, $J = 19.8$), 105.2 (d, $J = 24.4$), 64.5, 28.9, 24.4, 21.6, 19.9; $^{19}\text{F NMR}$ (376 MHz, CDCl_3): δ –134.7 (ddd, $J = 20.8, 11.3, 7.8$, 1F), –143.2 (ddd; $J = 20.8, 9.6, 6.9$, 1F); IR (film): 2936, 1610, 1599, 1487, 1359 cm^{-1} ; HRMS-APCI (m/z) $[\text{M} + \text{H}]^+$ calcd for $\text{C}_{19}\text{H}_{18}\text{F}_2\text{NO}_2\text{S}^+$, 362.10208; found 362.10203.

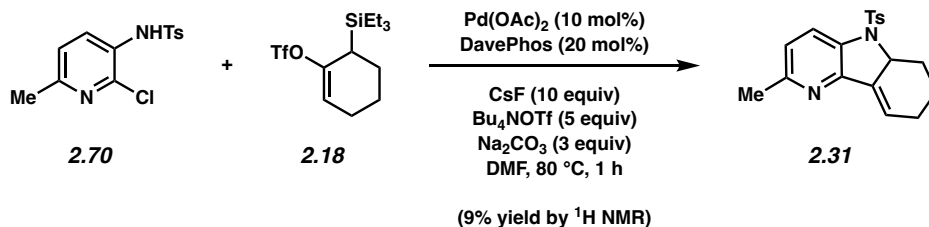


2.31. Followed General Procedure 2.5. Purification by preparative thin layer chromatography (9:1 benzene:MeCN) afforded annulation product **2.31** (99% yield, average of two experiments) as a white solid. **Annulation product 2.31:** Mp: 168–170 °C; R_f 0.27 (4:1 hexanes:acetone); $^1\text{H NMR}$

(500 MHz, C₆D₆): δ 8.04 (d, J = 8.3, 1H), 7.65 (d, J = 8.2, 2H), 6.59 (d, J = 8.1, 2H), 6.49 (d, J = 8.4, 1H), 6.32 (q, J = 3.5, 1H), 4.24–4.17 (m, 1H), 2.89 (m, J = 4.1, 1H), 2.27 (s, 3H), 1.79–1.73 (m, 2H), 1.72 (s, 3H), 1.61–1.52 (m, 1H), 1.48–1.41 (m, 1H), 1.30–1.18 (m, 1H); ¹³C NMR (125 MHz, CDCl₃): δ 154.1, 148.1, 144.6, 136.2, 135.1, 132.9, 129.8, 127.7, 122.7, 122.4, 121.6, 63.1, 29.0, 24.6, 23.8, 21.6, 20.2; IR (film): 3034, 2933, 1425, 1360, 1166 cm⁻¹; HRMS-APCI (m/z) [M + H]⁺ calcd for C₁₉H₂₁N₂O₂S⁺, 341.13183; found 341.13129.

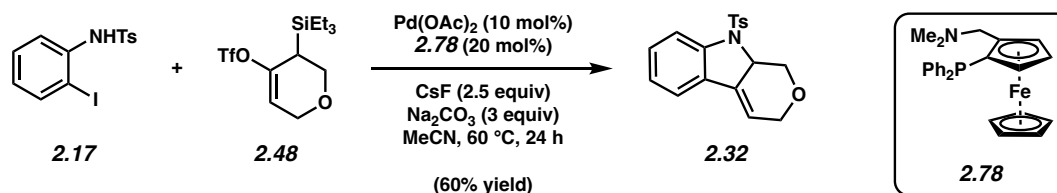


2.31. Followed General Procedure 2.5. Purification by preparative thin layer chromatography (9:1 benzene:MeCN) generated annulation product **2.31** (78% yield, average of two experiments) as a white solid. **Annulation product 2.31:** Spectral data matched those observed for the product obtained from the annulation of **2.45**.

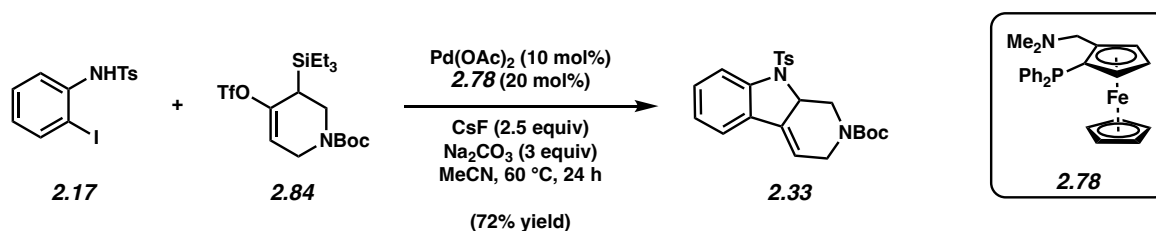


2.31. Followed modified version of General Procedure 2.5 by adding 1,3,5-trimethoxybenzene (0.33 equiv) as an external standard following the workup. Analysis of the crude reaction material by ¹H NMR showed annulation product **2.31** (9% yield, average of two experiments). **Annulation**

product 2.31: Spectral data matched those observed for the product obtained from the annulation of **2.45**.



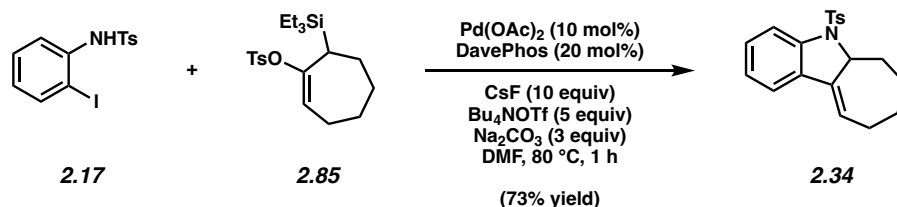
2.32. Followed General Procedure 2.6. Purification by preparative thin layer chromatography (9:1 benzene:Et₂O) afforded annulation product **2.32** (60% yield, average of two experiments) as a white solid. **Annulation product 2.32:** Mp: 161–163 °C; R_f 0.47 (9:1 benzene:Et₂O); ¹H NMR (500 MHz, CDCl₃): δ 7.79 (d, *J* = 8.1, 1H), 7.73 (d, *J* = 8.3, 2H), 7.28–7.22 (m, 4H), 7.02 (t, *J* = 7.5, 1H), 5.81 (q, *J* = 2.8, 1H), 4.77 (dd, *J* = 10.1, 5.1, 1H), 4.46–4.23 (m, 3H), 3.57 (t, *J* = 9.8, 1H), 2.36 (s, 3H); ¹³C NMR (125 MHz, CDCl₃): δ 144.7, 143.5, 133.8, 132.4, 129.8, 129.7, 128.4, 127.9, 124.2, 120.7, 115.6, 115.3, 67.4, 65.5, 59.9, 21.6; IR (film): 2925, 2874, 1599, 1459, 1354 cm⁻¹; HRMS-APCI (*m/z*) [M + H]⁺ calcd for C₁₈H₁₈NO₃S⁺, 328.10019; found 328.09993.



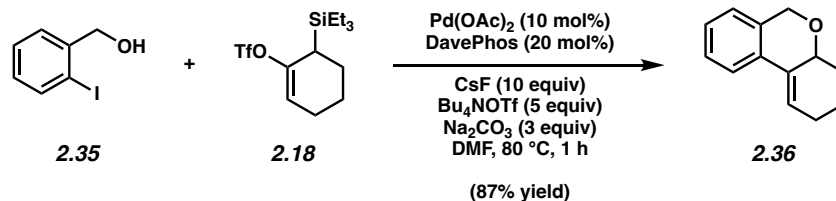
2.33. Followed General Procedure 2.6. Purification by preparative thin layer chromatography (9:1 benzene:Et₂O) afforded annulation product **2.33** (72% yield, average of two experiments) as a beige solid. **Annulation product 2.33:** Mp: 185–188 °C; R_f 0.41 (9:1 benzene:Et₂O); ¹H NMR (600 MHz, CDCl₃): δ 7.81 (d, *J* = 8.3, 1H), 7.79–7.63 (m, 2H), 7.29–7.26 (m, 1H), 7.26–7.21 (m,

3H), 7.02 (t, $J = 7.6$, 1H), 5.90–5.75 (m, 1H), 5.25–4.96 (m, 1H), 4.58–4.25 (m, 1H), 4.25–4.02 (m, 1H), 3.91–3.67 (m, 1H), 2.99–2.78 (m, 1H), 2.37 (s, 3H), 1.61–1.40 (m, 9H); ^{13}C NMR (125 MHz, CDCl_3): δ 154.8, 144.7, 143.7, 135.0, 132.8, 132.5, 129.8, 129.7, 128.1, 127.8, 124.3, 120.6, 115.4, 114.5, 113.9, 80.4, 60.9, 46.4, 45.1, 43.9, 43.3, 29.7, 28.5, 21.6; IR (film): 2976, 2930, 1698, 1459, 1365 cm^{-1} ; HRMS-APCI (m/z) [$\text{M} + \text{H}$] $^+$ calcd for $\text{C}_{23}\text{H}_{27}\text{N}_2\text{O}_4\text{S}^+$, 427.16860; found 427.16787.

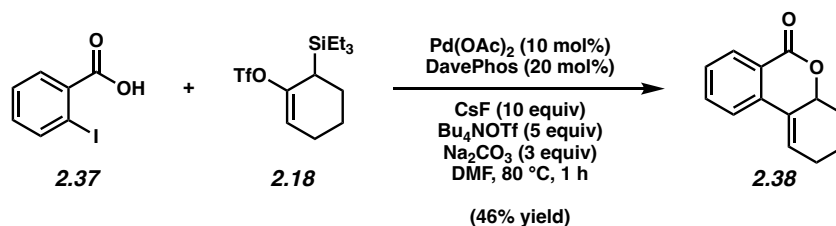
Note: 2.33 was obtained as a mixture of rotamers. These data represent empirically observed chemical shifts from the ^1H and ^{13}C -NMR spectra.



2.34. Followed General Procedure 2.5. Purification by preparative thin layer chromatography (97:3 benzene: Et_2O) afforded annulation product **2.34** (73% yield, average of two experiments) as a white solid. **Annulation product 2.34:** Mp: 186–188 °C; R_f 0.36 (9:1 hexanes: EtOAc); ^1H NMR (500 MHz, CDCl_3): δ 7.69 (d, $J = 8.3$, 1H), 7.60 (d, $J = 8.3$, 2H), 7.23–7.15 (m, 4H), 6.99 (t, $J = 7.6$, 1H), 6.20 (ddd, $J = 9.0, 5.2, 2.9$, 1H), 4.63 (dq, $J = 11.1, 1.8$, 1H), 2.50–2.43 (m, 1H), 2.32 (s, 3H), 2.31–2.28 (m, 1H), 2.18–2.04 (m, 2H), 1.85–1.74 (m, 2H), 1.68–1.60 (m, 1H), 1.37–1.23 (m, 1H); ^{13}C NMR (125 MHz, CDCl_3): δ 143.9, 143.1, 141.7, 134.3, 129.7, 129.6, 128.8, 127.3, 124.2, 119.9, 119.8, 116.2, 68.1, 34.7, 30.0, 28.6, 27.5, 21.6; IR (film): 2923, 1462, 1353, 1168, 578 cm^{-1} ; HRMS-APCI (m/z) [$\text{M} + \text{H}$] $^+$ calcd for $\text{C}_{20}\text{H}_{22}\text{NO}_2\text{S}^+$, 340.13658; found 340.13645.

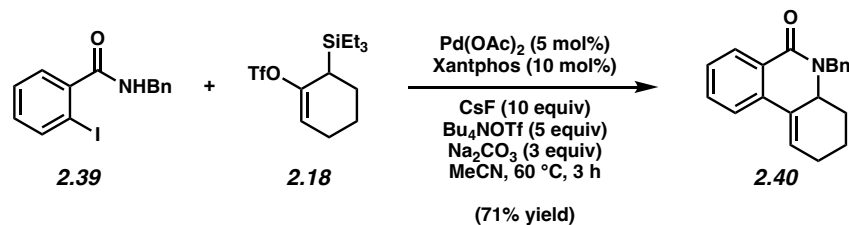


2.36. Followed General Procedure 2.5. Purification by preparative thin layer chromatography (9:1 hexanes:EtOAc, eluted twice) generated annulation product **2.36** (87% yield, average of two experiments) as a colorless oil. **Annulation product 2.36:** R_f 0.58 (4:1 hexanes:acetone); ¹H NMR (500 MHz, CDCl₃): δ 7.58 (d, J = 7.9, 1H), 7.23–7.13 (m, 2H), 7.00 (d, J = 7.4, 1H), 6.40–6.34 (m, 1H), 4.89 (d, J = 15.0, 1H), 4.81 (d, J = 14.8, 1H), 4.26–4.17 (m, 1H), 2.39–2.17 (m, 3H), 1.96–1.83 (m, 1H), 1.68–1.59 (m, 2H); ¹³C NMR (100 MHz, CDCl₃): δ 133.8, 132.1, 131.4, 126.9, 126.8, 124.6, 122.6, 121.3, 73.9, 68.3, 29.7, 26.0, 20.3; IR (film): 3032, 2938, 2863, 1721, 1447 cm⁻¹; HRMS-APCI (m/z) [$M + H$]⁺ calcd for C₁₃H₁₅O⁺, 187.1174; found 187.1172.

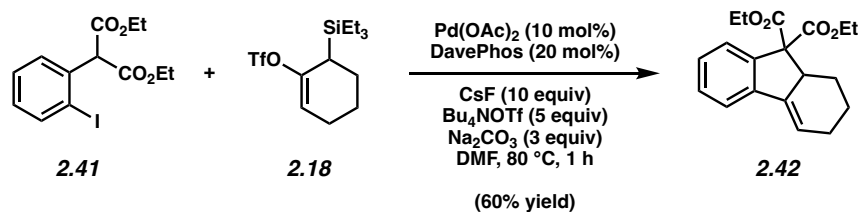


2.38. Followed General Procedure 2.5. Purification by preparative thin layer chromatography (19:1 benzene:Et₂O) generated annulation product **2.38** (46% yield, average of two experiments) as a colorless oil. **Annulation product 2.38:** R_f 0.44 (CH₂Cl₂); ¹H NMR (500 MHz, CDCl₃): δ 8.11 (d, J = 7.8, 1H), 7.57 (t, J = 7.6, 1H), 7.50 (d, J = 7.8, 1H), 7.40 (t, J = 7.6, 1H), 6.52–6.43 (m, 1H), 5.11 (app. s, 1H), 2.44–2.21 (m, 3H), 2.03–1.86 (m, 2H), 1.75–1.62 (m, 1H); ¹³C NMR (100 MHz, CDCl₃): δ 165.3, 137.9, 133.9, 130.3, 129.3, 128.9, 128.2, 123.4, 122.7, 75.3, 29.0, 25.8,

19.8; IR (film): 3063, 1719, 1657, 1599, 1276 cm^{-1} ; HRMS-APCI (m/z) [$M + H$] $^+$ calcd for $\text{C}_{13}\text{H}_{13}\text{O}_2^+$, 201.09101; found 201.08884.

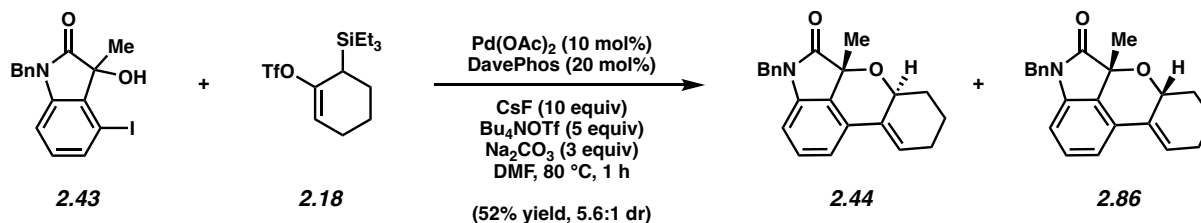


2.40. A 1-dram vial containing a magnetic stir bar was charged with benzamide **2.39** (16.9 mg, 0.05 mmol, 1.0 equiv), Bu_4NOTf (98.7 mg, 0.25 mmol, 5.0 equiv), and Xantphos (2.9 mg, 0.005 mmol, 10 mol%). A separate 1-dram vial was charged with silyl triflate **2.18** (17.2 mg, 0.075 mmol, 1.5 equiv). Both vials were taken into a glovebox where Na_2CO_3 (15.9 mg, 0.150 mmol, 3.0 equiv) and CsF (76.0 mg, 0.500 mmol, 10.0 equiv) were added to the vial containing benzamide **2.39**. The vial containing silyl triflate **2.18** was then treated with an aliquot of MeCN (0.33 mL) and agitated to ensure full dissolution. $\text{Pd}(\text{OAc})_2$ (0.6 mg, 0.0025 mmol, 5 mol%) in MeCN (0.33 mL) was then added to the vial containing benzamide **2.39** from a freshly prepared stock solution. Subsequently, silyl triflate **2.18** in MeCN was also transferred to the reaction vial containing benzamide **2.39**. The vial was sealed with a Teflon-lined cap, removed from the glovebox, and stirred for 3 h at 60 °C. The mixture was then filtered through a pad of silica gel, eluting with EtOAc (10 mL). The eluate was concentrated and purified by preparative thin layer chromatography (9:1 benzene:MeCN) to provide annulation product **2.40** as a white solid (71% yield, average of two experiments). **Annulation product 2.40:** Spectral data matched those reported in the literature.³³



2.42. Followed General Procedure 2.5. Purification by preparative thin layer chromatography (99:1 benzene:MeCN, eluted twice) generated annulation product **2.42** (60% yield, average of two experiments) as a colorless oil. **Annulation product 2.42:** R_f 0.77 (CH_2Cl_2); ^1H NMR (500 MHz, CDCl_3): δ 7.64 (d, $J = 7.7$, 1H), 7.45 (d, $J = 7.7$, 1H), 7.30 (dt, $J = 7.5$, 1.0, 1H), 7.24 (dt, $J = 7.5$, 1.0, 1H), 6.10 (q, $J = 3.5$, 1H), 4.38–4.29 (m, 2H), 4.18 (dq, $J = 10.9$, 7.1, 1H), 4.10 (dq, $J = 10.9$, 7.1, 1H), 3.64–3.54 (m, 1H), 2.32–2.15 (m, 3H), 2.03–1.95 (m, 1H), 1.76–1.65 (m, 1H), 1.37 (t, $J = 7.0$, 3H), 1.35–1.27 (m, 1H), 1.20 (t, $J = 7.1$, 3H); ^{13}C NMR (100 MHz, CDCl_3): δ 170.0, 169.6, 141.5, 140.1, 139.7, 128.7, 127.8, 125.9, 120.1, 118.6, 67.1, 61.7, 61.3, 47.6, 25.1, 24.9, 22.6, 14.2; IR (film): 2981, 2833, 1728, 1467, 1248 cm^{-1} ; HRMS-APCI (m/z) $[\text{M} + \text{H}]^+$ calcd for $\text{C}_{19}\text{H}_{23}\text{O}_4^+$, 315.15909; found 315.15538.

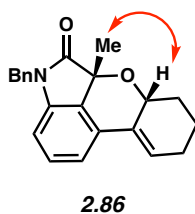
2.8.2.5 Diastereoselective Annulation



2.44 and **2.86.** Followed General Procedure 2.5. Purification by preparative TLC (4:1 hexanes:acetone, eluted 3 times) afforded major diastereomer **2.44** and minor diastereomer **2.86**, each as a waxy amorphous solid (52% combined yield, 5.6:1 dr (determined by ^1H NMR analysis of the crude mixture), average of two experiments). **Annulation Product 2.44** (major

diastereomer): R_f 0.35 (4:1 hexanes:acetone); ^1H NMR (500 MHz, CDCl_3): δ 7.33–7.23 (m, 5H), 7.14 (t, $J = 7.8$, 1H), 6.91 (d, $J = 7.7$, 1H), 6.53 (d, $J = 7.7$, 1H), 6.25–6.21 (m, 1H), 5.07 (d, $J = 15.6$, 1H), 4.58 (d, $J = 15.6$, 1H), 4.34–4.28 (m, 1H), 2.40–2.18 (m, 3H), 1.93–1.80 (m, 2H), 1.75–1.63 (m, 1H), 1.57 (s, 3H); ^{13}C NMR (125 MHz, CDCl_3): δ 178.8, 139.9, 136.0, 132.4, 131.9, 129.4, 129.2, 128.8, 127.7, 127.4, 126.5, 117.1, 107.4, 74.6, 74.4, 43.8, 32.2, 25.9, 25.7, 21.1; IR (film): 2924, 2854, 1730, 1608, 1473 cm^{-1} ; HRMS-APCI (m/z) $[\text{M}+\text{H}]^+$ calcd for $\text{C}_{22}\text{H}_{22}\text{NO}_2^+$, 332.16451; found 332.16337. **Annulation product 2.86** (minor diastereomer): R_f 0.32 (4:1 hexanes:acetone); ^1H NMR (500 MHz, CDCl_3): δ 7.34–7.28 (m, 5H), 7.13–7.03 (m, 2H), 6.44 (d, $J = 7.2$, 1H), 6.35–6.31 (m, 1H), 5.13 (d, $J = 15.7$, 1H), 4.88–4.83 (m, 1H), 4.46 (d, $J = 15.7$, 1H), 2.32–2.23 (m, 3H), 2.01–1.93 (m, 1H), 1.83–1.71 (m, 1H), 1.77 (s, 3H), 1.68–1.61 (m, 1H); ^{13}C NMR (125 MHz, CDCl_3): δ 179.2, 140.9, 136.0, 131.1, 129.2, 129.1, 128.8, 128.4, 127.7, 127.4, 124.2, 114.9, 106.7, 75.4, 71.1, 43.7, 29.3, 25.8, 22.5, 20.7; IR (film): 2930, 2865, 1729, 1604, 1469 cm^{-1} ; HRMS-APCI (m/z) $[\text{M}+\text{H}]^+$ calcd for $\text{C}_{22}\text{H}_{22}\text{NO}_2^+$, 332.16451; found 332.16383.

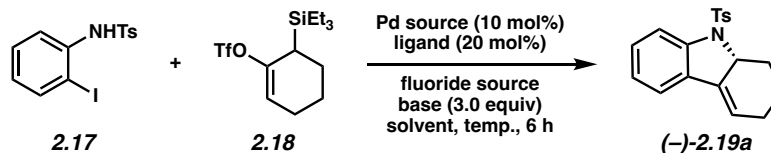
The structure of **2.86** was verified by 2D-NOESY, as the following interaction was observed:



2.8.2.6 Optimization of the Asymmetric Annulation

Results from the optimization of the asymmetric annulation reaction between **2.17** and **2.18** appear below. Ligand, solvent, fluoride source, palladium source, and base were varied using General Procedure 2.7, and results appear below in Tables 2.6, 2.7, 2.8, 2.9, and 2.10 respectively.

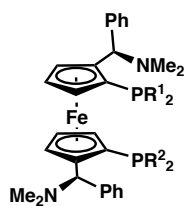
General Procedure 2.7 for the optimization of the asymmetric annulation:



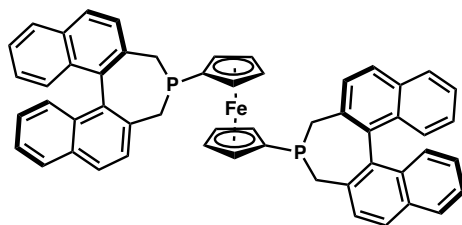
(-)-2.19a. Inside a glovebox, a 1-dram vial was charged with the base (0.09 mmol, 3.0 equiv), the ligand (0.006 mmol, 20 mol%), and the fluoride source as solids. The vial was then treated sequentially with separate freshly prepared stock solutions of iodoaniline **2.17** (11.3 mg, 0.03 mmol, 1.0 equiv), the palladium source (10 mol% Pd), and silyl triflate **2.18** (10.3 mg, 0.03 mmol, 1.0 equiv) to give a final reaction concentration of 0.075 M. The vial was sealed with a Teflon-lined cap, removed from the glovebox, and stirred for 6 h at the desired reaction temperature. After 6 h, 6-acetylbenzothiophene (2.0 mg, 0.011 mmol, 0.38 equiv) was added to the reaction as an external standard for subsequent quantitative analysis by SFC. The mixture was then filtered through a pad of silica gel, eluting with MeCN (10 mL). The eluate was analyzed directly by SFC to determine the yield of **(-)-2.19a** and degree of enantioenrichment.

*The stereochemistry depicted for **(-)-2.19a** is not necessarily representative of the major enantiomer observed for all ligands screened. Any modification of the conditions shown in the general procedure above are specified in the following tables.*

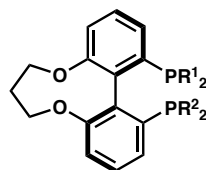
A range of ligands (see Figure 2.5 below for ligand structures) were screened using General Procedure 2.7, and results of these screening reactions appear below in Table 2.6.



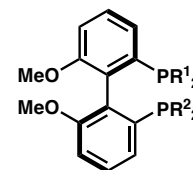
Mandyphos



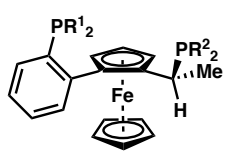
BINAPHANE



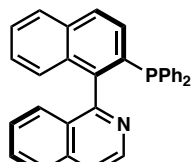
Tunephos



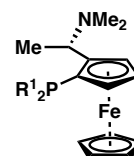
MeO-BIPHEP



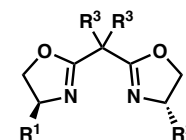
Wallphos



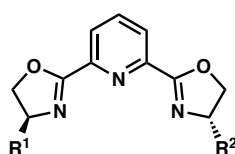
QUINAP



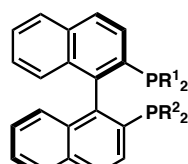
PPFA



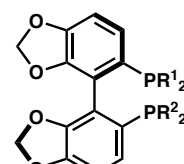
BOX



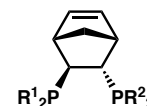
PyBOX



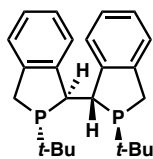
BINAP



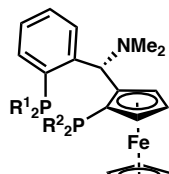
SEGPHOS



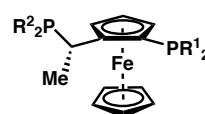
Norphos



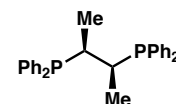
DuanPhos



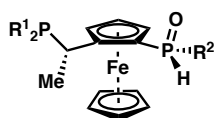
Taniaphos



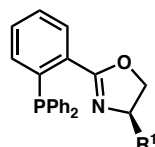
Josiphos



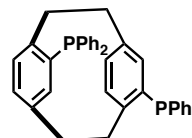
Chiraphos



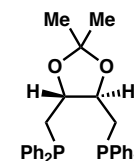
JosPOphos



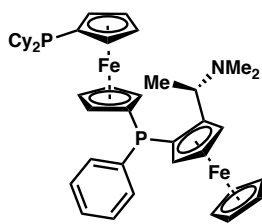
PHOX



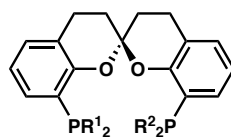
Phanephos



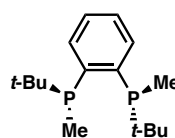
DIOP



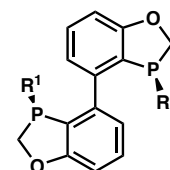
Chenphos



SKP



BenzP*



BABIBOP

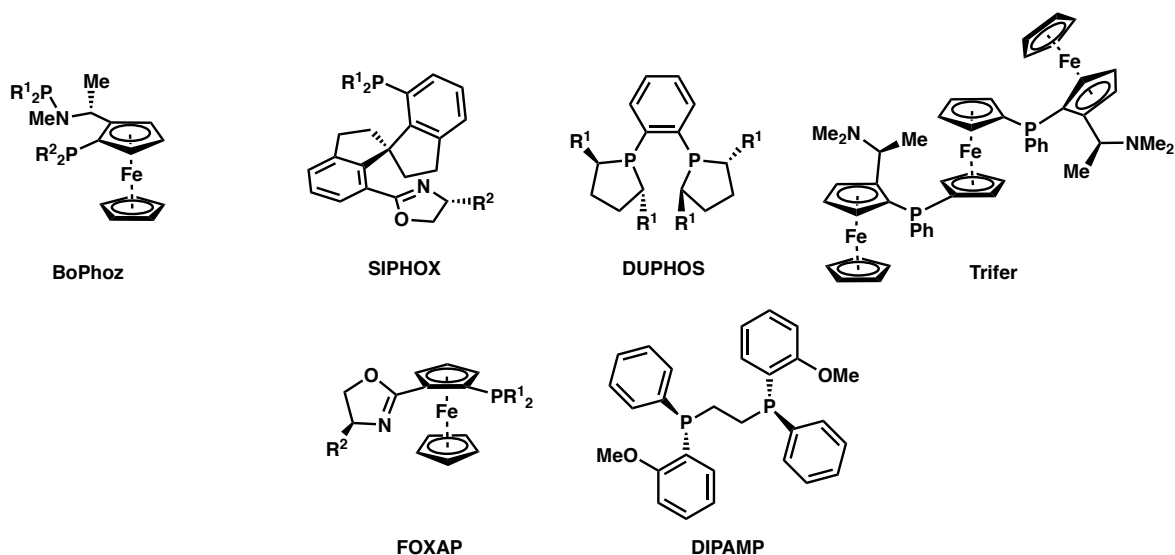
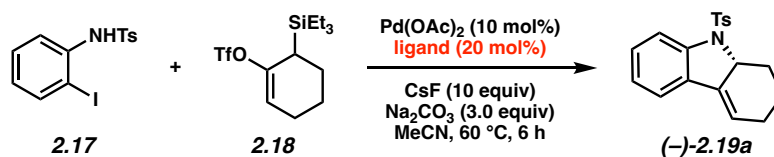


Figure 2.5. Ligand families evaluated during asymmetric reaction development.

Table 2.6. Chiral ligand screen results. See Figure 2.5 above for ligand classes (absolute stereochemistry of product may differ between table entries).

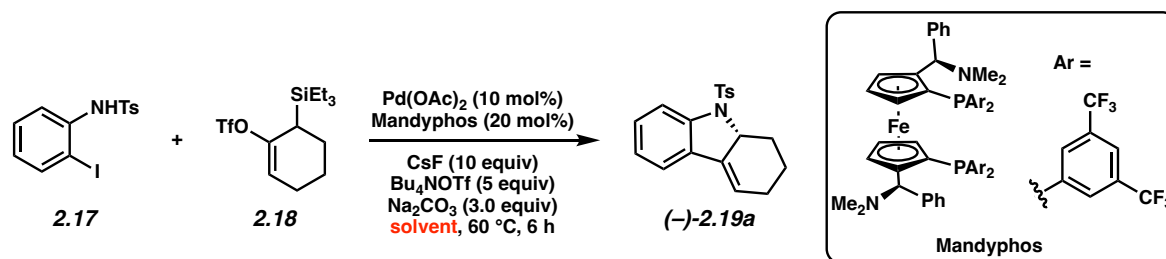


Entry	Ligand Class	R ¹	R ²	Yield ^a	%ee
1	Mandyphos	3,5-bis(trifluoro methyl)pheny 1	3,5-bis(trifluoro methyl)pheny 1	69%	69%
2	Mandyphos	3,5-xylyl	3,5-xylyl	74%	41%
3	Mandyphos	4-methoxy-3,5-xylyl	4-methoxy-3,5-xylyl	63%	47%
4	Mandyphos	Cy	Cy	68%	47%
5	Mandyphos	Ph	Ph	52%	35%
6	Binaphane	N/A	N/A	28%	4%
7	Tunephos	Ph	Ph	37%	5%
8	MeO-BIPHEP	Ph	Ph	40%	1%
9	Walphos	Ph	3,5-bis(trifluoro methyl)pheny 1	14%	13%
10	QUINAP	N/A	N/A	29%	8%

11	PPFA	Cy	N/A	95%	40%
12	BOX (R ³ = Me)	<i>t</i> -Bu	<i>t</i> -Bu	18%	1%
13	PyBOX	<i>i</i> -Pr	<i>i</i> -Pr	6%	6%
14	BINAP	3,5-xylyl	3,5-xylyl	4%	21%
15	SEGPPOS	Ph	Ph	6%	38%
16	Norphos	Ph	Ph	1%	33%
17	Duanphos	N/A	N/A	7%	28%
18	Taniaphos	Ph	Ph	43%	9%
19	Josiphos	Ph	Cy	0%	N/A
20	Chiraphos	N/A	N/A	0%	N/A
21	JosPOphos	<i>t</i> -Bu	Ph	12%	15%
22	PHOX	<i>i</i> -Pr	N/A	7%	23%
23	Phanephos	N/A	N/A	61%	18%
24	DIOP	N/A	N/A	13%	3%
25	Chenphos	N/A	N/A	77%	26%
26	SKP	Ph	Ph	71%	10%
27	BenzP*	N/A	N/A	0%	N/A
28	BABIBOP	<i>t</i> -Bu	<i>t</i> -Bu	4%	73%
29	BoPhoz	Ph	Ph	74%	0%
30	SiPHOX	Ph	Bn	3%	6%
31	DUPHOS	Me	N/A	18%	6%
32	Trifer	N/A	N/A	80%	60%
33	FOXAP	Ph	<i>i</i> -Pr	9%	12%
34	DIPAMP	N/A	N/A	10%	15%

^a Yield determined by quantitative SFC analysis using 6-acetylbenzothiophene as an external standard.

Table 2.7. Solvent screening results.

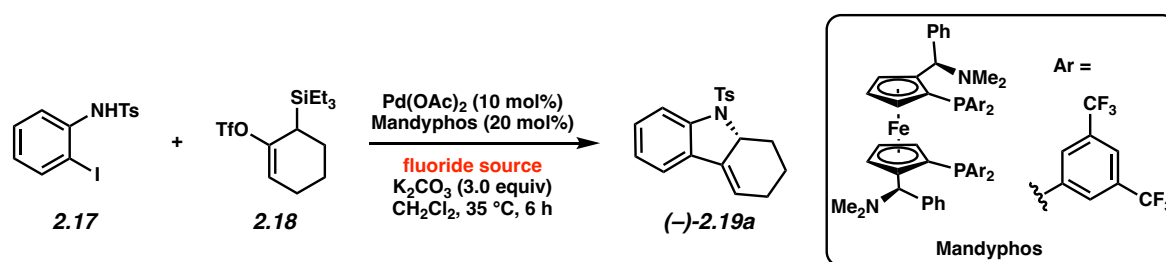


Entry	Solvent	Yield ^a	%ee
1 ^b	CH ₂ Cl ₂	24%	80%
2	1,2-dichloroethane	16%	72%
3	acetonitrile	90%	65%

4	THF	63%	65%
5	1,2-dimethoxyethane	40%	61%
6	1,4-dioxane	79%	61%
7	DMF	28%	45%
8	PhMe	68%	43%
9	pyridine	42%	34%

^a Yield determined by quantitative SFC analysis using 6-acetylbenzothiophene as an external standard. ^b Reaction carried out at 35 °C due to solvent volatility.

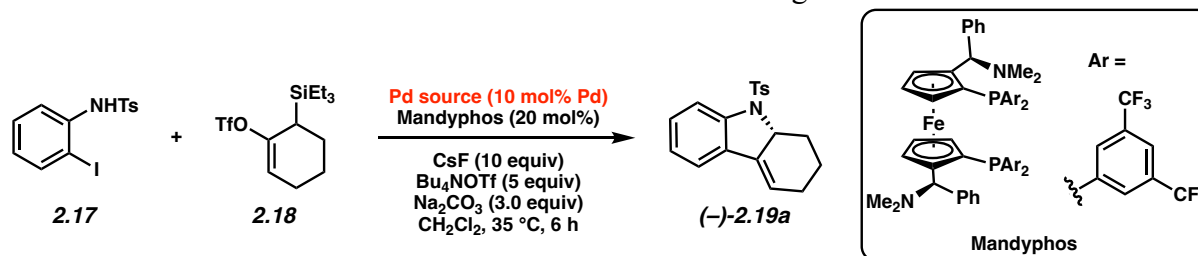
Table 2.8. Fluoride source screening results.



Entry	Fluoride source	NMR Yield ^a	%ee
1	CsF (10 equiv) Bu ₄ NOTf (5 equiv)	14%	85%
2	TBAF•H ₂ O (1.5 equiv)	22%	85%
3	TASF (1.5 equiv)	38%	83%
4	TBAT (1.5 equiv)	29%	78%
5	KF (5 equiv) 18-crown-6 (5 equiv)	14%	79%

^a Yield determined by quantitative SFC analysis using 6-acetylbenzothiophene as an external standard.

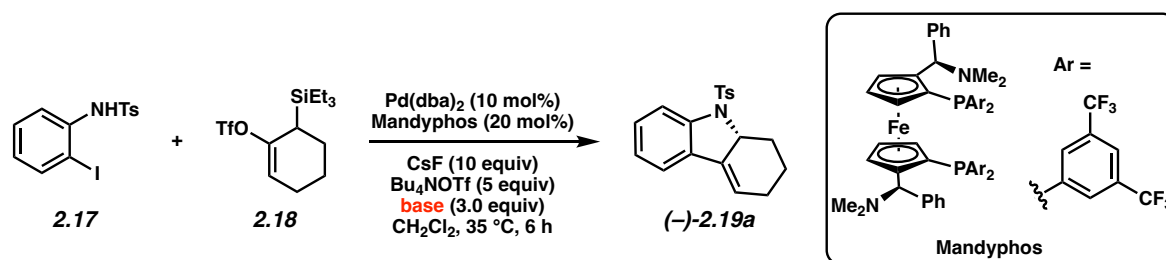
Table 2.9. Palladium source screening results.



Entry	Pd source	Yield ^a	%ee
1	Pd ₂ (dba) ₃	20%	83%
2	Pd(dba) ₂	43%	82%
3	[Pd(allyl)Cl] ₂	49%	80%
4	Pd(OAc) ₂	37%	76%
5	PdCl ₂	44%	67%
6	Pd(acac) ₂	16%	63%

^a Yield determined by quantitative SFC analysis using 6-acetylbenzothiophene as an external standard.

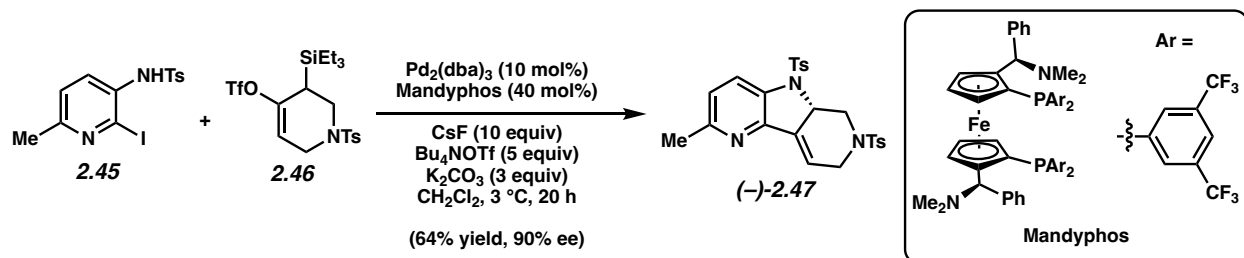
Table 2.10. Base screening results.



Entry	Base	Yield ^a	%ee
1	K ₂ CO ₃	14%	85%
2	K ₂ HPO ₄	15%	85%
3	KOtBu	12%	84%
4	Et ₃ N	27%	82%
5	NaOAc•3H ₂ O	15%	79%
6	NaHMDS	4%	51%

^a Yield determined by quantitative SFC analysis using 6-acetylbenzothiophene as an external standard.

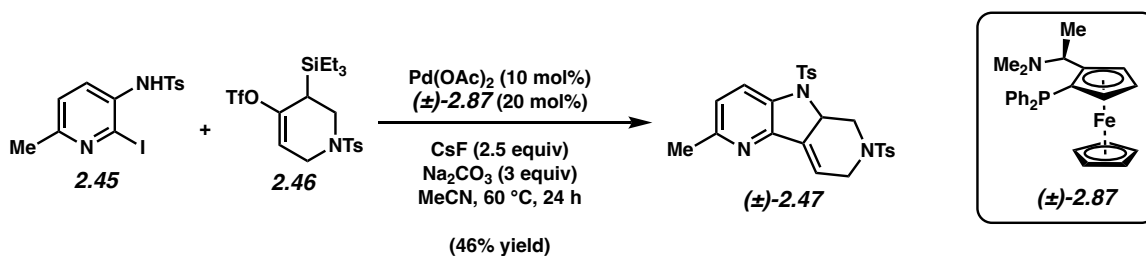
2.8.2.7 Synthesis of (-)-2.47 via Asymmetric Annulation



(-)-2.47. A 1-dram vial containing a magnetic stir bar was charged with iodopyridine **2.45** (23.3 mg, 0.06 mmol, 1.2 equiv) and Bu_4NOTf (98.7 mg, 0.25 mmol, 5.0 equiv). A separate 1-dram vial was charged with silyl triflate **2.46** (25.0 mg, 0.05 mmol, 1.0 equiv). Both vials were taken into a glovebox where K_2CO_3 (20.7 mg, 0.15 mmol, 3.0 equiv) and CsF (76.0 mg, 0.50 mmol, 10 equiv) were added to the vial containing iodopyridine **2.45**. An empty vial equipped with a stir bar was then charged with Mandyphos (27.3 mg, 0.020 mmol, 40 mol%) and $\text{Pd}_2(\text{dba})_3$ (4.6 mg, 0.005 mmol, 10 mol%) then treated with CH_2Cl_2 (0.33 mL) to give a deep purple solution. This vial was sealed with a Teflon-lined cap and stirred at 45 °C for 45 min then cooled back to 23 °C, yielding a yellow/brown solution. The vial containing silyl triflate **2.46** was then treated with an aliquot of CH_2Cl_2 (0.33 mL) and agitated to ensure full dissolution. The solution of $\text{Pd}_2(\text{dba})_3$ /Mandyphos and the solution of silyl triflate were then transferred sequentially to the reaction vial containing iodopyridine **2.45**, and the vial was sealed with a Teflon-lined cap, removed from the glovebox, and stirred for 20 h at 3 °C. The mixture was then filtered through a pad of silica gel, eluting with 9:1 benzene:MeCN (30 mL). The eluate was concentrated and purified by preparative thin layer chromatography (9:1 benzene:MeCN) to provide annulation product (-)-2.47 (64% yield, average of two experiments) as a white solid. **Annulation product (-)-2.47**: Mp: 161–163 °C; R_f 0.29 (9:1 benzene:MeCN); $^1\text{H NMR}$ (500 MHz, CDCl_3): δ 7.89 (d, $J = 8.5$, 1H), 7.76 (d, $J = 8.3$, 2H), 7.66 (d, $J = 8.3$, 2H), 7.35 (d, $J = 8.0$, 2H), 7.27 (d, $J = 8.0$, 2H), 6.98 (d, $J = 8.5$, 1H), 6.22 (q, $J = 3.2$,

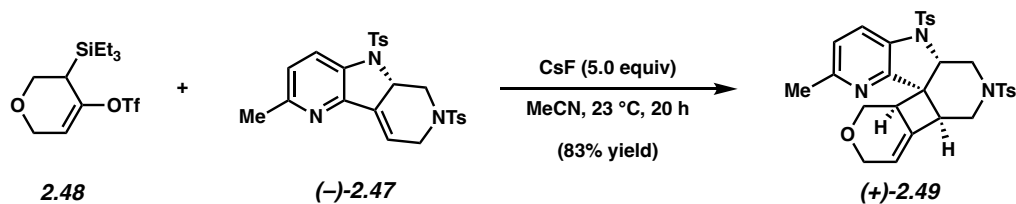
1H), 4.84 (dd, $J = 11.3, 5.1$, 1H), 4.41 (dt, $J = 18.5, 3.6$, 1H), 4.29–4.22 (m, 1H), 3.54 (dt, $J = 18.5, 3.6$, 1H), 2.70 (dd, $J = 11.3, 9.9$, 1H), 2.452 (s, 3H), 2.448 (s, 3H), 2.40 (s, 3H); ^{13}C NMR (125 MHz, CDCl_3): δ 154.8, 146.4, 145.3, 143.9, 136.6, 134.5, 134.2, 131.7, 130.1, 129.9, 127.9, 127.4, 123.3, 122.7, 116.2, 60.0, 47.0, 44.9, 23.8, 21.63, 21.59; IR (film): 2924, 1441, 1360, 1166, 1093 cm^{-1} ; HRMS-APCI (m/z) [$M + H$] $^+$ calcd for $\text{C}_{25}\text{H}_{26}\text{N}_3\text{O}_4\text{S}_2^+$, 496.13592; found 496.13508; $[\alpha]^{20.9}_{\text{D}} -168^\circ$ ($c = 0.500$, CH_2Cl_2).

Note: 3 °C was selected for the practical convenience of being able to perform long reactions in a refrigerator.

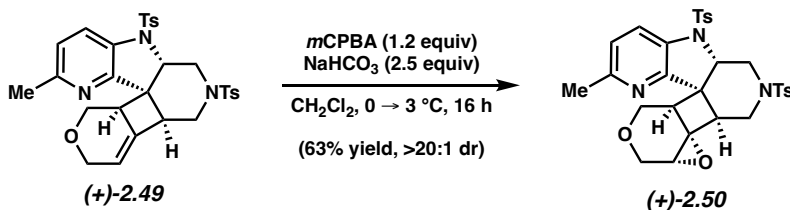


(\pm)-**2.47**. Followed a modified version of General Procedure 2.6 by using ligand (\pm)-**2.87**. Purification by preparative thin layer chromatography (9:1 benzene:MeCN) afforded annulation product (\pm)-**2.47** (46% yield) as a white solid. **Annulation product (\pm)-2.47**: Spectral data matched those obtained for ($-$)-**2.47**.

2.8.2.8 Elaboration of Annulation Product ($-$)-**2.47**



Pentacycle (+)-2.49. A 1-dram vial was charged with annulation product (–)-2.47 (17.3 mg, 0.035 mmol, 1.0 equiv) and silyl triflate 2.48 (18.2 mg, 0.053 mmol, 1.5 equiv) then purged with nitrogen for 5 min. The reactants were then dissolved in MeCN (0.35 mL, 0.10 M) before the rapid addition of CsF (26.6 mg, 0.175 mmol, 5.0 equiv) in a single portion. The vial was sealed with a Teflon-lined cap and stirred at 23 °C for 20 h. The mixture was then filtered through pad of silica gel, eluting with EtOAc (10 mL). The eluate was concentrated to provide a crude residue, which was purified by flash column chromatography (19:1 benzene:Et₂O → 7:3 benzene:Et₂O) to provide a single diastereomer of pentacycle (+)-2.49 (16.8 mg, 83% yield) as a white crystalline solid. Relative and absolute stereochemistry were assigned by single crystal X-ray diffraction studies of epoxide (+)-2.50. **Pentacycle (+)-2.49:** Mp: 110 °C; R_f 0.21 (9:1 benzene:MeCN); ¹H NMR (500 MHz, CDCl₃): δ 7.77 (d, *J* = 8.3, 1H), 7.65 (d, *J* = 8.1, 2H), 7.61 (d, *J* = 8.1, 2H), 7.29 (app t, *J* = 8.9, 4H), 6.99 (d, *J* = 8.3, 1H), 5.63–5.58 (m, 1H), 4.38 (dd, *J* = 10.0, 6.7, 1H), 4.23 (dd, *J* = 11.8, 7.1, 1H), 4.17–4.05 (m, 2H), 4.04–3.92 (m, 2H), 3.01–2.91 (m, 1H), 2.59 (app. d, *J* = 2.59, 2H), 2.48 (s, 3H), 2.40 (s, 6H), 2.28 (dd, *J* = 12.4, 4.8, 1H), 1.93 (t, *J* = 11.4, 1H); ¹³C NMR (125 MHz, CDCl₃): δ 155.3, 152.8, 145.0, 143.8, 135.1, 133.4, 132.44, 132.37, 130.1, 129.8, 127.6, 126.9, 123.0, 122.6, 113.3, 65.1, 61.6, 58.3, 50.5, 49.9, 48.1, 45.8, 44.3, 23.8, 21.6, 21.5; IR (film): 2922, 2850, 1447, 1357, 1164 cm⁻¹; HRMS-APCI (*m/z*) [M + H]⁺ calcd for C₃₀H₃₂N₃O₅S₂⁺, 578.17779; found 578.17515; [α]_D^{23.8} +38.7° (*c* = 0.500, CH₂Cl₂).



Epoxide (+)-2.50. A 1-dram vial was charged with pentacycle (+)-**2.49** (11.2 mg, 0.019 mmol, 1.0 equiv) and CH₂Cl₂ (0.28 mL, 0.07 M) then cooled to 0 °C. NaHCO₃ (4.1 mg, 0.049 mmol, 2.5 equiv) and *m*CPBA (77 wt% purity, 5.0 mg, 0.022 mmol, 1.2 equiv) were added sequentially as solids, and the reaction was moved to a cold room set to 3 °C where it was stirred for 16 h. The reaction was quenched by addition of EtOAc (5 mL), and the organic layer was washed with saturated aqueous NaHCO₃ (3 x 5 mL), dried with Na₂SO₄, filtered, and concentrated under reduced pressure. The resulting crude solid was purified by preparative thin layer chromatography (9:1 benzene:MeCN) to provide epoxide (+)-**2.50** (7.4 mg, 63% yield) as a white crystalline solid. Crystals suitable for X-ray diffraction studies were obtained by recrystallization from a mixture of EtOAc and cyclohexane. **Epoxide (+)-2.50:** Mp: decomposes at 220 °C; R_f 0.69 (4:1 benzene:MeCN); ¹H NMR (500 MHz, CDCl₃): δ 7.78 (d, *J* = 8.3, 1H), 7.68 (d, *J* = 8.2, 2H), 7.62 (d, *J* = 8.2, 2H), 7.29 (app. t, *J* = 7.6, 4H), 6.98 (d, *J* = 8.3, 1H), 4.89 (dd, *J* = 10.4, 6.5, 1H), 4.36 (ddd, *J* = 11.7, 6.5, 1.3, 1H), 4.30 (dd, *J* = 13.2, 4.3, 1H), 3.79 (t, *J* = 3.2, 1H), 3.68 (d, *J* = 4.2, 1H), 3.58 (d, *J* = 12.6, 1H), 3.29 (dd, *J* = 13.4, 2.4, 1H), 2.66–2.56 (m, 2H), 2.46 (s, 3H), 2.393 (s, 3H), 2.390 (s, 3H), 2.19 (dd, *J* = 12.7, 4.6, 1H), 2.14 (dd, *J* = 12.4, 2.2, 1H), 1.97 (t, *J* = 11.6, 1H); ¹³C NMR (125 MHz, CDCl₃): δ 155.2, 152.2, 144.9, 144.0, 134.8, 132.7, 132.6, 130.1, 129.9, 127.7, 127.0, 122.9, 122.1, 68.0, 60.5, 58.2, 53.7, 50.6, 48.9, 46.4, 44.5, 43.3, 42.0, 23.7, 21.6, 21.5; IR (film): 2924, 2848, 1597, 1449, 1358 cm⁻¹; HRMS-APCI (*m/z*) [M + H]⁺ calcd for C₃₀H₃₂N₃O₆S₂⁺, 594.17270; found 594.16951; [α]_D^{24.8} +50.0° (*c* = 1.00, CH₂Cl₂).

Crystal Structure Analysis

Diffraction intensities were collected at 100 K on a Bruker Smart ApexII CCD diffractometer with CuKα radiation, 1.54178 Å. Absorption corrections were applied by SADABS⁵⁶. All calculations

were performed by the SHELXL-2014 packages⁵⁷. Deposition Number 2065022 contains the supplementary crystallographic data for this paper. These data are provided free of charge by the joint Cambridge Crystallographic Data Centre and Fachinformationszentrum Karlsruhe Access Structures service www.ccdc.cam.ac.uk/structures.

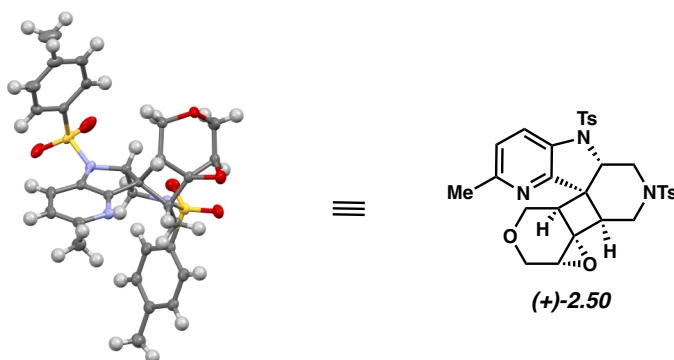


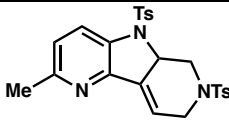
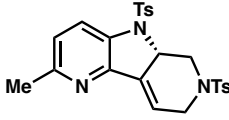
Figure 2.6. ORTEP representation of X-ray crystallographic structure (+)-2.50. EtOAc omitted for clarity. (CCDC Registry # 2065022).

Table 2.11. Crystal data and structure refinement for epoxide (+)-2.50.

Identification code	cu_garg2006s	
Empirical formula	C ₃₄ H ₃₉ N ₃ O ₈ S ₂	
Formula weight	681.80	
Temperature	100(2) K	
Wavelength	1.54178 Å	
Crystal system	Monoclinic	
Space group	P2 ₁	
Unit cell dimensions	a = 10.0508(2) Å	a = 90°.
	b = 14.2935(3) Å	b = 105.5148(7)°.
	c = 12.0393(3) Å	g = 90°.
Volume	1666.56(6) Å ³	
Z	2	
Density (calculated)	1.359 Mg/m ³	
Absorption coefficient	1.917 mm ⁻¹	
F(000)	720	
Crystal size	0.300 x 0.200 x 0.200 mm ³	
Theta range for data collection	3.810 to 69.338°.	
Index ranges	-12 ≤ h ≤ 12, -16 ≤ k ≤ 17, -14 ≤ l ≤ 12	
Reflections collected	27146	
Independent reflections	5940 [R(int) = 0.0190]	
Completeness to theta = 67.679°	97.4 %	
Absorption correction	Semi-empirical from equivalents	
Max. and min. transmission	0.75 and 0.60	

Refinement method	Full-matrix least-squares on F ²
Data / restraints / parameters	5940 / 1 / 463
Goodness-of-fit on F ²	1.054
Final R indices [I>2sigma(I)]	R1 = 0.0308, wR2 = 0.0828
R indices (all data)	R1 = 0.0311, wR2 = 0.0831
Absolute structure parameter	0.031(2)
Extinction coefficient	n/a
Largest diff. peak and hole	0.428 and -0.291 eÅ ⁻³

Table 2.12. SFC conditions and data.

Compound	Column	Solvent	Flow Rate	Retention Times (min)	Enantiomeric Ratio (er)
 (+)-2.47	ChiralPak AD-H/40 °C	20% isopropanol in CO ₂	3.5 mL/min	3.61/5.00	49.8 : 50.2
 (-)-2.47	ChiralPak AD-H/40 °C	20% isopropanol in CO ₂	3.5 mL/min	3.64/5.03	4.9 : 95.1

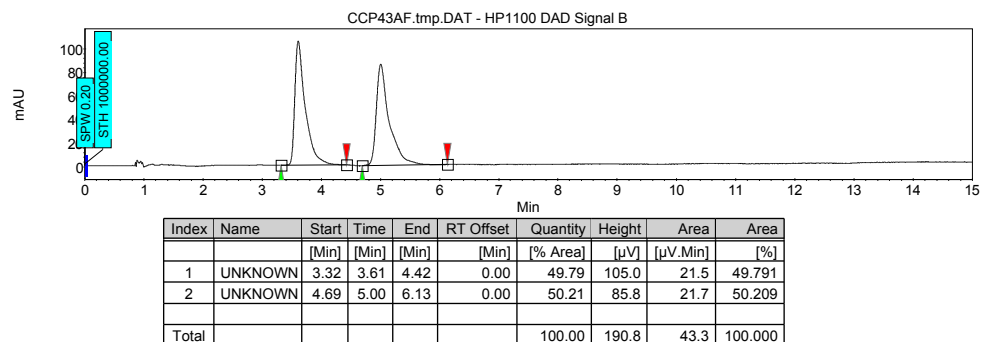
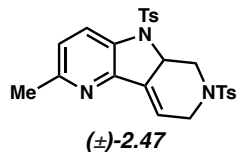


Figure 2.7. SFC trace for (±)-2.47.

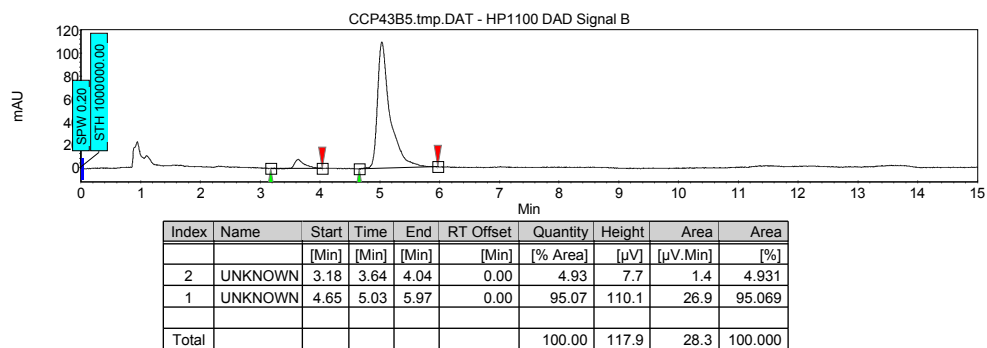
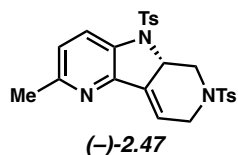


Figure 2.8. SFC trace for (-)-2.47.

2.9 Spectra Relevant to Chapter Two:

Palladium-Catalyzed Annulations of Strained Cyclic Allenes

Andrew V. Kelleghan, Dominick C. Witkowski, Matthew S. McVeigh, and Neil K. Garg

J. Am. Chem. Soc. **2021**, *143*, 9338–9342.

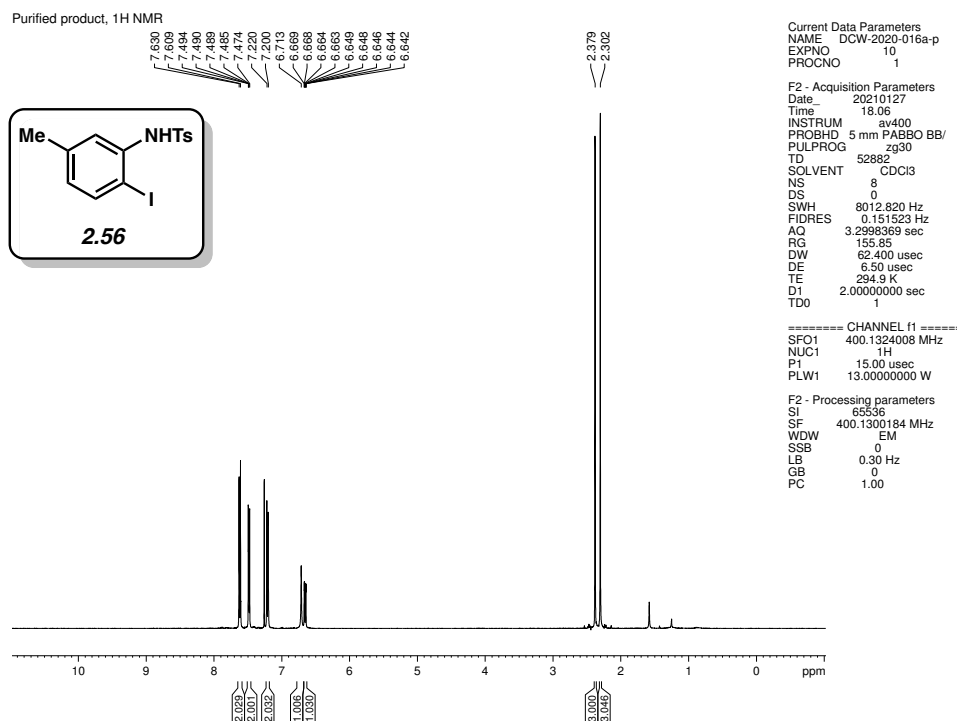


Figure 2.9. ¹H NMR (400 MHz, CDCl₃) of compound 2.56.

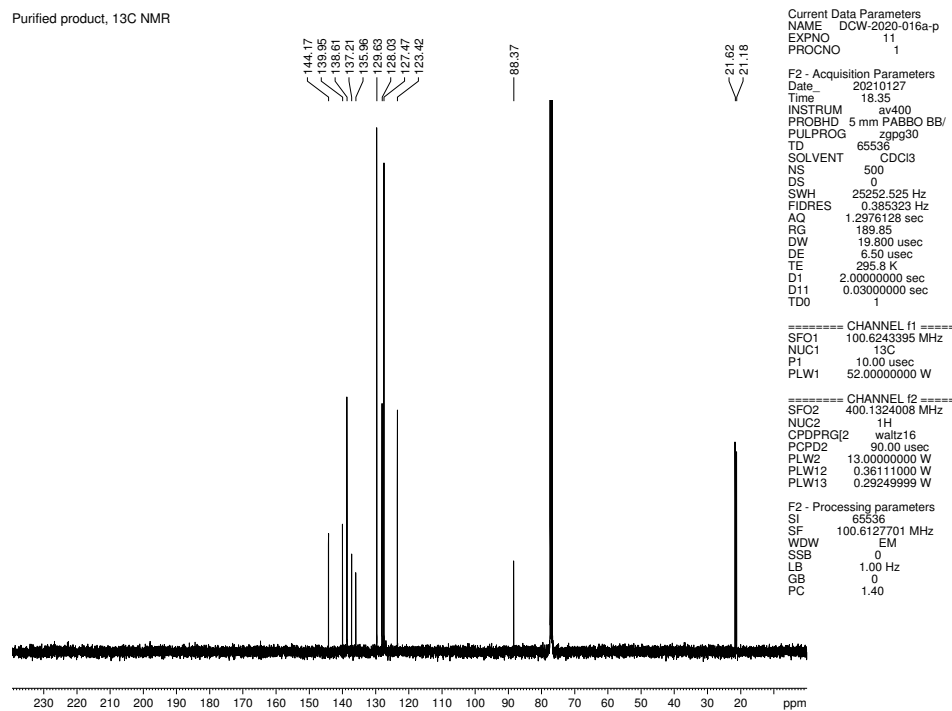


Figure 2.10. ¹³C NMR (100 MHz, CDCl₃) of compound 2.56.

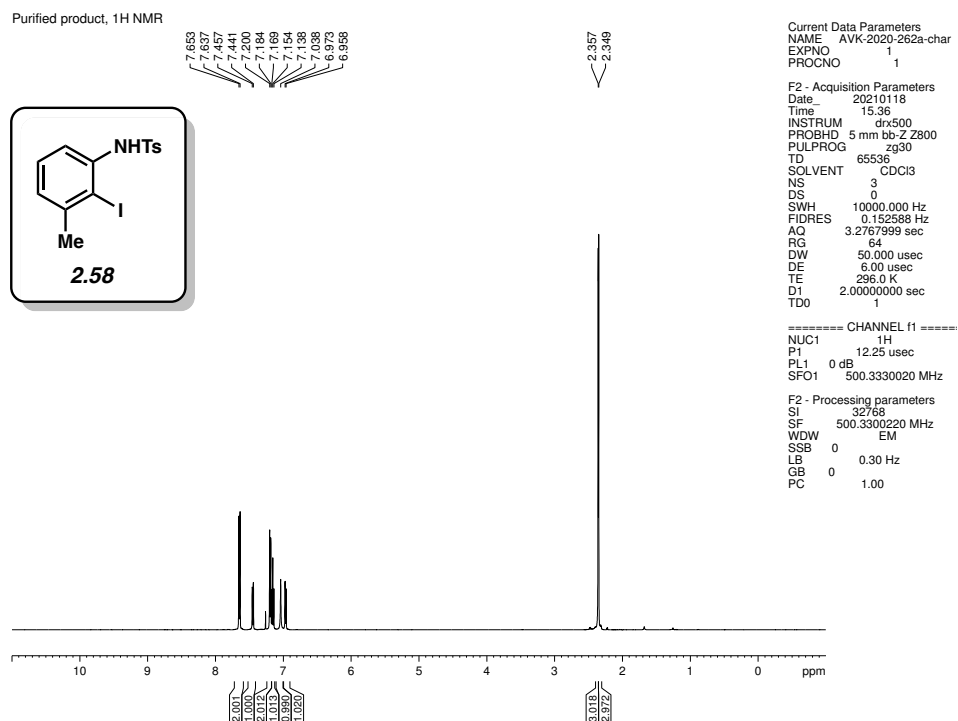


Figure 2.11. ¹H NMR (500 MHz, CDCl₃) of compound **2.58**.

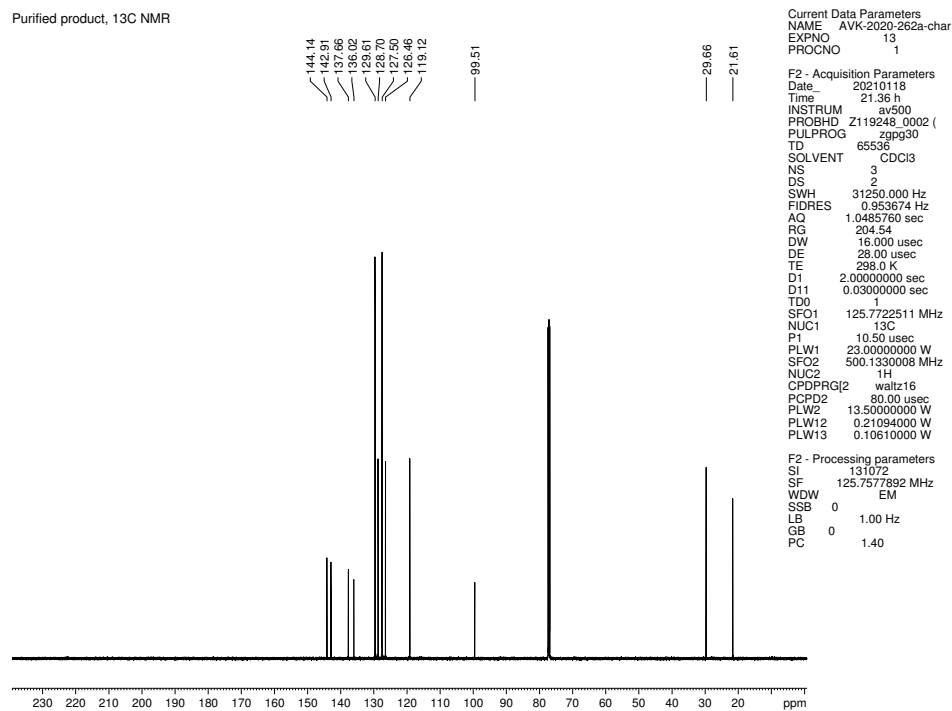


Figure 2.12. ¹³C NMR (125 MHz, CDCl₃) of compound **2.58**.

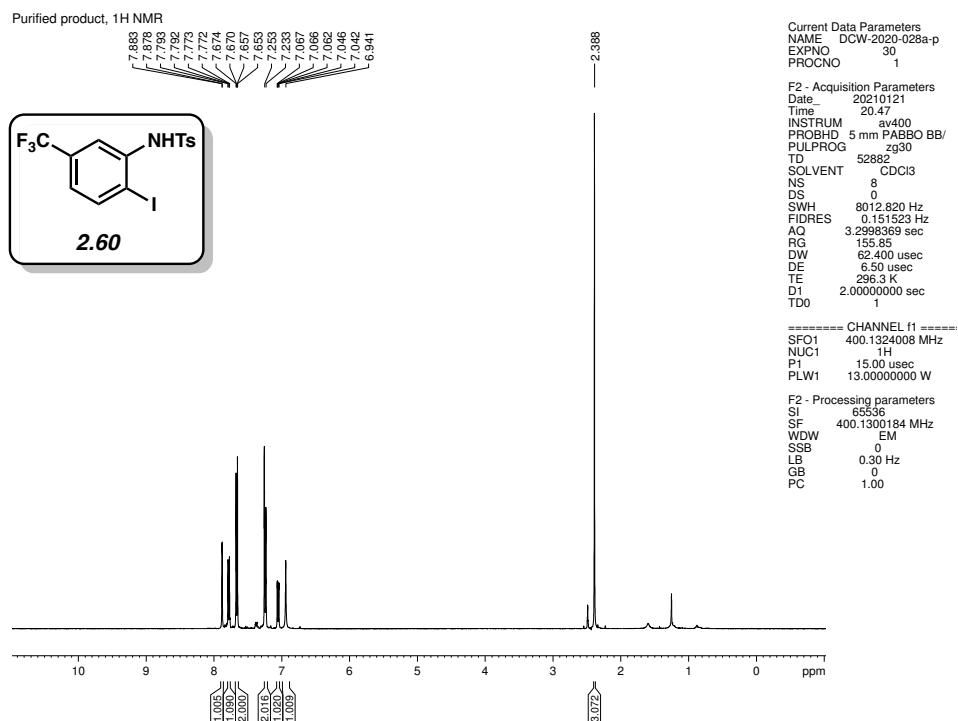


Figure 2.13. ¹H NMR (400 MHz, CDCl₃) of compound **2.60**.

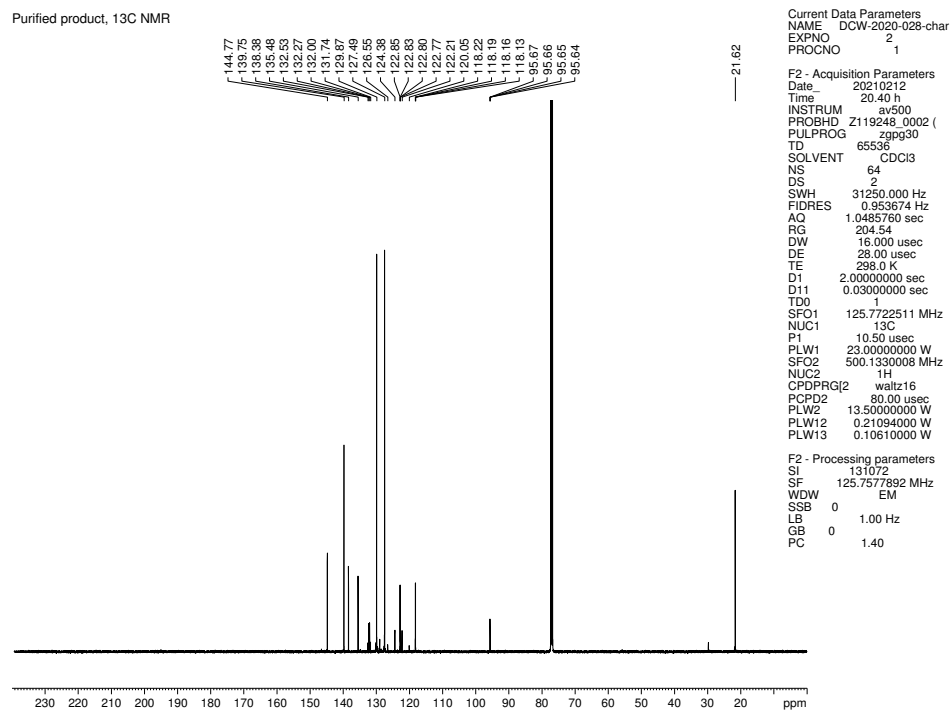


Figure 2.14. ¹³C NMR (125 MHz, CDCl₃) of compound **2.60**.

Purified product, ^{19}F NMR

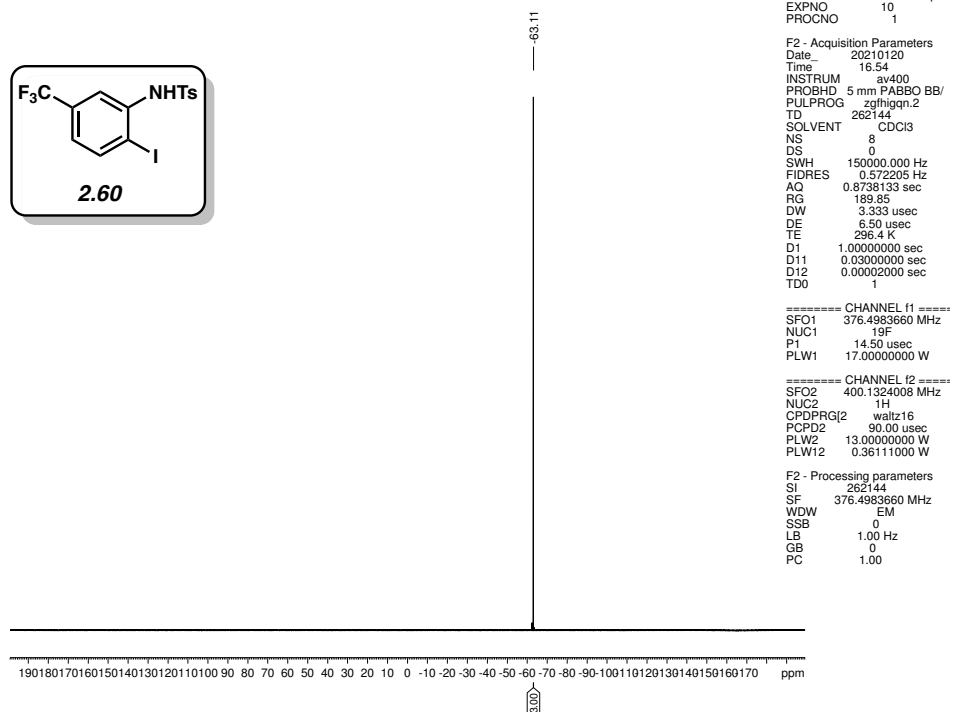
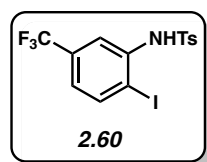


Figure 2.15. ^{19}F NMR (376 MHz, CDCl_3) of compound **2.60**.

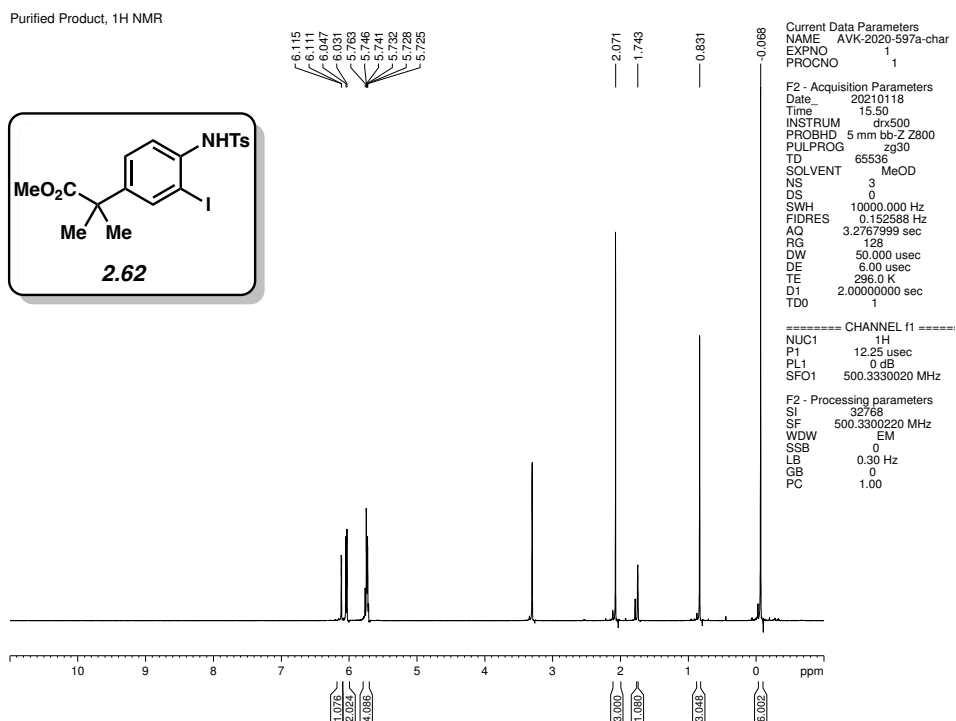


Figure 2.16. ¹H NMR (500 MHz, CD₃OD) of compound 2.62.

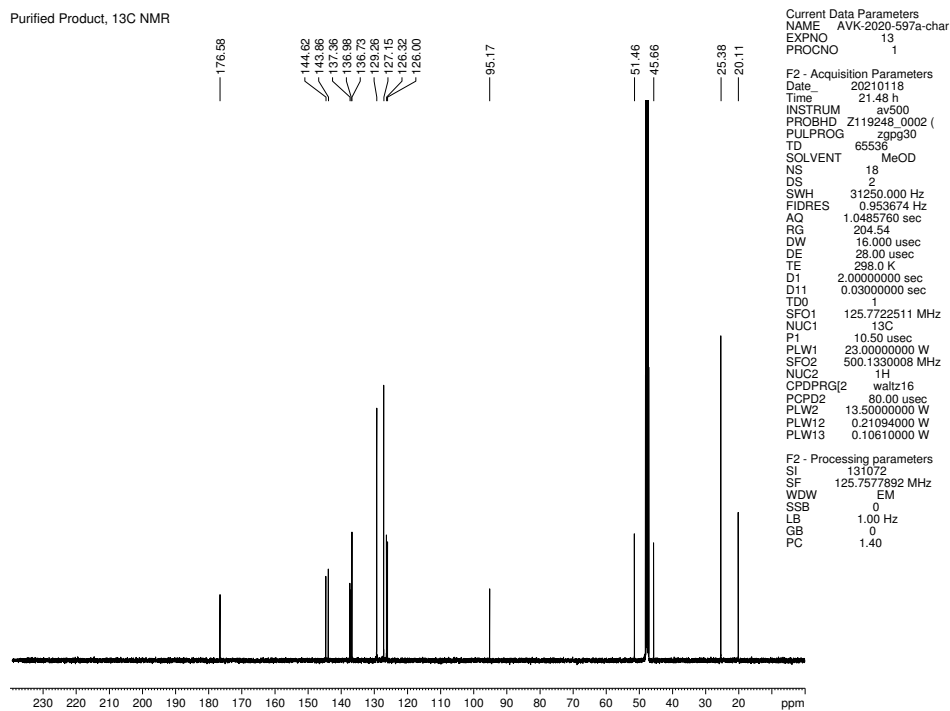


Figure 2.17. ¹³C NMR (125 MHz, CD₃OD) of compound 2.62.

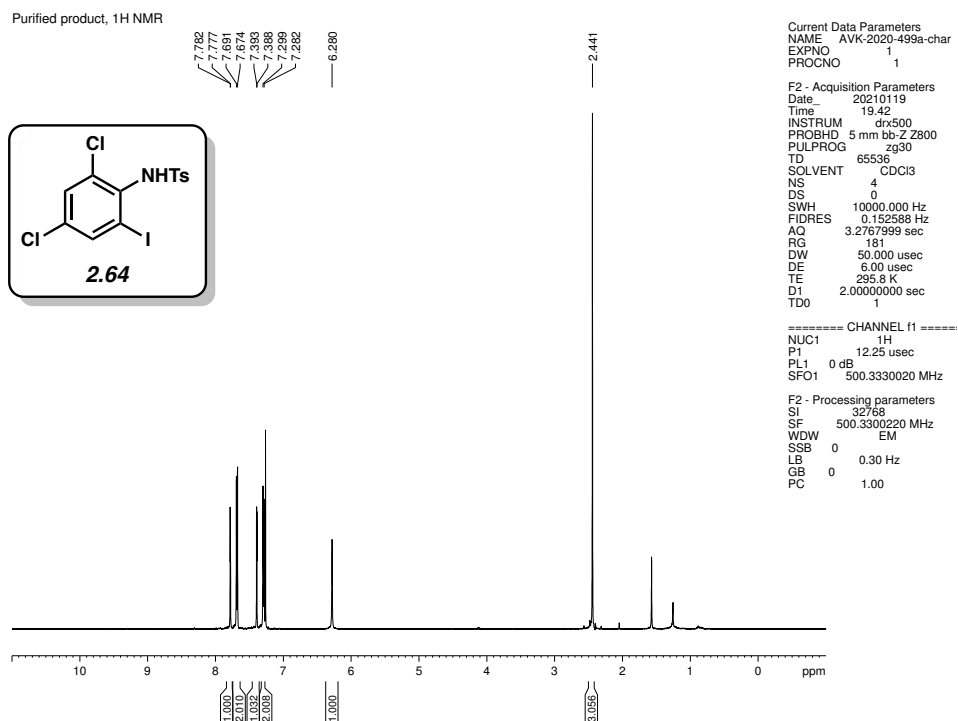


Figure 2.18. ¹H NMR (500 MHz, CDCl₃) of compound 2.64.

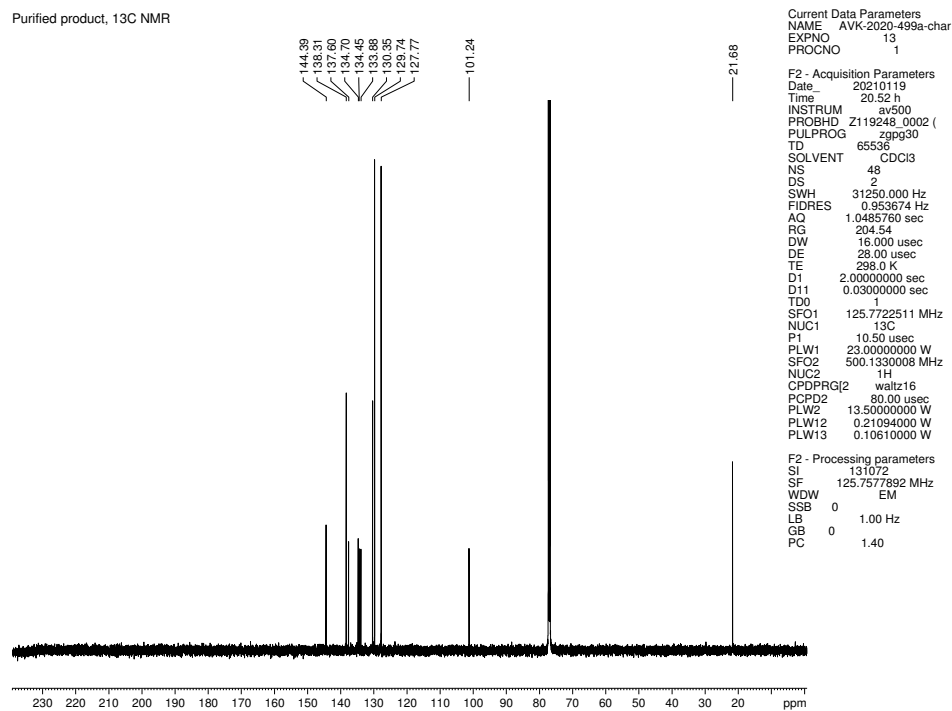


Figure 2.19. ¹³C NMR (125 MHz, CDCl₃) of compound 2.64.

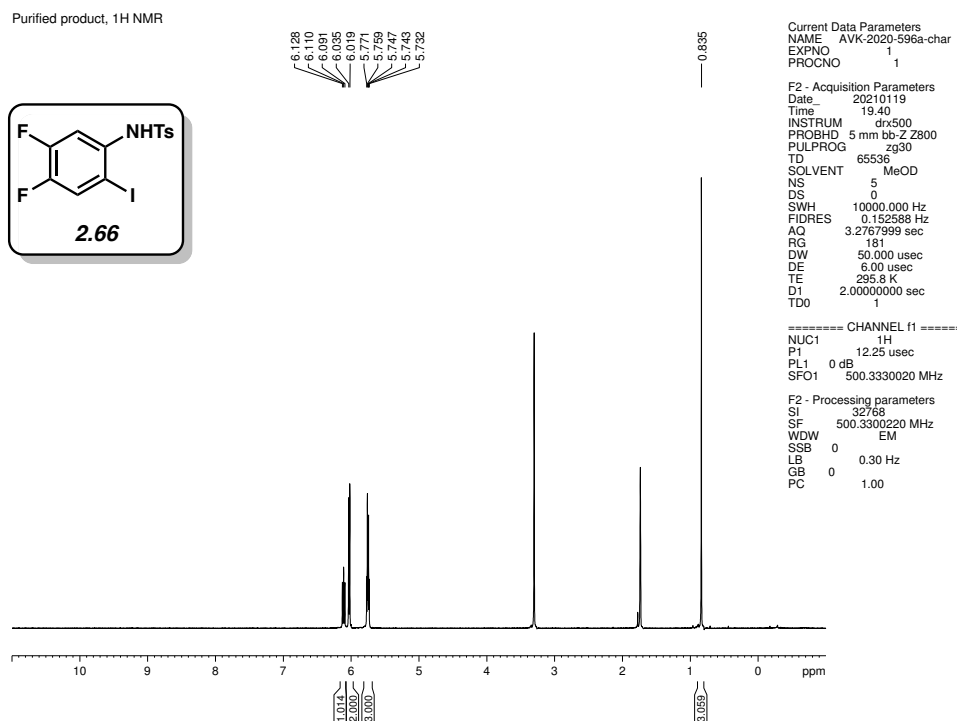


Figure 2.20. ^1H NMR (500 MHz, CD_3OD) of compound **2.66**.

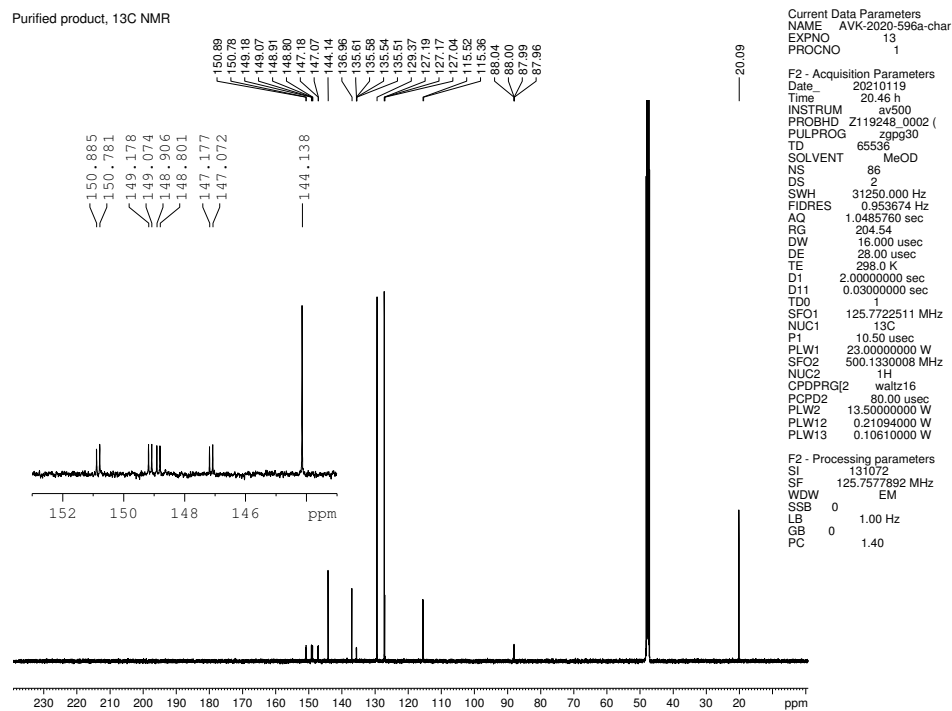


Figure 2.21. ^{13}C NMR (125 MHz, CD_3OD) of compound **2.66**.

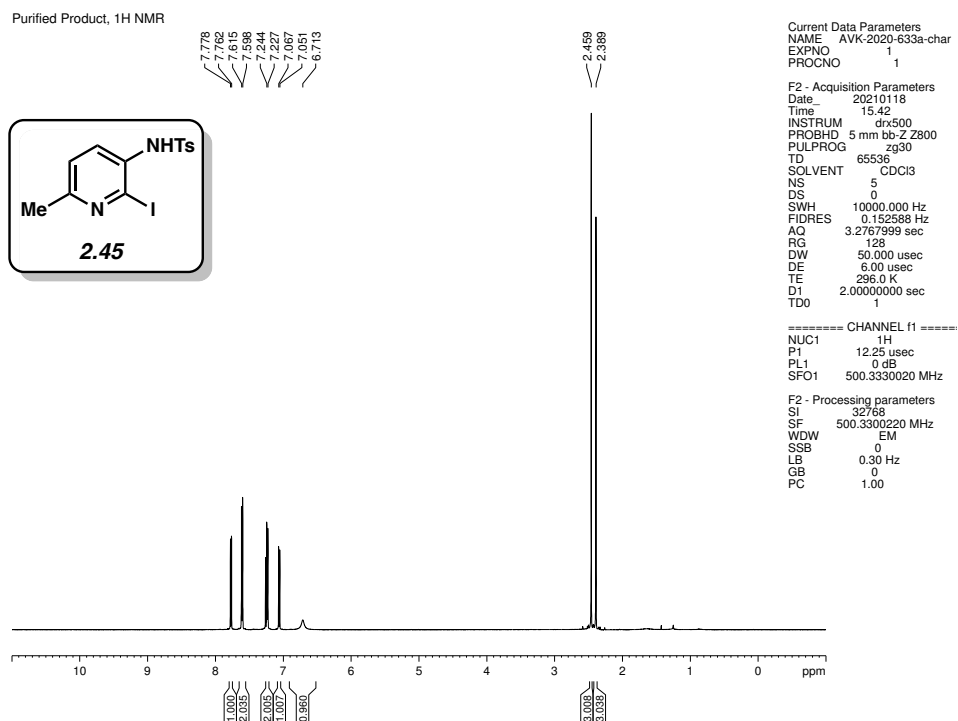


Figure 2.22. ¹H NMR (500 MHz, CDCl₃) of compound 2.45.

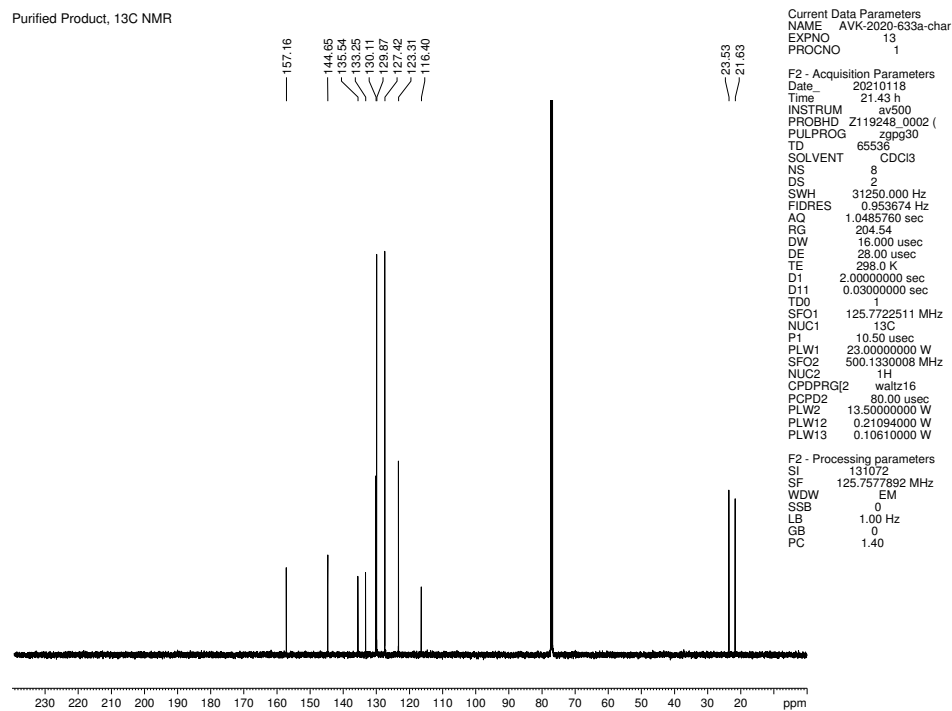


Figure 2.23. ¹³C NMR (125 MHz, CDCl₃) of compound 2.45.

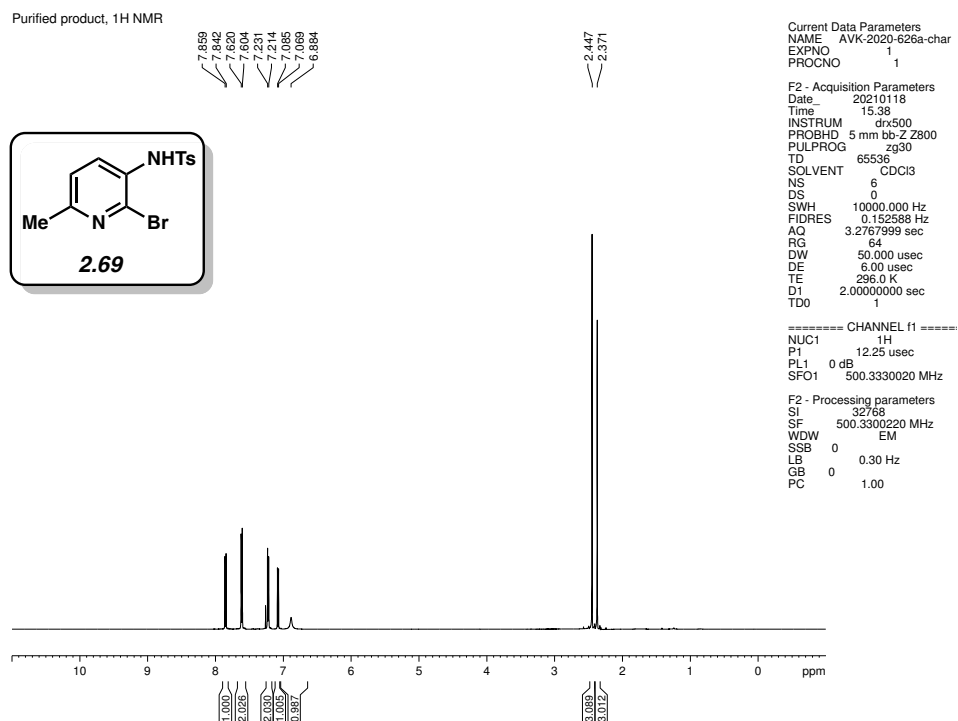


Figure 2.24. ¹H NMR (500 MHz, CDCl₃) of compound **2.69**.

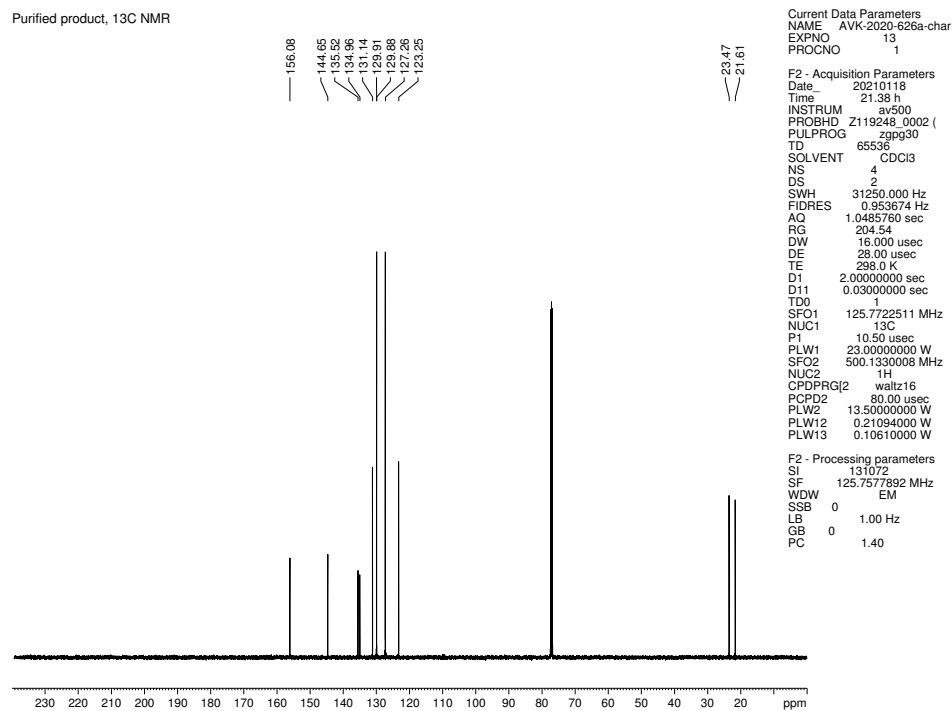


Figure 2.25. ¹³C NMR (125 MHz, CDCl₃) of compound **2.69**.

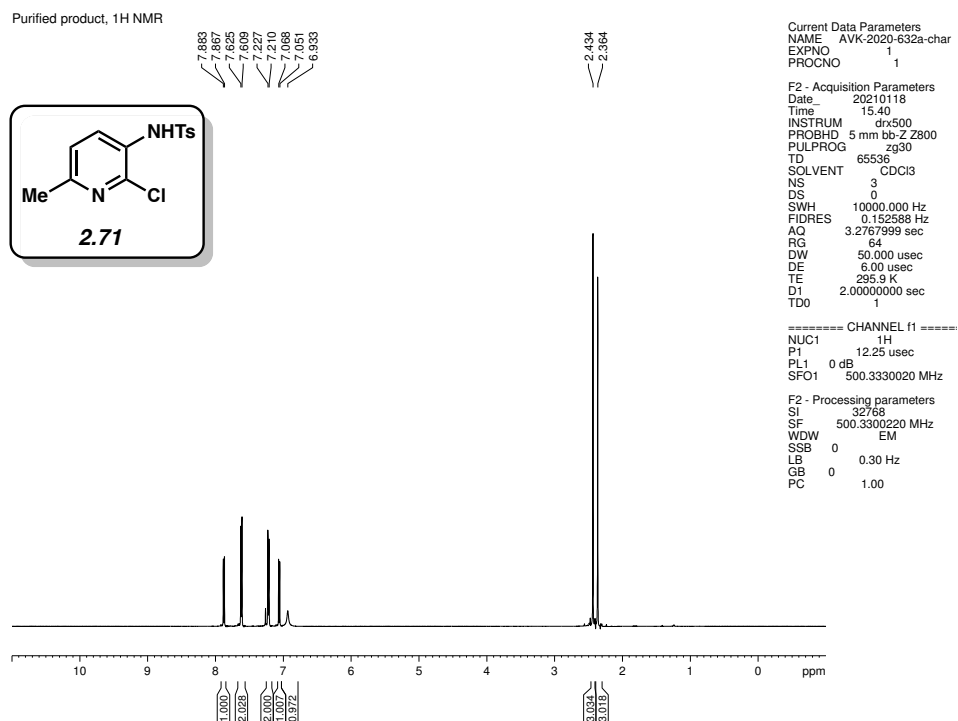


Figure 2.26. ¹H NMR (500 MHz, CDCl₃) of compound 2.71.

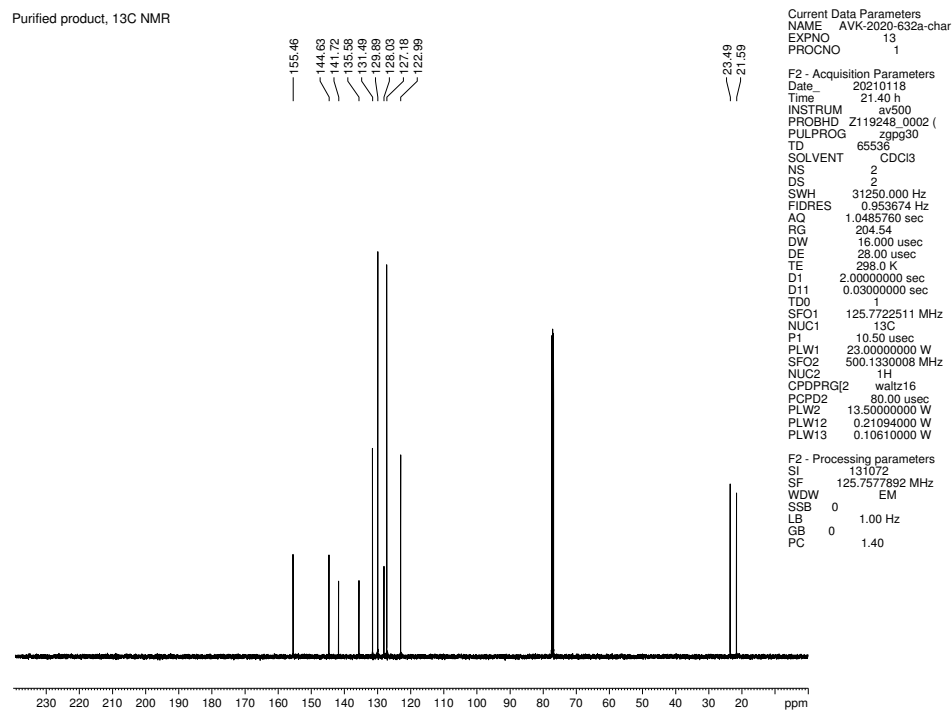


Figure 2.27. ¹³C NMR (125 MHz, CDCl₃) of compound 2.71.

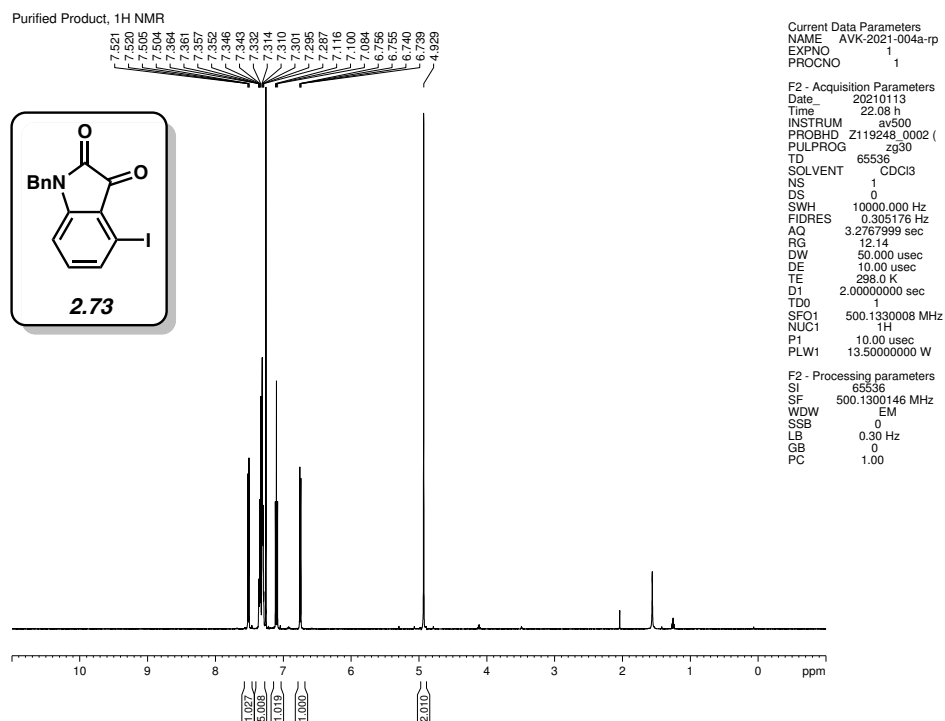


Figure 2.28. ¹H NMR (500 MHz, CDCl₃) of compound **2.73**.

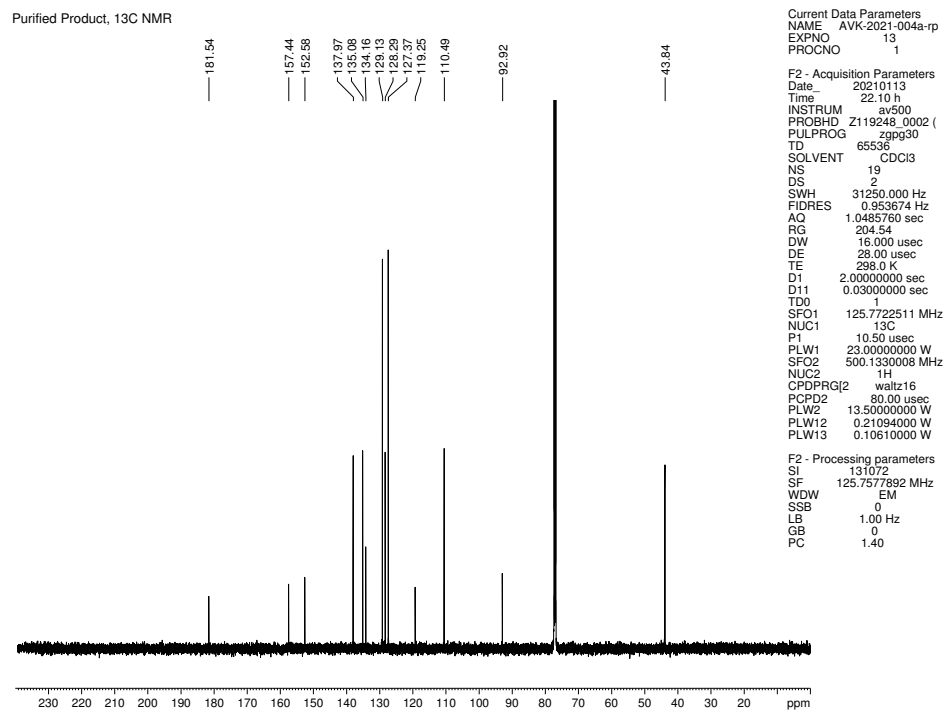


Figure 2.29. ¹³C NMR (125 MHz, CDCl₃) of compound **2.73**.

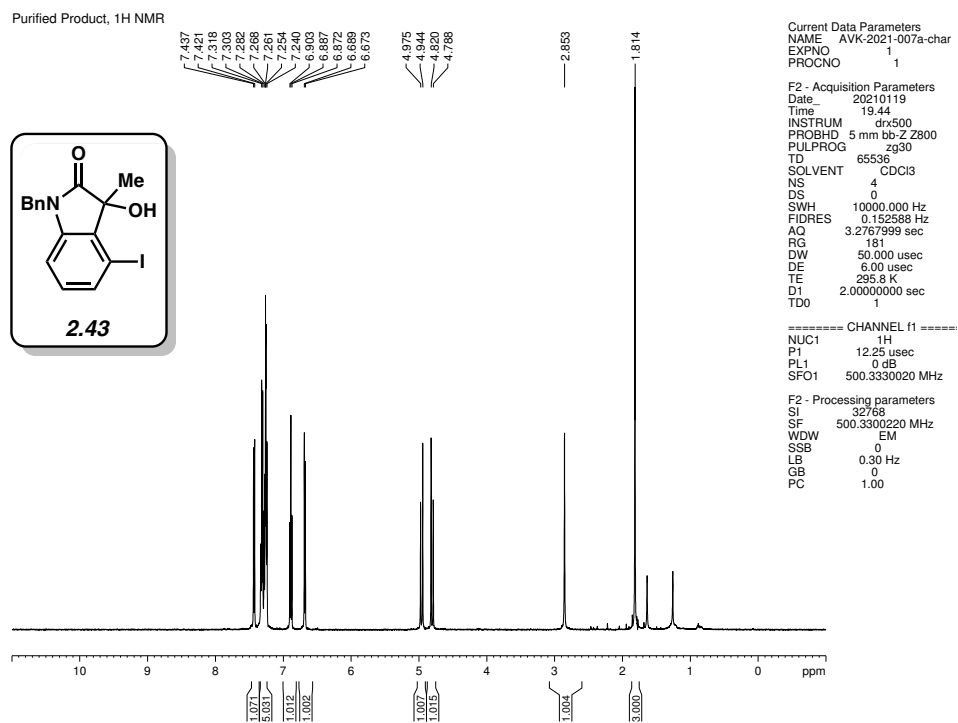


Figure 2.30. ¹H NMR (500 MHz, CDCl₃) of compound 2.43.

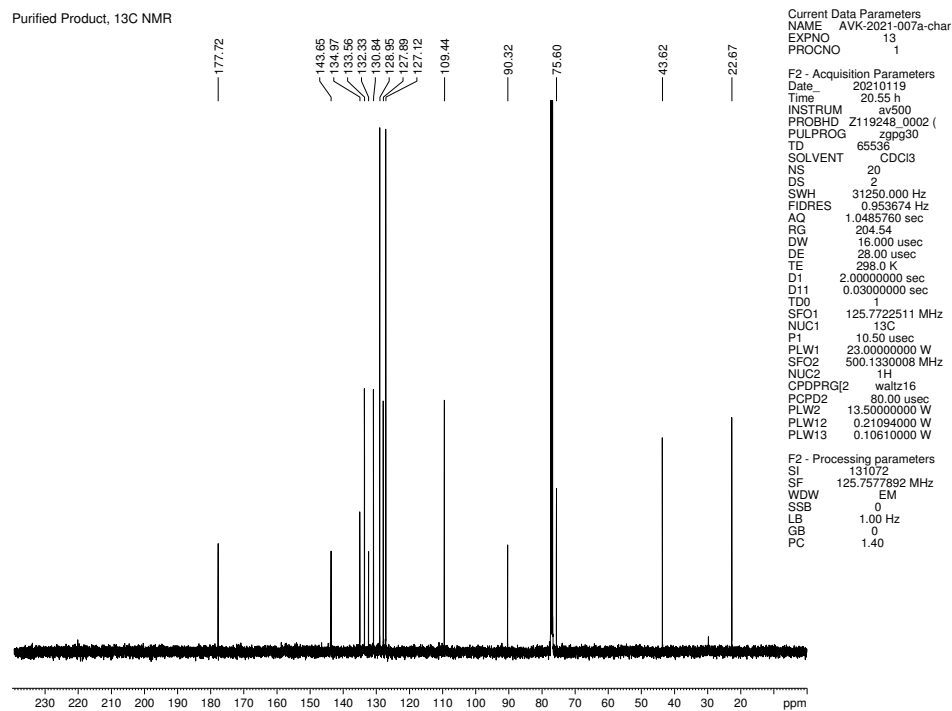


Figure 2.31. ¹³C NMR (125 MHz, CDCl₃) of compound 2.43.

Purified product, ¹H NMR

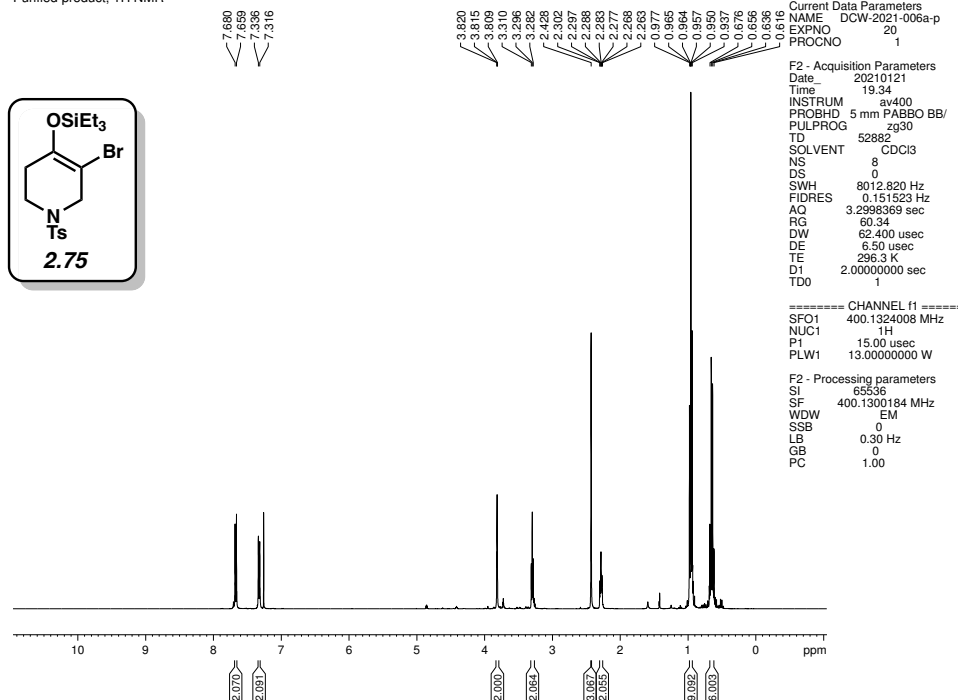


Figure 2.32. ¹H NMR (400 MHz, CDCl₃) of compound 2.75.

Purified product, ¹³C NMR

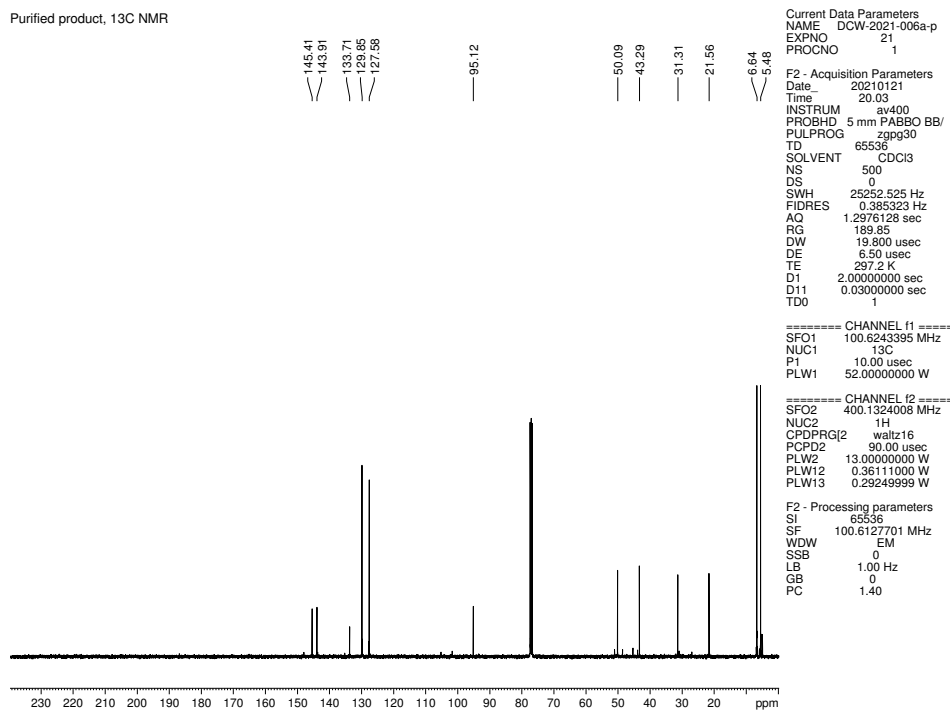


Figure 2.33. ¹³C NMR (100 MHz, CDCl₃) of compound 2.75.

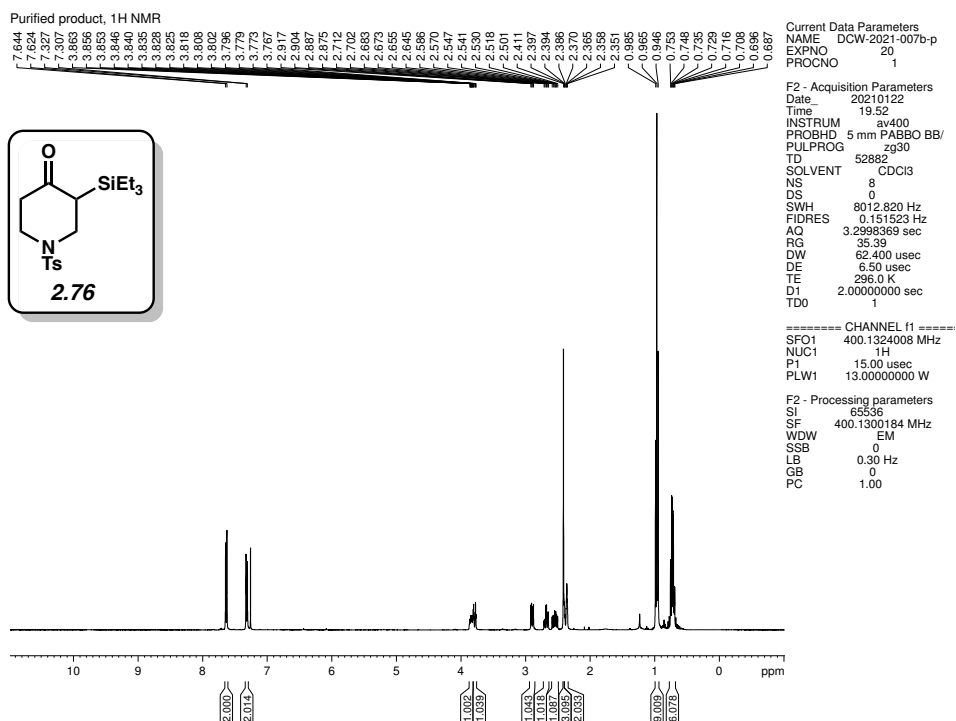


Figure 2.34. ¹H NMR (400 MHz, CDCl₃) of compound 2.76.

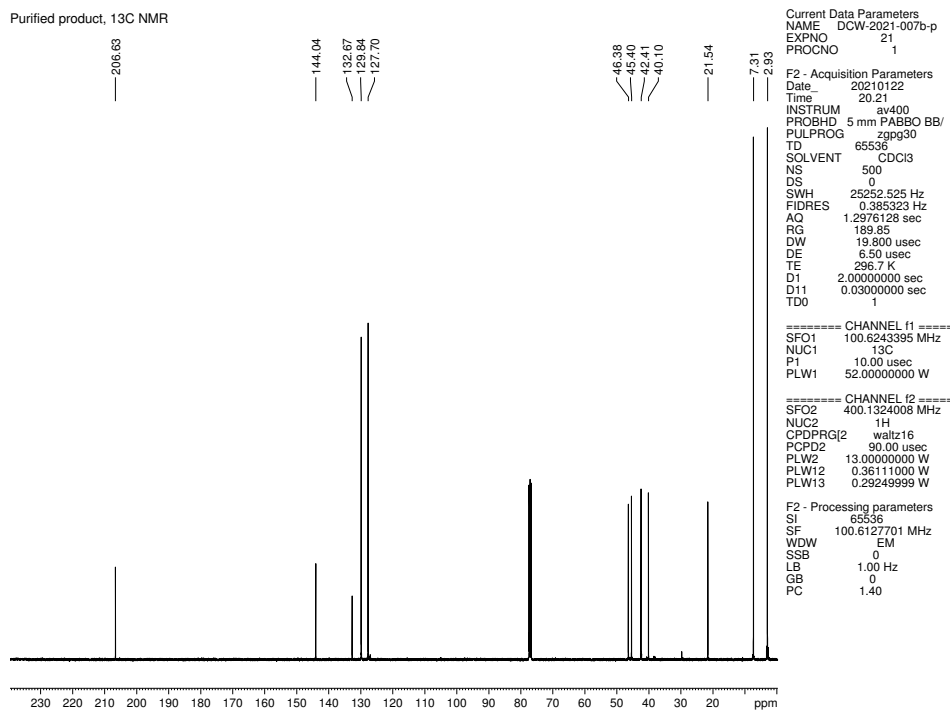


Figure 2.35. ¹³C NMR (100 MHz, CDCl₃) of compound 2.76.

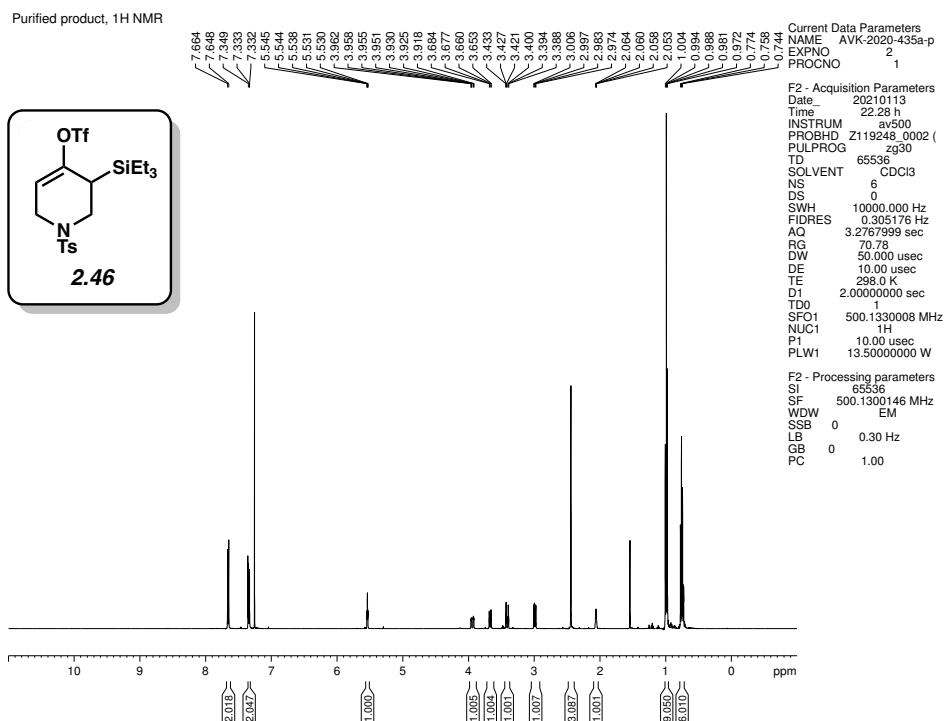


Figure 2.36. ¹H NMR (500 MHz, CDCl₃) of compound 2.46.

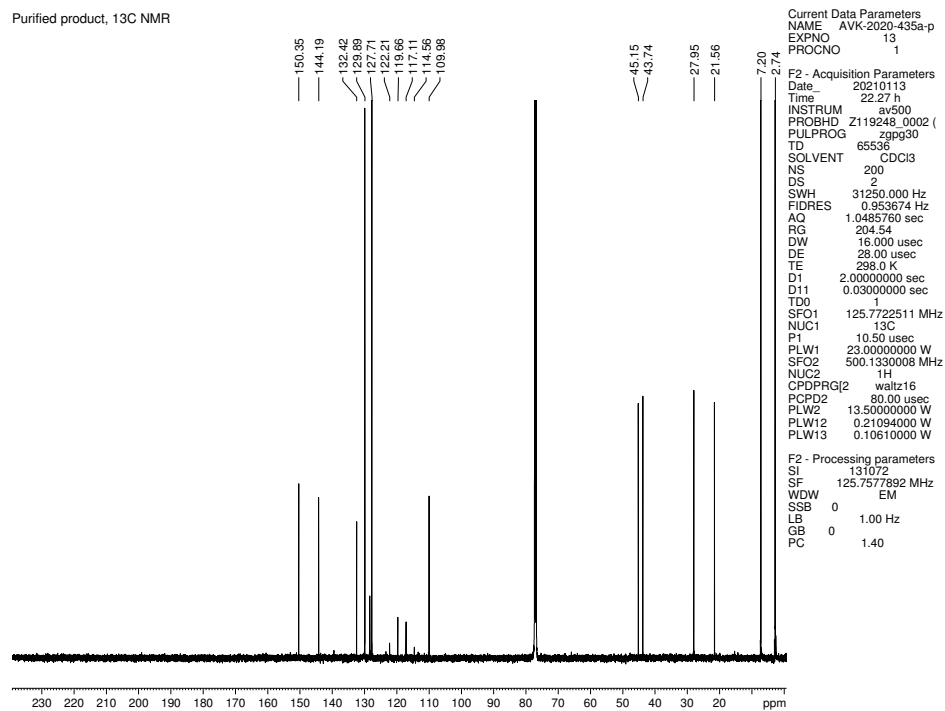


Figure 2.37. ¹³C NMR (125 MHz, CDCl₃) of compound 2.46.

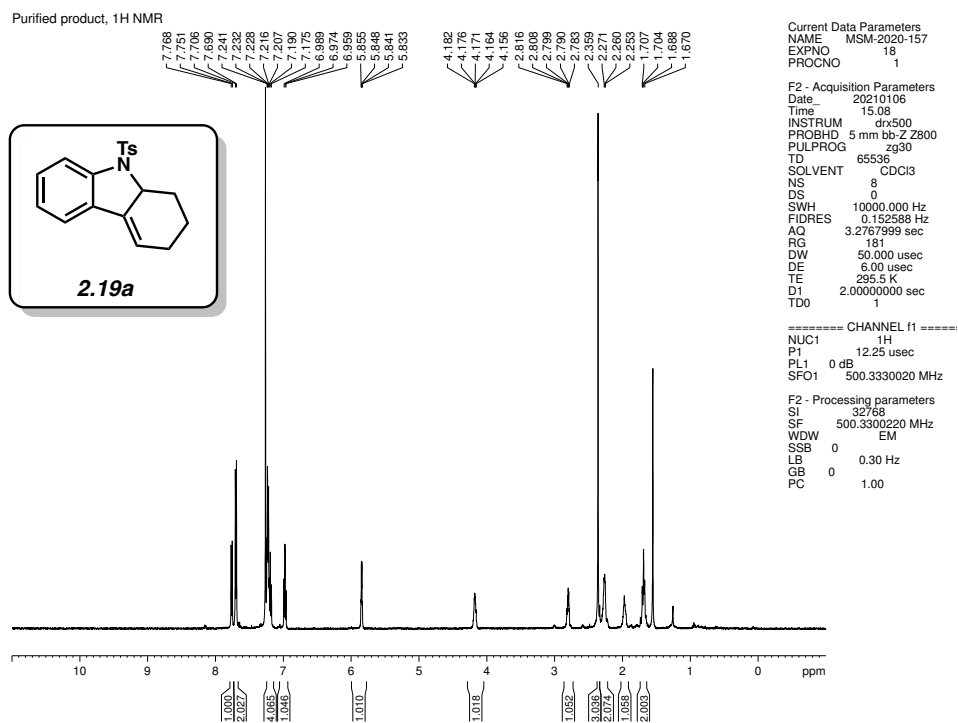


Figure 2.38. ¹H NMR (500 MHz, CDCl₃) of compound **2.19a**.

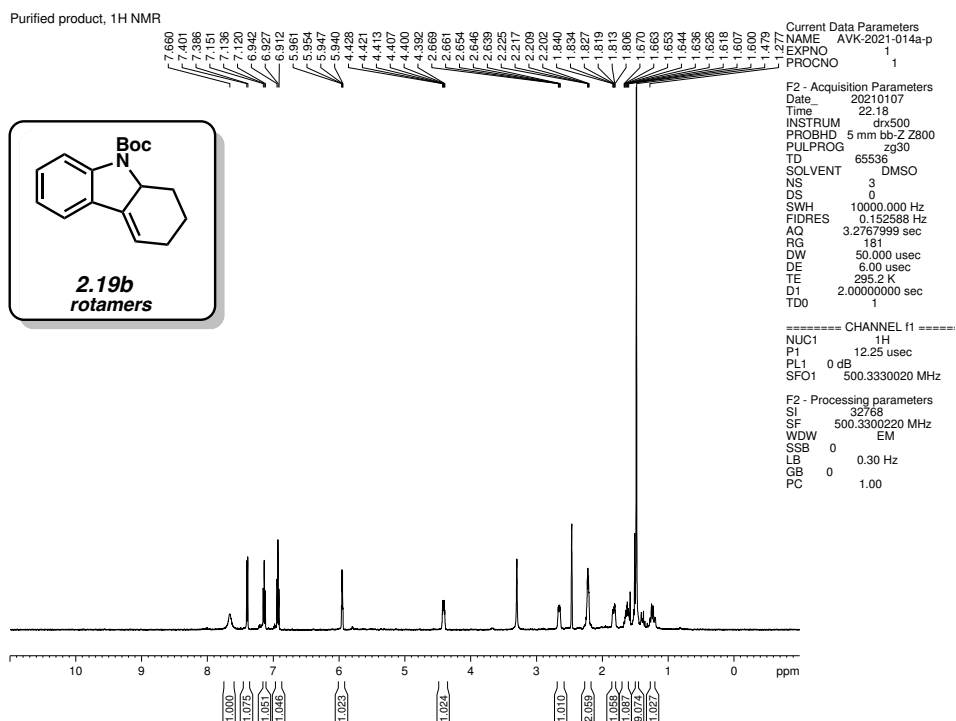


Figure 2.39. ¹H NMR (500 MHz, DMSO-d₆) of compound 2.19b.

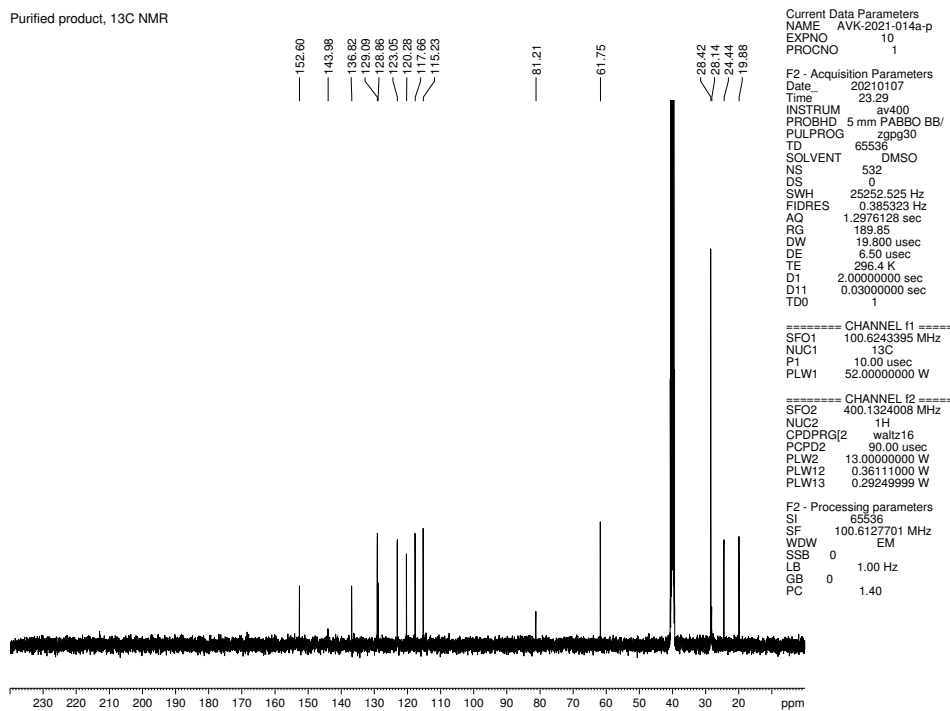


Figure 2.40. ¹³C NMR (100 MHz, DMSO-d₆) of compound 2.19b.

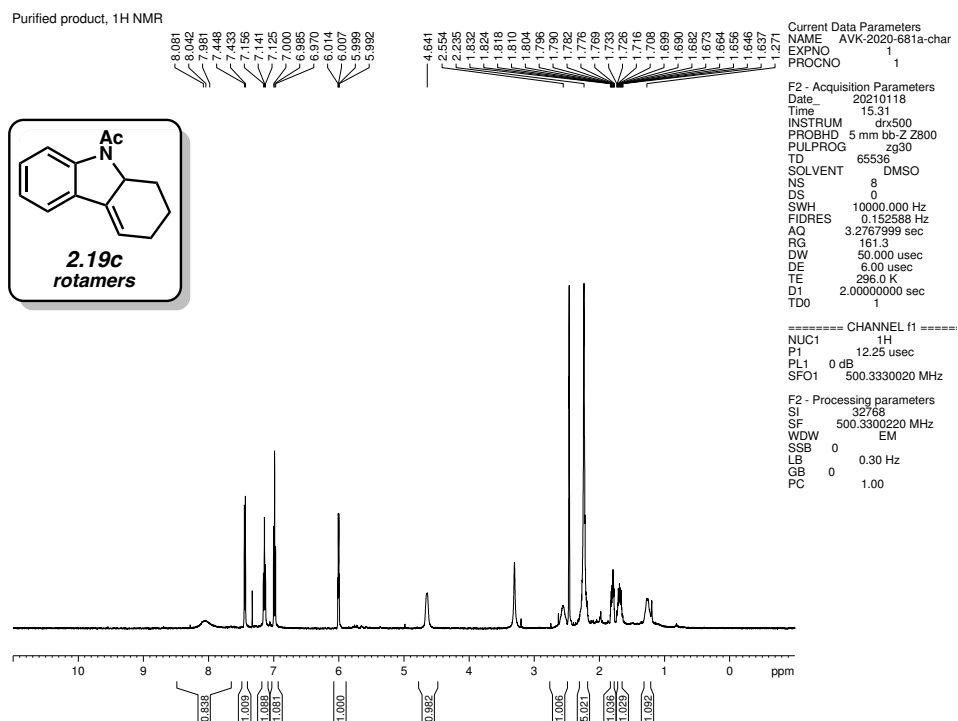


Figure 2.41. ¹H NMR (500 MHz, DMSO-d₆) of compound **2.19c**.

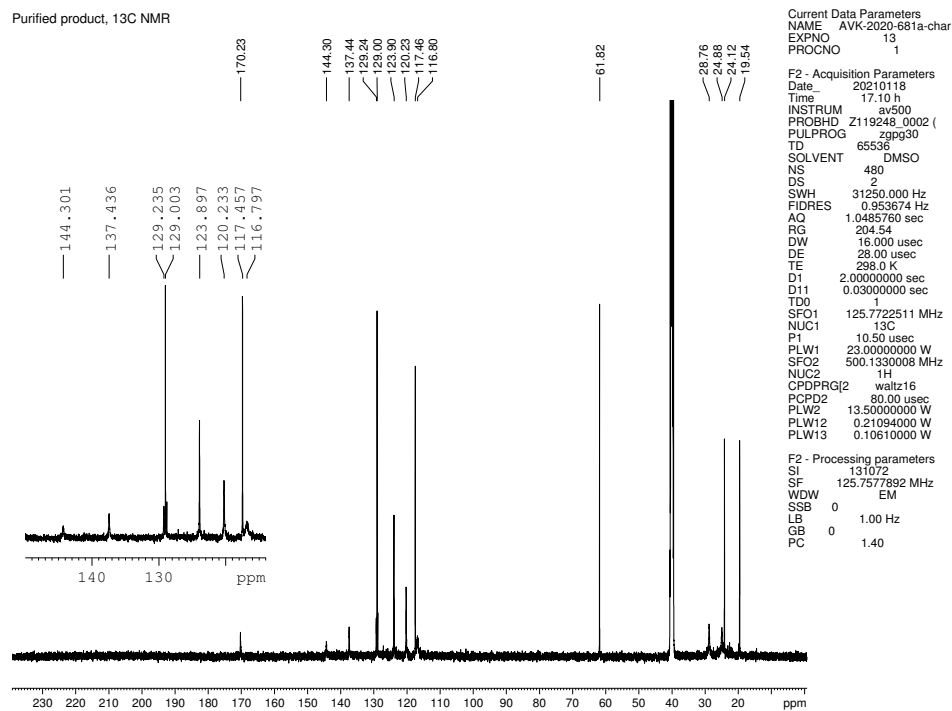


Figure 2.42. ¹³C NMR (125 MHz, DMSO-d₆) of compound **2.19c**.

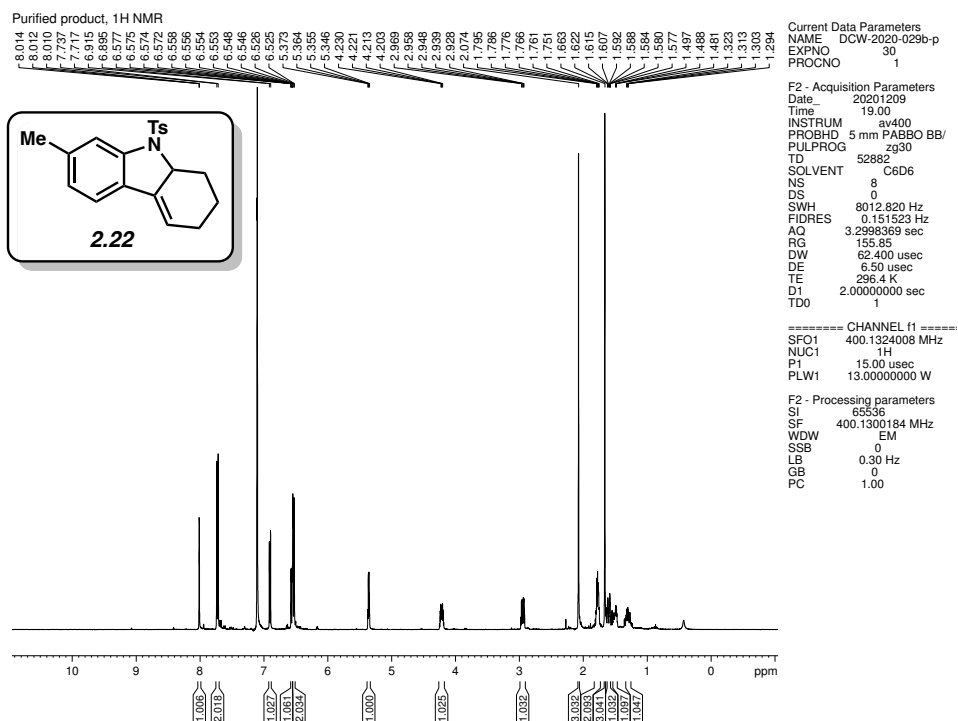


Figure 2.43. ¹H NMR (400 MHz, CDCl₃) of compound 2.22.

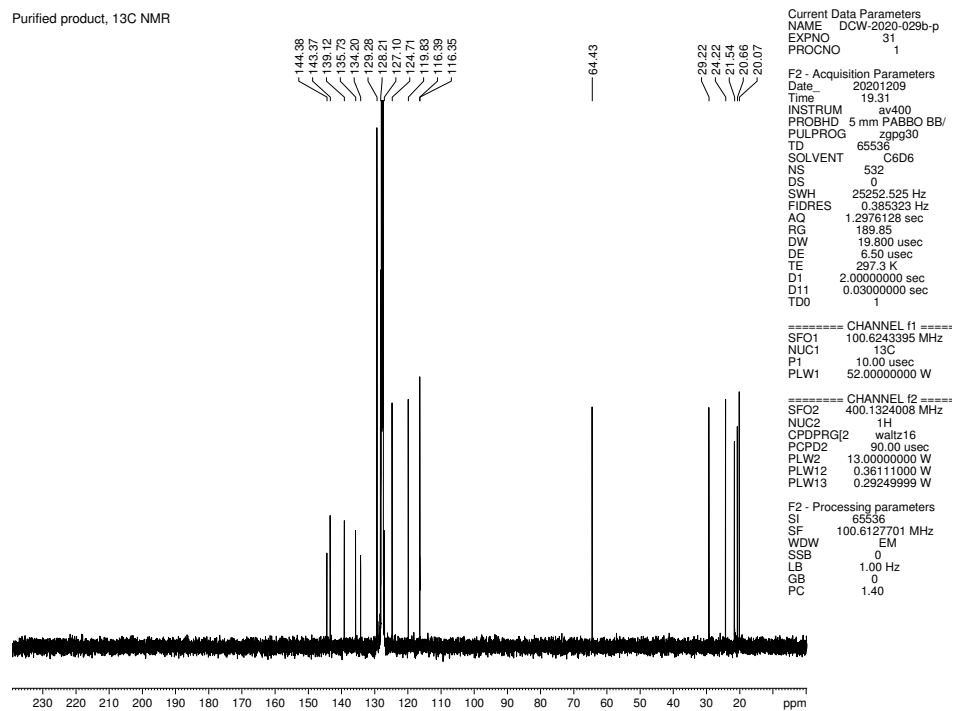


Figure 2.44. ¹³C NMR (100 MHz, CDCl₃) of compound 2.22.

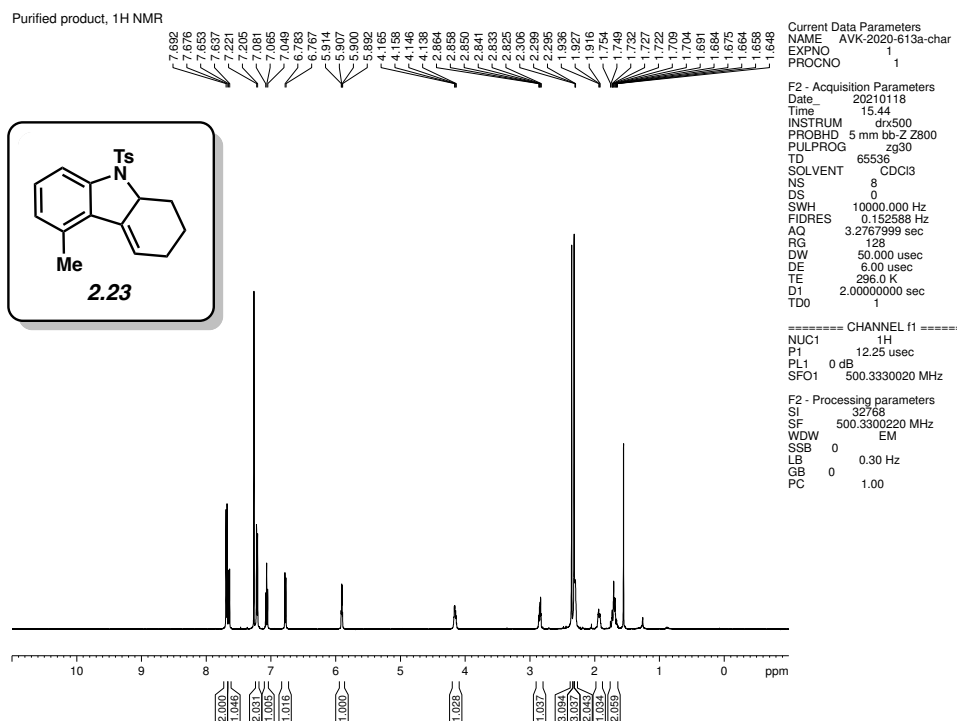


Figure 2.45. ¹H NMR (500 MHz, CDCl₃) of compound 2.23.

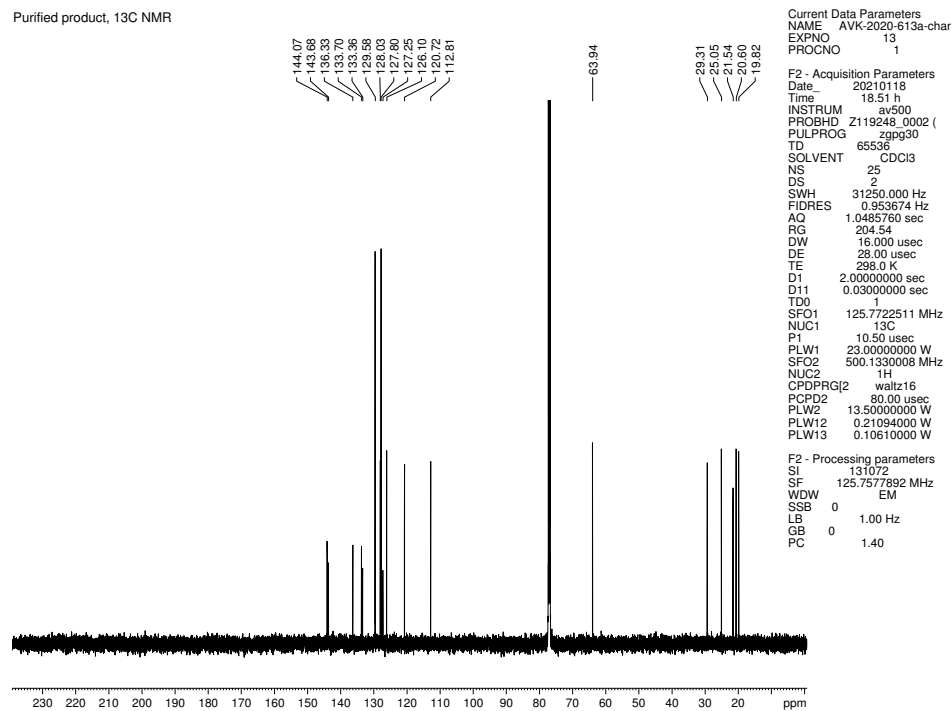


Figure 2.46. ¹³C NMR (125 MHz, CDCl₃) of compound 2.23.

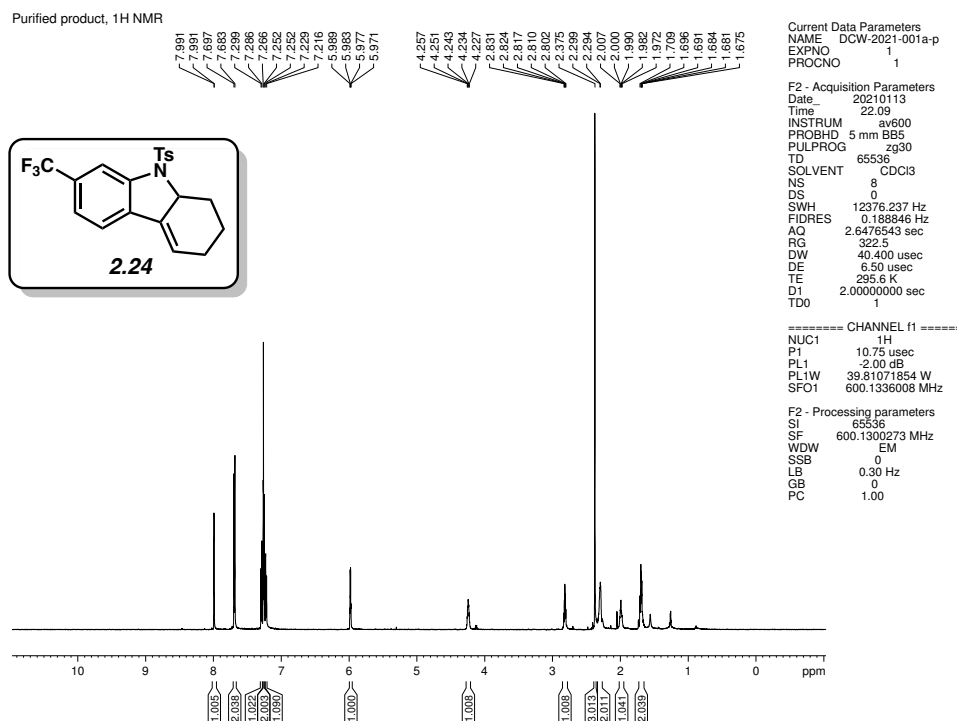


Figure 2.47. ¹H NMR (600 MHz, CDCl₃) of compound 2.24.

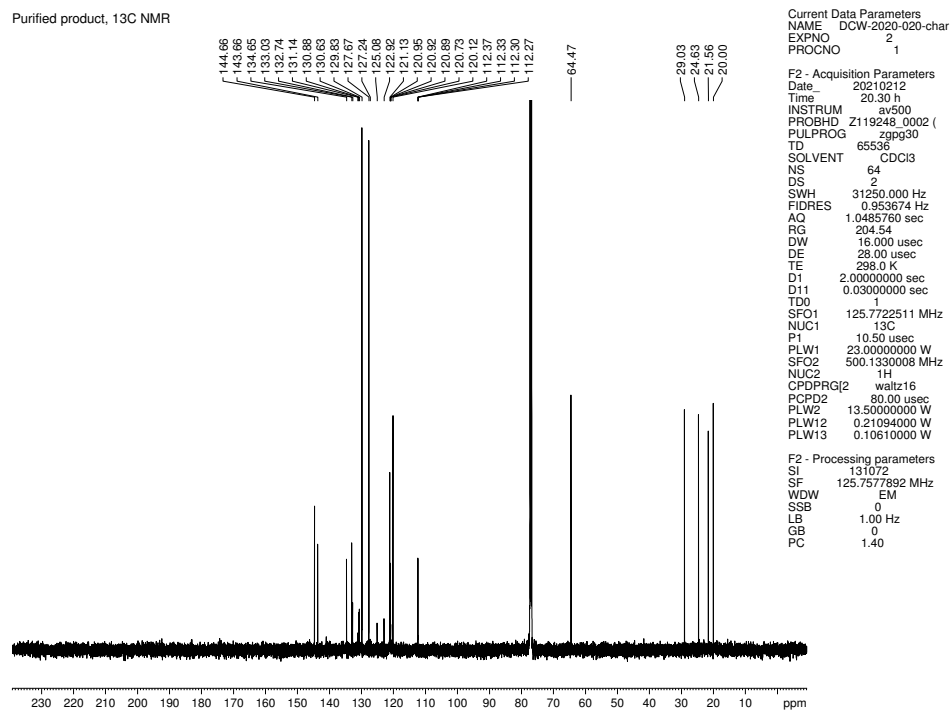


Figure 2.48. ¹³C NMR (125 MHz, CDCl₃) of compound 2.24.

Purified product, ^{19}F NMR

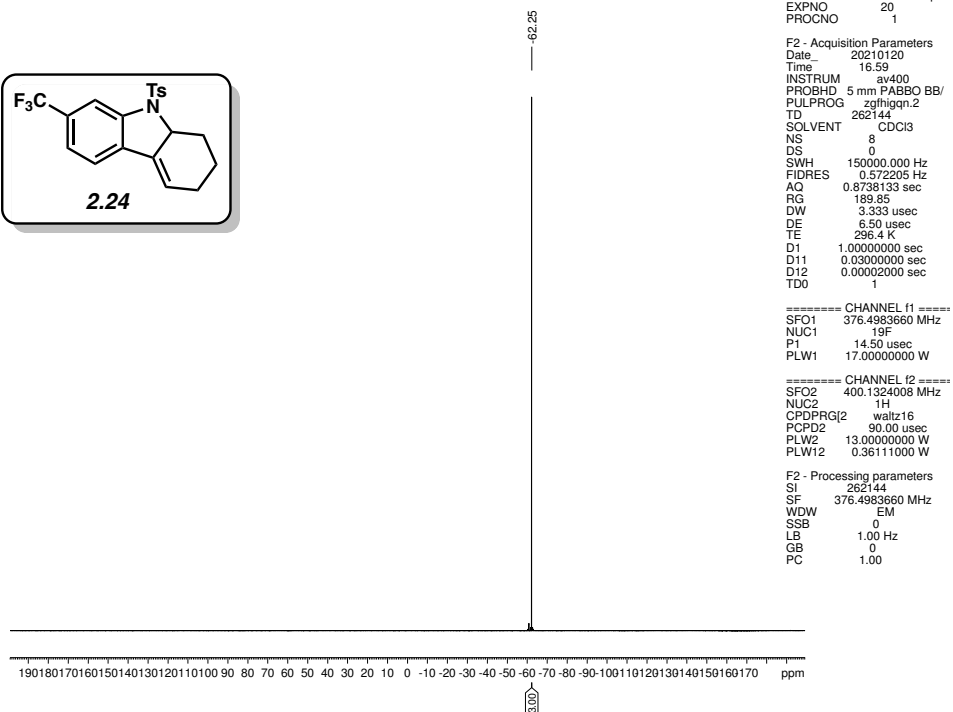
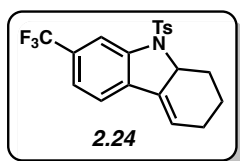


Figure 2.49. ^{19}F NMR (376 MHz, CDCl_3) of compound 2.24.

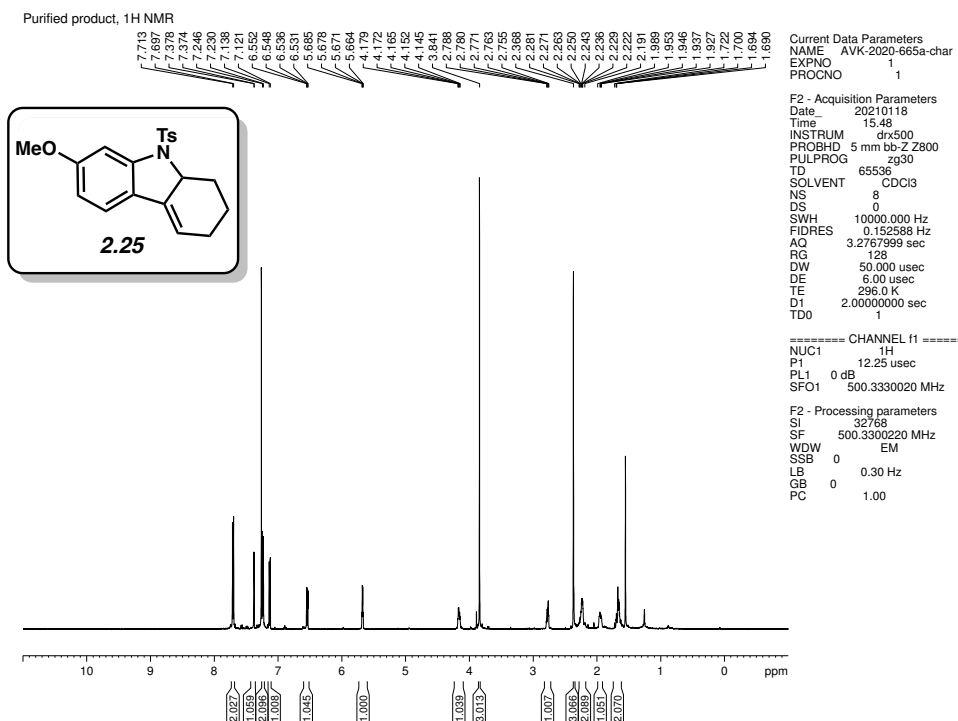


Figure 2.50. ¹H NMR (500 MHz, CDCl₃) of compound 2.25.

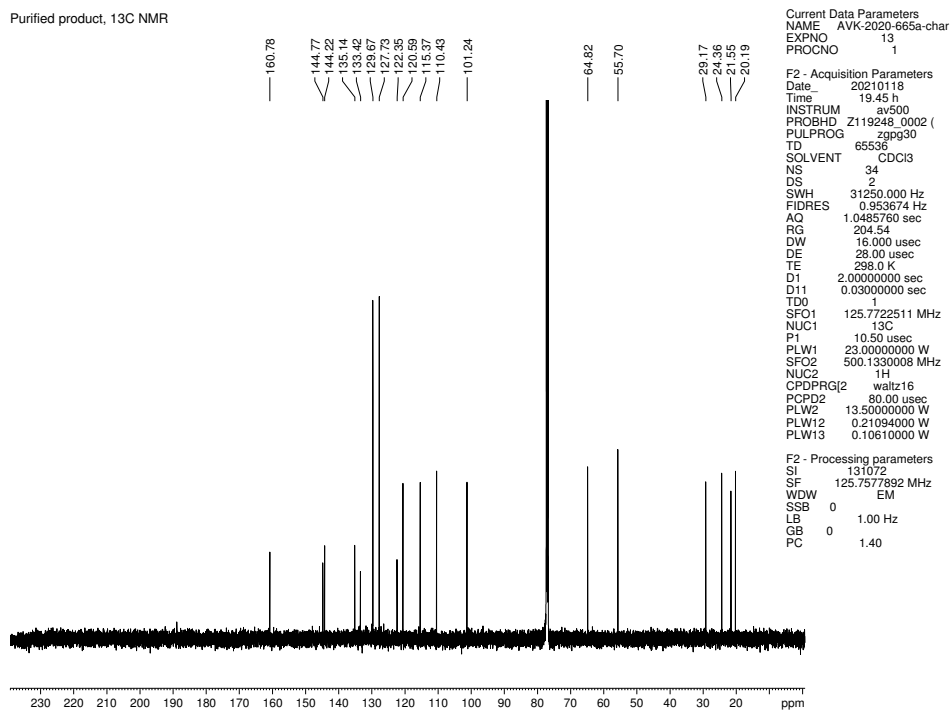


Figure 2.51. ¹³C NMR (125 MHz, CDCl₃) of compound 2.25.

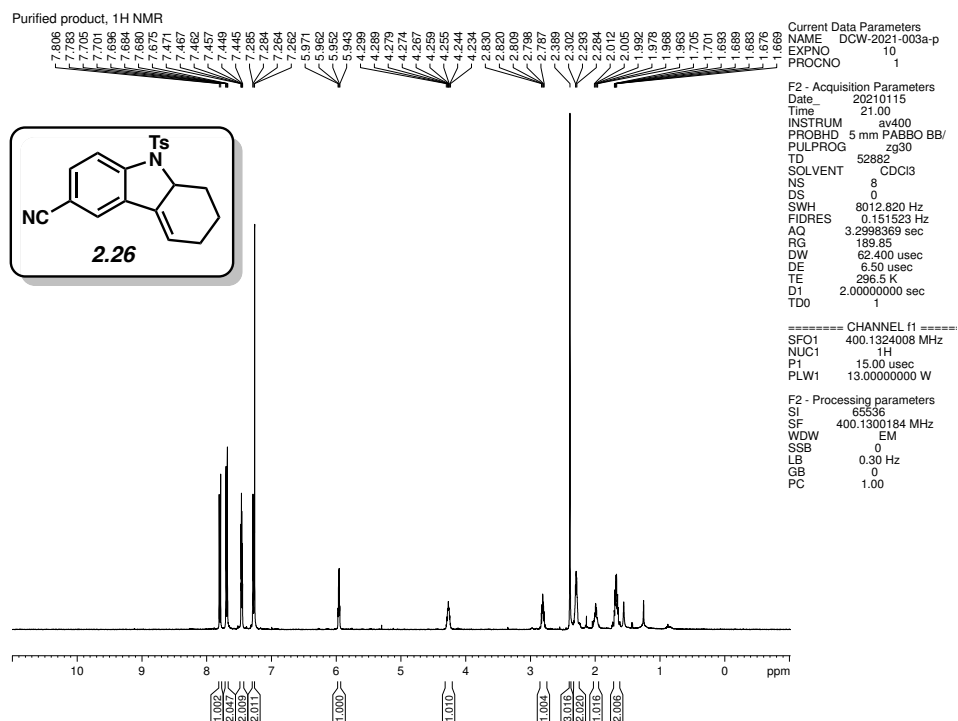


Figure 2.52. ¹H NMR (400 MHz, CDCl₃) of compound 2.26.

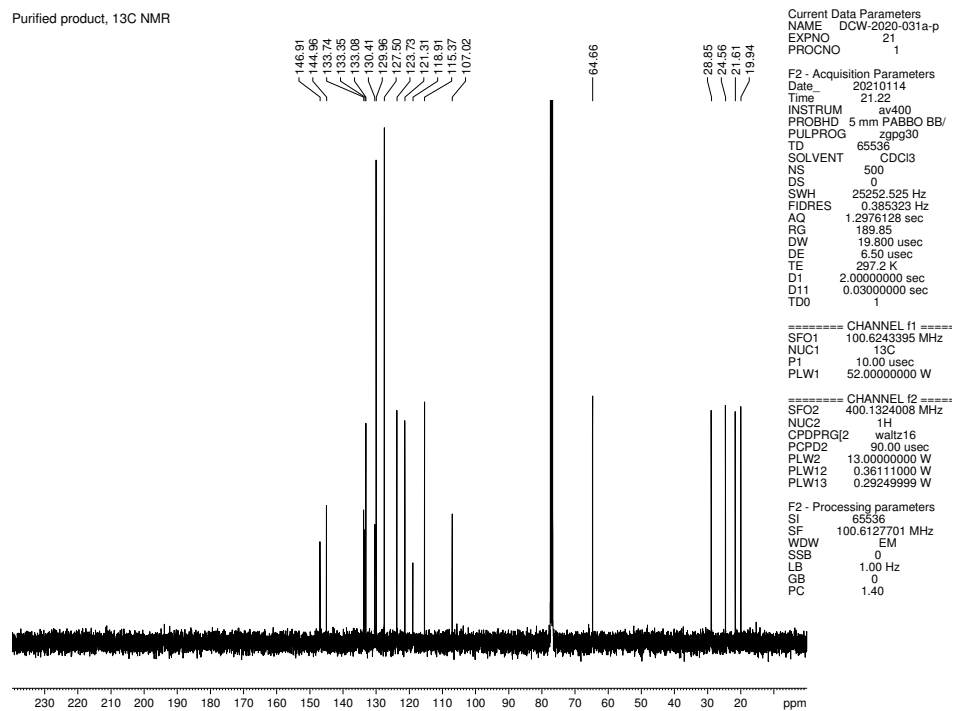


Figure 2.53. ¹³C NMR (100 MHz, CDCl₃) of compound 2.26.

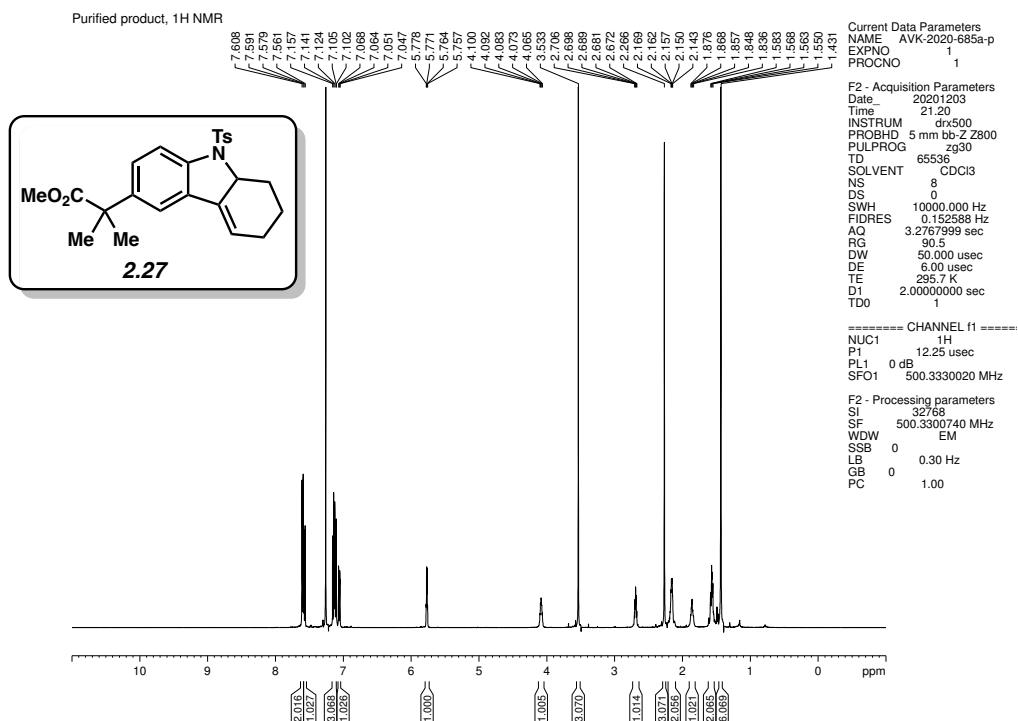


Figure 2.54. ¹H NMR (500 MHz, CDCl₃) of compound 2.27.

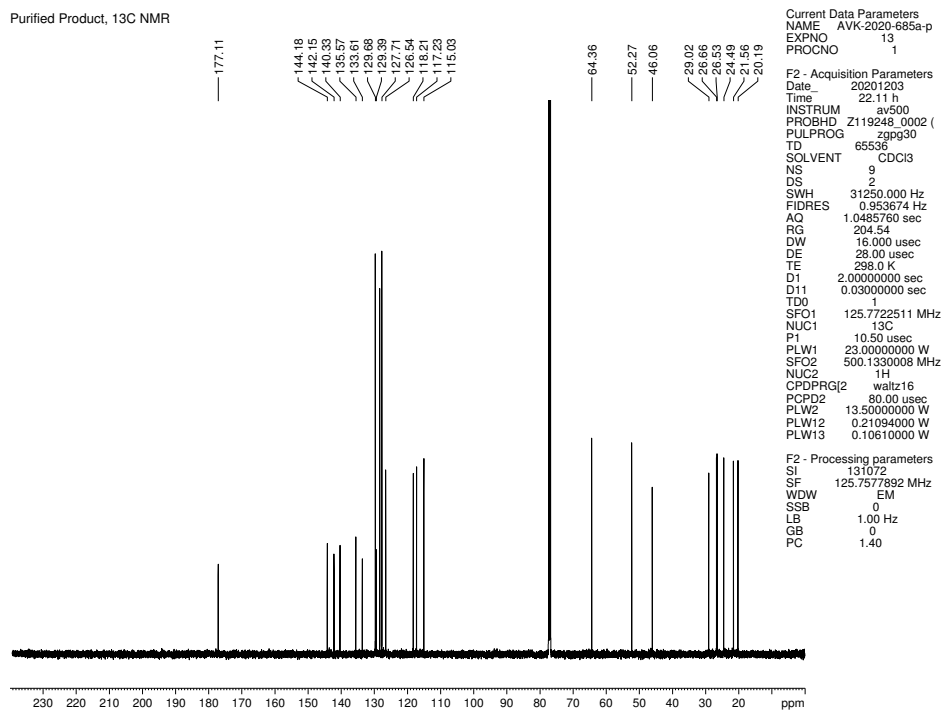


Figure 2.55. ¹³C NMR (125 MHz, CDCl₃) of compound 2.27.

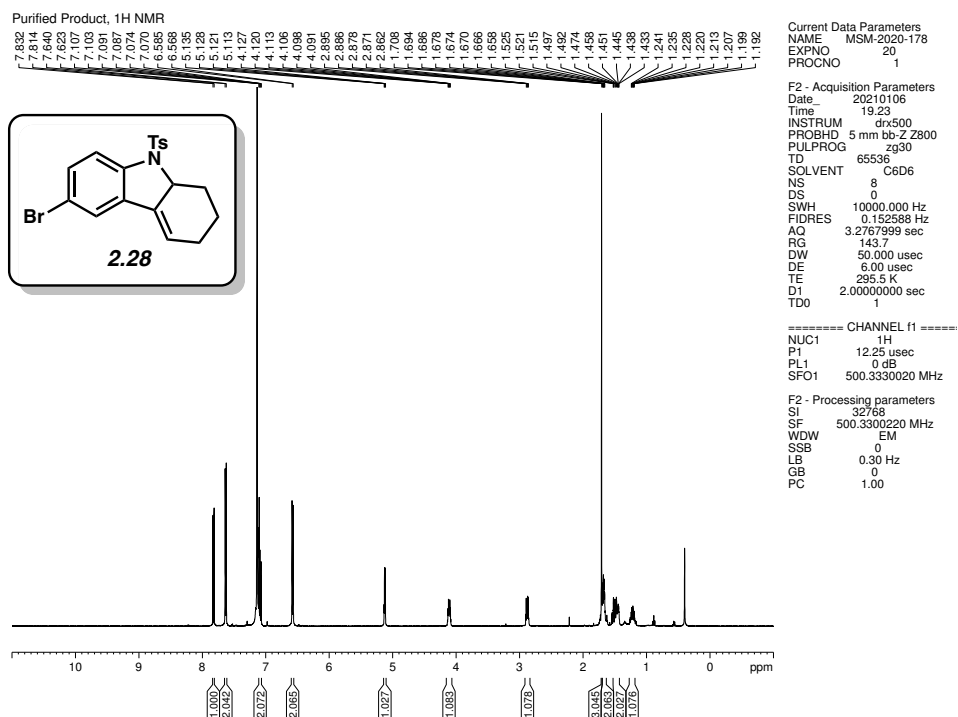


Figure 2.56. ¹H NMR (500 MHz, CDCl₃) of compound 2.28.

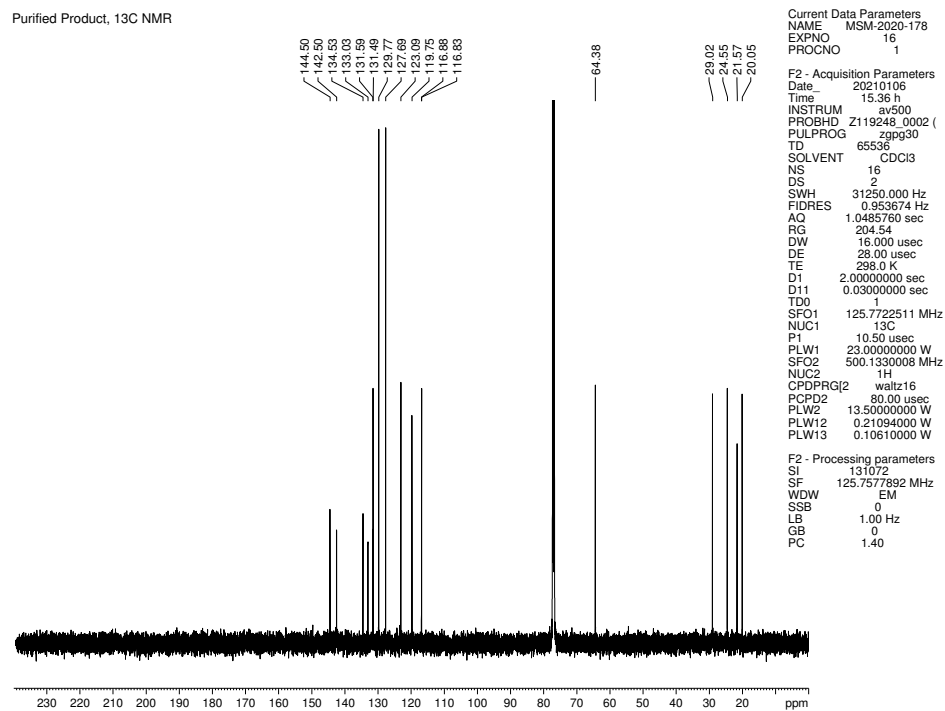


Figure 2.57. ¹³C NMR (125 MHz, CDCl₃) of compound 2.28.

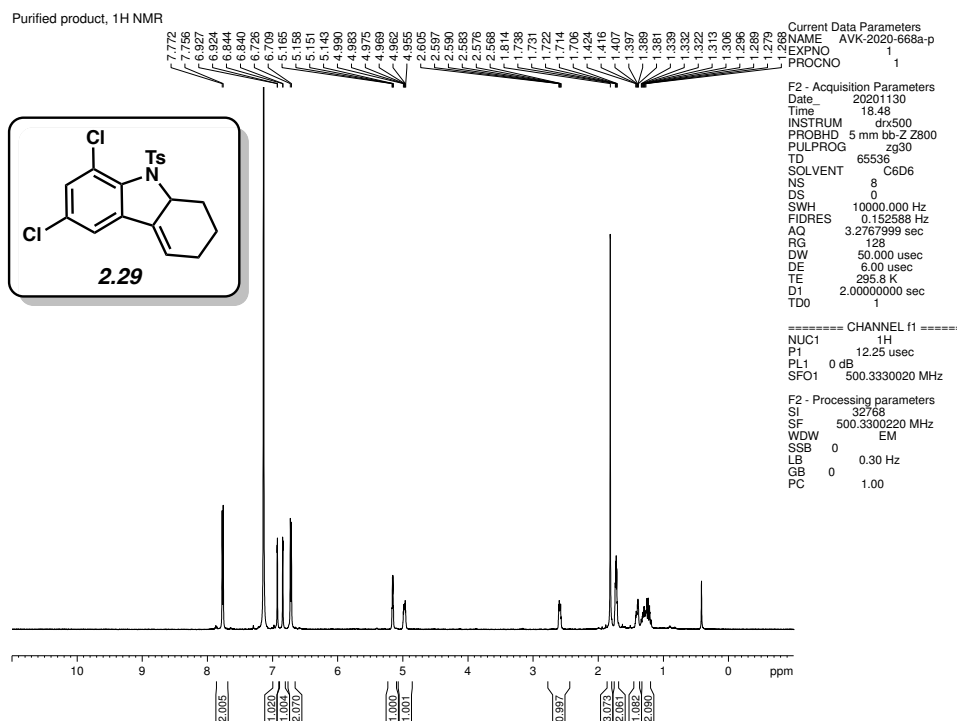


Figure 2.58. ¹H NMR (500 MHz, CDCl₃) of compound 2.29.

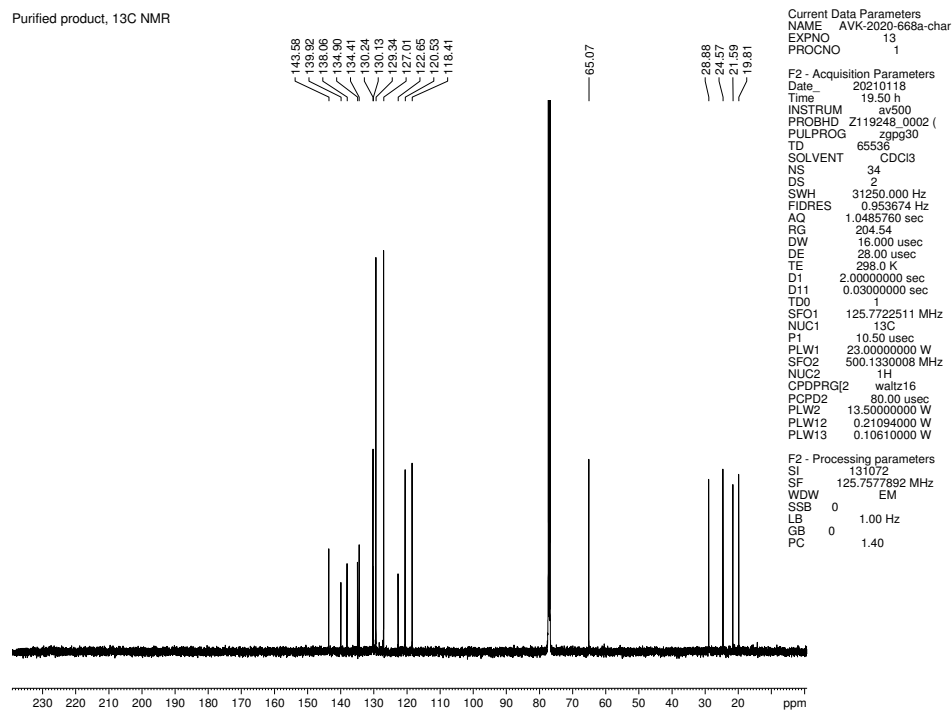


Figure 2.59. ¹³C NMR (125 MHz, CDCl₃) of compound 2.29.

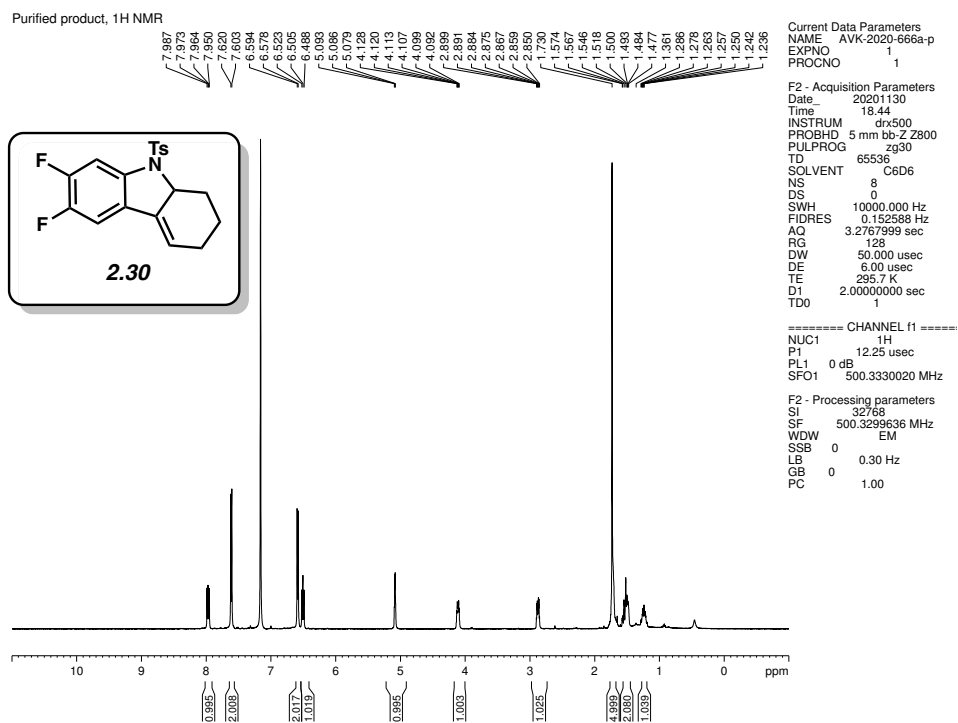


Figure 2.60. ¹H NMR (500 MHz, CDCl₃) of compound 2.30.

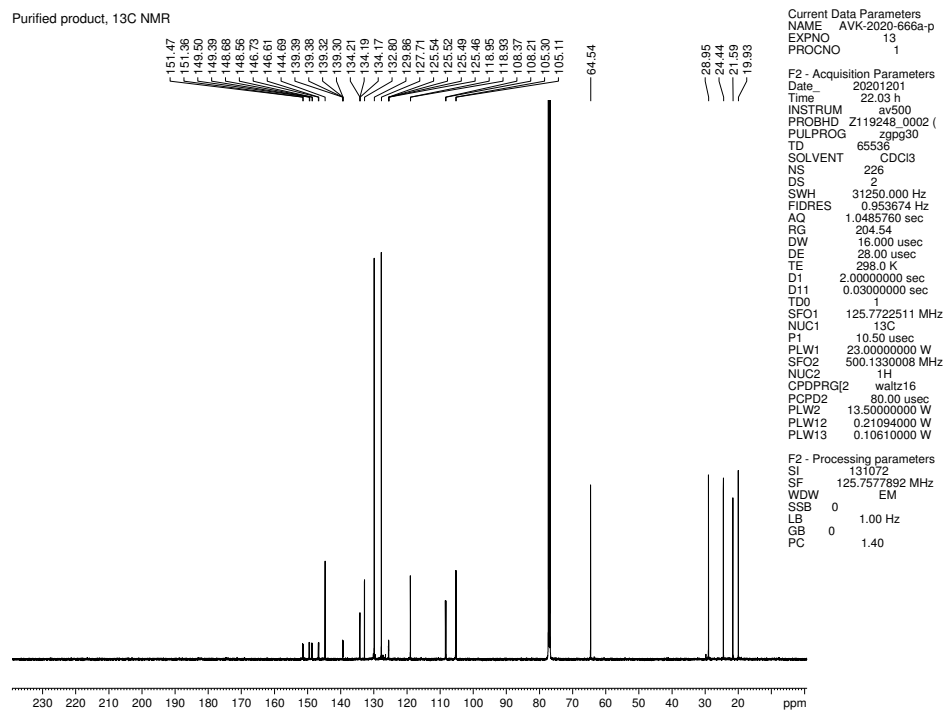


Figure 2.61. ¹³C NMR (125 MHz, CDCl₃) of compound 2.30.

Purified product, ¹⁹F NMR

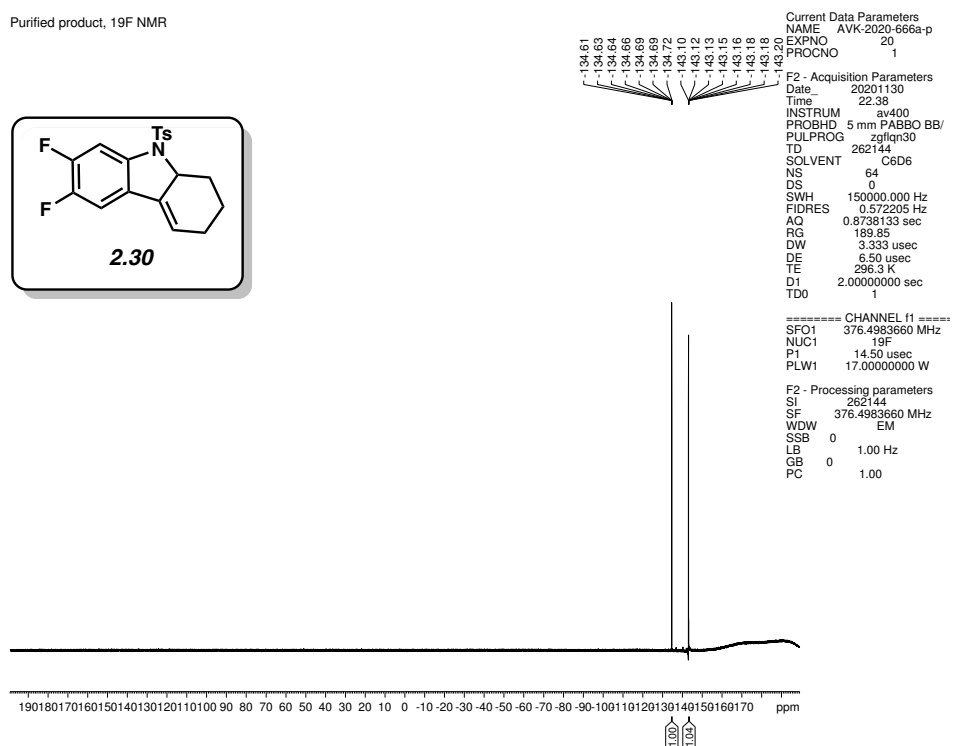
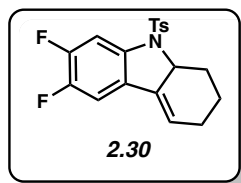


Figure 2.62. ¹⁹F NMR (376 MHz, CDCl₃) of compound **2.30**.

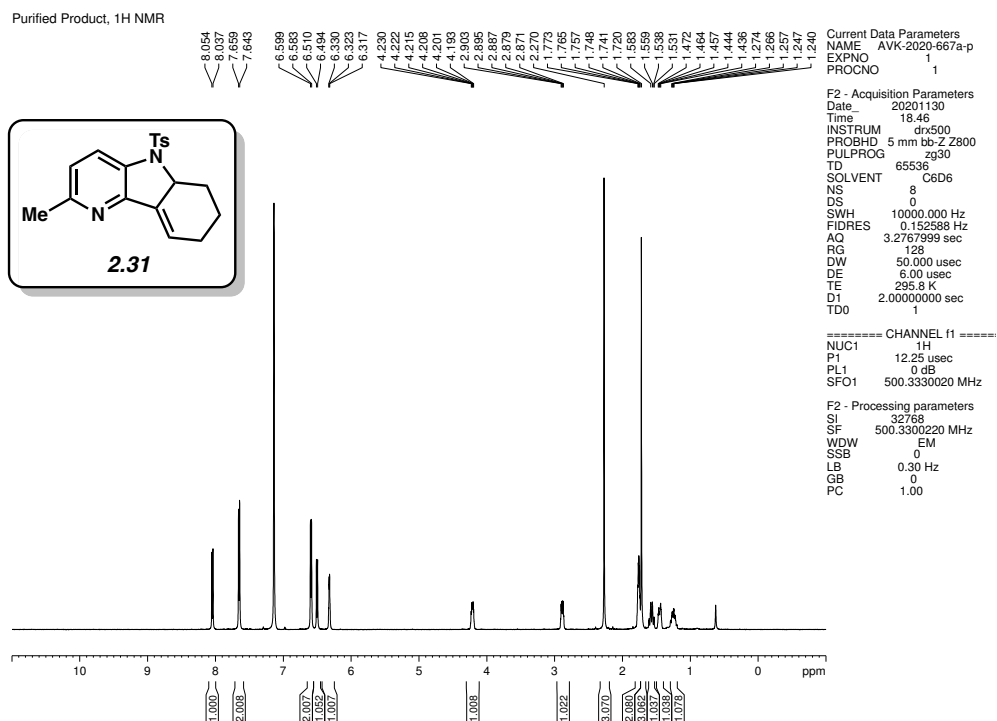


Figure 2.63. ¹H NMR (500 MHz, CDCl₃) of compound 2.31.

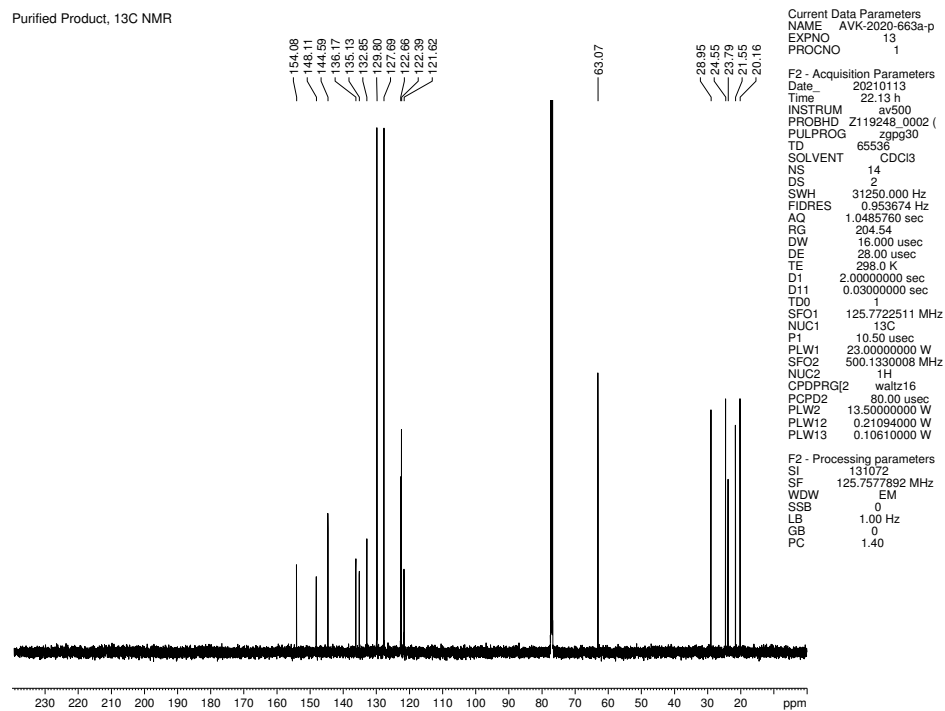


Figure 2.64. ¹³C NMR (125 MHz, CDCl₃) of compound 2.31.

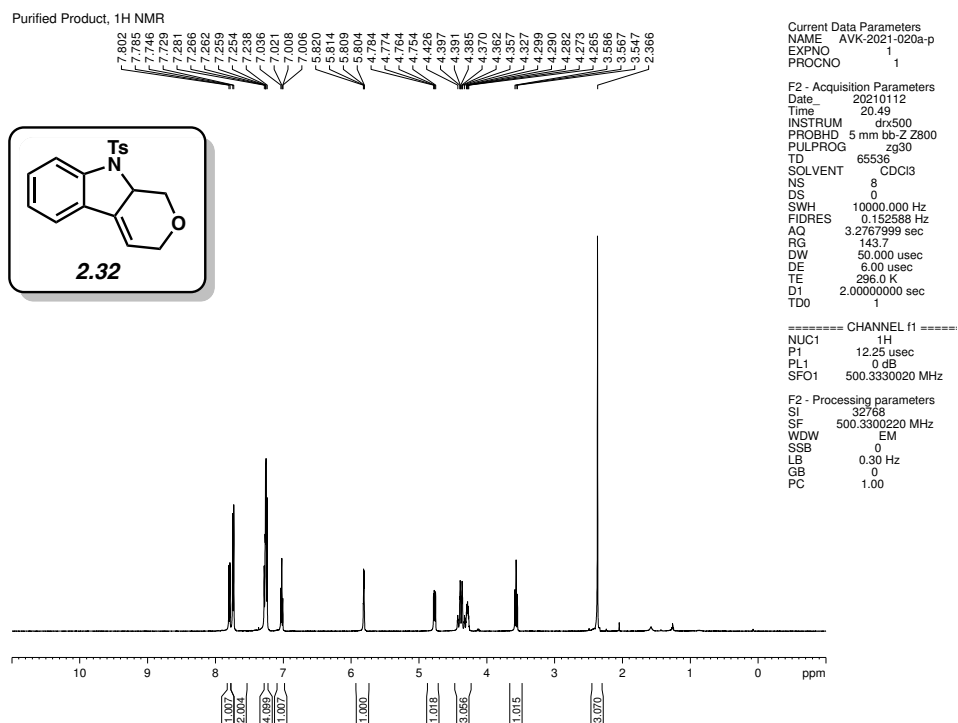


Figure 2.65. ¹H NMR (500 MHz, CDCl₃) of compound 2.32.

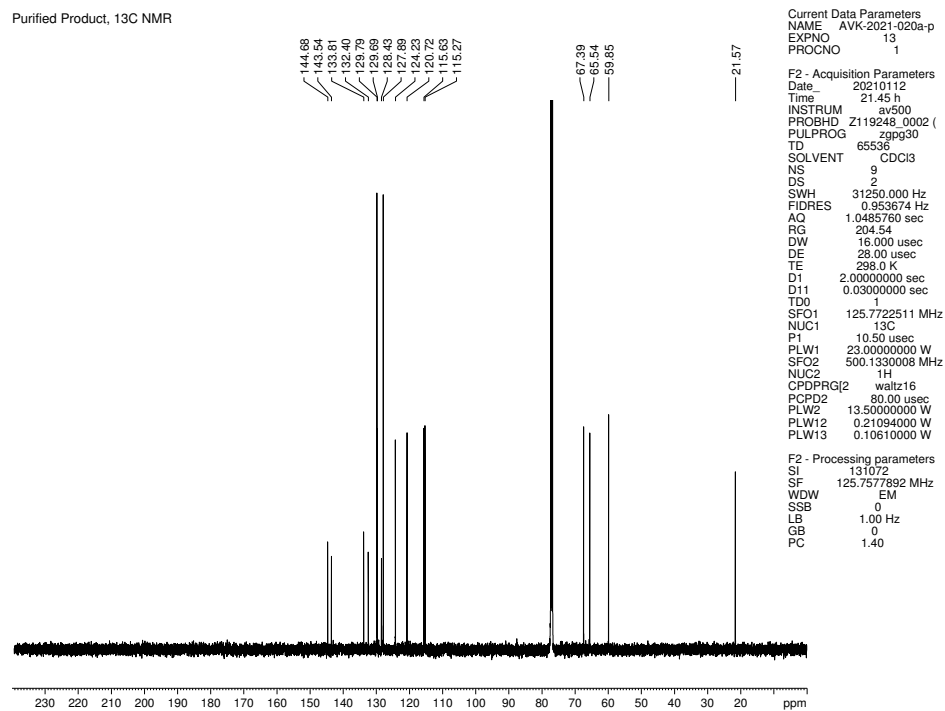


Figure 2.66. ¹³C NMR (125 MHz, CDCl₃) of compound 2.32.

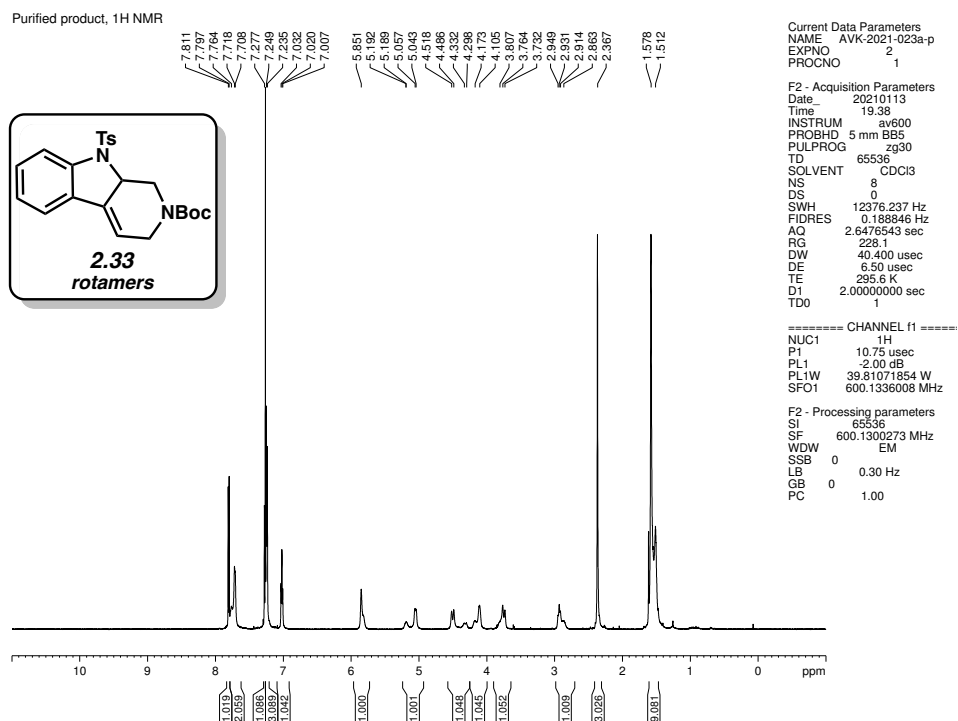


Figure 2.67. ¹H NMR (600 MHz, CDCl₃) of compound 2.33.

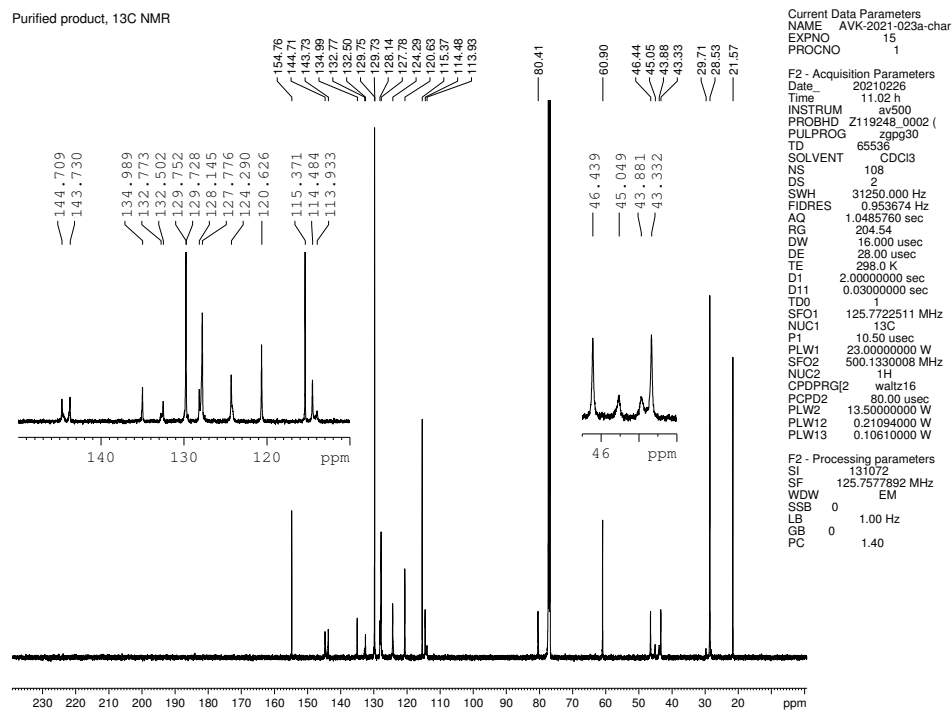


Figure 2.68. ¹³C NMR (125 MHz, CDCl₃) of compound 2.33.

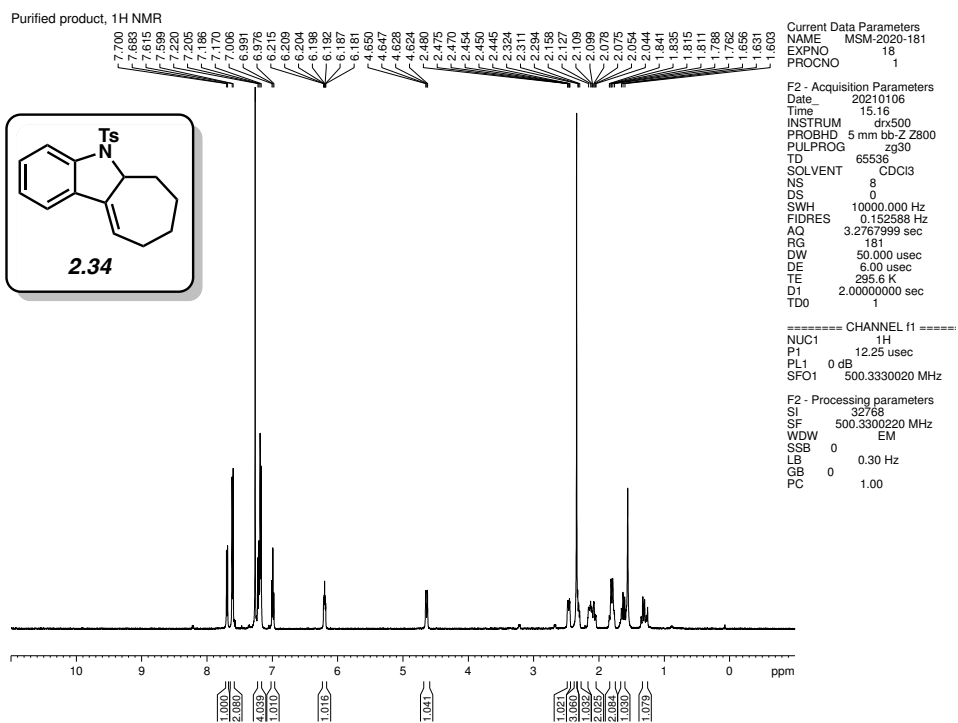


Figure 2.69. ¹H NMR (500 MHz, CDCl₃) of compound 2.34.

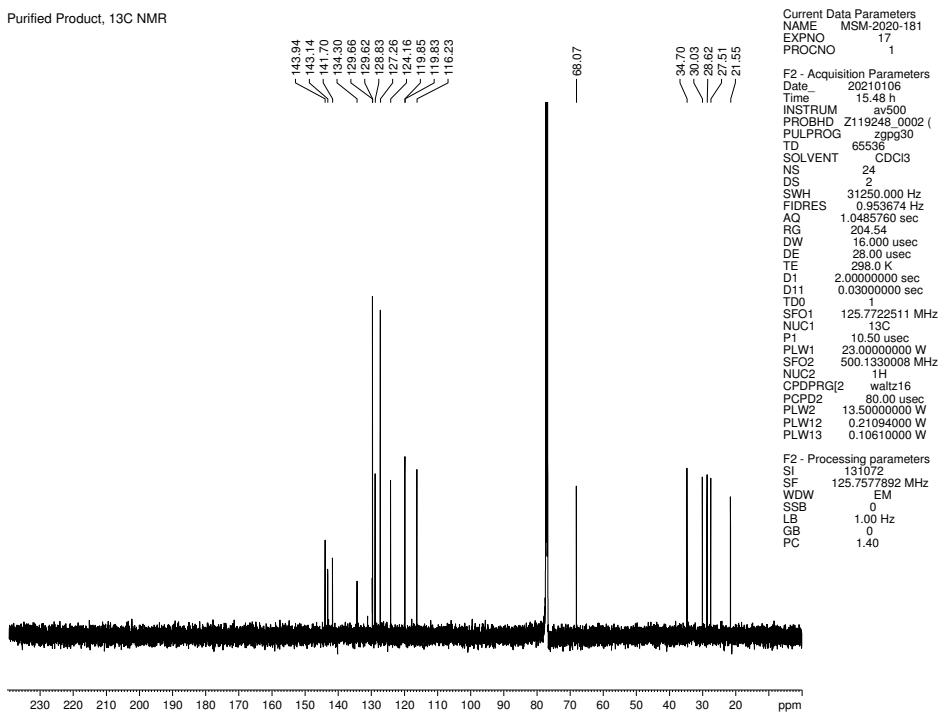


Figure 2.70. ¹³C NMR (125 MHz, CDCl₃) of compound 2.34.

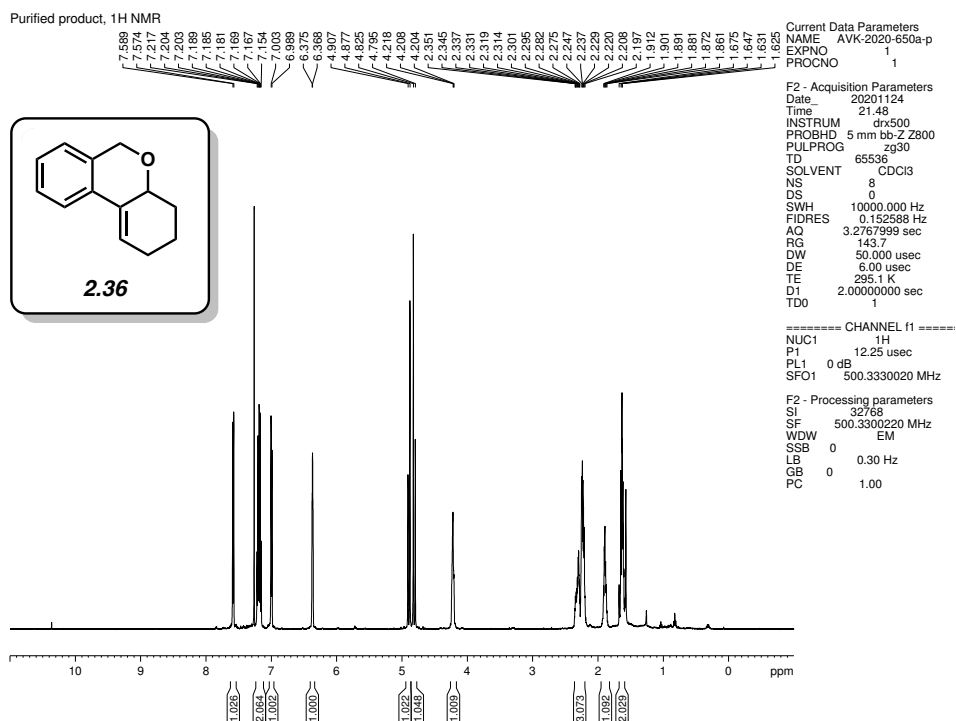


Figure 2.71. ¹H NMR (500 MHz, CDCl₃) of compound 2.36.

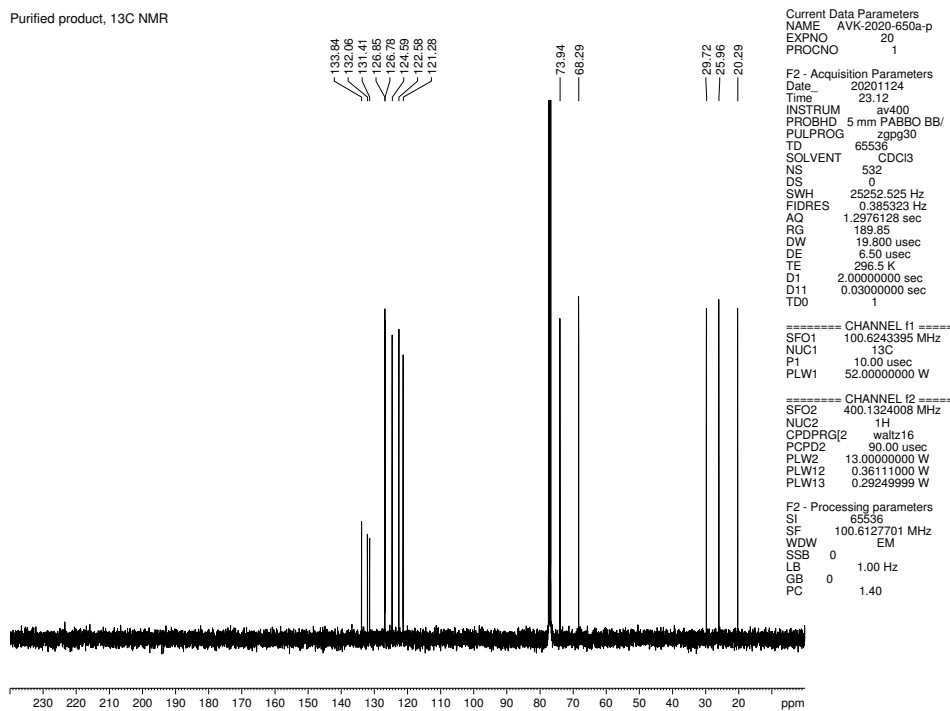


Figure 2.72. ¹³C NMR (100 MHz, CDCl₃) of compound 2.36.

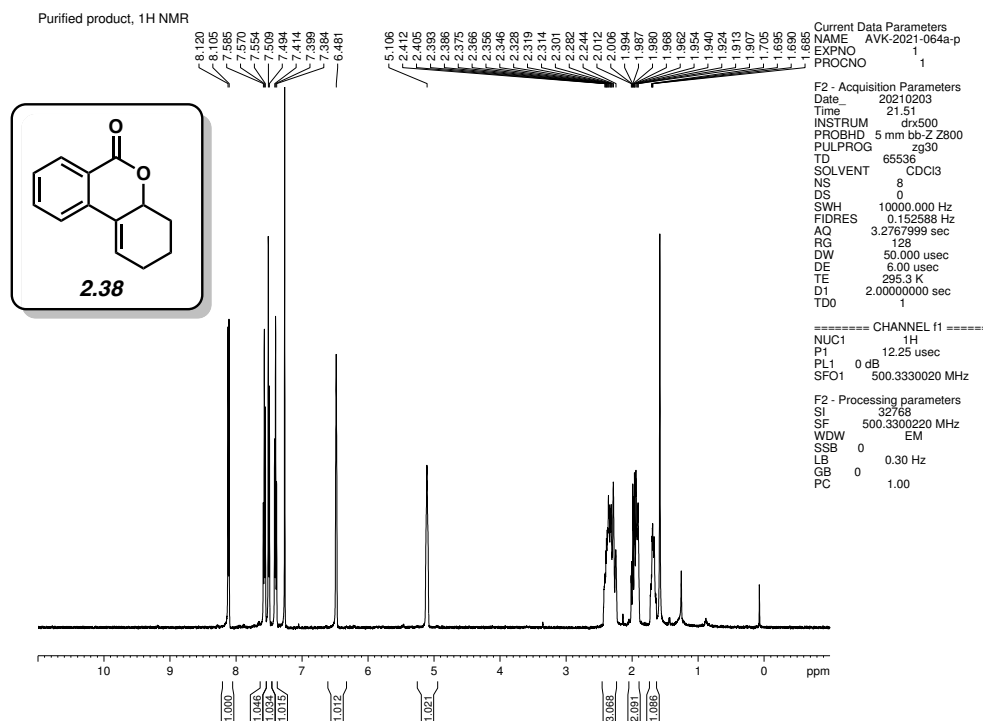


Figure 2.73. ¹H NMR (500 MHz, CDCl₃) of compound 2.38.

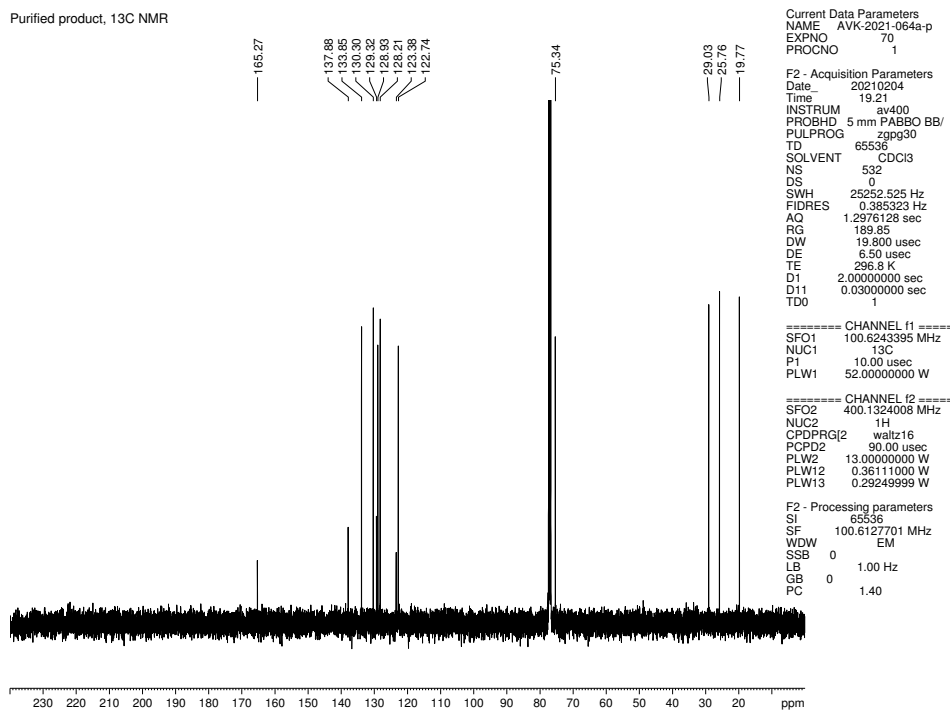


Figure 2.74. ¹³C NMR (100 MHz, CDCl₃) of compound 2.38.

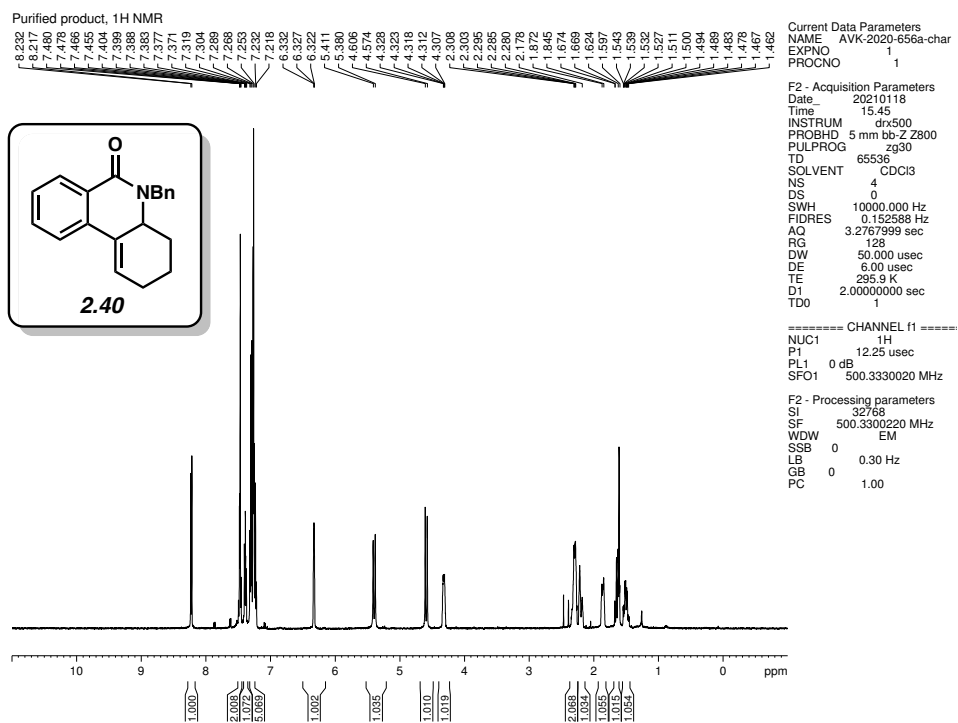


Figure 2.75. ¹H NMR (500 MHz, CDCl₃) of compound 2.40.

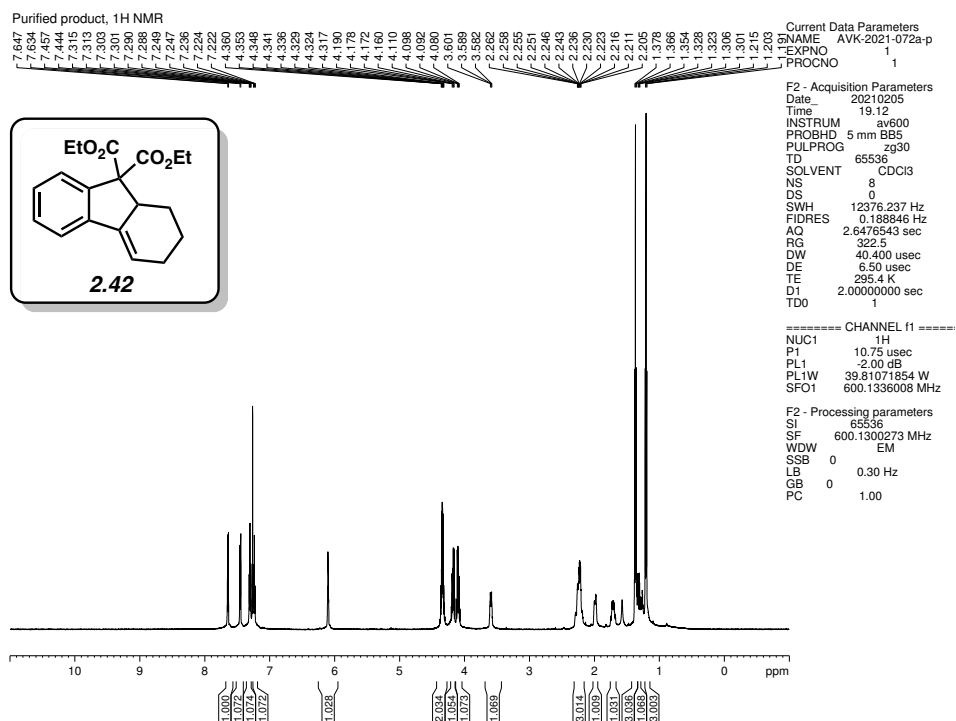


Figure 2.76. ¹H NMR (600 MHz, CDCl₃) of compound 2.42.

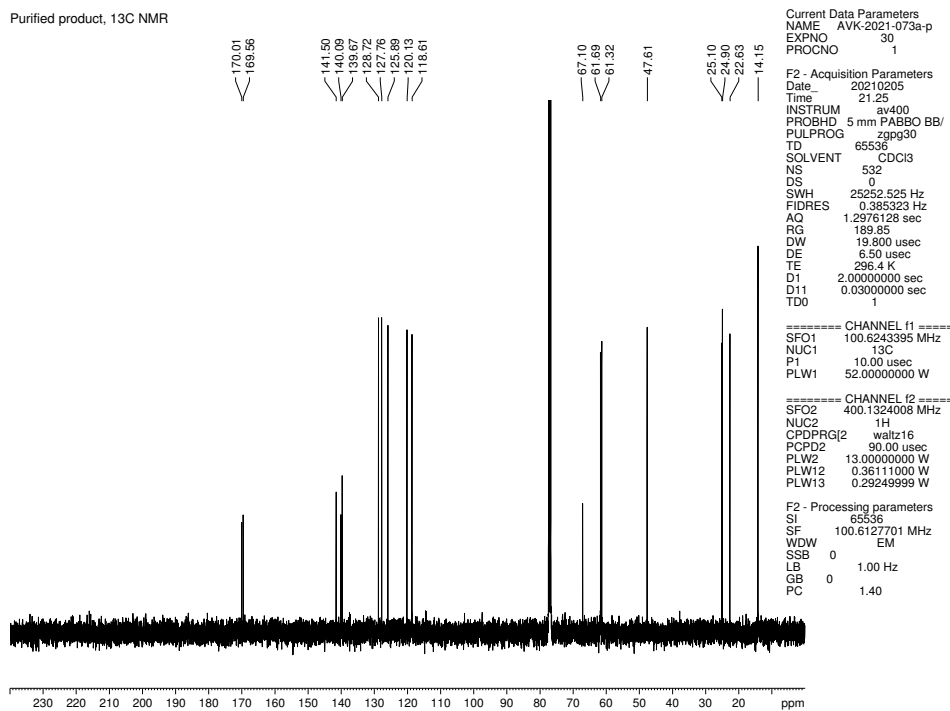


Figure 2.77. ¹³C NMR (100 MHz, CDCl₃) of compound 2.42.

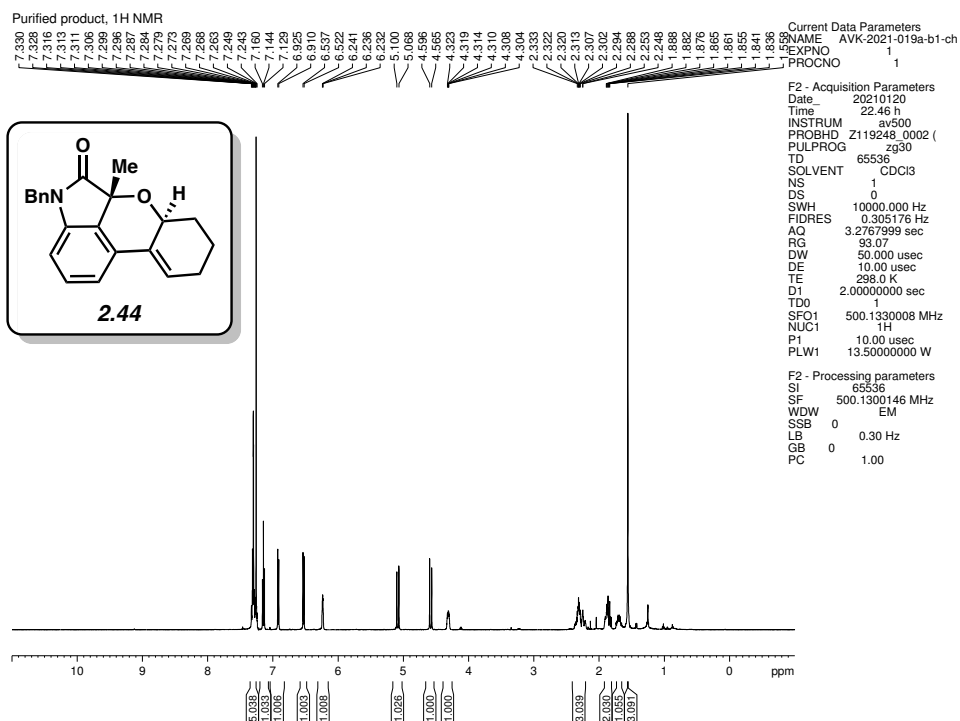


Figure 2.78. ¹H NMR (500 MHz, CDCl₃) of compound 2.44.

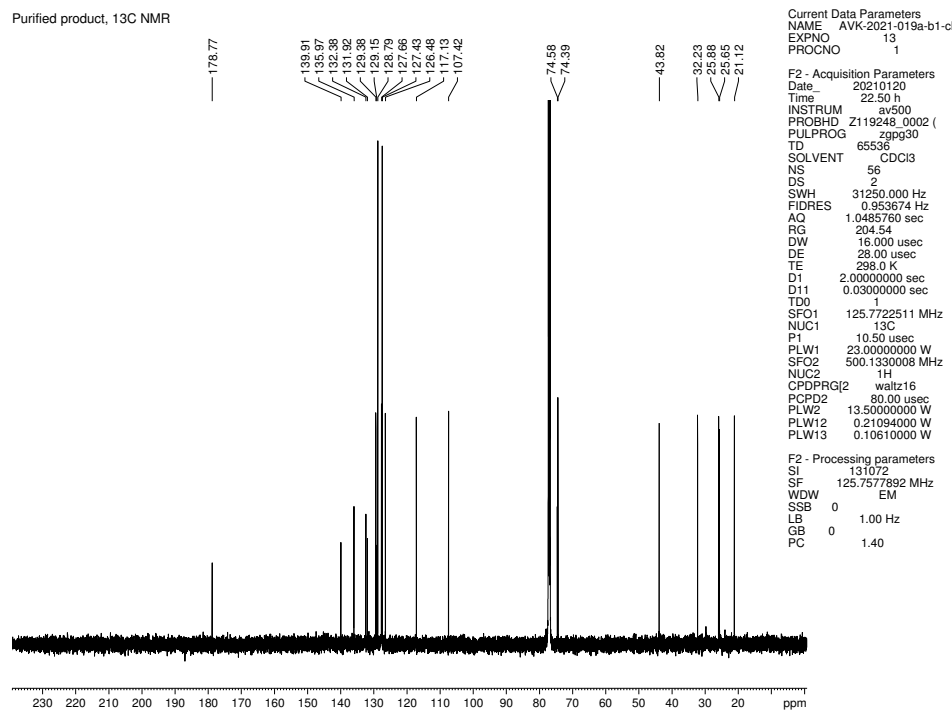


Figure 2.79. ¹³C NMR (125 MHz, CDCl₃) of compound 2.44.

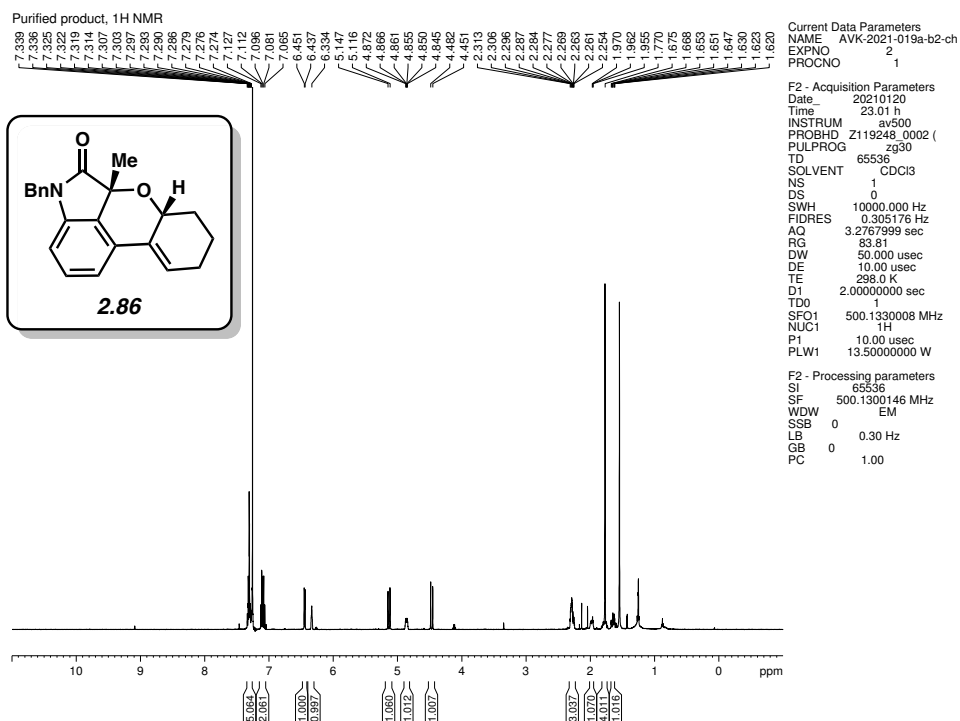


Figure 2.80. ¹H NMR (500 MHz, CDCl₃) of compound **2.86**.

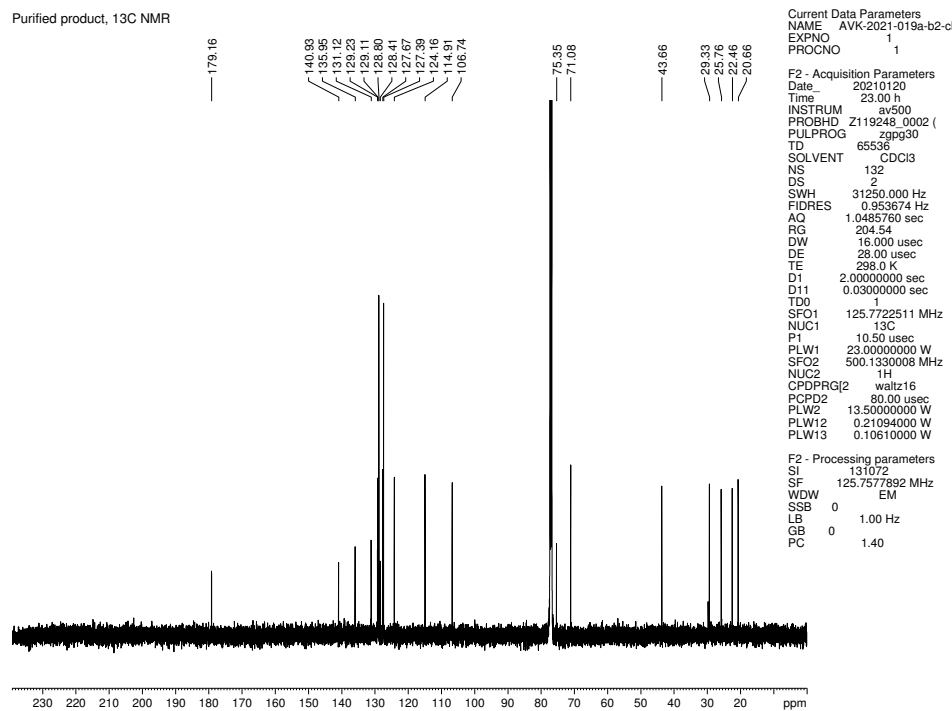
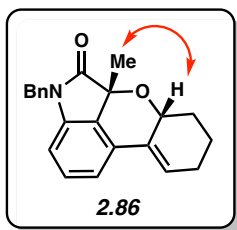


Figure 2.81. ¹³C NMR (125 MHz, CDCl₃) of compound **2.86**.



Purified product, NOESY

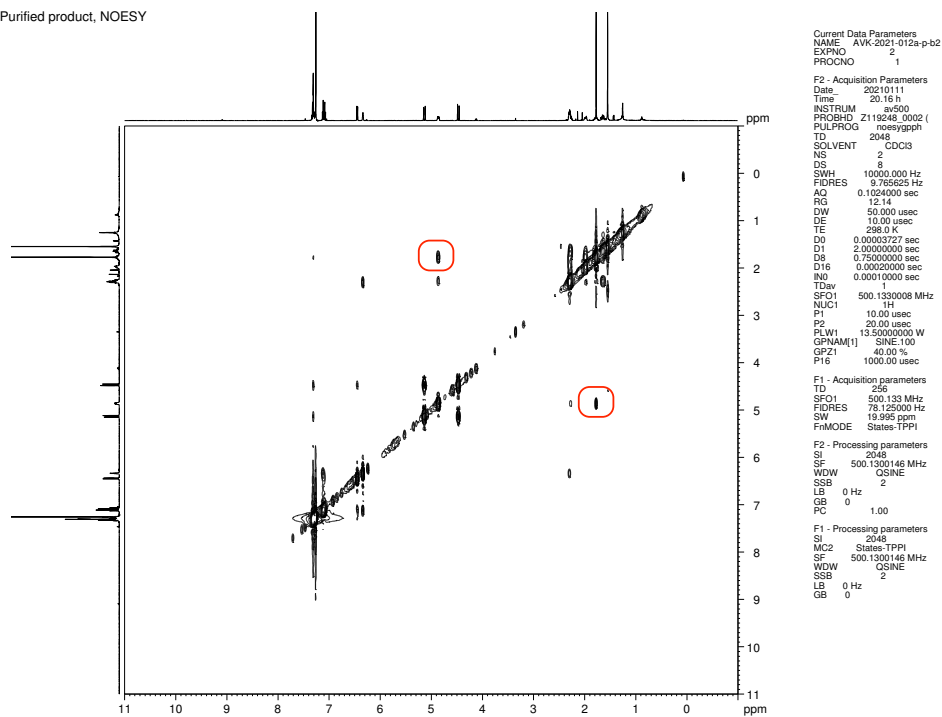


Figure 2.82. NOESY (500 MHz, CDCl_3) of compound **2.86**.

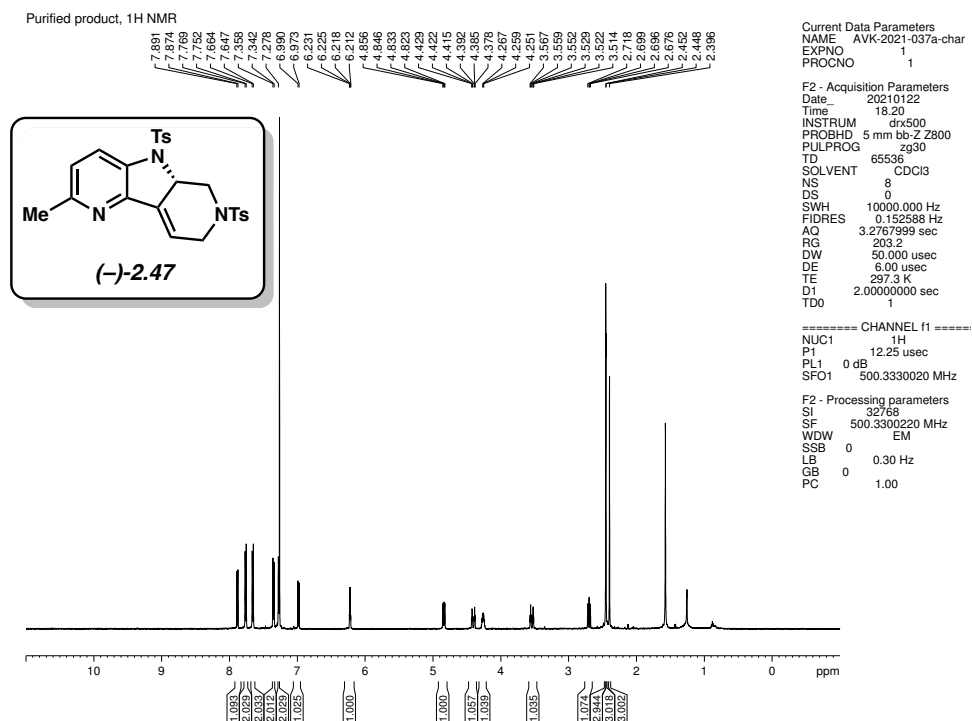


Figure 2.83. ¹H NMR (500 MHz, CDCl₃) of compound (-)-2.47.

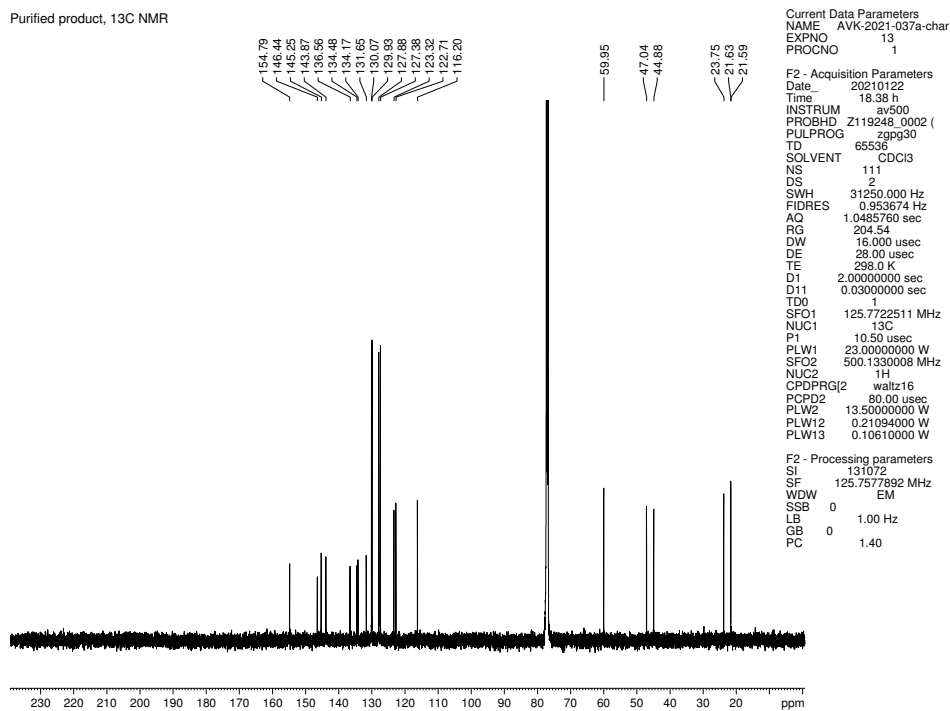


Figure 2.84. ¹³C NMR (125 MHz, CDCl₃) of compound (-)-2.47.

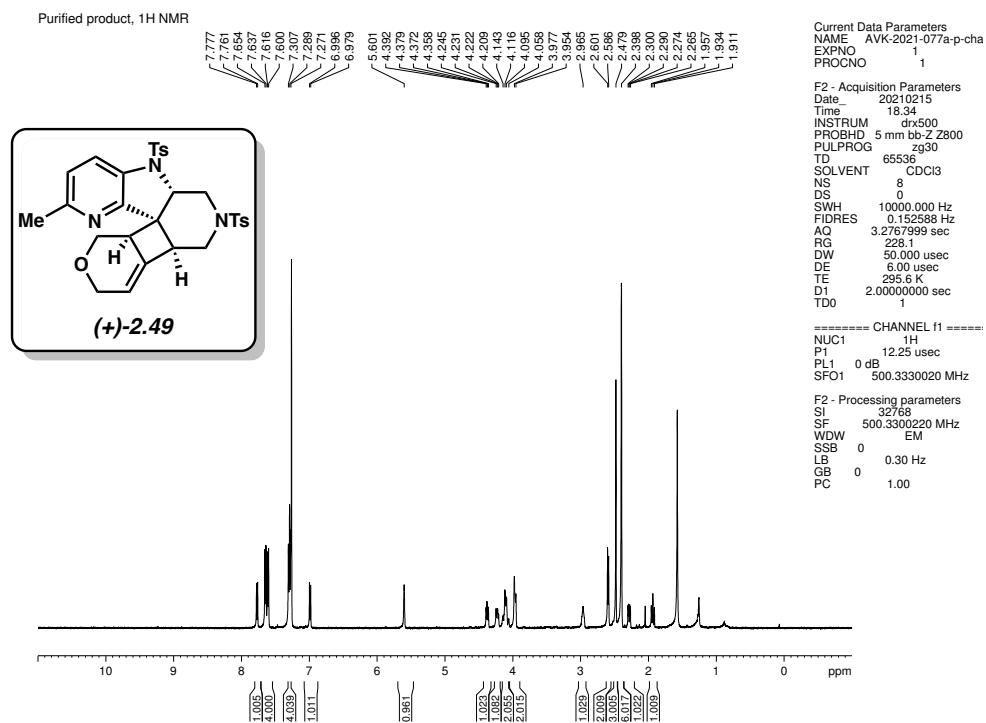


Figure 2.85. ¹H NMR (500 MHz, CDCl₃) of compound (+)-2.49.

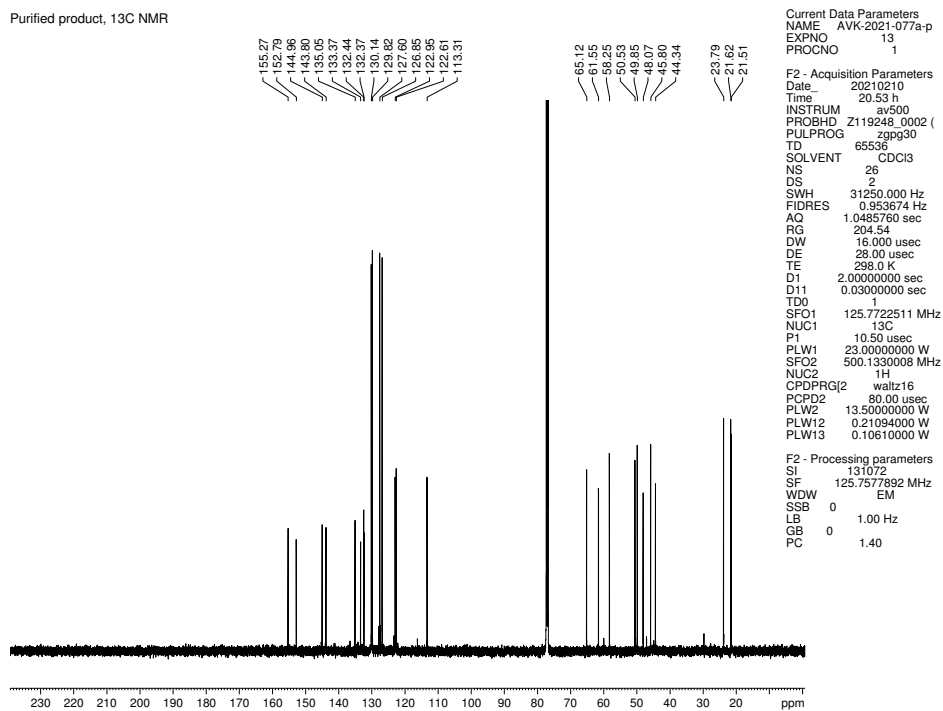


Figure 2.86. ¹³C NMR (125 MHz, CDCl₃) of compound (+)-2.49.

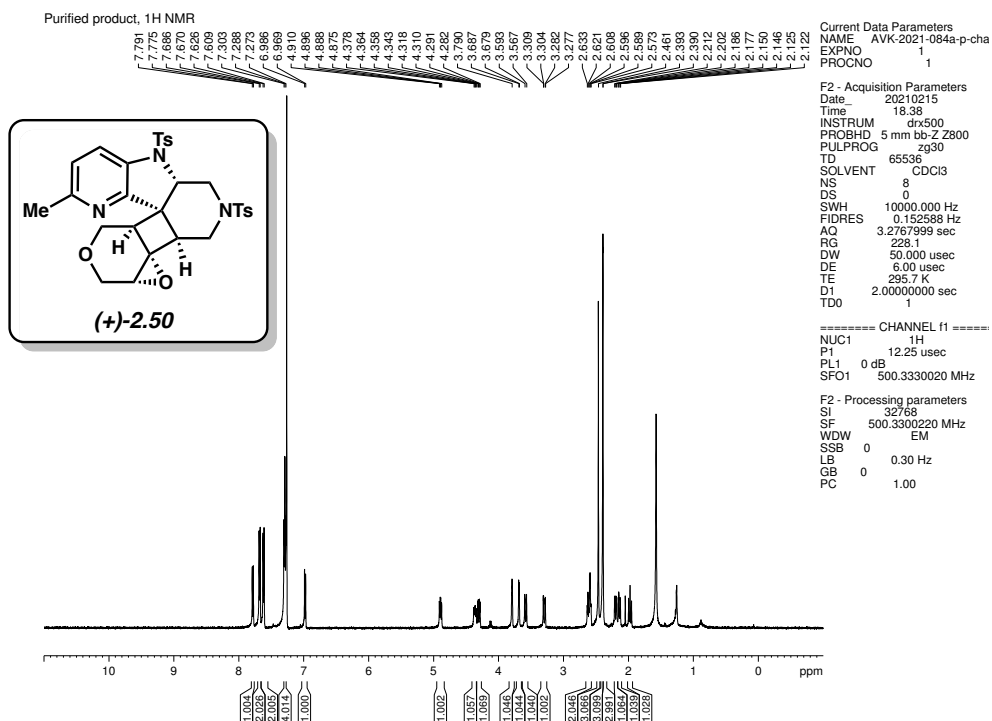


Figure 2.87. ¹H NMR (500 MHz, CDCl₃) of compound (+)-2.50.

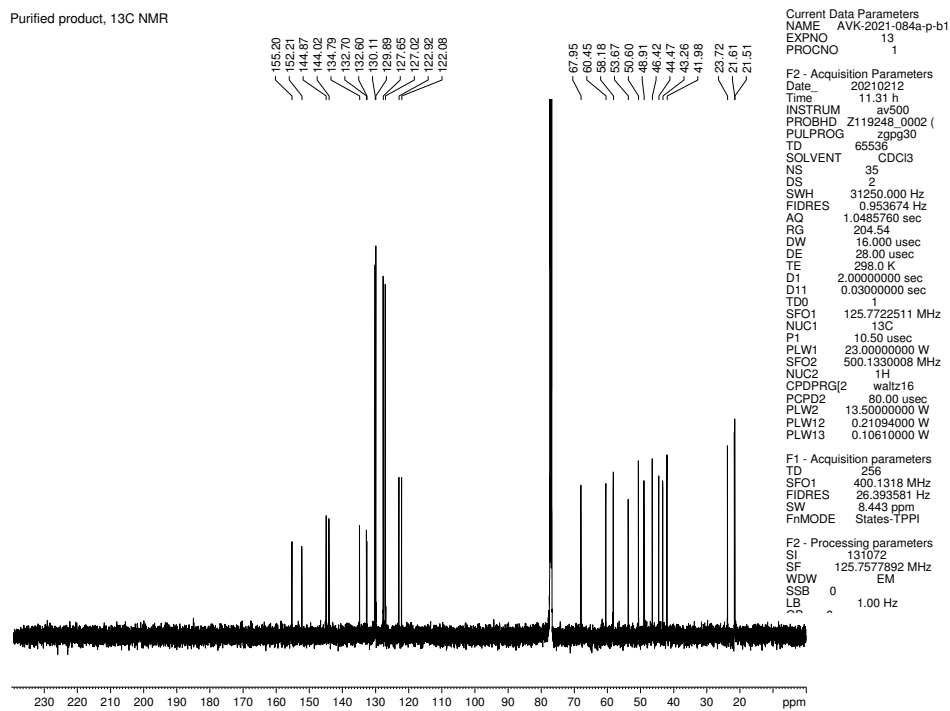


Figure 2.88. ¹³C NMR (125 MHz, CDCl₃) of compound (+)-2.50.

2.10 Notes and References

- (1) Wenk, H. H.; Winkler, M.; Sander, W. One century of aryne chemistry. *Angew. Chem., Int. Ed.* **2003**, *42*, 502–528.
- (2) Roberts, J. D.; Simmons, H. E.; Carlsmith, L. A.; Vaughan, C. W. Rearrangement in the reaction of chlorobenzene-1-C¹⁴ with potassium amide. *J. Am. Chem. Soc.* **1953**, *75*, 3290–3291.
- (3) Wittig, G. Phenyl-lithium, der Schlüssel zu einer neuen Chemie metallorganischer Verbindungen. *Naturwissenschaften* **1942**, *30*, 696–703.
- (4) Wittig, G.; Pohmer, L. Intermediäre Bildung von Dehydrobenzol (Cyclohexa-dienin). *Angew. Chem.* **1955**, *67*, 348.
- (5) Julia, M.; Huang, Y.; Igolen, J. Synthesis of 4- or 5-aminoindoles by arsenic substitution. *C. R. Acad. Sci., Ser. C* **1967**, *265*, 110–112.
- (6) Shah, T. K.; Medina, J. M.; Garg, N. K. Expanding the strained alkyne toolbox: Generation and utility of oxygen-containing strained alkynes. *J. Am. Chem. Soc.* **2016**, *138*, 4948–4954.
- (7) Scardiglia, F.; Roberts, J. D. Evidence for cyclohexyne as an intermediate in the coupling of phenyllithium with 1-chlorocyclohexene. *Tetrahedron* **1957**, *1*, 343–344.

- (8) For a review describing a wide range of in-situ-generated strained intermediates, see: Shi, J.; Li, L.; Li, Y. *o*-Silylaryl triflates: A journey of Kobayashi aryne precursors. *Chem. Rev.* **2021**, *121*, 3892–4044.
- (9) Dubrovskiy, A. V.; Markina, N. A.; Larock, R. C. Use of benzyne for the synthesis of heterocycles. *Org. Biomol. Chem.* **2013**, *11*, 191–218.
- (10) Mauger, C. C.; Mignani, G. A. An efficient and safe procedure for the large-scale Pd-catalyzed hydrazonation of aromatic chlorides using Buchwald technology. *Org. Process Res. Dev.* **2004**, *8*, 1065–1071.
- (11) Takikawa, H.; Nishii, A.; Sakai, T.; Suzuki, K. Aryne-based strategy in the total synthesis of naturally occurring polycyclic compounds. *Chem. Soc. Rev.* **2018**, *47*, 8030–8056.
- (12) Tadross, P. M.; Stoltz, B. M. A comprehensive history of arynes in natural product total synthesis. *Chem. Rev.* **2012**, *112*, 3550–3577.
- (13) Gampe, C. M.; Carreira, E. M. Arynes and cyclohexyne in natural product synthesis. *Angew. Chem., Int. Ed.* **2012**, *51*, 3766–3778.
- (14) Schleth, F.; Vettiger, T.; Rommel, M.; Tobler, H. Process for the preparation of pyrazole carboxylic acid amides. International patent WO2011131544 A1, Oct 27, 2011.

- (15) Lin, J. B.; Shah, T. J.; Goetz, A. E.; Garg, N. K.; Houk, K. N. Conjugated trimeric scaffolds accessible from indolyne cyclotrimerizations: synthesis, structures, and electronic properties. *J. Am. Chem. Soc.* **2017**, *139*, 10447–10455.
- (16) Whereas cyclic allenes have not seen synthetic development to the extent that their alkyne counterparts have, invaluable studies on methods for allene generation and trapping have been put forward by Christl, Balci & Jones, Elliot, Guitián, West, and many others. For a comprehensive view of strained cyclic allene chemistry through 2003, see: Christl, M. Cyclic allenes up to seven-membered rings. in *Modern Allene Chemistry*; Krause, N.; Kashmi, S. A. K., Eds.; Wiley-VCH: Weinheim, 2004; pp 243–357.
- (17) The disparity between the development of these related intermediates is clearly seen by comparison of the wealth of reactions discovered for cyclic alkynes (nucleophilic trappings, cycloadditions, ene reactions, C–H insertions, transition-metal-catalyzed processes, multicomponent couplings, and many others – see ref. 8) to the few known modes of cyclic allene reactivity.
- (18) Wittig, G.; Fritze, P. On the intermediate occurrence of 1,2-cyclohexadiene. *Angew. Chem., Int. Ed. Engl.* **1966**, *5*, 846.
- (19) Lovering, F.; Bikker, J.; Humblet, C. Escape from flatland: Increasing saturation as an approach to improving clinical success. *J. Med. Chem.* **2009**, *52*, 6752–6756.

- (20) Quintana, I.; Peña, D.; Pérez, D.; Guitián, E. Generation and reactivity of 1,2-cyclohexadiene under mild reaction conditions. *Eur. J. Org. Chem.* **2009**, 2009, 5519–5524.
- (21) Peña, D.; Iglesias, B.; Quintana, I.; Pérez, D.; Guitián, E.; Castedo, L. Synthesis and reactivity of new strained cyclic allene and alkyne precursors. *Pure Appl. Chem.* **2009**, 78, 451–455.
- (22) Lofstrand, V. A.; West, F. G. Efficient trapping of 1,2-cyclohexadienes with 1,3-dipoles. *Chem. Eur. J.* **2016**, 22, 10763–10767.
- (23) Lofstrand, V. A.; McIntosh, K. C.; Almehmadi, Y. A.; West, F. G. Strain-activated Diels–Alder trapping of 1,2-cyclohexadienes: Intramolecular capture by pendent furans. *Org. Lett.* **2019**, 21, 6231–6234.
- (24) Almehmadi, Y. A.; West, F. G. A mild method for the generation and interception of 1,2-cycloheptadienes with 1,3-dipoles. *Org. Lett.* **2020**, 22, 6091–6095.
- (25) Wang, B.; Constantin, M.-G.; Singh, S.; Zhou, Y.; Davis, R. L.; West, F. G. Generation and trapping of electron-deficient 1,2-cyclohexadienes. Unexpected hetero-Diels–Alder reactivity. *Org. Biomol. Chem.* **2021**, 19, 399–405.

- (26) Hioki, Y.; Mori, A.; Okano, K. Steric effects on deprotonative generation of cyclohexynes and 1,2-cyclohexadienes from cyclohexenyl triflates by magnesium amides. *Tetrahedron* **2020**, *76*, 131103.
- (27) Inoue, K.; Nakura, R.; Okano, K.; Mori, A. One-pot synthesis of silylated enol triflates from silyl enol ethers for cyclohexynes and 1,2-cyclohexadienes. *Eur. J. Org. Chem.* **2018**, *2018*, 3343–3347.
- (28) Westphal, M. V.; Hudson, L.; Mason, J. W.; Pradeilles, J. A.; Zecri, F. J.; Briner, K.; Schreiber, S. L. Water-compatible cycloadditions of oligonucleotide-conjugated strained allenes for DNA-encoded library synthesis. *J. Am. Chem. Soc.* **2020**, *142*, *17*, 7776–7782.
- (29) Barber, J. S.; Styduhar, E. D.; Pham, H. V.; McMahon, T. C.; Houk, K. N.; Garg, N. K. Nitrene cycloadditions of 1,2-cyclohexadiene. *J. Am. Chem. Soc.* **2016**, *138*, 2512–2515.
- (30) Barber, J. S.; Yamano, M. M.; Ramirez, M.; Darzi, E. R.; Knapp, R. R.; Liu, F.; Houk, K. N.; Garg, N. K. Diels–Alder cycloadditions of strained azacyclic allenes. *Nat. Chem.* **2018**, *10*, 953–960.
- (31) Yamano, M. M.; Knapp, R. R.; Ngamnithiporn, A.; Ramirez, M.; Houk, K. N.; Stoltz, B. M.; Garg, N. K. Cycloadditions of oxacyclic allenes and a catalytic asymmetric entryway to enantioenriched cyclic allenes. *Angew. Chem., Int. Ed.* **2019**, *58*, 5653–5657.

- (32) McVeigh, M. S.; Kelleghan, A. V.; Yamano, M. M.; Knapp, R. R.; Garg, N. K. Silyl tosylate precursors to cyclohexyne, 1,2-cyclohexadiene, and 1,2-cycloheptadiene. *Org. Lett.* **2020**, *22*, 4500–4504.
- (33) Yamano, M. M.; Kelleghan, A. V.; Shao, Q.; Giroud, M.; Simmons, B. J.; Li, B.; Chen, S.; Houk, K. N.; Garg, N. K. Intercepting fleeting cyclic allenes with asymmetric nickel catalysis. *Nature* **2020**, *586*, 242–247.
- (34) Analogous transformations of linear allenes have been reported. For a representative study, see: Larock, R. C.; Berrios-Peña, N. G.; Fried, C. A. Regioselective, palladium-catalyzed hetero- and carboannulation of 1,2-dienes using functionally substituted aryl halides. *J. Org. Chem.* **1991**, *56*, 2615–2617.
- (35) When the experiment shown in entry 4 was performed in the absence of exogenous ligand, product **2.19a** was obtained in 17% yield.
- (36) 2-(*N,N*-dimethylaminomethyl)-1-diphenylphosphinoferrocene was found to provide similar results to Davephos, but the latter was chosen for further study given its widespread commercial availability.
- (37) Tetrabutylammonium salts have been shown to increase the rate of strained intermediate generation, presumably by improving CsF solubility; for a relevant study, see: Feng, M.; Tang, B.; Wang, N.; Xiu, H.-X.; Jiang, X. Ligand controlled regiodivergent C₁ insertion

on arynes for construction of phenanthridinone and acridone alkaloids. *Angew. Chem., Int. Ed.* **2015**, *54*, 14960–14964.

- (38) Despite the general ability of Pd to activate Ar–Br and Ar–Cl bonds, brominated and chlorinated products **2.28** and **2.29** were obtained in synthetically useful yields, thus highlighting the chemoselectivity of this transformation. Moreover, the halides provide versatile synthetic handles for further functionalization.
- (39) The bromo derivative of **2.17** performs modestly in the annulation reaction to give 41% yield of **2.19a**. We attribute the nearly twofold increase in yield when using the 2-bromopyridine to the well-documented 2-halopyridine effect. Of note, even a chloride electrophile could generate product **2.31** in this pyridyl system, albeit in 9% yield, see Section 2.8.2.4 for details. For a reference documenting the origins of such effects, see: Legault, C. Y.; Garcia, Y.; Merlic, C. A.; Houk, K. N. Origin of regioselectivity in palladium-catalyzed cross-coupling reactions of polyhalogenated heterocycles. *J. Am. Chem. Soc.* **2007**, *129*, 12664–12665.
- (40) The corresponding silyl triflate has been found to be unstable, leading to the development of a silyl tosylate as an alternative allene precursor, see ref. 24.
- (41) We hypothesize that the *trans* diastereomer is obtained as the major product due to a destabilizing steric interaction in the presumed transition state leading to the *cis*

diastereomer. Specifically, a steric interaction between the methyl group adjacent to the alcohol and the π -allyl fragment may disfavor formation of the *cis* product.

- (42) The origin of asymmetric induction is presumed to be similar to that recently reported in the Ni-catalyzed annulation of benzotriazinones involving desymmetrization of an intermediate π -allyl metal complex (e.g., **2.16**); see ref 33.
- (43) Zenner, Z. M.; Larock, R. C. Palladium-catalyzed, asymmetric hetero- and carboannulation of allenes using functionally-substituted aryl and vinylic iodides. *J. Org. Chem.* **1999**, *64*, 7312–7322.
- (44) Fra, L.; Millán, A.; Souto, J. A.; Muñoz, K. Indole synthesis based on a modified Koser Reagent. *Angew. Chem., Int. Ed.* **2014**, *53*, 7349–7353.
- (45) Zhang, L.; Si, X.; Rominger, F.; Hashmi, A. S. K. Visible-light-induced radical carbocyclization/*gem*-diborylation through triplet energy transfer between a gold catalyst and aryl iodides. *J. Am. Chem. Soc.* **2020**, *142*, 10485–10493.
- (46) Shen, H.; Fu, J.; Yuan, H.; Gong, J.; Yang, Z. Synthesis of 2,3-disubstituted indoles and benzofurans by the tandem reaction of rhodium(II)-catalyzed intramolecular C–H insertion and oxygen-mediated oxidation. *J. Org. Chem.* **2016**, *81*, 10180–10192.
- (47) Ji, Q.; Peng, X.; Wong, H. N. C. Brønsted acid-catalyzed synthesis of carbazoles from 2-substituted indoles. *Org. Chem. Front.* **2014**, *1*, 1197–1200.

- (48) Seath, C. P.; Wilson, K. L.; Campbell, A.; Mowat, J. M.; Watson, A. J. B. Synthesis of 2-BMIDA 6,5-bicyclic heterocycles by Cu(I)/Pd(0)/Cu(II) cascade catalysis of 2-iodoaniline/phenols. *Chem. Commun.* **2016**, *52*, 8703–8706.
- (49) Chen, C.; Chandru Senadi, G.; Liu, M-C.; Wang, J-J. Halogenation of arenes via an in situ generated hypohalous acid from *m*-CPBA and HX: Mechanistic insights from cyclic voltammetry. *ChemistrySelect* **2016**, *1*, 2207–2211.
- (50) Medina, J. M.; Moreno, J.; Racine, S.; Du, S.; Garg, N. K. Mizoroki-Heck cyclizations of amide derivatives for the introduction of quaternary centers. *Angew. Chem., Int. Ed.* **2017**, *56*, 6567–6571.
- (51) Zhang, D.; Yum, E. K.; Liu, Z.; Larock, R. C. Synthesis of indenenes by the palladium-catalyzed carboannulation of internal alkynes. *Org. Lett.* **2005**, *7*, 4963–4966.
- (52) Alekseyev, R. S.; Kurkin, A. V.; Yuroskaya, M. A. The Piloty-Robinson reaction of *N*-substituted piperidin-4-one azines. A novel route for the synthesis of 3,6-diazacarbazole. *Chem. Heterocycl. Comp.* **2011**, *47*, 584–596.
- (53) Marr, G.; Hunt, T. Unsymmetrically disubstituted ferrocenes. Part VIII. Synthesis and reactivity of some 2-substituted ferrocenylphosphines. *J. Chem. Soc. C* **1969**, 1070–1072.
- (54) Tamio, H.; Takaya, M.; Motoo, F.; Masahiro, K.; Nobuo, N.; Yuji, H.; Akira, M.; Sota, K.; Mitsuo, K.; Keiji, Y.; Makoto, K. Asymmetric synthesis catalyzed by chiral

- ferrocenylphosphine-transition metal complexes. I. Preparation of chiral ferrocenylphosphines. *Bull. Chem. Soc. Jpn.* **1980**, *53*, 1138–1151.
- (55) Arisawa, M.; Terada, Y.; Takahashi, K.; Nakagawa, M.; Nishida, A. Development of isomerization and cycloisomerization with use of ruthenium hydride with *N*-heterocyclic carbene and its application to the synthesis of heterocycles. *J. Org. Chem.* **2006**, *71*, 4255–4261.

CHAPTER THREE

Catalyst-Controlled Annulations of Strained Cyclic Allenes with π -Allylpalladium Complexes

Dominick C. Witkowski, Matthew S. McVeigh, Georgia M. Scherer, Sarah M. Anthony, and

Neil K. Garg

J. Am. Chem. Soc. **2023**, *145*, 10491–10496.

3.1 Abstract

Strained cyclic allenes are a class of in situ-generated fleeting intermediates that, despite being discovered more than 50 years ago, has received significantly less attention from the synthetic community compared to related strained intermediates. Examples of trapping strained cyclic allenes that involve transition metal catalysis are especially rare. We report the first annulations of highly reactive cyclic allenes with in situ-generated π -allylpalladium species. By varying the ligand employed, either of two isomeric polycyclic scaffolds can be obtained with high selectivity. The products are heterocyclic, sp^3 -rich, and bear two or three new stereocenters. This study should encourage the further development of fragment couplings that rely on transition metal catalysis and strained cyclic allenes for the rapid assembly of complex scaffolds.

3.2 Introduction

In situ-generated strained intermediates that bear a functional group with a preferred linear geometry within a small ring have emerged as valuable synthetic building blocks. Arynes^{1,2,3,4,5,6} and cyclic alkynes^{7,8} (e.g., **3.1–3.3**, Figure 3.1A) have been most well-studied with applications

spanning the synthesis of heterocycles,^{9,10} ligands (such as XPhos),¹¹ natural products,^{12,13,14} agrochemicals,¹⁵ and organic materials.^{16,17} A related class of strained intermediates discovered around the same time as arynes and cyclic alkynes is strained cyclic allenes, such as 1,2-cyclohexadiene (**3.4**).^{18,19} The cumulated diene confined to a small ring leads to ~30 kcal/mol of strain energy, making cyclic allenes well-suited for strain-promoted reactions.^{20,21,22} However, these intermediates have received significantly less attention compared to arynes and cyclic alkynes despite possessing many attractive attributes²³ that substantiate their value as building blocks for the synthesis of complex sp³-rich scaffolds. Recent studies of strained cyclic allenes have led to advances in cyclic allene generation protocols,^{24,25,26} cycloaddition reactions,^{27,28,29,30,31,32,33,34,35,36} metal-catalyzed processes,^{37,38} trapping in a single-electron process,³⁹ DNA-encoded library synthesis,⁴⁰ and total synthesis.⁴¹

An attractive yet underdeveloped approach to leveraging strained cyclic allenes in synthesis utilizes transition metal catalysis.^{42,43} Only three reports of such transformations have been demonstrated in the literature.⁴⁴ In these reactions, an organometallic intermediate **3.5** is generated catalytically and intercepts a transient cyclic allene (e.g., **3.6**) (Figure 3.1B). This gives rise to annulated product **3.7**. In the known literature reports, only σ -bound metal species have been used, namely, palladacycle **3.8**,^{24,45} nickelacycle **3.9**,³⁷ and arylpalladium species **3.10**.³⁸ With the aim of expanding the types of organometallic intermediates that can be used in reactions of strained cyclic allenes, we became interested in the use of π -allylpalladium species **3.11**. The ability of **3.11** to undergo C–C bond formation at either of its termini^{46,47,48} is distinct from the reactivity of organometallic intermediates used previously in cyclic allene annulations. As will be described herein, the use of π -allylpalladium complexes^{49,50} to trap cyclic allenes provides

opportunities to control regiochemistry and stereoselectivity, while building diverse and sp^3 -rich scaffolds.

In this chapter, we demonstrate the first use of π -allylmetal complexes to trap strained cyclic allenes (3.12 and 3.6, respectively, Figure 3.1C). By varying the ligand employed, either of two different polycyclic scaffolds, 3.13 or 3.14, can be formed preferentially, via the formation of multiple bonds and stereocenters. Studies toward an enantioselective variant are also reported. These studies demonstrate the merger of transition metal catalysis and strained cyclic allenes for the rapid assembly of complex, sp^3 -rich scaffolds.

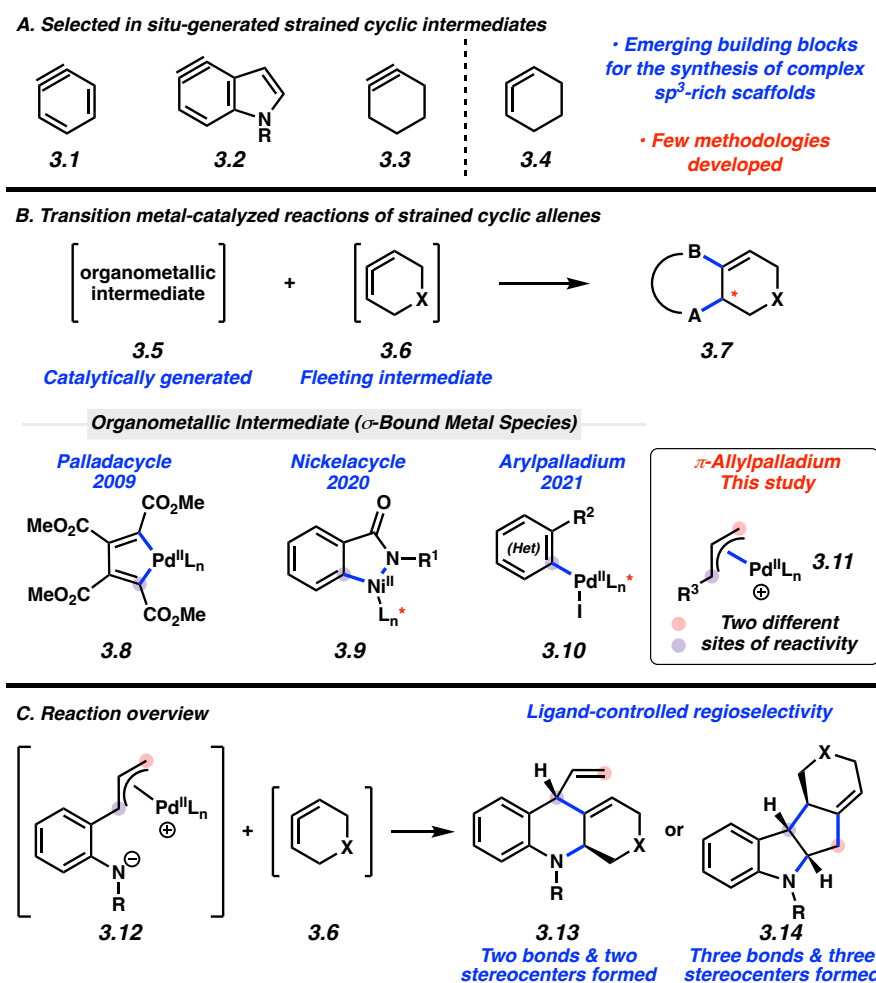


Figure 3.1. (A) Strained cyclic intermediates 3.1–3.4, (B) approaches for metal-catalyzed reactions of strained cyclic allenes, and (C) overview of current study.

3.3 Reaction Optimization

To initiate our studies, we investigated the reaction of vinyl benzoxazinone **3.15** with silyl triflate **3.16** using palladium catalysis (Table 3.1). Of note, benzoxazinone **3.15**, a known π -allylmetal precursor,^{51,52,53,54,55} was selected for these studies as it had been demonstrated to be compatible with fluoride-mediated generation of benzyne.⁵⁶ Based on known reactivity of **3.15**, two products could plausibly arise, tricycle **3.17** or tetracycle **3.18**. To generate soluble fluoride ions, CsF and Bu₄NOTf⁵⁷ were used in combination. Furthermore, elevated temperatures were employed to facilitate efficient generation of reactive intermediates. Select key results from reaction optimization are depicted, and additional data are available in Section 3.8.2.2.

The use of the dialkylbiaryl ligand DavePhos, which had previously been identified as a competent ligand in a cyclic allene annulation,³⁸ did not lead to a productive reaction (Table 3.1, entry 1). However, switching to the PPh₃ ligand gave tricyclic annulation product **3.17**, albeit in a low yield of 20% (entry 2). Alternatively, the use of the bidentate ferrocene ligand dppf delivered constitutional isomer **3.18** as the major product (entry 3). With initial results for the selective formation of annulation products **3.17** or **3.18**, we performed optimization to selectively access each of the constitutional isomers. For practical reasons, we elected to pursue the use of Pd(PPh₃)₄, which gave **3.17** in slightly improved yield and excellent selectivity (entry 4; compared with entry 2). Because a significant amount of decomposition of benzoxazinone **3.15** was observed under these conditions,⁵⁸ we explored additives to mitigate deleterious side reactions. Empirically, the addition of water led to significant improvement, generating tricycle **3.17** in 65% yield after 2 h (entry 5). Extensive efforts were made to selectively generate tetracycle **3.18**. We ultimately identified that the use of Buchwald precatalyst dppf Pd G3 and water as an additive delivered **3.18** in 73% yield after 2 h (entry 6; compared with entry 3). Thus, either tricycle **3.17** or tetracycle

3.18 could be accessed by the judicious choice of ligand. It should be noted that the annulation of benzyne with benzoxazinone **3.15** only delivers the tetracyclic counterpart to **3.18**, without formation of the tricyclic counterpart to **3.17**.⁵⁶

Table 3.1. Select Results from Optimization Studies.

Entry	Catalyst	Ligand	Additive	Yield ^b	3.17:3.18 ^c
1	Pd(OAc) ₂	DavePhos (10 mol%)	–	0%	–
2	Pd(OAc) ₂	PPh ₃ (10 mol%)	–	20%	>20:1
3	Pd(OAc) ₂	dppf (10 mol%)	–	10%	1:14
4	Pd(PPh ₃) ₄	–	–	24%	18:1
5	Pd(PPh ₃) ₄	–	H ₂ O (9.0 equiv)	65%	19:1
6 ^d	dppf Pd G3	–	H ₂ O (9.0 equiv)	73%	1:13

^a Reactions conditions: **3.15** (3.0 equiv), **3.16** (1.0 equiv), catalyst (5 mol%), ligand (as shown), CsF (10 equiv), Bu₄NOTf (5.0 equiv), additive (as shown), DMF (0.050 M), 70 °C, 2 h. ^b Yield determined by an isolation experiment. ^c Ratio of **3.17**:**3.18** and dr were determined by ¹H NMR analysis. In entries where **3.17** is the major product, dr = 11:1; in entries where **3.18** is the major product dr = >20:1. ^d [Pd] (10 mol%), 0.025 M.

3.4 Scope of Annulation Reactions

Having identified suitable reaction conditions for the selective formation of either constitutional isomer **3.17** or **3.18**, we examined the scope of the methodology beginning with the formation of tricyclic products **3.21** (Figure 3.2). The parent substrate, along with its *N*-mesyl derivative, each gave 60% yield of tricyclic product (**3.17** and **3.22**, respectively). A variety of substituents on the arene (R² = Me, F, OMe, Ph, 2-thiophene) were also tolerated, as evidenced by the formation of tricycles **3.23–3.29**.⁵⁹ The use of a naphthalene-derived substrate proceeded smoothly to furnish **3.30** in 64% yield. Additionally, we evaluated a benzoxazinone bearing an isopropenyl group, which afforded tricycle **3.31**. Lastly, heterocyclic allene precursors (i.e., **3.20**)

could be employed under modified reaction conditions to enable further modulation of the product structure. More specifically, interception of oxa-²⁹ and aza-derivatives²⁸ of **3.20** delivered heterocycles **3.32** and **3.33**, respectively. It should be noted that formation of the corresponding tetracyclic products was either negligible or not observed for the results shown in Figure 3.2. Additionally, in most cases, the observed diastereoselectivities are synthetically useful.

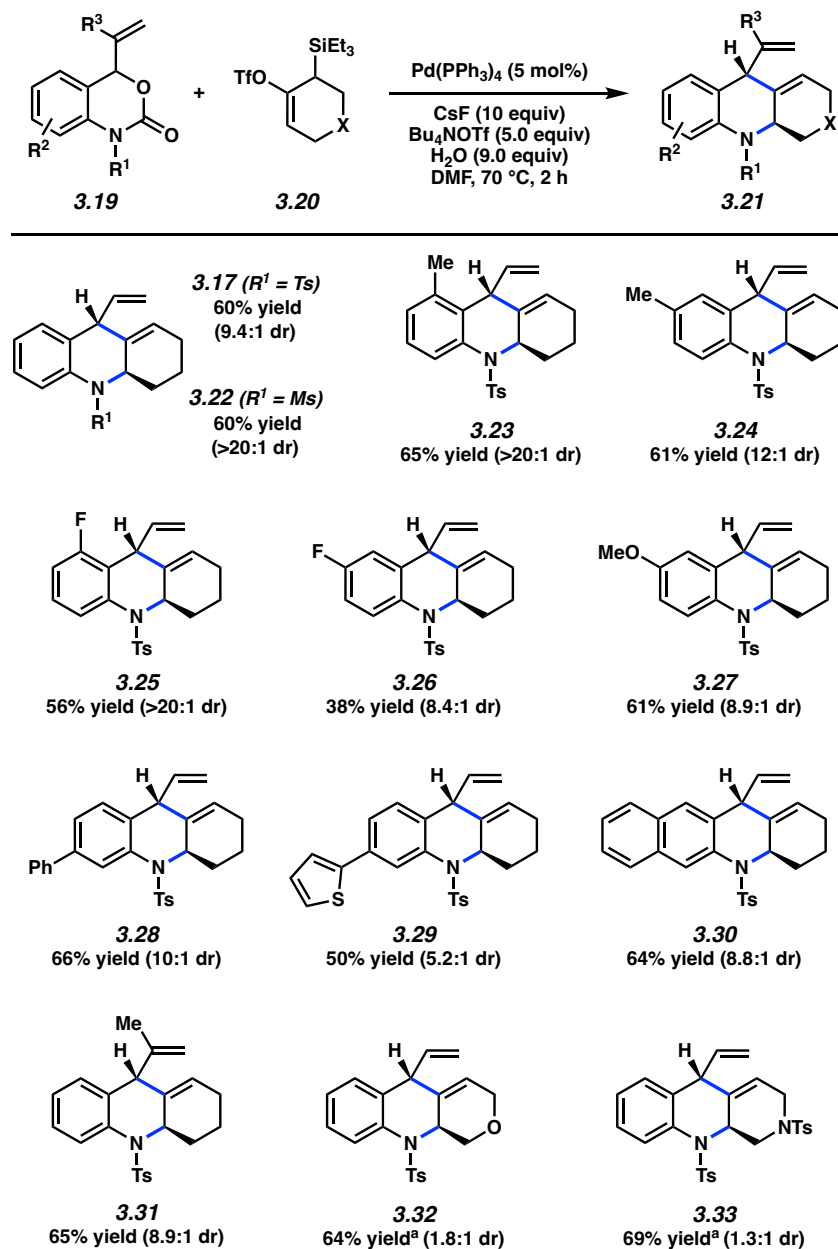


Figure 3.2. Scope of the annulation reaction using PPh_3 as the ligand. Reactions performed on 0.05 mmol scale with **3.19** (3.0 equiv) and **3.20** (1.0 equiv) at 0.050 M. Yields reflect an average of two isolation experiments. ^aReactions were performed with CsF (5.0 equiv) in MeCN (0.050 M) at 60 °C for 6 h, without Bu_4NOTf additive.

Subsequently, the scope of the methodology for preparing tetracycles utilizing the dppf Pd G3 catalyst was assessed (Figure 3.3). Although our conditions shown in Table 3.1, entry 6 were generally useful, some modifications were made to obtain optimal yields based on empirical

observations. Beginning with the parent substrate combination, **3.18** was isolated in 70% yield and >20:1 dr. Variation of the *N*-substituent, as well as steric and electronic perturbations of the aryl ring, were tolerated as seen by the formation of **3.35–3.43** in good yields. Finally, trapping of an oxacyclic allene gave tetracycle **3.44**. Notably, the annulations to afford tetracycles **3.34** proceed via the formation of three new bonds and three stereocenters with excellent diastereoselectivity (>20:1 dr in all cases).

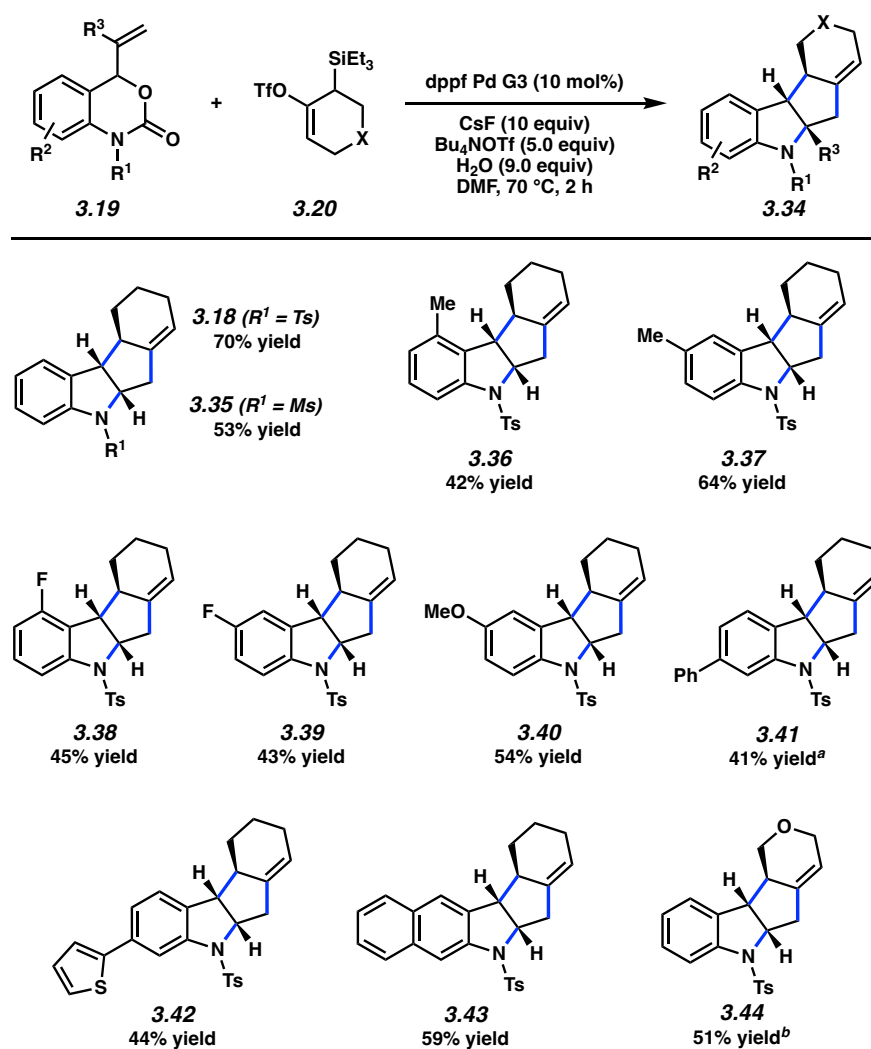


Figure 3.3. Scope of the annulation reaction using *dppf* as the ligand. Reactions performed on 0.05 mmol scale with **3.19** (3.0 equiv) and **3.20** (1.0 equiv) at 0.025 M. Yields reflect an average of two isolation experiments. For all isolations, dr = >20:1 and ratios of **3.34**:**3.21** range from

6.3:1 to >20:1; see Section 3.8.2.3 for details. ^a Reaction was performed at 100 °C. ^b Reaction was performed in MeCN (0.0125 M) at 30 °C for 14 h, without Bu₄NOTf additive.

3.5 Reaction Mechanism

Plausible mechanisms for the transformations we have developed are depicted in Figure 3.4. The Pd(0) catalyst coordinates to **3.45**. Oxidative addition of the Pd(0) catalyst into the allylic C–O bond of **3.46** followed by decarboxylation affords zwitterionic π -allylpalladium intermediate **3.12**.⁵¹ Ligand-controlled migratory insertion of cyclic allene **3.6** (formed from fluoride-mediated 1,2-elimination of silyl triflate **3.20**) gives π -allylpalladium intermediates **3.47** and **3.48**.⁶⁰ These intermediates arise from C–C bond formation at either of the two sites of reactivity of π -allylpalladium species **3.12**. The branched or linear selectivity of the migratory insertion is proposed to be a result of the ligands employed.⁶¹ Cyclizations of **3.47** and **3.48** afford tricycle **3.13**⁶² and tetracycle **3.14**, respectively, through the formation of one or two new bonds.

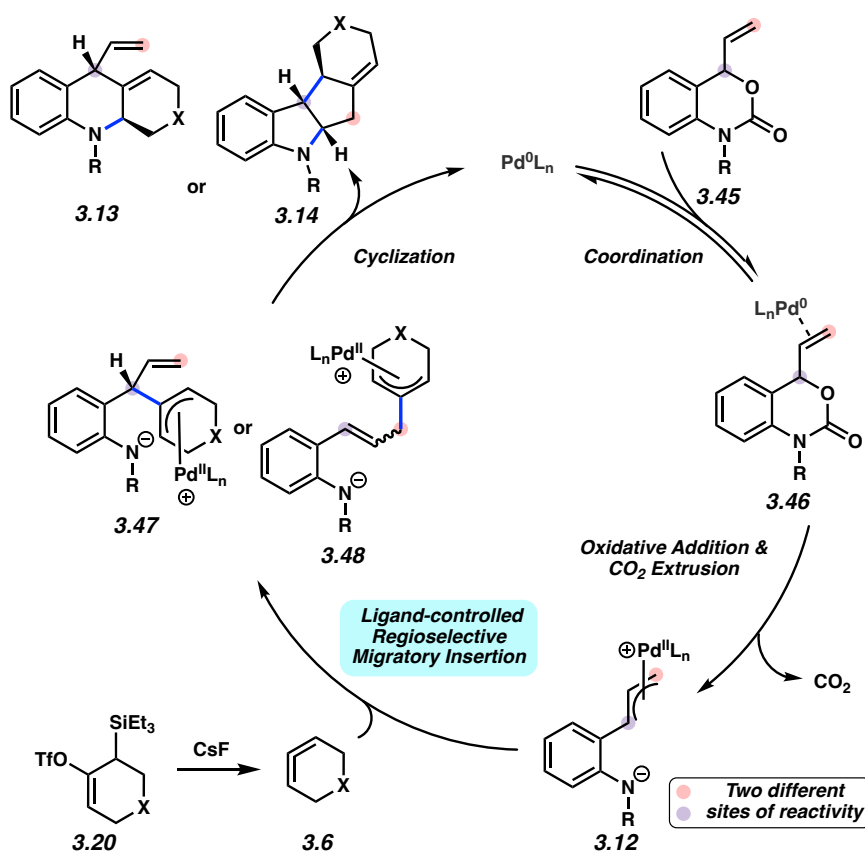


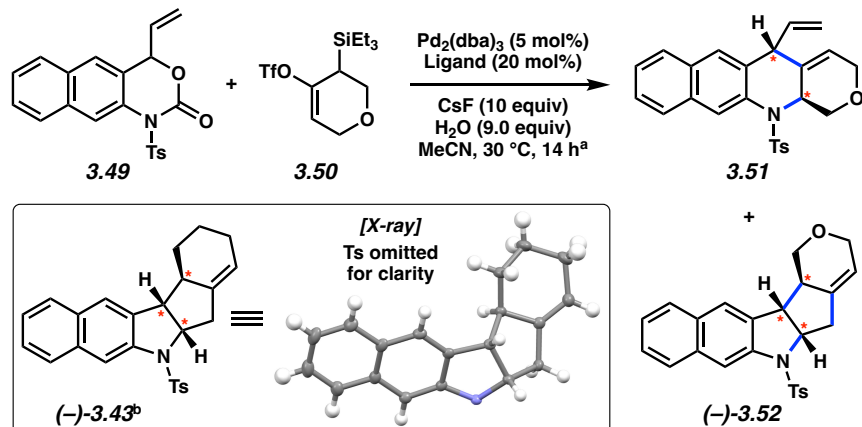
Figure 3.4. Proposed catalytic cycle.

3.6 Investigating the Feasibility of an Enantioselective Variant

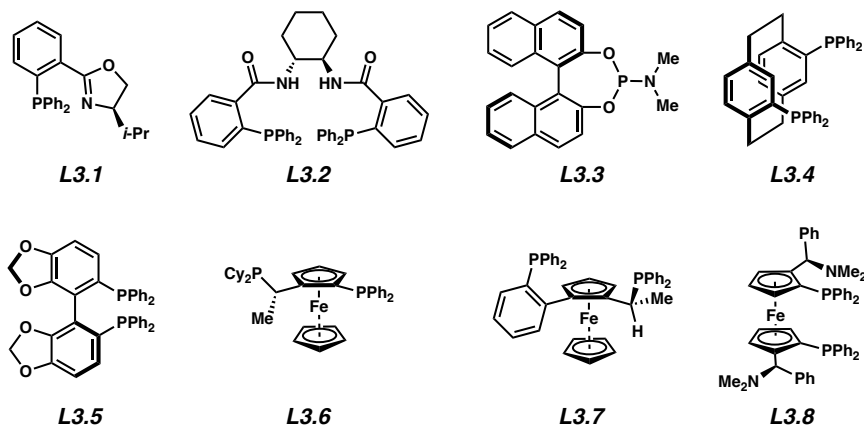
Given the notable impact of ligands on selectivity in these transformations, the feasibility of an enantioselective variant was investigated using vinyl benzoxazinone **3.49** and oxacyclic allene precursor **3.50**. Notably, the use of two chiral racemic starting materials would represent a departure from previous studies that use an achiral trapping partner.^{37,38} Select key results are shown in Table 3.2, with additional information being available in the Section 3.8.2.5.⁶³ The use of PHOX ligand **L3.1** and Trost's ligand **L3.2**, which are commonly employed in π -allylpalladium chemistry,⁵⁰ provided no desired reactivity (entries 1 and 2, respectively). However, using phosphoramidite ligand **L3.3** (entry 3), annulation product **3.51** was formed as the major isomer, thus demonstrating the feasibility of rendering the annulation to form both products

enantioselective. Given the greater structural complexity of isomer (–)-**3.52**, we elected to assess other chiral diphosphine ligands in pursuit of (–)-**3.52**. The use of Phanephos **L3.4**, Segphos ligand **L3.5**, and Josiphos ligand **L3.6** each gave the desired product (–)-**3.52** in varying yields and enantioselectivities. The employment of Walphos ligand **L3.7** and Mandyphos ligand **L3.8** each resulted in increased yields and enantioselectivities. Of these, use of **L3.8** provided superior results and delivered (–)-**3.52** in 54% yield and 70% ee.⁶⁴ We surmise that the absolute configuration of (–)-**3.52** is as depicted, on the basis of an X-ray crystal structure obtained for carbocyclic derivative (–)-**3.43**. Although improving the enantioselectivity was challenging in our initial efforts,⁶⁵ the results shown provide the most structurally complex products accessible from the merger of strained cyclic allenes and asymmetric catalysis to date. As enantioselective transformations of fleeting strained cyclic intermediates remain exceedingly rare, we hope these results will promote further efforts in this area.

Table 3.2. Evaluation of Select Chiral Ligands in the Annulation Reaction.



Entry	Ligand	Yield (51/52) ^c	dr (3.51/3.52)	ee (3.51/3.52)
1	L3.1	- / -	- / -	- / -
2	L3.2	- / -	- / -	- / -
3	L3.3	26% / 11%	2.8:1 / >20:1	~38% / 12%
4	L3.4	- / 32%	- / >20:1	- / 14%
5	L3.5	- / 24%	- / >20:1	- / 82%
6	L3.6	- / 10%	- / >20:1	- / 14%
7	L3.7	- / 34%	- / >20:1	- / 60%
8	L3.8	- / 54%	- / >20:1	- / 70%



^a Reaction conditions: **3.49** (3.0 equiv), **3.50** (1.0 equiv), $\text{Pd}_2(\text{dba})_3$ (5 mol%), ligand (20 mol%), CsF (10 equiv), H_2O (9.0 equiv), MeCN (0.0125 M), 30 °C, 14 h. ^b See Section 3.8.2.6 for details and crystallographic data. ^c Yield determined by an isolation experiment.

3.7 Conclusion

We have developed the first strategy for engaging strained cyclic allenes with π -allyl metal species. These are rare examples of cyclic allene reactions in transition metal-catalyzed processes. By the judicious choice of ligands, selectivity can be controlled, leading to the preferential formation of tri- or tetracyclic heterocycles with significant structural complexity. Of note, the transformations proceed by formation of either two or three new bonds and two or three new stereocenters. We also demonstrate the feasibility of an enantioselective variant, thus providing a crucial proof-of-principle study for further asymmetric reaction development. Overall, the union of strained cyclic allenes and π -allylpalladium chemistry expands the types of organometallic intermediates that can be used in cyclic allene reactions to access complex sp^3 -rich scaffolds. We hope this study promotes the further development and understanding of transition metal-catalyzed reactions of strained cyclic allenes.

3.8 Experimental Section

3.8.1 Materials and Methods

Unless stated otherwise, reactions were conducted in flame-dried glassware under an atmosphere of nitrogen, and commercially obtained reagents were used as received unless otherwise specified. Anhydrous solvents were either freshly distilled or passed through activated alumina columns, unless otherwise stated. Non-commercially available substrates were synthesized according to known preparations or following protocols specified in the Experimental Procedures. Prior to use, acetonitrile (MeCN), dimethylformamide (DMF), 1,4-dioxane, methanol (MeOH), methylene chloride, and tetrahydrofuran (THF) were passed through activated alumina columns and degassed by five freeze-pump-thaw cycles. Water and 1,4-dioxane were degassed by sparging with N_2 gas before use. Hydrochloric acid, sodium bicarbonate, sodium hydride, ethyl

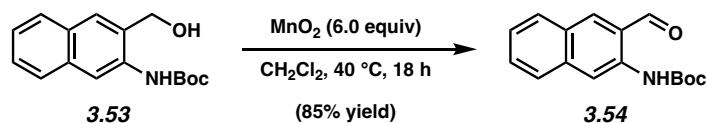
chloroformate, phenylboronic acid pinacol ester (**3.59**), and thiophene-2-boronic acid (**3.64**) pinacol ester were obtained from Sigma-Aldrich. Sodium carbonate was obtained from EMD Millipore. 4-Toluenesulfonyl chloride (TsCl) was obtained from Oakwood Chemical. Vinylmagnesium bromide (**3.55**) was obtained from Acros Organics. Palladium(II) acetate, tris(dibenzylideneacetone)dipalladium(0) ($\text{Pd}_2(\text{dba})_3$), methanesulfonato[1,1'-bis(diphenylphosphino)ferrocene]](2'-amino-1,1'-biphenyl-2-yl)palladium(II) (DPPF Palladacycle Gen. 3), cesium fluoride, manganese dioxide, and tetrakis(triphenylphosphine)palladium(0) were obtained from Strem Chemicals. Tetrabutylammonium trifluoromethanesulfonate (Bu_4NOTf) was obtained from TCI America. Potassium carbonate was obtained from Fisher Scientific. 2-Amino-4-bromobenzaldehyde (**3.58**) was obtained from AmBeed. All ligands used for reaction optimization (Sections 3.8.2.2, 3.8.2.4, and 3.8.2.5) were obtained from Strem Chemicals, TCI America, Sigma-Aldrich, or Solvias. Ethyl chloroformate was distilled over CaH_2 prior to use. MnO_2 , Na_2CO_3 , and K_2CO_3 were dried in an oven heated to 120 °C for 48 h prior to use. Reaction temperatures at or above 23 °C were controlled using an IKA Mag temperature modulator, and unless stated otherwise, performed at room temperature (approximately 23 °C). Thin-layer chromatography (TLC) was conducted with EMD gel 60 F₂₅₄ pre-coated plates (0.25 mm for analytical chromatography and 0.50 mm for preparative chromatography) and visualized using a combination of UV light and potassium permanganate staining techniques. Silicycle Siliaflash P60 (particle size 40–63 μm) was used for flash column chromatography. ¹H-NMR and 2D-NOESY spectra were recorded on Bruker spectrometers (at 400, 500, and 600 MHz) and are reported relative to the residual solvent signal. Data for ¹H-NMR spectra are reported as follows: chemical shift (δ ppm), multiplicity, coupling constant (Hz) and integration. ¹³C-NMR spectra were recorded on Bruker spectrometers (at 100,

125, and 150 MHz) and are reported relative to the residual solvent signal. Data for ^{13}C -NMR spectra are reported in terms of chemical shift (δ ppm) and, when necessary, multiplicity, and coupling constant (Hz). ^{19}F -NMR spectra were recorded on Bruker spectrometers (at 282 MHz) and are reported in terms of chemical shift (δ ppm), multiplicity, coupling constant (Hz) and integration. IR spectra were recorded on a Perkin-Elmer UATR Two FT-IR spectrometer and a JASCO FT/IR-4100 spectrometer and are reported in terms of frequency absorption (cm^{-1}). Uncorrected melting points were measured using a Digimelt MPA160 melting point apparatus. DART-MS spectra were collected on a Thermo Exactive Plus MSD (Thermo Scientific) equipped with an ID-CUBE ion source and a Vapur Interface (IonSense Inc.). Both the source and MSD were controlled by Excalibur software version 3.0. The analyte was spotted onto OpenSpot sampling cards (IonSense Inc.) using deuterated chloroform (CDCl_3) or CH_2Cl_2 as the solvent. Ionization was accomplished using UHP He plasma with no additional ionization agents. The mass calibration was carried out using Pierce LTQ Velos ESI (+) and (-) Ion calibration solutions (Thermo Fisher Scientific). Optical rotations were measured with a Rudolf Autopol III Automatic Polarimeter. Determination of enantiopurity was carried out on a JASCO SFC (supercritical fluid chromatography) using a Daicel ChiralPak ID column and a Daicel ChiralPak IE column. Data for SFC chromatograms are reported in enantiomeric excess (ee).

Alcohol **3.53**,⁶⁶ vinyl benzoxazinone derivatives **3.15**⁶⁷, **3.69**⁵⁶, **3.70**⁵⁶, **3.71**⁶⁸, **3.73**⁶⁷, **3.74**⁶⁸, **3.76**⁶⁸, **3.81**⁶⁹, **3.86**⁷⁰, **3.87**⁶⁹, **3.89**⁶⁷, and **3.90**⁶⁹, and allene precursors **3.16**²⁷, **3.50**²⁹, **3.84**³⁸, and **3.88**²⁵ are all known compounds. The ^1H NMR spectral data matched those reported in literature.

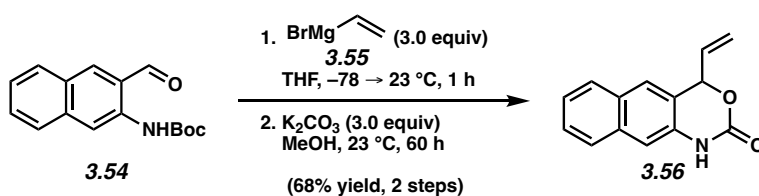
3.8.2 Experimental Procedures

3.8.2.1 Synthesis of *N*-Tosyl-vinyl Benzoxazinones



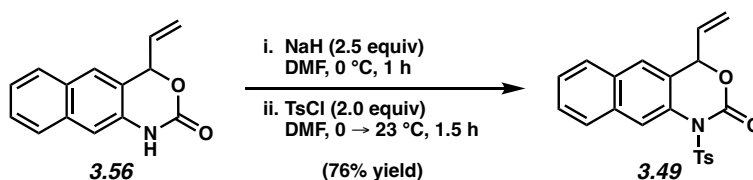
Aldehyde 3.54. To a solution of alcohol **3.53** (2.37 g, 8.67 mmol, 1.0 equiv) in CH_2Cl_2 (28.9 mL, 0.30 M) was added MnO_2 (4.52 g, 52.0 mmol, 6.0 equiv) in a single portion. The reaction vessel was fitted with an air condenser and the resulting mixture was stirred at 40 °C for 18 h. After 18 h, the reaction mixture was cooled to 23 °C and filtered over a celite plug eluting with ethyl acetate (500 mL). The filtrate was then concentrated under reduced pressure to afford aldehyde **3.54** (1.99 g, 85% yield) as a yellow solid, which was used in the subsequent step without purification.

Aldehyde 3.54: Mp: 132–133 °C; R_f 0.57 (5:1 hexanes:EtOAc); ^1H NMR (500 MHz, CDCl_3): δ 10.19 (br s, 1H), 10.07 (s, 1H), 8.78 (s, 1H), 8.18 (s, 1H), 7.87 (d, $J = 8.2$, 1H), 7.82 (d, $J = 8.3$, 1H), 7.59 (t, $J = 7.3$, 1H), 7.42 (t, $J = 7.5$, 1H), 1.57 (s, 9H); ^{13}C NMR (125 MHz, CDCl_3): δ 195.2, 153.4, 140.4, 137.5, 136.5, 130.4, 129.1, 128.2, 127.8, 125.4, 122.8, 115.2, 80.9, 28.5; IR (film): 3314, 2980, 1728, 1673, 1541 cm^{-1} ; HRMS-APCI (m/z) $[\text{M} - \text{H}]^-$ calcd for $\text{C}_{16}\text{H}_{16}\text{NO}_3^-$, 270.1125; found 270.1112.



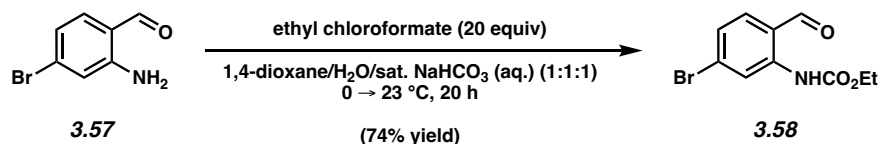
Vinyl benzoxazinone 3.56. To a solution of aldehyde **3.54** (750 mg, 2.77 mmol, 1.0 equiv) in THF (6.0 mL, 0.46 M) at $-78\text{ }^\circ\text{C}$ was added vinylmagnesium bromide **3.55** (0.32 M in THF, 25.9 mL, 8.29 mmol, 3.0 equiv) dropwise over 25 min. The solution was warmed to 23 °C and stirred at this temperature for 1 h. The reaction was then cooled to 0 °C and quenched with dropwise addition of saturated aqueous NaHCO_3 (40 mL). The resulting mixture was extracted with diethyl

ether (3 x 50 mL). The combined organic layers were dried with Na₂SO₄, filtered, and concentrated under reduced pressure to afford a dark orange oil (828 mg). To a solution of the dark orange oil in MeOH (9.1 mL, 0.30 M) was added K₂CO₃ (1.15 g, 8.30 mmol, 3.0 equiv) and the resulting heterogeneous mixture was allowed to stir at 23 °C for 60 h. The reaction was then neutralized with 2 M HCl (4 mL) and the resulting mixture was extracted with EtOAc (3 x 50 mL). The combined organic layers were washed with brine (1 x 50 mL), dried with Na₂SO₄, filtered, and concentrated under reduced pressure. The crude material was purified by flash column chromatography (5:1 → 4:1 hexanes:EtOAc) to provide vinyl benzoxazinone **3.56** (425 mg, 68% yield over 2 steps) as an off-white solid. **Vinyl benzoxazinone 3.56**: Mp: 165 °C; R_f 0.33 (2:1 hexanes:EtOAc); ¹H NMR (500 MHz, CDCl₃): δ 9.33 (s, 1H), 7.77 (d, *J* = 8.1, 1H), 7.74 (d, *J* = 8.2, 1H), 7.58 (s, 1H), 7.47 (ddd, *J* = 8.1, 6.9, 1.2, 1H), 7.40 (ddd, *J* = 8.1, 6.9, 1.2, 1H), 7.29 (s, 1H), 6.17 (ddd, *J* = 17.0, 10.4, 6.4, 1H), 5.97 (dd, *J* = 6.4, 1.0, 1H), 5.49 (dt, *J* = 10.4, 0.9, 1H), 5.44 (dt, *J* = 17.1, 1.0, 1H); ¹³C NMR (125 MHz, CDCl₃): δ 153.4, 133.9, 133.8, 132.9, 130.2, 128.1, 127.4, 127.1, 125.2, 124.8, 121.1, 120.3, 110.4, 80.3; IR (film): 3099, 2927, 1706, 1379, 1032 cm⁻¹; HRMS-APCI (*m/z*) [M + H]⁺ calcd for C₁₄H₁₂NO₂⁺, 226.0863; found 226.0866.



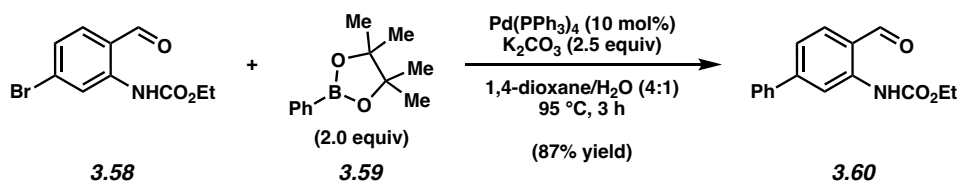
N-tosyl-vinyl benzoxazinone 3.49. To a solution of vinyl benzoxazinone **3.56** (350 mg, 1.55 mmol, 1.0 equiv) in DMF (10.4 mL, 0.15 M) at 0 °C was added NaH (60 wt% dispersion in mineral oil, 160 mg, 3.88 mmol, 2.5 equiv) in one portion. The mixture was stirred at this temperature for 1 h prior to the addition of TsCl (592 mg, 3.11 mmol, 2.0 equiv) in one portion. The resulting

mixture was gradually warmed to 23 °C over 1.5 h then quenched by pouring into an Erlenmeyer flask filled with ice. The resulting mixture was extracted with EtOAc (3 x 50 mL). The combined organic layers were washed with water (3 x 40 mL), dried with Na₂SO₄, filtered, and concentrated under reduced pressure. The crude material was purified by flash column chromatography (9:1 hexanes:EtOAc) to provide *N*-tosyl-vinyl benzoxazinone **3.49** (449 mg, 76% yield) as a white solid. ***N*-tosyl-vinyl benzoxazinone 3.49**: Mp: 148–149 °C; R_f 0.57 (2:1 hexanes:EtOAc); ¹H NMR (500 MHz, CDCl₃): δ 8.14 (dt, *J* = 8.7, 1.9, 2H), 8.04 (s, 1H), 7.88 (d, *J* = 8.0, 1H), 7.81 (d, *J* = 8.0, 1H), 7.65 (s, 1H), 7.55 (ddd, *J* = 8.2, 6.9, 1.4, 1H), 7.51 (ddd, *J* = 8.1, 7.0, 1.5, 1H), 7.43–7.38 (m, 2H), 6.11 (ddd, *J* = 17.2, 10.5, 6.0, 1H), 5.78 (dd, *J* = 6.1, 1.1, 1H), 5.52 (dt, *J* = 10.6, 1.1, 1H), 5.42 (ddd, *J* = 17.2, 1.3, 0.7, 1H), 2.47 (s, 3H); ¹³C NMR (125 MHz, CDCl₃): δ 149.4, 145.8, 135.7, 133.2, 132.2, 131.1, 130.8, 129.8, 129.3, 128.3, 127.8, 127.5, 126.9, 126.0, 124.7, 121.7, 118.9, 79.8, 21.9; IR (film): 3065, 2927, 1744, 1368, 1168 cm⁻¹; HRMS-APCI (*m/z*) [M + H]⁺ calcd for C₂₁H₁₈NO₄S⁺, 380.0951; found 380.0957.



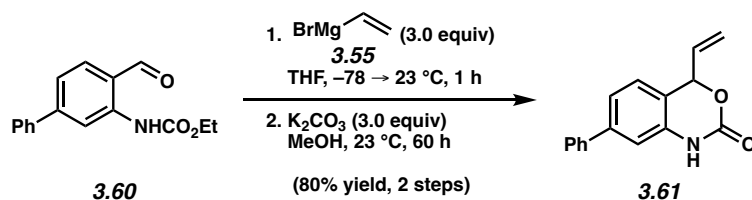
Carbamate 3.58. To a solution of amino benzaldehyde **3.57** (1.50 g, 7.50 mmol, 1.0 equiv) in 1:1:1 1,4-dioxane/water/sat. NaHCO₃ (30 mL, 0.25 M) at 0 °C was added ethyl chloroformate (8.00 mL, 80.0 mmol, 20.0 equiv) dropwise over 5 min. The reaction was then warmed to 23 °C over 20 h before being diluted with brine (40 mL). The resulting mixture was extracted with EtOAc (3 x 30 mL). The combined organic layers were dried with Na₂SO₄, filtered, and concentrated under reduced pressure. The crude material was purified by flash column chromatography (49:1 hexanes:EtOAc) to provide carbamate **3.58** (1.51 g, 74% yield) as a pale yellow solid. **Carbamate**

3.58: Mp: 66–67 °C; R_f 0.58 (5:1 hexanes:EtOAc); ^1H NMR (600 MHz, CDCl_3): δ 10.60 (br s, 1H), 9.86 (s, 1H), 8.73 (d, $J = 1.2$, 1H), 7.48 (d, $J = 8.2$, 1H), 7.31 (dd, $J = 8.2$, 1.7, 1H), 4.26 (q, $J = 7.2$, 2H), 1.34 (t, $J = 7.2$, 3H); ^{13}C NMR (125 MHz, CDCl_3): δ 194.3, 153.6, 142.2, 137.0, 131.9, 125.4, 121.6, 120.1, 61.9, 14.6; IR (film): 3231, 2995, 1728, 1515, 1216 cm^{-1} ; HRMS-APCI (m/z) $[\text{M} + \text{H}]^+$ calcd for $\text{C}_{10}\text{H}_{11}\text{BrNO}_3^+$, 271.9917; found 271.9919.



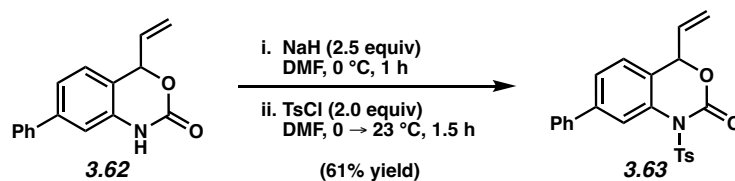
Carbamate 3.60. An 8-dram vial containing a magnetic stir bar was charged with carbamate **3.58** (600 mg, 2.21 mmol, 1.0 equiv), potassium carbonate (762 mg, 5.51 mmol, 2.5 equiv), and phenylboronic acid pinacol ester **3.59** (900 mg, 4.41 mmol, 2.0 equiv). The vial was taken into a glovebox where $\text{Pd}(\text{PPh}_3)_4$ (255 mg, 0.221 mmol, 0.1 equiv) was added. The reaction was sealed with a septum cap, removed from the glovebox, and placed under a flow of N_2 . Then, 4:1 1,4-dioxane:water (16 mL, 0.138 M) was added. The septum cap was then carefully replaced with a Teflon-lined cap and stirred for 3 h at 95 °C. The reaction mixture was then cooled to 23 °C, concentrated under reduced pressure, diluted with water (10 mL) and extracted with CH_2Cl_2 (3 x 20 mL). The combined organic layers were dried with Na_2SO_4 , filtered, and concentrated under reduced pressure. The crude material was purified by flash column chromatography (49:1 hexanes:EtOAc) to provide carbamate **3.60** (515 mg, 87% yield) as a white solid. **Carbamate 3.60**: Mp: 109–110 °C; R_f 0.66 (5:1 hexanes:EtOAc); ^1H NMR (500 MHz, CDCl_3): δ 10.65 (br s, 1H), 9.94 (d, $J = 0.6$, 1H), 8.78 (d, $J = 1.5$, 1H), 7.73–7.66 (m, 3H), 7.49–7.44 (m, 2H), 7.44–7.38 (m, 2H), 4.27 (q, $J = 7.1$, 2H), 1.36 (t, $J = 7.1$, 3H); ^{13}C NMR (125 MHz, CDCl_3): δ 194.7, 154.0,

148.8, 141.9, 139.7, 136.6, 129.1, 128.9, 127.7, 120.7, 120.3, 117.0, 61.6, 14.6; IR (film): 3272, 2928, 1724, 1564, 1211 cm^{-1} ; HRMS-APCI (m/z) $[\text{M} + \text{H}]^+$ calcd for $\text{C}_{16}\text{H}_{16}\text{NO}_3^+$, 270.1125; found 270.1127.



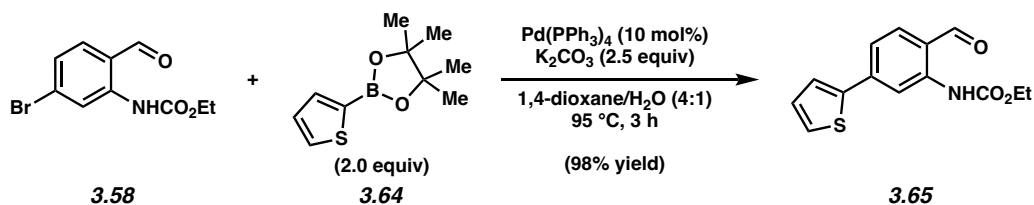
Vinyl benzoxazinone 3.61. To a solution of aldehyde **3.60** (495 mg, 1.84 mmol, 1.0 equiv) in THF (1.0 mL, 2 M) at $-78 \text{ }^\circ\text{C}$ was added vinylmagnesium bromide **3.55** (0.46 M in THF, 12.0 mL, 5.51 mmol, 3.0 equiv) dropwise over 7 min. The solution was warmed to $23 \text{ }^\circ\text{C}$ and stirred at this temperature for 30 min. The reaction was then cooled to $0 \text{ }^\circ\text{C}$ and quenched with dropwise addition of saturated aqueous NaHCO_3 (6 mL). The resulting mixture was extracted with diethyl ether (3 x 7 mL). The combined organic layers were dried with Na_2SO_4 , filtered, and concentrated under reduced pressure to afford an oil (550 mg). To a solution of the oil in MeOH (6.17 mL, 0.30 M) was added K_2CO_3 (767 mg, 5.55 mmol, 3.0 equiv) and the resulting heterogeneous mixture was allowed to stir at $23 \text{ }^\circ\text{C}$ for 60 h. The reaction was neutralized with 1 M HCl (6 mL), and the resulting mixture was extracted with EtOAc (3 x 20 mL). The combined organic layers were washed with brine (10 mL), dried with Na_2SO_4 , filtered, and concentrated under reduced pressure. The crude product was purified by flash column chromatography (5:1 hexanes:EtOAc) to provide vinyl benzoxazinone **3.61** (373 mg, 80% yield over 2 steps) as a pale yellow solid. **Vinyl benzoxazinone 3.61:** Mp: $159\text{--}161 \text{ }^\circ\text{C}$; R_f 0.15 (5:1 hexanes:EtOAc); ^1H NMR (500 MHz, CDCl_3): δ 7.62 (br s, 1H), 7.57–7.53 (m, 2H), 7.48–7.42 (m, 2H), 7.38 (tt, $J = 7.4, 1.3$, 1H), 7.30 (dd, $J = 7.9, 1.7$, 1H), 7.17 (d, $J = 7.8$, 1H), 7.00 (d, $J = 1.7$, 1H), 6.10 (ddd, $J = 16.9, 10.3, 6.4$,

1H), 5.87–5.84 (m, 1H), 5.56–5.38 (m, 2H); ¹³C NMR (125 MHz, CDCl₃, 13 of 14 signals observed): δ 143.0, 139.9, 135.5, 133.9, 129.0, 128.1, 127.3, 125.6, 122.4, 119.9, 118.9, 113.0, 80.3; IR (film): 3235, 2971, 1704, 1366, 760 cm⁻¹; HRMS-APCI (*m/z*) [M + H]⁺ calcd for C₁₆H₁₄NO₂⁺, 252.1019; found 252.1018.

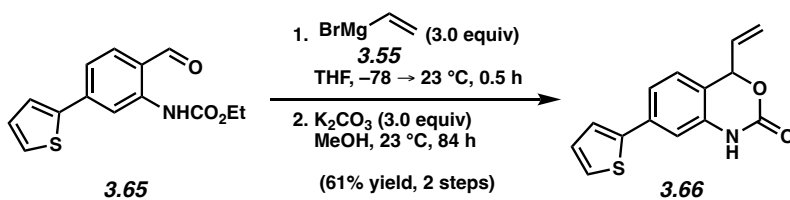


***N*-tosyl-vinyl benzoxazinone 3.63.** To a solution of vinyl benzoxazinone **3.62** (370 mg, 1.47 mmol, 1.0 equiv) in DMF (9.82 mL, 0.15 M) at 0 °C was added NaH (60 wt% dispersion in mineral oil, 150 mg, 3.68 mmol, 2.5 equiv) in one portion. The mixture was stirred at this temperature for 1 h prior to the addition of TsCl (561 mg, 2.94 mmol, 2.0 equiv) in one portion. The resulting mixture was gradually warmed to 23 °C over 3 h then quenched by pouring into an Erlenmeyer flask filled with ice. The resulting mixture was extracted with EtOAc (3 x 20 mL). The combined organic layers were washed with water (3 x 30 mL), dried with Na₂SO₄, filtered, and concentrated under reduced pressure. The crude material was purified by flash column chromatography (7:1 hexanes:EtOAc) to provide *N*-tosyl-vinyl benzoxazinone **3.63** (365 mg, 61% yield) as a yellow solid. ***N*-tosyl-vinyl benzoxazinone 3.63:** Mp: 120–121 °C; *R_f* 0.23 (5:1 hexanes:EtOAc); ¹H NMR (500 MHz, CDCl₃): δ 8.12 (d, *J* = 8.3, 2H), 7.85 (s, 1H), 7.59 (d, *J* = 7.4, 2H), 7.51–7.45 (m, 3H), 7.44–7.37 (m, 3H), 7.25 (overlapped with residual solvent peak, 1H), 6.07 (ddd, *J* = 16.9, 10.4, 6.2, 1H), 5.69 (d, *J* = 6.0, 1H), 5.49 (d, *J* = 10.4, 1H), 5.41 (d, *J* = 17.1, 1H), 2.47 (s, 3H); ¹³C NMR (125 MHz, CDCl₃): δ 149.3, 145.8, 142.8, 140.0, 135.8, 134.6, 132.2, 129.9, 129.3,

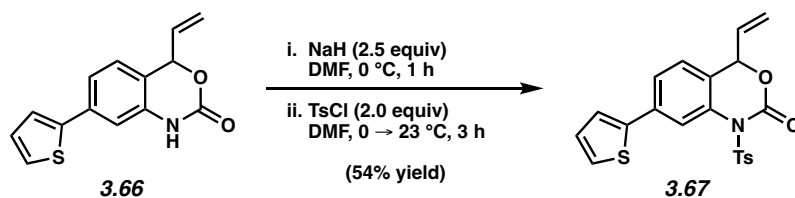
129.2, 128.3, 127.4, 125.5, 125.3, 124.9, 121.4, 119.9, 79.5, 21.9; IR (film): 3025, 2970, 1747, 1364, 1166 cm^{-1} ; HRMS-APCI (m/z) [$M + H$] $^+$ calcd for $\text{C}_{23}\text{H}_{20}\text{NO}_4\text{S}^+$, 406.1108; found 406.1109.



Carbamate 3.65. A 50-mL round-bottomed flask containing a magnetic stir bar was charged with carbamate **3.58** (750 mg, 2.76 mmol, 1.0 equiv), potassium carbonate (952 mg, 6.89 mmol, 2.5 equiv), and thiophene-2-boronic acid pinacol ester **3.64** (1.16 g, 5.51 mmol, 2.0 equiv). The flask was taken into a glovebox where $\text{Pd}(\text{PPh}_3)_4$ (319 mg, 0.276 mmol, 0.10 equiv) was added. The reaction was sealed with a septum cap, removed from the glovebox, and placed under a flow of N_2 . Then, 4:1 1,4-dioxane:water (18.8 mL, 0.147 M) was added. The reaction mixture was stirred for 3 h at 95 °C. The reaction mixture was then cooled to 23 °C, concentrated under reduced pressure, diluted with water (10 mL), and extracted with CH_2Cl_2 (3 x 20 mL). The combined organic layers were dried with Na_2SO_4 , filtered, and concentrated under reduced pressure. The crude material was purified by flash column chromatography (19:1 hexanes:EtOAc) to provide carbamate **3.65** (745 mg, 98% yield) as a yellow solid. **Carbamate 3.65:** Mp: 105–106 °C; R_f 0.68 (1:1 hexanes: CH_2Cl_2); ^1H NMR (600 MHz, CDCl_3): δ 10.66 (br s, 1H), 9.87 (s, 1H), 8.82 (d, $J = 1.4$, 1H), 7.62 (d, $J = 8.0$, 1H), 7.54 (dd, $J = 3.7, 1.1$, 1H), 7.43–7.38 (m, 2H), 7.13 (dd, $J = 5.0, 3.7$, 1H), 4.27 (q, $J = 7.2$, 2H), 1.36 (t, $J = 7.2$, 3H); ^{13}C NMR (125 MHz, CDCl_3): δ 194.2, 153.9, 142.9, 142.1, 141.7, 136.9, 128.6, 127.5, 125.9, 120.2, 119.1, 115.0, 61.7, 14.6; IR (film): 3263, 1734, 1610, 1212, 703 cm^{-1} ; HRMS-APCI (m/z) [$M + H$] $^+$ calcd for $\text{C}_{14}\text{H}_{14}\text{NO}_3\text{S}^+$, 276.0694; found 276.0690.



Vinyl benzoxazinone 3.66. To a solution of aldehyde **3.65** (500 mg, 1.82 mmol, 1.0 equiv) in THF (22.7 mL, 0.080 M) at -78 °C was added vinylmagnesium bromide **3.55** (0.46 M in THF, 11.8 mL, 5.45 mmol, 3.0 equiv) dropwise over 7 min. The solution was warmed to 23 °C and stirred at this temperature for 30 min. The reaction was then cooled to 0 °C and quenched with dropwise addition of saturated aqueous NaHCO₃ (8 mL). The resulting mixture was extracted with diethyl ether (3 x 10 mL). The combined organic layers were dried with Na₂SO₄, filtered, and concentrated under reduced pressure to afford an oil (551 mg). To a solution of the oil in MeOH (20.0 mL, 0.091 M) was added K₂CO₃ (753 mg, 5.45 mmol, 3.0 equiv) and the resulting heterogeneous mixture was allowed to stir at 23 °C for 84 h. The reaction was neutralized with 1 M HCl (6 mL), and the resulting mixture was extracted with EtOAc (3 x 20 mL). The combined organic layers were washed with brine (10 mL), dried with Na₂SO₄, filtered, and concentrated under reduced pressure. The crude product was purified by flash column chromatography (5:1 hexanes:EtOAc) to provide vinyl benzoxazinone **3.66** (284 mg, 61% yield over 2 steps) as an off-white solid. **Vinyl benzoxazinone 3.66:** Mp: 163 °C; R_f 0.11 (5:1 hexanes:EtOAc); ¹H NMR (500 MHz, CDCl₃): δ 7.57 (br s, 1H), 7.33–7.30 (m, 3H), 7.12–7.07 (m, 2H), 7.02 (d, *J* = 1.4, 1H), 6.08 (ddd, *J* = 16.9, 10.3, 6.4, 1H), 5.82 (d, *J* = 6.4, 1H), 5.44 (d, *J* = 10.3, 1H), 5.39 (d, *J* = 17.1, 1H); ¹³C NMR (125 MHz, CDCl₃): δ 151.8, 142.9, 136.0, 135.6, 133.8, 128.3, 125.9, 125.8, 124.1, 121.2, 120.0, 119.0, 111.4, 80.2; IR (film): 3108, 2925, 1706, 1376, 1268 cm⁻¹; HRMS-APCI (*m/z*) [M + H]⁺ calcd for C₁₄H₁₂NO₂S⁺, 258.0589; found 258.0590.



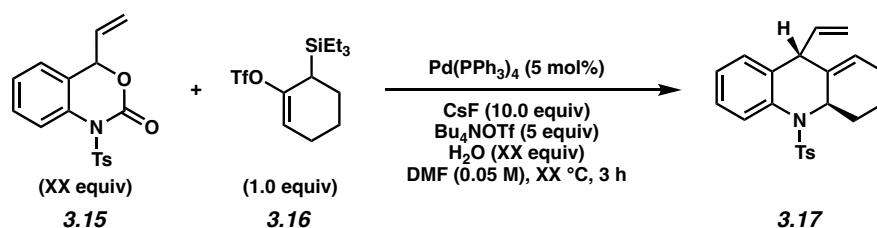
***N*-tosyl-vinyl benzoxazinone 3.67.** To a solution of vinyl benzoxazinone **3.66** (284 mg, 1.10 mmol, 1.0 equiv) in DMF (7.35 mL, 0.15 M) at 0 °C was added NaH (60 wt% dispersion in mineral oil, 110 mg, 2.75 mmol, 2.5 equiv) in one portion. The mixture was stirred at this temperature for 1 h prior to the addition of TsCl (420 mg, 2.20 mmol, 2.0 equiv) in one portion. The resulting mixture was gradually warmed to 23 °C over 3 h then quenched by pouring into an Erlenmeyer flask filled with ice. The resulting mixture was extracted with EtOAc (3 x 20 mL). The combined organic layers were washed with water (30 mL), dried with Na₂SO₄, filtered, and concentrated under reduced pressure. The crude material was purified by flash column chromatography (7:1 hexanes:EtOAc) to provide *N*-tosyl-vinyl benzoxazinone **3.67** (246 mg, 54% yield) as a white solid. ***N*-tosyl-vinyl benzoxazinone 3.67:** Mp: 119 °C; *R_f* 0.18 (5:1 hexanes:EtOAc); ¹H NMR (600 MHz, CDCl₃): δ 8.15 (dt, *J* = 8.7, 2.0, 2H), 7.84 (d, *J* = 1.6, 1H), 7.48 (dd, *J* = 8.0, 1.6, 1H), 7.44–7.39 (m, 2H), 7.37–7.33 (m, 2H), 7.18 (d, *J* = 8.0, 1H), 7.12 (dd, *J* = 5.0, 3.7, 1H), 6.05 (ddd, *J* = 17.0, 10.4, 6.1, 1H), 5.58–5.63 (m, 1H), 5.52–5.46 (m, 1H), 5.40 (ddd, *J* = 17.2, 1.3, 0.6, 1H), 2.48 (s, 3H); ¹³C NMR (150 MHz, CDCl₃): δ 149.2, 145.9, 142.9, 135.87, 135.86, 134.9, 132.1, 129.9, 129.3, 128.5, 126.1, 125.7, 125.4, 124.5, 123.5, 121.5, 118.3, 79.5, 21.9; IR (film): 2977, 2367, 1758, 1173, 823 cm⁻¹; HRMS-APCI (*m/z*) [M + H]⁺ calcd for C₂₁H₁₈NO₄S₂⁺, 412.0677; found 412.0668.

3.8.2.2. Optimization of the Racemic Annulation

Results from the optimization of the reactions between **3.15** and **3.16** and between **3.15** and **3.50** appear below. Reactant stoichiometry and temperature were varied using General Procedure 3.1, and results appear below in Table 3.3 and 3.4, respectively. Water loading, catalyst loading, and concentration were varied using General Procedure 3.2, and results appear below in Table 3.5, 3.6, and 3.7, respectively. Ligands were varied using General Procedure 3.3, and results appear below in Table 3.8. Initial efforts to use other metals (e.g., Ir and Ni) were unsuccessful. As such, we focused on Pd.

Any modification of the conditions shown in the general procedures above are specified in the following schemes. Although reactions were performed in a glovebox for consistency, reactions setup on the bench-top did not suffer from a significant loss in yield.

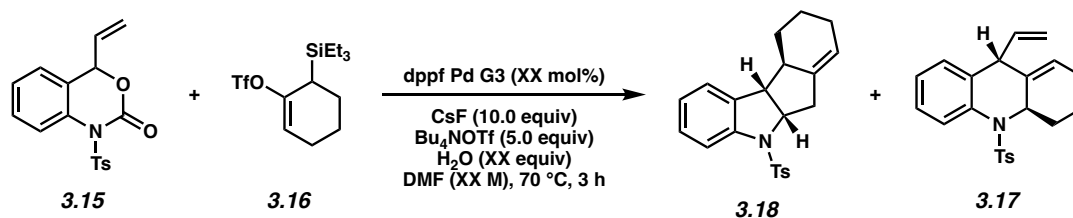
General Procedure 3.1 for the optimization of the racemic annulation:



Annulation Product 3.17. A 1-dram vial containing a magnetic stir bar was charged with vinyl benzoxazinone **3.15** and Bu₄NOTf (49 mg, 0.13 mmol, 5.0 equiv). A separate 1-dram vial was charged with silyl triflate **3.16**. The two vials were taken into a glovebox where Pd(PPh₃)₄ (1.4 mg, 0.0013 mmol, 0.05 equiv) and CsF (38 mg, 0.25 mmol, 10.0 equiv) were added to the vial containing vinyl benzoxazinone **3.15**. To the vial containing silyl triflate **3.16** was added the appropriate amount of DMF to afford a 0.05 M solution. The vial was capped and shaken to ensure

full dissolution. The necessary amount of the solution of silyl triflate **3.16** (0.05 M in DMF, 500 μ L, 8.6 mg, 0.025 mmol, 1.0 equiv) was then transferred via micropipette to the reaction vial containing vinyl benzoxazinone **3.15**. The reaction was sealed with a septum cap, removed from the glovebox, and placed under a flow of N₂. Then, deionized water was added to the reaction vessel via microsyringe. The septum cap was then carefully replaced with a Teflon-lined cap under a stream of N₂ and stirred for 3 h at the desired reaction temperature. The mixture was then filtered through a pad of silica gel, eluting with EtOAc (8 mL). The eluate was concentrated by iteratively azeotroping with *n*-heptane (4 x 5 mL). The crude residue was then redissolved in CH₂Cl₂ (1 mL) and filtered through a pad of silica gel eluting with CH₂Cl₂ (20 mL) to remove excess Bu₄NOTf. The eluate was concentrated to afford a crude residue, which was analyzed by ¹H NMR using mesitylene as an external standard.

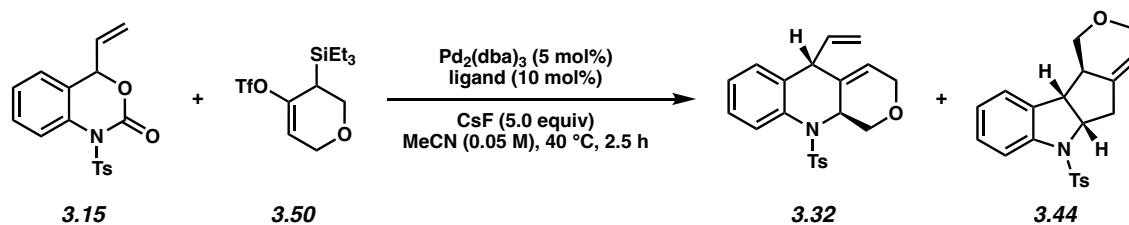
General Procedure 3.2 for the optimization of the racemic annulation:



Annulation Products 3.17 and 3.18. A 1-dram vial containing a magnetic stir bar was charged with vinyl benzoxazinone **3.15** (25 mg, 0.075 mmol, 3.0 equiv) and Bu₄NOTf (49 mg, 0.13 mmol, 5.0 equiv). A separate 1-dram vial was charged with silyl triflate **3.16**. The two vials were taken into a glovebox where dppf Pd G3 and CsF (38 mg, 0.25 mmol, 10.0 equiv) were added to the vial containing vinyl benzoxazinone **3.15**. To the vial containing silyl triflate **3.16** was added the appropriate amount of DMF to afford a solution of desired concentration. The vial was capped and shaken to ensure full dissolution. The necessary amount of the solution of silyl triflate **3.16** (8.6

mg, 0.025 mmol, 1.0 equiv) was then transferred via micropipette to the reaction vial containing vinyl benzoxazinone **3.15**. The reaction was sealed with a septum cap, removed from the glovebox, and placed under a flow of N₂. Then, deionized water was added to the reaction vessel via microsyringe. The septum cap was then carefully replaced with a Teflon-lined cap under a stream of N₂ and stirred for 3 h at 70 °C. The mixture was then filtered through a pad of silica gel, eluting with EtOAc (8 mL). The eluate was washed with water (2 x 5 mL), dried with Na₂SO₄, filtered, and concentrated under reduced pressure. The crude residue was redissolved in CH₂Cl₂ (1 mL) and filtered through a pad of silica gel eluting with CH₂Cl₂ (20 mL) to remove excess Bu₄NOTf. The eluate was concentrated and purified by preparative thin layer chromatography (4:1:1 hexanes:CH₂Cl₂:Et₂O) to provide annulation products **3.17** and **3.18**.

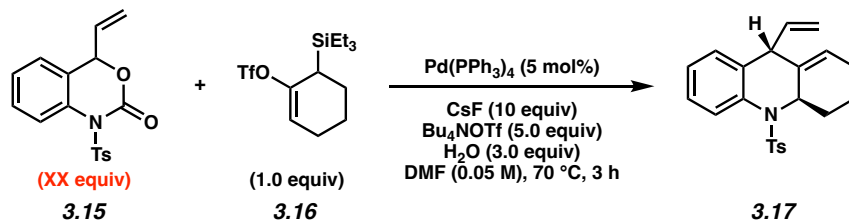
General Procedure 3.3 for the optimization of the racemic annulation:



Annulation Products 3.32 and 3.44. A 1-dram vial containing a magnetic stir bar was charged with vinyl benzoxazinone **3.15** (25 mg, 0.075 mmol, 3.0 equiv). A separate 1-dram vial was charged with silyl triflate **3.50**. The two vials were taken into a glovebox where Pd₂(dba)₃ (1.1 mg, 0.0013 mmol, 5 mol%), ligand (0.0025 mmol, 10 mol%) and CsF (38 mg, 0.25 mmol, 10.0 equiv) were added to the vial containing vinyl benzoxazinone **3.15**. To the vial containing silyl triflate **3.50** was added the appropriate amount of MeCN to afford a 0.05 M solution. The vial was capped and shaken to ensure full dissolution. The necessary amount of the solution of silyl triflate **3.50** (0.05 M in MeCN, 500 μL, 8.6 mg, 0.025 mmol, 1.0 equiv) was then transferred via micropipette

to the reaction vial containing vinyl benzoxazinone **3.15**. The reaction was sealed with a Teflon-lined cap, removed from the glovebox, and stirred for 2.5 h at 40 °C. The mixture was then filtered through a pad of silica gel, eluting with EtOAc (8 mL). The eluate was concentrated to provide a crude residue, which was analyzed by ¹H NMR using mesitylene as an external standard.

Table 3.3. Evaluation of Vinyl Benzoxazinone Equivalents.



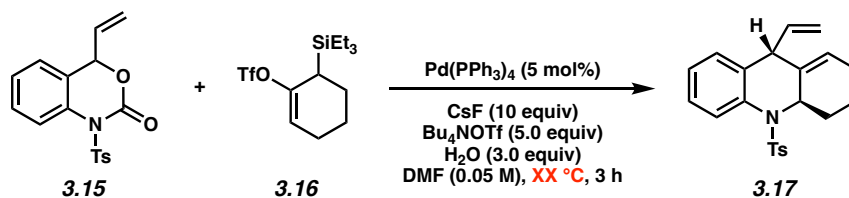
Entry	Equiv. 3.15	¹ H NMR Yield ^a	dr
1	1.0	31%	7.4:1 ^b
2	3.0	54%	11:1 ^b
3	5.0	47%	9.3:1 ^c

^a ¹H NMR yield determined using mesitylene as an external standard.

^b dr was determined by ¹H NMR analysis of crude reaction mixture.

^c dr was determined by ¹H NMR analysis of isolated mixture of diastereomers.

Table 3.4. Evaluation of Temperature.

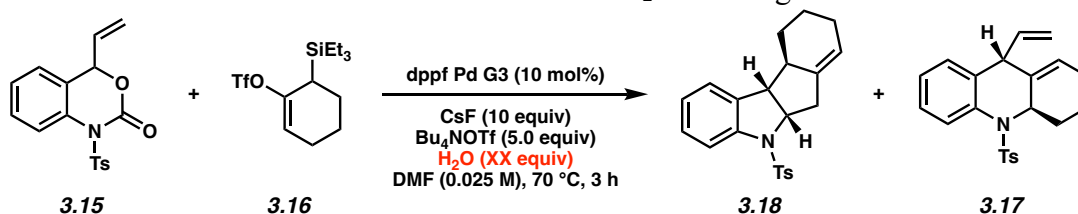


Entry	Temperature (°C)	¹ H NMR Yield ^a	dr ^b
1	50	46%	8.4:1
2	70	54%	11:1
3	90	47%	7.8:1

^a ¹H NMR yield determined using mesitylene as an external standard.

^b dr was determined by ¹H NMR analysis of crude reaction mixture.

Table 3.5. Evaluation of H₂O Loading.

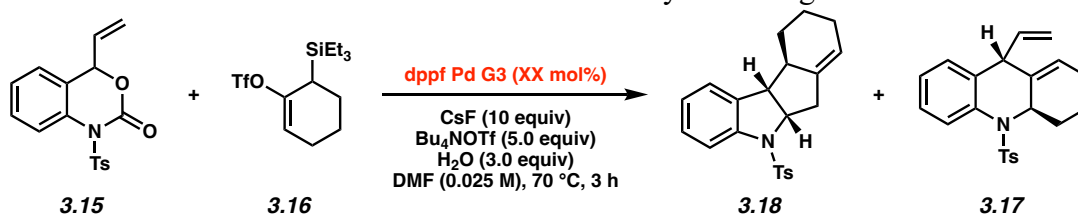


Entry	Equiv. H ₂ O	Isolated Yield ^a	3.18:3.17 ^b
1	0.0	28%	>20:1
2	3.0	59%	10:1
3	6.0	65%	11:1
4	9.0	74%	10:1
5	12.0	73%	3.8:1

^a Products isolated as a mixture.

^b For **3.18** dr = >20:1. For **3.17** dr could not be determined. Ratio of **3.18:3.17** and dr were determined by ¹H NMR analysis of the isolated mixture.

Table 3.6. Evaluation of Catalyst Loading.

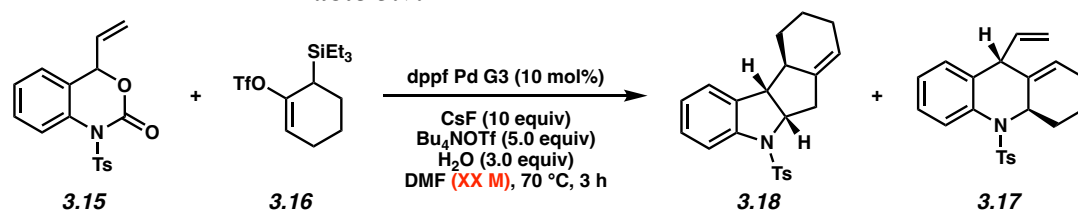


Entry	Mol% [Pd]	Isolated Yield ^a	3.18:3.17 ^b
1	5 mol%	44%	11:1
2	10 mol%	59%	10:1
3	15 mol%	61%	11:1

^a Products isolated as a mixture.

^b For **3.18** dr = >20:1. For **3.17** dr could not be determined. Ratio of **3.18:3.17** and dr were determined by ¹H NMR analysis of the isolated mixture.

Table 3.7. Evaluation of Concentration.

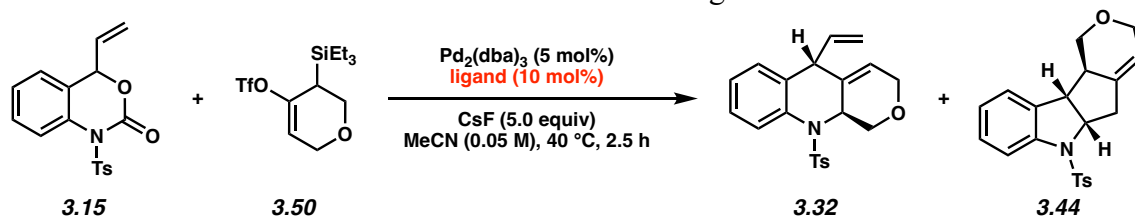


Entry	Concentration	Isolated Yield ^a	3.18:3.17 ^b
1	0.05	64%	7.6:1
2	0.025	59%	10:1
3	0.0125	51%	15:1

^a Products isolated as a mixture.

^b For **3.18** dr = >20:1. For **3.17** dr could not be determined. Ratio of **3.18:3.17** and dr were determined by ¹H NMR analysis of the isolated mixture.

Table 3.8. Evaluation of Ligands.



Entry	Ligand	¹ H NMR Yield (3.32) ^{a,b}	¹ H NMR Yield (3.44) ^{a,c}
1	Pd(PPh ₃) ₄ (5 mol%) ^d	54%	0%
2	PCy ₃	18%	4%
3	DavePhos	13%	0%
4	Ruphos	10%	0%
5	Xantphos	8%	0%
6	SPhos	8%	0%
7	XPhos	6%	0%
8	dppe	0%	0%
9	dtbpf	0%	0%
10	rac-BINAP	0%	0%
11	DPEphos	0%	8%
12	dppf	0%	36%
13	dppf Pd G3 (5 mol%) ^d	0%	44%

^a ¹H NMR yield determined using mesitylene as an external standard.

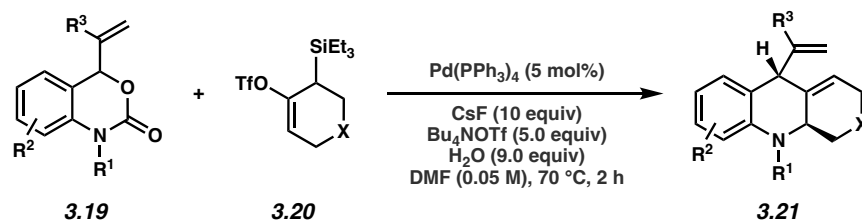
^b ~1:1 dr as determined by ¹H NMR analysis of crude reaction mixture.

^c >20:1 dr as determined by ¹H NMR analysis of crude reaction mixture.

^d Pd₂(dba)₃ omitted from the reaction.

3.8.2.3. Scope of the Racemic Annulation

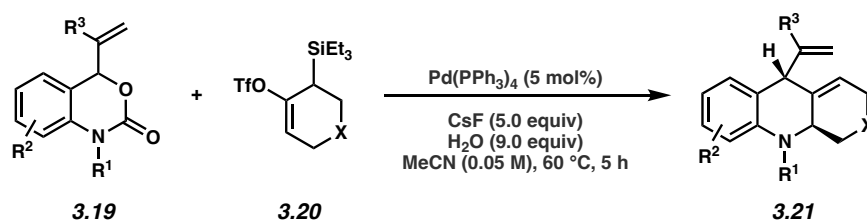
General Procedure 3.4 for the scope of the racemic annulation:



Annulation Products 3.21. A 1-dram vial containing a magnetic stir bar was charged with vinyl benzoxazinone **3.19** (0.15 mmol, 3.0 equiv) and Bu₄NOTf (98 mg, 0.25 mmol, 5.0 equiv). A separate 1-dram vial was charged with silyl triflate **3.20**. The two vials were taken into a glovebox where Pd(PPh₃)₄ (2.9 mg, 0.0025 mmol, 5 mol%) and CsF (76 mg, 0.50 mmol, 10.0 equiv) were

added to the vial containing vinyl benzoxazinone **3.19**. To the vial containing silyl triflate **3.20** was added the appropriate amount of DMF to afford a 0.05 M solution. The vial was capped and shaken to ensure full dissolution. The necessary amount of the solution of silyl triflate **3.20** (0.05 M in DMF, 1.0 mL, 0.05 mmol, 1.0 equiv) was then transferred via micropipette to the reaction vial containing vinyl benzoxazinone **3.19**. The reaction was sealed with a septum cap, removed from the glovebox, and placed under a flow of N₂. Then, deionized water (8.1 μL, 0.45 mmol, 9.0 equiv) was added to the reaction vessel via microsyringe. The septum cap was then carefully replaced with a Teflon-lined cap under a stream of N₂ and stirred for 2 h at 70 °C. The mixture was then filtered through a pad of silica gel, eluting with EtOAc (8 mL). The eluate was washed with water (4 x 5 mL), dried with Na₂SO₄, filtered, and concentrated under reduced pressure. The crude residue was redissolved in CH₂Cl₂ (1 mL) and filtered through a pad of silica gel eluting with CH₂Cl₂ (20 mL) to remove excess Bu₄NOTf. The eluate was concentrated and purified by preparative thin layer chromatography to provide annulation products **3.21**.

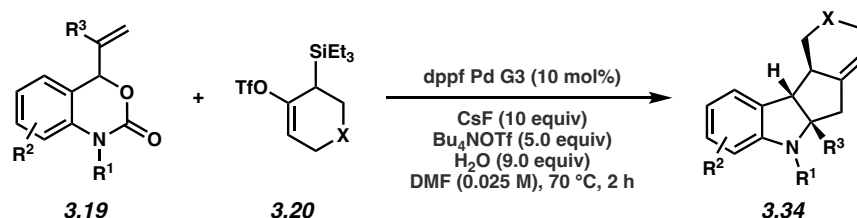
General Procedure 3.5 for the scope of the racemic annulation:



Annulation Products 3.21. A 1-dram vial containing a magnetic stir bar was charged with vinyl benzoxazinone **3.19** (0.15 mmol, 3.0 equiv). A separate 1-dram vial was charged with silyl triflate **3.20**. The two vials were taken into a glovebox where Pd(PPh₃)₄ (2.9 mg, 0.0025 mmol, 5 mol%) and CsF (38 mg, 0.25 mmol, 5.0 equiv) were added to the vial containing vinyl benzoxazinone **3.19**. To the vial containing silyl triflate **3.20** was added the appropriate amount of MeCN to afford

a 0.05 M solution. The vial was capped and shaken to ensure full dissolution. The necessary amount of the solution of silyl triflate **3.20** (0.05 M in MeCN, 1.0 mL, 0.05 mmol, 1.0 equiv) was then transferred via micropipette to the reaction vial containing vinyl benzoxazinone **3.19**. The reaction was sealed with a septum cap, removed from the glovebox, and placed under a flow of N₂. Then, deionized water (8.1 μL, 0.45 mmol, 9.0 equiv) was added to the reaction vessel via microsyringe. The septum cap was then carefully replaced with a Teflon-lined cap under a stream of N₂ and stirred for 5 h at 60 °C. The mixture was then filtered through a pad of silica gel, eluting with EtOAc (8 mL). The eluate was concentrated and purified by preparative thin layer chromatography to provide annulation products **3.21**.

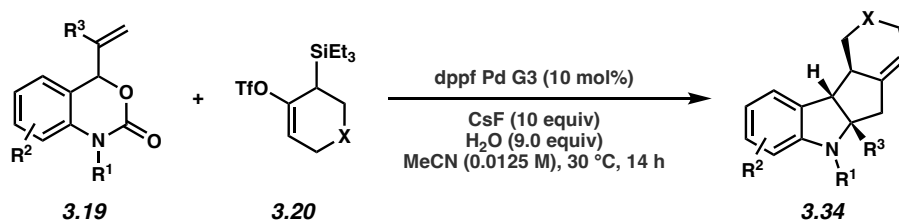
General Procedure 3.6 for the scope of the racemic annulation:



Annulation Products 3.34. A 1-dram vial containing a magnetic stir bar was charged with vinyl benzoxazinone **3.19** (0.15 mmol, 3.0 equiv) and Bu₄NOTf (98 mg, 0.25 mmol, 5.0 equiv). A separate 1-dram vial was charged with silyl triflate **3.20**. The two vials were taken into a glovebox where dppf Pd G3 (4.7 mg, 0.0050 mmol, 10 mol%) and CsF (76 mg, 0.50 mmol, 10.0 equiv) were added to the vial containing vinyl benzoxazinone **3.19**. To the vial containing silyl triflate **3.20** was added the appropriate amount of DMF to afford a 0.025 M solution. The vial was capped and shaken to ensure full dissolution. The necessary amount of the solution of silyl triflate **3.20** (0.025 M in DMF, 2.0 mL, 0.05 mmol, 1.0 equiv) was then transferred via micropipette to the reaction vial containing vinyl benzoxazinone **3.19**. The reaction was sealed with a septum cap, removed

from the glovebox, and placed under a flow of N₂. Then, deionized water (8.1 μL, 0.45 mmol, 9.0 equiv) was added to the reaction vessel via microsyringe. The septum cap was then carefully replaced with a Teflon-lined cap under a stream of N₂ and stirred for 2 h at 70 °C. The mixture was then filtered through a pad of silica gel, eluting with EtOAc (8 mL). The eluate was washed with water (4 x 5 mL), dried with Na₂SO₄, filtered, and concentrated under reduced pressure. The crude residue was redissolved in CH₂Cl₂ (1 mL) and filtered through a pad of silica gel eluting with CH₂Cl₂ (20 mL) to remove excess Bu₄NOTf. The eluate was concentrated and purified by preparative thin layer chromatography to provide annulation products **3.34**.

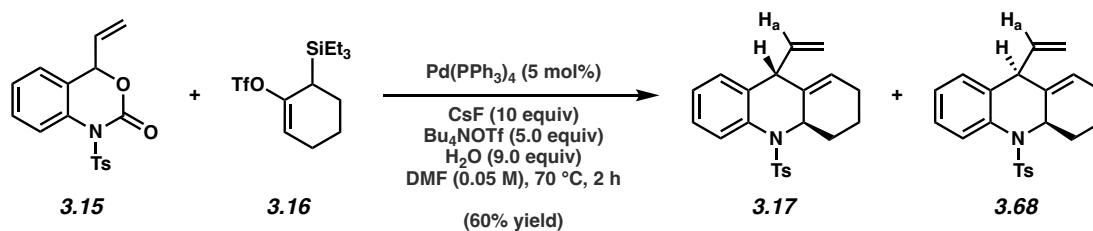
General Procedure 3.7 for the scope of the racemic annulation:



Annulation Products 3.34. A 2-dram vial containing a magnetic stir bar was charged with vinyl benzoxazinone **3.19** (0.15 mmol, 3.0 equiv). A separate 1-dram vial was charged with silyl triflate **3.20**. The two vials were taken into a glovebox where dppf Pd G3 (4.7 mg, 0.0050 mmol, 10 mol%) and CsF (75 mg, 0.50 mmol, 10.0 equiv) were added to the vial containing vinyl benzoxazinone **3.19**. To the vial containing silyl triflate **3.20** was added the appropriate amount of MeCN to afford a 0.0125 M solution. The vial was capped and shaken to ensure full dissolution. The necessary amount of the solution of silyl triflate **3.20** (0.0125 M in MeCN, 4.0 mL, 0.05 mmol, 1.0 equiv) was then transferred via micropipette to the reaction vial containing vinyl benzoxazinone **3.19**. The reaction was sealed with a septum cap, removed from the glovebox, and placed under a flow of N₂. Then, deionized water (8.1 μL, 0.45 mmol, 9.0 equiv) was added to the reaction vessel via

microsyringe. The septum cap was then carefully replaced with a Teflon-lined cap under a stream of N₂ and stirred for 14 h at 30 °C. The mixture was then filtered through a pad of silica gel, eluting with EtOAc (8 mL). The eluate was concentrated and purified by preparative thin layer chromatography to provide annulation products **3.34**.

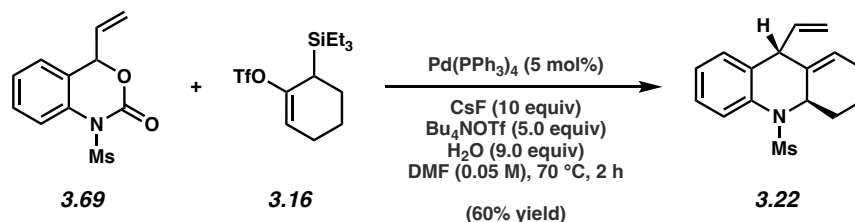
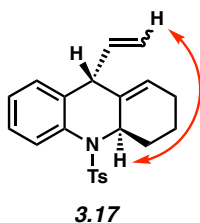
Any modification of the conditions shown in the general procedures above are specified in the following schemes. Although reactions were performed in a glovebox for consistency, reactions setup on the bench-top did not suffer from a significant loss in yield.



3.17 and **3.68**. Followed General Procedure 3.4. Purification by preparative thin layer chromatography (4:1:1 hexanes:CH₂Cl₂:Et₂O) afforded a mixture of major diastereomer **3.17** and minor diastereomer **3.68** (60% combined yield, 9.4:1 dr, average of two experiments) as a white solid. Diastereomeric ratio was determined by integrating the following peaks in the ¹H NMR spectrum of the isolated mixture (H_a **3.17**: 4.81 ppm; **3.68**: 5.88 ppm). **Annulation Products 3.17 and 3.68**: R_f 0.70 (4:1:1 hexanes:CH₂Cl₂:Et₂O); ¹H NMR (500 MHz, CDCl₃, **3.17**): 7.85 (dd, *J* = 8.2, 0.9, 1H), 7.43 (dt, *J* = 8.3, 1.7, 2H), 7.26–7.21 (overlapped with residual solvent peak, 1H), 7.16–7.12 (m, 2H), 7.10 (td, *J* = 7.4, 1.2, 1H), 6.96 (dd, *J* = 7.5, 1.5, 1H), 5.57–5.53 (m, 1H), 4.81 (ddd, *J* = 17.1, 10.0, 5.4, 1H), 4.70–4.58 (m, 2H), 4.42 (dt, *J* = 9.9, 1.8, 1H), 3.68–3.65 (m, 1H), 2.60 (dq, *J* = 11.7, 4.3, 1H), 2.35 (s, 3H), 2.08–1.90 (m, 2H), 1.85–1.79 (m, 1H), 1.77–1.65 (m, 1H), 1.62–1.52 (overlapped with residual H₂O peak, 1H); ¹³C NMR (125 MHz, CDCl₃, **3.17**): δ

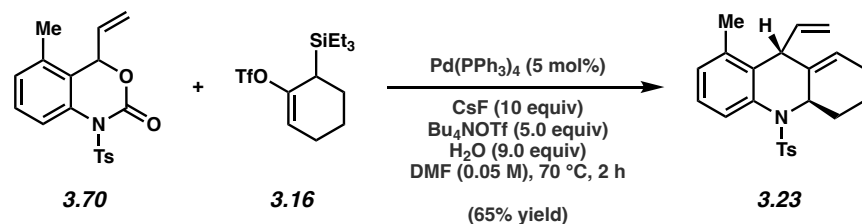
143.5, 137.5, 136.3, 136.2, 135.9, 134.9, 129.4, 127.8, 127.7, 127.5, 126.0, 125.7, 124.8, 115.2, 56.4, 51.8, 32.7, 24.5, 21.6, 21.2; IR (film): 2972, 2864, 1484, 1359, 1164 cm^{-1} ; HRMS-APCI (m/z) $[\text{M} + \text{H}]^+$ calcd for $\text{C}_{22}\text{H}_{24}\text{NO}_2\text{S}^+$, 366.1522; found 366.1522.

The structure of **3.17** was verified by 2D-NOESY, as the following interaction was observed:

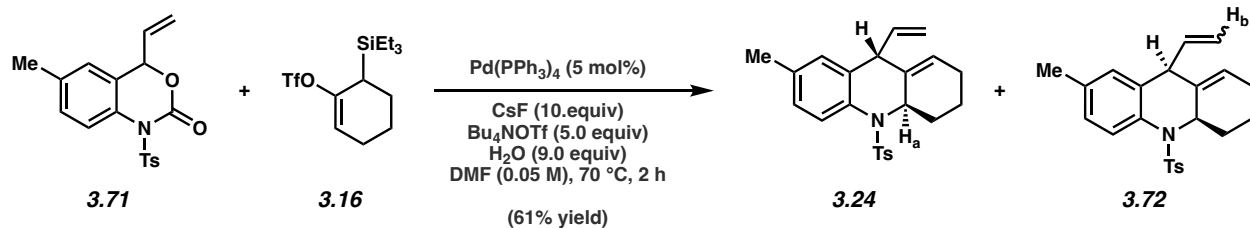


3.22. Followed General Procedure 3.4. Purification by preparative thin layer chromatography (4:1:1 hexanes: CH_2Cl_2 : Et_2O) afforded **3.22** (60% yield, >20:1 dr (determined by ^1H NMR analysis of the crude mixture), average of two experiments) as a white solid. **Annulation Product 3.22:** Mp: 107–108 $^\circ\text{C}$; R_f 0.52 (4:1:1 hexanes: CH_2Cl_2 : Et_2O); ^1H NMR (500 MHz, CDCl_3): δ 7.70 (d, $J = 8.2$, 1H), 7.26–7.22 (overlapped with residual solvent peak, 1H), 7.17–7.10 (m, 2H), 5.94 (ddd, $J = 17.3$, 10.3, 3.6, 1H), 5.69–5.64 (m, 1H), 5.20–5.15 (m, 1H), 5.08–5.02 (m, 1H), 4.75–4.69 (m, 1H), 3.93–3.89 (m, 1H), 2.80 (s, 3H), 2.44 (dq, $J = 11.7$, 3.9, 1H), 2.11–2.05 (m, 1H), 2.04–1.94 (m, 1H), 1.84–1.79 (m, 1H), 1.77–1.65 (m, 1H), 1.56–1.46 (overlapped with residual H_2O peak, 1H); ^{13}C NMR (125 MHz, CDCl_3): δ 139.0, 135.7, 135.2, 135.0, 128.1, 128.0, 125.7, 125.4, 124.6, 116.8, 56.5, 51.3, 39.5, 32.5, 24.5, 21.1; IR (film): 2931, 2862, 1485, 1341, 1155 cm^{-1} ; HRMS-

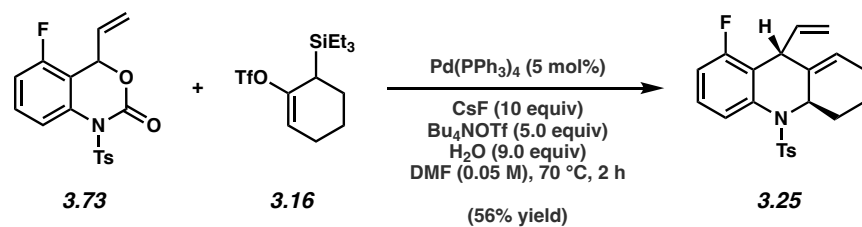
APCI (m/z) $[M + H]^+$ calcd for $C_{16}H_{20}NO_2S^+$, 290.1209; found 290.1209. Relative stereochemistry was assigned by analogy to the 1H NMR data of **3.17** and **3.68**.



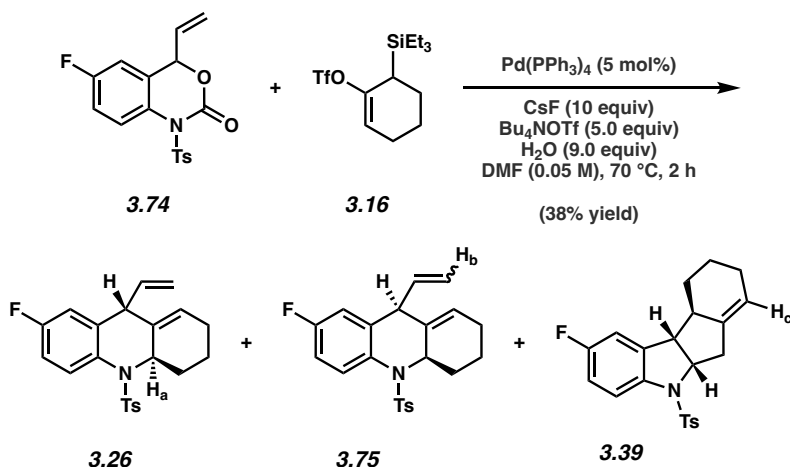
3.23. Followed General Procedure 3.4. Purification by preparative thin layer chromatography (4:1:1 hexanes:CH₂Cl₂:Et₂O) afforded **3.23** (65% yield, >20:1 dr (determined by 1H NMR analysis of the crude mixture), average of two experiments) as a white solid. **Annulation Product 3.23:** Mp: 109–111 °C; R_f 0.62 (4:1:1 hexanes:CH₂Cl₂:Et₂O); 1H NMR (500 MHz, CDCl₃): δ 7.69 (d, J = 8.2, 1H), 7.43 (dt, J = 8.3, 1.9, 2H), 7.16–7.09 (m, 3H), 6.96 (d, J = 7.4, 1H), 5.57–5.53 (m, 1H), 4.83 (ddd, J = 17.1, 10.1, 5.5, 1H), 4.68–4.60 (m, 2H), 4.48 (dt, J = 10.0, 1.8, 1H), 3.89–3.84 (m, 1H), 2.58 (dq, J = 12.0, 4.3, 1H), 2.35 (s, 3H), 2.19 (s, 3H), 2.07–1.90 (m, 2H), 1.84–1.79 (m, 1H), 1.76–1.65 (m, 1H), 1.60–1.52 (overlapped with residual H₂O peak, 1H); ^{13}C NMR (125 MHz, CDCl₃): δ 143.4, 136.6, 136.5, 136.3, 134.92, 134.89, 134.1, 129.3, 127.9, 127.3, 126.7, 124.6, 123.9, 115.6, 56.2, 48.0, 32.6, 24.5, 21.6, 21.2, 19.0; IR (film): 2926, 1739, 1351, 1163, 665 cm⁻¹; HRMS-APCI (m/z) $[M + H]^+$ calcd for $C_{23}H_{26}NO_2S^+$, 380.1684; found 380.1685. Relative stereochemistry was assigned by analogy to the 1H NMR data of **3.17** and **3.68**.



3.24 and **3.72**. Followed General Procedure 3.4. Purification by preparative thin layer chromatography (4:1:1 hexanes:CH₂Cl₂:Et₂O) afforded a mixture of major diastereomer **3.24** and minor diastereomer **3.72** (61% combined yield, 12:1 dr, average of two experiments) as a white solid. Diastereomeric ratio was determined by integrating the following peaks in the ¹H NMR spectrum of the crude reaction mixture (H_a **3.24**: 4.62–4.55 ppm; H_b **3.72**: 5.16 ppm). **Annulation Products 3.24 and 3.72**: R_f 0.69 (4:1:1 hexanes:CH₂Cl₂:Et₂O); ¹H NMR (600 MHz, CDCl₃, **3.24**): δ 7.72 (d, *J* = 8.2, 1H), 7.43 (dt, *J* = 8.3, 1.6, 2H), 7.17–7.13 (m, 2H), 7.04 (dd, *J* = 8.3, 1.8, 1H), 6.77 (d, *J* = 1.8, 1H), 5.54–5.52 (m, 1H), 4.76 (ddd, *J* = 17.0, 9.9, 5.5, 1H), 4.68 (dt, *J* = 17.1, 1.8, 1H), 4.62–4.55 (m, 1H), 4.40 (dt, *J* = 9.8, 1.8, 1H), 3.62–3.59 (m, 1H), 2.58 (dq, *J* = 11.9, 4.3, 1H), 2.36 (s, 3H), 2.29 (s, 3H), 2.04–1.90 (m, 2H), 1.83–1.78 (m, 1H), 1.75–1.65 (m, 1H), 1.60–1.52 (overlapped with residual H₂O peak, 1H); ¹³C NMR (150 MHz, CDCl₃, **3.24**): δ 143.4, 137.6, 136.42, 136.36, 135.7, 135.6, 132.2, 129.4, 128.20, 128.19, 127.8, 126.0, 124.6, 115.0, 56.3, 52.0, 32.6, 24.5, 21.6, 21.2, 21.0; IR (film): 2925, 1494, 1351, 1166, 567 cm⁻¹; HRMS-APCI (*m/z*) [M + H]⁺ calcd for C₂₃H₂₆NO₂S⁺, 380.1684; found 380.1685. Relative stereochemistry was assigned by analogy to the ¹H NMR data of **3.17** and **3.68**.

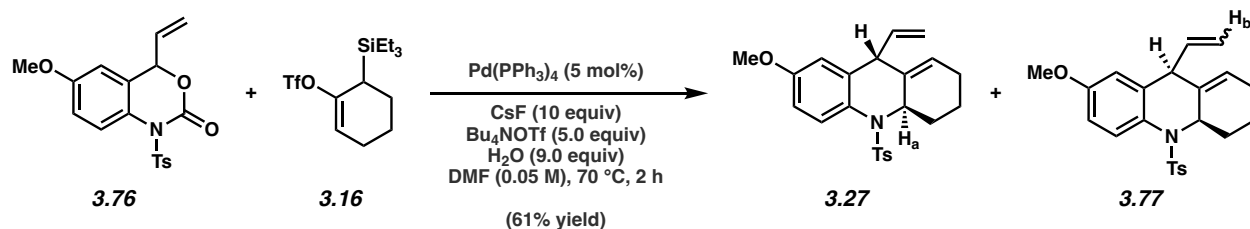


3.25. Followed General Procedure 3.4. Purification by preparative thin layer chromatography (4:1:1 hexanes:CH₂Cl₂:Et₂O) afforded **3.25** (56% yield, >20:1 dr (determined by ¹H NMR analysis of the crude mixture), average of two experiments) as a white solid. **Annulation Product 3.25:** Mp: 150–154 °C; R_f 0.67 (4:1:1 hexanes:CH₂Cl₂:Et₂O); ¹H NMR (500 MHz, CDCl₃): δ 7.67 (d, *J* = 8.4, 1H), 7.47–7.39 (m, 2H), 7.21–7.13 (m, 3H), 6.85 (td, *J* = 8.5, 0.7, 1H), 5.64–5.60 (m, 1H), 4.79 (ddd, *J* = 17.1, 9.8, 5.1, 1H), 4.68 (dt, *J* = 17.1, 1.5, 1H), 4.65–4.58 (m, 1H), 4.46 (dt, *J* = 9.9, 1.8, 1H), 4.10–4.06 (m, 1H), 2.62 (dq, *J* = 11.8, 4.3, 1H), 2.36 (s, 3H), 2.08–1.92 (m, 2H), 1.86–1.80 (m, 1H), 1.77–1.65 (m, 1H), 1.62–1.52 (overlapped with residual H₂O peak, 1H); ¹³C NMR (125 MHz, CDCl₃): δ 158.8 (d, *J* = 244.1), 143.8, 136.5 (d, *J* = 6.4), 136.1, 136.0, 135.0, 129.5, 127.8, 127.6 (d, *J* = 9.3), 125.8, 123.2 (d, *J* = 19.9), 121.6 (d, *J* = 3.2), 115.8, 112.1 (d, *J* = 22.0), 56.3, 43.4 (d, *J* = 3.7), 32.8, 24.5, 21.6, 21.1; ¹⁹F NMR (282 MHz, CDCl₃): δ –121.39 (m, 1F); IR (film): 2928, 2864, 1584, 1465, 1352 cm⁻¹; HRMS-APCI (*m/z*) [M + H]⁺ calcd for C₂₂H₂₃FNO₂S⁺, 384.1428; found 384.1428. Relative stereochemistry was assigned by analogy to the ¹H NMR data of **3.17** and **3.68**.

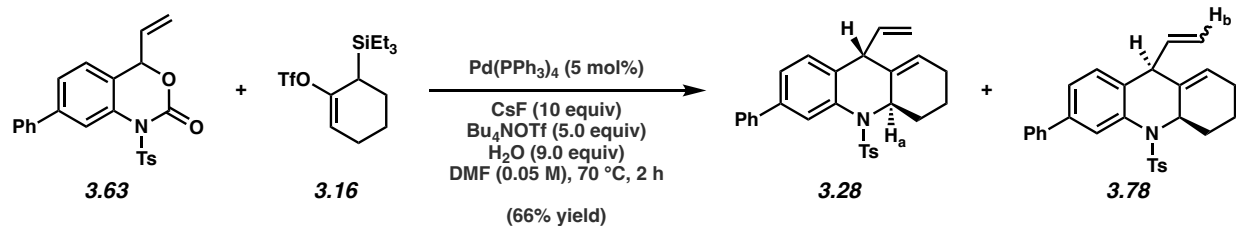


3.26, **3.75**, and **3.39**. Followed General Procedure 3.4. Purification by preparative thin layer chromatography (4:1:1 hexanes:CH₂Cl₂:Et₂O) afforded a mixture of major diastereomer **3.26**, minor diastereomer **3.75**, and constitutional isomer **3.39** (38% combined yield, 8.4:1 dr, 14:2.3:1.0 **3.26**:**3.75**:**3.39**, average of two experiments) as a waxy white solid. Diastereomeric ratio was determined by integrating the following peaks in the ¹H-NMR spectrum of the crude reaction mixture (H_a **3.26**: 4.59–4.54 ppm; H_b **3.75**: 5.25 ppm). Ratio of constitutional isomers was determined by integrating the following peaks in the ¹H-NMR spectrum of the isolated mixture (H_a **3.26**: 4.59–4.54 ppm; H_b **3.75**: 5.25 ppm; H_c **3.39**: 5.51–5.49 ppm). **Annulation Products 3.26**, **3.75**, and **3.39**: R_f 0.63 (4:1:1 hexanes:CH₂Cl₂:Et₂O); ¹H NMR (500 MHz, CDCl₃, **3.26**): δ 7.82 (dd, *J* = 9.0, 5.1, 1H), 7.43–7.39 (m, 2H), 7.18–7.14 (m, 2H), 6.93 (td, *J* = 8.5, 3.0, 1H), 6.68 (dd, *J* = 8.3, 3.0, 1H), 5.57–5.54 (m, 1H), 4.77–4.64 (m, 2H), 4.59–4.54 (m, 1H), 4.41 (dt, *J* = 9.3, 2.1, 1H), 3.63–3.60 (m, 1H), 2.59 (dq, *J* = 11.7, 4.1, 1H), 2.37 (s, 3H), 2.07–1.91 (m, 2H), 1.85–1.80 (m, 1H), 1.76–1.64 (m, 1H), 1.60–1.50 (overlapped with residual H₂O peak, 1H); ¹³C NMR (125 MHz, CDCl₃, **3.26**): δ 160.4 (d, *J* = 246.6), 143.7, 138.1 (d, *J* = 7.4), 136.7, 136.1, 135.7, 129.5, 127.9, 127.8, 127.1, 125.4, 115.6, 114.3 (d, *J* = 16.7), 114.1 (d, *J* = 16.2), 56.2, 51.8, 32.6, 24.5, 21.6, 21.2; ¹⁹F NMR (282 MHz, CDCl₃): δ –116.79 (m, 1F); IR (film): 2929, 1741, 1488,

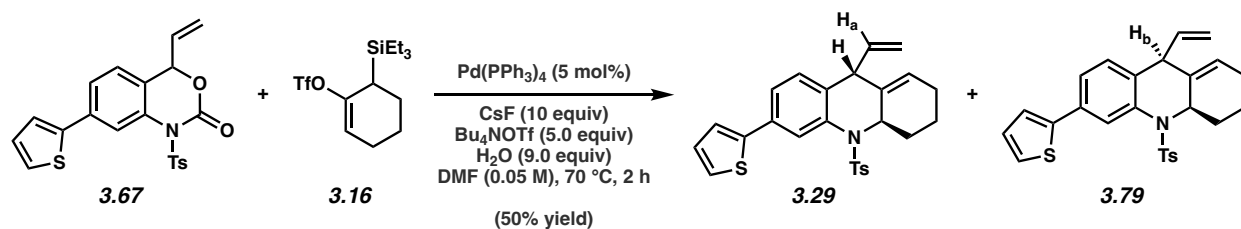
1351, 1164 cm^{-1} ; HRMS-APCI (m/z) $[\text{M} + \text{H}]^+$ calcd for $\text{C}_{22}\text{H}_{23}\text{FNO}_2\text{S}^+$, 384.1428; found 384.1430. Relative stereochemistry was assigned by analogy to the ^1H NMR data of **3.17** and **3.68**.



3.27 and **3.77**. Followed General Procedure 3.4. Purification by preparative thin layer chromatography (4:1:1 hexanes: CH_2Cl_2 : Et_2O) afforded a mixture of major diastereomer **3.27** and minor diastereomer **3.77** (61% combined yield, 8.9:1 dr, average of two experiments) as a colorless clear oil. Diastereomeric ratio was determined by integrating the following peaks in the ^1H NMR spectrum of the crude reaction mixture (H_a **3.27**: 4.59–4.51 ppm; H_b **3.77**: 5.23 ppm). **Annulation Products 3.27** and **3.77**: R_f 0.54 (4:1:1 hexanes: CH_2Cl_2 : Et_2O); ^1H NMR (500 MHz, CDCl_3 , **3.27**): δ 7.76 (d, $J = 9.0$, 1H), 7.40 (dt, $J = 8.3, 2.0$, 2H), 7.17–7.13 (m, 2H), 6.78 (dd, $J = 9.0, 3.0$, 1H), 6.51 (d, $J = 3.0$, 1H), 5.55–5.51 (m, 1H), 4.72–4.67 (m, 2H), 4.59–4.51 (m, 1H), 4.39–4.35 (m, 1H), 3.78 (s, 3H), 3.61–3.58 (m, 1H), 2.57 (dq, $J = 11.8, 4.3$, 1H), 2.36 (s, 3H), 2.06–1.90 (m, 2H), 1.84–1.78 (m, 1H), 1.75–1.64 (m, 1H), 1.61–1.50 (overlapped with residual H_2O peak, 1H); ^{13}C NMR (125 MHz, CDCl_3 , **3.27**): δ 157.5, 143.4, 137.5, 137.2, 136.24, 136.18, 129.4, 127.8, 127.7, 127.5, 124.9, 115.2, 112.9, 112.5, 56.2, 55.5, 52.1, 32.6, 24.5, 21.6, 21.2; IR (film): 2935, 1600, 1494, 1163, 567 cm^{-1} ; HRMS-APCI (m/z) $[\text{M} + \text{H}]^+$ calcd for $\text{C}_{23}\text{H}_{26}\text{NO}_3\text{S}^+$, 396.1633; found 396.1631. Relative stereochemistry was assigned by analogy to the ^1H NMR data of **3.17** and **3.68**.

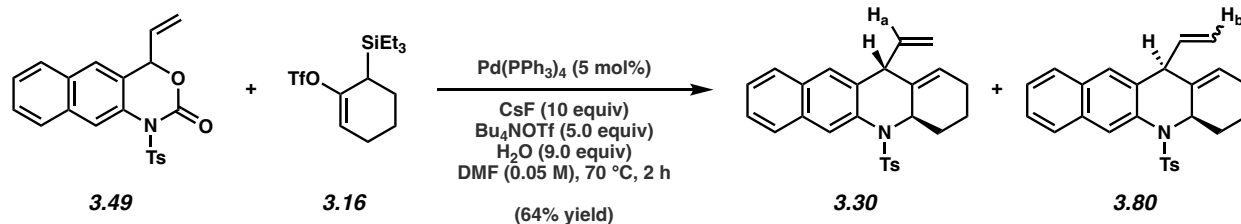


3.28 and **3.78**. Followed General Procedure 3.4. Purification by preparative thin layer chromatography (4:1:1 hexanes:CH₂Cl₂:Et₂O) afforded a mixture of major diastereomer **3.28** and minor diastereomer **3.78** (66% combined yield, 10:1 dr, average of two experiments) as a colorless clear oil. Diastereomeric ratio was determined by integrating the following peaks in the ¹H NMR spectrum of the crude reaction mixture (H_a **3.28**: 4.67–4.63 ppm; H_b **3.78**: 5.27 ppm). **Annulation Products 3.28** and **3.78**: R_f 0.76 (4:1:1 hexanes:CH₂Cl₂:Et₂O); ¹H NMR (500 MHz, CDCl₃, **3.28**): δ 8.12 (d, *J* = 1.8, 1H), 7.66–7.62 (m, 2H), 7.49–7.42 (m, 4H), 7.37–7.33 (m, 2H), 7.17–7.13 (m, 2H), 7.03 (d, *J* = 7.8, 1H), 5.60–5.56 (m, 1H), 4.85 (ddd, *J* = 17.1, 10.0, 5.4, 1H), 4.70 (dt, *J* = 17.1, 1.6, 1H), 4.67–4.63 (m, 1H), 4.45 (dt, *J* = 10.0, 1.8, 1H), 3.73–3.70 (m, 1H), 2.63 (dq, *J* = 11.8, 4.3, 1H), 2.35 (s, 3H), 2.05–1.95 (m, 2H), 1.86–1.81 (m, 1H), 1.78–1.67 (m, 1H), 1.66–1.59 (overlapped with residual H₂O peak, 1H); ¹³C NMR (125 MHz, CDCl₃, **3.28**): δ 143.6, 140.54, 140.52, 137.5, 136.3, 136.1, 135.3, 134.8, 129.4, 128.9, 128.0, 127.9, 127.6, 127.2, 125.0, 124.7, 124.3, 115.3, 56.4, 51.6, 32.7, 24.6, 21.6, 21.2; IR (film): 2927, 1599, 1482, 1165, 665 cm⁻¹; HRMS-APCI (*m/z*) [M + H]⁺ calcd for C₂₈H₂₈NO₂S⁺, 442.1841; found 442.1841. Relative stereochemistry was assigned by analogy to the ¹H NMR data of **3.17** and **3.68**.

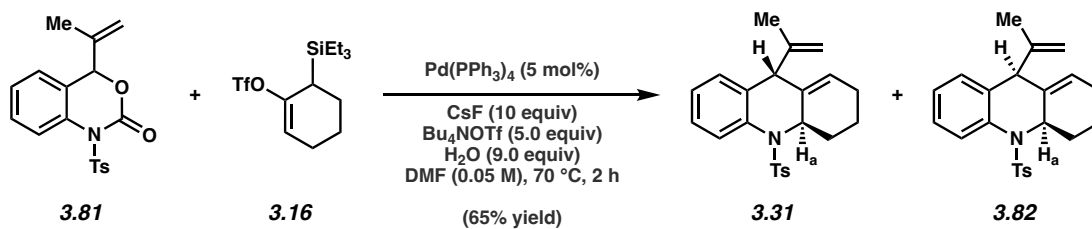


3.29 and **3.79**. Followed General Procedure 3.4. Purification by preparative thin layer chromatography (4:1:1 hexanes:CH₂Cl₂:Et₂O) afforded a mixture of major diastereomer **3.29** and minor diastereomer **3.79** (50% combined yield, 5.2:1 dr, average of two experiments) as an off-white solid. Diastereomeric ratio was determined by integrating the following peaks in the ¹H NMR spectrum of the crude reaction mixture (H_a **3.29**: 4.88 ppm; H_b **3.79**: 4.59–4.55 ppm).

Annulation Products 3.29 and **3.79**: R_f 0.57 (4:1:1 hexanes:CH₂Cl₂:Et₂O); ¹H NMR (500 MHz, CDCl₃, **3.29**): δ 8.12 (d, *J* = 1.8, 1H), 7.50 (dt, *J* = 8.3, 1.9, 2H), 7.36–7.31 (m, 2H), 7.28 (dd, *J* = 5.1, 1.1, 1H), 7.17–7.14 (m, 2H), 7.11–7.07 (m, 1H), 6.96 (d, *J* = 7.8, 1H), 5.59–5.56 (m, 1H), 4.88 (ddd, *J* = 17.0, 10.1, 5.3, 1H), 4.71–4.64 (m, 2H), 4.47 (dt, *J* = 10.0, 1.9, 1H), 3.70–3.67 (m, 1H), 2.64 (dq, *J* = 11.6, 4.2, 1H), 2.35 (s, 3H), 2.05–1.95 (m, 2H), 1.86–1.81 (m, 1H), 1.78–1.67 (m, 1H), 1.65–1.56 (overlapped with residual H₂O peak, 1H); ¹³C NMR (125 MHz, CDCl₃, **3.29**, 23 of 24 signals observed): δ 144.0, 143.7, 137.4, 136.2, 136.0, 135.5, 134.8, 133.8, 129.4, 128.2, 128.1, 128.0, 125.01, 125.00, 123.5, 123.1, 115.4, 56.4, 51.5, 32.7, 24.5, 21.6, 21.2; IR (film): 2973, 2363, 1742, 1165, 667 cm⁻¹; HRMS-APCI (*m/z*) [M + H]⁺ calcd for C₂₆H₂₆NO₂S₂⁺, 448.1405; found 448.1408. Relative stereochemistry was assigned by analogy to the ¹H NMR data of **3.17** and **3.68**.

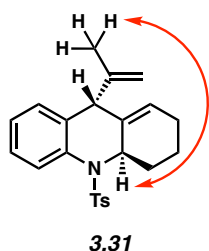


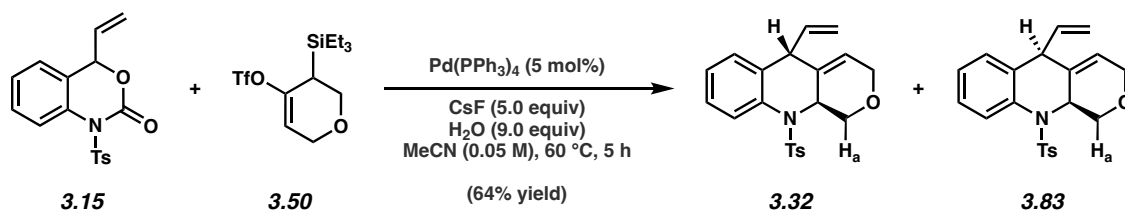
3.30 and **3.80**. Followed General Procedure 3.4. Purification by preparative thin layer chromatography (4:1:1 hexanes:CH₂Cl₂:Et₂O) afforded a mixture of major diastereomer **3.30** and minor diastereomer **3.80** (64% combined yield, 8.8:1 dr, average of two experiments) as a white solid. Diastereomeric ratio was determined by integrating the following peaks in the ¹H NMR spectrum of the crude reaction mixture (H_a **3.30**: 5.03 ppm; H_b **3.80**: 5.30 ppm). **Annulation Products 3.30** and **3.80**: R_f 0.61 (4:1:1 hexanes:CH₂Cl₂:Et₂O); ¹H NMR (500 MHz, CDCl₃, **3.30**): δ 8.32 (s, 1H), 7.86–7.82 (m, 1H), 7.72–7.68 (m, 1H), 7.48 (dt, *J* = 8.3, 2.0, 2H), 7.47–7.38 (m, 3H), 7.11–7.07 (m, 2H), 5.64–5.60 (m, 1H), 5.03 (ddd, *J* = 17.1, 10.1, 5.0, 1H), 4.82–4.75 (m, 1H), 4.71 (ddd, *J* = 17.2, 1.9, 1.7, 1H), 4.52 (ddd, *J* = 10.1, 2.1, 1.6, 1H), 3.90–3.87 (m, 1H), 2.64 (dq, *J* = 11.8, 4.3, 1H), 2.31 (s, 3H), 2.09–2.02 (m, 1H), 2.01–1.90 (m, 1H), 1.87–1.81 (m, 1H), 1.81–1.69 (m, 1H), 1.65–1.55 (m, 1H); ¹³C NMR (125 MHz, CDCl₃, **3.30**): δ 143.6, 137.6, 136.5, 136.0, 135.0, 133.1, 132.9, 131.4, 129.3, 128.2, 127.9, 127.1, 126.0, 125.8, 125.5, 123.4, 115.7, 56.6, 52.0, 32.5, 24.7, 21.6, 21.2; IR (film): 2927, 2862, 1460, 1353, 1165 cm⁻¹; HRMS-APCI (*m/z*) [M + H]⁺ calcd for C₂₆H₂₆NO₂S⁺, 416.1679; found 416.1676. Relative stereochemistry was assigned by analogy to the ¹H NMR data of **3.17** and **3.68**.



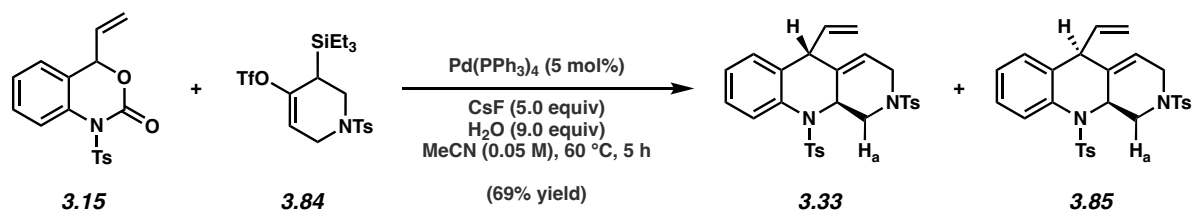
3.31 and **3.82**. Followed General Procedure 3.4. Purification by preparative thin layer chromatography (4:1:1 hexanes:CH₂Cl₂:Et₂O) afforded a mixture of major diastereomer **3.31** and minor diastereomer **3.82** (65% combined yield, 8.9:1 dr, average of two experiments) as a white solid. Diastereomeric ratio was determined by integrating the following peaks in the ¹H NMR spectrum of the isolated mixture (H_a **3.31**: 4.78–4.71 ppm; **3.82**: 4.56–4.51 ppm). **Annulation Products 3.31 and 3.82**: R_f 0.63 (4:1:1 hexanes:CH₂Cl₂:Et₂O); ¹H NMR (500 MHz, CDCl₃, **3.31**): δ 7.86–7.83 (m, 1H), 7.50 (dt, *J* = 8.3, 2.0, 2H), 7.24–7.19 (m, 1H), 7.12–7.08 (m, 2H), 7.05 (td, *J* = 7.5, 1.2, 1H), 6.95 (dd, *J* = 7.5, 1.6, 1H), 5.60–5.57 (m, 1H), 4.78–4.71 (m, 1H), 4.35–4.30 (m, 1H), 4.15–4.13 (m, 1H), 3.60 (s, 1H), 2.59 (dq, *J* = 11.8, 4.3, 1H), 2.34 (s, 3H), 2.11–2.04 (m, 1H), 2.04–1.93 (m, 1H), 1.86–1.81 (m, 1H), 1.80–1.68 (m, 1H), 1.59–1.54 (m, 1H), 1.26–1.24 (m, 3H); ¹³C NMR (125 MHz, CDCl₃, **3.31**): δ 143.3, 143.0, 136.9, 135.8, 135.01, 134.95, 129.5, 129.1, 129.0, 128.1, 127.4, 127.0, 126.0, 125.05, 125.01, 112.5, 56.7, 54.5, 32.6, 24.6, 21.7, 21.6, 21.3; IR (film): 2928, 2863, 1484, 1344, 1160 cm⁻¹; HRMS-APCI (*m/z*) [M + H]⁺ calcd for C₂₃H₂₆NO₂S⁺, 380.1679; found 380.1678.

The structure of **3.31** was verified by 2D-NOESY, as the following interaction was observed:





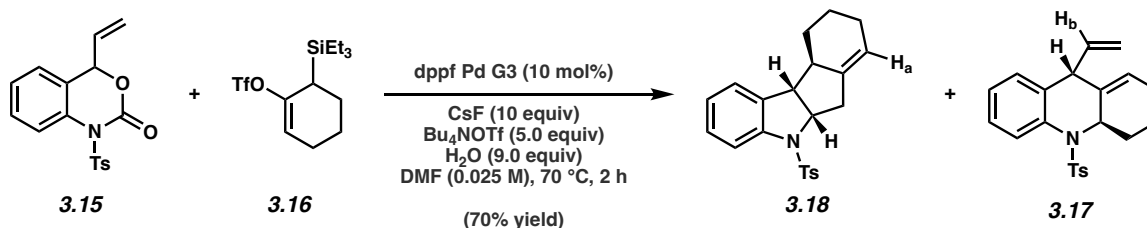
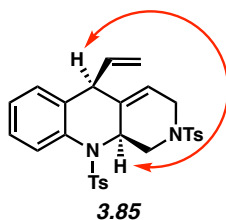
3.32 and **3.83**. Followed General Procedure 3.5. Purification by preparative thin layer chromatography (4:1:1 hexanes:CH₂Cl₂:Et₂O) afforded a mixture of major diastereomer **3.32** and minor diastereomer **3.83** (64% combined yield, 1.8:1 dr, average of two experiments) as a white solid. Diastereomeric ratio was determined by integrating the following peaks in the ¹H NMR spectrum of the crude reaction mixture (H_a **3.32**: 3.36 ppm; **3.83**: 3.30 ppm). **Annulation Products 3.32** and **3.83**: R_f 0.37 (4:1:1 hexanes:CH₂Cl₂:Et₂O); ¹H NMR (500 MHz, CDCl₃, **3.32**): δ 7.91–7.88 (m, 1H), 7.40 (dt, *J* = 8.3, 2.0, 2H), 7.31–7.27 (m, 1H), 7.17–7.11 (m, 3H), 6.98 (dd, *J* = 7.5, 1.6, 1H), 5.58 (q, *J* = 2.7, 1H), 4.71 (ddd, *J* = 17.1, 9.9, 5.0, 1H), 4.67–4.55 (m, 3H), 4.35 (dt, 9.8, 2.0, 1H), 4.20–4.10 (m, 1H), 4.05 (ddd, *J* = 16.7, 3.9, 2.0, 1H), 3.76–3.73 (m, 1H), 3.36 (dd, *J* = 10.0, 9.3, 1H), 2.36 (s, 3H); ¹H NMR (500 MHz, CDCl₃, **3.83**): δ 7.66 (dd, *J* = 8.0, 1.2, 1H), 7.34–7.30 (m, 3H), 7.22–7.17 (m, 3H), 6.94 (dt, *J* = 7.7, 1.3, 1H), 5.85 (dt, *J* = 16.8, 10.0, 1H), 5.32–5.27 (m, 2H), 4.76 (ddd, *J* = 17.0, 1.8, 0.3, 1H), 4.67–4.55 (m, 1H), 4.39 (dd, *J* = 10.4, 5.6, 1H), 4.20–4.10 (m, 1H), 3.98 (ddt, *J* = 18.6, 4.1, 2.3, 1H), 3.30 (t, *J* = 10.0, 1H), 2.40 (s, 3H), 2.28 (d, *J* = 9.3, 1H); ¹³C NMR (125 MHz, CDCl₃, **3.32** and **3.83**): δ 144.0, 143.9, 137.4, 136.7, 136.6, 135.3, 135.2, 134.8, 134.6, 134.4, 134.2, 133.3, 129.7, 129.6, 128.6, 128.0, 127.9, 127.8, 127.6, 127.2, 126.9, 126.4, 126.1, 124.3, 122.3, 120.2, 118.5, 115.6, 69.1, 68.6, 64.9, 64.9, 54.0, 52.2, 50.5, 45.3, 21.63, 21.61; IR (film): 2925, 2852, 1349, 1165, 1088 cm⁻¹; HRMS-APCI (*m/z*) [M + H]⁺ calcd for C₂₁H₂₂NO₃S⁺, 368.1315; found 368.1332. Relative stereochemistry was assigned by analogy to the ¹H NMR data of **3.33** and **3.85**.



3.33 and **3.85**. Followed General Procedure 3.5. Purification by preparative thin layer chromatography (4:1:1 hexanes:CH₂Cl₂:Et₂O) afforded a mixture of major diastereomer **33** and minor diastereomer **3.85** (69% combined yield, 1.3:1 dr, average of two experiments) as a waxy white-yellow solid. Diastereomeric ratio was determined by integrating the following peaks in the ¹H NMR spectrum of the crude reaction mixture (H_a **3.33**: 3.14 ppm; **3.85**: 3.05 ppm). To obtain an analytical sample, the mixture of diastereomers was then purified by preparative thin layer chromatography (2:1 Et₂O:hexanes) to afford **3.85** as a waxy pale yellow solid. **Annulation Products 3.33 and 3.85**: R_f 0.33 (4:1:1 hexanes:CH₂Cl₂:Et₂O); ¹H NMR (500 MHz, CDCl₃, **3.33**): δ 7.85 (dd, *J* = 8.2, 1.0, 1H), 7.74 (dt, *J* = 8.3, 1.9, 2H), 7.37 (dt, *J* = 8.3, 1.9, 2H), 7.35–7.27 (m, 2H), 7.26–7.21 (overlapped with residual solvent peak, 1H), 7.21–7.13 (m, 2H), 7.10 (td, *J* = 7.5, 1.2, 1H), 6.92 (dd, *J* = 7.5, 1.6, 1H), 5.50 (dt, *J* = 4.0, 2.3, 1H), 4.68–4.58 (m, 3H), 4.53–4.47 (m, 1H), 4.29 (ddd, *J* = 9.9, 2.1, 1.4, 1H), 4.14–4.07 (m, 1H), 3.71–3.66 (m, 1H), 3.14 (ddd, *J* = 17.2, 3.5, 2.3, 1H), 2.43–2.35 (m, 7H); ¹H NMR (500 MHz, CDCl₃, **3.85**): δ 7.70 (dt, *J* = 8.3, 1.9, 2H), 7.62 (dd, *J* = 8.0, 1.2, 1H), 7.35–7.27 (m, 5H), 7.21–7.13 (m, 3H), 6.88 (dt, *J* = 7.6, 1.2, 1H), 5.76 (dt, *J* = 16.9, 9.9, 1H), 5.27 (dd, *J* = 10.1, 1.8, 1H), 5.20 (sext, *J* = 2.3, 1H), 4.71 (dd, *J* = 17.0, 1.3, 1H), 4.68–4.58 (m, 1H), 4.43–4.39 (m, 1H), 4.03 (dq, *J* = 16.9, 3.1, 1H), 3.05 (ddt, *J* = 17.1, 3.5, 2.5, 1H), 2.43–2.35 (m, 6H), 2.31 (dd, *J* = 11.1, 10.1, 1H), 2.21 (d, *J* = 9.2, 1H); ¹³C NMR (125 MHz, CDCl₃, **3.33** and **3.85**): δ 144.0, 143.9, 143.72, 143.70, 137.3, 137.1, 136.1, 135.2, 135.1, 135.0, 134.6, 134.2, 133.84, 133.77, 133.4, 132.7, 129.8, 129.6, 129.4, 128.5, 127.81, 127.75, 127.70, 127.66, 127.5, 127.1, 127.0, 126.3, 126.1, 124.1, 120.4, 119.5, 115.7, 115.5, 54.9, 52.9,

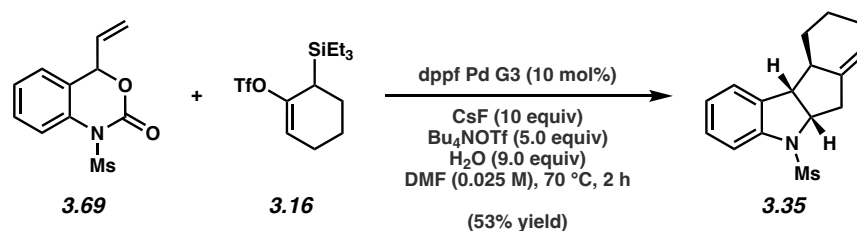
50.2, 48.7, 48.3, 45.1, 44.1, 44.0, 21.53, 21.50; IR (film): 3065, 2923, 1483, 1348, 1162 cm^{-1} ; HRMS-APCI (m/z) $[M + H]^+$ calcd for $\text{C}_{28}\text{H}_{29}\text{N}_2\text{O}_4\text{S}_2^+$, 521.1563; found 521.1567.

The structure of **3.85** was verified by 2D-NOESY, as the following interaction was observed:

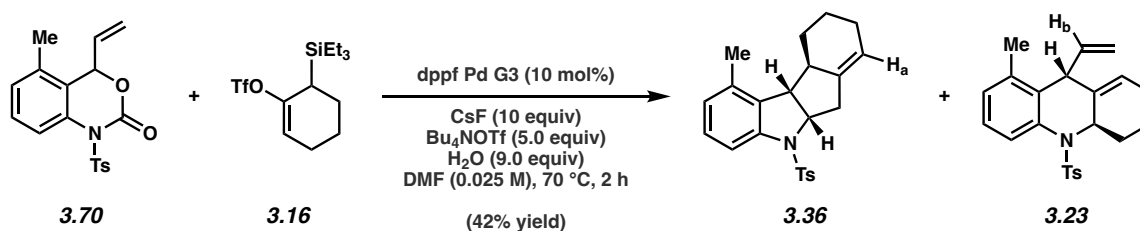


3.18. Followed General Procedure 3.6. Purification by preparative thin layer chromatography (4:1:1 hexanes: CH_2Cl_2 : Et_2O) afforded a mixture of **3.18** and constitutional isomer **3.17** (70% combined yield, >20:1 dr, 12:1 **3.18**:**3.17**, average of two experiments) as a white solid. Ratio of constitutional isomers was determined by integrating the following peaks in the ^1H NMR spectrum of the isolated mixture (H_a **3.18**: 5.51–5.49 ppm; H_b **3.17**: 4.81 ppm). **Annulation Products 3.18** and **3.17**: R_f 0.57 (4:1:1 hexanes: CH_2Cl_2 : Et_2O); ^1H NMR (500 MHz, CDCl_3 , **3.18**): 7.67–7.63 (m, 3H), 7.23–7.17 (m, 3H), 7.09 (d, $J = 7.3$, 1H), 7.00 (t, $J = 7.4$, 1H), 5.51–5.49 (br m, 1H), 4.42 (dt, $J = 10.2$, 7.6, 1H), 3.09–3.03 (m, 1H), 2.98 (dd, $J = 15.6$, 7.9, 1H), 2.75–2.69 (m, 1H), 2.35 (s, 3H), 2.24–2.17 (m, 2H), 2.01–1.99 (m, 2H), 1.82–1.78 (m, 1H), 1.50–1.39 (m, 1H), 1.23–1.14 (m, 1H); ^{13}C NMR (125 MHz, CDCl_3 , **3.18**): δ 143.9, 141.2, 140.3, 135.4, 134.7, 129.6, 128.0, 127.3, 124.2, 124.0, 118.9, 115.4, 65.7, 52.1, 46.0, 41.3, 29.2, 24.7, 22.3, 21.5; IR (film): 2924, 2854,

1478, 1355, 1167 cm^{-1} ; HRMS-APCI (m/z) $[\text{M} + \text{H}]^+$ calcd for $\text{C}_{22}\text{H}_{24}\text{NO}_2\text{S}^+$, 366.1522; found 366.1523. Relative stereochemistry was assigned by analogy to the ^1H NMR data of **3.43**.

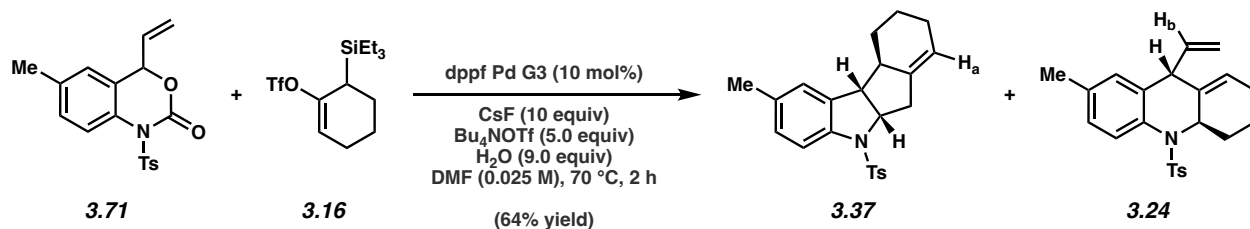


3.35. Followed General Procedure 3.6. Purification by preparative thin layer chromatography (4:1:1 hexanes: CH_2Cl_2 : Et_2O) afforded **3.35** (53% yield, >20:1 dr, average of two experiments) as a white solid. **Annulation Product 3.35**: Mp: $126\text{--}128^\circ\text{C}$; R_f 0.42 (4:1:1 hexanes: CH_2Cl_2 : Et_2O); ^1H NMR (500 MHz, CDCl_3): δ 7.41 (d, $J = 8.2$, 1H), 7.25–7.20 (m, 2H), 7.05 (t, $J = 7.4$, 1H), 5.52–5.50 (br m, 1H), 4.55 (dt, $J = 10.1$, 7.3, 1H), 3.34 (t, $J = 9.3$, 1H), 2.94 (dd, $J = 15.9$, 8.0, 1H), 2.86 (s, 3H), 2.73–2.68 (m, 1H), 2.30–2.27 (m, 2H), 2.05–2.01 (m, 2H), 1.87–1.82 (m, 1H), 1.53–1.42 (m, 1H), 1.34–1.24 (m, 1H); ^{13}C NMR (125 MHz, CDCl_3): δ 141.3, 140.3, 135.0, 128.5, 124.7, 124.1, 119.3, 114.2, 66.7, 52.7, 46.2, 41.3, 35.5, 29.2, 24.9, 22.4; IR (film): 2926, 2854, 1479, 1348, 1159 cm^{-1} ; HRMS-APCI (m/z) $[\text{M} + \text{H}]^+$ calcd for $\text{C}_{16}\text{H}_{20}\text{NO}_2\text{S}^+$, 290.1209; found 290.1211. Relative stereochemistry was assigned by analogy to the ^1H NMR data of **3.43**.



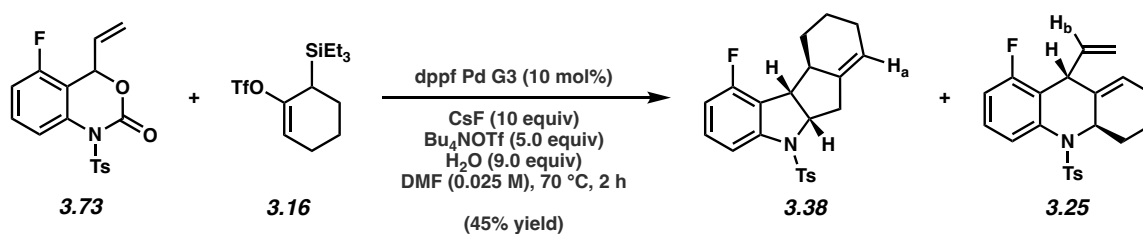
3.36. Followed General Procedure 3.6. Purification by preparative thin layer chromatography (4:1:1 hexanes: CH_2Cl_2 : Et_2O) afforded a mixture of **3.36** and constitutional isomer **3.23** (42%

combined yield, >20:1 dr, 7.6:1 **3.36:3.23**, average of two experiments) as a white solid. Ratio of constitutional isomers was determined by integrating the following peaks in the ^1H NMR spectrum of the isolated mixture (H_a **3.36**: 5.52–5.50 ppm; H_b **3.23**: 4.83 ppm). **Annulation Products 3.36 and 3.23**: R_f 0.61 (4:1:1 hexanes: CH_2Cl_2 : Et_2O); ^1H NMR (500 MHz, CDCl_3 , **3.36**): δ 7.62 (d, $J = 8.2$, 2H), 7.49 (d, $J = 8.0$, 1H), 7.18 (d, $J = 8.0$, 2H), 7.10 (t, $J = 7.9$, 1H), 6.80 (d, $J = 7.6$, 1H), 5.52–5.50 (br m, 1H), 4.41 (dt, $J = 9.8, 7.5$, 1H), 3.12–3.07 (m, 1H), 2.96 (dd, $J = 15.6, 7.7$, 1H), 2.79–2.73 (m, 1H), 2.35 (s, 3H), 2.31–2.26 (m, 2H), 2.23 (s, 3H), 2.02–1.99 (m, 2H), 1.83–1.78 (m, 1H), 1.51–1.40 (m, 1H), 1.26–1.17 (m, 1H); ^{13}C NMR (125 MHz, CDCl_3 , **3.36**): δ 143.9, 141.4, 140.6, 134.9, 134.8, 133.8, 129.7, 128.0, 127.5, 125.6, 119.2, 113.0, 66.1, 51.9, 45.1, 41.2, 30.1, 24.9, 22.7, 21.7, 20.2; IR (film): 2923, 1739, 1355, 1166, 663 cm^{-1} ; HRMS-APCI (m/z) [$\text{M} + \text{H}$] $^+$ calcd for $\text{C}_{23}\text{H}_{26}\text{NO}_2\text{S}^+$, 380.1684; found 380.1683. Relative stereochemistry was assigned by analogy to the ^1H NMR data of **3.43**.



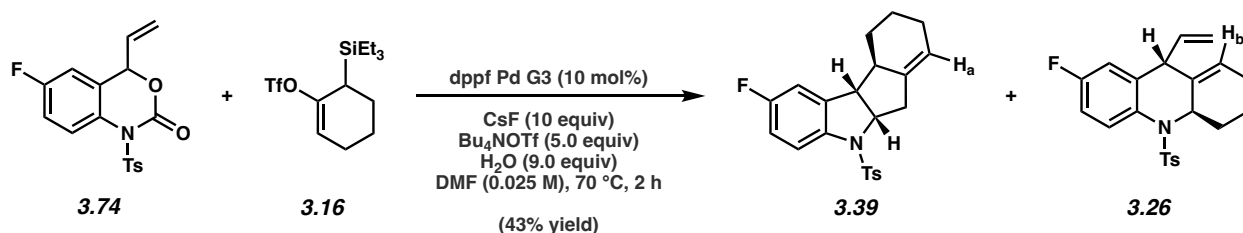
3.37. Followed General Procedure 3.6. Purification by preparative thin layer chromatography (4:1:1 hexanes: CH_2Cl_2 : Et_2O) afforded a mixture of **3.37** and constitutional isomer **3.24** (64% combined yield, >20:1 dr, 6.3:1 **3.37:3.24**, average of two experiments) as a colorless clear oil. Ratio of constitutional isomers was determined by integrating the following peaks in the ^1H NMR spectrum of the isolated mixture (H_a **3.37**: 5.50–5.48 ppm; H_b **3.24**: 4.76 ppm). **Annulation Products 3.37 and 3.24**: R_f 0.74 (4:1:1 hexanes: CH_2Cl_2 : Et_2O); ^1H NMR (500 MHz, CDCl_3 , **37**):

δ 7.63 (dt, $J = 8.3, 1.9, 2\text{H}$), 7.53 (d, $J = 8.3, 1\text{H}$), 7.20–7.16 (m, 2H), 7.03–6.99 (m, 1H), 6.91–6.88 (m, 1H), 5.50–5.48 (br m, 1H), 4.39 (dt, $J = 10.0, 7.7, 1\text{H}$), 3.02–2.93 (m, 2H), 2.73–2.66 (m, 1H), 2.35 (s, 3H), 2.28 (s, 3H), 2.24–2.17 (m, 2H), 2.02–1.98 (m, 2H), 1.83–1.77 (m, 1H), 1.51–1.40 (m, 1H), 1.23–1.13 (m, 1H); ^{13}C NMR (125 MHz, CDCl_3 , **37**): δ 143.9, 140.5, 139.0, 135.8, 134.7, 133.9, 129.7, 128.7, 127.4, 124.9, 119.0, 115.4, 65.9, 52.2, 46.1, 41.3, 29.4, 24.9, 22.4, 21.7, 21.1; IR (film): 2922, 1739, 1485, 1354, 1165 cm^{-1} ; HRMS-APCI (m/z) $[\text{M} + \text{H}]^+$ calcd for $\text{C}_{23}\text{H}_{26}\text{NO}_2\text{S}^+$, 380.1684; found 380.1684. Relative stereochemistry was assigned by analogy to the ^1H NMR data of **3.43**.



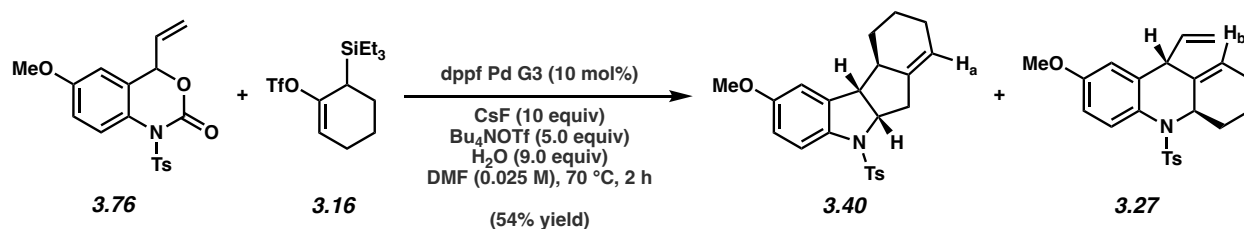
3.38. Followed General Procedure 3.6. Purification by preparative thin layer chromatography (4:1:1 hexanes: CH_2Cl_2 : Et_2O) afforded a mixture of **3.38** and constitutional isomer **3.25** (45% combined yield, >20:1 dr, 11:1 **3.38**:**3.25**, average of two experiments) as a waxy light yellow solid. Ratio of constitutional isomers was determined by integrating the following peaks in the ^1H NMR spectrum of the isolated mixture (H_a **3.38**: 5.54–5.50 ppm; H_b **3.25**: 4.79 ppm). **Annulation Products 3.38 and 3.25**: R_f 0.65 (4:1:1 hexanes: CH_2Cl_2 : Et_2O); ^1H NMR (500 MHz, CDCl_3 , **3.38**): δ 7.65 (dt, $J = 8.3, 2.2, 2\text{H}$), 7.44 (d, $J = 8.1, 1\text{H}$), 7.23–7.14 (m, 3H), 6.73–6.67 (m, 1H), 5.54–5.50 (br m, 1H), 4.46 (dt, $J = 10.5, 7.6, 1\text{H}$), 3.20 (dd, $J = 10.3, 7.7, 1\text{H}$), 3.00 (dd, $J = 15.6, 8.0, 1\text{H}$), 2.75–2.67 (m, 1H), 2.37 (s, 3H), 2.35–2.31 (m, 2H), 2.02–1.96 (m, 2H), 1.83–1.76 (m, 1H), 1.51–1.39 (m, 1H), 1.23–1.13 (m, 1H); ^{13}C NMR (125 MHz, CDCl_3 , **3.38**): δ 159.6 (d, $J = 246.1$),

144.3, 144.0 (d, $J = 8.7$), 139.9, 134.6, 129.8, 129.7, 127.4, 121.7 (d, $J = 22.4$), 119.6, 111.1 (d, $J = 3.4$), 110.9 (d, $J = 20.3$), 66.5, 49.7 (d, $J = 1.4$), 45.5, 41.5, 29.1 (d, $J = 2.4$), 24.9, 22.4, 21.7; ^{19}F NMR (282 MHz, CDCl_3): δ -116.72 (m, 1F); IR (film): 2926, 2856, 1620, 1457, 1355 cm^{-1} ; HRMS-APCI (m/z) $[\text{M} + \text{H}]^+$ calcd for $\text{C}_{22}\text{H}_{23}\text{FNO}_2\text{S}^+$, 384.1428; found 384.1431. Relative stereochemistry was assigned by analogy to the ^1H NMR data of **3.43**.

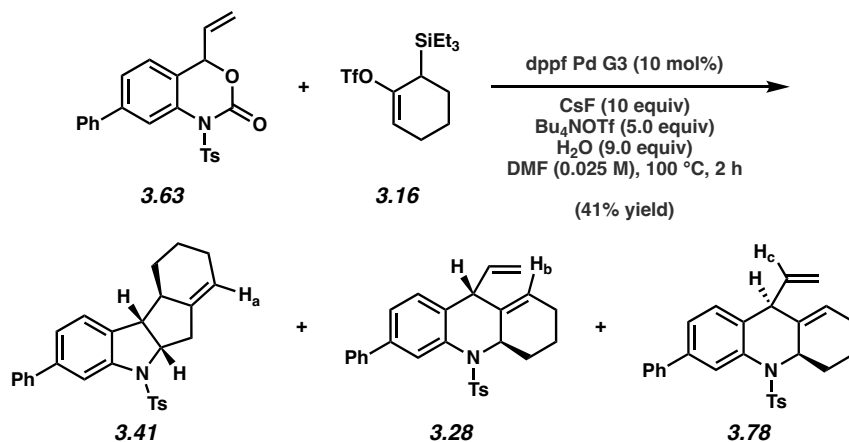


3.39. Followed General Procedure 3.6. Purification by preparative thin layer chromatography (4:1:1 hexanes: CH_2Cl_2 : Et_2O) afforded a mixture of **3.39** and constitutional isomer **3.26** (43% combined yield, >20:1 dr, 13:1 **3.39**:**3.26**, average of two experiments) as a light yellow solid. Ratio of constitutional isomers was determined by integrating the following peaks in the ^1H NMR spectrum of the isolated mixture (H_a **3.39**: 5.51–5.49 ppm; H_b **3.26**: 5.57–5.54 ppm). **Annulation Products 3.39 and 3.26**: R_f 0.72 (4:1:1 hexanes: CH_2Cl_2 : Et_2O); ^1H NMR (500 MHz, CDCl_3 , **3.39**): δ 7.62–7.58 (m, 3H), 7.22–7.18 (m, 2H), 6.90 (tdd, $J = 8.8, 2.7, 0.6$, 1H), 6.78 (ddd, $J = 8.0, 2.6, 0.8$, 1H), 5.51–5.49 (br m, 1H), 4.42 (dt, $J = 10.3, 7.5$, 1H), 3.02–2.93 (m, 2H), 2.73–2.65 (m, 1H), 2.36 (s, 3H), 2.24–2.14 (m, 2H), 2.03–1.96 (m, 2H), 1.83–1.78 (m, 1H), 1.51–1.39 (m, 1H), 1.21–1.12 (m, 1H); ^{13}C NMR (125 MHz, CDCl_3 , **3.39**): δ 160.1 (d, $J = 242.5$), 144.2, 139.9, 137.7 (d, $J = 8.1$), 137.4, 134.4, 129.8, 127.4, 119.4, 116.8 (d, $J = 8.6$), 114.7 (d, $J = 23.4$), 111.5 (d, $J = 23.7$), 66.3, 52.1 (d, $J = 1.7$), 46.0, 41.2, 29.3, 24.8, 22.3, 21.7; ^{19}F NMR (282 MHz, CDCl_3): δ -119.18 (m, 1F); IR (film): 2926, 2853, 1479, 1355, 1166 cm^{-1} ; HRMS-APCI (m/z) $[\text{M} + \text{H}]^+$ calcd for

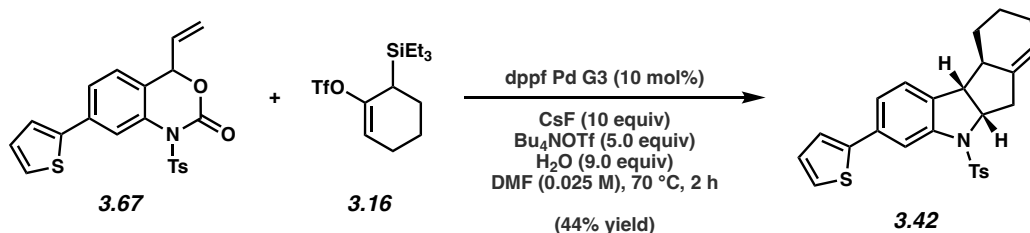
$C_{22}H_{23}FNO_2S^+$, 384.1428; found 384.1430. Relative stereochemistry was assigned by analogy to the 1H NMR data of **3.43**.



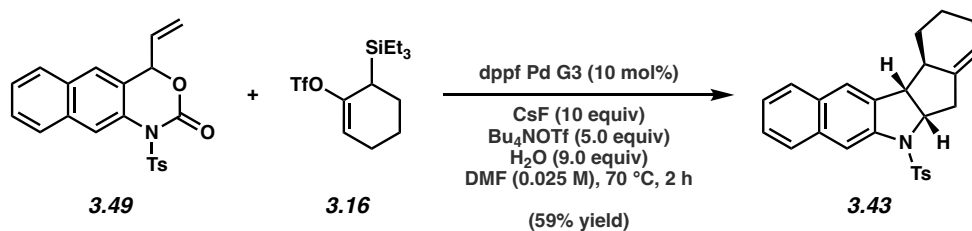
3.40. Followed General Procedure 3.6. Purification by preparative thin layer chromatography (4:1:1 hexanes:CH₂Cl₂:Et₂O) afforded a mixture of **3.40** and constitutional isomer **3.27** (54% combined yield, >20:1 dr, 8.5:1 **3.40**:**3.27**, average of two experiments) as a colorless clear oil. Ratio of constitutional isomers was determined by integrating the following peaks in the 1H NMR spectrum of the isolated mixture (H_a **3.40**: 5.49–5.47 ppm; H_b **3.27**: 5.55–5.51 ppm). **Annulation Products 3.40 and 3.27**: *R_f* 0.57 (4:1:1 hexanes:CH₂Cl₂:Et₂O); 1H NMR (600 MHz, CDCl₃, **3.40**): δ 7.60–7.56 (m, 3H), 7.19–7.16 (m, 2H), 6.75 (dd, *J* = 8.8, 2.4, 1H), 6.63–6.61 (m, 1H), 5.49–5.47 (br m, 1H), 4.37 (dt, *J* = 10.2, 7.6, 1H), 3.77 (s, 3H), 2.98–2.91 (m, 2H), 2.71–2.65 (m, 1H), 2.35 (s, 3H), 2.24–2.14 (m, 2H), 2.02–1.98 (m, 2H), 1.82–1.77 (m, 1H), 1.49–1.40 (m, 1H), 1.20–1.12 (m, 1H); ^{13}C NMR (150 MHz, CDCl₃, **3.40**): δ 157.1, 143.9, 140.3, 137.6, 134.7, 134.4, 129.7, 127.5, 119.1, 116.9, 113.0, 110.2, 66.1, 55.8, 52.2, 45.9, 41.1, 29.4, 24.8, 22.4, 21.7; IR (film): 2928, 1597, 1485, 1164, 665 cm⁻¹; HRMS-APCI (*m/z*) [M + H]⁺ calcd for C₂₃H₂₆NO₃S⁺, 396.1633; found 396.1632. Relative stereochemistry was assigned by analogy to the 1H NMR data of **3.43**.



3.41. Followed a modified version of General Procedure 3.6 by altering the temperature (100 °C). Purification by preparative thin layer chromatography (4:1:1 hexanes:CH₂Cl₂:Et₂O) afforded a mixture of **3.41** and constitutional isomers **3.28** and **3.78** (41% combined yield, >20:1 dr, 20:1.1:1.0 **3.41**:**3.28**:**3.78**, average of two experiments) as an off-white solid. Ratio of constitutional isomers was determined by integrating the following peaks in the ¹H NMR spectrum of the isolated mixture (H_a **3.41**: 5.53–5.49ppm; H_b **3.28**: 5.60–5.56 ppm; H_c **3.78**: 5.92 ppm). **Annulation Products 3.41, 3.28, and 3.78**: R_f 0.82 (4:1:1 hexanes:CH₂Cl₂:Et₂O); ¹H NMR (500 MHz, CDCl₃, **3.41**): δ 7.90 (d, *J* = 1.6, 1H), 7.68 (dt, *J* = 8.4, 1.6, 2H), 7.63–7.59 (m, 2H), 7.48–7.43 (m, 2H), 7.39–7.34 (m, 1H), 7.24 (dd, *J* = 7.8, 1.7, 1H), 7.22–7.18 (m, 2H), 7.15 (d, *J* = 7.8, 1H), 5.53–5.49 (br m, 1H), 4.48 (dt, *J* = 10.2, 7.6, 1H), 3.09 (dd, *J* = 10.1, 8.0, 1H), 3.01 (dd, *J* = 15.6, 7.9, 1H), 2.79–2.72 (m, 1H), 2.35 (s, 3H), 2.30–2.21 (m, 2H), 2.05–1.99 (m, 2H), 1.85–1.78 (m, 1H), 1.53–1.43 (m, 1H), 1.27–1.17 (m, 1H); ¹³C NMR (125 MHz, CDCl₃, **3.41**): δ 144.0, 142.0, 141.4, 140.9, 140.3, 134.7, 134.6, 129.7, 128.8, 127.4, 127.3, 127.2, 124.4, 123.1, 119.0, 113.9, 66.1, 51.9, 46.0, 41.3, 29.2, 24.8, 22.3, 21.5; IR (film): 3220, 2928, 2367, 1483, 1356 cm⁻¹; HRMS-APCI (*m/z*) [M + H]⁺ calcd for C₂₈H₂₈NO₂S⁺, 442.1841; found 442.1842. Relative stereochemistry was assigned by analogy to the ¹H NMR data of **3.43**.

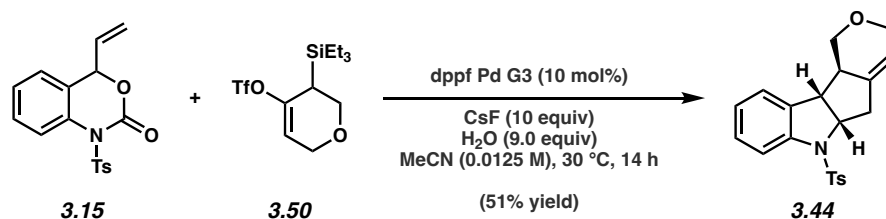


3.42. Followed General Procedure 3.6. Purification by preparative thin layer chromatography (4:1:1 hexanes:CH₂Cl₂:Et₂O) afforded **3.42** (44% yield, >20:1 dr, average of two experiments) as a white solid. **Annulation Product 3.42:** Mp: 188–190 °C; *R_f* 0.74 (4:1:1 hexanes:CH₂Cl₂:Et₂O); ¹H NMR (500 MHz, CDCl₃): δ 7.92 (s, 1H), 7.68 (d, *J* = 8.1, 2H), 7.35 (d, *J* = 3.5, 1H), 7.29 (d, *J* = 5.0, 1H), 7.25–7.23 (overlapped with residual solvent peak, 1H), 7.20 (d, *J* = 8.0, 2H), 7.11–7.06 (m, 2H), 5.52–5.50 (br m, 1H), 4.47 (dt, *J* = 10.0, 7.6, 1H), 3.09–2.97 (m, 2H), 2.78–2.71 (m, 1H), 2.35 (s, 3H), 2.27–2.19 (m, 2H), 2.03–1.99 (m, 2H), 1.84–1.79 (m, 1H), 1.51–1.41 (m, 1H), 1.26–1.15 (m, 1H); ¹³C NMR (125 MHz, CDCl₃): δ 144.4, 144.2, 142.2, 140.3, 134.9, 134.73, 134.66, 129.8, 128.2, 127.5, 125.0, 124.7, 123.5, 122.1, 119.2, 112.7, 66.3, 52.1, 46.2, 41.4, 29.3, 24.9, 22.4, 21.7; IR (film): 2965, 2367, 1423, 1356, 1212 cm⁻¹; HRMS-APCI (*m/z*) [M + H]⁺ calcd for C₂₆H₂₆NO₂S₂⁺, 448.1405; found 448.1409. Relative stereochemistry was assigned by analogy to the ¹H NMR data of **3.42**.



3.43. Followed General Procedure 3.6. Purification by preparative thin layer chromatography (4:1:1 hexanes:CH₂Cl₂:Et₂O) afforded **3.43** (59% yield, >20:1 dr, average of two experiments) as a white solid. **Annulation Product 3.43:** Mp: 181–183 °C; *R_f* 0.64 (4:1:1 hexanes:CH₂Cl₂:Et₂O);

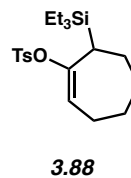
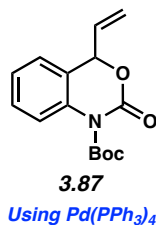
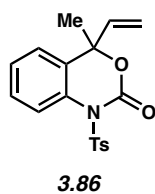
^1H NMR (500 MHz, CDCl_3): δ 8.01 (s, 1H), 7.84–7.80 (m, 1H), 7.72 (dt, $J = 8.3, 2.0$, 2H), 7.71–7.67 (m, 1H), 7.53–7.5 (m, 1H), 7.43 (ddd, $J = 8.2, 6.9, 1.3$, 1H), 7.36 (ddd, $J = 8.1, 6.8, 1.2$, 1H), 7.19–7.15 (m, 2H), 5.54–5.50 (br m, 1H), 4.53 (ddd, $J = 10.3, 7.5, 6.8$, 1H), 3.24–3.19 (m, 1H), 3.03 (dd, $J = 15.8, 7.9$, 1H), 2.83–2.76 (m, 1H), 2.35–2.28 (m, 5H), 2.07–2.00 (m, 2H), 1.88–1.81 (m, 1H), 1.52–1.42 (m, 1H), 1.33–1.22 (m, 1H); ^{13}C NMR (125 MHz, CDCl_3): δ 144.2, 140.7, 140.2, 136.4, 134.8, 133.9, 131.1, 129.8, 127.9, 127.41, 127.39, 126.0, 124.8, 122.9, 119.2, 111.3, 66.2, 51.9, 46.5, 41.4, 29.3, 24.9, 22.4, 21.6; IR (film): 2923, 2852, 1454, 1356, 1163 cm^{-1} ; HRMS-APCI (m/z) [$\text{M} + \text{H}$] $^+$ calcd for $\text{C}_{26}\text{H}_{26}\text{NO}_2\text{S}^+$, 416.1678; found 416.1682. Relative stereochemistry was assigned by X-ray crystallography; see Section 3.8.2.6 for details. See Table 3.11, Entry 1 and Figure 3.8 for SFC data.



3.44. Followed General Procedure 3.7. Purification by preparative thin layer chromatography (4:1:1 hexanes: CH_2Cl_2 : Et_2O) afforded **3.44** (51% yield, >20:1 dr (determined by ^1H NMR analysis of the crude mixture), average of two experiments) as a white solid. **Annulation Product 3.44:** Mp: 128–130 $^\circ\text{C}$; R_f 0.22 (4:1:1 hexanes: CH_2Cl_2 : Et_2O); ^1H NMR (600 MHz, CDCl_3): δ 7.68–7.62 (m, 3H), 7.25–7.22 (m, 1H), 7.21–7.18 (m, 2H), 7.05–7.00 (m, 2H), 5.54–5.51 (m, 1H), 4.45 (dt, $J = 10.4, 7.5$, 1H), 4.33 (dd, $J = 10.5, 6.1$, 1H), 4.16 (dq, $J = 16.2, 3.0$, 1H), 4.10–4.03 (m, 1H), 3.19 (t, $J = 10.3$, 1H), 3.10–3.04 (m, 2H), 2.77–2.70 (m, 1H), 2.60–2.56 (m, 1H), 2.35 (s, 3H); ^{13}C NMR (125 MHz, CDCl_3): δ 144.2, 141.3, 138.3, 134.8, 134.5, 129.8, 128.5, 127.4, 124.53, 124.52,

117.4, 115.8, 69.0, 65.6, 65.0, 47.9, 44.6, 40.9, 21.7; IR (film): 2955, 2819, 1460, 1349, 1158 cm^{-1} ; HRMS-APCI (m/z) $[\text{M} + \text{H}]^+$ calcd for $\text{C}_{21}\text{H}_{22}\text{NO}_3\text{S}^+$, 368.1315; found 368.1331. Relative stereochemistry was assigned by analogy to the ^1H NMR data of **3.43**.

A. Unsuccessful substrates



B. Low yielding substrates

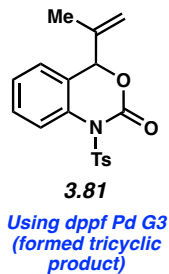
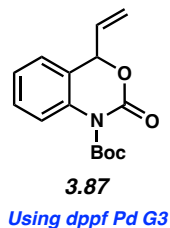
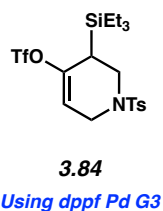
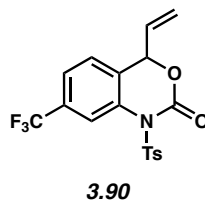
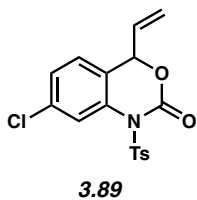
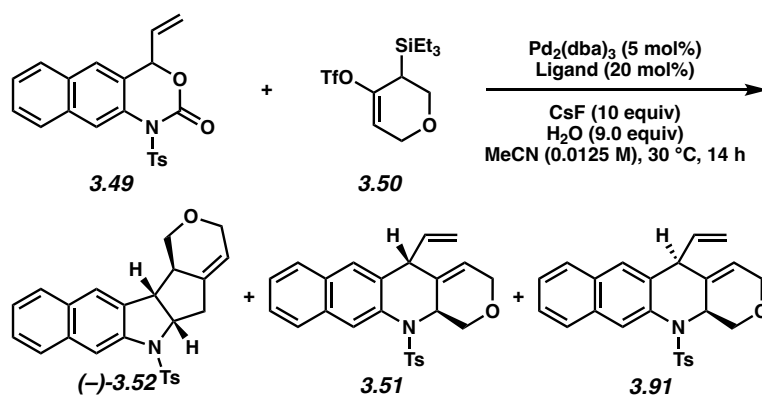


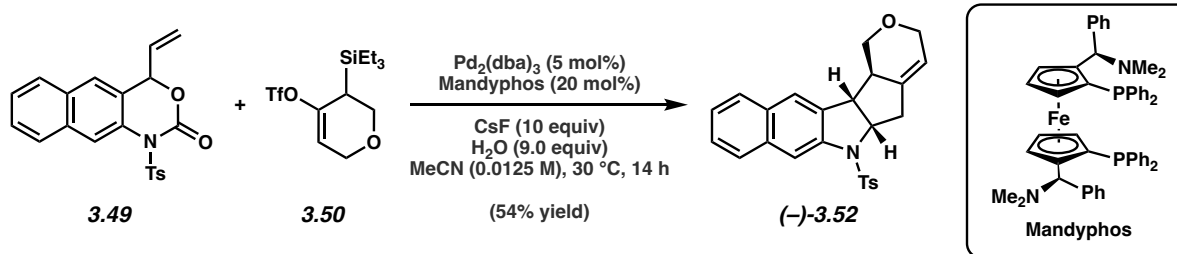
Figure 3.5. Unsuccessful and low yielding substrates evaluated during scope studies.

3.8.2.4 Representative Asymmetric Annulations

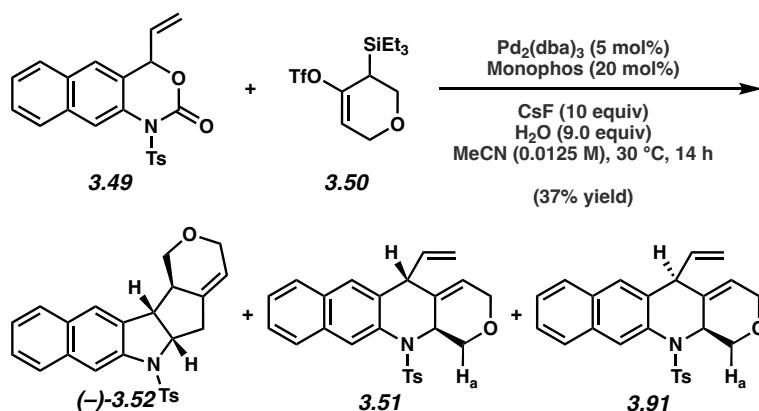
General Procedure 3.8 for the asymmetric annulation:



A 1-dram vial containing a magnetic stir bar was charged with vinyl benzoxazinone **3.49** (28 mg, 0.075 mmol, 3.0 equiv). A separate 1-dram vial was charged with silyl triflate **3.50**. The two vials were taken into a glovebox where $\text{Pd}_2(\text{dba})_3$ (1.1 mg, 0.0013 mmol, 5 mol%), ligand (0.005 mmol, 20 mol%), and CsF (38 mg, 0.25 mmol, 10 equiv) were added to the vial containing vinyl benzoxazinone **3.49**. To the vial containing silyl triflate **3.50** was added the appropriate amount of MeCN to afford a 0.0125 M solution. The vial was capped and shaken to ensure full dissolution. The necessary amount of the solution of silyl triflate **3.50** (0.0125 M in MeCN, 2.0 mL, 8.7 mg, 0.025 mmol, 1.0 equiv) was then transferred via micropipette to the reaction vial containing vinyl benzoxazinone **3.49**. The reaction was sealed with a septum cap, removed from the glovebox, and placed under a flow of N_2 . Then, deionized water (4.1 μL , 0.23 mmol, 9.0 equiv) was added to the reaction vessel via microsyringe. The septum cap was then carefully replaced with a Teflon-lined cap under a stream of N_2 and stirred for 14 h at 30 °C. The mixture was then filtered through a pad of silica gel, eluting with EtOAc (8 mL). The eluate was concentrated and purified by preparative thin layer chromatography to provide annulation products **(-)-3.52**, **3.51**, and **3.91** which were analyzed by SFC using a chiral stationary phase.

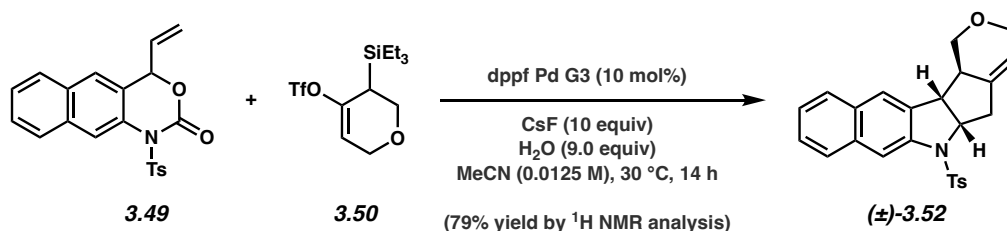


(-)-**3.52**. Followed General Procedure 3.8. Purification by preparative thin layer chromatography (8:3:3 hexanes:CH₂Cl₂:Et₂O) afforded annulation product (-)-**3.52** (54% yield, >20:1 dr, 70% ee) as a white solid. (-)-**3.52**: Mp: 157–159 °C; *R_f* 0.37 (8:3:3 hexanes:CH₂Cl₂:Et₂O); ¹H NMR (500 MHz, CDCl₃): δ 8.02, (s, 1H), 7.83 (d, *J* = 8.1, 1H), 7.73–7.68 (m, 3H), 7.47–7.42 (m, 2H), 7.40–7.35 (m, 1H), 7.17 (d, *J* = 8.0, 2H), 5.56–5.54 (br m, 1H), 4.56 (dt, *J* = 10.0, 7.5, 1H), 4.44 (dd, *J* = 10.4, 6.1, 1H), 4.21–4.15 (m, 1H), 4.12–4.06 (m, 1H), 3.31–3.20 (m, 2H), 3.11 (dd, *J* = 15.6, 7.7, 1H), 2.84–2.76 (m, 1H), 2.69–2.65 (m, 1H), 2.33 (s, 3H); ¹³C NMR (125 MHz, CDCl₃): δ 144.4, 140.0, 138.6, 135.4, 134.8, 134.0, 131.2, 129.9, 127.9, 127.5, 127.3, 126.3, 125.0, 123.3, 117.6, 111.7, 69.0, 66.0, 65.0, 47.5, 44.9, 40.9, 21.7; IR (film): 2926, 1457, 1356, 1164, 590 cm⁻¹; HRMS-APCI (*m/z*) [*M* + H]⁺ calcd for C₂₅H₂₄NO₃S⁺, 418.1471; found 418.1505. [*α*]_D^{19.9} –8.0° (*c* = 1.00, CH₂Cl₂). Relative stereochemistry was assigned by analogy to the ¹H NMR data of **3.43**. See Table 3.11, Entry 5 and Figure 3.12 for SFC data.

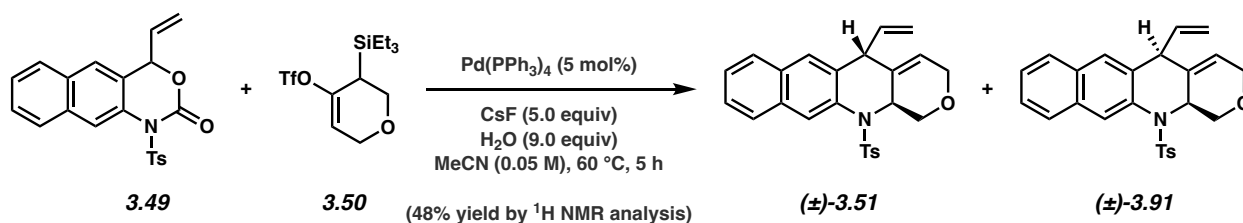


(-)-**3.52**, **3.51**, and **3.91**. Followed General Procedure 3.8. Purified by preparative thin layer chromatography (8:3:3 hexanes:CH₂Cl₂:Et₂O) afforded (-)-**3.52** (11% yield, >20:1 dr (determined by ¹H NMR analysis of the crude mixture), 12% ee) as a white solid and an mixture of major diastereomer **3.51** and minor diastereomer **3.91** (26% yield, 2.8:1 dr, ~38% ee and ~38% ee, respectively) as an off-white solid. Diastereomeric ratio was determined by integrating the following peaks in the ¹H-NMR spectrum of the crude reaction mixture (H_a **3.51**: 3.41–3.31 ppm; **3.91**: 3.41–3.31 ppm). Spectral data matched those obtained for (-)-**3.52**, **3.51** and **3.91**: R_f 0.54 (8:3:3 hexanes:CH₂Cl₂:Et₂O); ¹H NMR (500 MHz, CDCl₃, **3.51**): δ 8.37 (s, 1H), 7.91–7.86 (m, 1H), 7.76–7.70 (m, 1H), 7.50–7.41 (m, 3H), 7.35–7.31 (m, 2H), 7.13–7.09 (m, 2H), 5.65 (q, *J* = 2.7, 1H), 4.89 (ddd, *J* = 17.1, 10.1, 4.9, 1H), 4.81–4.72 (m, 1H), 4.67 (ddd, *J* = 17.2, 2.0, 1.4, 1H), 4.62 (dd, *J* = 10.4, 5.5, 1H), 4.45–4.39 (m, 1H), 4.22–4.11 (m, 1H), 4.04 (ddd, 16.9, 3.9, 1.9, 1H), 4.01–3.94 (m, 1H), 3.41–3.31 (m, 1H), 2.33 (s, 3H); ¹H NMR (500 MHz, CDCl₃, **3.91**): δ 8.15 (s, 1H), 7.91–7.86 (m, 1H), 7.76–7.70 (m, 1H), 7.50–7.41 (m, 5H), 7.19–7.15 (m, 2H), 5.99 (dt, *J* = 19.4, 9.9, 1H), 5.40–5.34 (m, 2H), 4.83 (dd, *J* = 17.1, 1.5, 1H), 4.81–4.72 (m, 1H), 4.45–4.39 (m, 1H), 4.22–4.11 (m, 1H), 4.01–3.94 (m, 1H), 3.41–3.31 (m, 1H), 2.48–2.44 (m, 1H), 2.39 (s, 3H); ¹³C NMR (125 MHz, CDCl₃, **3.51** and **3.91**, 45 of 46 signals observed): δ 144.0, 143.9, 136.7, 136.1, 136.0, 135.7, 135.6, 134.3, 133.9, 133.2, 133.1, 132.7, 132.4, 132.0, 131.5, 129.7, 129.5,

128.3, 128.2, 127.9, 127.5, 127.2, 127.11, 127.05, 126.6, 126.3, 126.22, 126.21, 126.17, 124.1, 123.0, 122.9, 120.3, 119.1, 116.1, 69.0, 68.5, 65.1, 65.1, 54.3, 52.4, 50.7, 45.7, 21.63, 21.60; IR (film): 2926, 2853, 1356, 1167, 1091 cm^{-1} ; HRMS-APCI (m/z) $[\text{M} + \text{H}]^+$ calcd for $\text{C}_{25}\text{H}_{24}\text{NO}_3\text{S}^+$, 418.1471; found 418.1465. Optical rotation could not be determined for **3.51** and **3.91** due to difficulty of separation. Relative stereochemistry was assigned by analogy to the ^1H NMR data of **3.33** and **3.85**. See Table 3.11, Entry 7 and Figure 3.14 for SFC data for **3.51** and see Table 3.11, Entry 9 and Figure 3.16 for SFC data for **3.91**.



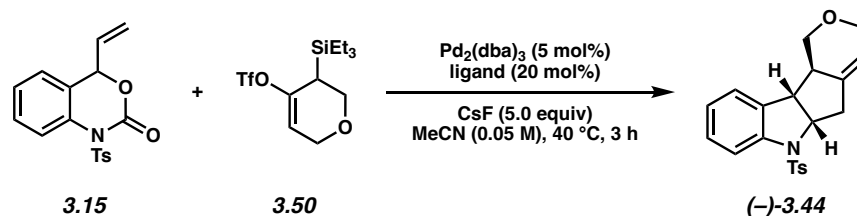
(±)-3.52. Followed a modified version of General Procedure 3.7 by performing on 0.025 mmol scale. Purification by preparative thin layer chromatography (4:1:1 hexanes: CH_2Cl_2 : Et_2O) afforded an analytical sample of annulation product **(±)-3.52** (79% yield by ^1H NMR using mesitylene as an internal standard, >20:1 dr (determined by ^1H NMR analysis of the crude mixture)) as a white solid. **Annulation Product (±)-3.52**: Spectral data matched those obtained for **(−)-3.52**. See Table 3.11, Entry 4 and Figure 3.11 for SFC data.



$(\pm)\text{-3.51}$ and $(\pm)\text{-3.91}$. Followed a modified version of General Procedure 3.5 by performing on 0.025 mmol scale. Purification by preparative thin layer chromatography (8:3:3 hexanes: CH_2Cl_2 : Et_2O) afforded an analytical sample of a mixture of major diastereomer $(\pm)\text{-3.51}$ and minor diastereomer $(\pm)\text{-3.91}$ (48% yield by $^1\text{H NMR}$ using mesitylene as an internal standard, 1.3:1 dr) as a white solid. Diastereomeric ratio was determined by integrating the following peaks in the $^1\text{H-NMR}$ spectrum of the crude reaction mixture (H_a $(\pm)\text{-3.51}$: 3.41–3.31 ppm; $(\pm)\text{-3.91}$: 3.41–3.31 ppm). Spectral data matched those obtained for **3.51** and **3.91**. See Table 3.11, Entry 6 and Figure 3.13 for SFC data for $(\pm)\text{-3.51}$ and see Table 3.11, Entry 8 and Figure 3.15 for SFC data for $(\pm)\text{-3.91}$.

3.8.2.5. Extended Evaluation of Chiral Ferrocenyl Phosphine Ligands

General Procedure 3.9 for the evaluation of the asymmetric annulation:



A 1-dram vial containing a magnetic stir bar was charged with vinyl benzoxazinone **3.15** (28 mg, 0.075 mmol, 3.0 equiv). A separate 1-dram vial was charged with silyl triflate **3.50**. The two vials were taken into a glovebox where $\text{Pd}_2(\text{dba})_3$ (1.1 mg, 0.0013 mmol, 5 mol%), ligand (0.005 mmol, 20 mol%), and CsF (17 mg, 0.13 mmol, 5.0 equiv) were added to the vial containing vinyl

benzoxazinone **3.15**. To the vial containing silyl triflate **3.50** was added the appropriate amount of MeCN to afford a 0.05 M solution. The vial was capped and shaken to ensure full dissolution. The necessary amount of the solution of silyl triflate **3.50** (0.05 M in MeCN, 500 μ L, 8.7 mg, 0.025 mmol, 1.0 equiv) was then transferred via micropipette to the reaction vial containing vinyl benzoxazinone **3.15**. The reaction was sealed with a Teflon-lined cap, removed from the glovebox, and stirred for 3 h at 40 °C. The mixture was then filtered through a pad of silica gel, eluting with EtOAc (8 mL). The eluate was concentrated and purified by preparative thin layer chromatography to provide annulation products (–)-**3.44** which were analyzed by SFC using a chiral stationary phase.

The stereochemistry depicted for (–)-3.44 is not necessarily representative of the major enantiomer observed for all ligands evaluated. Any modification of the conditions shown in the general procedure above are specified in the following scheme.

A range of ligands (see Figure 3.6 below for ligand structures) were tested using General Procedure 3.9, and results of these studies appear below in Table 3.9.

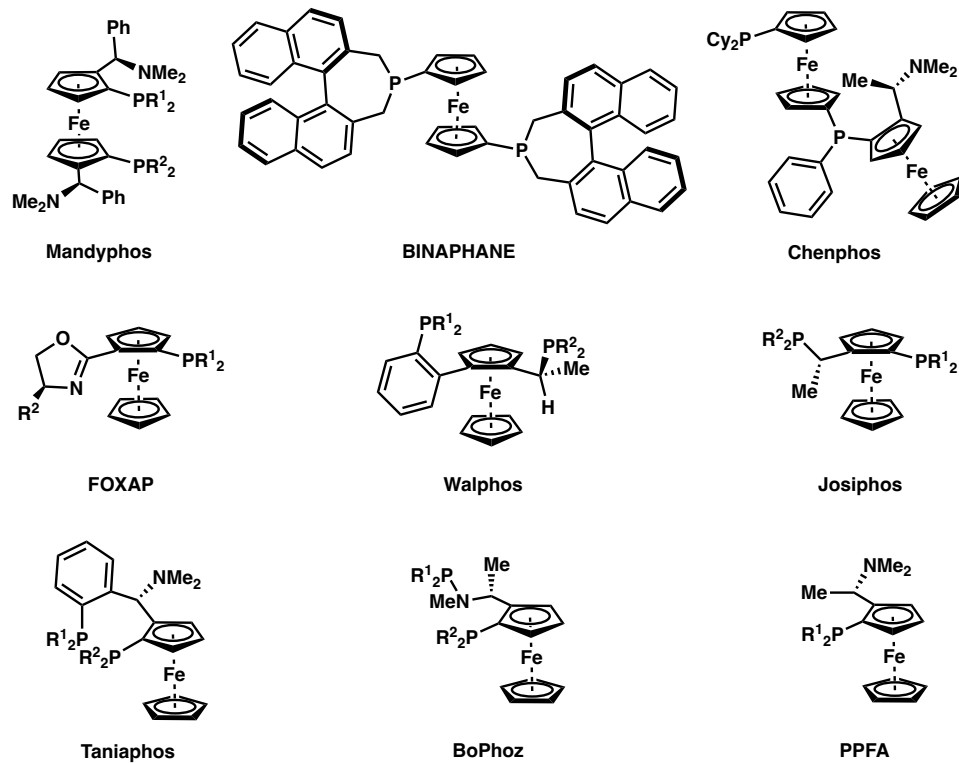
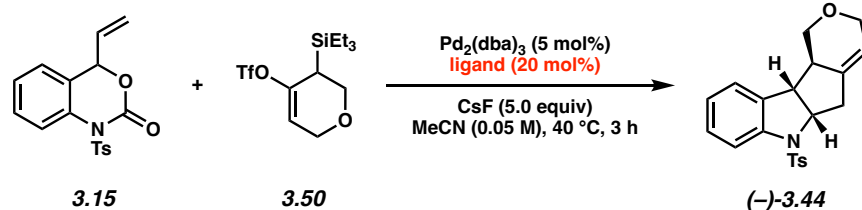


Figure 3.6. Ligand families evaluated during asymmetric reaction development.

Table 3.9. Ligand evaluation results. See Figure 3.6 above for ligand classes (absolute stereochemistry of product may differ between table entries).



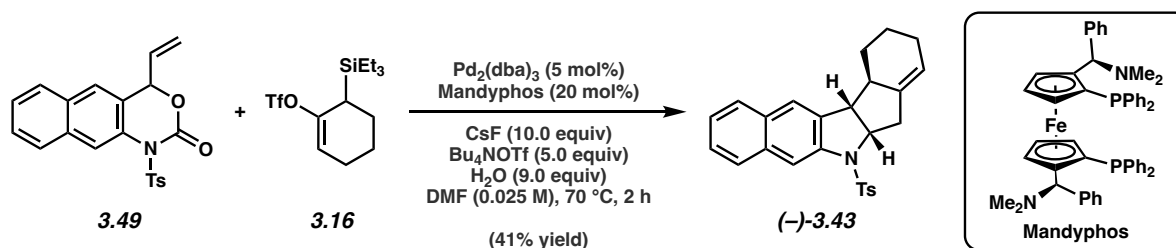
Entry	Ligand Class	R ¹	R ²	Yield ^a	%ee
1	Mandyphos ^b	Ph	Ph	19%	77%
2	Mandyphos ^b	4-methoxy-3,5-xylyl	4-methoxy-3,5-xylyl	18%	73%
3	Mandyphos ^b	3,5-bis(trifluoromethyl)phenyl	3,5-bis(trifluoromethyl)phenyl	0%	N/A
4	Mandyphos ^b	3,5-xylyl	3,5-xylyl	5%	19%
5	Mandyphos ^b	Cy	Cy	0%	N/A
6	BINAPHAN E	N/A	N/A	0%	N/A
7	Chenphos	N/A	N/A	0%	N/A
8	FOXAP	Ph	<i>i</i> -Pr	0%	N/A
9	Walphos	Ph	Ph	13%	46%
10	Walphos	Ph	3,5-xylyl	5%	N/A
11	Walphos	3,5-xylyl	3,5-xylyl	5%	N/A
12	Walphos	Ph	Cy	10%	N/A
13	Josiphos ^b	Ph	Cy	0%	N/A
14	Josiphos	2-furyl	3,5-xylyl	16%	N/A
15	Josiphos	1-naphthyl	3,5-xylyl	4%	N/A
16	Josiphos	Ph	<i>t</i> -Bu	8%	N/A
17	Taniaphos	Ph	Ph	0%	N/A
18	BoPhoz	Ph	Ph	18%	0%

19	PPFA ^b	Ph	N/A	0%	N/A
20 ^c	No ligand	N/A	N/A	0%	N/A

^a ¹H NMR yield determined using mesitylene as an external standard. ^b 10 mol% ligand.
^c Conditions: Pd₂(dba)₃ (2.5 mol%), CsF (10 equiv), H₂O (3.0 equiv), MeCN (0.0125 M), 30 °C, 16 h.

3.8.2.6. Assignment of Absolute Stereochemical Configuration

To determine the major enantiomer formed in the annulation reaction, annulation product (–)-**3.43** was synthesized.



(–)-**3.43**. A 1-dram vial containing a magnetic stir bar was charged with vinyl benzoxazinone **3.49** (28 mg, 0.075 mmol, 3.0 equiv) and Bu₄NOTf (49 mg, 0.13 mmol, 5.0 equiv). A separate 1-dram vial was charged with silyl triflate **3.16**. The two vials were taken into a glovebox where Pd₂(dba)₃ (1.1 mg, 0.0013 mmol, 5 mol%), Mandyphos (4.1 mg, 0.005 mmol, 20 mol%), and CsF (38 mg, 0.25 mmol, 10.0 equiv) were added to the vial containing vinyl benzoxazinone **3.49**. To the vial containing silyl triflate **3.16** was added the appropriate amount of DMF to afford a 0.025 M solution. The vial was capped and shaken to ensure full dissolution. The necessary amount of the solution of silyl triflate **3.16** (0.025 M in DMF, 1.0 mL, 8.6 mg, 0.025 mmol, 1.0 equiv) was then transferred via micropipette to the reaction vial containing vinyl benzoxazinone **3.49**. The reaction was sealed with a septum cap, removed from the glovebox, and placed under a flow of N₂. Then, deionized water (4.1 μL, 0.23 mmol, 9.0 equiv) was added to the reaction vessel via microsyringe. The septum cap was then carefully replaced with a Teflon-lined cap under a stream of N₂ and

stirred for 2 h at 70 °C. The mixture was then filtered through a pad of silica gel, eluting with EtOAc (8 mL). The eluate was washed with water (2 x 5 mL), dried with Na₂SO₄, filtered, and concentrated under reduced pressure. The crude residue was redissolved in CH₂Cl₂ (1 mL) and filtered through a pad of silica gel eluting with CH₂Cl₂ (20 mL) to remove excess Bu₄NOTf. The eluate was concentrated and purified by preparative thin layer chromatography (4:1:1 hexanes:CH₂Cl₂:Et₂O) to provide annulation product (–)-**3.43** (41% yield, >20:1 dr, 58% ee) as an off-white solid. Crystals suitable for X-ray diffraction studies were obtained by liquid diffusion crystallization: (–)-**3.43** in a 1-dram vial was dissolved in minimal amounts of CH₂Cl₂ then EtOH was layered on top resulting in ~1:5 CH₂Cl₂:EtOH (solvents were filtered through a 0.22 μm filter prior to use). The ee for the crystals of (–)-**3.43** evaluated by X-ray analysis was ~80%, with the major enantiomer seen by SFC analysis corresponding to the major enantiomer observed after chromatography. (–)-**3.43**: Spectral data matched those previous reported in Section 3.8.2.3 for **3.43**. [α]^{18.1}_D–203° (c = 1.00, CH₂Cl₂). See Table 3.11, Entries 2 and 3 and Figures 3.9 and 3.10 for SFC data.

Crystal Structure Analysis

Diffraction intensities were collected at 100 K on a Bruker Smart ApexII CCD diffractometer with CuKα radiation, 1.54178 Å. Absorption corrections were applied by SADABS.⁷¹ All calculations were performed by the SHELXL-2014 packages.⁷² Deposition Number 2238913 contains the supplementary crystallographic data for this paper. These data are provided free of charge by the joint Cambridge Crystallographic Data Centre and Fachinformationszentrum Karlsruhe Access Structures service www.ccdc.cam.ac.uk/structures.

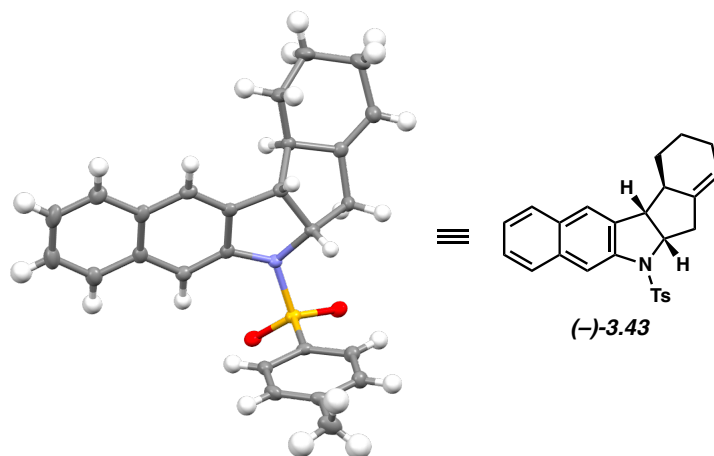


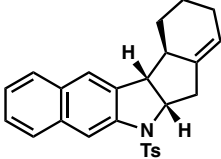
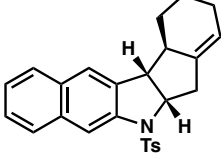
Figure 3.7. ORTEP representation of X-ray crystallographic structure (-)-3.43. (CCDC Registry # 2238913).

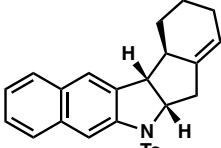
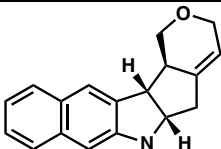
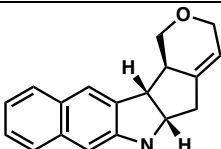
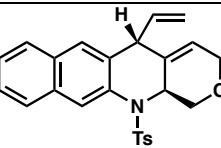
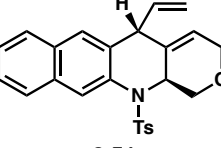
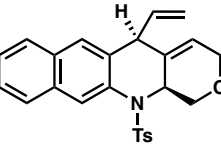
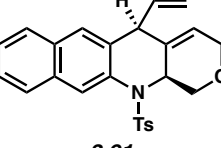
Table 3.10. Crystal data and structure refinement for compound (-)-3.43.

Identification code	cu_garg2209_a	
Empirical formula	C ₂₆ H ₂₅ N O ₂ S	
Formula weight	415.53	
Temperature	100(2) K	
Wavelength	1.54178 Å	
Crystal system	Monoclinic	
Space group	P2 ₁	
Unit cell dimensions	a = 14.1629(10) Å	α = 90°
	b = 5.4284(4) Å	β = 107.696(3)°
	c = 14.3334(10) Å	γ = 90°
Volume	1049.84(13) Å ³	
Z	2	
Density (calculated)	1.314 Mg/m ³	
Absorption coefficient	1.544 mm ⁻¹	
F(000)	440	
Crystal size	0.400 x 0.030 x 0.030 mm ³	
Theta range for data collection	3.236 to 69.429 °	

Index ranges	-17<=h<=15, -5<=k<=6, -14<=l<=17
Reflections collected	13355
Independent reflections	3750 [R(int) = 0.0405]
Completeness to theta = 67.679°	97.9
Absorption correction	Semi-empirical from equivalents
Max. and min. transmission	0.75 and 0.58
Refinement method	Full-matrix least-squares on F ²
Data / restraints / parameters	3750 / 1 / 272
Goodness-of-fit on F ²	1.061
Final R indices [I>2sigma(I)]	R1 = 0.0295, wR2 = 0.0742
R indices (all data)	R1 = 0.0311, wR2 = 0.0748
Absolute structure parameter	0.037(7)
Extinction coefficient	n/a
Largest diff. peak and hole	0.180 and -0.333 e.Å ⁻³

Table 3.11. SFC conditions and data.

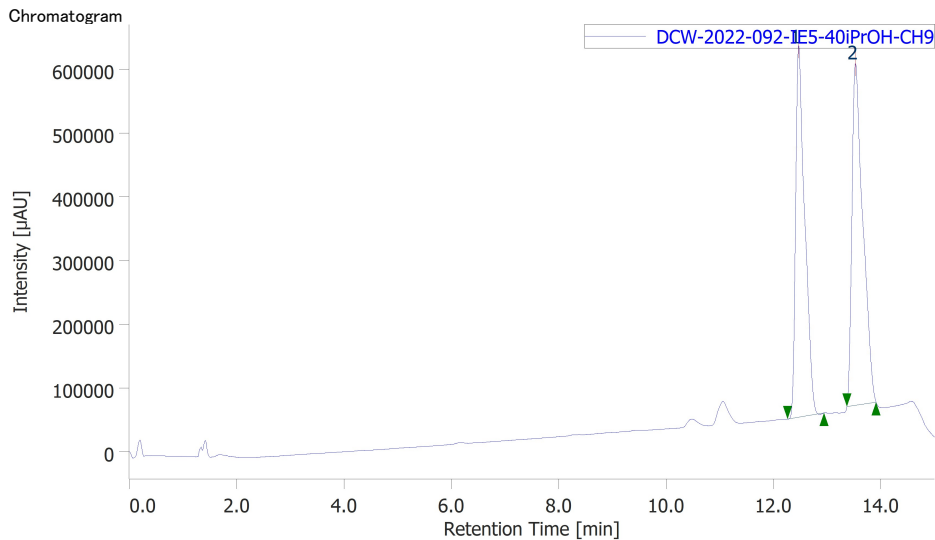
Compound	Column	Solvent	Flow Rate	Retention Times (min)	Enantiomeric Ratio (er)
 <p>(±)-3.43</p>	Daicel ChiralPak IE / 30 °C	5–40% isopropanol in CO ₂	4.0 mL/min	12.463/13.523	47.7 : 52.3
 <p>(-)-3.43 <i>From reaction mixture</i></p>	Daicel ChiralPak IE / 30 °C	5–40% isopropanol in CO ₂	4.0 mL/min	12.485/13.522	20.9 : 79.1

 (-)-3.43 <i>Crystals used for X-ray analysis</i>	Daicel ChiralPak IE / 30 °C	5–40% isopropanol in CO ₂	4.0 mL/min	12.507/13.567	10 : 90 ^a
 (±)-3.52	Daicel ChiralPak ID / 30 °C	5–40% isopropanol in CO ₂	4.0 mL/min	11.740/12.933	49.2 : 50.8
 (-)-3.52	Daicel ChiralPak ID / 30 °C	5–40% isopropanol in CO ₂	4.0 mL/min	11.730/12.940	84.9 : 15.1
 (±)-3.51	Daicel ChiralPak ID / 30 °C	5–40% isopropanol in CO ₂	4.0 mL/min	9.830/10.103	48.6 : 51.4 ^b
 3.51	Daicel ChiralPak ID / 30 °C	5–40% isopropanol in CO ₂	4.0 mL/min	9.890/10.170	69 : 31 ^b
 (±)-3.91	Daicel ChiralPak ID / 30 °C	5–40% isopropanol in CO ₂	4.0 mL/min	9.017/9.453	52.3 : 47.7 ^b
 3.91	Daicel ChiralPak ID / 30 °C	5–40% isopropanol in CO ₂	4.0 mL/min	9.070/9.500	69 : 31 ^b

^a The ee for (-)-**3.43** (Crystals) is approximated due to low concentration and a non-zero baseline.

^b Due to difficulty resolving peaks, the ee reported for **3.51** and **3.94** (see Section 3.8.2.4) is approximated.

DCW-2022-092_112 DCW-2022-092-IE5-40iPrOH 1/20/2023 11:26:46 AM

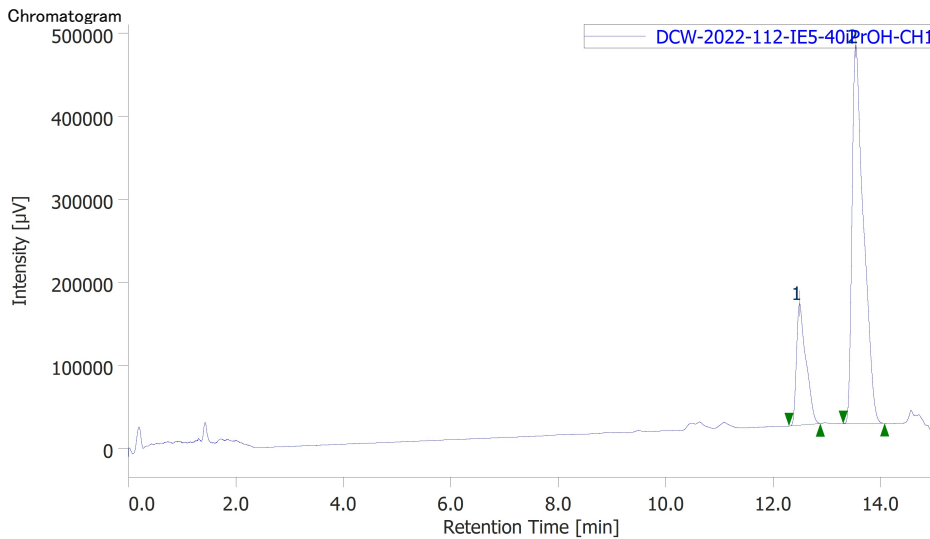


Peak Information

#	Peak Name	CH	tR [min]	Area [µV.sec]	Height [µV]	Area%	Height%	Quantity	NTP	Resolution	Symmetry Factor	Warning
1	Unknown	9	12.463	6871405	583880	47.675	52.105	N/A	25133	3.072	1.669	
2	Unknown	9	13.523	7541748	536710	52.325	47.895	N/A	20546	N/A	1.713	

Figure 3.8. SFC trace of (±)-3.43.

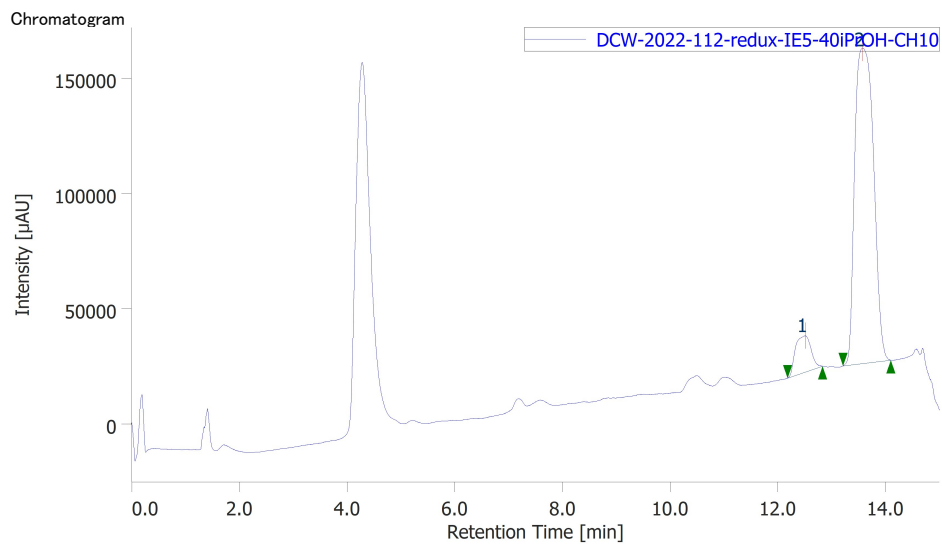
DCW-2022-092_112 DCW-2022-112-IE5-40iPrOH 1/20/2023 11:30:46 AM



Peak Information

#	Peak Name	CH	tR [min]	Area [µV.sec]	Height [µV]	Area%	Height%	Quantity	NTP	Resolution	Symmetry Factor	Warning
1	Unknown	1	12.485	1792991	146467	20.943	24.323	N/A	23046	2.900	1.692	
2	Unknown	1	13.528	6768170	455706	79.057	75.677	N/A	19000	N/A	1.770	

Figure 3.9. SFC trace of (-)-3.43 (from reaction mixture).

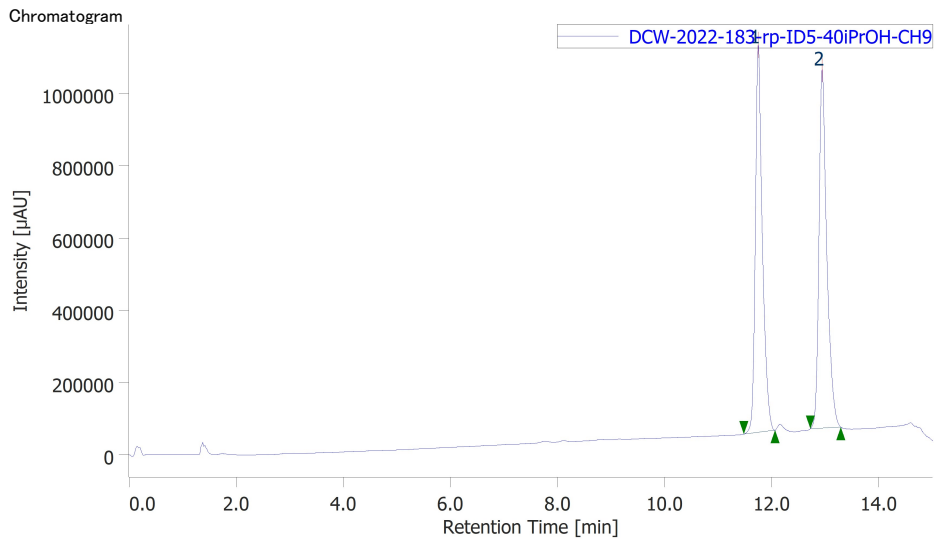


Peak Information

#	Peak Name	CH	tR [min]	Area [µV·sec]	Height [µV]	Area%	Height%	Quantity	NTP	Resolution	Symmetry Factor	Warning
1	Unknown	10	12.507	322576	15742	8.856	10.315	N/A	7675	1.696	0.951	
2	Unknown	10	13.567	3319743	136876	91.144	89.685	N/A	6319	N/A	1.274	

Figure 3.10. SFC trace of (-)-**3.43** (Crystals used for X-ray analysis).

DCW-2022-183-rp DCW-2022-183-rp-ID5-40iPrOH 1/20/2023 11:32:36 AM

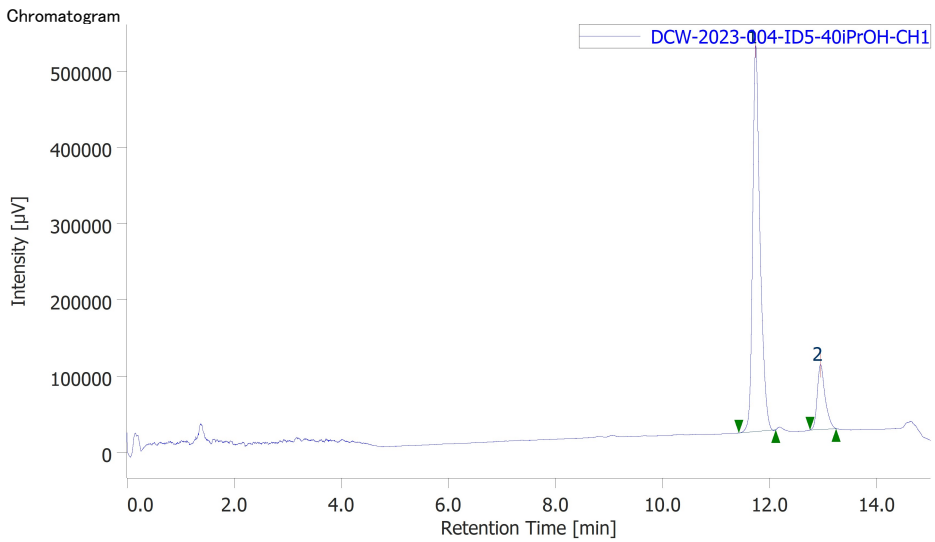


Peak Information

#	Peak Name	CH	tR [min]	Area [µV·sec]	Height [µV]	Area%	Height%	Quantity	NTP	Resolution	Symmetry Factor	Warning
1	Unknown	9	11.740	9762221	1072140	49.248	51.904	N/A	43994	5.060	1.362	
2	Unknown	9	12.933	10060552	993464	50.752	48.096	N/A	43154	N/A	1.404	

Figure 3.11. SFC trace of (±)-3.52.

DCW-2023-004.005.006 DCW-2023-004-ID5-40iPrOH 1/20/2023 11:33:43 AM

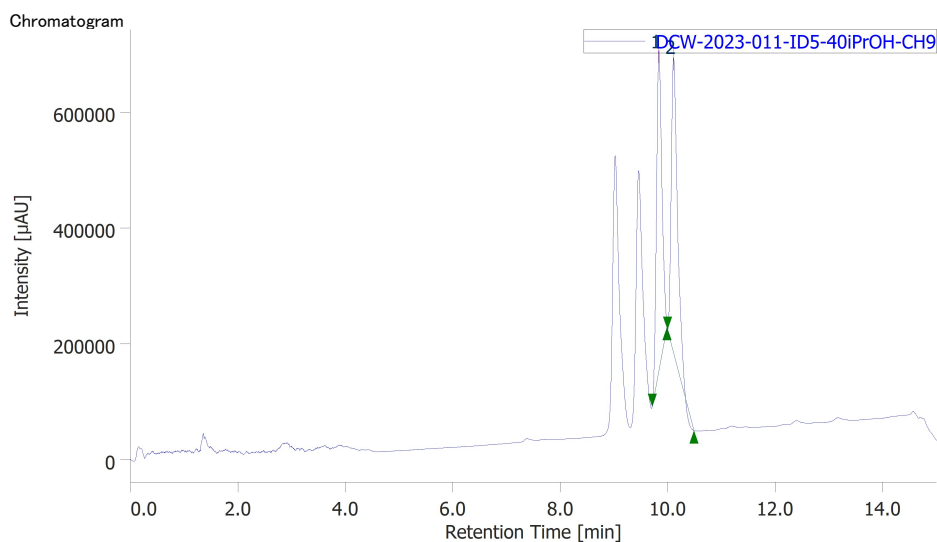


Peak Information

#	Peak Name	CH	tR [min]	Area [µV·sec]	Height [µV]	Area%	Height%	Quantity	NTP	Resolution	Symmetry Factor	Warning
1	Unknown	1	11.730	4861803	506817	84.904	85.612	N/A	38918	4.927	1.359	
2	Unknown	1	12.940	864424	85178	15.096	14.388	N/A	41315	N/A	1.339	

Figure 3.12. SFC trace of (-)-3.52.

DCW-2023-011 DCW-2023-011-ID5-40iPrOH 1/20/2023 11:34:21 AM

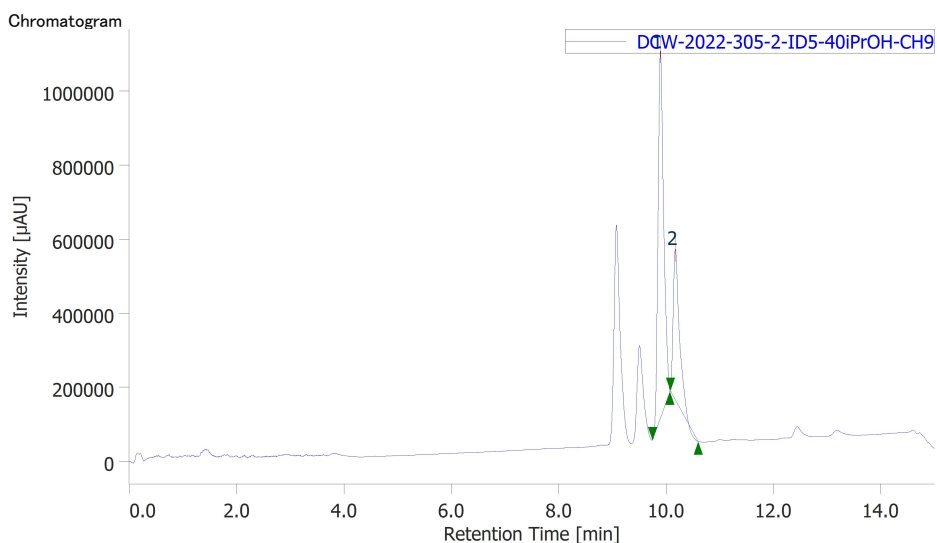


Peak Information

#	Peak Name	CH	tR [min]	Area [µV·sec]	Height [µV]	Area%	Height%	Quantity	NTP	Resolution	Symmetry Factor	Warning
1	Unknown	9	9.830	3912441	554563	48.564	52.160	N/A	44701	1.399	1.217	
2	Unknown	9	10.103	4143789	508642	51.436	47.840	N/A	38548	N/A	1.579	

Figure 3.13. SFC trace of (±)-3.51.

DCW-2022-305 DCW-2022-305-2-ID5-40iPrOH 1/20/2023 11:41:20 AM

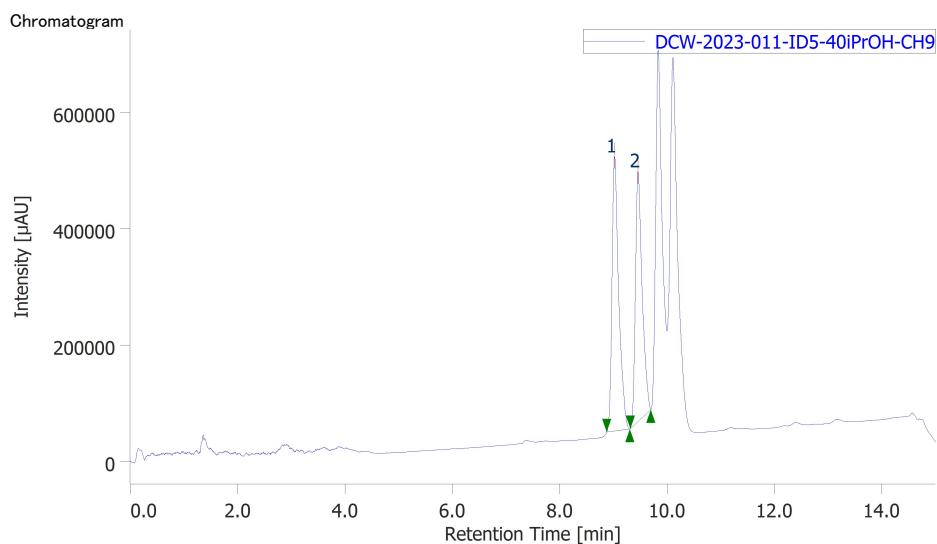


Peak Information

#	Peak Name	CH	tR [min]	Area [µV·sec]	Height [µV]	Area%	Height%	Quantity	NTP	Resolution	Symmetry Factor	Warning
1	Unknown	9	9.890	7222036	993611	68.556	70.879	N/A	44561	1.465	1.280	
2	Unknown	9	10.170	3312508	408236	31.444	29.121	N/A	43101	N/A	1.785	

Figure 3.14. SFC trace of 3.51.

DCW-2023-011 DCW-2023-011-ID5-40iPrOH 1/20/2023 11:38:42 AM

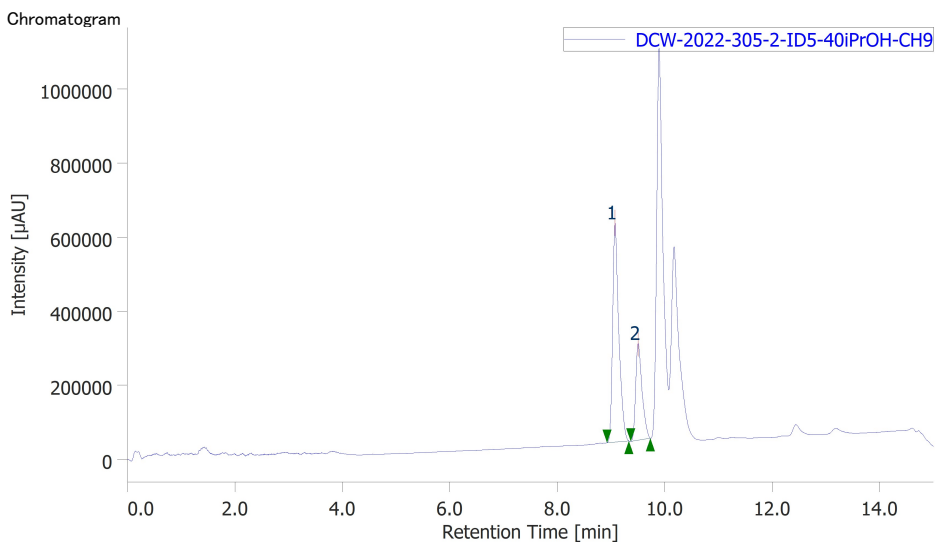


Peak Information

#	Peak Name	CH	tR [min]	Area [μV·sec]	Height [μV]	Area%	Height%	Quantity	NTP	Resolution	Symmetry Factor	Warning
1	Unknown	9	9.017	4091997	472755	52.309	52.338	N/A	28612	2.019	1.522	
2	Unknown	9	9.453	3730678	430511	47.691	47.662	N/A	29389	N/A	1.484	

Figure 3.15. SFC trace of (±)-3.91.

DCW-2022-305 DCW-2022-305-2-ID5-40iPrOH 1/20/2023 11:40:05 AM



Peak Information

#	Peak Name	CH	tR [min]	Area [μV·sec]	Height [μV]	Area%	Height%	Quantity	NTP	Resolution	Symmetry Factor	Warning
1	Unknown	9	9.070	4706828	591021	68.734	69.396	N/A	33228	2.102	1.464	
2	Unknown	9	9.500	2141035	260642	31.266	30.604	N/A	32369	N/A	1.450	

Figure 3.16. SFC trace of 3.91.

3.9 Spectra Relevant to Chapter Three:

Catalyst-Controlled Annulations of Strained Cyclic Allenes with π -Allylpalladium Complexes

Dominick C. Witkowski, Matthew S. McVeigh, Georgia M. Scherer, Sarah M. Anthony, and

Neil K. Garg

J. Am. Chem. Soc. **2023**, *145*, 10491–10496.

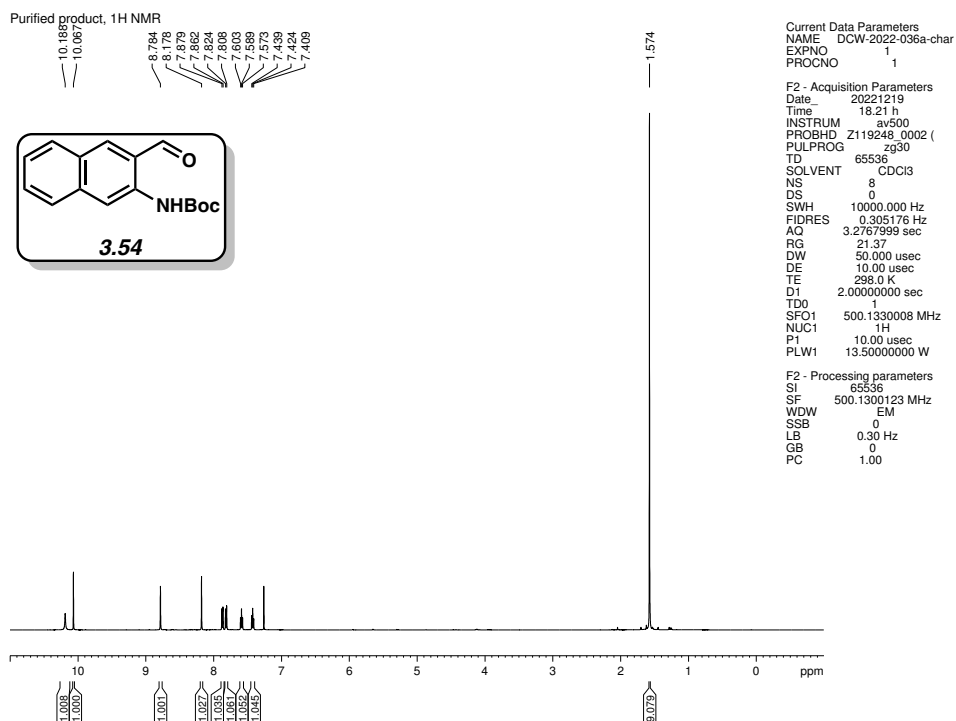


Figure 3.17. ¹H NMR (500 MHz, CDCl₃) of compound **3.54**.

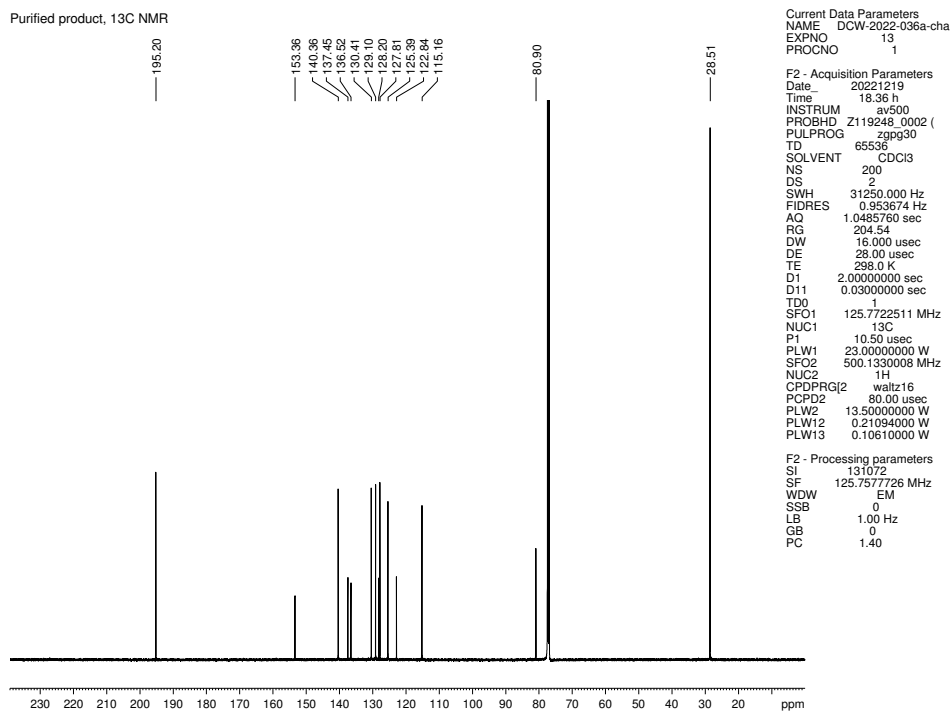


Figure 3.18. ¹³C NMR (125 MHz, CDCl₃) of compound **3.54**.

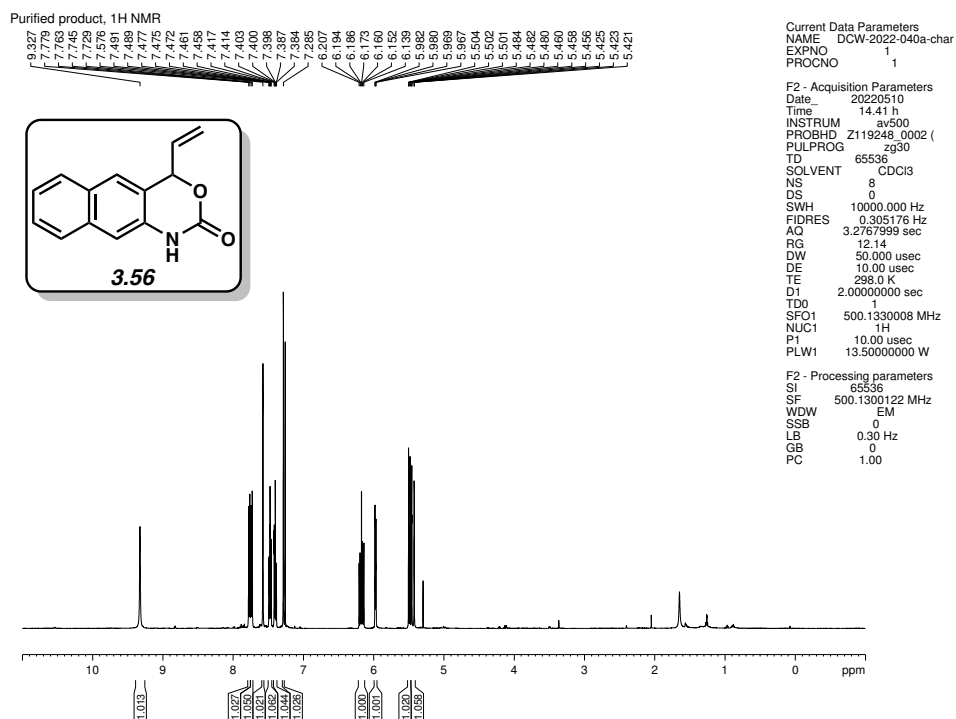


Figure 3.19. ¹H NMR (500 MHz, CDCl₃) of compound 3.56.

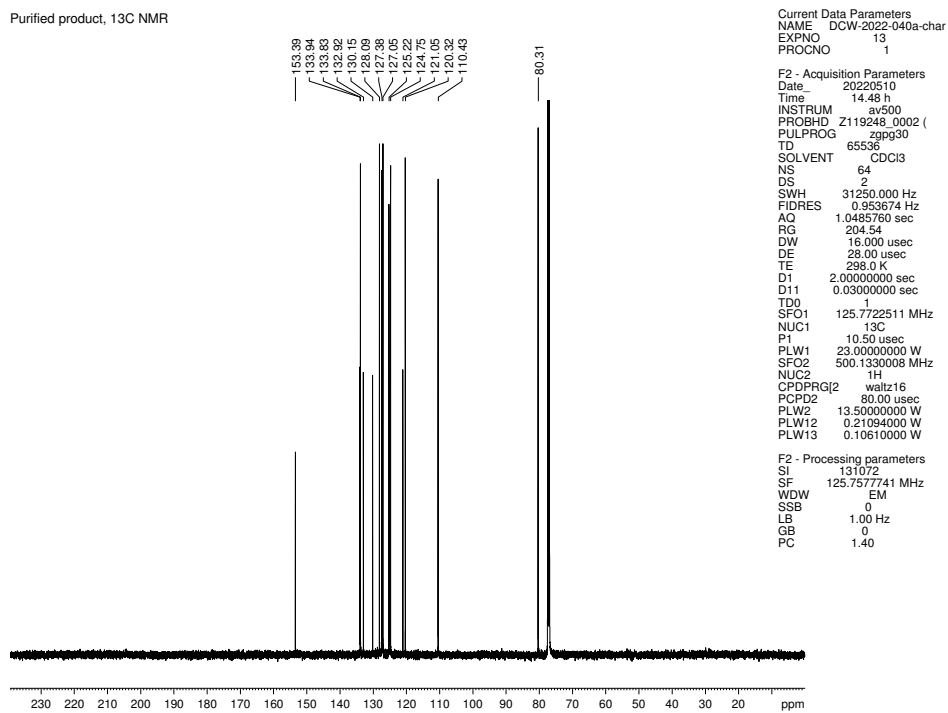


Figure 3.20. ¹³C NMR (125 MHz, CDCl₃) of compound 3.56.

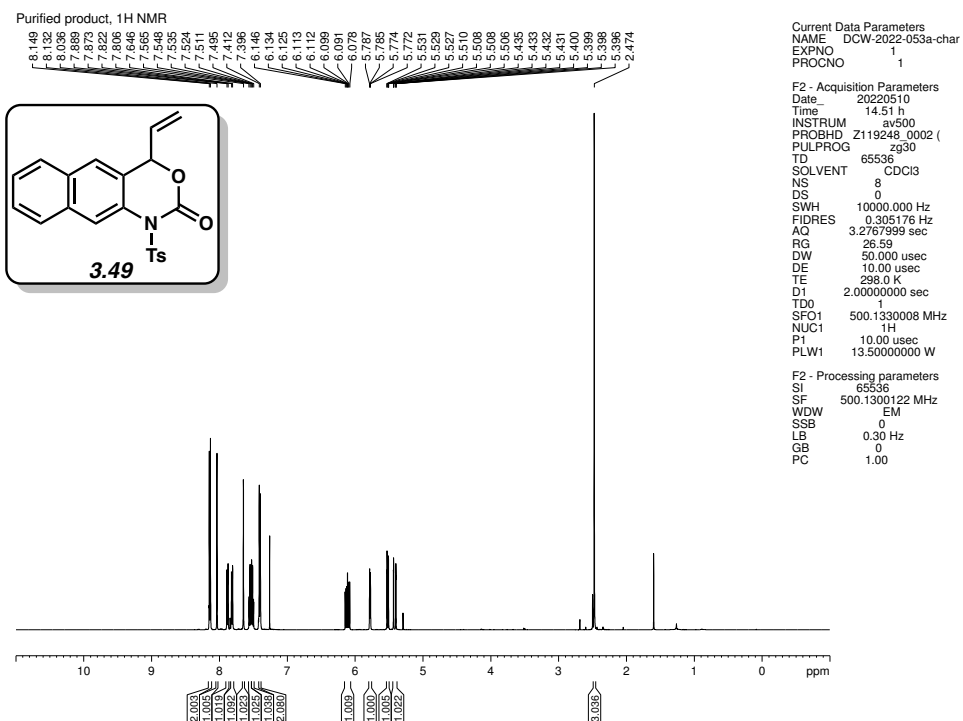


Figure 3.21. ¹H NMR (500 MHz, CDCl₃) of compound 3.49.

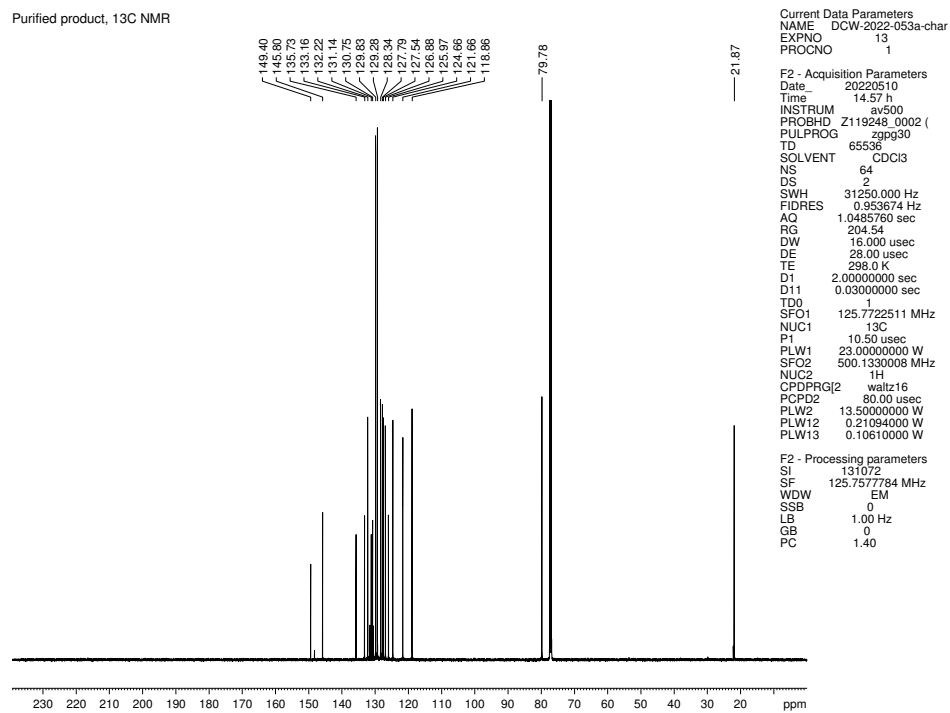


Figure 3.22. ¹³C NMR (125 MHz, CDCl₃) of compound 3.49.

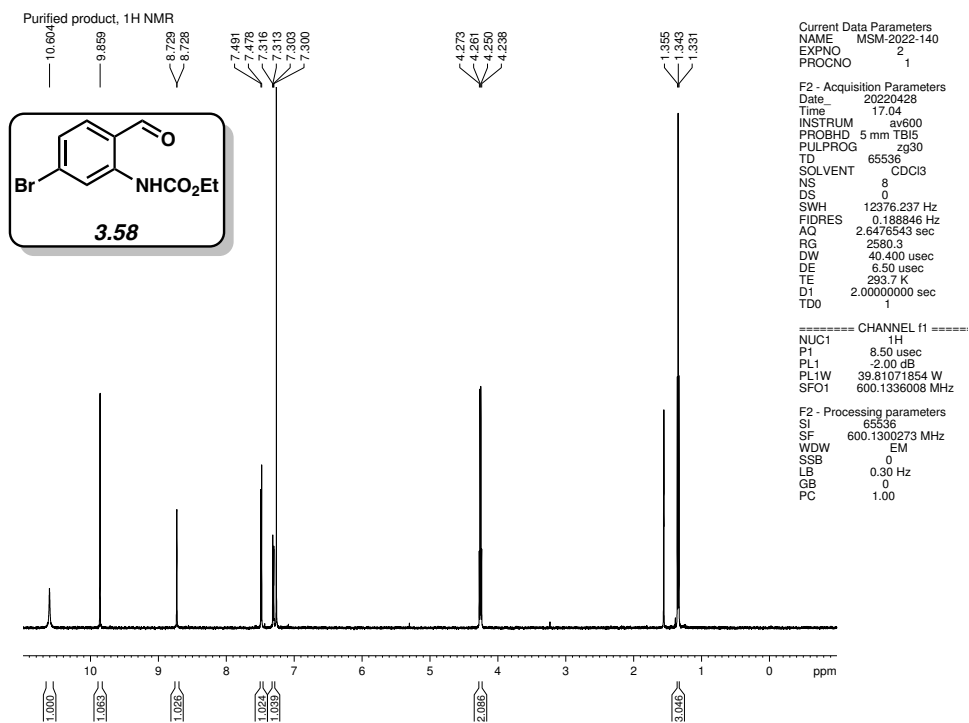


Figure 3.23. ¹H NMR (600 MHz, CDCl₃) of compound 3.58.

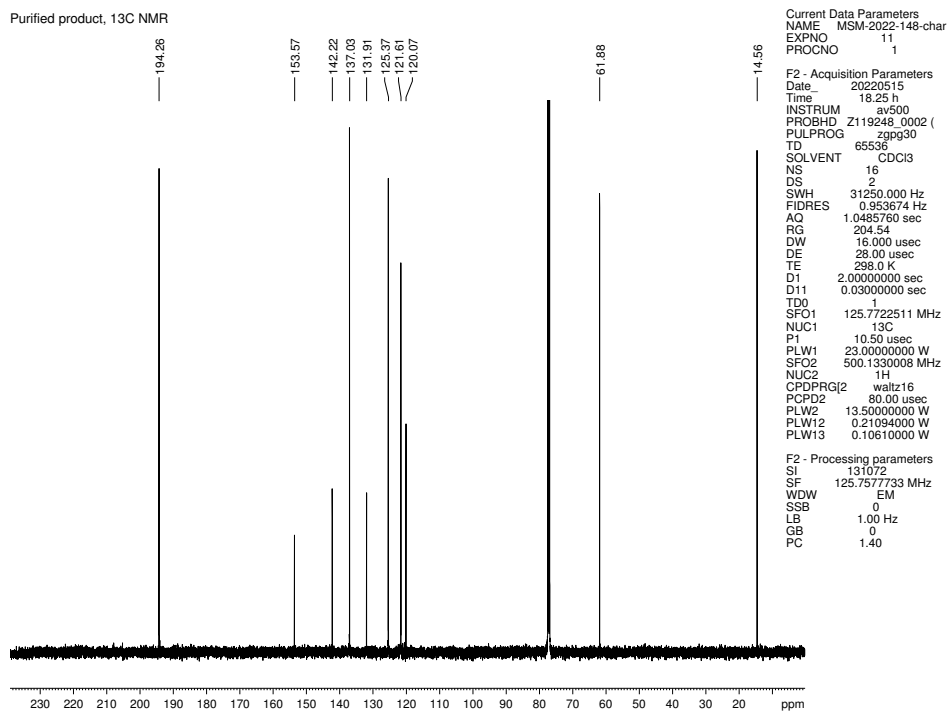


Figure 3.24. ¹³C NMR (125 MHz, CDCl₃) of compound 3.58.

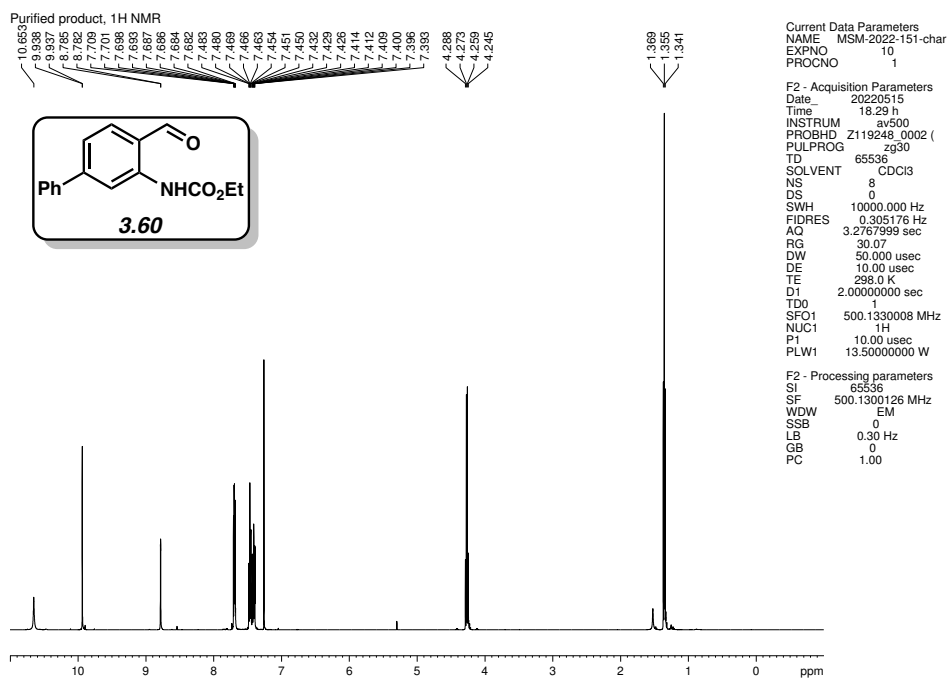


Figure 3.25. ¹H NMR (500 MHz, CDCl₃) of compound 3.60.

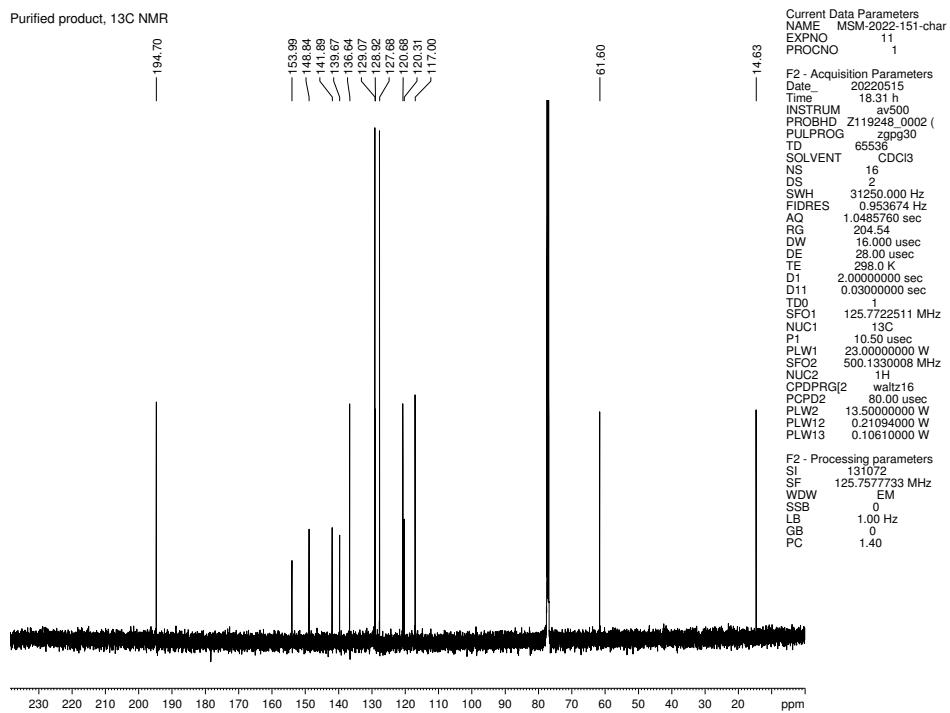


Figure 3.26. ¹³C NMR (125 MHz, CDCl₃) of compound 3.60.

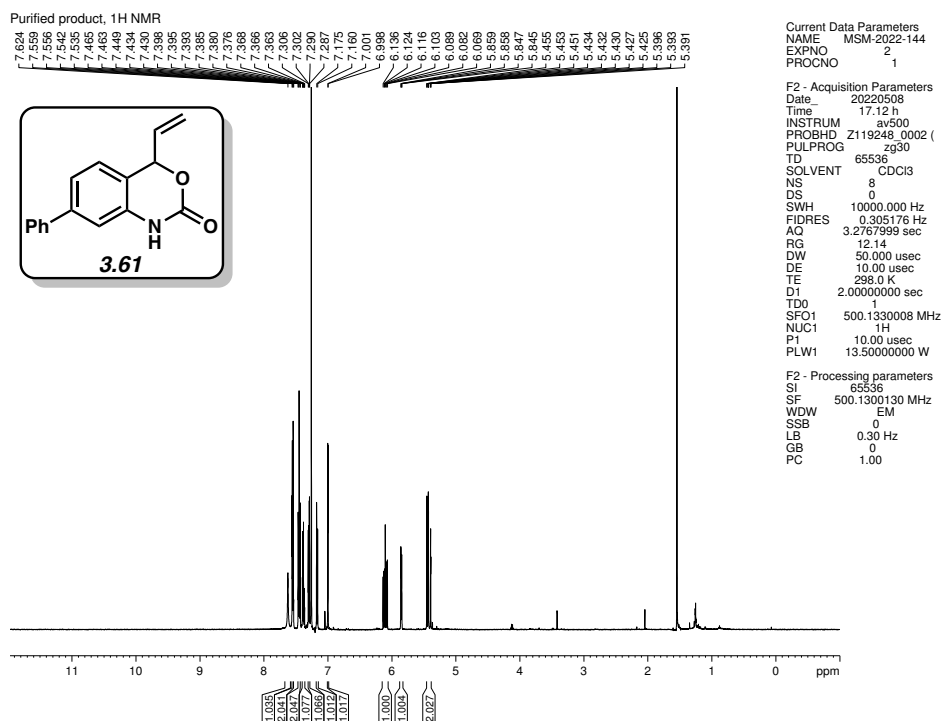


Figure 3.27. ¹H NMR (500 MHz, CDCl₃) of compound 3.61.

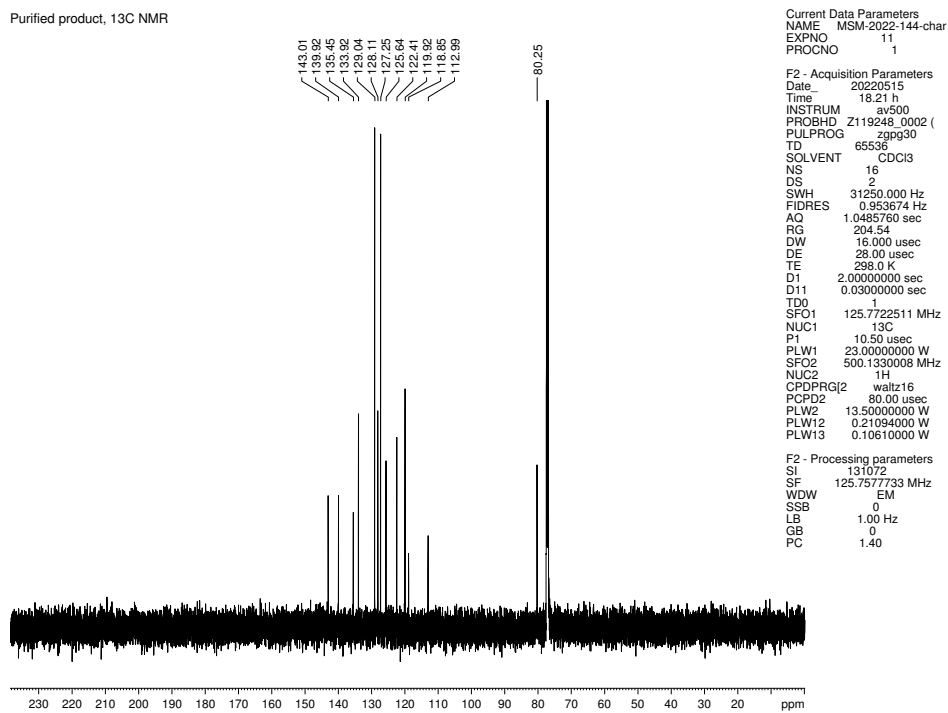


Figure 3.28. ¹³C NMR (125 MHz, CDCl₃) of compound 3.61.

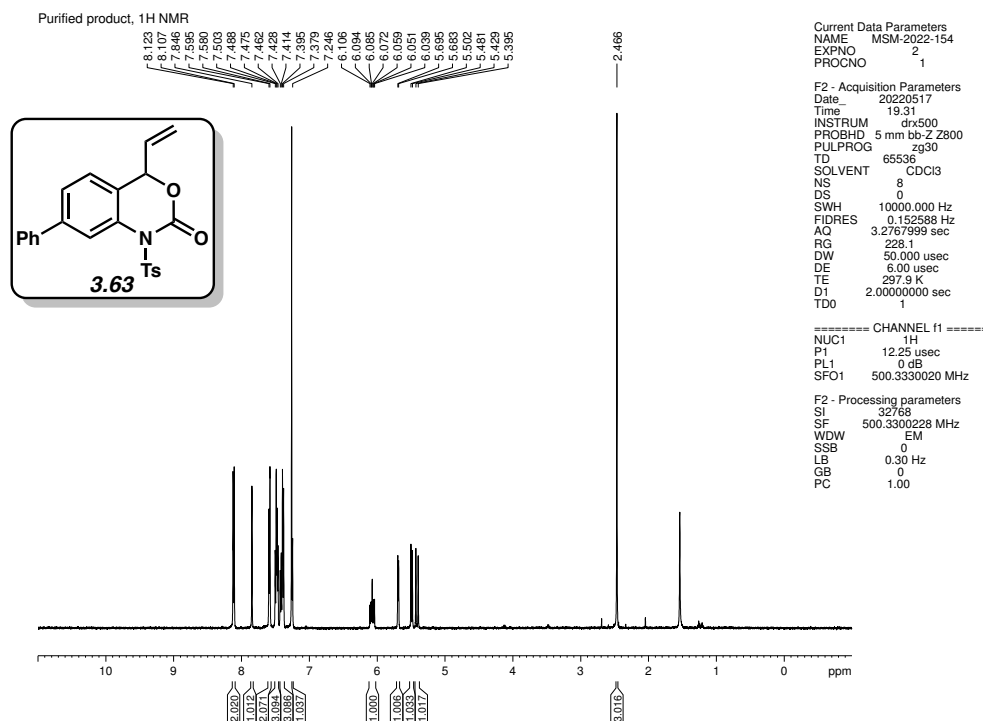


Figure 3.29. ¹H NMR (500 MHz, CDCl₃) of compound 3.63.

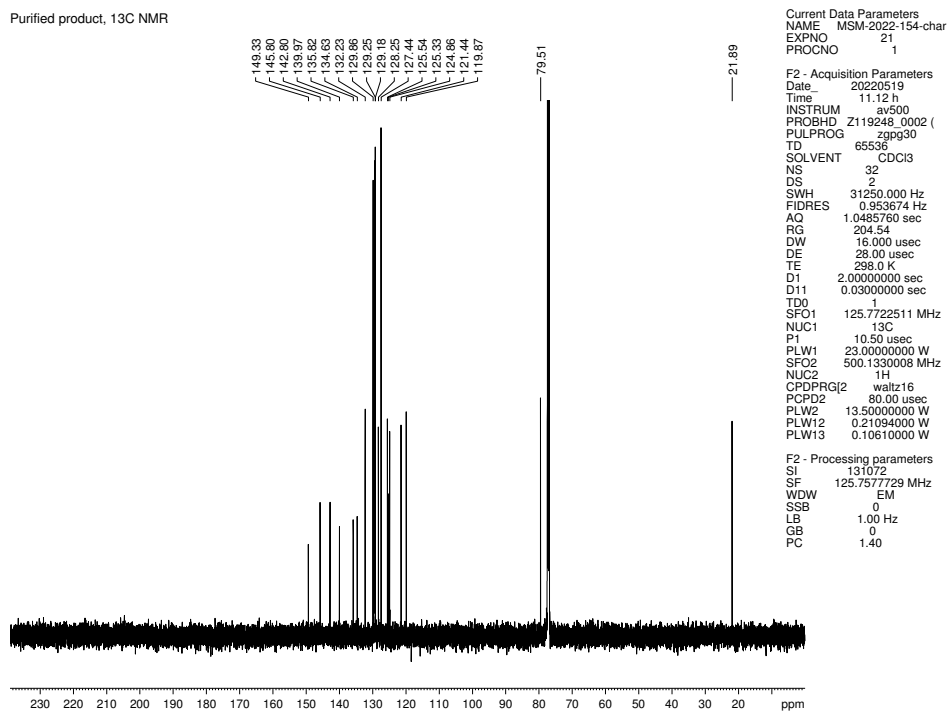


Figure 3.30. ¹³C NMR (125 MHz, CDCl₃) of compound 3.63.

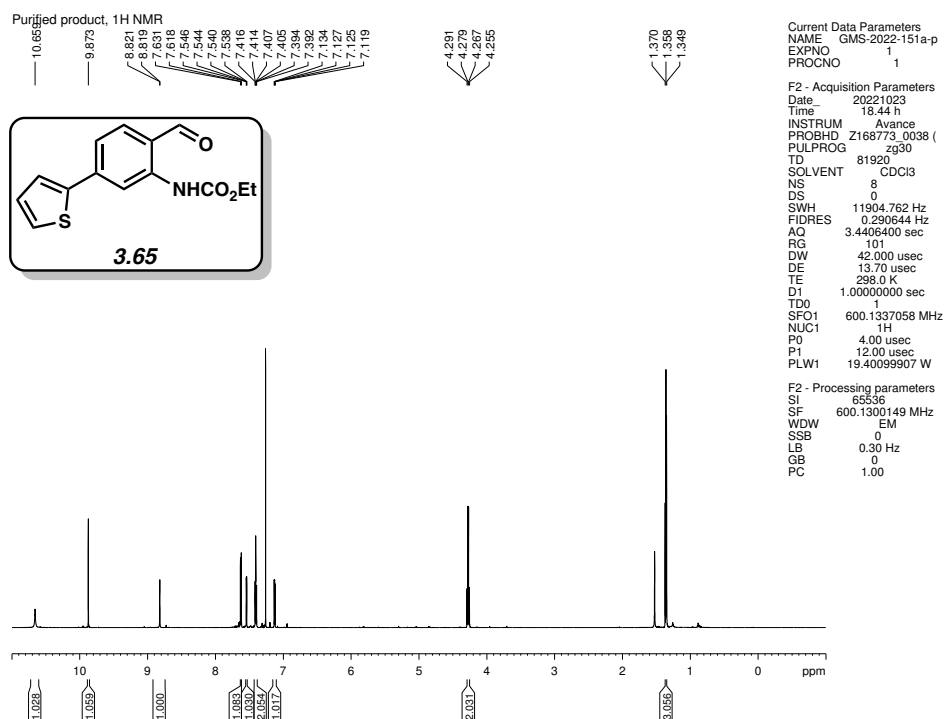


Figure 3.31. ¹H NMR (600 MHz, CDCl₃) of compound 3.65.

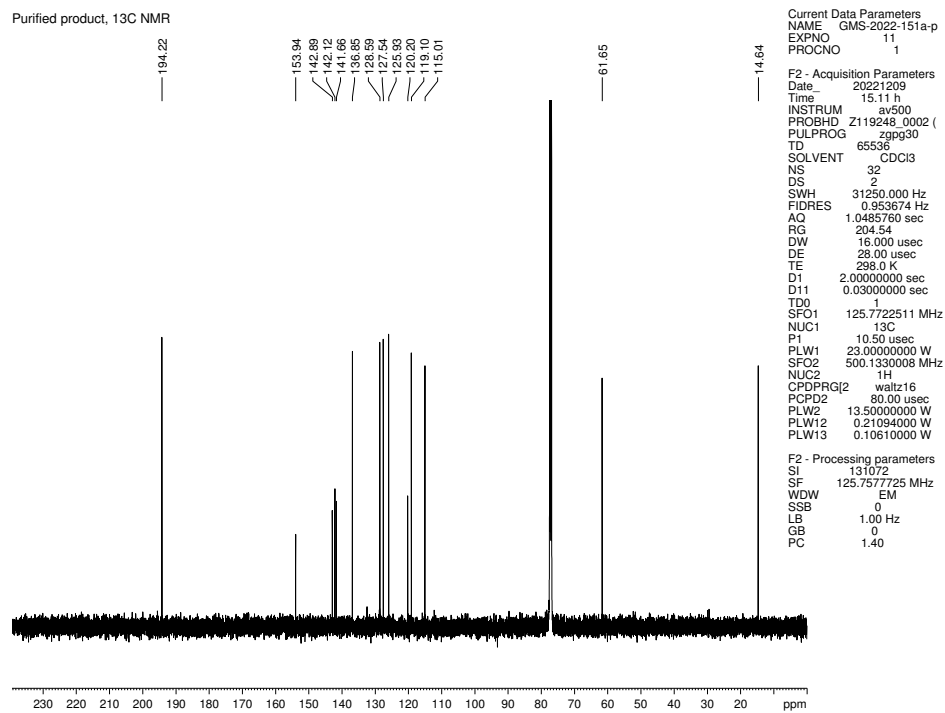


Figure 3.32. ¹³C NMR (125 MHz, CDCl₃) of compound 3.65.

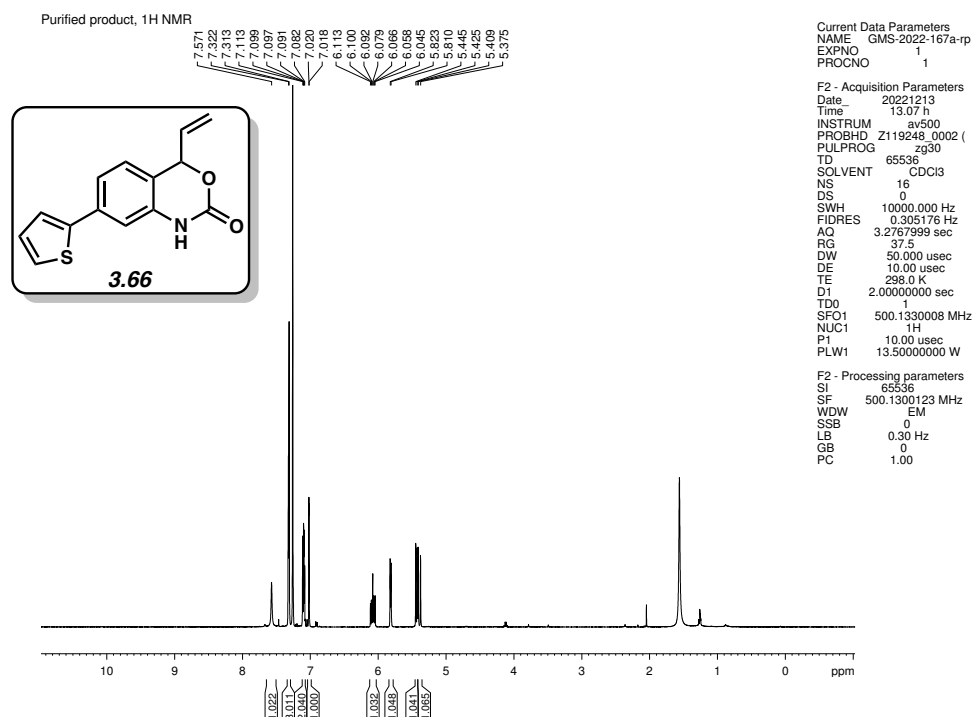


Figure 3.33. ¹H NMR (500 MHz, CDCl₃) of compound 3.66.

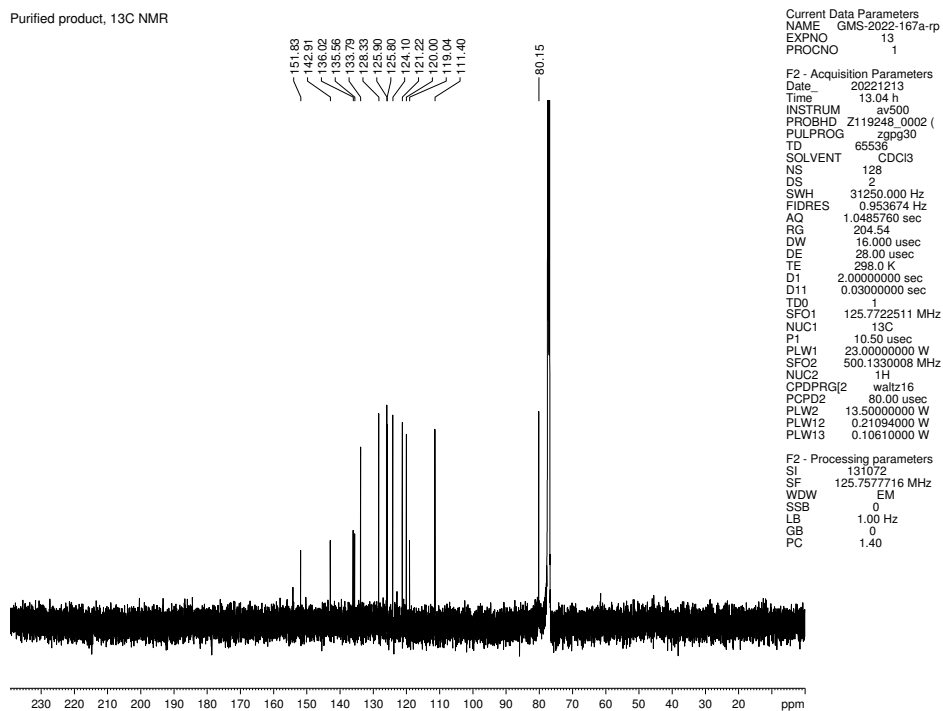


Figure 3.34. ¹³C NMR (125 MHz, CDCl₃) of compound 3.66.

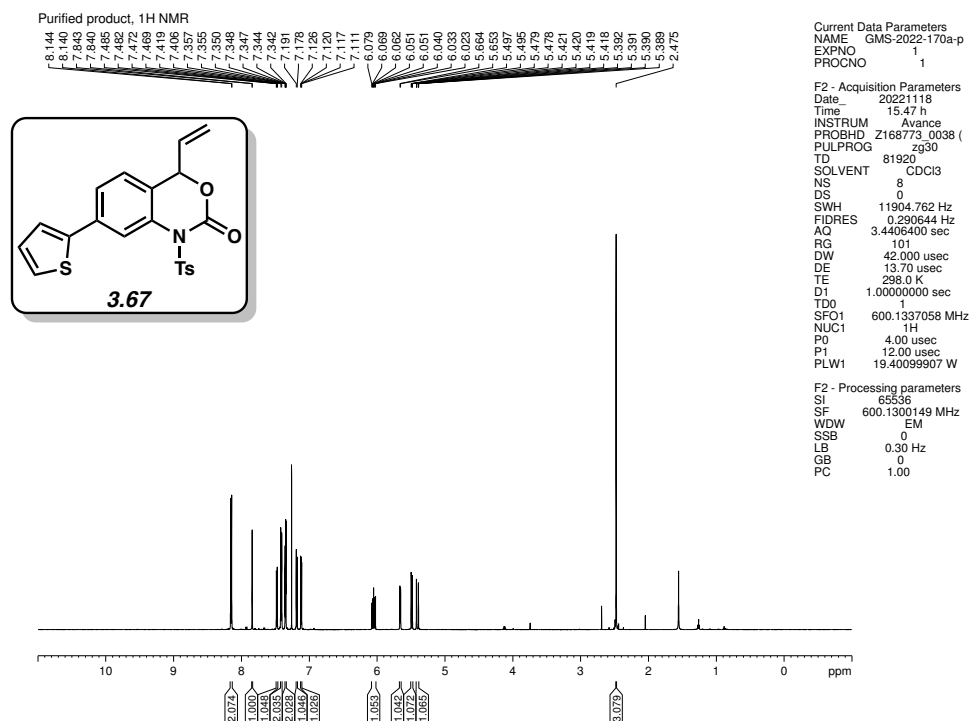


Figure 3.35. ¹H NMR (600 MHz, CDCl₃) of compound 3.67.

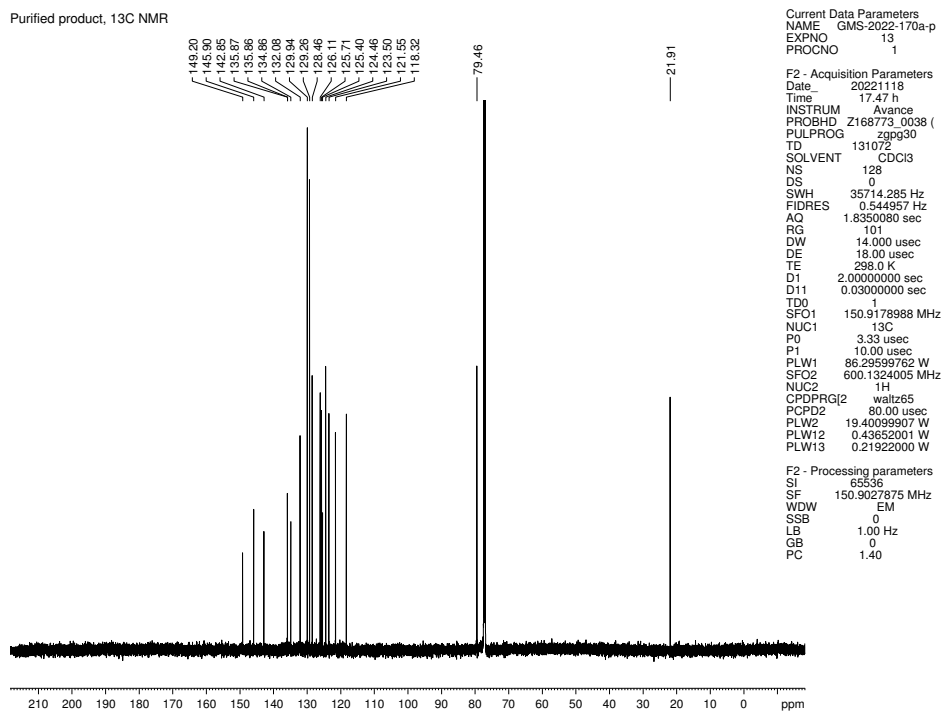


Figure 3.36. ¹³C NMR (150 MHz, CDCl₃) of compound 3.67.

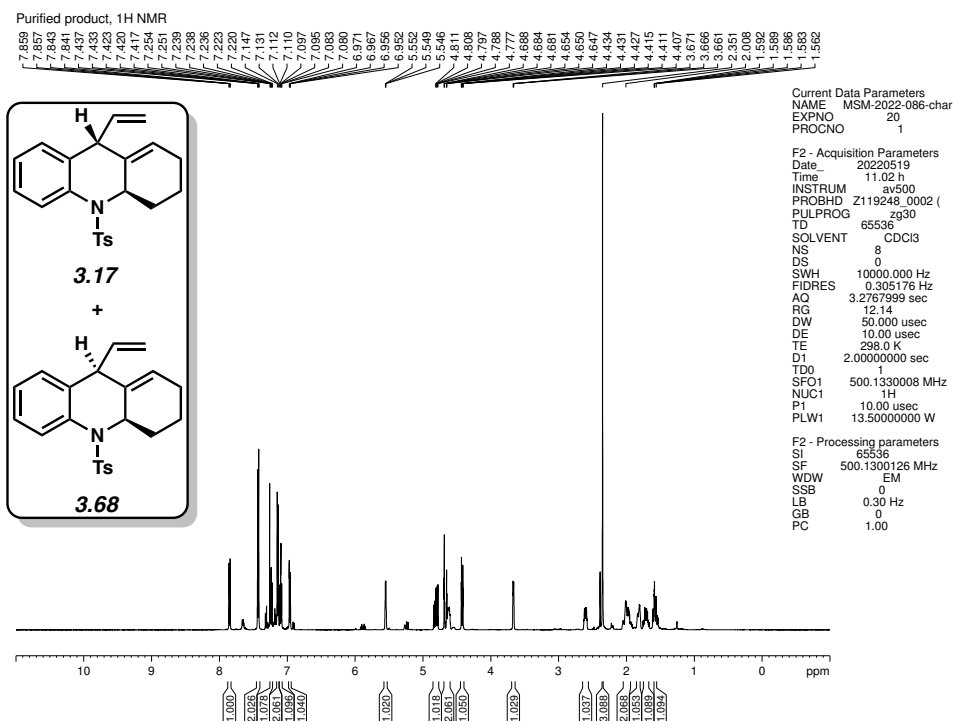


Figure 3.37. ¹H NMR (500 MHz, CDCl₃) of compounds **3.17** and **3.68**.

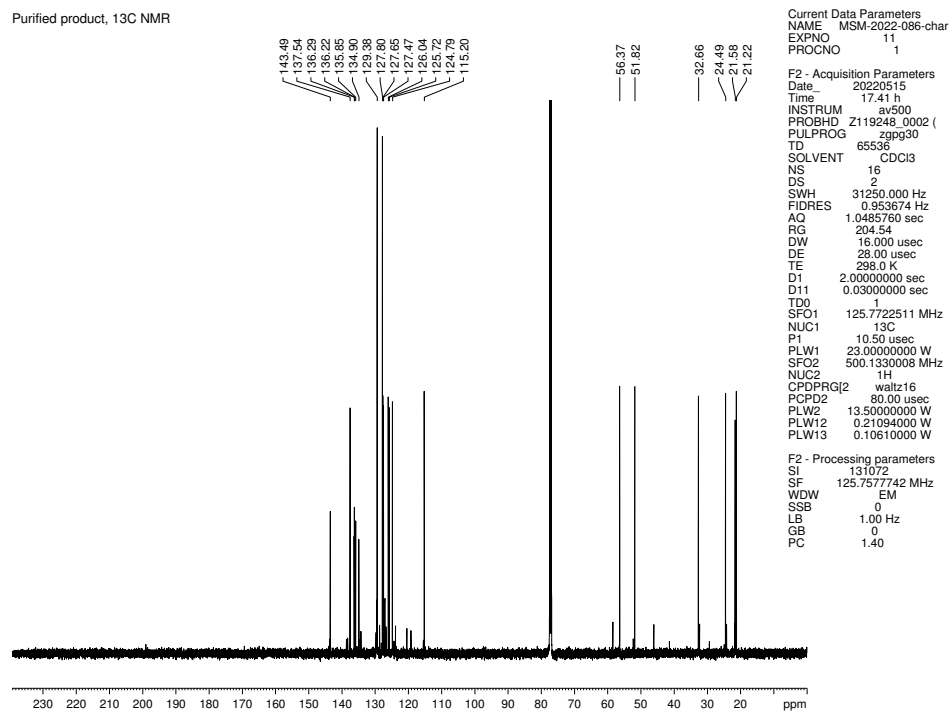


Figure 3.38. ¹³C NMR (125 MHz, CDCl₃) of compounds **3.17** and **3.68**.

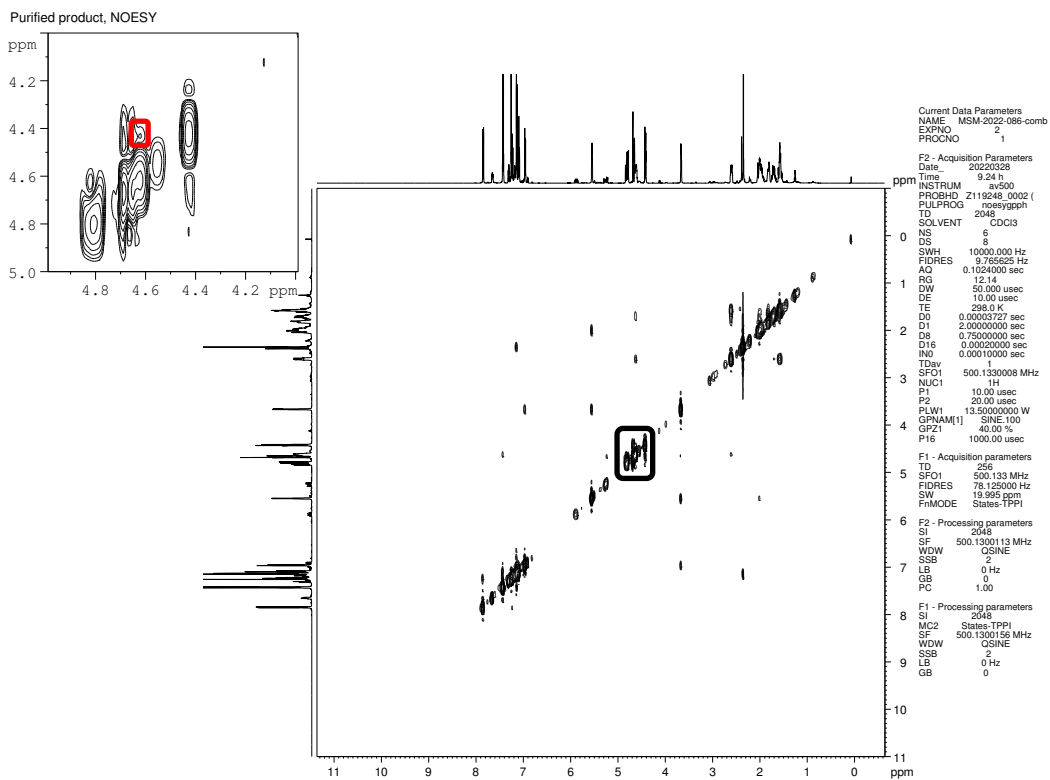
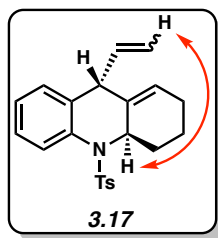


Figure 3.39. NOESY (500 MHz, CDCl₃) of compound **3.17**.

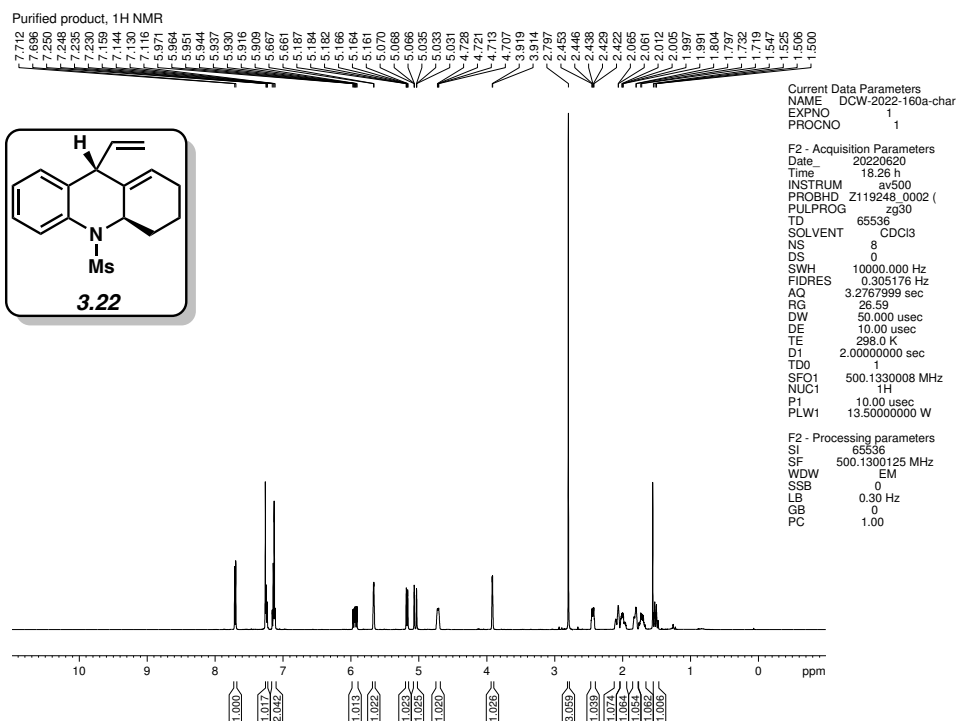


Figure 3.40. ¹H NMR (500 MHz, CDCl₃) of compound 3.22.

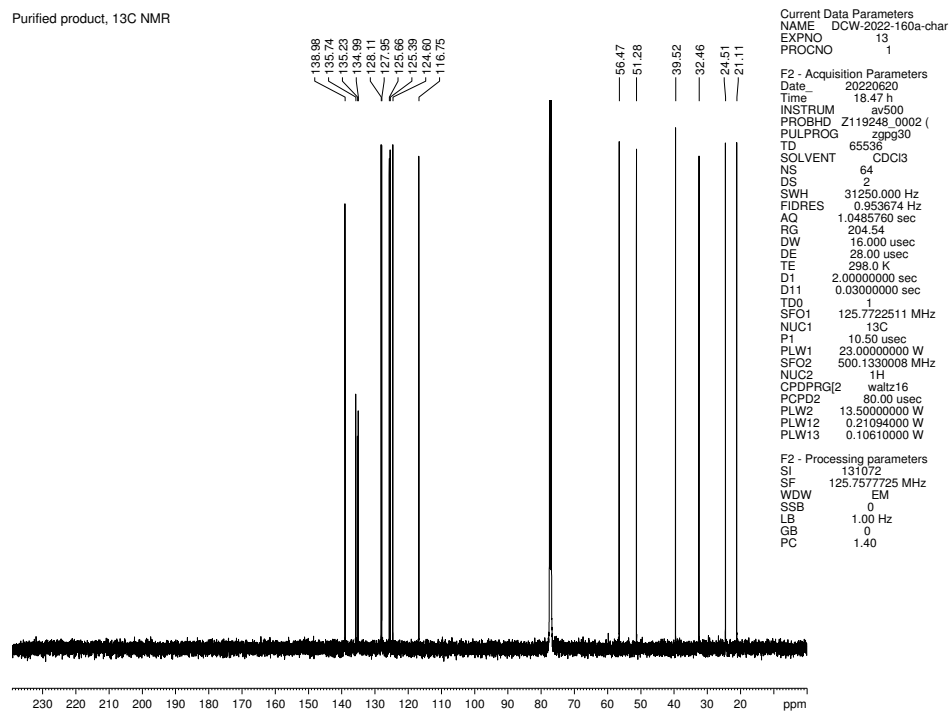


Figure 3.41. ¹³C NMR (125 MHz, CDCl₃) of compound 3.22.

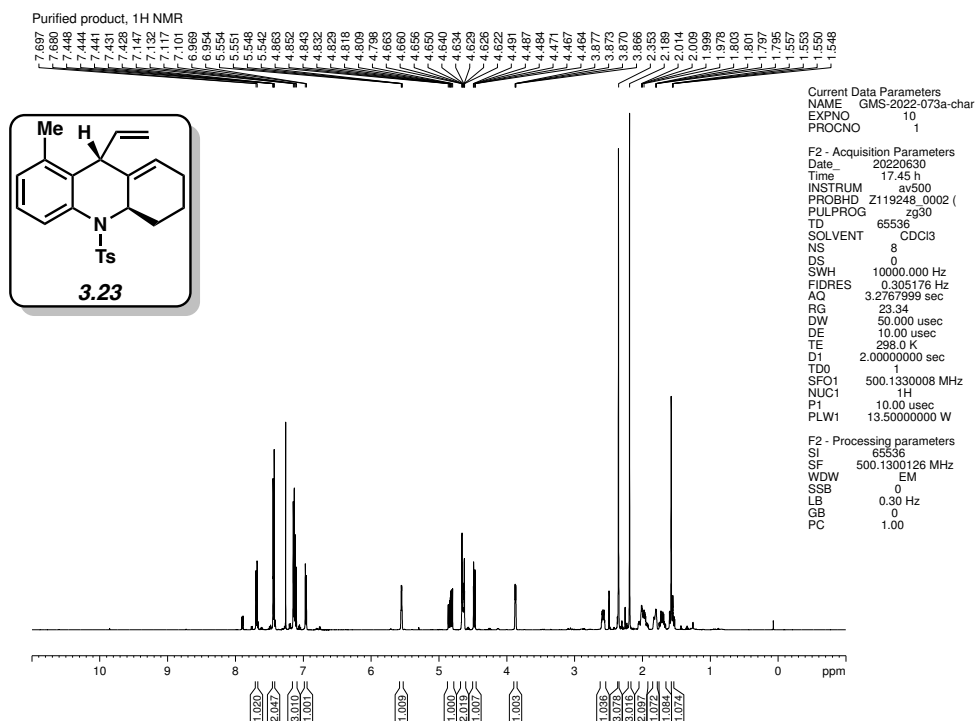


Figure 3.42. ¹H NMR (500 MHz, CDCl₃) of compound 3.23.

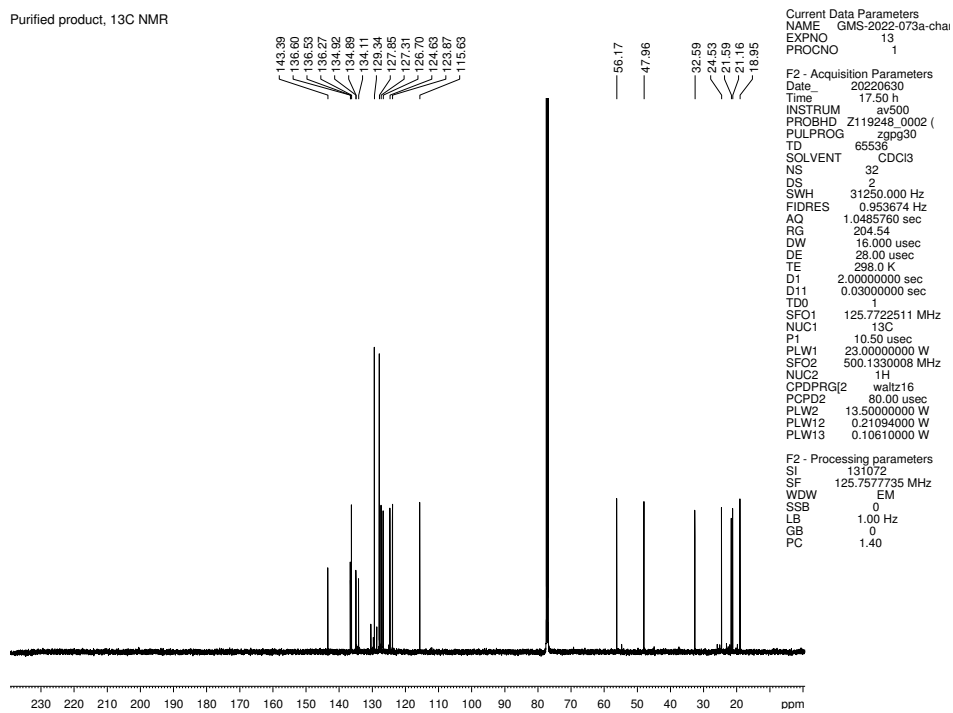


Figure 3.43. ¹³C NMR (125 MHz, CDCl₃) of compound 3.23.

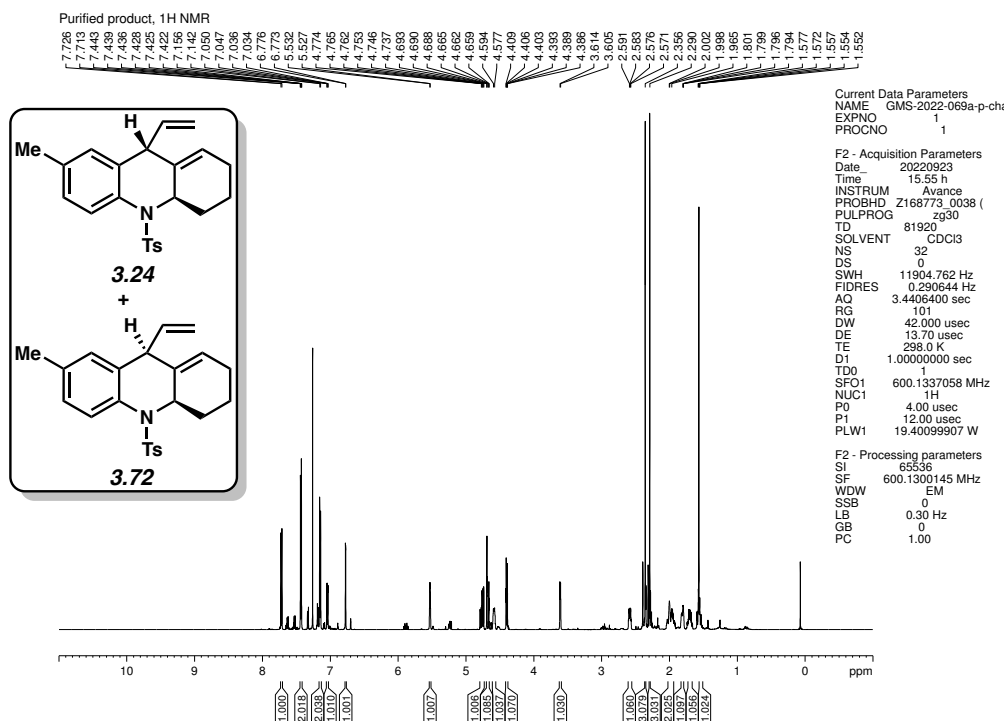


Figure 3.44. ¹H NMR (600 MHz, CDCl₃) of compounds 3.24 and 3.72.

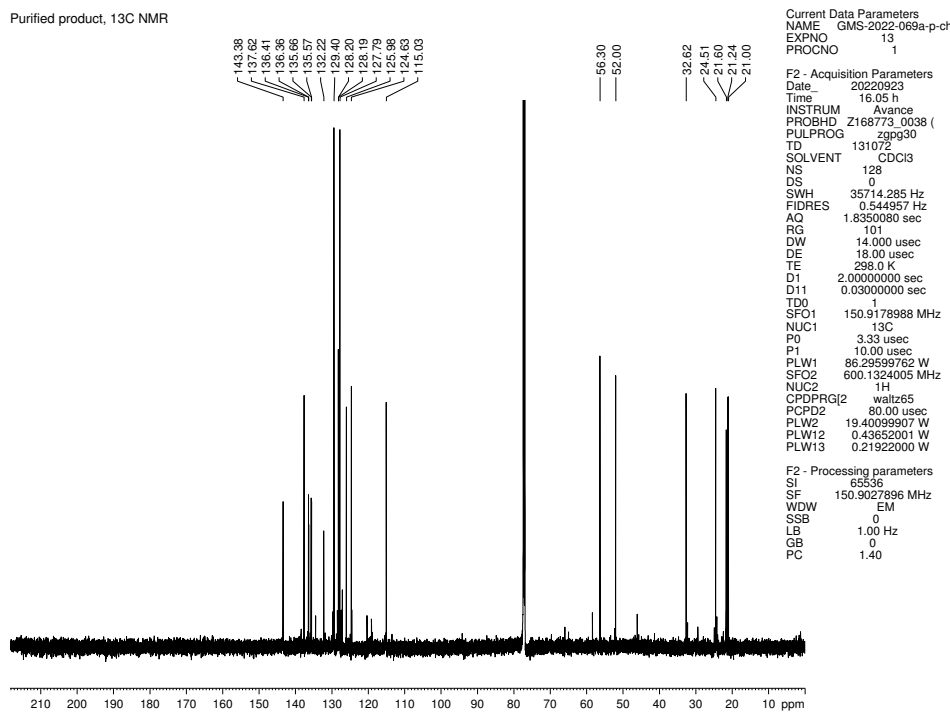
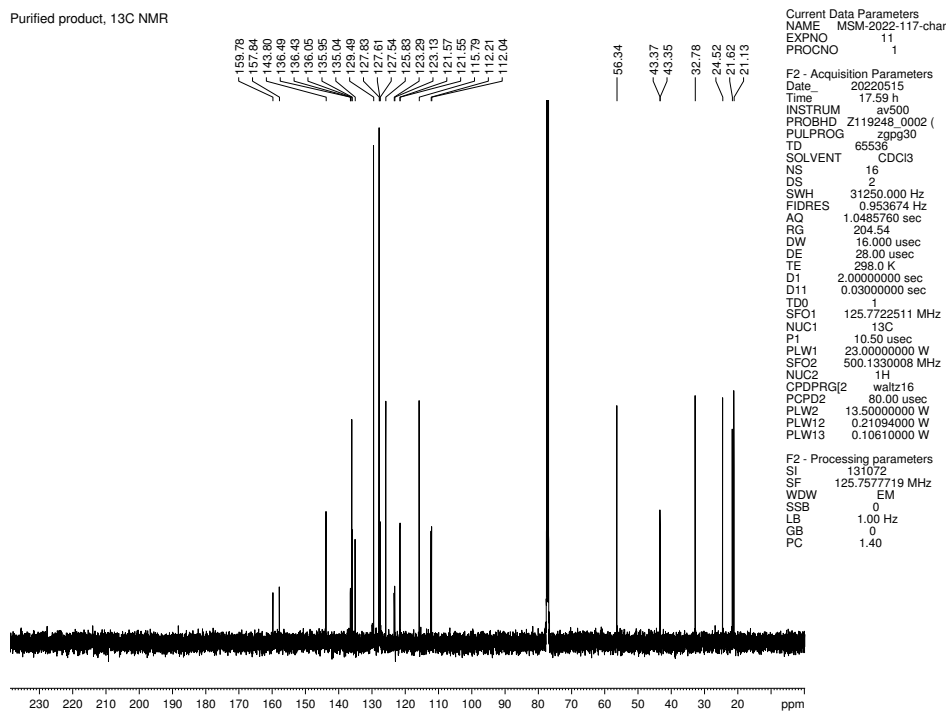
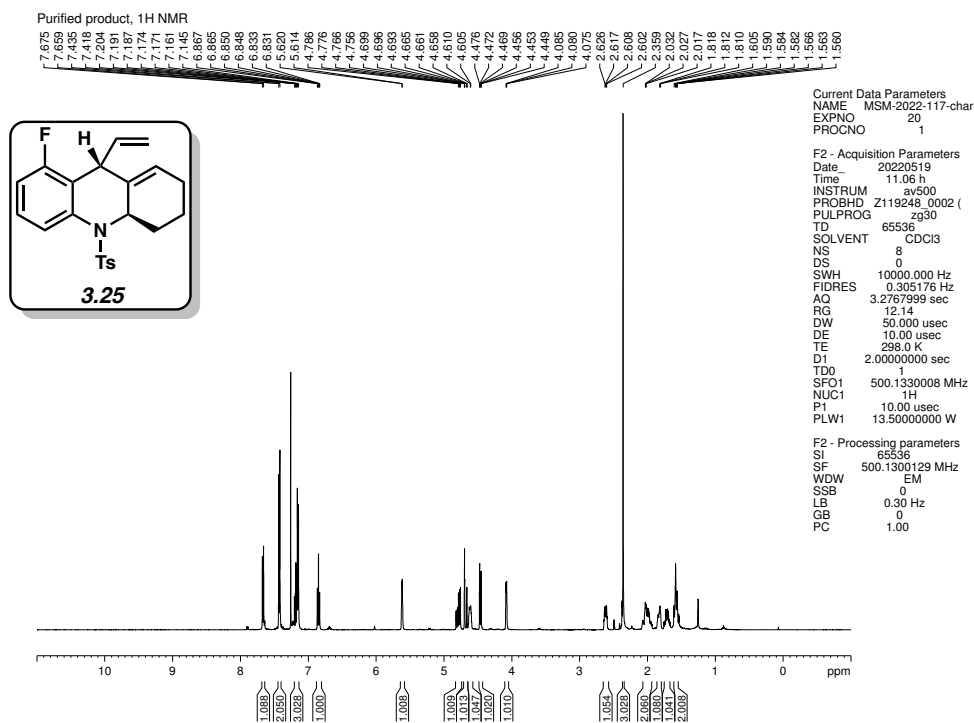


Figure 3.45. ¹³C NMR (150 MHz, CDCl₃) of compounds 3.24 and 3.72.



Purified product, ^{19}F NMR

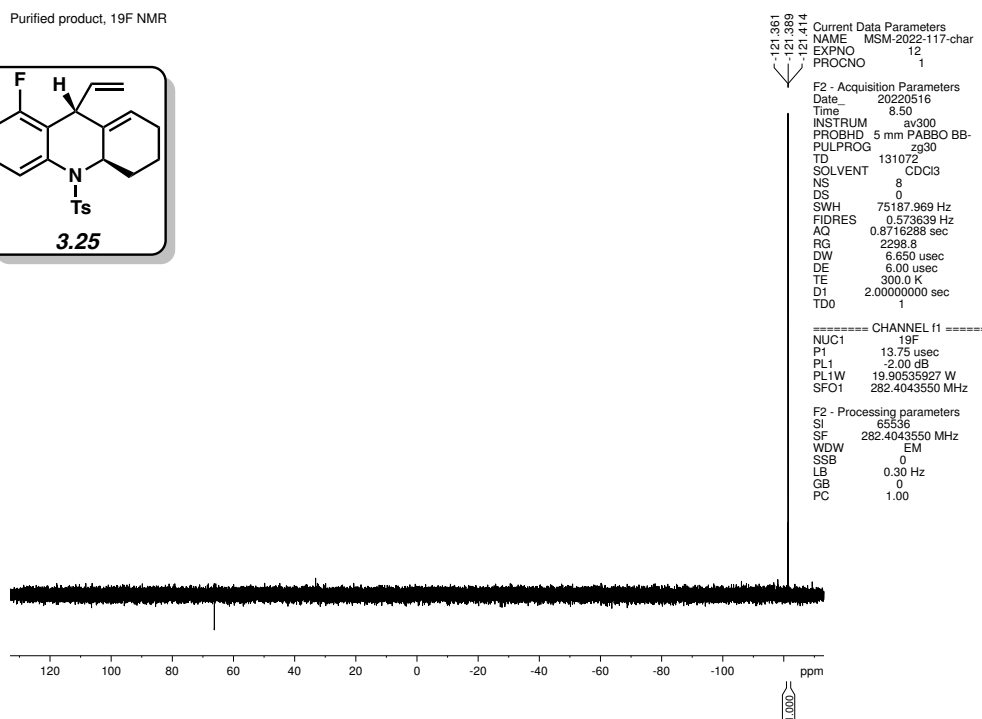
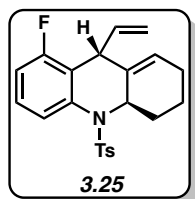


Figure 3.48. ^{19}F NMR (282 MHz, CDCl_3) of compound 3.25.

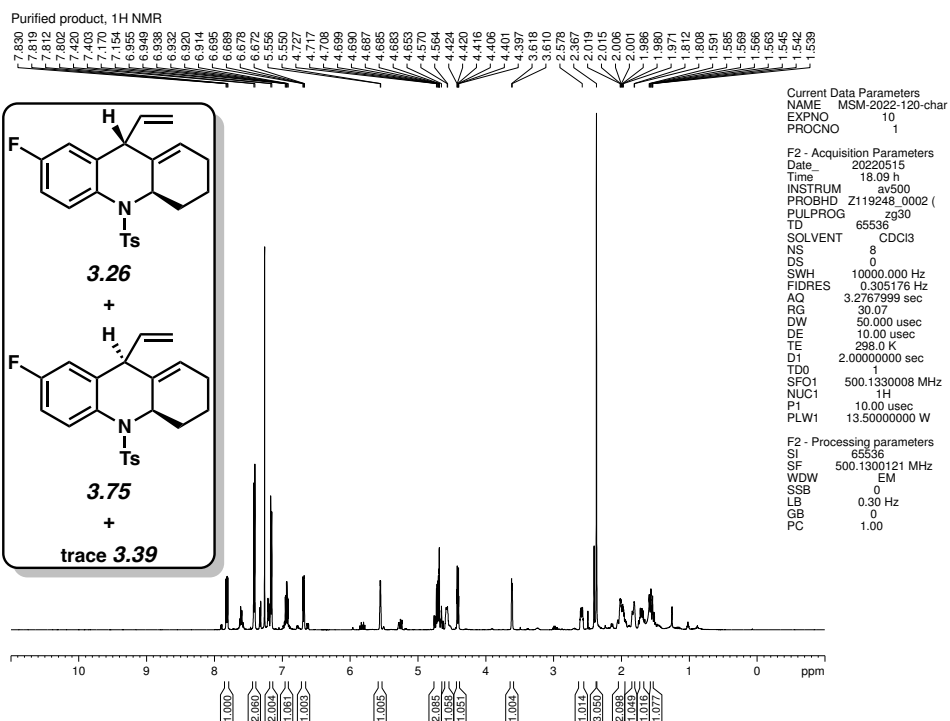


Figure 3.49. ¹H NMR (500 MHz, CDCl₃) of compounds 3.26, 3.75, and 3.39 (trace).

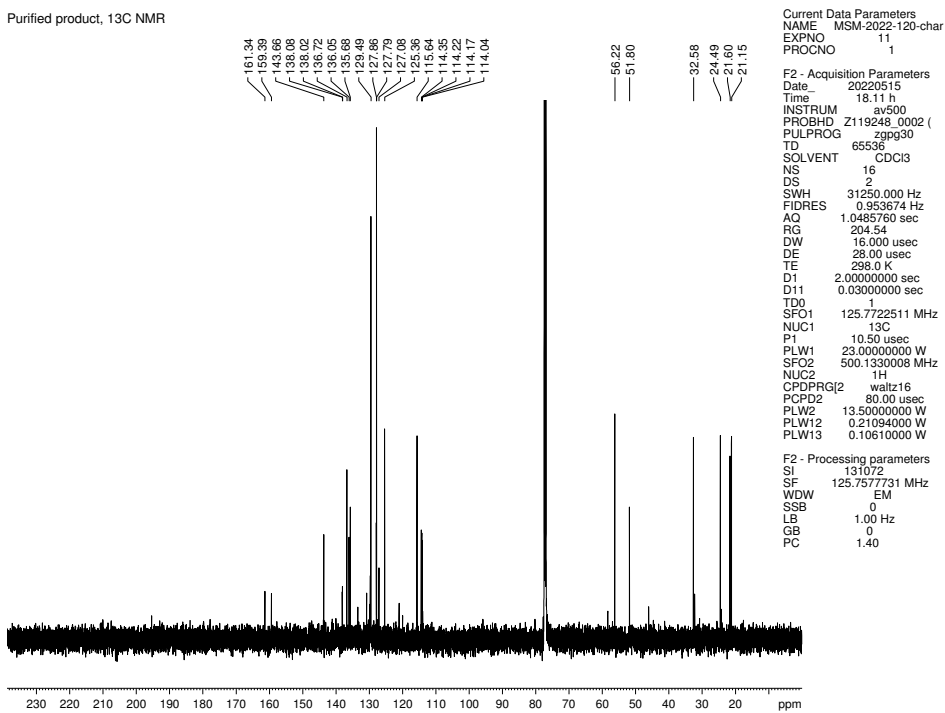
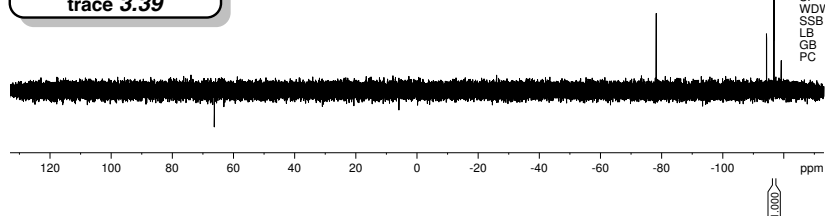
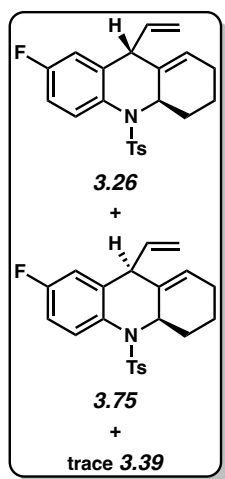


Figure 3.50. ¹³C NMR (125 MHz, CDCl₃) of compounds 3.26, 3.75, and 3.39 (trace).

Purified product, ^{19}F NMR



-116.748
-116.778
-116.798
-116.798
-116.808
-116.825

Current Data Parameters
NAME MSM-2022-120-char
EXPNO 30
PROCNO 1

F2 - Acquisition Parameters
Date_ 20220516
Time 8.59
INSTRUM av300
PROBHD 5 mm PABBO BB-
PULPROG zg30
TD 131072
SOLVENT CDCl3
NS 8
DS 0
SWH 75187.969 Hz
FIDRES 0.573639 Hz
AQ 0.8716288 sec
RG 2298.8
DW 6.650 usec
DE 6.00 usec
TE 300.0 K
D1 2.00000000 sec
TD0 1

===== CHANNEL f1 =====
NUC1 ^{19}F
P1 13.75 usec
PL1 -2.00 dB
PL1W 19.90535927 W
SFO1 282.4043550 MHz

F2 - Processing parameters
SI 65536
SF 282.4043550 MHz
WDW EM
SSB 0
LB 0.30 Hz
GB 0
PC 1.00

Figure 3.51. ^{19}F NMR (282 MHz, CDCl_3) of compounds **3.26**, **3.75**, and **3.39** (trace).

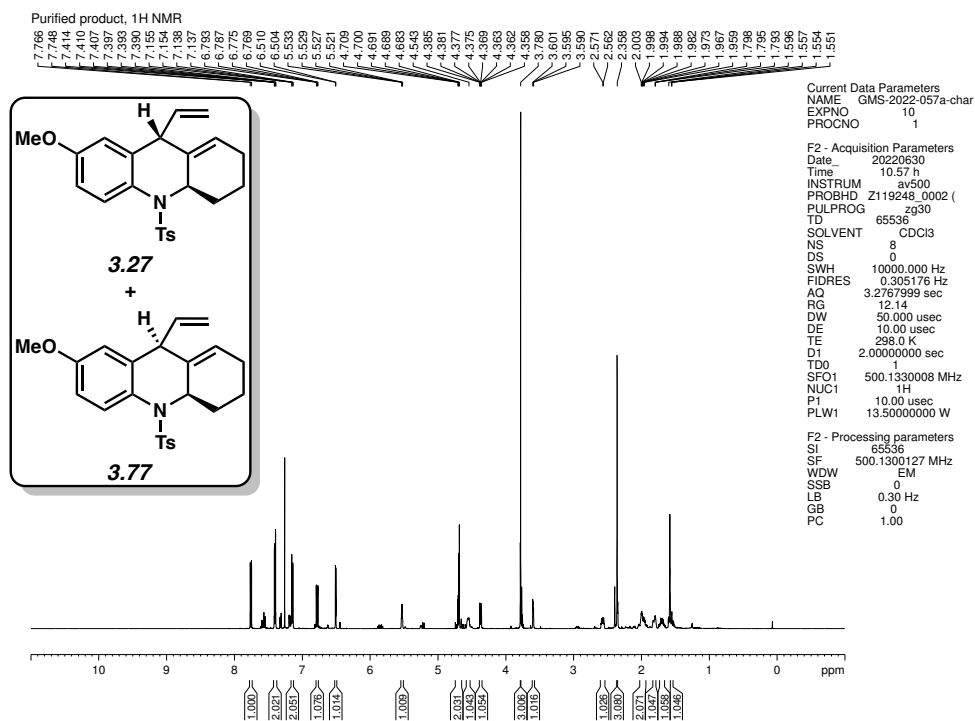


Figure 3.52. ¹H NMR (500 MHz, CDCl₃) of compounds 3.27 and 3.77.

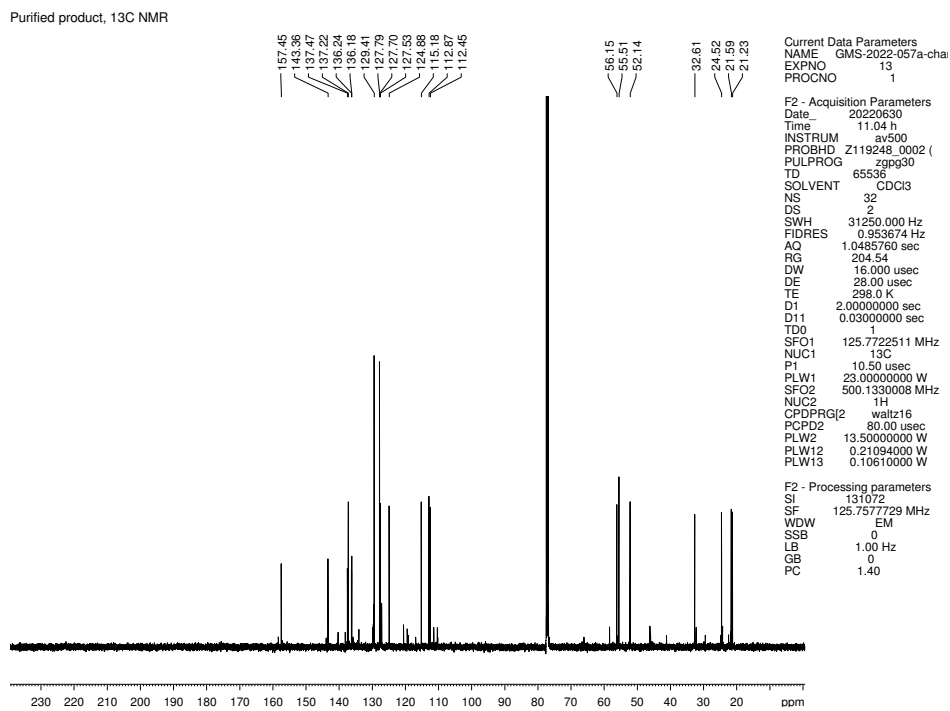


Figure 3.53. ¹³C NMR (125 MHz, CDCl₃) of compounds 3.27 and 3.77.

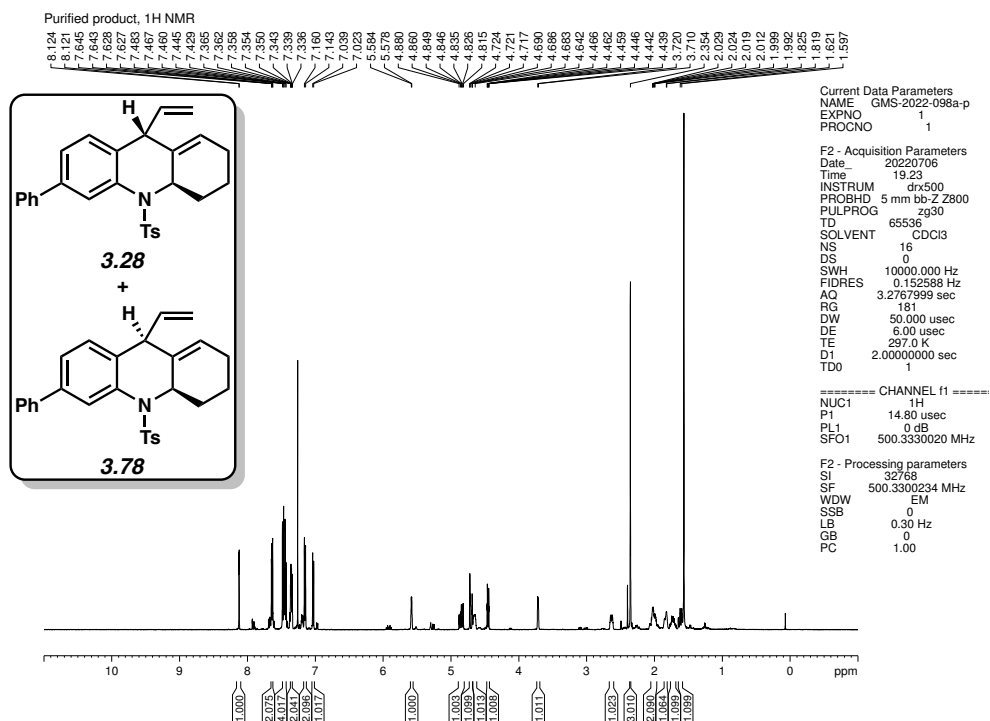


Figure 3.54. ¹H NMR (500 MHz, CDCl₃) of compounds 3.28 and 3.78.

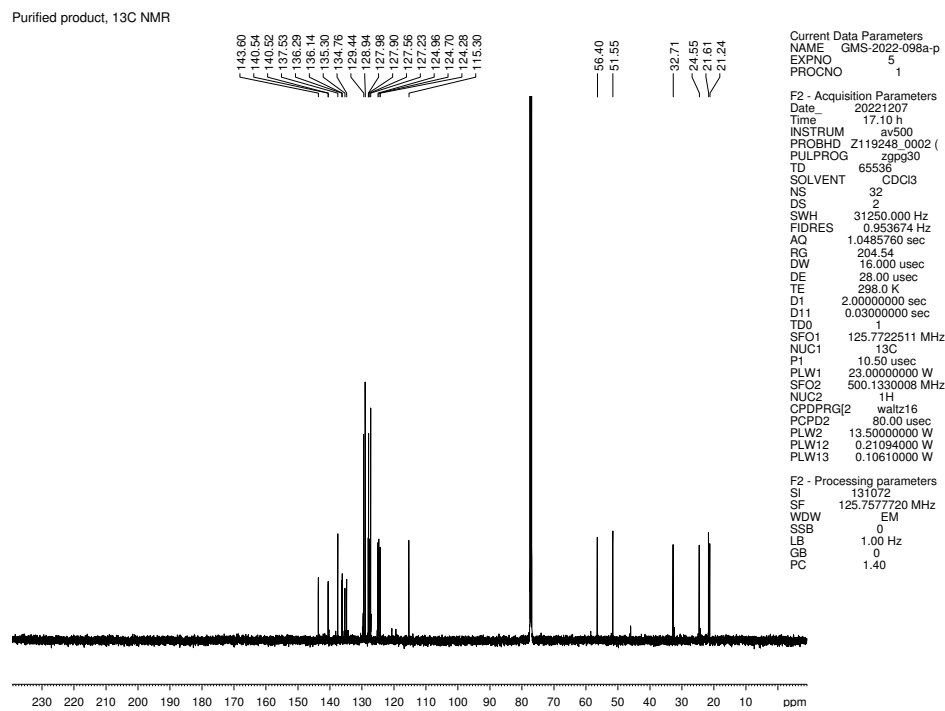


Figure 3.55. ¹³C NMR (125 MHz, CDCl₃) of compounds 3.28 and 3.78.

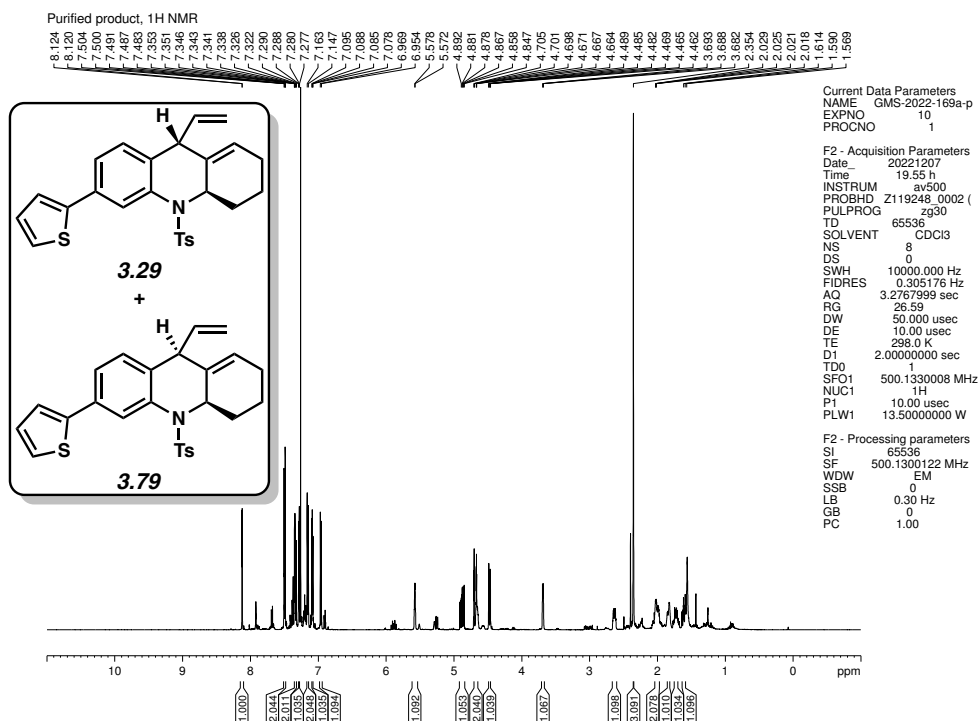


Figure 3.56. ¹H NMR (500 MHz, CDCl₃) of compounds 3.29 and 3.79.

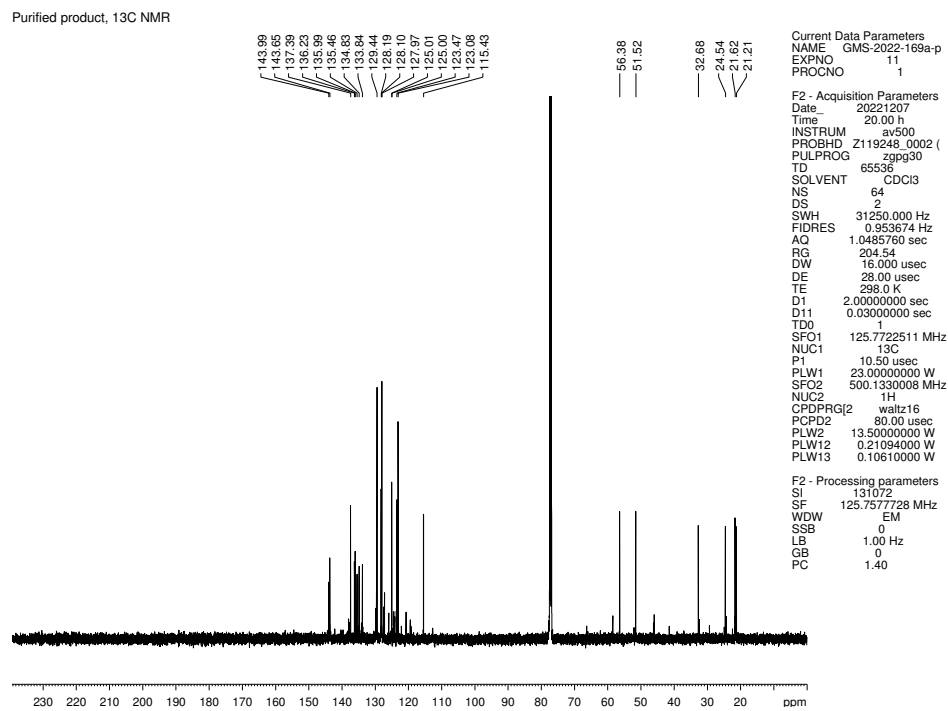


Figure 3.57. ¹³C NMR (125 MHz, CDCl₃) of compounds 3.29 and 3.79.

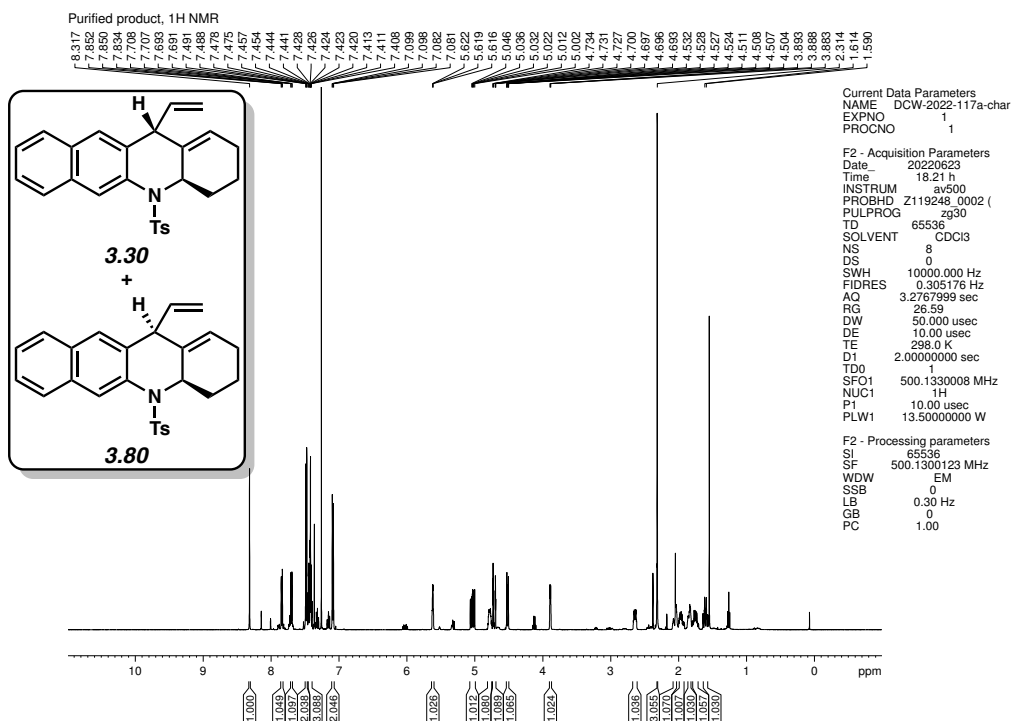


Figure 3.58. ¹H NMR (500 MHz, CDCl₃) of compounds 3.30 and 3.80.

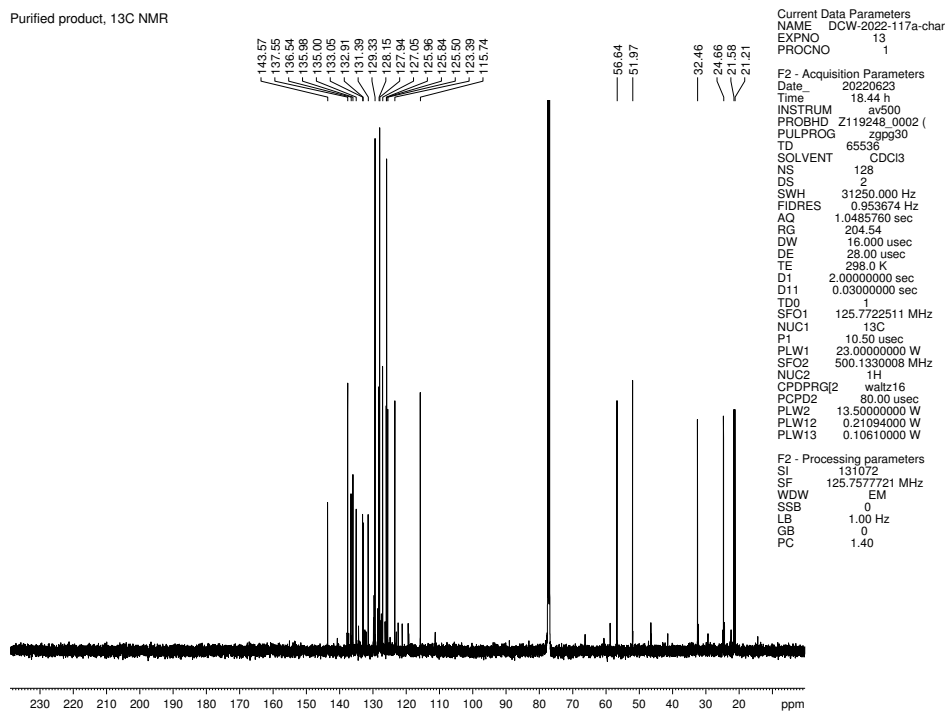


Figure 3.59. ¹³C NMR (125 MHz, CDCl₃) of compounds 3.30 and 3.80.

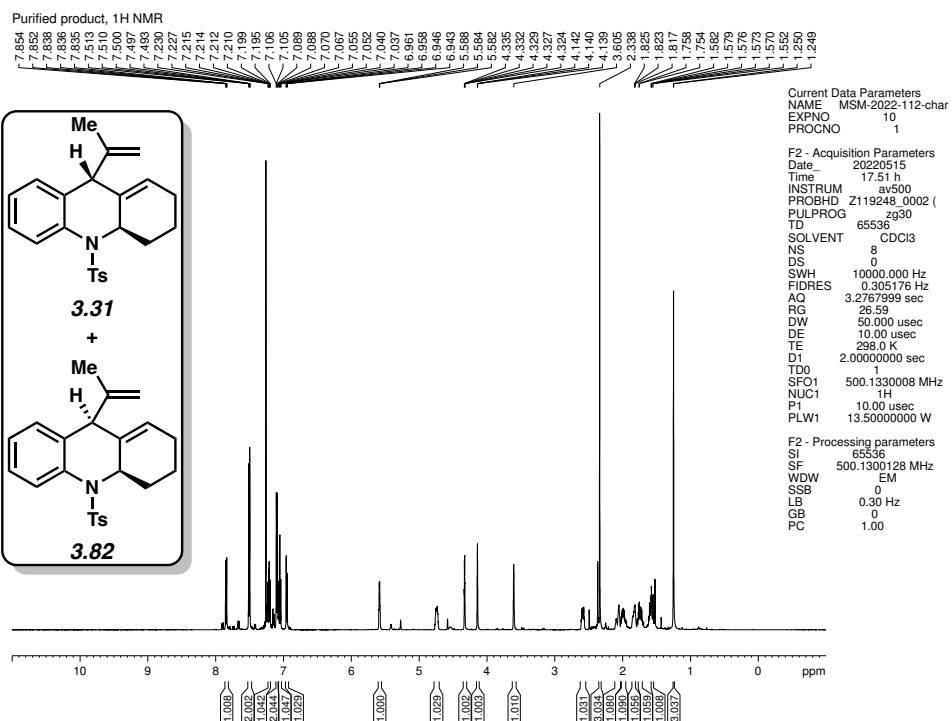


Figure 3.60. ¹H NMR (500 MHz, CDCl₃) of compounds 3.31 and 3.82.

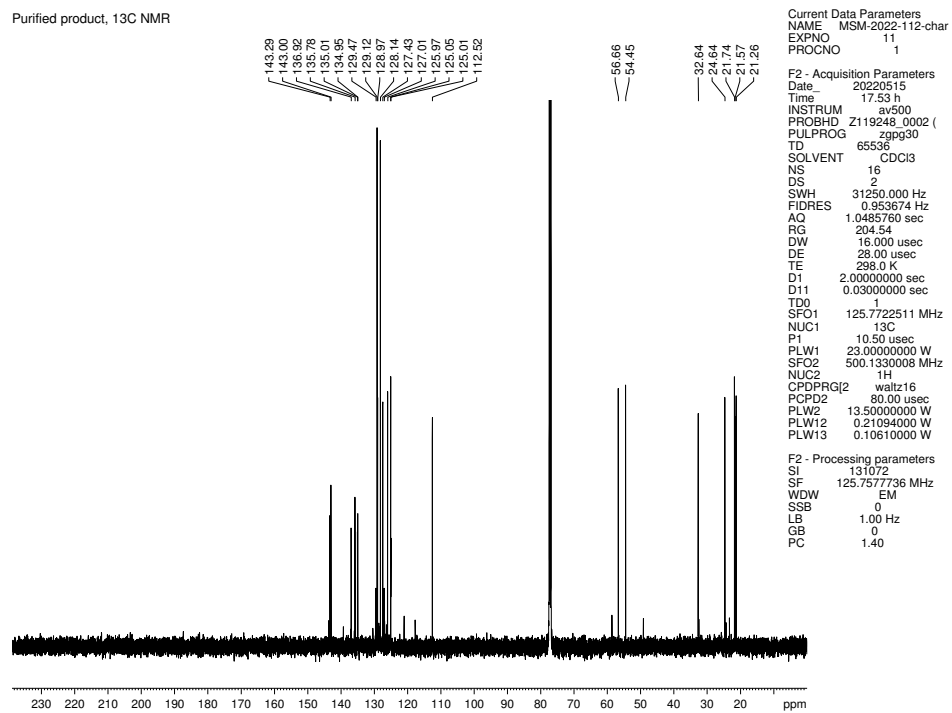
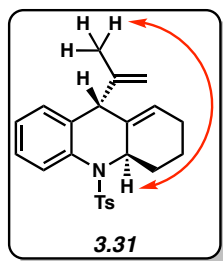


Figure 3.61. ¹³C NMR (125 MHz, CDCl₃) of compounds 3.31 and 3.82.



Purified product, NOESY

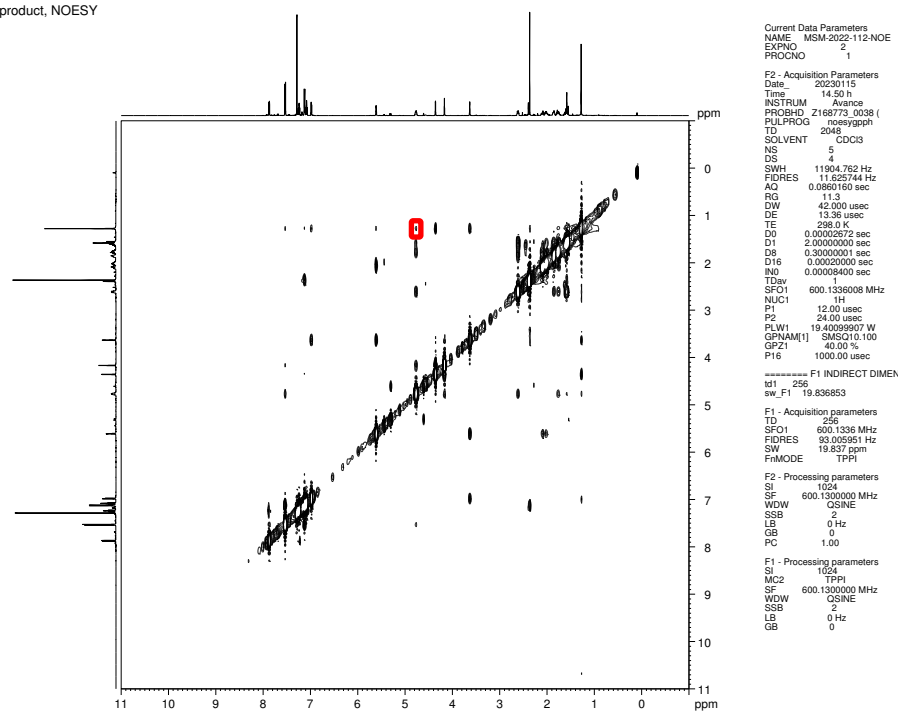


Figure 3.62. NOESY (600 MHz, CDCl₃) of compound **3.31**.

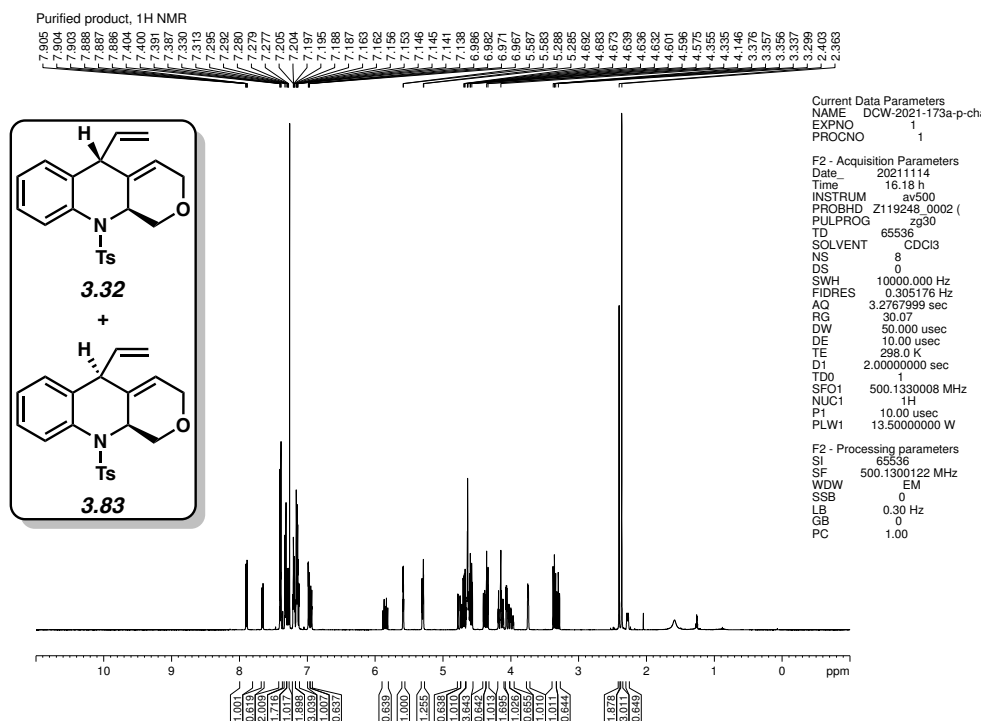


Figure 3.63. ¹H NMR (500 MHz, CDCl₃) of compounds **3.32** and **3.83**.

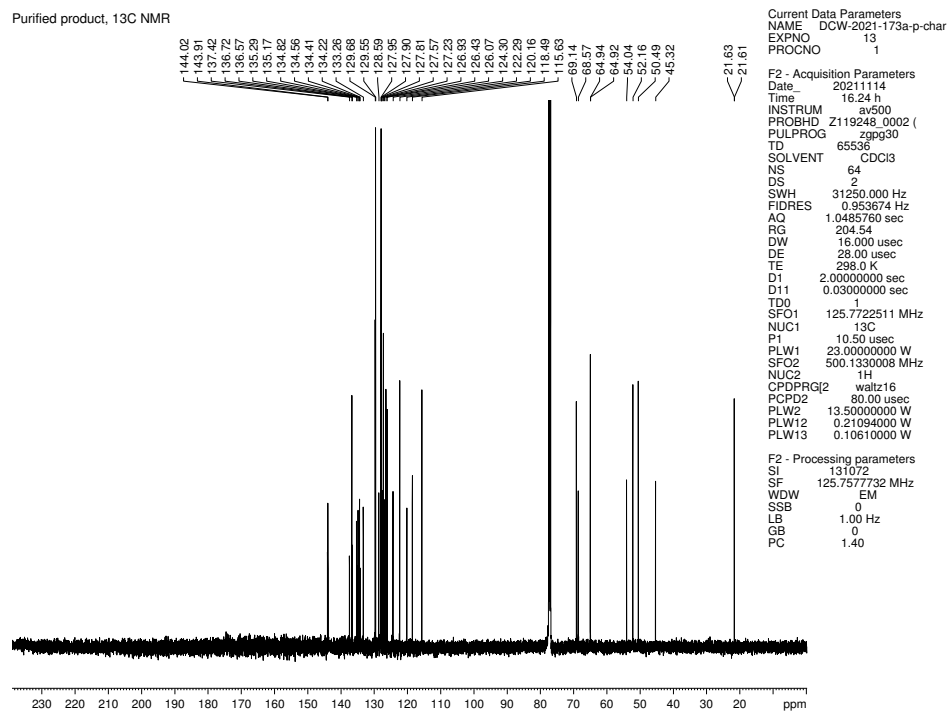


Figure 3.64. ¹³C NMR (125 MHz, CDCl₃) of compounds **3.32** and **3.83**.

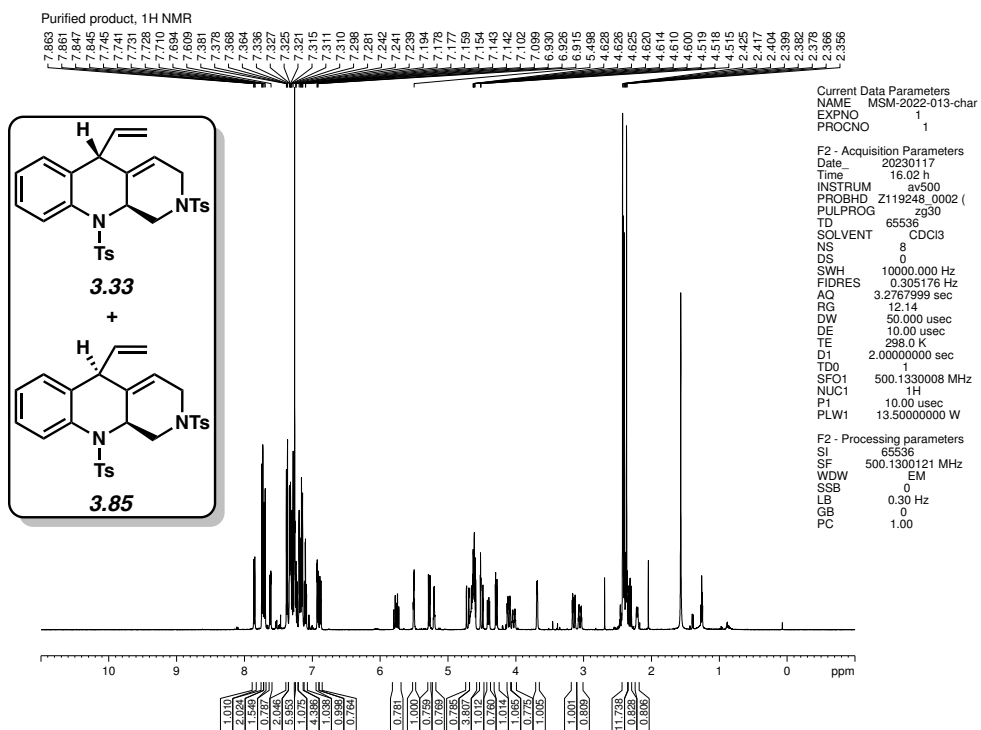


Figure 3.65. ¹H NMR (500 MHz, CDCl₃) of compounds 3.33 and 3.85.

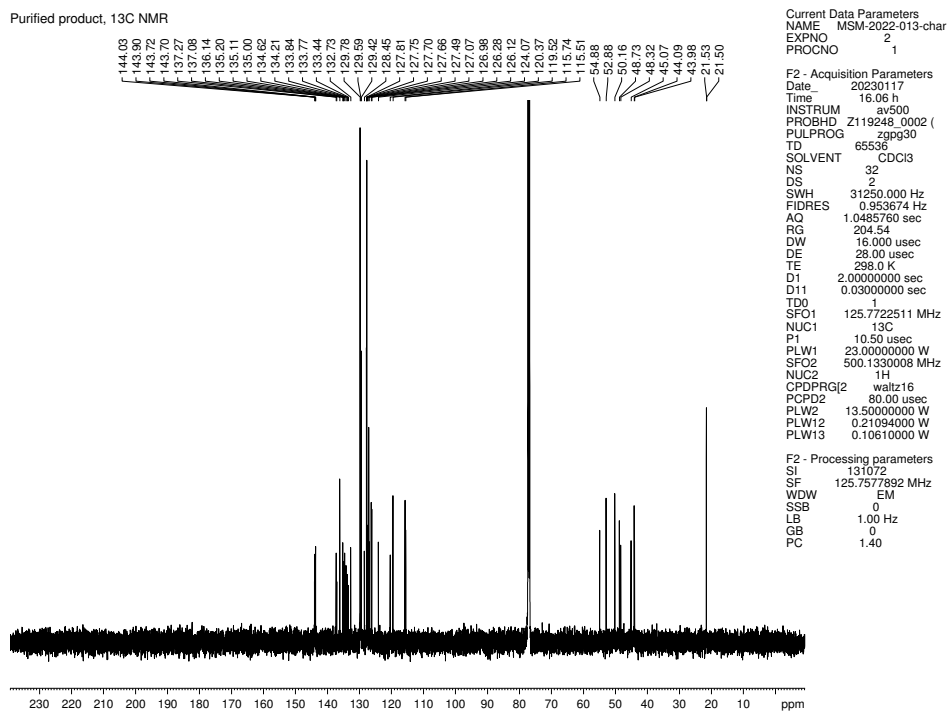
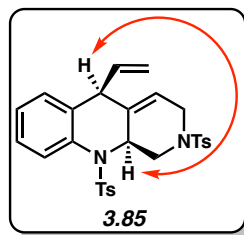
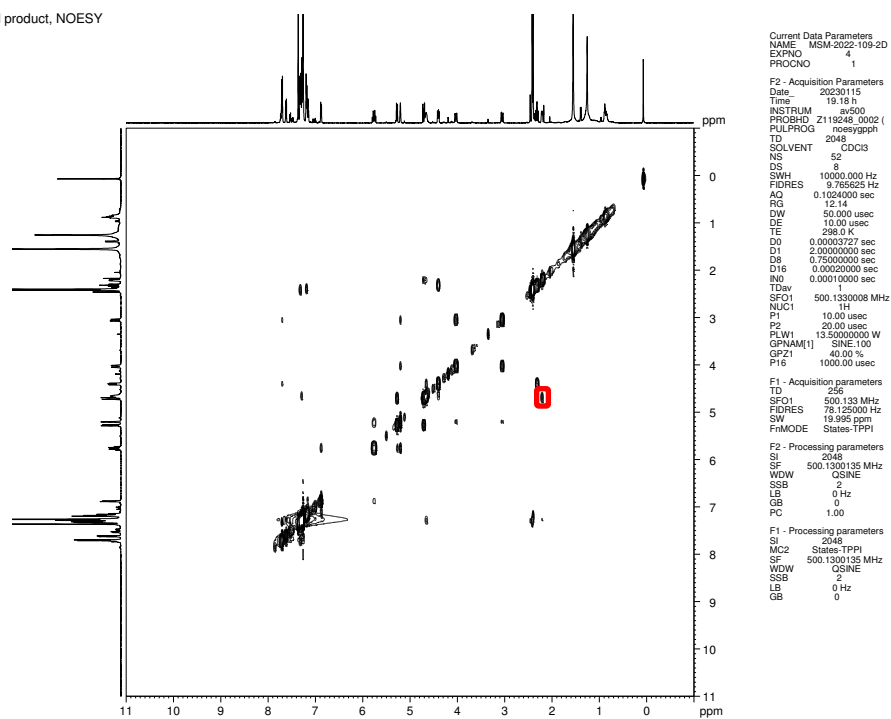


Figure 3.66. ¹³C NMR (125 MHz, CDCl₃) of compounds 3.33 and 3.85.



Purified product, NOESY



```

Current Data Parameters
NAME      MSM-2022-109-2D
EXPNO    4
PROCNO   1

F2 - Acquisition Parameters
Date_    20230115
Time     19.18 h
INSTRUM  sxt50
PROBHD   Z119248_0002 (
PULPROG  noesypph
TD        2048
SOLVENT  CDCl3
NS        52
DS        8
SWH       10000.000 Hz
FIDRES    9.765625 Hz
AQ        0.1024000 sec
RG         12.14
DW         50.000 usec
DE         10.00 usec
TE         298.0 K
D0         0.00000000 sec
D1         2.00000000 sec
D8         0.75000000 sec
D16        0.00020000 sec
IN0        0.00010000 sec
TD0av
SFO1      500.1330008 MHz
NUC1       1H
P1         10.00 usec
P2         20.00 usec
PL1        13.50000000 W
GPNAM[1]  SINE 100
GFZ1       40.00 %
PT6        1000.00 usec

F1 - Acquisition parameters
TD         256
SFO1      500.133 MHz
FIDRES     78.125000 Hz
SW         19.985 ppm
FhMODE     States-TPPI

F2 - Processing parameters
SI         2048
SE         500.1300135 MHz
WDW        CSINE
SSB         2
LB          0 Hz
GB          0
PC          1.00

F1 - Processing parameters
SI         2048
MC2        States-TPPI
SF         500.1300135 MHz
WDW        CSINE
SSB         2
LB          0 Hz
GB          0
  
```

Figure 3.67. NOESY (500 MHz, CDCl₃) of compound **3.85**.

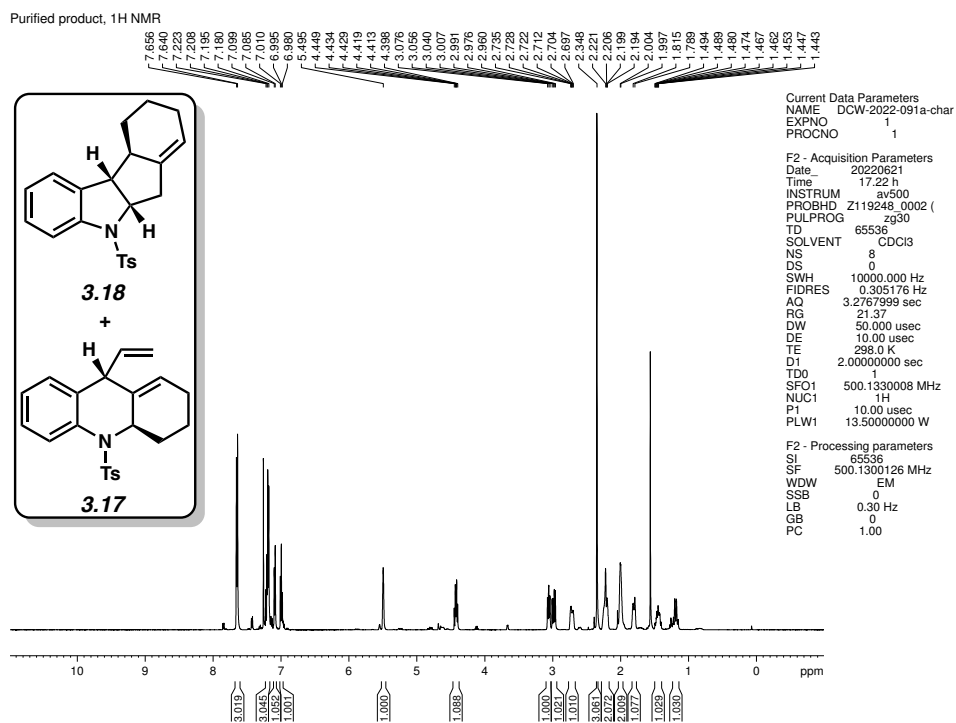


Figure 3.68. ¹H NMR (500 MHz, CDCl₃) of compounds 3.18 and 3.17.

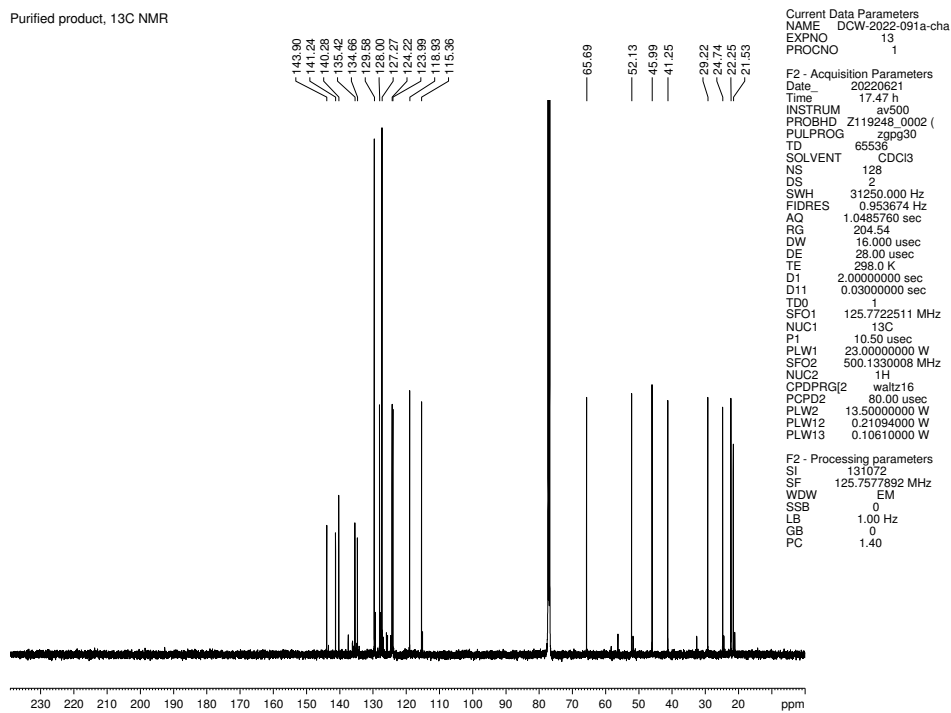


Figure 3.69. ¹³C NMR (125 MHz, CDCl₃) of compounds 3.18 and 3.17.

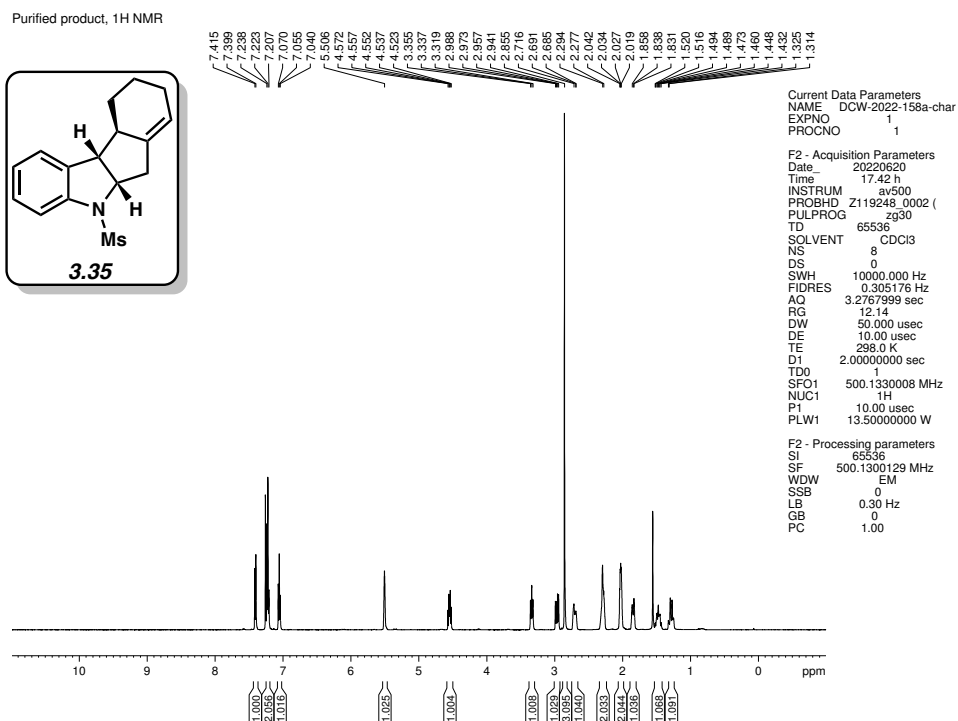


Figure 3.70. ¹H NMR (500 MHz, CDCl₃) of compound 3.35.

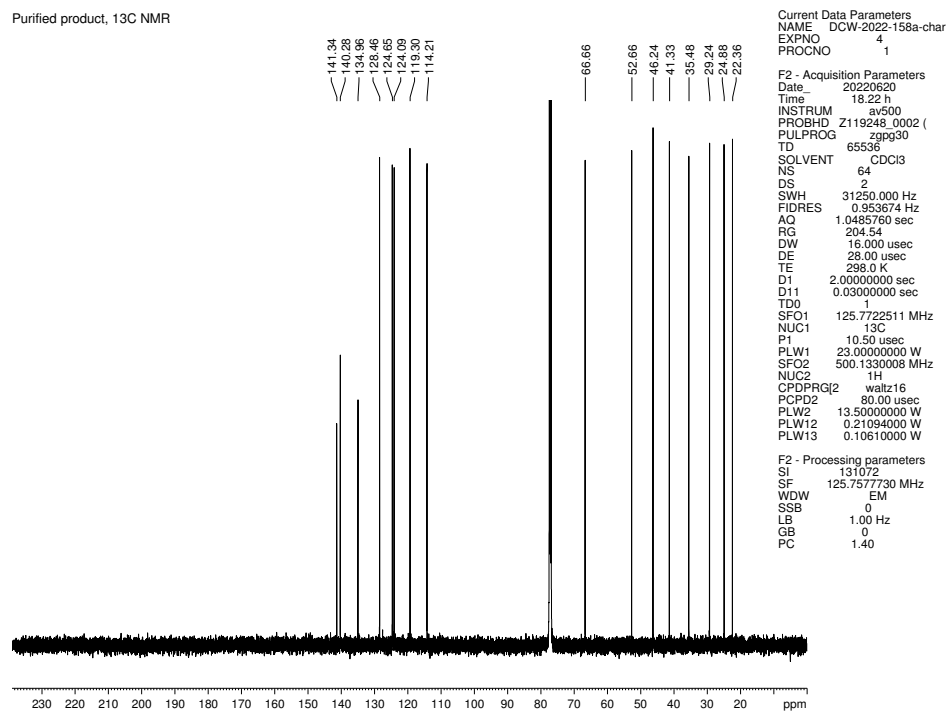


Figure 3.71. ¹³C NMR (125 MHz, CDCl₃) of compound 3.35.

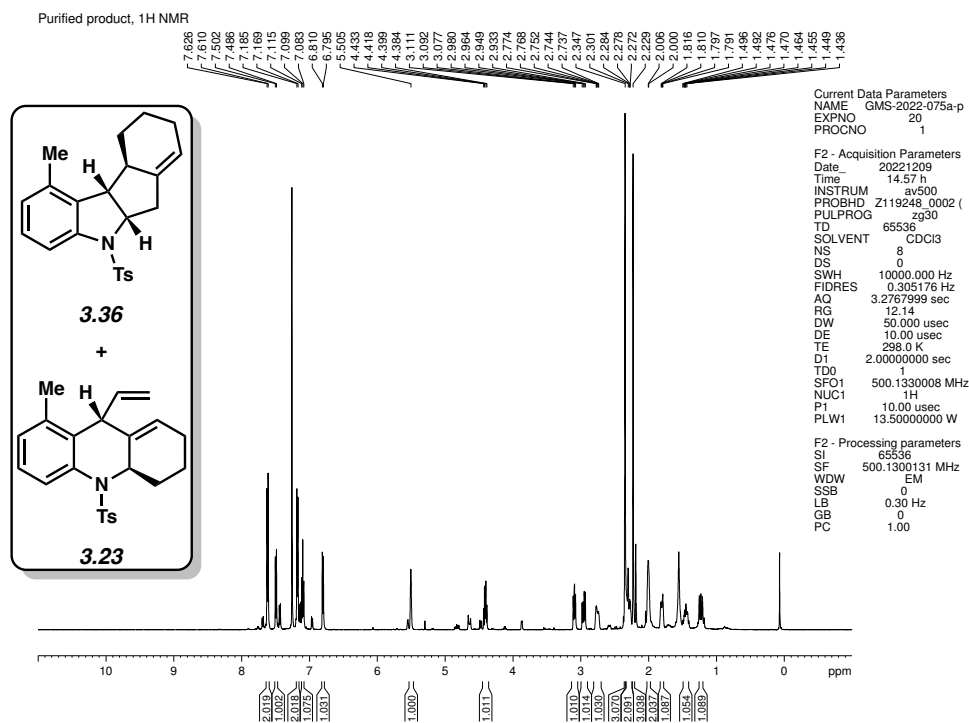


Figure 3.72. ¹H NMR (500 MHz, CDCl₃) of compounds **3.36** and **3.23**.

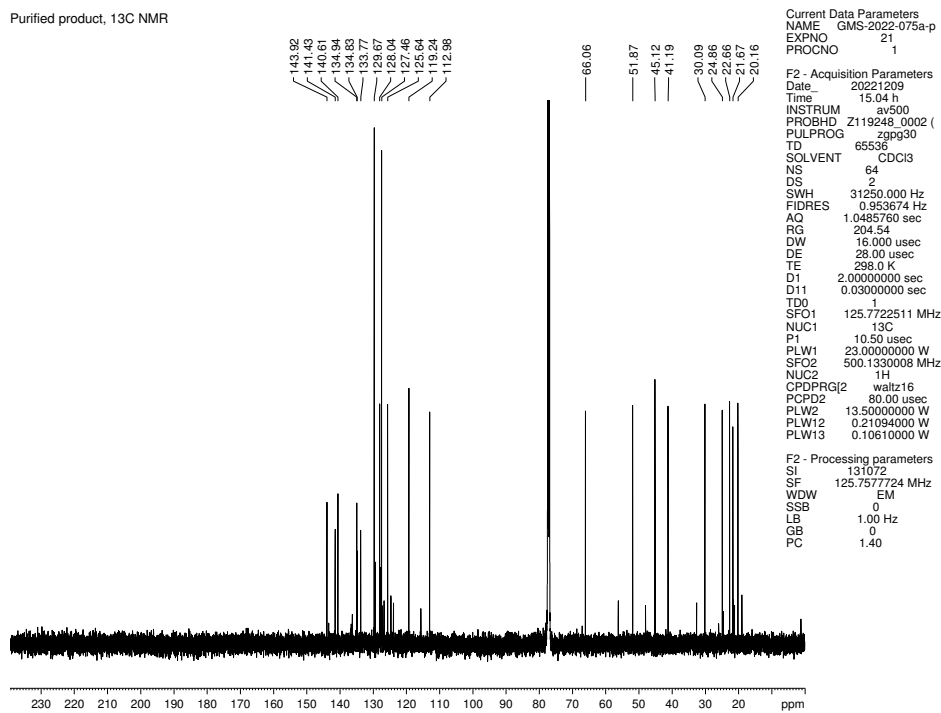


Figure 3.73. ¹³C NMR (125 MHz, CDCl₃) of compound **3.36** and **3.23**.

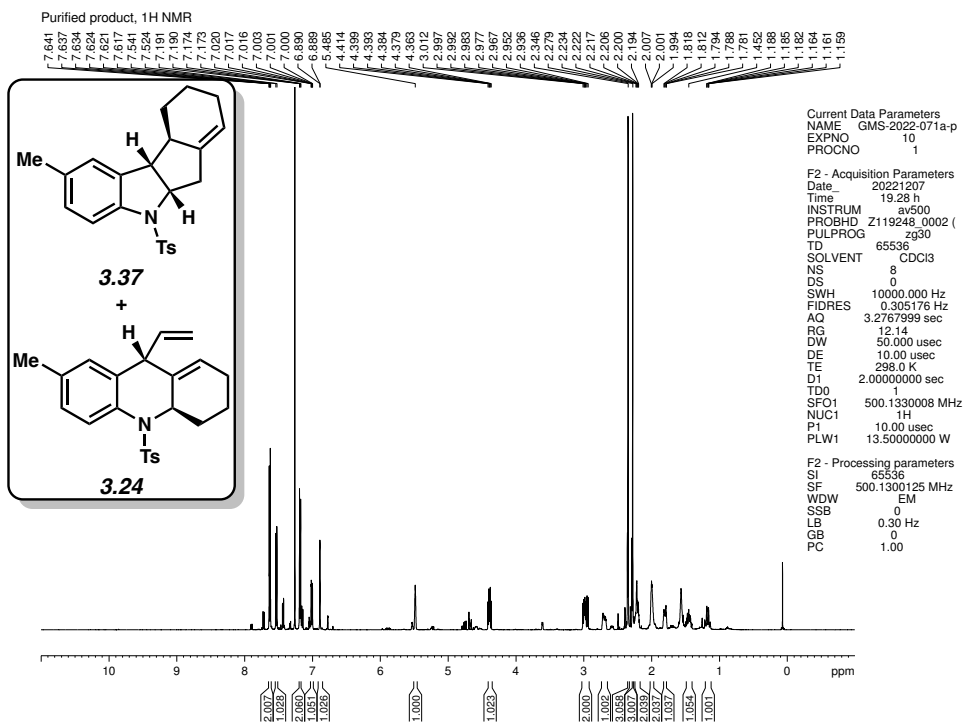


Figure 3.74. ¹H NMR (500 MHz, CDCl₃) of compounds 3.37 and 3.24.

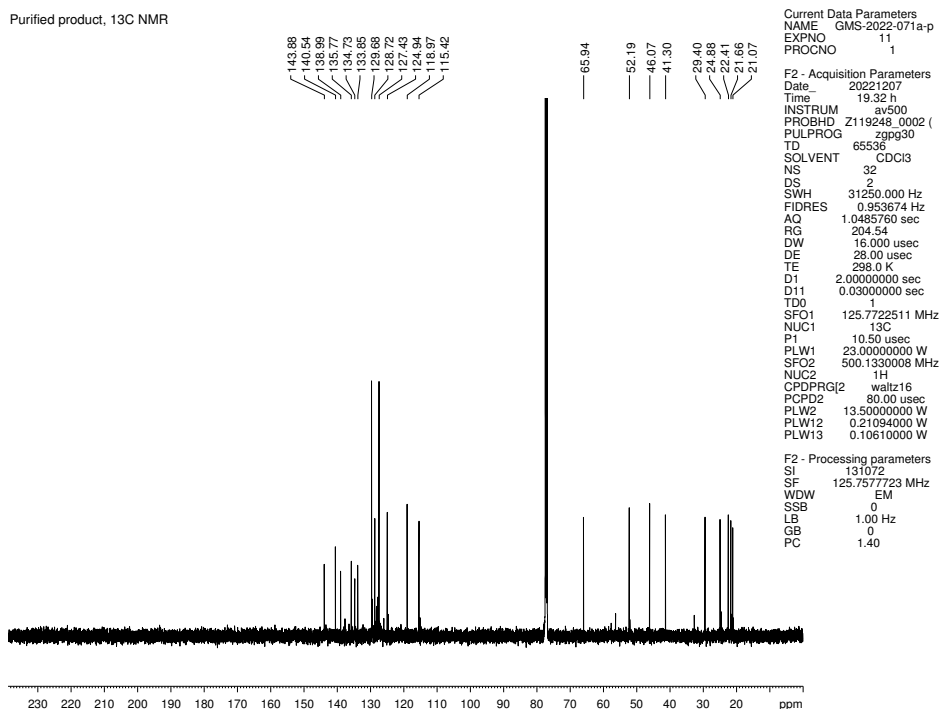
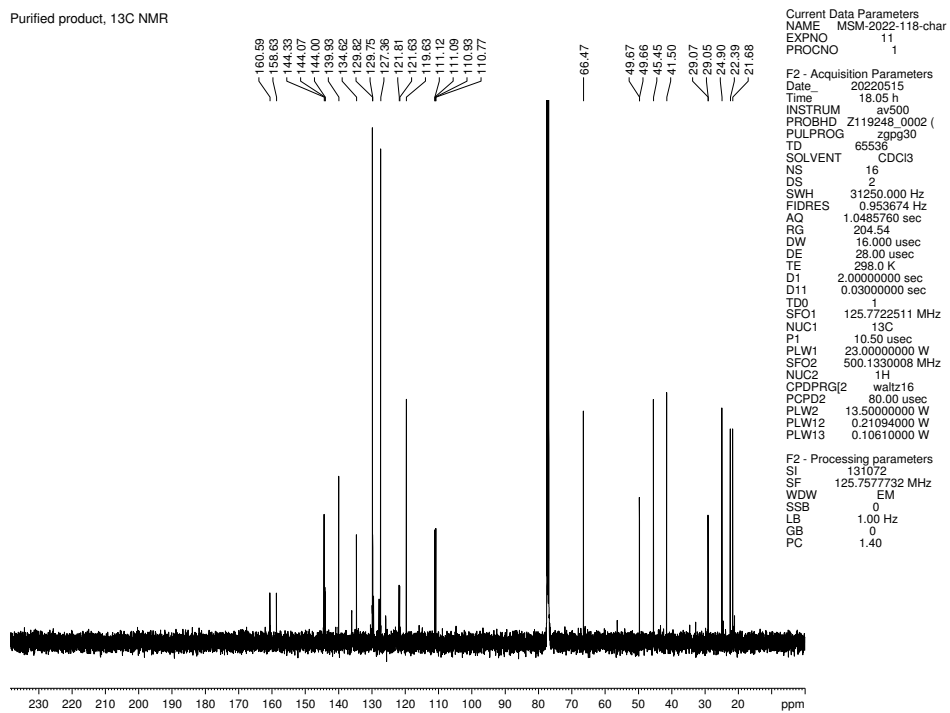
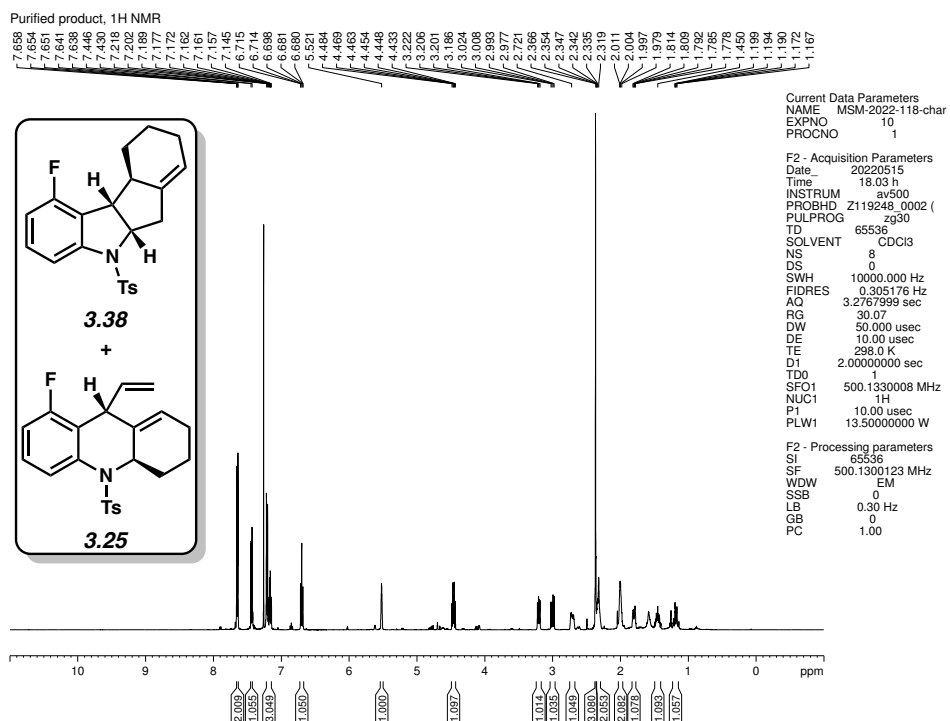


Figure 3.75. ¹³C NMR (125 MHz, CDCl₃) of compound 3.37 and 3.24.



Purified product, ^{19}F NMR

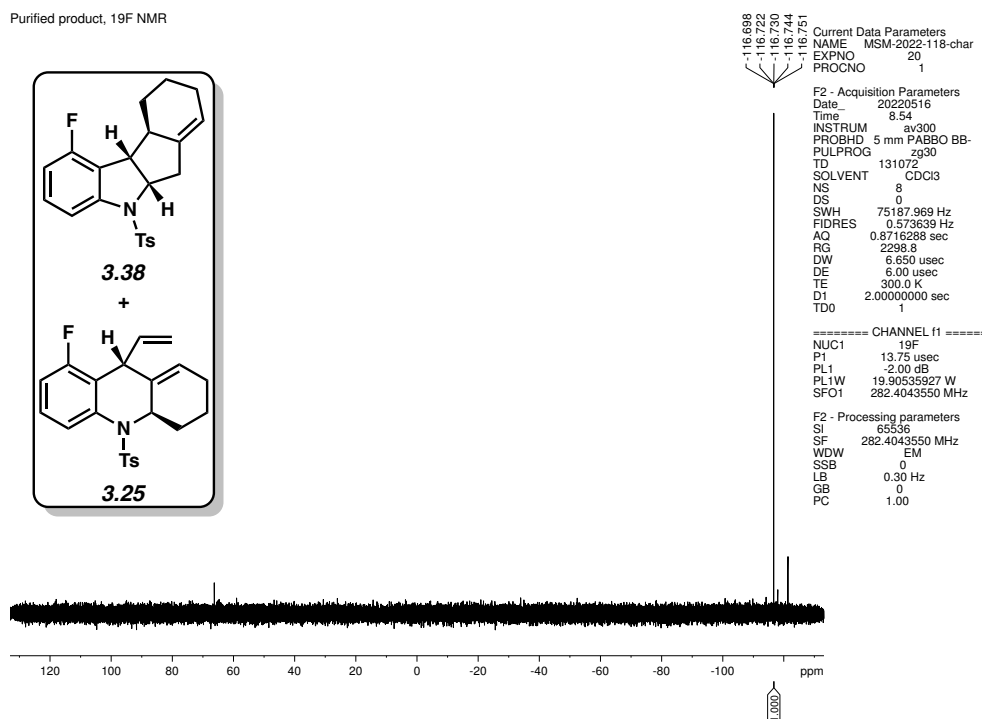


Figure 3.78. ^{19}F NMR (282 MHz, CDCl_3) of compound **3.38** and **3.25**.

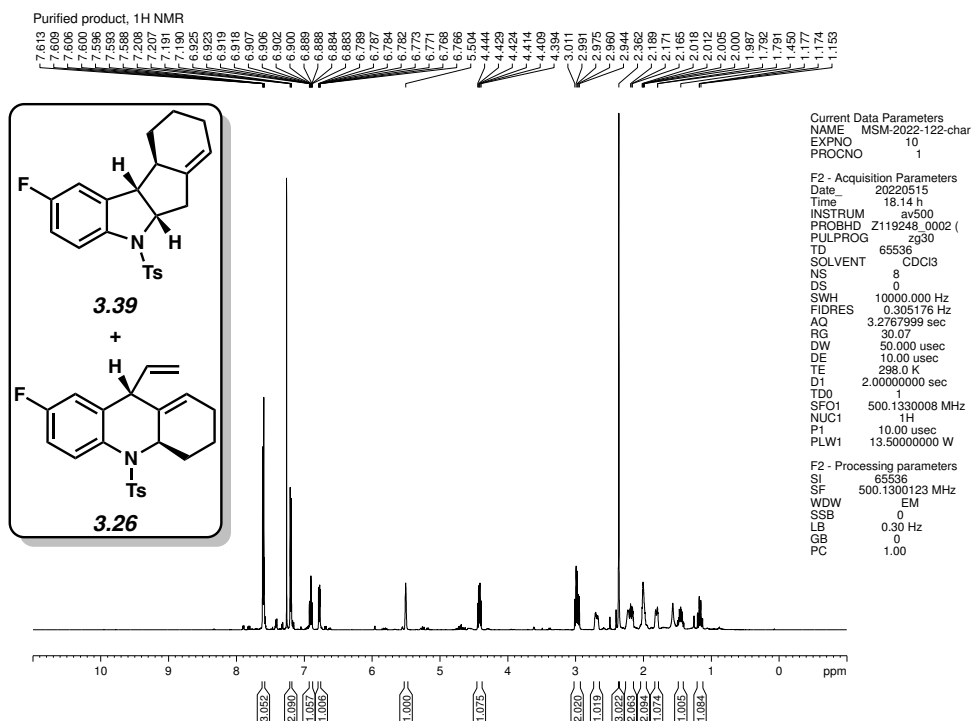


Figure 3.79. ¹H NMR (500 MHz, CDCl₃) of compounds 3.39 and 3.26.

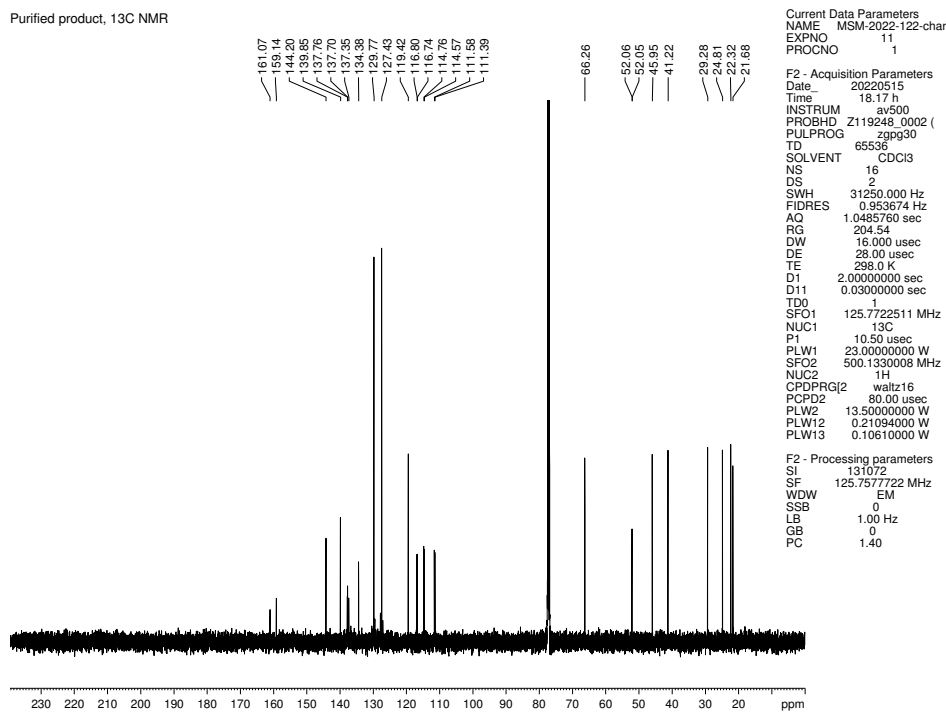
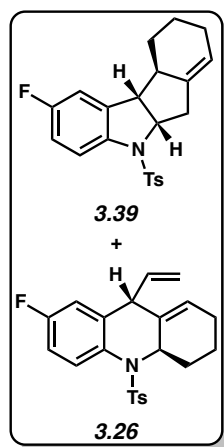


Figure 3.80. ¹³C NMR (125 MHz, CDCl₃) of compound 3.39 and 3.26.

Purified product, ^{19}F NMR



-119.140
-119.157
-119.170
-119.187
-119.200
-119.217

Current Data Parameters
NAME MSM-2022-122-char
EXPNO 40
PROCNO 1

F2 - Acquisition Parameters
Date_ 20220516
Time 9.03
INSTRUM av300
PROBHD 5 mm PABBO BB-
PULPROG zg30
TD 131072
SOLVENT CDCl3
NS 8
DS 0
SWH 75187.969 Hz
FIDRES 0.573639 Hz
AQ 0.8716288 sec
RG 2298.8
DW 6.650 usec
DE 6.00 usec
TE 300.0 K
D1 2.0000000 sec
TD0 1

===== CHANNEL f1 =====
NUC1 ^{19}F
P1 13.75 usec
PL1 -2.00 dB
PL1W 19.90535927 W
SFO1 282.4043550 MHz

F2 - Processing parameters
SI 65536
SF 282.4043550 MHz
WDW EM
SSB 0
LB 0.30 Hz
GB 0
PC 1.00

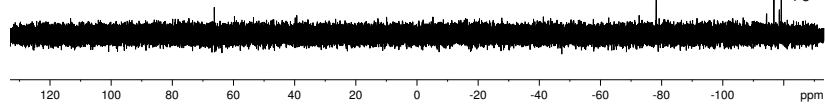


Figure 3.81. ^{19}F NMR (282 MHz, CDCl_3) of compound **3.39** and **3.26**.

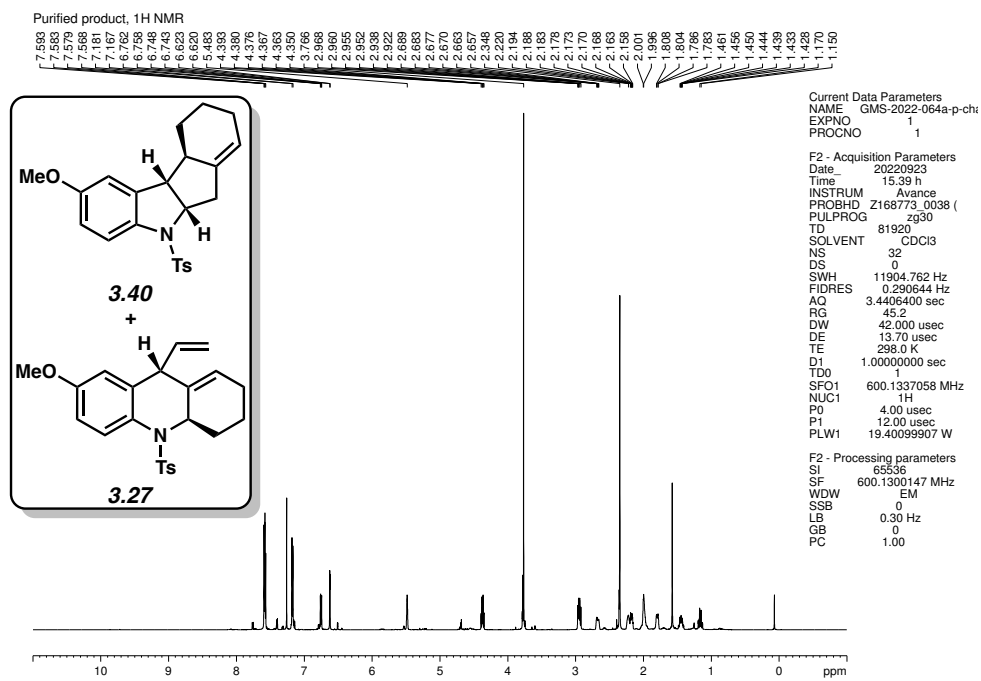


Figure 3.82. ¹H NMR (600 MHz, CDCl₃) of compounds **3.40** and **3.27**.

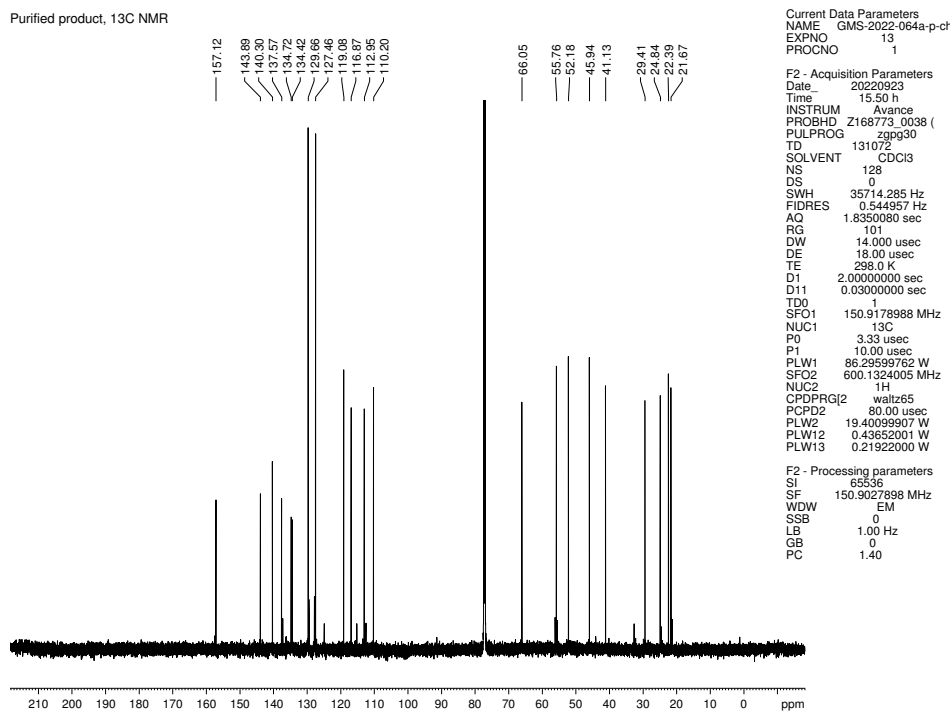


Figure 3.83. ¹³C NMR (150 MHz, CDCl₃) of compound **3.40** and **3.27**.

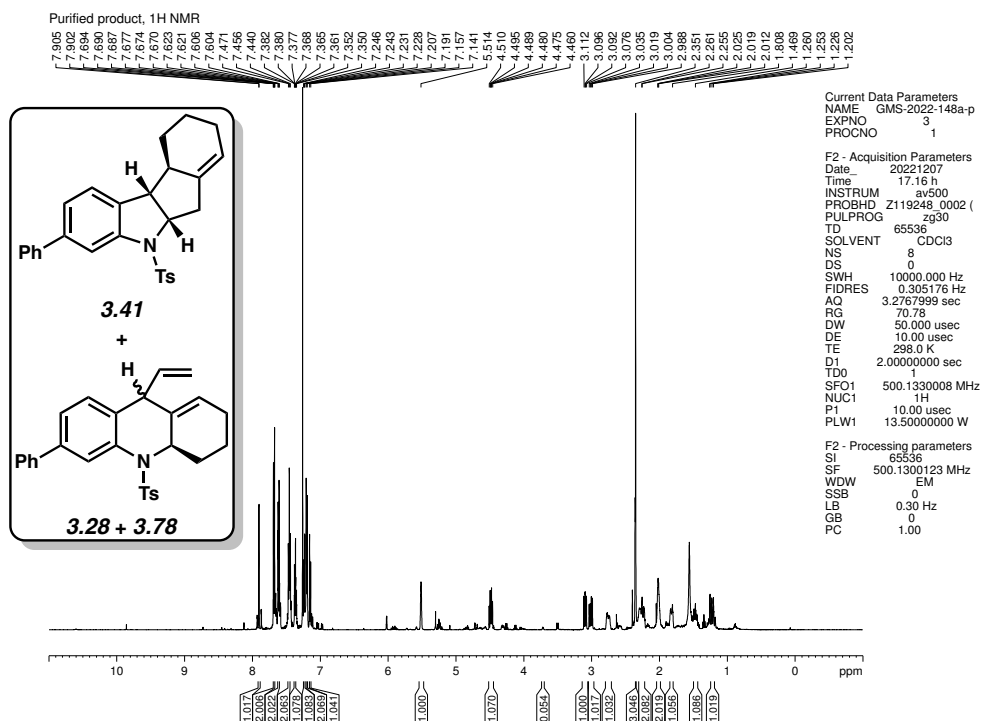


Figure 3.84. ¹H NMR (500 MHz, CDCl₃) of compounds 3.41, 3.28, and 3.78.

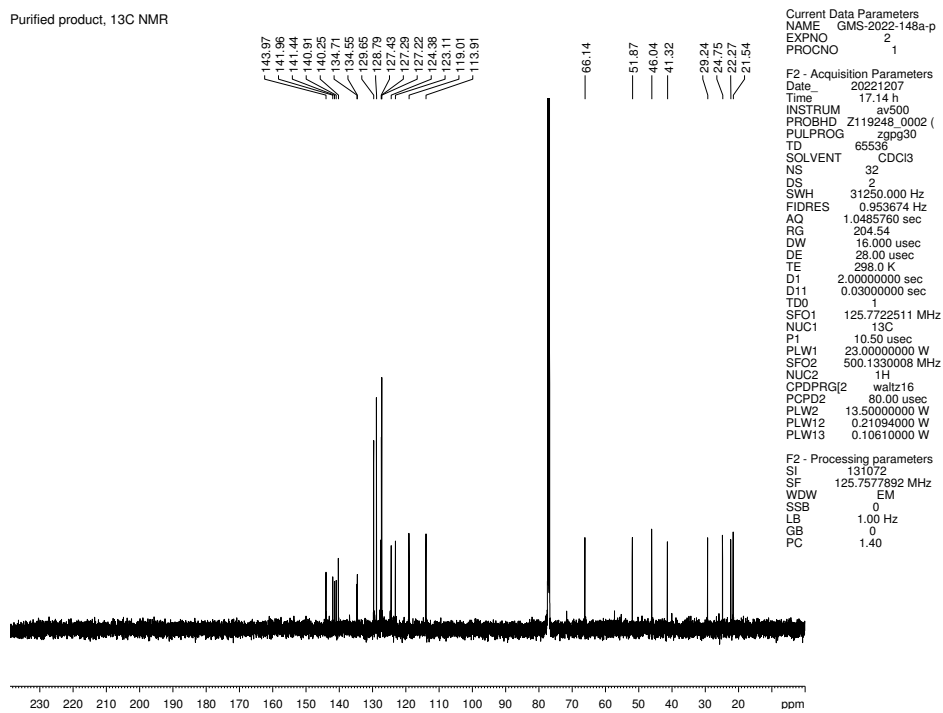


Figure 3.85. ¹³C NMR (125 MHz, CDCl₃) of compounds 3.41, 3.28, and 3.78.

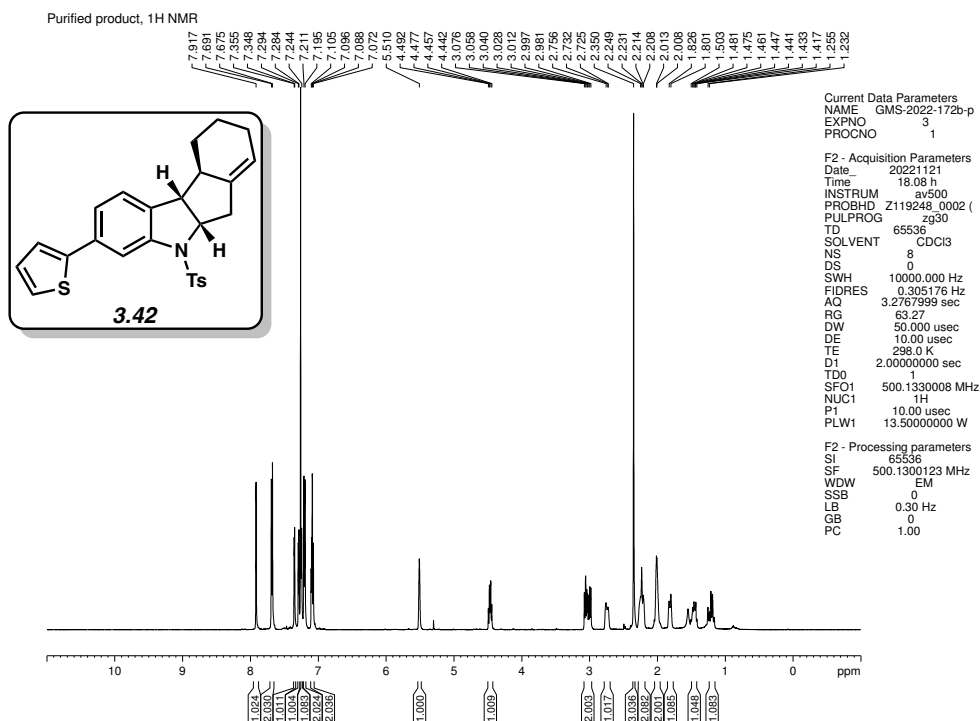


Figure 3.86. ¹H NMR (500 MHz, CDCl₃) of compound 3.42.

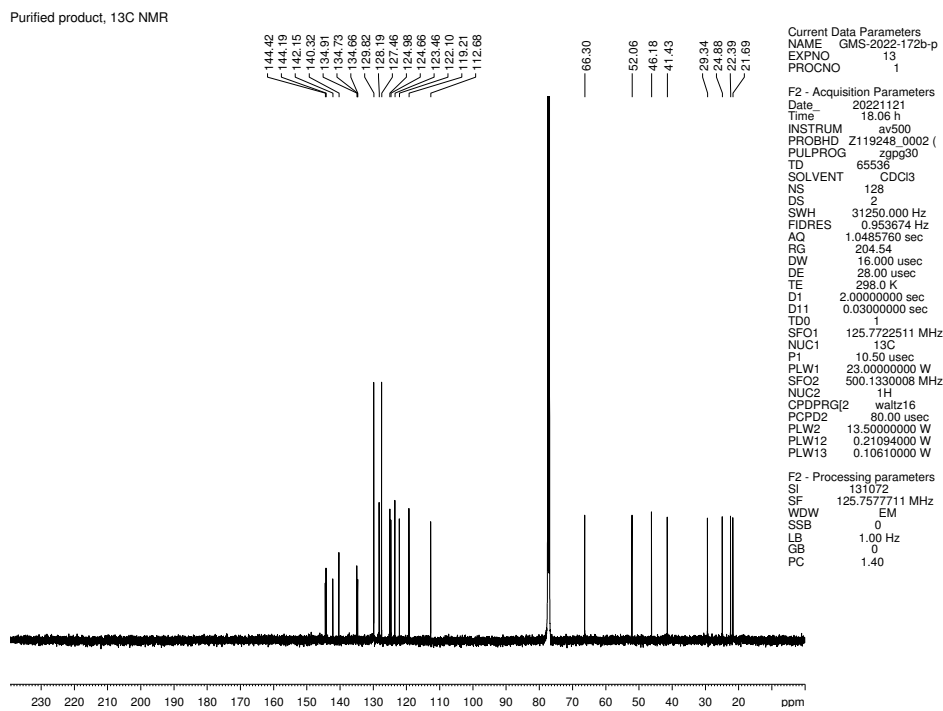


Figure 3.87. ¹³C NMR (125 MHz, CDCl₃) of compound 3.42.

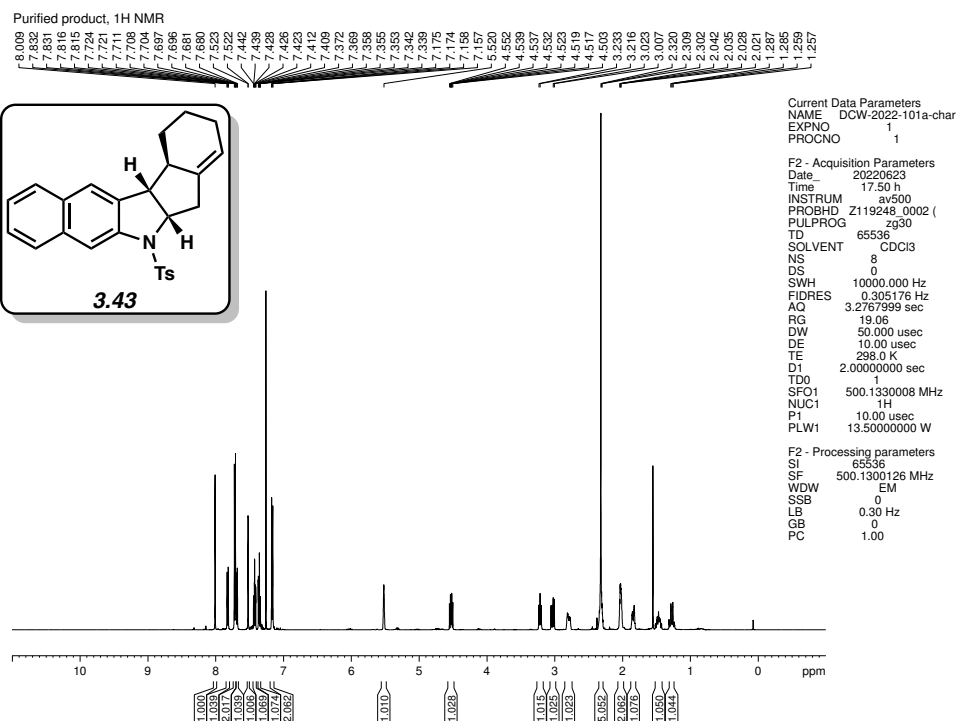


Figure 3.88. ¹H NMR (500 MHz, CDCl₃) of compound 3.43.

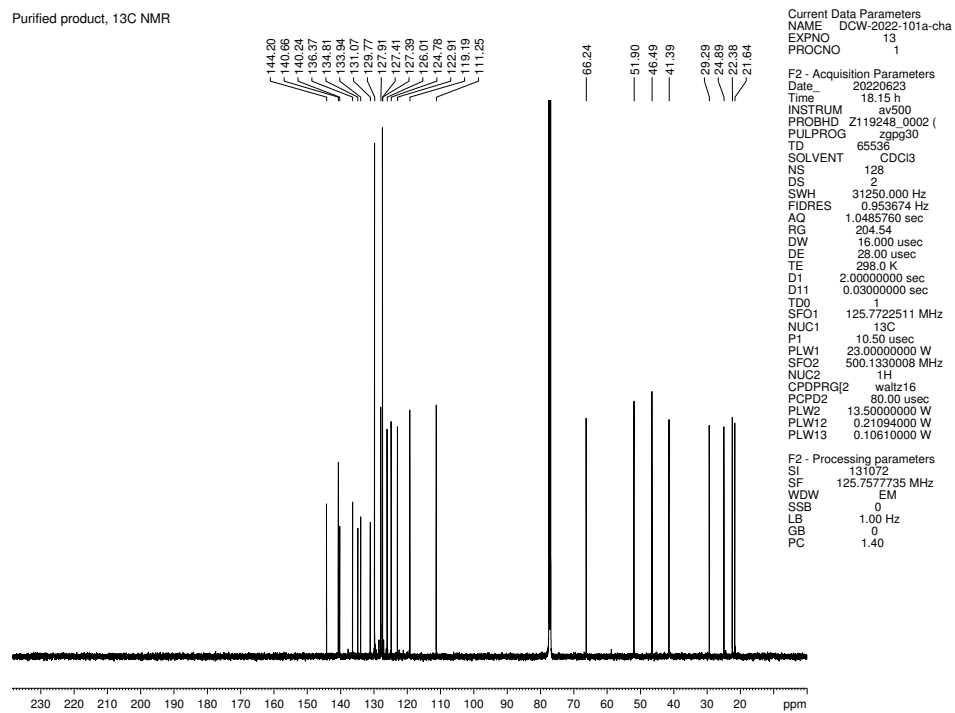


Figure 3.89. ¹³C NMR (125 MHz, CDCl₃) of compound 3.43.

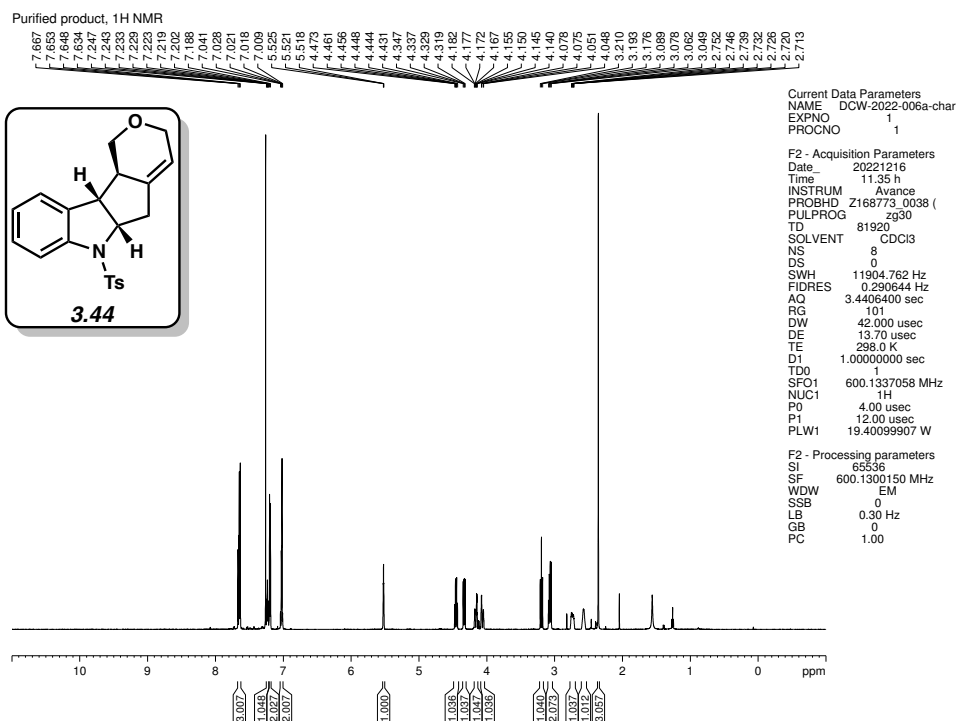


Figure 3.90. ¹H NMR (600 MHz, CDCl₃) of compound 3.44.

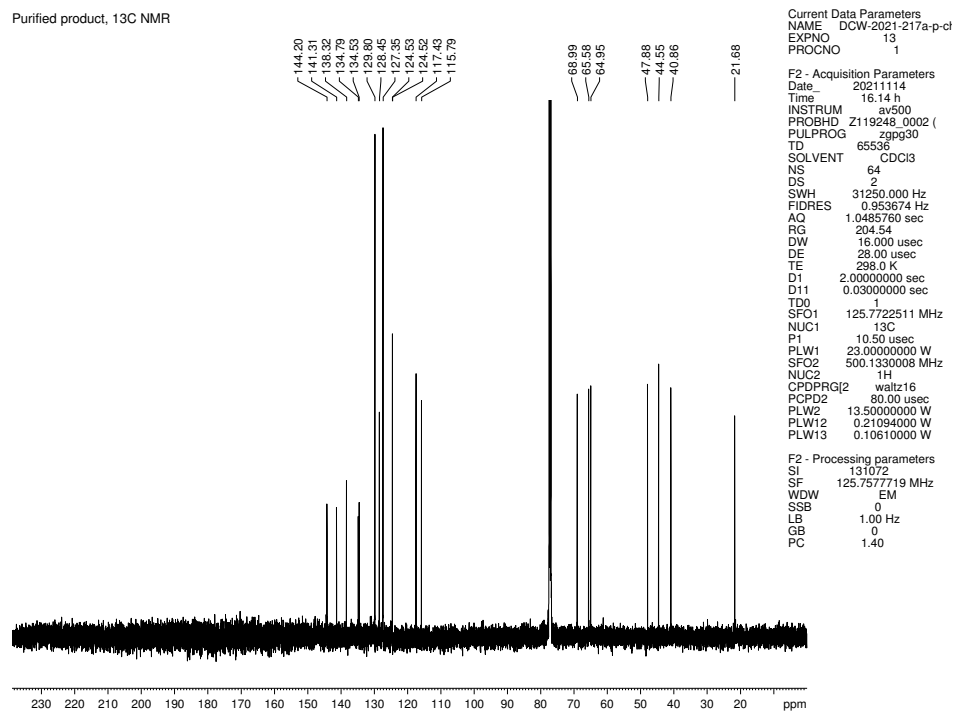


Figure 3.91. ¹³C NMR (125 MHz, CDCl₃) of compound 3.44.

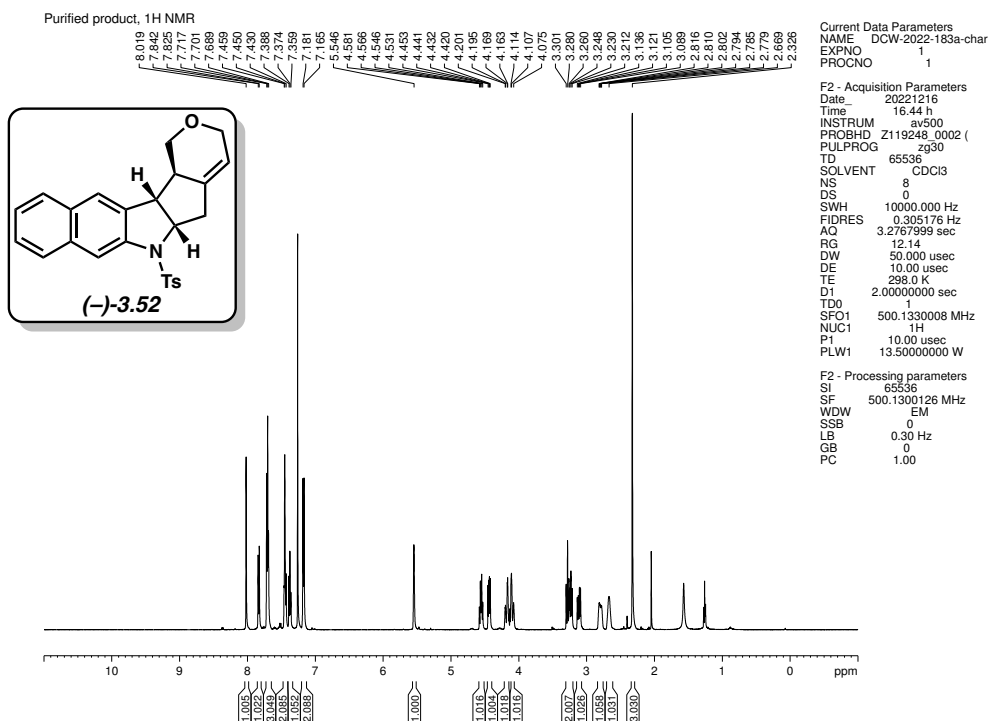


Figure 3.92. ¹H NMR (500 MHz, CDCl₃) of compound 3.52.

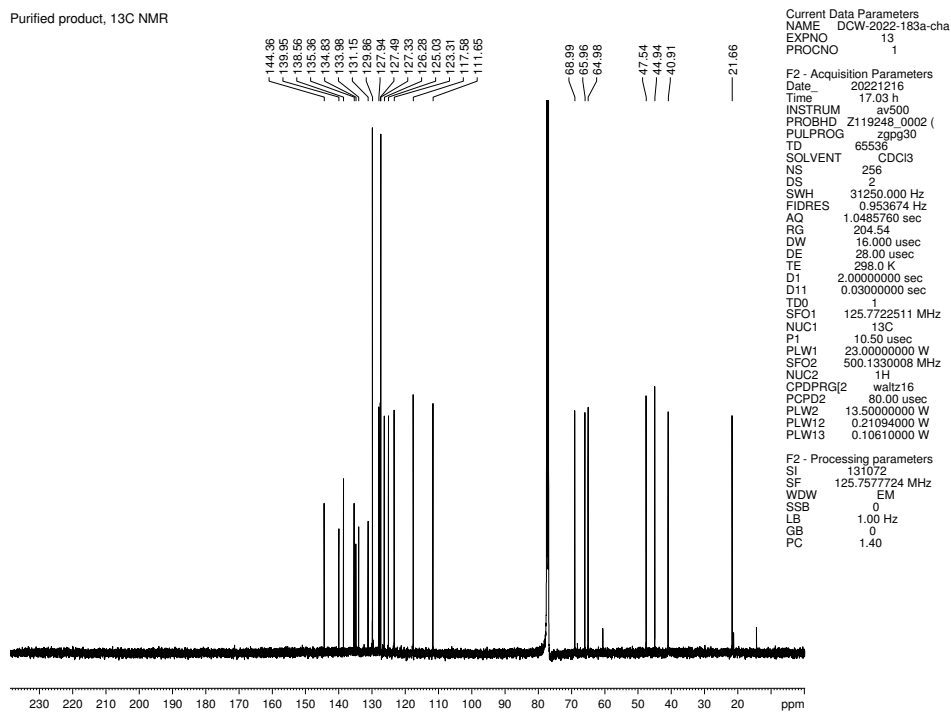
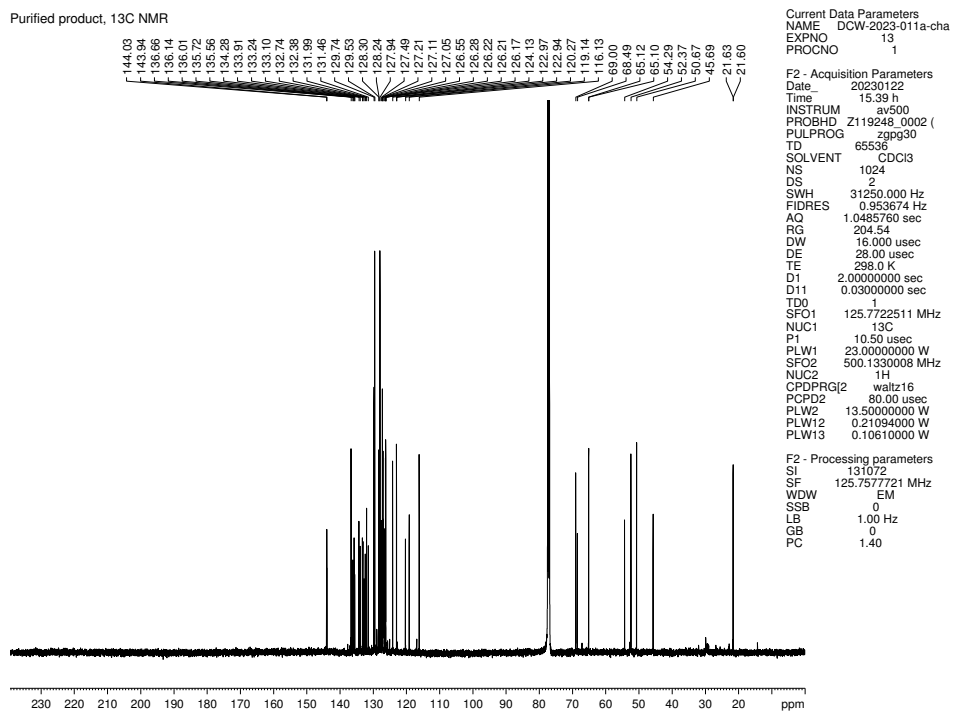
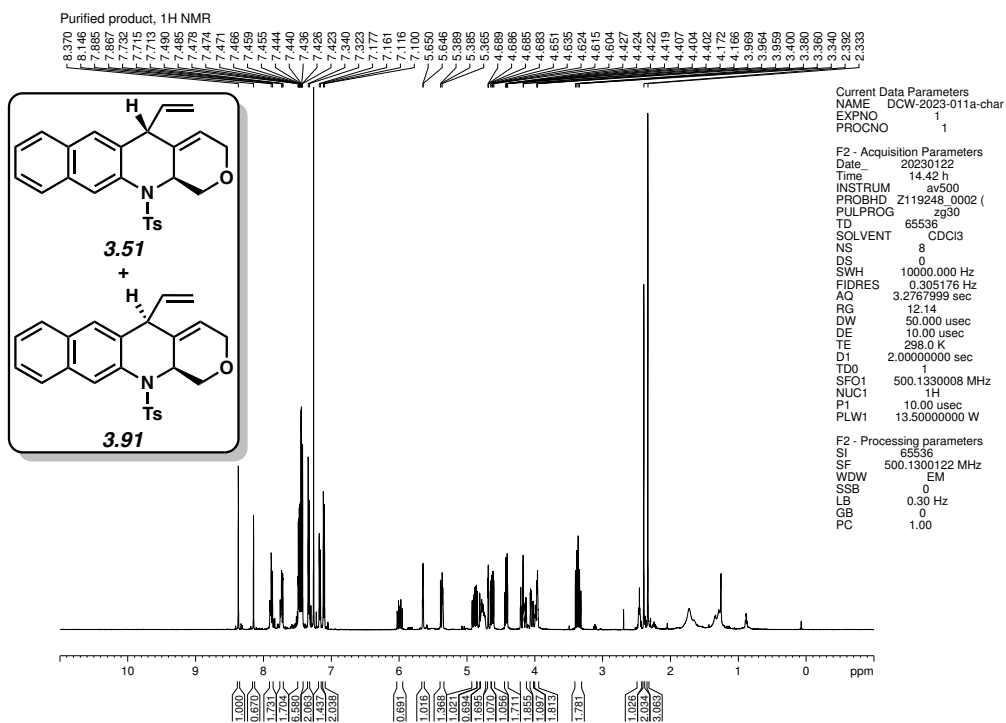


Figure 3.93. ¹³C NMR (125 MHz, CDCl₃) of compound 3.52.



3.10 Notes and References

- (1) Roberts, J. D.; Simmons, H. E.; Carlsmith, L. A.; Vaughn, C. W. Rearrangement in the reaction of chlorobenzene-1- C^{14} with potassium amide. *J. Am. Chem. Soc.* **1953**, *75*, 3290–3291.
- (2) Wenk, H. H.; Winkler, M.; Sander, W. One century of aryne chemistry. *Angew. Chem., Int. Ed.* **2003**, *42*, 502–528.
- (3) Dhokale, R. A.; Mhaske, S. B. Transition-metal-catalyzed reactions involving arynes. *Synthesis* **2018**, *50*, 1–16.
- (4) Bhunia, A.; Yetra, S. R.; Biju, A. T. Recent advances in transition-metal-free carbon–carbon and carbon–heteroatom bond-forming reaction using arynes. *Chem. Soc. Rev.* **2012**, *41*, 3140–3152.
- (5) Goetz, A. E.; Garg, N. K.; Enabling the use of heterocyclic arynes in chemical synthesis. *J. Org. Chem.* **2014**, *79*, 846–851.
- (6) Nakamura, Y.; Yoshida, S.; Hosya, T. Recent advances in synthetic hetaryne chemistry. *Heterocycles* **2019**, *98*, 1623–1677.
- (7) Scardiglia, F.; Roberts, J. D. Evidence for cyclohexyne as an intermediate in the coupling of phenyllithium with 1-chlorocyclohexene. *Tetrahedron* **1957**, *1*, 343–344.

- (8) For a review describing a wide range of in situ generated strained intermediates, see: Shi, J.; Li, L.; Li, Y. *o*-Silylaryl triflates: A journey of Kobayashi aryne precursors. *Chem. Rev.* **2021**, *121*, 3892–4044.
- (9) Dubrovskiy, A. V.; Markina, N. A.; Larock, R. C. Use of benzyne for the synthesis of heterocycles. *Org. Biomol. Chem.* **2013**, *11*, 191–218.
- (10) Goetz, A. E.; Shah, T. K.; Garg, N. K. Pyridynes and indolynes as building blocks for functionalized heterocycles and natural products. *Chem. Commun.* **2015**, *51*, 34–45.
- (11) Mauger, C. C.; Mignani, G. A. An efficient and safe procedure for the large-scale Pd-catalyzed hydrazonation of aromatic chlorides using Buchwald technology. *Org. Proc. Res. Dec.* **2004**, *8*, 1065–1071.
- (12) Tadross, P. M.; Stoltz, B. M. A comprehensive history of arynes in natural product total synthesis. *Chem. Rev.* **2012**, *112*, 3550–3577.
- (13) Gampe, C. M.; Carreira, E. M. Arynes and cyclohexyne in natural product total synthesis. *Angew. Chem., Int. Ed.* **2012**, *112*, 3550–3577.
- (14) Takikawa, H.; Nishii, A.; Sakai, T.; Suzuki, K. Aryne-based strategy in the total synthesis of naturally occurring polycyclic compounds. *Chem. Soc. Rev.* **2018**, *47*, 8030–8056.

- (15) Schleth, F.; Vettiger, T.; Rommel, M.; Tobler, H. Process for the preparation of pyrazole carboxylic acid amides. International patent WO 2011131544 A1, Oct 27, 2011.
- (16) Lin, J. B.; Shah, T. J.; Goetz, A. E.; Garg, N. K.; Houk, K. N. Conjugated trimeric scaffolds accessible from indolyne cyclotrimerizations: Synthesis, structures, and electronic properties. *J. Am. Chem. Soc.* **2017**, *139*, 10447–10455.
- (17) Darzi, E. R.; Barber, J. S.; Garg, N. K. Cyclic alkyne approach to heteroatom-containing polycyclic aromatic hydrocarbon scaffolds. *Angew. Chem., Int. Ed.* **2019**, *58*, 9419–9424.
- (18) Wittig, G.; Fritze, P. On the intermediate occurrence of 1,2-cyclohexadiene. *Angew. Chem., Int. Ed.* **1966**, *5*, 846.
- (19) Moser, W. R. The reactions of *gem*-dihalocyclopropanes with organometallic reagents. Ph.D. Dissertation, Massachusetts Institute of Technology Cambridge, MA, 1964.
- (20) Christl, M. Cyclic allenes up to seven-membered rings. *Modern Allene Chemistry*; Krause, N., Kashmi, S. A. K., Eds.; Wiley-VCH: Weinheim, 2004; pp 243–357.
- (21) Angus, R. O., Jr.; Schmidt, M. W.; Johnson, R. P. Small-ring cyclic cumulenes: Theoretical studies of the structure and barrier to inversion of cyclic allenes. *J. Am. Chem. Soc.* **1985**, *107*, 532–537.

- (22) Daoust, K. J.; Hernandez, S. M.; Konrad, K. M.; Mackie, I. D.; Winstanley, J.; Johnson, R. P. Strain estimates for small-ring cyclic allenes and butatrienes. *J. Org. Chem.* **2006**, *71*, 5708–5714.
- (23) Strained cyclic allenes have several attractive attributes that include their: (a) generation under mild reaction conditions, (b) ability to undergo two or one electron processes leading to a wide scope of reactions, (c) inherent chirality, which can allow for stereoselective transformations, (d) participation in regioselective reactions based on substituent effects, and (e) relatively understudied nature, which allows numerous opportunities for discovery.
- (24) Quintana, I.; Peña, D.; Pérez, D.; Guitián, E. Generation and reactivity of 1,2-cyclohexadiene under mild reaction conditions. *Eur. J. Org. Chem.* **2009**, 5519–5524.
- (25) McVeigh, M. S.; Kelleghan, A. V.; Yamano, M. M.; Knapp, R. R.; Garg, N. K. Silyl tosylate precursors to cyclohexynes, 1,2-cyclohexadienes, and 1,2-cycloheptadiene. *Org. Lett.* **2020**, *22*, 4500–4504.
- (26) Hioki, Y.; Mori, A.; Okano, K. Steric effects on deprotonative generation of cyclohexynes and 1,2-cyclohexadienes from cyclohexenyl triflates by magnesium amides. *Tetrahedron* **2020**, *76*, 131103.
- (27) Barber, J. S.; Styduhar, E. D.; Pham, H. V.; McMahon, T. C.; Houk, K. N.; Garg, N. K. Nitrene cycloadditions of 1,2-cyclohexadiene. *J. Am. Chem. Soc.* **2016**, *138*, 2512–2515.

- (28) Barber, J. S.; Yamano, M. M.; Ramirez, M.; Darzi, E. R.; Knapp, R. R.; Liu, F.; Houk, K. N.; Garg, N. K. Diels–Alder cycloadditions of strained azacyclic allenes. *Nat. Chem.* **2018**, *10*, 953–960.
- (29) Yamano, M. M.; Knapp, R. R.; Ngamnithiporn, A.; Ramirez, M.; Houk, K. N.; Stoltz, B. M.; Garg, N. K. Cycloadditions of oxacyclic allenes and a catalytic asymmetric entryway to enantioenriched cyclic allenes. *Angew. Chem., Int. Ed.* **2019**, *58*, 5633–5657.
- (30) Ramirez, M.; Svatunek, D.; Liu, F.; Garg, N. K.; Houk, K. N. Origins of endo selectivity in Diels–Alder reactions of cyclic allene dienophiles. *Angew. Chem., Int. Ed.* **2021**, *60*, 14989–14997.
- (31) Lofstrand, V. A.; West, F. G. Efficient trapping of 1,2-cyclohexadienes with 1,3-dipoles. *Chem. Eur. J.* **2016**, *22*, 10763–10767.
- (32) Lofstrand, V. A.; McIntosh, K. C.; Almealmadi, Y. A.; West, F. G. Strain-activated Diels–Alder trapping of 1,2-cyclohexadienes: Intramolecular capture by pendant furans. *Org. Lett.* **2019**, *21*, 6231–6234.
- (33) Almealmadi, Y. A.; West, F. G. A mild method for the generation and interception of 1,2-cycloheptadienes with 1,3-dipoles. *Org. Lett.* **2020**, *22*, 6091–6095.

- (34) Wang, B.; Constantin, M.-G.; Singh, S.; Zhou, Y.; Davis, R. L.; West, F. G. Generation and trapping of electron-deficient 1,2-cyclohexadienes. Unexpected hetero-Diels–Alder reactivity. *Org. Biomol. Chem.* **2021**, *19*, 399–405.
- (35) Jankovic, C. L.; West, F. G. 2 + 2 Trapping of acyloxy-1,2-cyclohexadienes with styrenes and electron-deficient olefins. *Org. Lett.* **2022**, *24*, 9497–9501.
- (36) Nendel, M.; Tolbert, L. M.; Herring, L. E.; Islam, M. N.; Houk, K. N. Strained allenes as dienophiles in the Diels–Alder reaction: An experimental and computational study. *J. Org. Chem.* **1999**, *64*, 976–983.
- (37) Yamano, M. M.; Kelleghan, A. V.; Shao, Q.; Giroud, M.; Simmons, B. J.; Li, B.; Chen, S.; Houk, K. N.; Garg, N. K. Interception fleeting cyclic allenes with asymmetric nickel catalysis. *Nature* **2020**, *586*, 242–247.
- (38) Kelleghan, A. V.; Witkowski, D. C.; McVeigh, M. S.; Garg, N. K. Palladium-catalyzed annulations of strained cyclic allenes. *J. Am. Chem. Soc.* **2021**, *143*, 9338–9342.
- (39) McVeigh, M. S.; Garg, N. K. Interception of 1,2-cyclohexadiene with TEMPO radical. *Tetrahedron Lett.* **2021**, *87*, 153539–153543.
- (40) Westphal, M. V.; Hudson, L.; Mason, J. W.; Pradeilles, J. A.; Zécri, F. J.; Briner, K.; Schreiber, S. L. Water-compatible cycloadditions of oligonucleotide-conjugated strained allenes for DNA-encoded library synthesis. *J. Am. Chem. Soc.* **2020**, *142*, 7776–7782.

- (41) Ippoliti, F. M.; Adamson, N. J.; Wonilowicz, L. G.; Nasrallah, D. J.; Darzi, E. R.; Donaldson, J. S.; Garg, N. K. Total synthesis of lissodendoric acid A via stereospecific trapping of a strained cyclic allene. *Science* **2023**, *379*, 261–265.
- (42) Anthony, S. M.; Wonilowicz, L. G.; McVeigh, M. S.; Garg, N. K. Leveraging fleeting strained intermediates to access complex scaffolds. *JACS Au* **2021**, *1*, 897–912.
- (43) Spence, K. A.; Tena Meza, A.; Garg, N. K. Merging metals and strained intermediates. *Chem Catalysis* **2022**, *2*, 1870–1879.
- (44) In contrast, over 50 studies of cycloadditions or nucleophilic additions of 6-membered strained cyclic allenes are available in the literature. Similarly, arynes have been widely used in metal-catalyzed processes (for reviews, see: ref 3, 8, 42, 43).
- (45) For a report of palladacycle **3.8** being invoked in strained intermediate cocyclotrimerizations, see: Peña, D.; Pérez, D.; Guitián, E.; Castedo L. Selective palladium-catalyzed cocyclotrimerization of arynes with dimethyl acetylenedicarboxylate: A versatile method for the synthesis of polycyclic aromatic hydrocarbons. *J. Org. Chem.* **2000**, *65*, 6944–6950.
- (46) Baker, R. π -Allylmetal derivatives in organic synthesis. *Chem. Rev.* **1973**, *73*, 487–530.
- (47) Trost, B. Metal catalyzed allylic alkylations: Its development in the Trost laboratories. *Tetrahedron* **2015**, *71*, 5708–5733.

- (48) Dutta, S.; Bhattacharya, T.; Werz, D. B.; Maiti, D. Transition-metal-catalyzed C–H allylation reactions. *Chem* **2021**, *7*, 555–605.
- (49) Trost, B. M.; Crawley, M. L. Asymmetric transition-metal-catalyzed allylic alkylations: Applications in total synthesis. *Chem. Rev.* **2003**, *103*, 2921–2944.
- (50) Pàmies, O.; Margalef, J.; Cañellas, S.; James, J.; Judge, E.; Guiry, P. J.; Moberg, C.; Bäckvall, J.-E.; Pfaltz, A.; Pericàs, M. A.; Diégeuz, M. Recent advances in enantioselective Pd-catalyzed allylic substitution: From design to applications. *Chem. Rev.* **2021**, *121*, 4373–4505.
- (51) Wang, C.; Pahadi, N.; Tunge, J. A. Decarboxylative cyclizations and cycloadditions of palladium-polarized aza-*ortho*-xylylenes. *Tetrahedron* **2009**, *65*, 5102–5109.
- (52) Li, T.-R.; Wang, Y.-N.; Xiao, W.-J.; Lu, L.-Q. Transition-metal-catalyzed cyclization reactions using vinyl and ethynyl benzoxazinones as dipole precursors. *Tetrahedron Lett.* **2018**, *59*, 1521–1530.
- (53) Zuo, L.; Liu, T.; Chang, X.; Guo, W. An update of transition metal-catalyzed decarboxylative transformations of cyclic carbonates and carbamates. *Molecules* **2019**, *24*, 3930–3945.

- (54) Tian, Y.; Duan, M.; Liu, J.; Fu, S.; Dong, K.; Yue, H.; Hou, Y.; Zhao, Y. Recent advances in metal-catalyzed decarboxylative reactions of vinyl benzoxazinones. *Adv. Synth. Catal.* **2021**, *363*, 4461–4474.
- (55) You, Y.; Li, Q.; Zhang, Y.-P.; Zhao, J.-Q.; Wang, Z.-H.; Yuan, W.-C. Advances in palladium-catalyzed decarboxylative cycloadditions of cyclic carbonates, carbamates, and lactones. *ChemCatChem* **2022**, *14*, e202101887.
- (56) Duan, S.; Cheng, B.; Duan, X.; Bao, B.; Li, Y.; Zhai, H. Synthesis of *cis*-5,5a,6,10b-tetrahydroindeno[2,1-*b*]indoles through palladium-catalyzed decarboxylative coupling of vinyl benzoxazinones with arynes. *Org. Lett.* **2018**, *20*, 1417–1420.
- (57) Feng, M.; Tang, B.; Wang, N.; Xu, H.-X.; Jiang, X. Ligand controlled regiodivergent C₁ insertion on arynes for construction of phenanthridinone and acridone alkaloids. *Angew. Chem., Int. Ed.* **2015**, *54*, 14960–14964.
- (58) We hypothesize that fluoride-mediated detosylation of the vinyl benzoxazinone could be responsible for decomposition, see: Carato, P.; Yous, S.; Sellier, D.; Poupaert, J. H.; Lebegue, N.; Berthelot, P. Efficient and selective deprotection method for *N*-protected 2(3*H*)-benzoxazolones and 2(3*H*)-benzothiazolones. *Tetrahedron* **2004**, *60*, 10321–10324.
- (59) Yield of **3.26** represents a combined yield of tri- and tetracyclic isomers (16:1), see Section 3.8.2.3 for details.

- (60) Zimmer, R.; Dinesh, C. U.; Nandan, E.; Khan, F. A. Palladium-catalyzed reactions of allenes. *Chem. Rev.* **2000**, *100*, 3067–3125.
- (61) How specific ligands influence regioselectivity in the migratory insertion step of the proposed mechanism is not presently understood. However, ligand-guided regioselectivity in trapping π -allylpalladium species with conventional nucleophiles is not uncommon; see refs 46 and 47.
- (62) We hypothesize that the trans diastereomer is obtained as the major product due to a destabilizing steric interaction in the presumed transition state leading to the cis diastereomer. Specifically, a steric interaction between the vinyl group and the π -allyl fragment may disfavor formation of the cis product.
- (63) Empirically, **3.49** and **3.50** gave optimal yields and ee in comparison to other substrate combinations and, therefore, were used in subsequent optimization.
- (64) **3.49** was recovered (<30%) in 10% ee. This finding will be subject to further investigation.
- (65) Efforts to improve ee by varying easily-modifiable parameters such as solvent, concentration, and stoichiometry, led to no improvement. Future efforts beyond the present proof-of-principle study will be aimed toward improving enantioselectivity.
- (66) Havlík, M.; Dolenský, B.; Jakubek, M.; Král, V. Synthesis of unsymmetrical Tröger's bases bearing groups sensitive to reduction. *Eur. J. Org. Chem.* **2014**, *2014*, 2798–2805.

- (67) Li, T.-R.; Tan, F.; Lu, L.-Q.; Wei, Y.; Wang, Y.-N.; Liu, Y.-Y.; Yang, Q.-Q.; Chen, J.-R.; Shi, D.-Q.; Xiao, W.-J. Asymmetric trapping of zwitterionic intermediates by sulphur ylides in a palladium-catalysed decarboxylation-cycloaddition sequence. *Nat. Commun.* **2014**, *5*, 5500–5509.
- (68) Guo, C.; Fleige, M.; Janssen-Müller, D.; Daniliuc, C. G.; Glorius, F. Cooperative N-heterocyclic carbene/palladium-catalyzed enantioselective umpolung annulations. *J. Am. Chem. Soc.* **2016**, *138*, 7840–7843.
- (69) Tucker, Z. D.; Hill, H. M.; Smith, A. L.; Ashfeld, B. L. Diverting β -hydride elimination of a π -allyl Pd^{II} carbene complex for the assembly of disubstituted indolines via a highly diastereoselective (4+1)-cycloaddition. *Org. Lett.* **2020**, *22*, 6605–6609.
- (70) Lu, C.-H.; Darvishi, S.; Khakyzadeh, V.; Li, C. Pd-catalyzed enantioselective synthesis of 2-methy-3-methyleneindoline. *Chin. Chem. Lett.* **2021**, *32*, 405–407.
- (71) Sheldrick, G. M. (1996). *SADABS*. University of Göttingen, Germany.
- (72) Sheldrick, G. M. Crystal structure refinement with SHELXL. *Acta Cryst. C* **2015**, *71*, 3–8.

CHAPTER FOUR

Interception of 1,2-Cyclohexadiene with TEMPO Radical

Matthew S. McVeigh and Neil K. Garg

Tetrahedron Lett. **2021**, 87, 153539.

4.1 Abstract

Transient strained cyclic intermediates, such as strained cyclic allenes, are useful building blocks for the synthesis of structurally and stereochemically complex scaffolds. Trappings of strained cyclic allenes are thought to occur primarily through either two or one electron processes. Regarding the latter, diradical intermediates have been invoked in (2+2) cycloadditions and (3+2) nitrene cycloadditions. The present study questions if a monoradical pathway could exist for strained cyclic allene reactivity, as examined in the reaction of 1,2-cyclohexadiene and TEMPO radical. Our findings suggest the viability of this monoradical pathway.

4.2 Introduction

The structure and reactivity of transient strained cyclic intermediates, such as arynes, cyclic alkynes, and cyclic allenes (e.g., **4.1–4.5**, Figure 4.1A) have drawn interest from the scientific community over the last century.^{1,2,3} Of particular interest to our laboratory are strained cyclic allenes, such as 1,2-cyclohexadiene (**4.5**), which were first experimentally validated in the 1960s.^{4,5} Recently, a number of synthetic transformations using strained cyclic allenes have been reported,^{6,7,8,9,10,11,12,13,14,15,16,17,18,19,20} with cycloaddition reactions providing an opportunity to

generate structural and stereochemical complexity (Figure 4.1B). Notably, strained cyclic allenes are thought to react through both two and one electron pathways.²¹ For example, the (4+2) cycloaddition between **4.5** and furan (**4.6**) to afford **4.7** is suggested to be a concerted and asynchronous process,^{16,22} whereas the (3+2) cycloaddition between **4.5** and nitrene **4.8** to provide **4.9** is believed to involve competing two and one electron pathways.¹⁵ In the case of the (2+2) cycloaddition between styrene (**4.10**) and **4.5** to furnish **4.11**, one electron chemistry is thought to occur.²³ This latter example indicates the presence of diradical intermediate **4.12**. In the present study, we questioned if a strained cyclic allene could be intercepted to give monoradical intermediates **4.13**.^{24,25}

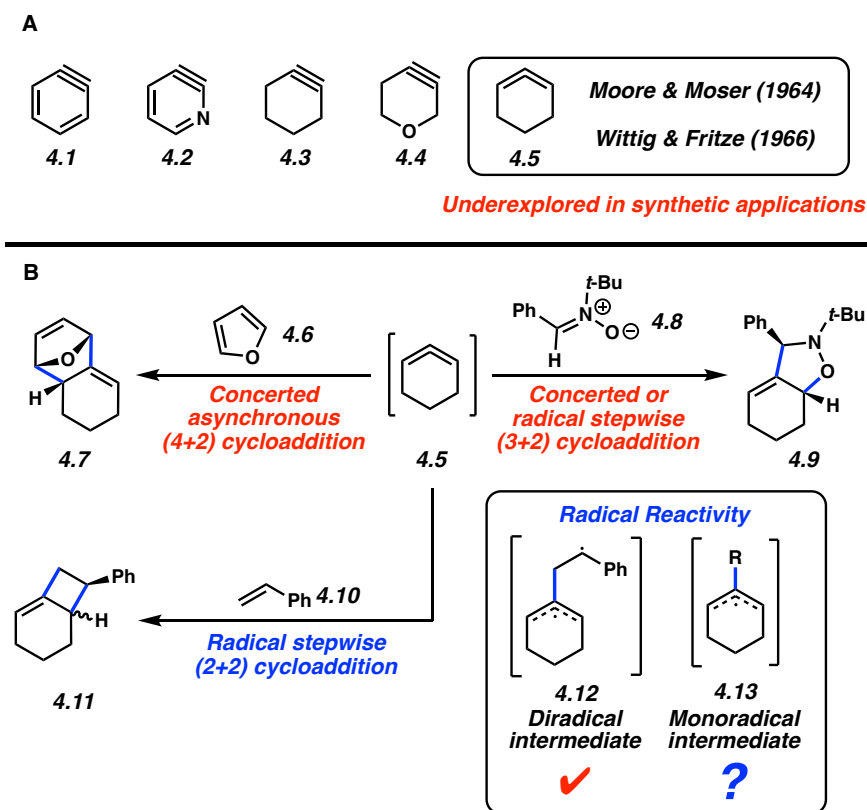


Figure 4.1. Selected *in situ* generated strained intermediates and the reactivity of 1,2-cyclohexadiene (**4.5**) in cycloaddition reactions.

4.3 Reactivity of 1,2-Cyclohexadiene with TEMPO Radical

To investigate the reactivity of strained cyclic allenes with monoradicals, we pursued the transformation shown in Figure 4.2. Silyl triflate **4.14**, a well-established precursor to 1,2-cyclohexadiene, was treated with (2,2,6,6-tetramethylpiperidin-1-yl)oxyl (TEMPO, **4.15**) in the presence of CsF at 80 °C. To our surprise, ketone **4.16** formed as the major product (>20:1 dr). Compound **4.16** had previously been prepared by Studer and co-workers, which provided validation of our structural assignment.²⁶

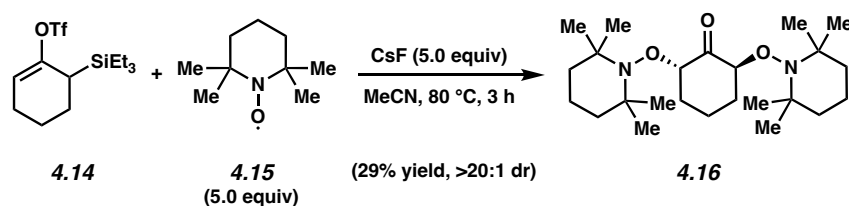


Figure 4.2. The reaction of *in situ* generated 1,2-cyclohexadiene and **4.15** to afford ketone **4.16**.

4.4 Reaction Mechanism

A plausible mechanism for the formation of ketone **4.16** is shown in Figure 4.3. Generation of **4.5** would occur *via* standard fluoride-mediated 1,2-elimination of silyl triflate **4.14**.⁶ Subsequently, one molecule of TEMPO (**4.15**) would react with **4.5** *in situ* to afford monoradical intermediate **4.17**. An additional equivalent of **4.15** would then combine with **4.17**, providing bis(alkoxyamine) **4.18**. Formation of α -carbonyl radical **4.19** would arise from homolytic fragmentation of **4.18**.²⁷ Trapping of radical **4.19** with a third equivalent of **4.15** would furnish the observed ketone **4.16**.²⁸

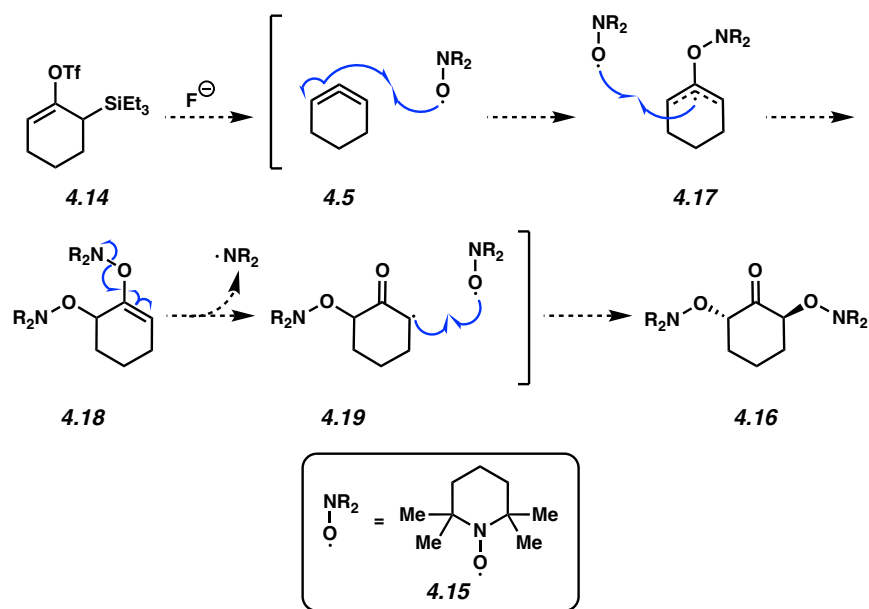


Figure 4.3. Potential mechanism for the formation of ketone **4.16**.

4.5 Isotopic Labeling Study

To provide evidence for the proposed mechanism, an isotope labeling study was performed, as summarized in Figure 4.4. ^{18}O -enriched **4.15**, prepared from the corresponding *N*-oxoammonium salt,²⁹ was combined with silyl triflate **4.14** and CsF at 80 °C to afford ketone **4.16**. Analysis of the isotopic distribution of ketone **4.16** by high resolution mass spectrometry demonstrated incorporation of ^{18}O at three sites in **4.16** (33% $^{18}\text{O}/^{18}\text{O}/^{18}\text{O}$). Additionally, the experimental isotopic distribution of **4.16** agreed with the expected distribution values when considering the proposed mechanism. We postulate that the observed labeling of the ketone oxygen arises from TEMPO (**4.15**) reacting with a strained cyclic allene intermediate to give monoradical **4.17**. Of note, no reaction between **4.14** and **4.15** occurs in the absence of CsF, which is indicative of cyclic allene formation en route to **4.16**. Moreover, exposure of non-labeled **4.16** to H_2^{18}O under standard reaction conditions did not lead to ^{18}O incorporation.

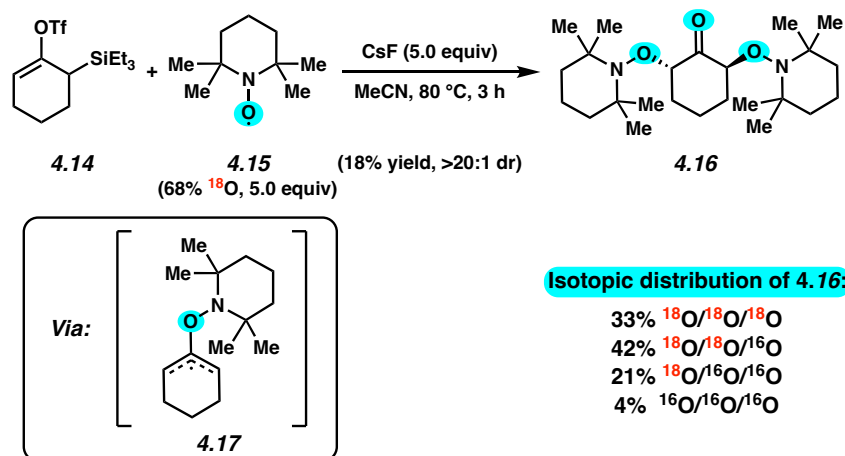


Figure 4.4. Isotope labeling study leveraging ^{18}O enriched TEMPO (**4.15**).

4.6 Conclusion

In summary, we have demonstrated the trapping of 1,2-cyclohexadiene (**4.5**) with TEMPO radical (**4.15**). The transformation gives rise to ketone **4.16**, which we surmise involves the consumption of three TEMPO (**4.15**) molecules. This suggests the possible trapping of a cyclic allene to give a monoradical intermediate and should prompt further investigation into one electron chemistry of strained cyclic allenes.

4.7 Experimental Section

4.7.1 Materials and Methods

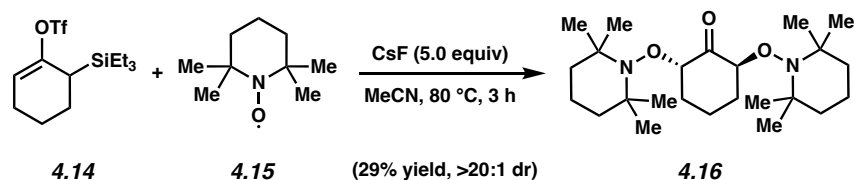
Unless stated otherwise, reactions were conducted in oven-dried glassware under an atmosphere of nitrogen using anhydrous solvents (passed through activated alumina columns). All commercially obtained reagents were used as received unless otherwise specified. (2,2,6,6-tetramethylpiperidin-1-yl)oxyl (TEMPO, **4.15**) was purchased from Sigma-Aldrich. Cesium fluoride (CsF) was obtained from Strem Chemicals. Reaction temperatures were controlled using an IKA Mag temperature modulator. Thin-layer chromatography (TLC) was conducted with EMD gel 60 F₂₅₄ pre-coated plates (0.25 mm for analytical chromatography and 0.50 mm for preparative

chromatography) and visualized using a combination of UV and potassium permanganate staining techniques. ^1H NMR spectra were recorded on Bruker spectrometers (500 and 600 MHz) and are reported relative to residual solvent signals. DART-MS spectra were collected on a Thermo Exactive Plus MSD (Thermo Scientific) equipped with an ID-CUBE ion source and a Vapor Interface (IonSense Inc.). Both the source and MSD were controlled by Excalibur software v. 3.0. The analyte was spotted onto OpenSpot sampling cards (IonSense Inc.) using CH_2Cl_2 as the solvent. Ionization was accomplished using UHP He plasma with no additional ionization agents. The mass calibration was carried out using Pierce LTQ Velos ESI (+) and (-) Ion calibration solutions (Thermo Fisher Scientific).

Note: Supporting information for the synthesis of silyl triflate **4.14**,¹³ has been published, and spectral data match those previously reported.

4.7.2 Experimental Procedures

4.7.2.1 1,2-Cyclohexadiene trapping with TEMPO (4.15)

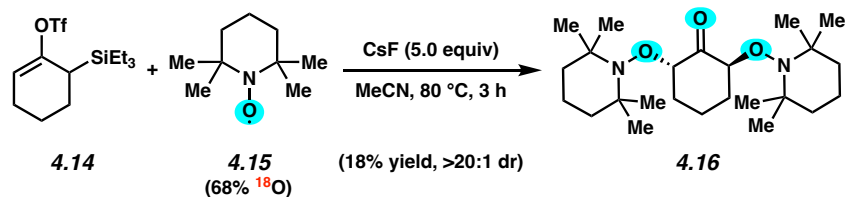


Ketone 4.16. To a stirred solution of silyl triflate **4.14** (17.2 mg, 50.0 μmol , 1.0 equiv) and TEMPO (**4.15**) (39.1 mg, 250 μmol , 5.0 equiv) in MeCN (0.5 mL, 0.1 M) was added CsF (38.0 mg, 250 μmol , 5.0 equiv). The reaction vessel was purged with N_2 , sealed with a teflon cap, and placed in a preheated, 80 $^\circ\text{C}$ aluminum heating block. After stirring for 3 h, the reaction was cooled to 23 $^\circ\text{C}$. The resultant dark red solution was filtered through a plug of silica gel (EtOAc eluent, 10 mL)

and concentrated under reduced pressure to afford a crude red solid. Purification by preparative thin layer chromatography (9:1 hexanes:ethyl acetate) provided ketone **4.16** (29% yield, >20:1 dr by ^1H NMR analysis of the crude material, average of two experiments) as a pale-brown solid. Ketone **4.16**: Spectral data match those previously reported.²⁶

4.7.2.2 Isotope labeling study with ^{18}O -enriched **4.15**

^{18}O -enriched TEMPO (**4.15**) was synthesized according to literature procedures.²⁹ Approximately 68% ^{18}O -enriched **4.15** was accessed (see Figure 4.5).



Ketone 4.16. To a stirred solution of silyl triflate **4.14** (8.0 mg, 23.2 μmol , 1.0 equiv) and ^{18}O enriched TEMPO (**4.15**) (18.1 mg, 116 μmol , 5.0 equiv) in MeCN (0.23 mL, 0.1 M) was added CsF (17.6 mg, 116 μmol , 5.0 equiv). The reaction vessel was purged with N_2 , sealed with a teflon cap, and placed in a preheated, 80 °C aluminum heating block. After stirring for 3 h, the reaction was cooled to 23 °C. The resultant dark red solution was filtered through a plug of silica gel (EtOAc eluent, 10 mL) and concentrated under reduced pressure to afford a crude red solid. Purification by preparative thin layer chromatography (9:1 hexanes:ethyl acetate) provided ketone **4.16** (18% yield, >20:1 dr by ^1H NMR analysis of the crude material) as a pale-brown solid. Ketone **4.16**: Spectral data match those previously reported.^{Error! Bookmark not defined.} The isotopic distribution of ketone **4.16** amounted to 33% $^{18}\text{O}/^{18}\text{O}/^{18}\text{O}$, 42% $^{18}\text{O}/^{18}\text{O}/^{16}\text{O}$, 21% $^{18}\text{O}/^{16}\text{O}/^{16}\text{O}$, 4% $^{16}\text{O}/^{16}\text{O}/^{16}\text{O}$ (see Figure 4.6).

4.8 Spectra Relevant to Chapter Four:

Interception of 1,2-Cyclohexadiene with TEMPO Radical

Matthew S. McVeigh and Neil K. Garg

Tetrahedron Lett. **2021**, 87, 153539.

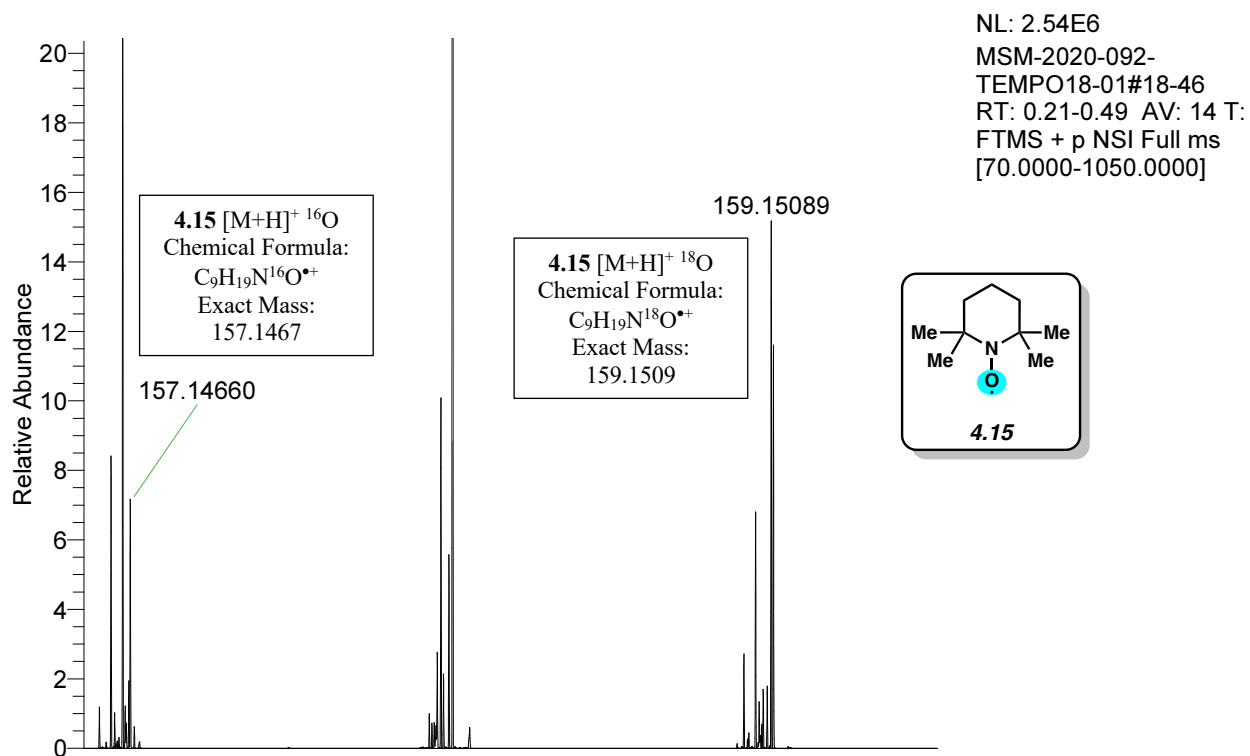


Figure 4.5. HRMS spectrum of compound **4.15**.

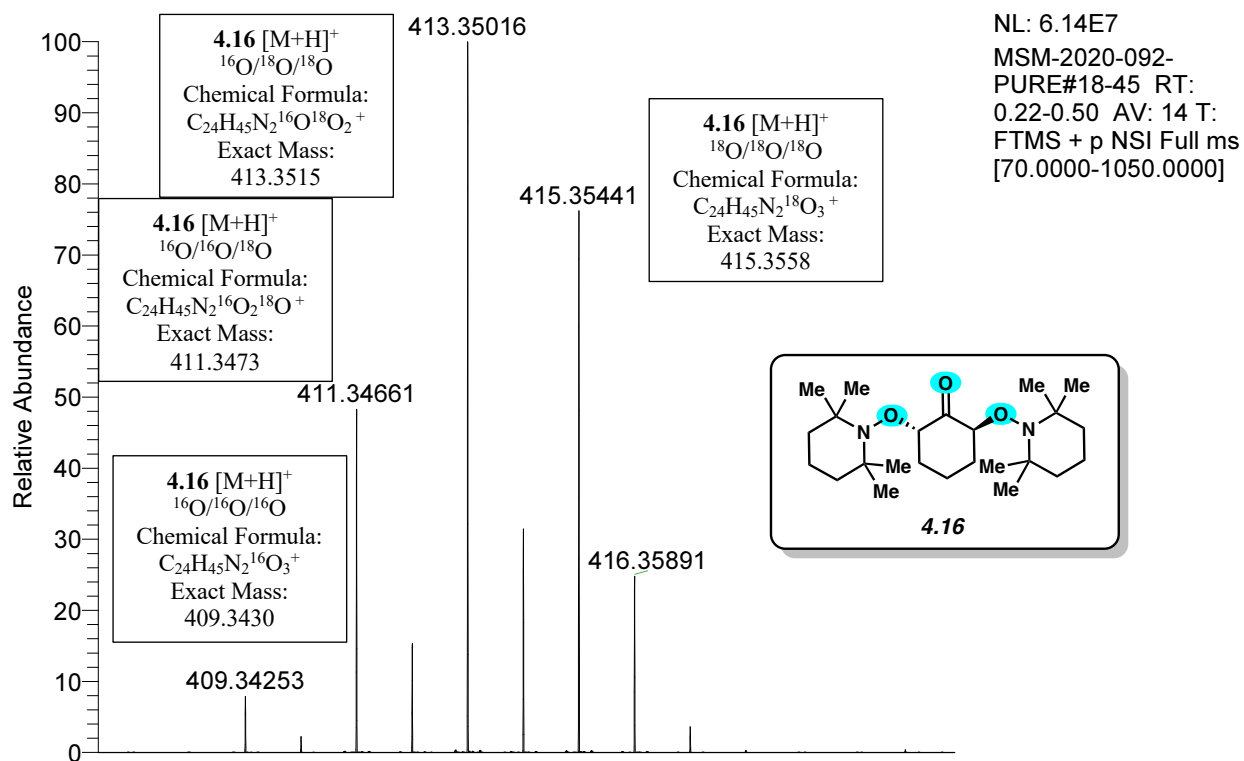
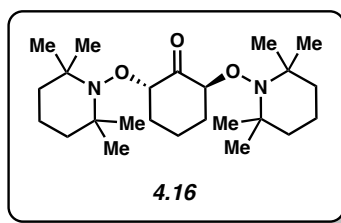


Figure 4.6. HRMS spectrum of compound **4.16**.



Purified product, ¹H NMR

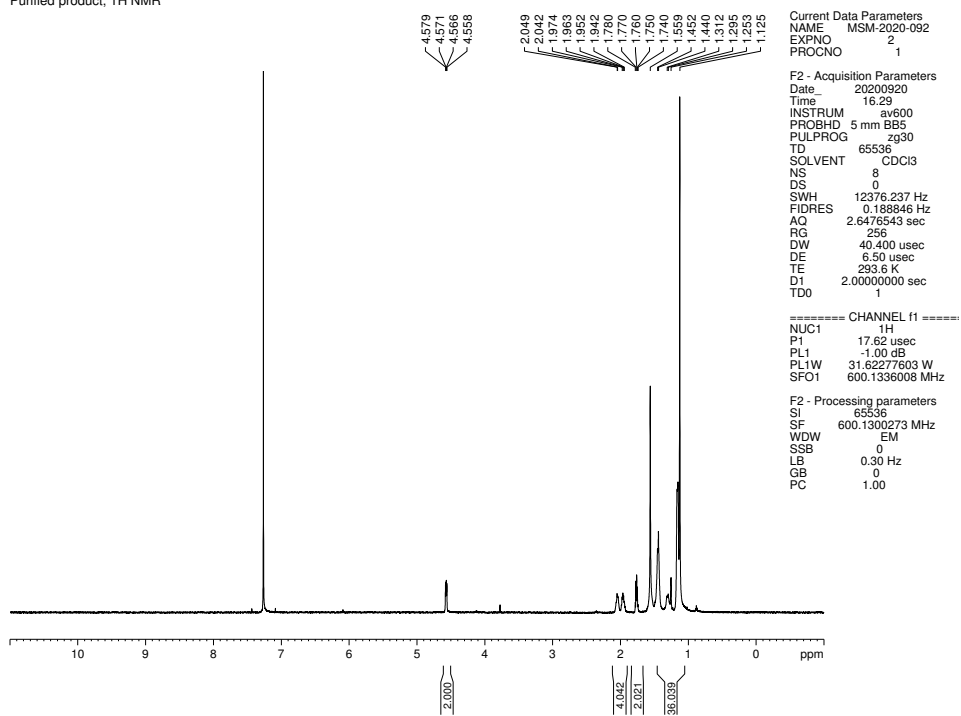


Figure 4.7. ¹H NMR (600 MHz, CDCl₃) of compound **4.16**.

4.9 Notes and References

- (1) Wenk, H. H.; Winkler, M.; Sander, W. One century of aryne chemistry. *Angew. Chem., Int. Ed.* **2003**, *42*, 502–528.
- (2) Shi, J.; Li, L.; Li, Y. *o*-Silylaryl triflates: A journey of Kobayashi aryne precursors. *Chem. Rev.* **2021**, *121*, 3892–4044.
- (3) Anthony, S. M.; Wonilowicz, L. G.; McVeigh, M. S.; Garg, N. K. Leveraging fleeting strained intermediates to access complex scaffolds. *JACS Au* **2021**, *1*, 897–912.
- (4) Moser, W. R. The reactions of *gem*-dihalocyclopropanes with organometallic reagents. Ph.D. Thesis, Massachusetts Institute of Technology: Cambridge, MA, January 1964.
- (5) Wittig, G.; Fritze, P. On the intermediate occurrence of 1,2-cyclohexadiene. *Angew. Chem., Int. Ed. Engl.* **1966**, *5*, 846.
- (6) Quintana, I.; Peña, D.; Pérez, D.; Guitián, E. Generation and reactivity of 1,2-cyclohexadiene under mild reaction conditions. *Eur. J. Org. Chem.* **2009**, *2009*, 5519–5524.
- (7) Peña, D.; Iglesias, B.; Quintana, I.; Pérez, D.; Guitián, E.; Castedo, L. Synthesis and reactivity of new strained cyclic allene and alkyne precursors. *Pure Appl. Chem.* **2009**, *78*, 451–455.
- (8) Lofstrand, V. A.; West, F. G. Efficient trapping of 1,2-cyclohexadienes with 1,3-dipoles. *Chem. Eur. J.* **2016**, *22*, 10763–10767.

- (9) Lofstrand, V. A.; McIntosh, K. C.; Almehmadi, Y. A.; West, F. G. Strain-activated Diels–Alder trapping of 1,2-cyclohexadienes: Intramolecular capture by pendent furans. *Org. Lett.* **2019**, *21*, 6231–6234.
- (10) Almehmadi, Y. A.; West, F. G. A mild method for the generation and interception of 1,2-cycloheptadienes with 1,3-dipoles. *Org. Lett.* **2020**, *22*, 6091–6095.
- (11) Wang, B.; Constantin, M.-G.; Singh, S.; Zhou, Y.; Davis, R. L.; West, F. G. Generation and trapping of electron-deficient 1,2-cyclohexadienes. Unexpected hetero-Diels–Alder reactivity. *Org. Biomol. Chem.* **2021**, *19*, 399–405.
- (12) Hioki, Y.; Mori, A.; Okano, K. Steric effects on deprotonative generation of cyclohexynes and 1,2-cyclohexadienes from cyclohexenyl triflates by magnesium amides. *Tetrahedron* **2020**, *76*, 131103.
- (13) Inoue, K.; Nakura, R.; Okano, K.; Mori, A. One-pot synthesis of silylated enol triflates from silyl enol ethers for cyclohexynes and 1,2-cyclohexadienes. *Eur. J. Org. Chem.* **2018**, *2018*, 3343–3347.
- (14) Westphal, M. V.; Hudson, L.; Mason, J. W.; Pradeilles, J. A.; Zecri, F. J.; Briner, K.; Schreiber, S. L. Water-compatible cycloadditions of oligonucleotide-conjugated strained allenes for DNA-encoded library synthesis. *J. Am. Chem. Soc.* **2020**, *142*, *17*, 7776–7782.
- (15) Barber, J. S.; Styduhar, E. D.; Pham, H. V.; McMahon, T. C.; Houk, K. N.; Garg, N. K. Nitronc cycloadditions of 1,2-cyclohexadiene. *J. Am. Chem. Soc.* **2016**, *138*, 2512–2515.

- (16) Barber, J. S.; Yamano, M. M.; Ramirez, M.; Darzi, E. R.; Knapp, R. R.; Liu, F.; Houk, K. N.; Garg, N. K. Diels–Alder cycloadditions of strained azacyclic allenes. *Nat. Chem.* **2018**, *10*, 953–960.
- (17) Yamano, M. M.; Knapp, R. R.; Ngamnithiporn, A.; Ramirez, M.; Houk, K. N.; Stoltz, B. M.; Garg, N. K. Cycloadditions of oxacyclic allenes and a catalytic asymmetric entryway to enantioenriched cyclic allenes. *Angew. Chem., Int. Ed.* **2019**, *58*, 5653–5657.
- (18) McVeigh, M. S.; Kelleghan, A. V.; Yamano, M. M.; Knapp, R. R.; Garg, N. K. Silyl tosylate precursors to cyclohexyne, 1,2-cyclohexadiene, and 1,2-cycloheptadiene. *Org. Lett.* **2020**, *22*, 4500–4504.
- (19) Yamano, M. M.; Kelleghan, A. V.; Shao, Q.; Giroud, M.; Simmons, B. J.; Li, B.; Chen, S.; Houk, K. N.; Garg, N. K. Intercepting fleeting cyclic allenes with asymmetric nickel catalysis. *Nature* **2020**, *586*, 242–247.
- (20) Kelleghan, A. V.; Witkowski, D. C.; McVeigh, M. S.; Garg, N. K. Palladium-catalyzed annulations of strained cyclic allenes. *J. Am. Chem. Soc.* **2021**, *143*, 9338–9342.
- (21) Nendel, M.; Tolbert, L. M.; Herring, L. E.; Islam, M. N.; Houk, K. N. Strained allenes as dienophiles in the Diels–Alder reaction: An experimental and computational study. *J. Org. Chem.* **1999**, *64*, 976–983.
- (22) Ramirez, M.; Svatunek, D.; Liu, F.; Garg, N. K.; Houk, K. N. Origins of endo selectivity in Diels–Alder reactions of cyclic allene dienophiles. *Angew. Chem, Int. Ed.* **2021**, *60*, 14989–14997.

- (23) For an extensive overview of the mechanistic investigations toward the (2+2) cycloadditions of strained cyclic allenes, see: Christl, M. Cyclic allenes up to seven-membered rings. *Modern Allene Chemistry*; Krause, N., Kashmi, S. A. K., Eds.; Wiley-VCH: Weinheim, 2004; pp 243–357.
- (24) For a recent study on monoradical-mediated cascade reactions of arynes, see: Scherübel, M.; Daniliuc, C. G.; Studer, A. Arynes as radical acceptors: TEMPO-mediated cascades comprising addition, cyclization, and trapping. *Angew. Chem., Int. Ed.* **2021**, *60*, 711–715.
- (25) For the trapping of cyclic allene dimerization intermediates with monoradicals, see: Bottini, A. T.; Cabral, L. J.; Dev, V. Role of added di-*t*-butylnitroxide in reactions of 1-iodocyclohexenes with potassium *t*-butoxide in dimethyl sulfoxide: Trapping of intermediate diradicals. *Tetrahedron Lett.* **1977**, 615–618.
- (26) Li, Y.; Pouliot, M.; Vogler, T.; Renaud, P.; Studer, A. α -Aminoxylation of ketones and β -chloro- α -aminoxylation of enones with TEMPO and chlorocatecholborane. *Org. Lett.* **2012**, *14*, 4474–4477.
- (27) This mode of homolytic fragmentation has been proposed in a TEMPO-mediated transformation, see: de la Torre, A.; Kaiser, D.; Maulide, N. Flexible and chemoselective oxidation of amides to α -keto amides and α -hydroxy amides. *J. Am. Chem. Soc.* **2017**, *139*, 6578–6581.

- (28) We propose that the high diastereoselectivity of the transformation could arise from the steric bias of the alkoxyamine substituent disfavoring *syn* addition of an additional TEMPO equivalent to intermediate **4.19**.
- (29) Jie, X.; Shang, Y.; Chen, Z.-N.; Zhang, X.; Zhuang, W.; Su, W. Differentiation between enamines and tautomerizable imines in the oxidation reaction with TEMPO. *Nat. Commun.* **2018**, *9*, 5002.

CHAPTER FIVE

Access to Complex Scaffolds Through [2+2] Cycloadditions of Strained Cyclic Allenes

Matthew S. McVeigh,[†] Jacob P. Sorrentino,[†] Allison T. Hands, and Neil K. Garg

J. Am. Chem. Soc. **2024**, *In Press*. doi.org/10.1021/jacs.4c03369

5.1 Abstract

We report the strain-induced [2+2] cycloadditions of cyclic allenes for the assembly of highly substituted cyclobutanes. By judicious choice of trapping agent, complex scaffolds bearing heteroatoms, fused rings, contiguous stereocenters, spirocycles, and quaternary centers are ultimately accessible. Moreover, we show that the resulting cycloadducts can undergo thermal isomerization. This study provides an alternative strategy to photochemical [2+2] cycloadditions for accessing highly functionalized cyclobutanes, while validating the use of underexplored strained intermediates for the assembly of complex architectures.

5.2 Introduction

Stereochemically complex scaffolds have become increasingly desirable in the discovery of bioactive molecules.^{1,2} One such motif, the substituted cyclobutane, is present in biologically relevant compounds and many natural products.^{3,4,5,6} Its rigid scaffold possesses distinct exit vectors that can be used to ultimately improve biological properties.^{3,6} Several representative cyclobutane-containing compounds are shown in Figure 5.1A: anti-viral agent Lobucavir (**5.1**),⁷ kinase inhibitor **5.2**,⁸ cannabinoid **5.3**,⁹ and natural products such as welwitindolinone A isonitrile (**5.4**),^{10,11} arnamial (**5.5**),¹² and scopariusicide A (**5.6**).¹³

Cyclobutanes are commonly introduced synthetically using feedstock fragments or cycloaddition reactions. Methods to introduce cyclobutanes have been reviewed^{3,14,15} and several elegant approaches have recently been reported, including those by Wilkerson–Hill,¹⁶ Yoon,^{17,18} and Brown.^{19,20,21} With regard to cycloadditions, photochemical [2+2] cycloadditions, which leverage in situ-generated photoexcited intermediates, are most common.^{22,23} Notably, harnessing these intermediates for regio- and stereoselective syntheses intermolecularly can be difficult, necessitating specialized reagents or catalysts.²⁴ As such, new methods for the synthesis of highly functionalized cyclobutanes bearing multiple stereocenters remain coveted.

An attractive yet underutilized approach to access highly functionalized cyclobutanes relies on strain-promoted reactivity. For example, arynes (e.g., **5.7a** and **5.7b**)^{25,26,27,28,29,30,31} and non-aromatic cyclic alkynes (e.g., **5.7c** and **5.7d**)^{32,33,34} are highly reactive, in situ-generated intermediates that can readily engage in [2+2] cycloadditions³⁵ due to their significant strain energies, typically ranging from 40–50 kcal/mol (Figure 5.1B).³⁶ A comparatively less well-studied class of compounds is strained cyclic allenes **5.8**.^{37,38,39} Like cyclic alkynes, strained cyclic allenes **5.8** contain a functional group that typically prefers a linear geometry, but is bent due to ring constraint, leading to significant strain energy (~30 kcal/mol).^{40,41} Although historically understudied, cyclic allenes **5.8** are emerging building blocks in the synthetic community.^{42,43,44,45,46,47,48,49} Recent advances include cycloaddition chemistry by West,^{44,50,51,52,53,54} the synthesis of DNA-encoded libraries by Schreiber,⁵⁵ and several studies from our laboratory,^{45,56,57,58,59,60,61,62,63,64,65,66,67} including the recent use of strained cyclic allenes in total synthesis.⁶⁸ With regard to [2+2] cycloadditions of strained cyclic allenes, seminal studies by Christl and others validated reactivity.^{69,70,71,72,73} More recently, elegant studies by West have demonstrated [2+2] cycloadditions of acetoxy-substituted carbocyclic allenes,⁵³ as well as

intramolecular trappings,⁵⁴ using silyl bromide precursors to cyclic allenes. Our laboratory has also reported scattered examples of [2+2] cycloadditions of cyclic allenes.^{56,57,62,66,74}

As part of a general program aimed at exploring the use of unconventional strained intermediates for the construction of complex scaffolds, we sought to investigate strain-driven [2+2] cycloadditions of cyclic allenes using the reaction design shown in Figure 5.1C. Cyclic allenes **5.8**, generated via fluoride-mediated 1,2-elimination of silyl triflates **5.9**, would engage with highly substituted alkenes **5.10** to afford densely functionalized cycloadducts **5.11**. As in other [2+2] cycloadditions, two new C–C bonds would form. Moreover, through the judicious choice of trapping partner, features indicative of structural complexity,^{75,76} such as heterocyclic frameworks,⁷⁷ spiro centers, contiguous stereocenters, and vicinal quaternary centers could be accessible under mild conditions. The transformation is accomplished without the need for metal-, Lewis acid-, or Brønsted acid catalysts; directing or auxiliary groups are also not required. Herein, we report the success of this approach to access highly functionalized cyclobutanes, which pushes the limits of complexity accessible from strained cyclic allene intermediates.

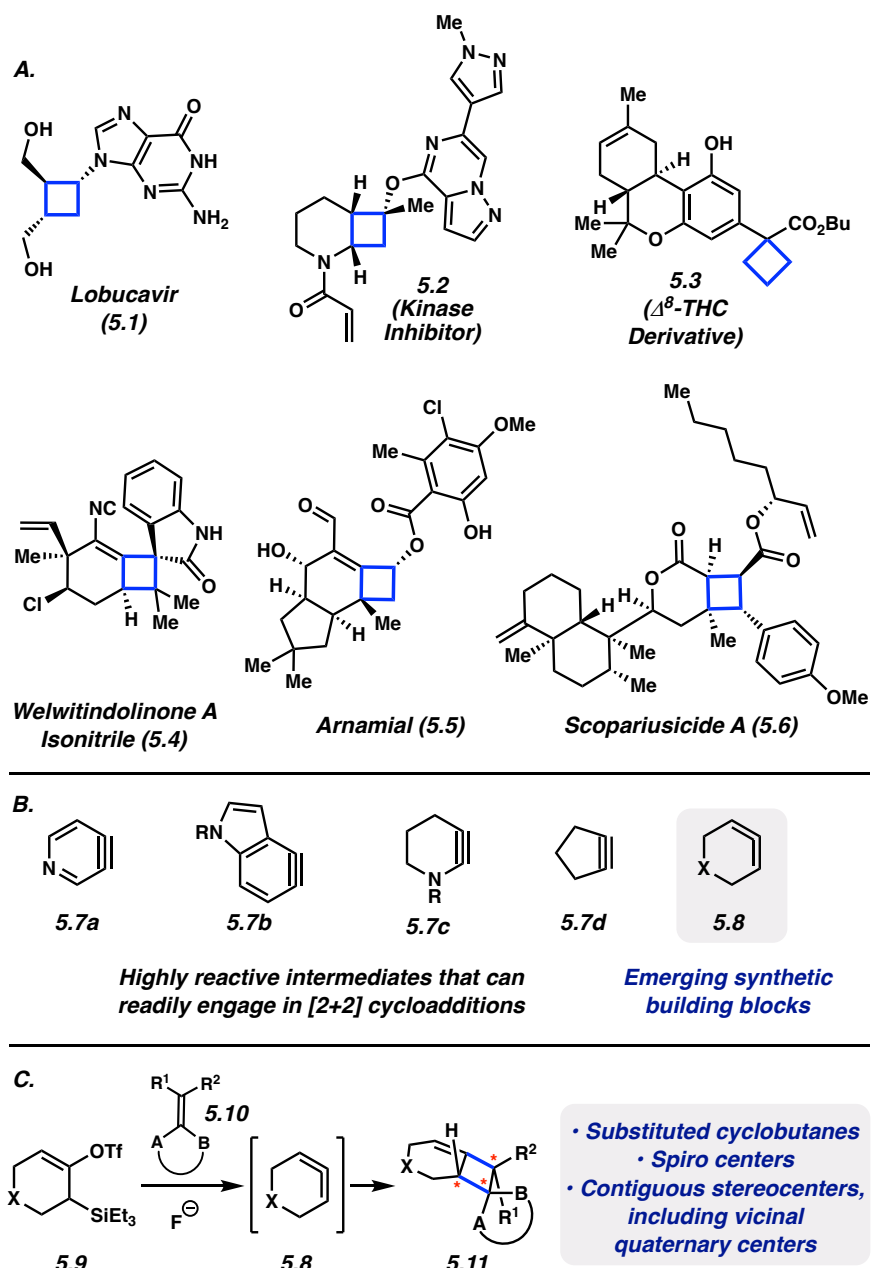


Figure 5.1. (A) Cyclobutane-containing, biologically relevant molecules **5.1–5.6**. (B) Strained cyclic intermediates **5.7a–d** and **5.8**. (C) Overview of the current study.

5.3 Surveying Exocyclic Alkenes in [2+2] Cycloaddition

To initiate these studies, we surveyed a range of exocyclic alkenes **5.14** in cyclic allene trapping experiments (Figure 5.2). Exocyclic alkenes are historically understudied in strained cyclic allene [2+2] cycloadditions, but if generally useful, would lead to the formation of desirable

spirocyclic products.^{6,78} Silyl triflate **5.12**, a precursor to oxacyclic allene **5.13**,^{57,79} was treated with CsF in the presence of exocyclic alkenes **5.14** at ambient temperatures to afford cycloadducts **5.15**. Reaction outcomes were then determined by ¹H NMR analysis. Notably, using unactivated alkene **5.16** afforded cycloadduct **5.17** in 42% yield (entry 1). Improved yields were seen when substrates containing an alkene with delocalized π -electrons were employed. For example, the electron-deficient alkene in α,β -unsaturated lactone **5.18** reacted to give cycloadduct **5.19** in high yield and moderate diastereoselectivity (entry 2). Similarly, electron-rich alkenes **5.20**, **5.22**, and **5.24** bearing heteroatoms could be employed and afforded cycloadducts **5.21**, **5.23**, and **5.25**, respectively (entries 3–5).⁸⁰ Lastly, leveraging styrene **5.26** in the transformation provided cycloadduct **5.27** in 94% yield and 2.8:1 diastereomeric ratio (dr) (entry 6). Based on the synthetic efficiency observed, we elected to further pursue trappings of substrates related to dienamine **5.24** and styrene **5.26** and further push the limits of complexity in the products.⁸¹

Several features of the reactions shown in Figure 5.2 should be noted: a) the reactions occur at ambient temperatures, b) yields and diastereomeric ratios are generally synthetically useful, although some variation in the latter was observed,⁸⁰ c) excellent regioselectivity is observed in each transformation,⁸² d) the general transformation allows for the formation of two new C–C bonds and typically two contiguous stereocenters, with access to further complexity being foreseeable based on the potential use of modified substrates, e) despite that strained cyclic allenes have historically been avoided, they can be used to readily access products containing three or more rings, including the desired spirocyclobutane and various heterocycles.

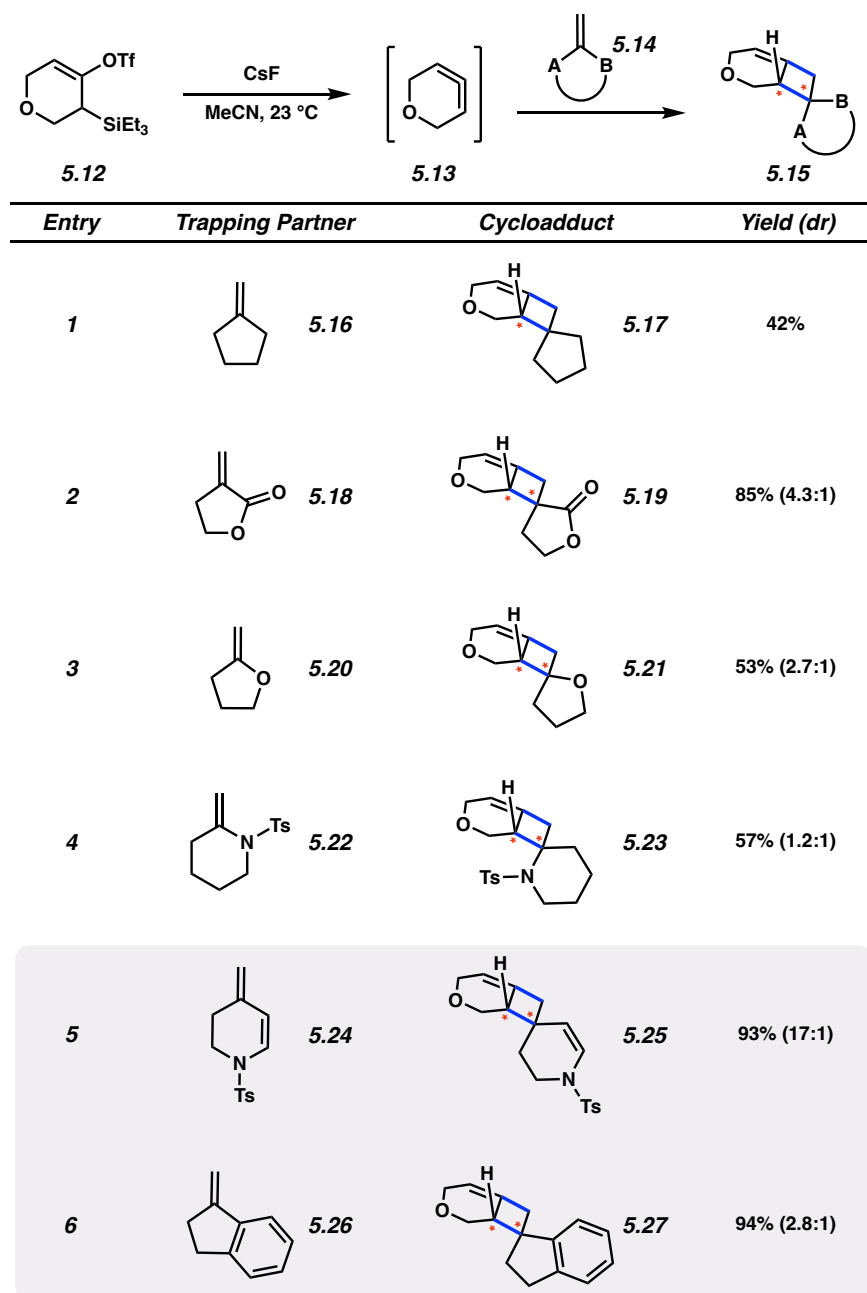


Figure 5.2. Survey of olefin partners **5.14** in [2+2] cycloaddition of oxacyclic allene **5.13**. Reactions conditions are as follows: **5.12** (1.0 equiv, 0.050 mmol), trapping partners **5.14** (5.0 equiv), CsF (5.0 equiv), MeCN (0.1 M), 23 °C, 3–4 h. Yields and dr determined by ^1H NMR analysis of the crude reaction mixture using mesitylene as an external standard.

5.4 Scope of [2+2] Cycloadditions with Dienamine Partners

Having selected two promising classes of cycloaddition partners (i.e., **5.24** and **5.26**)⁸¹ for further investigation, we assessed the scope of the methodology with respect to dienamines **5.28**

(Figure 5.3). Silyl triflate **5.12** and dienamines **5.28** were combined in the presence of CsF to afford cyclobutanes **5.29**. During early optimization efforts, it was found that a substoichiometric amount of tetrabutylammonium triflate (Bu₄NOTf) in dichloromethane as solvent was preferred when compared to acetonitrile.⁸³ Tetrabutylammonium salts are known to improve the solubility of fluoride ion in organic solvents^{84,85} and have been beneficial in prior studies of cyclic allene trapping reactions.^{60,62,64,68} Tosyl (Ts) and *tert*-butyloxycarbonyl (Boc) *N*-substituted substrates **5.24** and **5.30** could be employed, providing cycloadducts **5.25** and **5.31** in high yields and diastereoselectivities (entry 1). The use of tetrahydroazepine derivative **5.32** afforded **5.33** in 88% yield and 10:1 dr (entry 2). Increasingly substituted dienamines were tested as well. When **5.34** and **5.36** were utilized in the reaction, products **5.35** and **5.37** were obtained, which possess additional substitution on the cyclobutyl ring (entries 3 and 4, respectively). Notably, the trapping with **5.34** proceeds with moderate stereospecificity^{82,86} and results in cyclobutane **5.35**, containing three contiguous stereocenters. Substitution on the ring of the dienamine trapping partner was also tolerated. Employing iodo-substituted substrate **5.38** in the cycloaddition led to product **5.39**, whereas employment of **5.40** bearing a *gem*-dimethyl group furnished **5.41** (entries 5 and 6, respectively). The erosion in stereoselectivity when comparing the formation of **5.41** to **5.25** is attributed to the increased steric bulk from the *gem*-dimethyl group present in **5.41**.⁸⁷ Of note, cycloadduct **5.41** contains vicinal quaternary carbons.

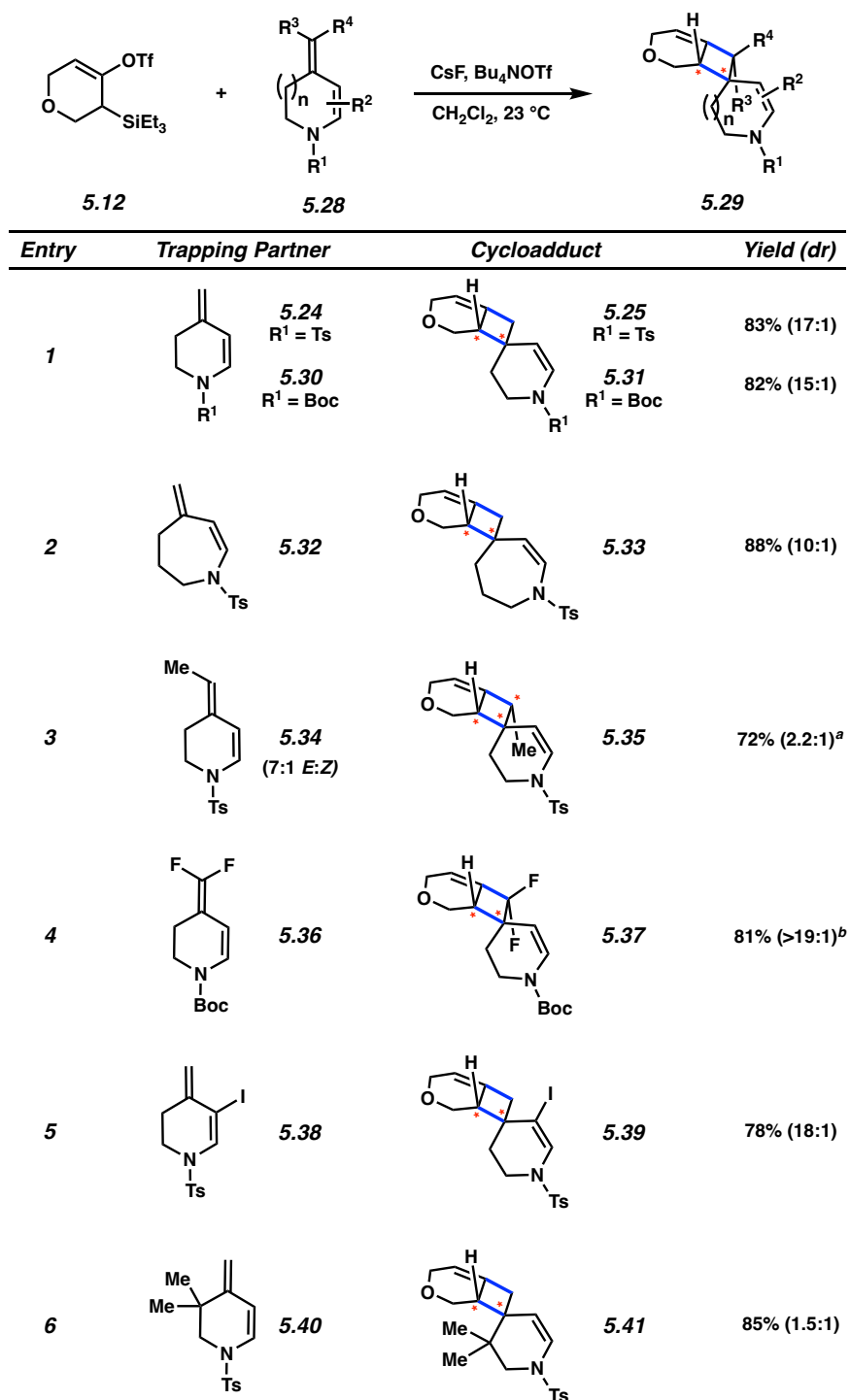


Figure 5.3. Scope of [2+2] cycloadditions with dienamine trapping partners **5.28**. Reaction conditions unless otherwise stated: **5.12** (1.0 equiv, 0.15 mmol), trapping partners **5.28** (3.0 equiv), CsF (5.0 equiv), Bu₄NOTf (50 mol%), CH₂Cl₂ (0.1 M), 23 °C, 24 h. Yields reflect an average of two isolation experiments; dr determined by ¹H NMR analysis. ^aThe 2.2:1 ratio reflects the ratio of the major diastereomer (2.2) to the sum of all minor diastereomers (1).

^bReaction was performed with CsF (5.0 equiv) in MeCN (0.1 M) at 23 °C for 24 h.

5.5 Scope of [2+2] Cycloadditions with Styrenyl Partners

The use of styrenyl trapping partners (Figure 5.4, i.e., **5.42** or **5.43**) in the methodology, including heterocyclic substrates, delivered structurally complex spiro cyclobutyl products bearing four or more interconnected rings. Using similar reaction conditions to those mentioned earlier (see Figure 5.3), employment of styrene **5.26** provided cycloadduct **5.27** in 80% yield and 4.0:1 dr (entry 1). Substrates **5.46** and **5.48**, which possess six-membered heterocyclic rings, could be employed, thus giving rise to cycloadducts **5.47** and **5.49** (entries 2 and 3). Moreover, employment of substrate **5.50** furnished pentacyclic product **5.51** containing a spiro tetrahydrocarbazole in 86% yield and 15:1 dr (entry 4). Substitution on the exocyclic alkene was also tolerated, as demonstrated by the cycloaddition of tri- and tetra-substituted alkenes **5.52**, **5.54**, **5.56**, and **5.58**. The use of these substrates generated cycloadducts **5.53**, **5.55**, **5.57**, and **5.59** (entries 5–8, respectively), which possess interesting features, such as three contiguous stereocenters (i.e., **5.53**), as well as vicinal fully substituted carbons (i.e., **5.55**, **5.57** and **5.59**). Lastly, we were delighted to find that trapping of the strained cyclic allene intermediate with pyridyl-substituted alkene **5.60** bearing a *gem*-dimethyl unit afforded cycloadduct **5.61** in high yield and excellent diastereoselectivity (entry 9). The structure of this product, bearing vicinal quaternary carbons, was verified by X-ray crystallography.

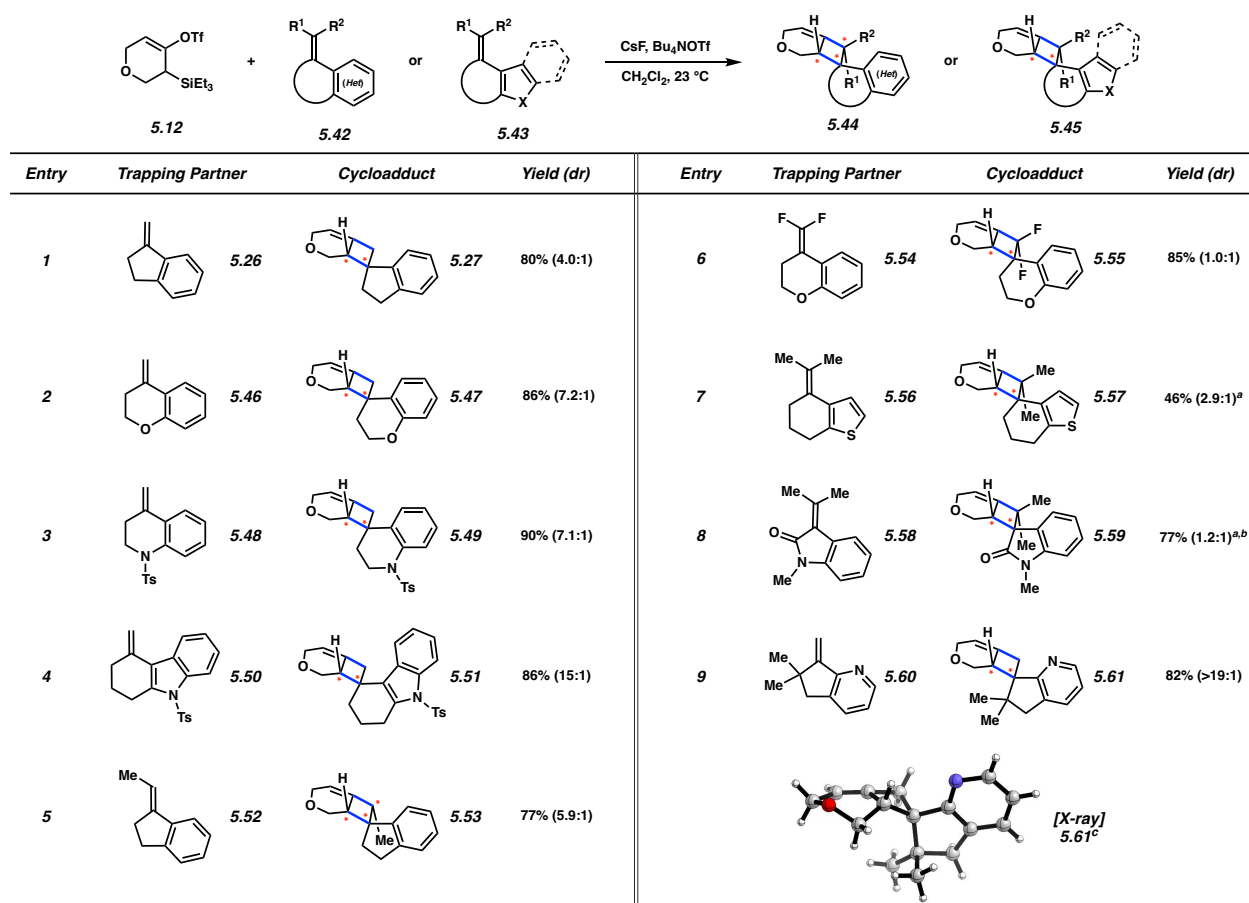


Figure 5.4. Scope of [2+2] cycloadditions with (het)aryl-substituted alkenes **5.42** and **5.43**. Reaction conditions unless otherwise stated: **5.12** (1.0 equiv, 0.15 mmol), trapping partners **5.42** or **5.43** (3.0 equiv), CsF (5.0 equiv), Bu₄NOTf (50 mol%), CH₂Cl₂ (0.1 M), 23 °C, 24 h. Yields reflect an average of two isolation experiments; dr determined by ¹H NMR analysis. ^aTrapping partner (5.0 equiv). ^bBu₄NOTf (20 mol%). ^cSee Section 5.10.2.6 for details and crystallographic data.

5.6 [2+2] Cycloadditions with Carbocyclic Allenes

Although our primary focus was on the use of heterocyclic allenenes to build medically-relevant heterocycles, we also examined carbocyclic allenenes (Figure 5.5). Treatment of silyl triflate **5.62** with dienamine **5.24** under conditions previously developed for carbocyclic allene generation,⁴⁵ delivered **5.64** in 75% yield and 7.1:1 dr, presumably via 1,2-cyclohexadiene (**5.63**). We were also intrigued by the possibility of using a larger, less strained cyclic allene in this methodology.⁴¹ As such, silyl tosylate **5.65** was subjected to conditions

previously developed to generate the corresponding 1,2-cycloheptadiene (**5.66**),⁵⁹ again using dienamine **5.24** as the trapping partner. These conditions resulted in the formation of cycloadduct **5.67** in 24% yield and 5.9:1 dr. Dimerization of the presumed allene intermediate **5.66** occurred competitively in this case.⁵¹ 1,2-Dienes in smaller rings (i.e., 5-membered rings) are not yet accessible for use in synthesis,^{88,89} but remain an opportunity for future discovery.

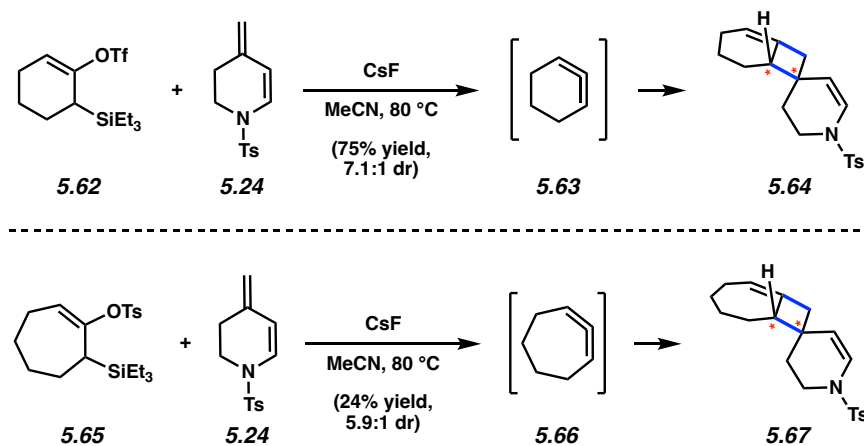


Figure 5.5. [2+2] cycloadditions of carbocyclic allenes **5.63** and **5.66** with dienamine **5.24**. Reaction conditions: **5.62** or **5.65** (1.0 equiv, 0.1 mmol), dienamine **5.24** (3.0–5.0 equiv), CsF (5.0 equiv), MeCN (0.1 M), 80 °C, 4–20 h.

5.7 Thermal Isomerization of Cycloadducts

Many products obtained from our studies possess strained alkylidene cyclobutanes with an adjacent π -system (i.e., alkene or aromatic ring), which could be susceptible to thermal isomerizations based on earlier studies by Christl and co-workers.⁷² Figure 5.6 highlights several key experimental findings, as well as computed ΔG values for each reaction shown. Cycloadduct **5.25**, which was accessed in high diastereoselectivity (see Figure 5.3, entry 1) was heated at 110 °C. We observed an erosion of dr, affording *epi*-**5.25** as the major isomer. This result was consistent with a computationally-determined ΔG value of -0.3 kcal/mol. Moreover, this finding suggested that comparing the ground state energetics of cycloadduct diastereomers could be used

to predict the results of thermal isomerization studies. Thus, we considered cycloadducts **5.41** and **5.61** obtained in our earlier experiments. Computational analysis indicated that *epi*-**5.41** and *epi*-**5.61** were each thermodynamically more stable relative to the major cycloadducts obtained in our cyclic allene trapping experiments ($\Delta G = -3.8$ and -2.7 kcal/mol, respectively). Gratifyingly, experimental results were consistent with computational predictions, allowing for the efficient conversion of **5.41** (1.5:1 dr) to *epi*-**5.41** (>19:1 dr) and **5.61** (>19:1 dr) to *epi*-**5.61** (>19:1 dr) under thermal conditions. Mechanistically, these isomerizations may occur by thermal homolytic cleavage of the strained bond between C6 and C4' indicated (see substrate **5.25**), followed by radical recombination, ultimately reaching a thermodynamic equilibrium of the two isomers. Our findings suggest that the selectivities observed in the aforementioned cyclic allene [2+2] trappings (see Figures 5.3 and 5.4) reflect kinetic distributions of products.

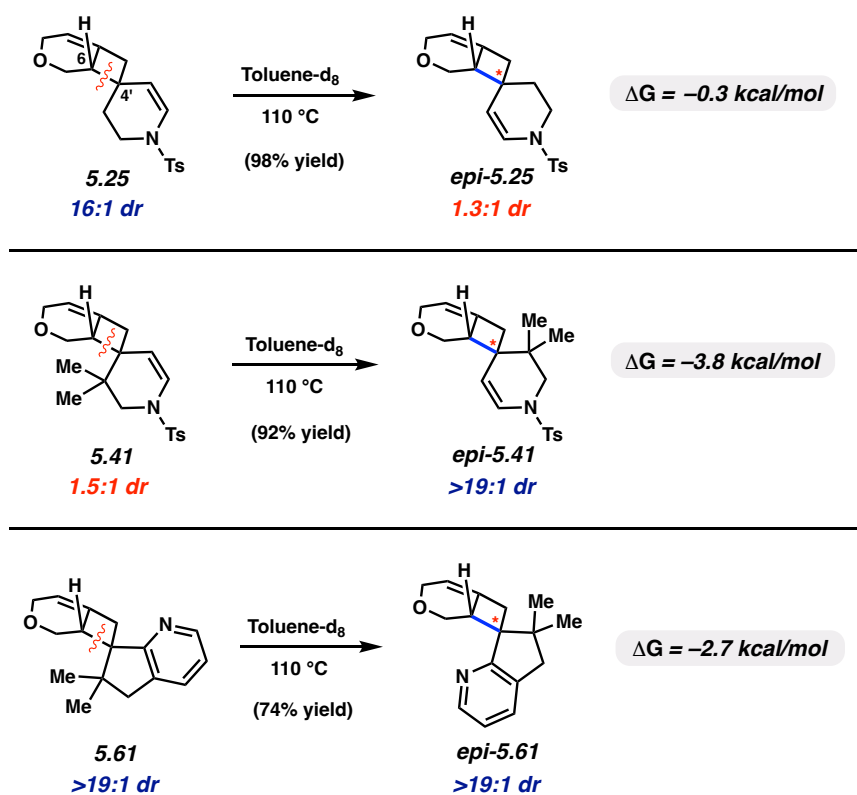


Figure 5.6. Thermal isomerization of cycloadducts **5.25**, **5.41**, and **5.61**. Yields and dr determined by ^1H NMR analysis using 1,3,5-trimethoxybenzene as an external standard. Free energies calculated using density functional theory (B3LYP/6-31G(d)).

5.8 Synthetic Elaborations of Cycloadducts

The [2+2] cycloadditions of strained cyclic allenes with highly substituted alkenes provides a platform to quickly access exceedingly complex cyclobutane-containing structures. Figure 5.7 showcases several such examples via the formation of polycycles **5.73**, **5.78**, and **5.82**, as well as their precursors. Ester-substituted cyclic allene precursor **5.68** was treated with trapping partner **5.38** under our usual reaction conditions to provide cycloadduct **5.70** in good yield and >19:1 dr. Of note, the reaction is also regioselective, favoring reaction of the alkene distal to the ester in the presumed cyclic allene intermediate **5.69** shown.⁹⁰ The α,β -unsaturated ester and vinyl iodide functional handles provide opportunities for further elaboration. Treatment of **5.70** with 1,8-diazabicyclo(5.4.0)undec-7-ene (DBU) in nitromethane delivered **5.71** in 51% yield and >19:1 dr,

introducing a quaternary stereocenter. By cross-coupling **5.71** with heterocyclic boronate **5.72**, highly decorated product **5.73** was obtained bearing four contiguous stereocenters, two of which are quaternary, and five rings in the core scaffold. In another example, azacyclic allene **5.75**, generated from silyl triflate **5.74**, was intercepted with cyclobutyl methyldene **5.76** to afford cycloadduct **5.77**. Subsequent epoxidation with *meta*-chloroperoxybenzoic acid (*m*-CPBA) yielded **5.78**, a polyspiro compound possessing four small rings and three contiguous stereocenters. Lastly, oxacyclic allene **5.13** was trapped with trisubstituted alkene **5.79**⁹¹ to provide cycloadduct **5.80** in 84% yield, introducing vicinal quaternary carbons and three contiguous stereocenters with a high degree of stereospecificity with respect to alkene geometry of **5.79**. Cycloadduct **5.80** was then subjected to nitrile oxide (3+2) cycloaddition to deliver **5.82**. This hexacyclic product possesses five contiguous stereocenters and three fully substituted carbons, including two quaternary centers. Cyclobutane-containing compounds **5.73**, **5.78**, and **5.82** are each accessible in either one or two steps from [2+2] cycloadducts, underscoring the structural complexity now readily accessible using strained cyclic allene methodology.

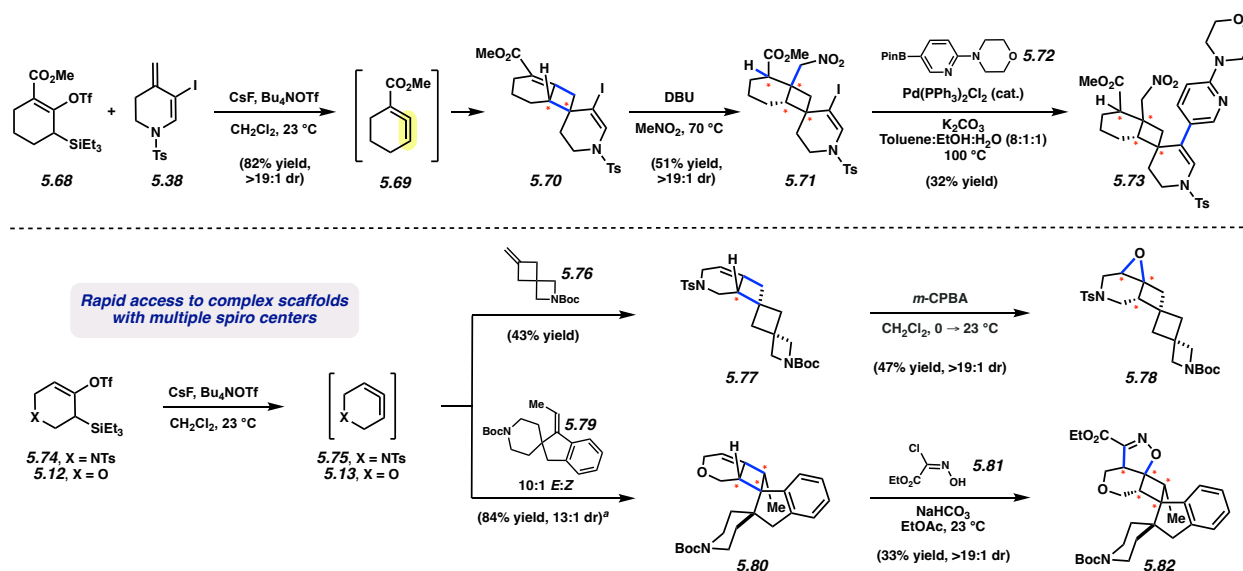


Figure 5.7. Synthetic elaborations of cycloadducts **5.70**, **5.77**, and **5.80** to access complex products **5.73**, **5.78**, and **5.82**, respectively. ^aThe 13:1 ratio reflects the ratio of the major diastereomer (13) to the sum of all minor diastereomers (1).

5.9 Conclusion

Cyclobutanes are desirable motifs typically introduced using photochemical cycloadditions. As an alternative approach, we utilize the strain-driven reactivity of cyclic allenes, which are emerging synthetic building blocks, to promote [2+2] cycloadditions. We have shown that exceedingly complex structures can be accessed by intercepting cyclic allenes with highly substituted exocyclic alkenes at ambient temperature. The products obtained directly from the methodology, along with their isomers and derivatives, contain the desirable cyclobutane motif and a number of attractive features, such as heterocycles, spiro centers, contiguous stereocenters, and vicinal quaternary centers. We expect this study should not only provide a versatile tool to access highly substituted cyclobutanes but should also prompt the further strategic use of unconventional strained intermediates for the rapid assembly of complex architectures.

5.10 Experimental Section

5.10.1 Materials and Methods

Unless stated otherwise, reactions were conducted in flame-dried glassware under an atmosphere of nitrogen, and commercially obtained reagents were used as received unless otherwise specified. Unless stated otherwise, anhydrous solvents were either freshly distilled or passed through activated alumina columns. Non-commercially available substrates were synthesized according to known preparations or following protocols specified in the Experimental Procedures. Acetonitrile (MeCN), dichloromethane, diethyl ether (Et₂O), benzene, triethylamine (Et₃N), toluene, dimethylformamide (DMF), and tetrahydrofuran (THF) were passed through an activated alumina column prior to use. Pyridine, diisopropylamine, and trifluoromethanesulfonic anhydride (Tf₂O) were distilled over CaH₂ prior to use. Ethyl acetate (EtOAc) was distilled over P₂O₅ prior to use. Tetrabutylammonium trifluoromethanesulfonate (Bu₄NOTf), *n*-butyllithium (*n*-BuLi), *p*-toluenesulfonyl chloride (TsCl), methylenecyclopentane (**5.16**), potassium *t*-butoxide (*t*-BuOK), isopropyltriphenylphosphonium iodide (*i*-PrPPh₃I), potassium bis(trimethylsilyl) amide (KHMDS), Hexamethylphosphoric acid triamide (HMPA), methyl cyanofornate, nitromethane (MeNO₂), 6-(Morpholin-4-yl)pyridine-3-boronic acid pinacol ester (**5.78**), sodium hydride (60 wt% in mineral oil), 1,8-diazabicyclo(5.4.0)undec-7-ene (DBU), and 3-chloroperoxybenzoic acid (*m*-CPBA, 77 wt%) were all purchased from Sigma-Aldrich and used as received. Cesium fluoride was obtained from Strem Chemicals, stored in a desiccator, and used as received. trans-Dichlorobis(triphenylphosphine)palladium(II) (Pd(PPh₃)₂Cl₂) was obtained from Strem Chemicals, stored in a glovebox, and used as received. 2-((difluoromethyl)sulfonyl)pyridine (**5.87**), 6,7-Dihydro-4-benzo[b]thiophenone (**5.92**), ethyltriphenylphosphonium bromide (EtPPh₃Br), methyltriphenylphosphonium bromide (MePPh₃Br), 3-methylenedihydrofuran-

2(3H)-one (**5.18**), chroman-4-one (**5.91**), and chromium(III) acetylacetonate ($\text{Cr}(\text{acac})_3$) were purchased from Combi Blocks. Iodine was obtained from Alpha Aesar. Iodomethane (MeI), sodium sulfate, sodium thiosulfate, and sodium bicarbonate were obtained from Thermo Fisher. 1-tosyl-2,3-dihydroquinolin-4(1H)-one (**5.90**) and *tert*-butyl 6-methylene-2-azaspiro[3.3]heptane-2-carboxylate (**5.76**) were obtained from Enamine. *tert*-Butyl 1-oxo-1,3-dihydrospiro[indene-2,4'-piperidine]-1'-carboxylate (**5.94**) was obtained from Ambeed. Ethyl 2-chloro-2-(hydroxyimino)acetate (**5.81**) was purchased from Tokyo Chemical Industry. Potassium carbonate and Tf_2O were obtained from Oakwood Chemical. Reaction temperatures at or above 23 °C were controlled using an IKAmag temperature modulator, and unless stated otherwise, performed at room temperature (approximately 23 °C). Thin layer chromatography (TLC) was conducted with EMD gel 60 F254 pre-coated plates (0.25 mm for analytical chromatography and 0.50 mm for preparative chromatography) and visualized using a combination of UV, anisaldehyde, and potassium permanganate staining techniques. Silicycle Siliaflash P60 (particle size 40–63 μm) was used for flash column chromatography and RediSep Gold Silica (20-40 μm) was used for automated chromatography on a CombiFlash NextGen 300+ instrument unless otherwise specified. ^1H -NMR and 2D-NOESY spectra were recorded on Bruker spectrometers (at 400, 500, and 600 MHz) and are reported relative to the residual solvent signal. Data for ^1H -NMR spectra are reported as follows: chemical shift (δ ppm), multiplicity, coupling constant (Hz), and integration. ^{13}C -NMR spectra were recorded on Bruker spectrometers (at 125 and 150 MHz) and are reported relative to the residual solvent signal. Data for ^{13}C -NMR spectra are reported in terms of chemical shift (δ ppm) and, when necessary, multiplicity, and coupling constant (Hz). ^{19}F -NMR spectra were recorded on a Bruker spectrometer (at 376 MHz) and are reported in terms of chemical shift (δ ppm), multiplicity, and integration. ^1H NMR Yields were determined by addition

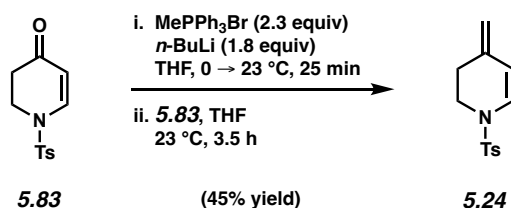
of trimethoxybenzene or an aliquot of a stock solution of external standard, mesitylene, in CDCl₃ to the concentrated crude reaction mixture followed by further dilution with CDCl₃ and subsequent ¹H NMR analysis. IR spectra were recorded on a Perkin-Elmer UATR Two FT-IR spectrometer and are reported in terms of frequency absorption (cm⁻¹). DART-MS spectra were collected on a Thermo Exactive Plus MSD (Thermo Scientific) equipped with an ID-CUBE ion source and a Vapor Interface (IonSense Inc.). Both the source and MSD were controlled by Excalibur software version 3.0. The analyte was spotted onto OpenSpot sampling cards (IonSense Inc.) using CDCl₃ or CH₂Cl₂ as the solvent. Ionization was accomplished using UHP He plasma with no additional ionization agents. The mass calibration was carried out using Pierce LTQ Velos ESI (+) and (-) Ion calibration solutions (Thermo Fisher Scientific). High-resolution mass spectra for compounds **5.64** and **5.67** were obtained on Agilent 6545 Q-TOF LC/MS with 1260 Infinity LC. Melting points were measured using a DigiMelt MPA160 melting point apparatus. To note, multiple stereoisomers are present in some NMR spectra. In these instances, the structures will be indicated on the spectrum.

3-(Triethylsilyl)-3,6-dihydro-2H-pyran-4-yl trifluoromethanesulfonate (**5.12**),⁵⁷ 2-methylenetetrahydrofuran (**5.20**),⁹² 2-methylene-1-tosylpiperidine (**5.22**),⁹³ 1-tosyl-2,3-dihydropyridin-4(1H)-one (**5.83**),⁹⁴ 1-methylene-2,3-dihydro-1H-indene (**5.26**),⁹⁵ *tert*-butyl 4-methylene-3,4-dihydropyridine-1(2H)-carboxylate (**5.30**),⁹⁶ 1,5,6,7-tetrahydro-4H-azepin-4-one (**5.84**),⁹⁷ 4-methylenechromane (**5.46**),⁹⁸ 4-methylene-9-tosyl-2,3,4,9-tetrahydro-1H-carbazole (**5.50**),⁹⁹ (E)-1-ethylidene-2,3-dihydro-1H-indene (**5.52**),¹⁰⁰ 4-(difluoromethylene)chromane (**5.54**),¹⁰¹ 1-methyl-3-(propan-2-ylidene)indolin-2-one (**5.58**),¹⁰² 6-(triethylsilyl)cyclohex-1-en-1-yl trifluoromethanesulfonate (**5.62**),⁴⁵ 7-(triethylsilyl)cyclohept-1-en-1-yl 4-

methylbenzenesulfonate (**5.65**),⁵⁹ 6,6-dimethyl-5,6-dihydro-7H-cyclopenta[*b*]pyridin-7-one (**5.93**),¹⁰³ 2-(triethylsilyl)cyclohexan-1-one (**5.95**),⁴⁶ and 1-tosyl-3-(triethylsilyl)-1,2,3,6-tetrahydropyridin-4-yl trifluoromethanesulfonate (**5.74**),⁶² are all known compounds. The ¹H NMR spectral data matched those reported in literature.

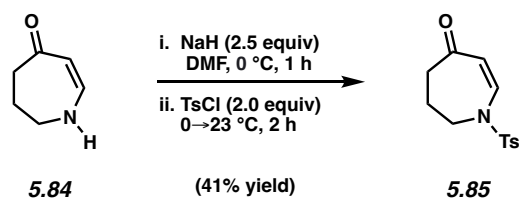
5.10.2 Experimental Procedures

5.10.2.1 Syntheses of Trapping Partners

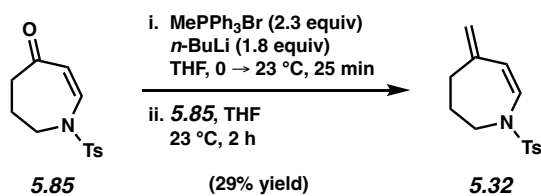


Dienamine 5.24. A 100 mL round bottom flask was charged with a magnetic stir bar, MePPh₃Br (4.90 g, 13.7 mmol, 2.3 equiv), and THF (30 mL). The flask was cooled to 0 °C. To the resulting stirring heterogeneous solution was added *n*-BuLi (2.4 M in hexanes, 4.50 mL, 10.8 mmol, 1.8 equiv) dropwise over 5 min. The orange heterogeneous solution was then allowed to warm to 23 °C over 25 min before dihydropyridone **5.83** (1.50 g, 5.97 mmol, 1.0 equiv) in THF (10 mL) was added dropwise over 2 min at this temperature for a final reaction concentration of 0.13 M. After 3.5 h, the reaction was filtered through a pad of silica, eluting with Et₂O (200 mL). The eluate was then concentrated under reduced pressure. The crude material was purified by flash column chromatography (4:1 hexanes:EtOAc) to afford dienamine **5.24** (670 mg, 45% yield) as a white solid. **Dienamine 5.24:** Mp: 109–110 °C; *R_f* 0.55 (5:1 hexanes:EtOAc); ¹H NMR (500 MHz, CDCl₃): δ 7.66 (d, *J* = 9.0, 2H), 7.30 (d, *J* = 8.2, 2H), 6.68 (d, *J* = 8.1, 1H), 5.52 (d, *J* = 8.2, 1H), 4.76 (s, 1H), 4.60 (s, 1H), 3.41 (t, *J* = 6.02, 2H), 2.43–2.36 (m, 5H); ¹³C NMR (150 MHz, CDCl₃): δ 144.1, 136.7, 134.8, 130.0, 127.2, 126.2, 111.0, 110.1, 44.1, 29.3, 21.7; IR (film): 2919, 1635,

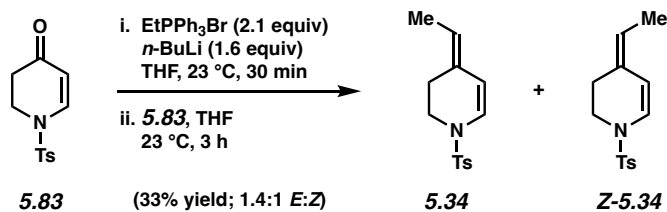
1596, 1346, 1164. HRMS-APCI (m/z) $[M + H]^+$ calcd for $C_{13}H_{16}NO_2S^+$, 250.0897; found 250.0899.



Azepinone 5.85. A 100 mL round bottom flask was charged with a magnetic stir bar, azepinone **5.84** (289 mg, 2.60 mmol, 1.0 equiv), and DMF (17 mL). Then, the flask was cooled to 0 °C. To the resulting stirring solution was added NaH (260 mg, 60% Wt, 6.50 mmol, 2.5 equiv) in one portion. The reaction was allowed to stir at this temperature for 1 h before TsCl (991 mg, 5.20 mmol, 2.0 equiv) was added in one portion. The resulting mixture was gradually warmed to 23 °C and stirred for 2 h before pouring the mixture into a 500 mL Erlenmeyer flask filled with ice (50 g) over 10 seconds. The resulting mixture was then extracted with EtOAc (3 x 75 mL). The combined organic layers were washed with water (5 x 75 mL) and brine (1 x 100 mL), dried with Na_2SO_4 , filtered, and concentrated under reduced pressure. The crude material was purified by flash column chromatography (3:1 → 1:1 Hexanes:EtOAc) to provide azepinone **5.85** (285 mg, 41% yield) as an off-white solid. **Azepinone 5.85:** Mp: 65–66 °C; Rf 0.37 (1:1 hexanes:EtOAc); 1H NMR (600 MHz, $CDCl_3$): δ 7.71–7.68 (m, 2H), 7.36 (d, $J = 8.1$, 2H), 7.33 (d, $J = 10.6$, 1H), 5.26 (d, $J = 10.8$, 1H), 3.72–3.69 (m, 2H), 2.58 (t, $J = 6.2$, 2H), 2.45 (s, 3H), 1.97–1.92 (m, 2H); ^{13}C NMR (150 MHz, $CDCl_3$): δ 199.9, 145.2, 136.2, 134.7, 130.3, 127.2, 109.1, 49.0, 42.7, 22.0, 21.7; IR (film): 1640, 1607, 1349, 1168, 931 cm^{-1} ; HRMS-APCI (m/z) $[M + H]^+$ calcd for $C_{13}H_{16}NO_3S^+$, 266.0845; found 266.0841.

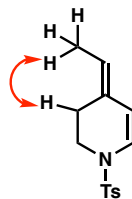


Dienamine 5.32. A 25 mL round bottom flask was charged with a magnetic stir bar, MePPh₃Br (310 mg, 867 μmol, 2.3 equiv), and THF (1.1 mL). Then, the flask was cooled to 0 °C. To the resulting stirring heterogeneous solution was then added *n*-BuLi (2.1 M in hexanes, 323 μL, 678 μmol, 1.8 equiv) dropwise over 5 min. The orange heterogeneous solution was then allowed to warm to 23 °C over 25 min before azepinone **5.85** (100 mg, 377 μmol, 1.0 equiv) in THF (5.0 mL) was added dropwise over 2 min at this temperature for a final reaction concentration of 0.06 M. After 2 h, the reaction filtered through a pad of silica, eluting with CH₂Cl₂ (50 mL). The eluate was then concentrated under reduced pressure. Purification of the crude material by flash column chromatography (hexanes → 1:1 hexanes:EtOAc) afforded dienamine **5.32** (28.5 mg, 29% yield) as a yellow solid. **Dienamine 5.32:** Mp: 109–110 °C; *R_f* 0.38 (3:1 hexanes:EtOAc); ¹H NMR (600 MHz, CDCl₃): δ 7.72–7.68 (m, 2H), 7.31 (d, *J* = 8.6, 2H), 6.50 (d, *J* = 9.5, 1H), 5.44 (d, *J* = 9.4, 1H), 4.82 (s, 1H), 4.80 (s, 1H), 3.63–3.57 (m, 2H), 2.43 (s, 3H), 2.31 (t, *J* = 6.5, 2H), 1.82–1.76 (m, 2H); ¹³C NMR (150 MHz, CDCl₃): δ 143.9, 143.6, 136.4, 130.0, 127.4, 127.0, 115.1, 115.0, 50.9, 34.7, 27.9, 21.7; IR (film): 2919, 1635, 11596, 1346, 1164 cm⁻¹. HRMS-APCI (*m/z*) [M + H]⁺ calcd for C₁₄H₁₈NO₂S⁺, 264.1053; found 264.1049.



Dienamine 5.34. A 100 mL round bottom flask was charged with a magnetic stir bar, EtPPh₃Br (7.51 g, 18.0 mmol, 2.1 equiv), and THF (42 mL). To the stirring heterogenous solution was then added *n*-BuLi (2.5 M in hexanes, 5.50 mL, 13.7 mmol, 1.6 equiv) dropwise over 5 min at 23 °C. The orange heterogenous solution was then stirred at this temperature for 30 min before dihydropyridone **5.83** (2.15 g, 8.56 mmol, 1.00 equiv) in THF (20 mL) was added dropwise over 2 min at 23 °C for a final reaction concentration of 0.15 M. After 15 h, the reaction was quenched with MeOH (4.0 mL) and the solution was concentrated under reduced pressure. The material was then filtered through a pad of silica, eluting with Et₂O (300 mL). The eluate was concentrated under reduced pressure. Purification of the crude material by flash column chromatography (hexanes → 4:1 hexanes:EtOAc) afforded a mixture of dienamines **5.34** and *Z*-**5.34** (**5.34**:*Z*-**5.34**, 1.4:1 (determined by ¹H NMR analysis of the isolated material); 748 mg, 33% yield) as a colorless oil. **5.34** and *Z*-**5.34** (2.1 g, 8.0 mmol) were then separated by preparative SFC (**5.34** rt 6.53 min, ColumnTek Enantiocel® AD-H; 250 (L) x 30 (ID) mm, 20% iPrOH (0.1% diethylamine), flow rate 85 mL/min, 35 °C) to give **5.34** (473 mg) which was then further purified by flash column chromatography (hexanes → 4:1 hexanes:EtOAc) to afford dienamine **5.34** (**5.34**:*Z*-**5.34**, 6.6:1 (determined by ¹H NMR analysis of the isolated material); 278 mg) as a colorless oil. **Dienamine 5.34:** R_f 0.83 (4:1 hexanes:EtOAc); ¹H NMR (600 MHz, C₆D₆): δ 7.68–7.65 (m, 2H), 7.31–7.28 (m, 2H), 6.54 (d, *J* = 8.1, 1H), 5.45 (d, *J* = 8.1, 1H), 5.29 (q, *J* = 7.0, 1H), 3.39 (t, *J* = 5.9, 2H), 2.41 (s, 3H), 2.36–2.33 (m, 2H), 1.59 (d, *J* = 7.1, 3H); ¹³C NMR (150 MHz, C₆D₆): δ 129.7, 128.3, 128.1, 128.0, 127.4, 124.1, 120.1, 113.2, 43.8, 23.7, 21.1, 12.9; IR (film) 2923, 2856, 1609, 1348, 1165, 1095, 678, 548 cm⁻¹; HRMS-APCI (*m/z*) [M + H]⁺ calcd for C₁₄H₁₈NO₂S⁺, 264.1053; found 264.1056.

The structure of **5.34** was verified by 2D-NOESY, as the following interaction was observed:



5.34

Compound **5.34** was separated by Lotus Separation on a 2.1 g scale.

Preparative Method:

Column: ColumnTek Enantiocel[®] AD-H; 250 (L) x 30 (ID) mm

Temperature: 35 °C

Moblile Phase CO₂ Modifier: 20% iPrOH (0.1% diethylamine)

Flow Rate: 85 mL/min

Back Pressure: 100 bar

Injection Volume: 1.0 mL of ~8 mg/mL solution in MeOH

Analytical Method:

Column: ColumnTek Enantiocel[®] AD-H; 250 (L) x 4.6 (ID) mm

Temperature: ambient

Moblile Phase CO₂ Modifier: 20% iPrOH (0.1% diethylamine)

Flow Rate: 2 mL/min

Back Pressure: 100 bar

Mixture of **5.34** and **Z-5.34**:

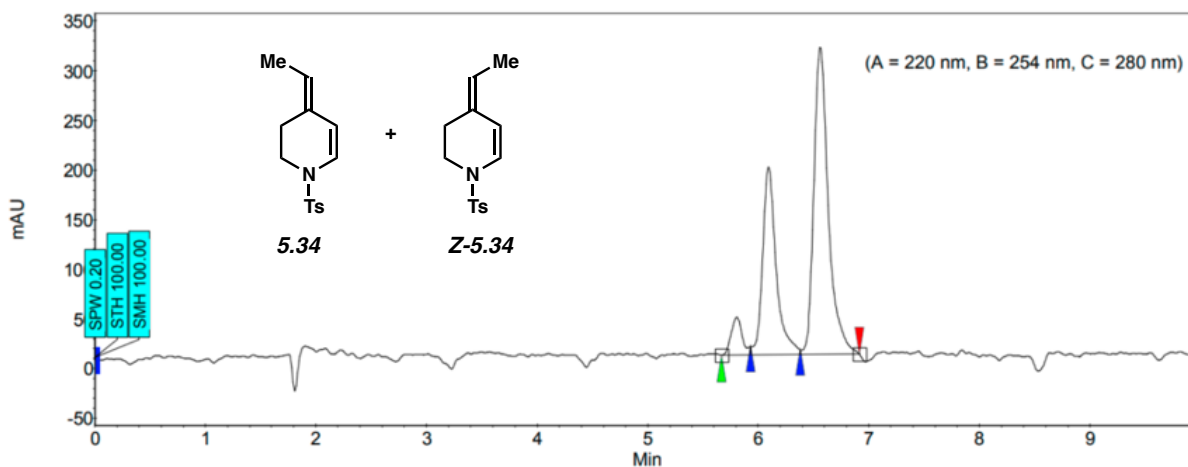


Figure 5.8. SFC trace for mixture of **5.34** and **Z-5.34**.

Enriched **5.34**:

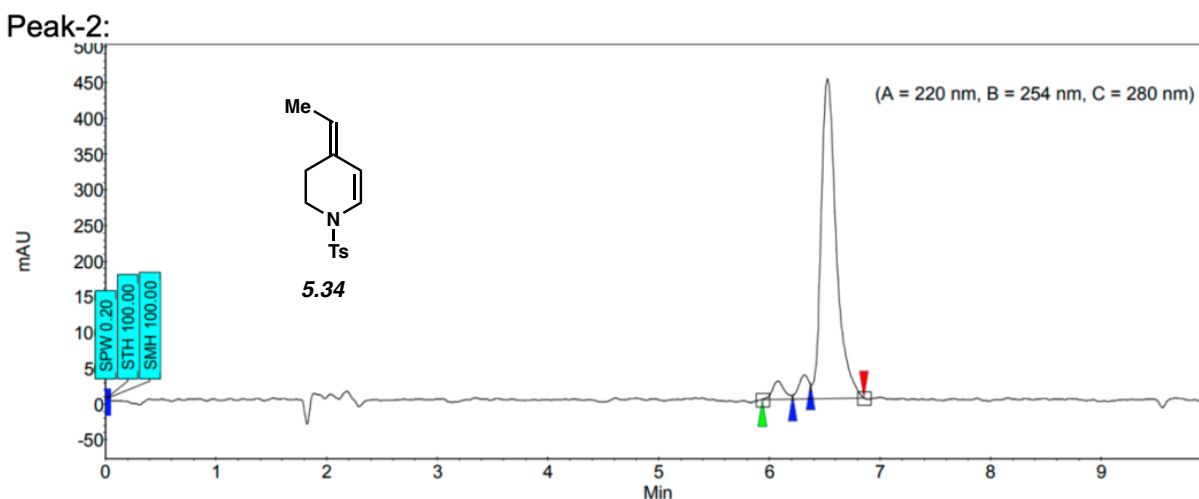
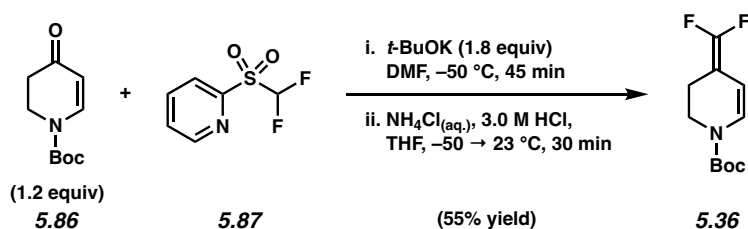


Figure 5.9. SFC trace for **5.34**.

Table 5.1. SFC data for **5.34**

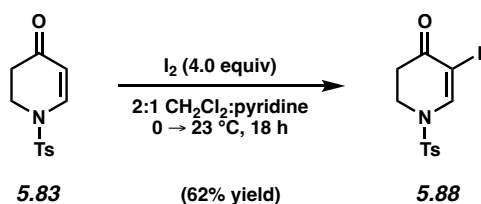
Index	Time (min)	Area (%)
<i>Z</i> - 5.34	6.08	4.0
Impurity	6.31	4.5
5.34	6.53	91.5
Total		100.0



Dienamine 5.36. A 100 mL round bottom flask was charged with a magnetic stir bar, dihydropyridone **5.86** (1.18 g, 6.00 mmol, 1.2 equiv), pyridine **5.87** (966 mg, 5.00 mmol, 1.0 equiv), and DMF (20 mL, 0.37 M). The flask was cooled to $-50 \text{ }^\circ\text{C}$. Then, a solution of *t*-BuOK (1.01 g, 9.00 mmol, 1.8 equiv) in DMF (10 mL) was added dropwise over 2 min to the reaction mixture. The solution was stirred at this temperature for 15 min where it turned a dark red color.

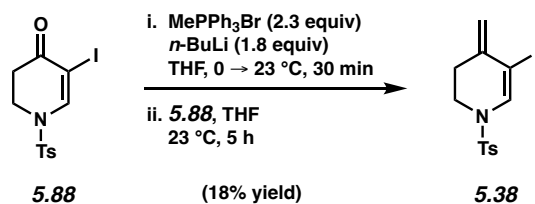
Then, ammonium chloride (saturated in H₂O, 10 mL) and HCl (3.0 M in H₂O, 10 mL) were subsequently added to the reaction mixture over 2 min, and the flask was warmed to 23 °C over 30 min, where the heterogeneous reaction mixture turned yellow. After this time, the mixture was extracted with Et₂O (2 x 100 mL) and washed with brine (1 x 100 mL). The combined organic layers were then dried over Na₂SO₄, filtered, and concentrated under reduced pressure. Purification of the crude material by flash column chromatography (4:1 hexanes:EtOAc → EtOAc) afforded dienamine **5.36** (631 mg, 55% yield) as a colorless oil. **Dienamine 5.36**: R_f 0.72 (9:1 hexanes:EtOAc); ¹H NMR (600 MHz, CDCl₃): δ 6.99–6.67 (m, 1H), 5.46–5.23 (m, 1H), 3.66–3.56 (m, 2H), 2.50–2.40 (m, 2H), 1.49 (s, 9H); ¹³C NMR (150 MHz, CDCl₃): δ 154.8, 152.5, 152.1, 151.6, 150.8 (dd, *J* = 291.7, 286.4), 126.2 (dd, *J* = 10.8, 3.0), 98.9, 98.5, 85.1, 84.6 (dd, *J* = 25.3, 18.7) 81.4, 79.9, 41.4, 40.1, 28.54, 28.48, 28.4, 28.3, 24.1, 20.9; ¹⁹F NMR (565 MHz, CDCl₃): δ -95.39 (dd, *J* = 84.6, 43.2), -96.64 (dd, *J* = 181.6, 43.8); IR (film) 2982, 1725, 1355, 1158, 763 cm⁻¹; HRMS-APCI (*m/z*) [M + H]⁺ calcd for C₁₁H₁₆F₂NO₂⁺, 232.1144; found 232.1136.

Note: 5.36 was obtained as a mixture of rotamers. These data represent empirically observed chemical shifts from the ¹H and ¹³C-NMR spectra.



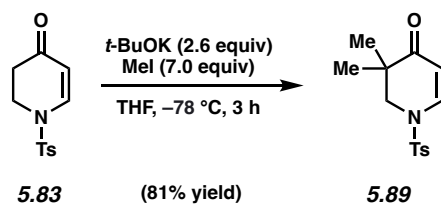
Dihydropyridone 5.88. A 50 mL round bottom flask was charged with a magnetic stir bar, dihydropyridone **5.83** (1.00, 3.98 mmol, 1.0 equiv), and a mixture of CH₂Cl₂:pyridine (2:1; 18 mL, 0.22 M). Subsequently, the flask was cooled to 0 °C. Then, iodine (4.04 g, 15.9 mmol, 4.0 equiv) was quickly added to the stirring solution in one portion. The reaction was stirred at this

temperature for 10 min before the flask was warmed to 23 °C and stirred for 18 h. The resulting mixture was then diluted with Et₂O (40 mL) and washed with a solution of saturated aqueous Na₂S₂O₃ (3 x 30 mL), and brine (30 mL). The organic layer was dried over Na₂SO₄, filtered, and concentrated under reduced pressure. The crude material was purified by flash column chromatography (3:1 → 1:1 hexanes:EtOAc) to afford dihydropyridone **5.88** (932 mg, 62% yield) as a pale yellow solid. **Dihydropyridone 5.88**: Mp: 138–139 °C; R_f 0.23 (3:1 hexanes:EtOAc); ¹H NMR (500 MHz, CDCl₃): δ 8.22 (s, 1H), 7.75–7.70 (m, 2H), 7.42–7.37 (m, 2H), 3.80 (t, *J* = 7.1, 2H), 2.72 (t, *J* = 6.7, 2H), 2.48 (s, 3H); ¹³C NMR (125 MHz, CDCl₃): 185.7, 148.3, 145.9, 133.3, 130.6, 127.4, 76.2, 44.1, 34.2, 21.7; IR (film): 2921, 1678, 1568, 1373, 1169. HRMS-APCI (*m/z*) [M – I]⁺ calcd for C₁₂H₁₂NO₃S⁺, 250.0532; found 250.0527.



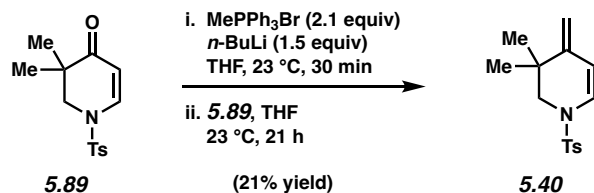
Dienamine 5.38. A 100 mL round bottom flask was charged with a magnetic stir bar, MePPh₃Br (3.40 g, 9.51 mmol, 2.3 equiv), and THF (20 mL). Then, the flask was cooled to 0 °C. To the stirring heterogeneous solution was added *n*-BuLi (1.9 M in hexanes, 3.94 mL, 7.44 mmol, 1.8 equiv) dropwise over 1 min. The orange heterogeneous solution was then allowed to warm to 23 °C over 30 min before dihydropyridone **5.88** (1.56 g, 4.14 mmol, 1.0 equiv) in THF (5.0 mL) was added dropwise over 2 min at this temperature for a final reaction concentration of 0.14 M. After 5 h, the reaction was filtered through a pad of silica, eluting with CH₂Cl₂ (200 mL). The eluate was then concentrated under reduced pressure. Purification of the crude material by flash column chromatography (30:1 hexanes:EtOAc → 9:1 hexanes:EtOAc) afforded dienamine **5.38** (275 mg,

18% yield) as yellow waxy solid. **Dienamine 5.38**: R_f 0.58 (3:1 hexanes:EtOAc); $^1\text{H NMR}$ (500 MHz, CDCl_3): δ 7.69–7.65 (m, 2H), 7.34 (d, $J = 8.0$, 2H), 7.31–7.29 (m, 1H), 5.06 (s, 1H), 4.92–4.90 (m, 1H), 3.49 (t, $J = 6.1$, 2H), 2.60–2.55 (m, 2H), 2.44 (s, 3 H); $^{13}\text{C NMR}$ (150 MHz, CDCl_3): δ 144.6, 137.2, 134.5, 133.1, 130.2, 127.2, 117.6, 77.0, 43.9, 29.3, 21.7; IR (film): 2924, 1738, 1618, 1365, 1161 cm^{-1} ; HRMS-APCI (m/z) $[\text{M} + \text{H}]^+$ calcd for $\text{C}_{13}\text{H}_{15}\text{INO}_2\text{S}^+$, 375.9863; found 375.9870.

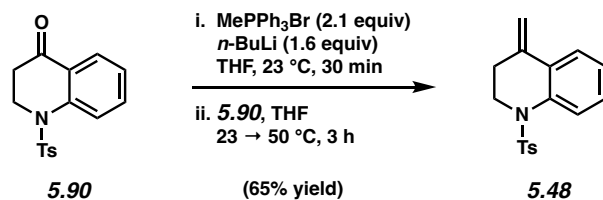


Dihydropyridone 5.89. A 100 mL round bottom flask was charged with a magnetic stir bar, *t*-BuOK (929 mg, 8.28 mmol, 2.6 equiv), and THF (24 mL). Then, the flask was cooled to $-78\text{ }^\circ\text{C}$. Subsequently, a solution of dihydropyridone **5.83** (800 mg, 3.18 mmol, 1.0 equiv) and MeI (1.39 mL, 22.3 mmol, 7.0 equiv) in THF (6.0 mL) was added dropwise over 2 min. After stirring for 3 h at this temperature, the flask was removed from the $-78\text{ }^\circ\text{C}$ bath and placed in an ice/water bath where it was warmed to $0\text{ }^\circ\text{C}$ before the reaction was quenched with a saturated aqueous solution of NH_4Cl (10 mL). The resulting mixture was extracted with EtOAc (3 x 30 mL), and the combined organic layers were dried over Na_2SO_4 , filtered, and concentrated under reduced pressure. The crude material was purified by flash column chromatography (3:1 hexanes:EtOAc) to provide dihydropyridone **5.89** (724 mg, 81% yield) as a white solid. **Dihydropyridone 5.89**: Mp: $83\text{ }^\circ\text{C}$; R_f 0.47 (3:1 hexanes:EtOAc); $^1\text{H NMR}$ (600 MHz, CDCl_3): 7.74–7.70 (m, 2H), 7.64 (d, $J = 8.4$, 1H), 7.38 (d, $J = 8.2$, 2H), 5.27 (d, $J = 8.8$, 1H), 3.38 (s, 2H), 2.46 (s, 3H), 1.03 (s, 6H); $^{13}\text{C NMR}$ (150 MHz, CDCl_3): 197.7, 145.4, 141.9, 134.1, 130.4, 127.4, 106.1, 55.0, 40.6, 22.2, 21.8; IR

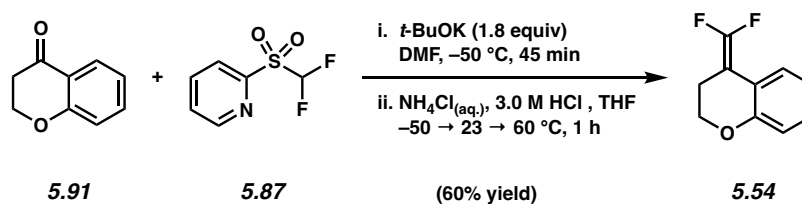
(film): 2970, 1671, 1597, 1364, 1169. HRMS-APCI (m/z) $[M + H]^+$ calcd for $C_{14}H_{18}NO_3S^+$, 280.1002; found 280.1005.



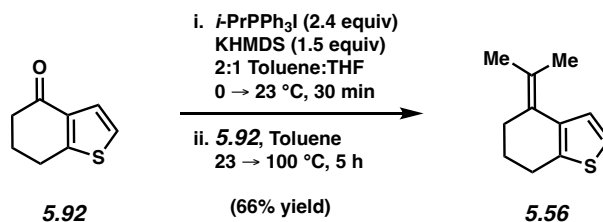
Dienamine 5.40. A 25 mL round bottom flask was charged with a magnetic stir bar, $MePPh_3Br$ (709 mg, 1.99 mmol, 2.1 equiv), and THF (3.1 mL). Then, to the stirring heterogeneous solution was added $n-BuLi$ (2.4 M in hexanes, (591 μ L, 1.42 mmol, 1.5 equiv) dropwise over 1 min at 23 °C. The orange heterogeneous solution was then stirred for 30 min before dihydropyridone **5.89** (264 mg, 945 μ mol, 1.0 equiv) in THF (3.1 mL) was added dropwise over 2 min for a final reaction concentration of 0.14 M. After 21 h, the reaction was filtered through a pad of silica, eluting with CH_2Cl_2 (100 mL). The eluate was then concentrated under reduced pressure. Purification of the crude material by flash column chromatography (9:1 hexanes:EtOAc) afforded dienamine **5.40** (55.1 mg, 21% yield) as a pale yellow solid. **Dienamine 5.40:** R_f 0.69 (3:1 hexanes:EtOAc); 1H NMR (500 MHz, $CDCl_3$): δ 7.68 (d, $J = 7.7$, 2H), 7.31 (d, $J = 7.7$, 2H), 6.66 (d, $J = 8.7$, 1H), 5.44 (d, $J = 8.2$, 1H), 4.76 (s, 1H), 4.70 (s, 1H), 2.98 (s, 2H), 2.42 (s, 3H), 1.04 (s, 6H); ^{13}C NMR (150 MHz, $CDCl_3$): δ 146.6, 143.9, 134.9, 129.8, 127.1, 124.5, 109.9, 106.7, 54.6, 34.2, 25.7, 21.6; IR (film): 2973, 1738, 1633, 1365, 1165 cm^{-1} ; HRMS-APCI (m/z) $[M + H]^+$ calcd for $C_{15}H_{20}NO_2S^+$, 278.1209; found 278.1216.



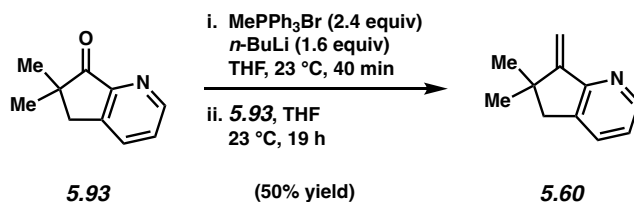
Olefin 5.48. A 50 mL round bottom flask was charged with a magnetic stir bar, MePPh₃Br (1.25 g, 3.48 mmol, 2.1 equiv), and THF (6 mL). Then, to the stirring heterogenous solution was added *n*-BuLi (2.5 M in hexanes, 1.06 mL, 2.66 mmol 1.60 equiv) dropwise over 1 min at 23 °C. The orange heterogenous solution was then allowed to stir at this temperature for 30 min until dihydroquinolinone **5.90** (500.0 mg, 1.659 mmol, 1.00 equiv) in THF (5 mL) was added dropwise over 2 min for a final reaction concentration of 0.15 M. The flask was then heated to 50 °C. After 3 h, the flask was cooled to 23 °C, then the reaction was quenched with methanol (4.0 mL), and the solution was concentrated under reduced pressure. The crude material was then filtered through a pad of silica, eluting with Et₂O (100 mL). The eluate was concentrated under reduced pressure. Purification of the crude material by flash column chromatography (4:1 hexanes:EtOAc) afforded olefin **5.48** (323 mg, 65% yield) as a colorless solid. **Olefin 5.48**: Mp: 101 °C; *R_f* 0.62 (7:3 hexanes:EtOAc); ¹H NMR (600 MHz, CDCl₃): δ 7.77 (dd, *J* = 8.3, 1.0, 1H), 7.59 (dd, *J* = 7.9, 1.4, 1H), 7.28–7.24 (m, 2H), 7.26 (overlapped with residual solvent peak, 1H), 7.20–7.16 (m, 2H), 7.16–7.11 (m, 2H), 5.45–5.43 (m, 1H), 4.79–4.76 (m, 1H), 3.90–3.86 (m, 2H), 2.37 (s, 3H), 2.36–2.33 (m, 2H); ¹³C NMR (150 MHz, CDCl₃): δ 143.6, 137.3, 137.2, 136.2, 129.6, 128.4, 128.2, 127.1, 125.4, 125.3, 124.4, 110.1, 46.2, 29.9, 21.5; IR (film) 3068, 2925, 1348, 1163, 1090, 577 cm⁻¹; HRMS-APCI (*m/z*) [*M* + *H*]⁺ calcd for C₁₇H₁₈NO₂S⁺, 300.1053; found 300.1042.



Olefin 5.54. A 100 mL round bottom flask was charged with a magnetic stir bar, chromanone **5.91** (920 mg, 6.21 mmol, 1.2 equiv), pyridine **5.87** (1.00 g, 5.18 mmol, 1.0 equiv), and DMF (20 mL, 0.31 M). Then, the flask was cooled to -50 °C. To the stirring solution was added a solution of *t*-BuOK (1.05 g, 9.32 mmol, 1.8 equiv) in DMF (10 mL) dropwise over 2 min. The reaction was then allowed to stir for 45 min at this temperature where it turned a dark red color. Then, ammonium chloride (saturated in H₂O, 11 mL) and HCl (3.0 M in H₂O, 10 mL) were subsequently added to the reaction over 2 min, and the flask was warmed to 23 °C over 30 min, where the heterogeneous reaction mixture turned yellow. Then, the flask was heated to 60 °C and stirred at this temperature for 30 min where the reaction became fully homogeneous. The flask was then cooled to 23 °C, and the mixture was extracted with Et₂O (1 x 100 mL) and washed with brine (1 x 100 mL) and 10% LiCl in H₂O (3 x 20 mL). The combined organic layers were then dried over Na₂SO₄, filtered, and concentrated under reduced pressure. Purification of the crude material by flash column chromatography (hexanes → 3:1 hexanes:EtOAc) afforded olefin **5.54** (570 mg, 3.13 mmol, 60% yield) as a colorless solid. The ¹H NMR spectral data matched those reported in literature.¹⁰¹

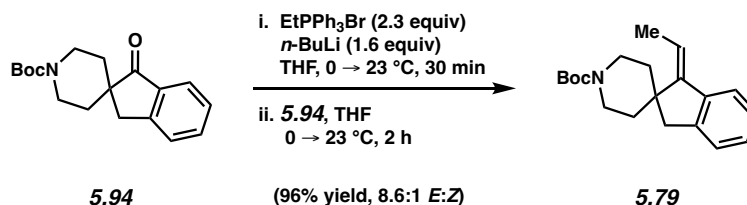


Olefin 5.56. A 100 mL round bottom flask was charged with a magnetic stir bar, *i*-PrPPh₃I (6.70 g, 15.0 mmol, 2.4 equiv), and toluene (20 mL). Then, the flask was cooled to 0 °C. To the stirring heterogenous solution was added KHMDS (1.0 M in THF, 10.0 mL, 10.0 mmol, 1.5 equiv) dropwise over 5 min. The red heterogenous solution then stirred at this temperature for 5 min before it was warmed to 23 °C over 30 min. Next, a solution of ketone **5.92** (1.00 g, 6.60 mmol, 1.0 equiv) in toluene (10 mL) was added dropwise over 4 min for a total reaction concentration of 0.16 M. Subsequently, a flame dried reflux condenser was attached to the reaction vessel. The stirring solution was heated to 100 °C, and the reaction stirred at this temperature for 5 h. The dark red solution was then cooled to 23 °C, and the mixture was filtered through a pad of silica, eluting with CH₂Cl₂ (200 mL) . The eluate was then concentrated under reduced pressure. Purification by flash column chromatography (hexanes) afforded olefin **5.56** (775 mg, 66% yield) as a pale brown oil. **Olefin 5.56:** *R*_f 0.90 (5:1 hexanes:EtOAc); ¹H NMR (600 MHz, CDCl₃): δ 7.18 (d, *J* = 5.4, 1H), 7.04 (d, *J* = 5.4, 1H), 2.87 (t, *J* = 6.5, 2H), 2.44–2.40 (m, 2H), 1.99 (s, 3H), 1.95–1.88 (m, 2H), 1.84 (s, 3H); ¹³C NMR (150 MHz, CDCl₃): δ 138.1, 136.5, 128.0, 126.3, 124.5, 120.4, 28.4, 25.9, 24.7, 23.2, 21.8; IR (film): 2927, 1444, 1367, 1049, 727 cm⁻¹; HRMS-APCI (*m/z*) [M + H]⁺ calcd for C₁₁H₁₅S⁺, 179.0889; found 179.0889.



Olefin 5.60. A 25 mL round bottom flask was charged with a magnetic stir bar, MePPh₃Br (1.33 g, 3.72 mmol, 2.4 equiv), and THF (4.0 mL). Then, to the stirring heterogenous solution was added *n*-BuLi (2.5 M in hexanes, 1.00 mL, 2.48 mmol, 1.6 equiv) dropwise over 2 min at 23 °C. The

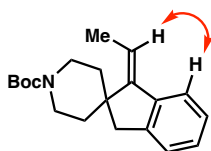
orange heterogenous solution then stirred for 40 min at this temperature. Subsequently, a solution of ketone **5.93** (250 mg, 1.55 mmol, 1.0 equiv) in THF (3.0 mL) was added dropwise over 4 min, for a total reaction concentration of 0.2 M. After 19 h, the purple solution was then filtered through a pad of silica, eluting with CH₂Cl₂ (200 mL). The eluate was then concentrated under reduced pressure. Purification of the crude material by flash column chromatography (5:1 hexanes:EtOAc) afforded olefin **5.60** (123 mg, 50% yield) as a pale yellow oil. **Olefin 5.60**: R_f 0.60 (5:1 hexanes:EtOAc); ¹H NMR (600 MHz, CDCl₃): δ 8.46–8.43 (m, 1H), 7.53–7.50 (m, 1H), 7.10 (dd, *J* = 7.3, 4.9, 1H), 5.97 (s, 1H), 5.08 (s, 1H), 2.80 (s, 2H), 1.25 (s, 6H); ¹³C NMR (150 MHz, CDCl₃): δ 158.7, 158.4, 148.6, 137.0, 133.3, 123.0, 105.0, 44.5, 40.9, 29.6; IR (film): 3064, 2925, 1647, 1424, 802 cm⁻¹; HRMS-APCI (*m/z*) [M + H]⁺ calcd for C₁₁H₁₄N⁺, 160.1121; found 160.1120.



Olefin 5.79. A 50 mL round bottom flask was charged with a magnetic stir bar, EtPPh₃Br (4.30 g, 12.0 mmol, 2.3 equiv), and THF (14 mL). Then, the flask was cooled to 0 °C. To the stirring heterogenous solution was added *n*-BuLi (2.5 M in hexanes, 3.20 mL, 8.00 mmol, 1.6 equiv) dropwise over 5 min. The red heterogenous solution was stirred at this temperature for 5 min before it was warmed to 23 °C over 30 min. After this time, the flask was cooled again to 0 °C, and a solution of ketone **5.94** (1.50 g, 5.00 mmol, 1.0 equiv) in THF (12 mL) was added dropwise over 7 min for a total reaction concentration of 0.17 M. The reaction was then warmed to 23 °C and stirred for 2 h. After this time, the solution was then filtered through a pad of silica, eluting with

CH₂Cl₂ (300 mL). The eluate was then concentrated under reduced pressure. Purification of the crude material by flash column chromatography (hexanes → 13:1 hexanes:EtOAc → 4:1 hexanes:EtOAc) and separation of two sets of fractions afforded olefin **5.79** (1.51 g, 96% yield, 8.6:1 *E:Z* mixture, determined by ¹H NMR analysis of isolated material) as a waxy white solid. **Olefin 5.79**: (10:1 *E:Z* mixture): Mp: 71–73 °C; R_f 0.66 (9:1 hexanes:EtOAc); ¹H NMR (600 MHz, CDCl₃): δ 7.38–7.33 (m, 1H), 7.21–7.13 (m, 3H), 6.11 (q, *J* = 7.5, 1H), 4.28–3.95 (m, 2H), 2.99 (s, 2H), 2.96–2.79 (m, 2H), 2.26–2.14 (m, 2H), 1.94 (d, *J* = 7.6, 3H), 1.50–1.45 (m, 11H); ¹³C NMR (125 MHz, CDCl₃): δ 155.1, 148.1, 141.6, 141.5, 128.4, 127.5, 126.7, 125.3, 119.7, 115.4, 79.5, 44.9, 42.3, 34.4, 28.5, 14.0; IR (film): 2932, 1689, 1421, 1169, 752 cm⁻¹; HRMS-APCI (*m/z*) [M + H]⁺ calcd for C₂₀H₂₈NO₂⁺, 314.2115; found 314.2115.

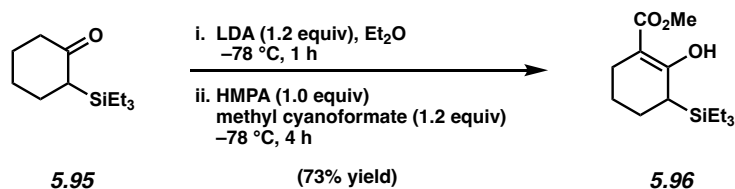
The structure of **5.79** was verified by 2D-NOESY, as the following interaction was observed:



5.79

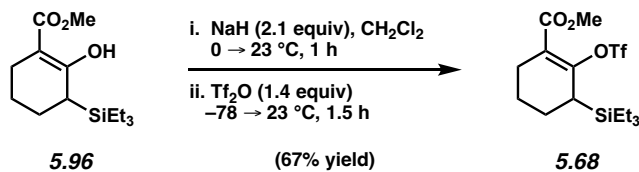
Note: 5.79 was obtained as a mixture of rotamers. These data represent empirically observed chemical shifts from the ¹H and ¹³C-NMR spectra.

5.10.2.2 Synthesis of Silyl Triflate **5.68**



Enol 5.96. A 25 mL round bottom flask was charged with a magnetic stir bar, diisopropylamine (410 μL, 2.85 mmol, 1.2 equiv), and Et₂O (2.4 mL). Then, the flask was cooled to -78 °C. To the

stirring solution was added *n*-BuLi (2.5 M in hexanes, 1.22 mL, 2.82 mmol, 1.2 equiv) dropwise over 1 min. The reaction was stirred at $-78\text{ }^{\circ}\text{C}$ for 20 min, then warmed to $23\text{ }^{\circ}\text{C}$ over 10 min. Then the flask was cooled to $-78\text{ }^{\circ}\text{C}$ and a solution of ketone **5.95** (500 mg, 2.35 mmol, 1.0 equiv) in Et₂O (10 mL) was added dropwise over 5 min. After stirring for 1 h at $-78\text{ }^{\circ}\text{C}$, HMPA (410 μL , 2.35 mmol, 1.0 equiv) and methyl cyanoformate (225 μL , 2.82 mmol, 1.2 equiv) were added dropwise sequentially over 2 min. The reaction was stirred at $-78\text{ }^{\circ}\text{C}$ for 2 h, then quenched by the addition of cooled deionized water ($0\text{ }^{\circ}\text{C}$, 8 mL) and allowed to warm to $23\text{ }^{\circ}\text{C}$. The layers were separated and the aqueous layer was extracted with Et₂O (3 x 15 mL). The combined organic layers were dried over Na₂SO₄, filtered, and concentrated under reduced pressure. Purification of the crude material by flash column chromatography (19:1 hexanes:EtOAc) afforded enol **5.96** (465 mg, 73% yield) as a yellow oil. **Enol 5.96**: *R_f* 0.80 (9:1 hexanes:EtOAc); ¹H NMR (500 MHz, CDCl₃): δ 12.46 (s, 1H), 3.73 (s, 3H), 2.34–2.27 (m, 1H), 2.17–2.09 (m, 1H), 2.06–2.00 (m, 1H), 1.87–1.76 (m, 1H), 1.72–1.65 (m, 1H), 1.65–1.56 (m, 1H), 1.54–1.42 (m, 1H), 0.96 (t, *J* = 7.9, 9H), 0.69–0.64 (m, 6H); ¹³C NMR (150 MHz, CDCl₃): δ 177.0, 173.2, 95.5, 51.2, 27.6, 24.3, 22.7, 22.6, 7.5, 3.3; IR (film): 2950, 1747, 1256, 1028, 716 cm⁻¹; HRMS-APCI (*m/z*) [*M* + *H*]⁺ calcd for C₁₄H₂₇O₃Si⁺, 271.1724; found 271.1721.

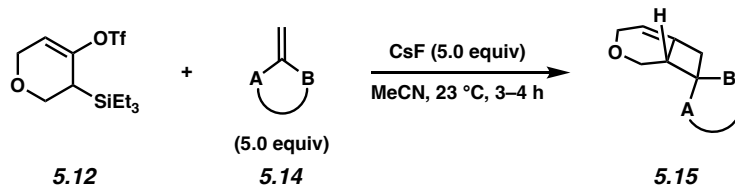


Silyl triflate 5.68. A 100 mL round bottom flask was charged with a magnetic stir bar, NaH (60 wt% dispersion in mineral oil, 320 mg, 8.00 mmol, 2.1 equiv), and CH₂Cl₂ (26 mL). Then, the flask was cooled to $0\text{ }^{\circ}\text{C}$. To the stirring heterogenous solution was added a solution of silyl alcohol

5.96 (1.02 g, 3.77 mmol, 1.0 equiv) in CH₂Cl₂ (8.0 mL) dropwise over 6 min for a total reaction concentration of 0.11 M. The flask was then allowed to warm to 23 °C. After 1 h, the reaction was cooled to -78 °C and Tf₂O (900 μL, 5.33 mmol, 1.4 equiv) was added dropwise over 1 min. After stirring for 5 min, the reaction was allowed to warm to 23 °C and stirred for 1.5 h. Then, the flask was cooled to 0 °C and the reaction was quenched with deionized water (15 mL). The layers were separated and the aqueous layer was extracted with CH₂Cl₂ (3 x 40 mL). The combined organic layers were dried over Na₂SO₄, filtered, and concentrated under reduced pressure. Purification of the crude material by flash column chromatography (hexanes → 5:1 hexanes:EtOAc) afforded silyl triflate **5.68** (1.01 g, 67% yield) as a colorless oil. **Silyl triflate 5.68**: ¹H NMR (500 MHz, CDCl₃): δ 3.76 (s, 3H), 2.8–2.71 (m, 1H), 2.25–2.14 (m, 1H), 2.14–2.06 (m, 1H), 2.03–1.91 (m, 1H), 1.79–1.70 (m, 1H), 1.70–1.61 (m, 1H), 1.53–1.44 (m, 1H), 0.97 (t, *J* = 7.9, 9H), 0.69 (q, *J* = 7.7, 6H); ⁹F NMR (282 MHz, CDCl₃): δ 74.2; ¹³C NMR (150 MHz, CDCl₃): δ 165.7, 156.6, 119.3, 118.6 (q, *J* = 320), 52.0, 28.4, 26.8, 25.6, 21.2, 7.2, 2.8; IR (film): 2956, 2880, 1722, 1645, 1422, 1206; HRMS-APCI (*m/z*) [M + H]⁺ calcd for C₁₅H₂₆F₃O₅SSi⁺, 403.1217; found 403.1198.

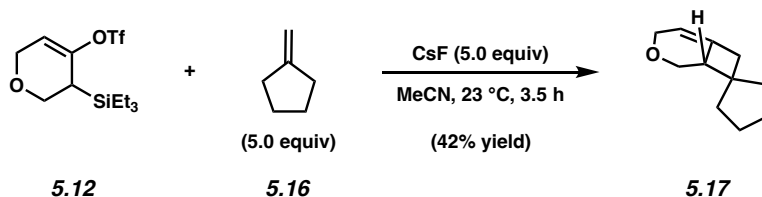
5.10.2.3 Survey of [2+2] Cycloadditions with Exocyclic Alkenes

General Procedure 5.1 for the survey of [2+2] cycloadditions with exocyclic alkenes

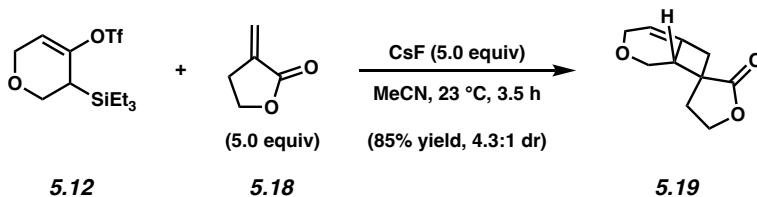


Cycloadducts 5.15. To a stirred solution of silyl triflate **5.12** (17.3 mg, 50 μmol, 1.0 equiv) and trapping partners **5.14** (250 μmol, 5.0 equiv) in MeCN (500 μL, 0.1 M) was added CsF (38.0 mg, 250 μmol, 5.0 equiv) in a single portion. The vial was then sealed with a Teflon-lined cap and

stirred at >900 RPM for 3–4 h at 23 °C. The mixture was then filtered through a pad of silica (monster pipette, ~2 cm silica), eluting with EtOAc (10 mL). The eluate was concentrated under reduced pressure to afford a crude residue, which was analyzed by ¹H NMR using mesitylene as an external standard.

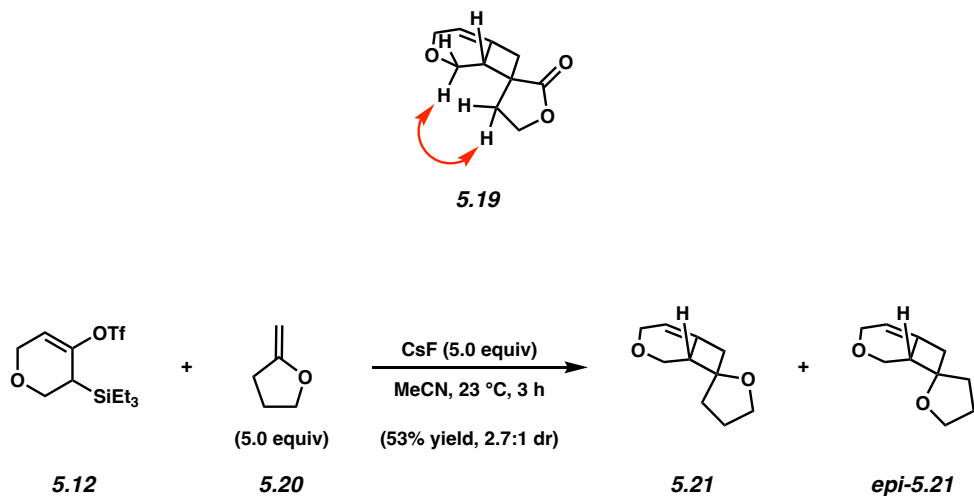


Cycloadduct 5.17. Followed General Procedure 5.1. Cycloadduct **5.17** was obtained in 42% yield by ¹H NMR analysis of the crude reaction mixture. An analytical sample was obtained by preparative thin layer chromatography (1:1 hexanes:CH₂Cl₂) to afford cycloadduct **5.17** as a colorless oil. **Cycloadduct 5.17:** R_f 0.50 (5:1 hexanes:EtOAc); ¹H NMR (500 MHz, CDCl₃): δ 5.33–5.29 (m, 1H), 4.24–4.17 (m, 1H), 4.13–4.07 (m, 1H), 3.91 (dd, *J* = 10.0, 6.6, 1H), 3.16 (app. t, *J* = 9.8, 1H), 2.99–2.91 (m, 1H), 2.74–2.69 (m, 1H), 2.43–2.37 (m, 1H), 1.69–1.64 (m, 2H), 1.65–1.53 (overlapped with residual H₂O peak, 2H), 1.53–1.43 (m, 4H); ¹³C NMR (125 MHz, CDCl₃): δ 136.1, 112.1, 65.5, 64.4, 48.8, 47.3, 44.2, 39.6, 32.0, 23.5, 23.3; IR (film): 2925, 2857, 1451, 1215, 1092 cm⁻¹; HRMS-APCI (*m/z*) [M + H]⁺ calcd for C₁₁H₁₇O⁺, 165.1274; found 165.1274.



Cycloadduct 5.19. Followed General Procedure 5.1. Cycloadduct **5.19** was obtained in 85% combined yield and 4.3:1 dr by ^1H NMR analysis of the crude reaction mixture. An analytical sample was obtained through two purifications by preparative thin layer chromatography (1:1 hexanes:EtOAc then 3:1 benzene:acetone, respectively) to afford cycloadduct **5.19** as a white solid. **Cycloadduct 5.19:** Mp: 77–79 °C; R_f 0.46 (1:1 hexanes:EtOAc); ^1H NMR (500 MHz, CDCl_3): δ 5.51–5.45 (m, 1H), 4.26–4.18 (m, 3H), 4.16–4.09 (m, 1H), 3.96 (dd, $J = 10.2, 6.6$, 1H), 3.60–3.52 (m, 1H), 3.37–3.30 (m, 1H), 3.20 (app. t, $J = 9.8$, 1H), 2.64 (d, $J = 13.6$, 1H), 2.32 (app. dt, $J = 13.0, 7.7$, 1H), 2.20 (app. dt, $J = 13.0, 5.7$, 1H); ^{13}C NMR (125 MHz, CDCl_3): δ 178.6, 133.3, 114.2, 65.7, 65.2, 63.0, 44.8, 44.6, 42.1, 29.4; IR (film): 2966, 1761, 1458, 1012, 886 cm^{-1} ; HRMS-APCI (m/z) [$M + \text{H}$] $^+$ calcd for $\text{C}_{10}\text{H}_{13}\text{O}_3^+$, 181.0859; found 181.0859.

The structure of **5.19** was verified by 2D-NOESY, as the following interaction was observed:



Cycloadducts 5.21 and epi-5.21. Followed General Procedure 5.1. Cycloadducts **5.21** and *epi*-**5.21** were obtained in 53% combined yield and 2.7:1 dr by ^1H NMR analysis of the crude reaction mixture. An analytical sample was obtained by preparative thin layer chromatography (2:1 hexanes:EtOAc, eluted 3 times) to afford a mixture of major diastereomer **5.21** and minor diastereomer *epi*-**5.21** as a colorless oil. Further purification by preparative thin layer

chromatography (2:1:1 hexanes:CH₂Cl₂:Et₂O, eluted 3 times) afforded **5.21** as a colorless oil (analytical sample used to determine ¹H NMR shifts and for 2D-NOESY experiment).

Cycloadducts 5.21 and *epi-5.21*: R_f 0.78 (1:1 hexanes:EtOAc); ¹H NMR (500 MHz, CDCl₃, **5.21**):

δ 5.45–5.42 (m, 1H), 4.22–4.17 (m, 1H), 4.10–4.00 (m, 2H), 3.86–3.82 (m, 1H), 3.82–3.76 (m, 1H), 3.26–3.21 (m, 1H), 3.17 (app. t, *J* = 9.7, 1H), 3.07–3.02 (m, 1H), 2.68–2.63 (m, 1H), 1.93–

1.72 (m, 4H); ¹H NMR (500 MHz, CDCl₃, *epi-5.21*, characterized from an inseparable mixture of

5.21 and *epi-5.21*): δ 5.46–5.41 (m, 1H), 4.25–4.12 (m, 2H), 3.90 (dd, *J* = 10.0, 6.8, 1H), 3.83–3.79 (m, 1H), 3.67–3.61 (m, 1H), 3.36 (app. t, *J* = 9.8, 1H), 3.04–2.98 (m, 2H), 2.73 (d, *J* = 14.4,

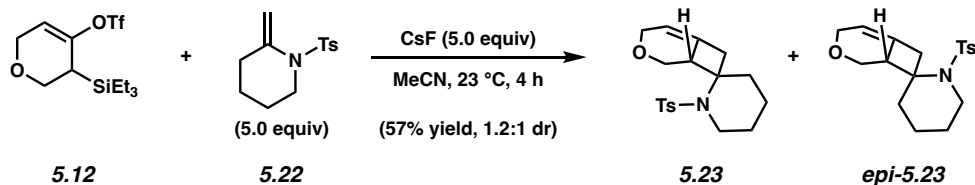
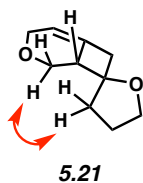
1H), 2.00–1.83 (m, 4H); ¹³C NMR (125 MHz, CDCl₃, **5.21** and *epi-5.21*, 19 out of 20 signals

observed): δ 134.6, 131.2, 113.9, 113.8, 85.7, 83.2, 67.6, 67.4, 65.3, 63.9, 62.3, 49.8, 49.5, 46.4,

44.0, 36.5, 30.4, 25.1, 24.8; IR (film): 2925, 1120, 1063, 1032, 732 cm⁻¹; HRMS-APCI (*m/z*) [*M*

+ H]⁺ calcd for C₁₀H₁₅O₂⁺, 167.1067; found 167.1063.

The structure of **5.21** was verified by 2D-NOESY, as the following interaction was observed:

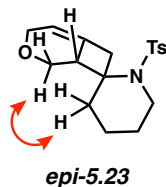


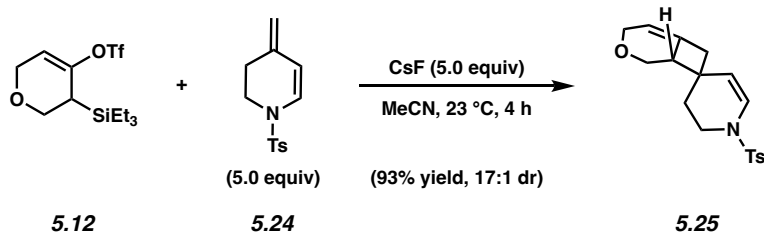
Cycloadduct 5.23. Followed General Procedure 5.1. Cycloadducts **5.23** and *epi-5.23* were obtained in 57% combined yield and 1.2:1 dr by ¹H NMR analysis of the crude reaction mixture.

An analytical sample was obtained by preparative thin layer chromatography (4:1:1

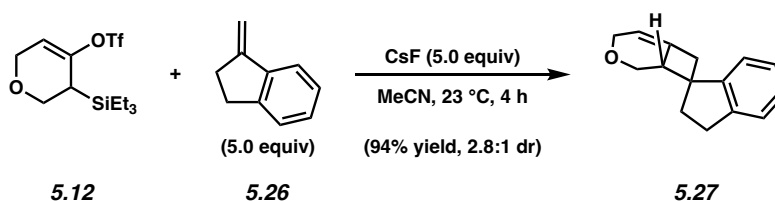
hexanes:CH₂Cl₂:Et₂O) which allowed for a separation of the diastereomers, affording cycloadducts **5.23** and *epi*-**5.23** as colorless oils. **Cycloadduct 5.23**: R_f 0.42 (4:1 hexanes:EtOAc); ¹H NMR (500 MHz, CDCl₃): δ 7.72–7.68 (m, 2H), 7.29–7.25 (overlapped with residual solvent peak, 2H), 5.43–5.40 (m, 1H), 4.20–4.00 (m, 3H), 3.71–3.64 (m, 1H), 3.31–3.23 (m, 2H), 3.22–3.12 (m, 1H), 2.88–2.77 (m, 2H), 2.41 (s, 3H), 1.80–1.58 (m, 6H); ¹³C NMR (150 MHz, CDCl₃): δ 142.8, 141.1, 133.4, 129.1, 126.9, 113.6, 67.2, 65.8, 64.7, 50.0, 47.6, 42.7, 39.5, 25.5, 22.5, 21.5; IR (film): 2929, 2865, 1321, 1150, 706 cm⁻¹; HRMS-APCI (*m/z*) [M+H]⁺ calcd for C₁₈H₂₄NO₃S⁺, 334.1471; found 334.1478. **Cycloadduct *epi*-5.23**: R_f 0.35 (4:1 hexanes:EtOAc); ¹H NMR (500 MHz, CDCl₃) δ 7.72–7.69 (m, 2H), 7.28–7.23 (overlapped with residual solvent peak, 2H), 4.68–4.63 (m, 1H), 4.34–4.26 (m, 1H), 4.17 (dd, *J* = 9.4, 6.3, 1H), 4.14–4.07 (m, 1H), 3.89–3.80 (m, 1H), 3.44 (d, *J* = 16.3, 1H), 3.15 (app. t, *J* = 9.7, 1H), 2.96–2.88 (m, 1H), 2.74–2.67 (m, 1H), 2.51–2.44 (m, 1H), 2.41 (s, 3H), 2.01 (app. td, *J* = 13.3, 4.0 Hz, 1H), 1.88–1.80 (m, 1H), 1.73 (dt, *J* = 13.3, 3.0, 1H), 1.68 – 1.43 (overlapped with residual water peak, 3H); ¹³C NMR (150 MHz, CDCl₃): δ 142.7, 141.2, 132.5, 129.7, 126.2, 114.7, 65.5, 63.5, 62.4, 47.9, 45.5, 43.2, 28.8, 25.4, 21.51, 21.46. IR (film) 2925, 2856, 1319, 1148, 882 cm⁻¹; HRMS-APCI (*m/z*) [M+H]⁺ calcd for C₁₈H₂₄NO₃S⁺, 334.1471; found 334.1477.

The structure of *epi*-**5.23** was verified by 2D-NOESY, as the following interaction was observed:





Cycloadduct 5.25. Followed General Procedure 5.1. Cycloadduct **5.25** was obtained in 93% combined yield and 17:1 dr by ^1H NMR analysis of the crude reaction mixture. **Cycloadduct 5.25:** See Section 5.10.2.5 Scope of [2+2] Cycloadditions with Dienamines for characterization data.

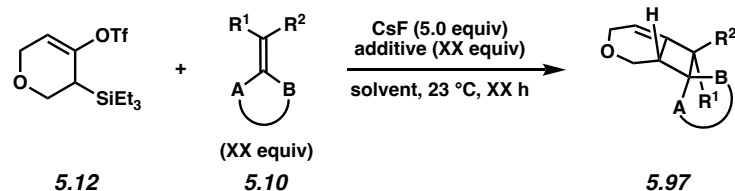


Cycloadducts 5.27. Followed General Procedure 5.1. Cycloadduct **5.27** was obtained in 94% combined yield and 2.8:1 dr by ^1H NMR analysis of the crude reaction mixture. **Cycloadduct 5.27:** See Section 5.10.2.6 Scope of [2+2] Cycloadditions with (Het)aryl-Substituted Alkenes for characterization data.

5.10.2.4 Optimization of [2+2] Cycloadditions with Exocyclic Alkenes

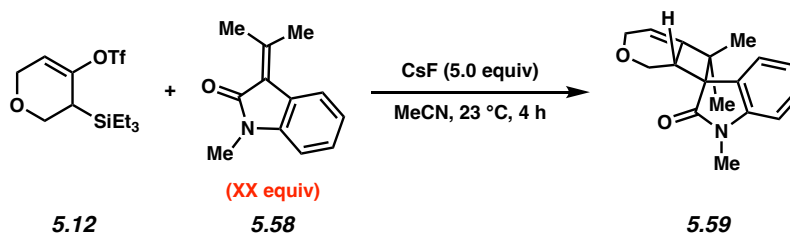
Results from the optimization of the reactions between **5.12** and **5.58** and between **5.12** and **5.24** appear below. Reactant stoichiometry, solvent, additive equivalents, and time were varied using General Procedure 5.2, and results appear below in Tables 5.2, 5.3, 5.4, and 5.5, respectively.

General Procedure 5.2 for the optimization of the [2+2] cycloaddition:



Cycloadducts 5.97. To a stirred solution of silyl triflate **5.12** (17.3 mg, 50.0 μmol , 1.0 equiv), additive, and trapping partners **5.10** in solvent (500 μL , 0.1 M) was added CsF (38.0 mg, 250 μmol , 5.0 equiv) in one portion. The vial was then sealed with a Teflon-lined cap and stirred at >900 RPM for the allotted time at 23 °C. The mixture was then filtered through a pad of silica (monster pipette, ~2 cm silica), eluting with EtOAc (10 mL). The eluate was concentrated under reduced pressure affording a crude residue, which was analyzed by ¹H NMR using mesitylene as an external standard.

Table 5.2. Evaluation of Equivalents of Trapping Partner **5.58**.

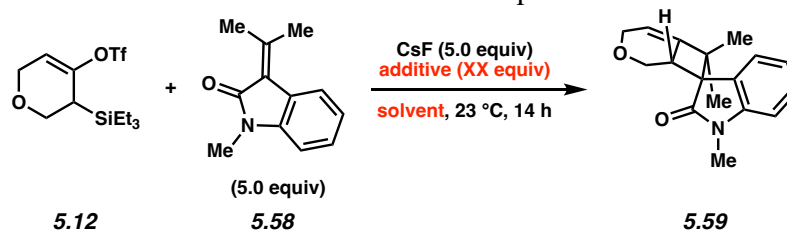


Entry	Equiv 5.58	¹ H NMR Yield ^{a,b}
1	1.0	17%
2	5.0	55%
3	10	72%

^aYield determined by ¹H NMR analysis of crude reaction mixture using mesitylene as an external standard

^bdr of cycloadduct ranges from 1.0:1–1.1:1 for all examples (determined by ¹H NMR analysis of crude reaction mixture)

Table 5.3. Evaluation of Solvent and Equivalents of Additive.



Entry	Solvent	Additive	¹ H NMR Yield ^{a,b}
1	MeCN	none	55% ^c
2	CH ₂ Cl ₂	Bu ₄ NOTf (1.0 equiv)	66%
3	CH ₂ Cl ₂	Bu ₄ NOTf (0.5 equiv)	70%
4	CH ₂ Cl ₂	Bu ₄ NOTf (0.2 equiv)	66%
5	CH ₂ Cl ₂	Bu ₄ NOTf (0.2 equiv)	81% ^d

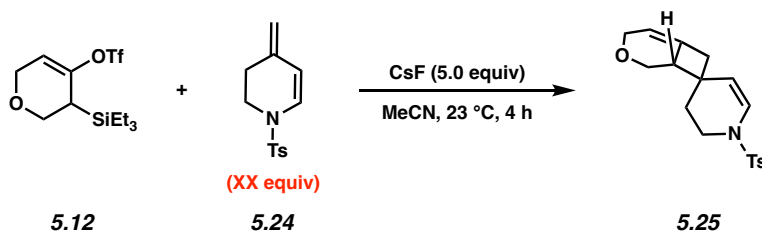
^aYield determined by ¹H NMR analysis of crude reaction mixture using mesitylene as an external standard

^bdr of cycloadduct ranges from 1.0:1–1.1:1 for all examples (determined by ¹H NMR analysis of crude reaction mixture)

^cReaction was performed for 4 h

^dReaction was performed for 21 h

Table 5.4. Evaluation of Equivalents of Trapping Partner **5.24**.

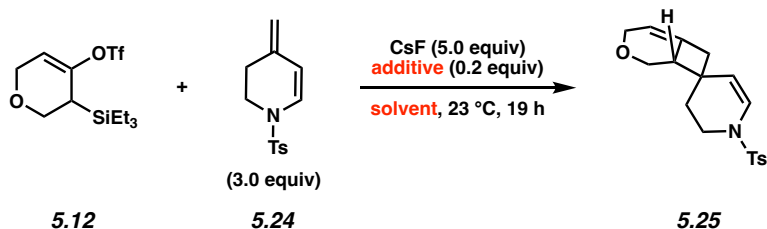


Entry	Equiv 5.24	¹ H NMR Yield ^{a,b}
1	1.2	62%
2	3.0	93%
3	5.0	93%

^aYield determined by ¹H NMR analysis of crude reaction mixture using mesitylene as an external standard

^bdr of cycloadduct >15:1 for all examples (determined by ¹H NMR analysis of crude reaction mixture)

Table 5.5. Evaluation of Solvent and Additive.



Entry	Solvent	Additive	¹ H NMR Yield ^{a,b}
1	MeCN	none	93% ^c
2	CH ₂ Cl ₂	Bu ₄ NOTf (0.2 equiv)	100%
3	CH ₂ Cl ₂	Bu ₄ NOTf (0.2 equiv)	76% ^d

^aYield determined by ¹H NMR analysis of crude reaction mixture using mesitylene as an external standard

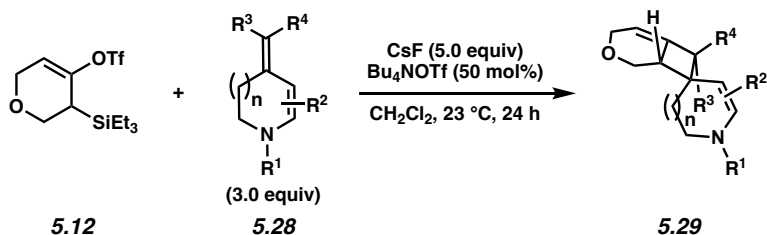
^bdr of cycloadduct >15:1 for all examples (determined by ¹H NMR analysis of crude reaction mixture)

^cReaction was performed for 4 h

^dReaction was performed with trapping partner **5.24** (1.3 equiv)

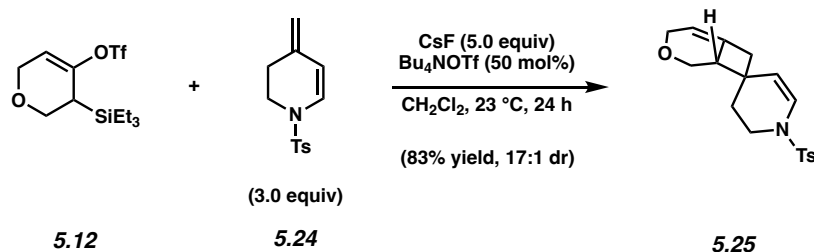
5.10.2.5 Scope of [2+2] Cycloadditions with Dienamines

General Procedure 5.3 for the scope of [2+2] cycloadditions with dienamines



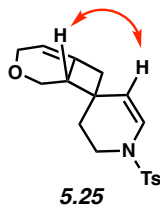
Cycloadducts 5.29. To a stirred solution of silyl triflate **5.12** (52.0 mg, 0.15 mmol, 1.0 equiv), trapping partner **5.28** (0.45 mmol, 3.0 equiv), and Bu₄NOTf (29.4 mg, 0.08 mmol, 0.5 equiv) in CH₂Cl₂ (1.5 mL, 0.1 M) was added CsF (114 mg, 0.75 mmol, 5.0 equiv). The vial was then sealed with a Teflon-lined cap and stirred at >900 RPM for 24 h at 23 °C. The mixture was then filtered through a pad of silica (monster pipette, ~2 cm silica) eluting with EtOAc (10 mL). The eluate was concentrated under reduced pressure then purified by silica chromatography to provide cycloadducts **5.29**.

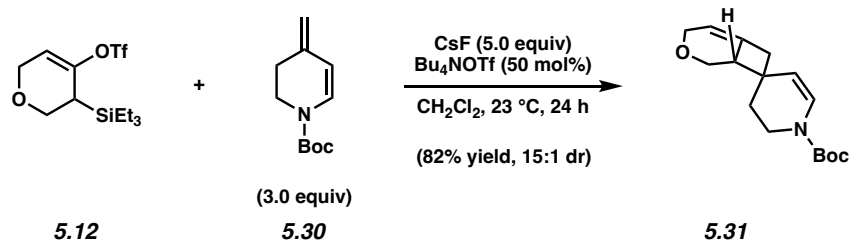
Any modification of the conditions shown in the general procedures above are specified in the following schemes.



Cycloadduct 5.25. Followed General Procedure 5.3. Purification by flash column chromatography (6:1 hexanes:EtOAc \rightarrow 1:1 hexanes:EtOAc) afforded cycloadduct **5.25** (83% combined yield, average of two experiments) as a clear oil. The dr, as determined by ^1H NMR analysis of each crude reaction mixture, was 17:1. **Cycloadduct 5.25:** R_f 0.36 (3:1 hexanes:EtOAc); ^1H NMR (600 MHz, CDCl_3): δ 7.66–7.62 (m, 2H), 7.31 (d, $J = 8.1$, 2H), 6.56 (d, $J = 8.2$, 1H), 5.37–5.35 (m, 1H), 5.03 (d, $J = 8.1$, 1H), 4.18–4.13 (m, 1H), 4.08–4.02 (m, 1H), 3.76 (dd, $J = 10.2, 6.4$, 1H), 3.38 (ddd, $J = 12.3, 6.4, 3.6$, 1H), 3.13 (ddd, $J = 12.0, 9.1, 3.4$, 1H), 3.05 (app. t, $J = 9.7$, 1H), 2.98–2.93 (m, 1H), 2.83–2.78 (m, 1H), 2.43 (s, 3H), 2.20 (d, $J = 14.1$ 1H), 1.68–1.58 (m, 2H); ^{13}C NMR (150 MHz, CDCl_3): δ 143.9, 135.0, 134.6, 129.9, 127.2, 124.0, 116.3, 114.0, 65.6, 63.0, 49.0, 46.3, 42.1, 38.2, 27.0, 21.7; IR (film): 2876, 1671, 1639, 1343, 1166 cm^{-1} ; HRMS-APCI (m/z) $[\text{M} + \text{H}]^+$ calcd for $\text{C}_{18}\text{H}_{22}\text{NO}_3\text{S}^+$, 332.1315; found 332.1314.

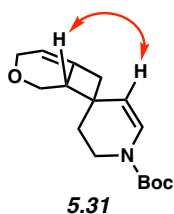
The structure of **5.25** was verified by 2D-NOESY, as the following interaction was observed:



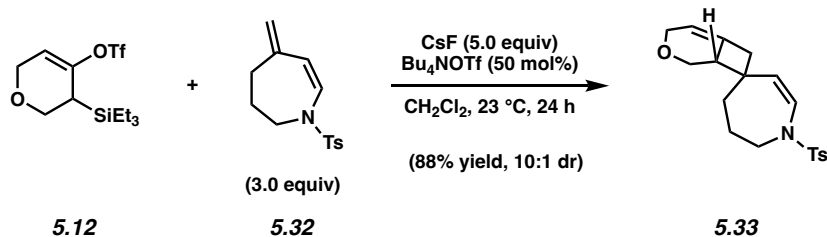


Cycloadduct 5.31. Followed General Procedure 5.3. Purification by flash column chromatography (30:1 hexanes:EtOAc → 15:1 hexanes:EtOAc) afforded cycloadduct **5.31** (82% combined yield, average of two experiments) as a pale yellow oil. The dr, as determined by ¹H NMR analysis of each crude reaction mixture, was 15:1. **Cycloadduct 5.31:** R_f 0.38 (3:1 hexanes:EtOAc); ¹H NMR (600 MHz, CDCl₃): δ 6.85–6.59 (m, 1H), 5.44–5.37 (m, 1H), 5.02–4.79 (m, 1H), 4.25–4.16 (m, 1H), 4.15–4.05 (m, 1H), 3.91 (dd, *J* = 9.6, 7.0, 1H), 3.68–3.49 (m, 1H), 3.38–3.27 (m, 1H), 3.20 (app. t, *J* = 9.9 1H), 3.07–3.00 (m, 1H), 2.92–2.82 (m, 1H), 2.40–2.31 (m, 1H), 1.81–1.69 (m, 2H), 1.48 (s, 9H); ¹³C NMR (125 MHz, CDCl₃): δ 152.5, 152.1, 135.1, 135.0, 124.4, 124.1, 114.0, 113.7, 113.6, 113.5 81.0, 80.8, 65.5, 63.1, 49.1, 46.2, 44.6, 40.6, 39.6, 38.5, 38.4, 28.3; IR (film): 2926, 1704, 1640, 1409, 1371 cm⁻¹; HRMS-APCI (*m/z*) [M + H]⁺ calcd for C₁₆H₂₄NO₃⁺, 278.1751; found 278.1749.

The structure of **5.31** was verified by 2D-NOESY, as the following interactions were observed:

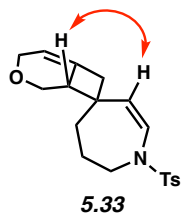


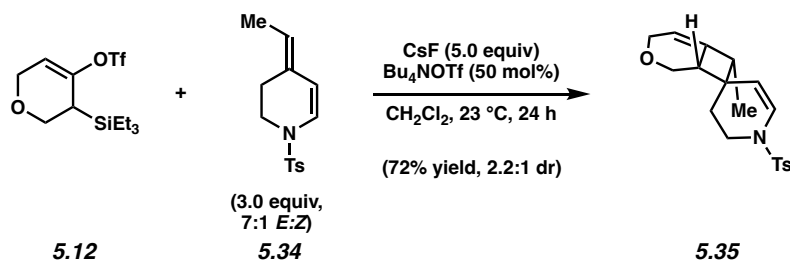
Note: 5.31 was obtained as a mixture of rotamers. These data represent empirically observed chemical shifts from the ¹H, and ¹³C-NMR spectra.



Cycloadducts 5.33. Followed General Procedure 5.3. Purification by flash column chromatography (13:1 hexanes:EtOAc \rightarrow 6:1 hexanes:EtOAc) afforded cycloadduct **5.33** (88% combined yield, average of two experiments) as a white solid. The dr, as determined by ^1H NMR analysis of each crude reaction mixture, was 10:1. **Cycloadduct 5.33:** Mp: 51–52 $^\circ\text{C}$; R_f 0.62 (3:1 hexanes:EtOAc); ^1H NMR (600 MHz, CDCl_3): δ 7.69–7.66 (m, 2H), 7.31 (d, $J = 8.1$, 2H), 6.37 (d, $J = 9.3$, 1H), 5.39–5.35 (m, 1H), 5.02 (d, $J = 9.3$, 1H), 4.17–4.13 (m, 1H), 4.09–4.03 (m, 1H), 3.80 (dd, $J = 10.3, 6.6$, 1H), 3.48–3.40 (m, 1H), 3.40–3.34 (m, 1H), 3.14 (app. t, $J = 9.8$, 1H), 3.05–2.96 (m, 1H), 2.78–2.72 (m, 1H), 2.49–2.43 (m, 1H), 2.43 (s, 3H), 1.71–1.65 (m, 3H), 1.54–1.50 (overlapped with residual water peak, 1H); ^{13}C NMR (125 MHz, CDCl_3): δ 143.7, 136.3, 135.2, 129.8, 126.9, 126.1, 123.4, 114.0, 65.4, 63.4, 51.4, 49.9, 45.2, 44.0, 29.2, 25.5, 21.6; IR (film): 2925, 1644, 1598, 2343, 1162 cm^{-1} ; HRMS-APCI (m/z) $[\text{M} + \text{H}]^+$ calcd for $\text{C}_{19}\text{H}_{24}\text{NO}_3\text{S}^+$, 346.1471; found 346.1477.

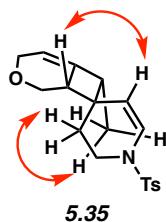
The structure of **5.33** was verified by 2D-NOESY, as the following interactions were observed:

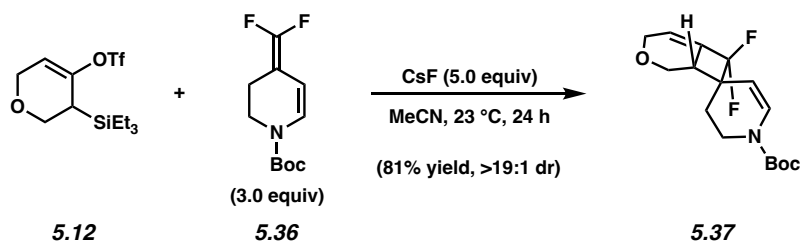




Cycloadduct 5.35. Followed General Procedure 5.3. Purification by preparative thin layer chromatography (9:1 hexanes:EtOAc) afforded cycloadduct **5.35** (72% combined yield, average of two experiments) as a colorless oil. The dr, as determined by ^1H NMR analysis of each crude reaction mixture, was 2.2:1. The 2.2:1 ratio reflects the ratio of the major diastereomer (2.2) to the sum of all minor diastereomers (1). **Cycloadduct 5.35:** R_f 0.16 (9:1 hexanes:EtOAc); ^1H NMR (500 MHz, CDCl_3): δ 7.66–7.60 (m, 2H), 7.30 (d, $J = 8.0$, 2H), 6.57 (d, $J = 8.2$, 1H), 5.31–5.27 (m, 1H), 4.96 (d, $J = 8.2$, 1H), 4.16–4.09 (m, 1H), 4.05–3.99 (m, 1H), 3.69 (dd, $J = 10.2, 6.5$, 1H), 3.35 (ddd, $J = 12.1, 6.8, 3.9$, 1H), 3.01–2.91 (m, 3H), 2.90–2.83 (m, 1H), 2.42 (s, 3H), 1.54–1.49 (m, 2H), 0.85 (d, $J = 6.9$, 3H); ^{13}C NMR (150 MHz, CDCl_3): δ 143.8, 140.7, 134.7, 129.7, 127.1, 124.3, 116.7, 110.8, 65.4, 62.8, 49.9, 48.1, 42.3, 40.4, 22.4, 21.6, 10.6; IR (film): 2910, 2842, 1335, 1144, 875 cm^{-1} . HRMS-APCI (m/z) $[\text{M} + \text{H}]^+$ calcd for $\text{C}_{19}\text{H}_{24}\text{NO}_3\text{S}^+$, 346.1471; found 346.1479.

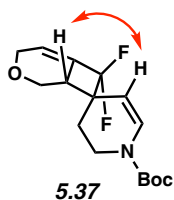
The structure of **5.35** was verified by 2D-NOESY, as the following interactions were observed:



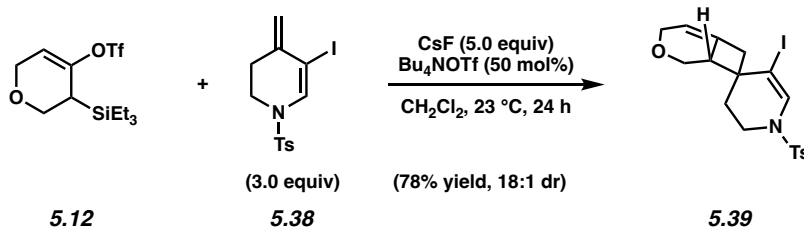


Cycloadduct 5.37. On 0.15 mmol scale, followed modified General Procedure 5.1 using three equivalents of dienamine **5.36** and an extended reaction time of 24 h. Purification by preparative thin layer chromatography (9:1 hexanes:EtOAc) afforded cycloadduct **5.37** (81% yield, average of two experiments) as a colorless oil. The dr, as determined by ^1H NMR analysis of each crude reaction mixture, was >19:1. **Cycloadduct 5.37:** R_f 0.45 (9:1 hexanes:EtOAc); ^1H NMR (600 MHz, CDCl_3): δ 7.05–6.83 (m, 1H), 6.08–6.05 (m, 1H), 4.96–4.77 (m, 1H), 4.35–4.26 (m, 1H), 4.18–4.12 (m, 1H), 4.09–4.02 (m, 1H), 3.70–3.57 (m, 1H), 3.46–3.36 (m, 1H), 3.10 (app. t, $J = 9.8$, 1H), 2.94–2.88 (m, 1H), 2.00–1.89 (m, 1H), 1.67–1.60 (m, 1H), 1.48 (s, 9H); ^{13}C NMR (150 MHz, CDCl_3): δ 152.2, 151.8, 134.8, 127.6, 127.4, 121.1 (dd, $J = 299.7, 273.0$), 120.1, 120.0, 103.7, 103.2, 81.3, 81.2, 64.6, 63.1, 49.6, 42.9, 42.8, 40.4, 39.4, 28.2, 22.9, 22.8; ^{19}F NMR (565 MHz, CDCl_3) δ –107.76 (dd, $J = 205.3, 103.6$), –109.51 (dd, $J = 205.3, 43.1$); IR (film) 2977, 2927, 1707, 1261, 770 cm^{-1} . HRMS-APCI (m/z) $[\text{M} + \text{H}]^+$ calcd for $\text{C}_{16}\text{H}_{22}\text{F}_2\text{NO}_3^+$, 314.1562; found 314.1570.

The structure of **5.37** was verified by 2D-NOESY, as the following interaction was observed:

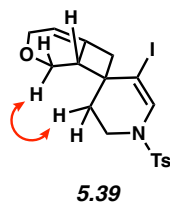


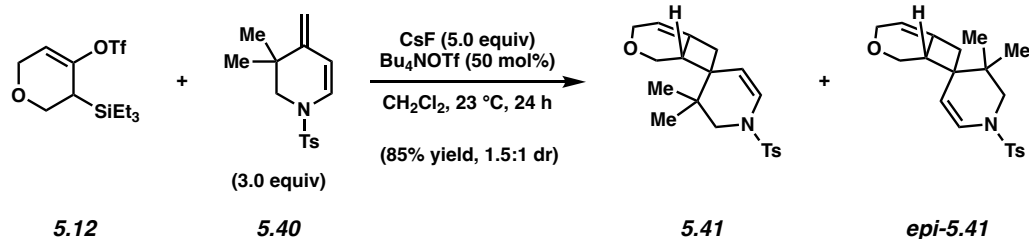
Note: 5.37 was obtained as a mixture of rotamers. These data represent empirically observed chemical shifts from the ^1H , ^{19}F , and ^{13}C -NMR spectra.



Cycloadduct 5.39. Followed General Procedure 5.3. Purification by flash column chromatography (30:1 hexanes:EtOAc \rightarrow 1:1 hexanes:EtOAc) afforded cycloadduct **5.39** (78% combined yield, average of two experiments) as a pale yellow oil. The dr, as determined by ^1H NMR analysis of each crude reaction mixture, was 18:1. **Cycloadduct 5.39:** R_f 0.38 (3:1 hexanes:EtOAc); ^1H NMR (500 MHz, CDCl_3): δ 7.65–7.61 (m, 2H), 7.33 (d, $J = 8.1$, 2H), 7.14 (s, 1H), 5.42–5.37 (m, 1H), 4.21–4.13 (m, 1H), 4.09–4.02 (m, 1H), 3.74 (dd, $J = 10.2, 6.6$, 1H), 3.38–3.26 (m, 3H), 3.10 (d, $J = 14.03$, 1H), 3.01 (app. t, 9.8, 1H), 2.44 (s, 3H), 2.11 (d, $J = 13.3$, 1H) 1.92–1.79 (m, 2H); ^{13}C NMR (125 MHz, CDCl_3): δ 144.3, 134.5, 133.8, 131.2, 130.0, 127.1, 114.6, 89.5, 65.4, 62.7, 49.1, 46.2, 43.5, 41.8, 27.5, 21.6; IR (film): 2965, 1599, 1345, 1168, 1647 cm^{-1} ; HRMS-APCI (m/z) [$\text{M} + \text{H}$] $^+$ calc'd for $\text{C}_{18}\text{H}_{21}\text{INO}_3\text{S}^+$, 458.0281; found 458.0288.

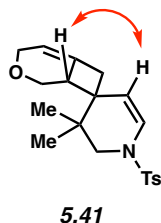
The structure of **5.39** was verified by 2D-NOESY, as the following interactions were observed:





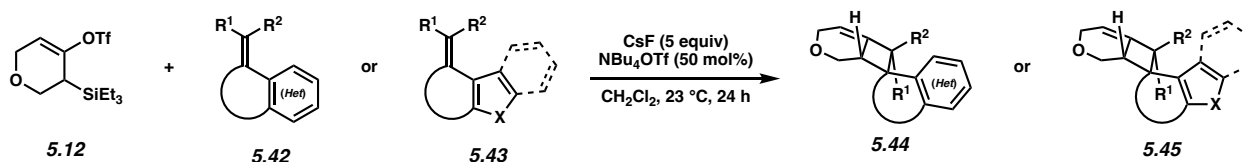
Cycloadducts 5.41 and *epi-5.41*. Followed General Procedure 5.3. Purification by flash column chromatography (30:1 hexanes:EtOAc → 9:1 hexanes:EtOAc) afforded a mixture of major diastereomer **5.41** and minor diastereomer *epi-5.41* (85% combined yield, average of two experiments) as a pale yellow oil. The dr, as determined by ¹H NMR analysis of each crude reaction mixture, was 1.5:1. An analytical sample of cycloadduct *epi-5.41* was obtained from the thermal isomerization experiment (see Section 5.10.2.8 Thermal Isomerizations of [2+2] Cycloadducts for details). **Cycloadducts 5.41** and *epi-5.41*: ¹H NMR (600 MHz, CDCl₃, **5.41**, characterized from an inseparable mixture of **5.41** and *epi-5.41*): δ 7.66–7.63 (m, 2H), 7.30 (d, *J* = 8.1, 2H), 6.48 (d, *J* = 7.9, 1H), 5.16–5.13 (m, 1H), 4.99 (d, *J* = 8.0, 1H), 4.26–4.18 (m, 1H), 4.13–4.12 (m, 1H), 3.96–3.85 (m, 1H), 3.55 (app. t, *J* = 10.0, 1H), 3.15–3.07 (m, 1H), 3.03–3.00 (m, 1H), 2.70–2.63 (m, 1H), 2.52–2.47 (m, 1H), 2.44–2.39 (m, 4H), 1.07 (s, 3H), 0.75 (s, 3H); ¹H NMR (500 MHz, CDCl₃, *epi-5.41*): δ 7.63 (d, *J* = 8.3, 2H), 7.30 (d, *J* = 8.1, 2H), 6.62 (d, *J* = 8.4, 1H), 5.45–5.39 (m, 1H), 4.94 (d, *J* = 8.2, 1H), 4.18–4.10 (m, 1H), 4.10–4.03 (m, 1H), 3.40–3.32 (m, 1H), 3.05 (d, *J* = 11.4, 1H), 3.01–2.93 (m, 2H), 2.92–2.85 (m, 1H), 2.57 (d, *J* = 11.4, 1H), 2.42 (s, 3H), 2.11 (d, *J* = 13.2, 1H), 0.92 (s, 3H), 0.83 (s, 3H); ¹³C NMR (150 MHz, CDCl₃, **5.41** and *epi-5.41*, 32 out of 36 signals observed): δ 143.8, 143.7, 136.1, 135.4, 134.8, 132.9, 129.74, 129.70, 127.01, 126.99, 123.5, 121.1, 117.6, 114.2, 111.0, 110.0, 66.1, 65.4, 64.7, 53.1, 52.3, 50.9, 47.2, 46.7, 44.2, 39.7, 33.33, 33.30, 22.6, 22.5, 21.6, 21.4. IR (film): 2965, 1647, 1598, 1345, 1167 cm⁻¹; HRMS-APCI (*m/z*) [*M* + *H*]⁺ calcd for C₂₀H₂₆NO₃S⁺, 360.1623; found 360.1635

The structure of **5.41** was verified by 2D-NOESY, as the following interactions were observed:



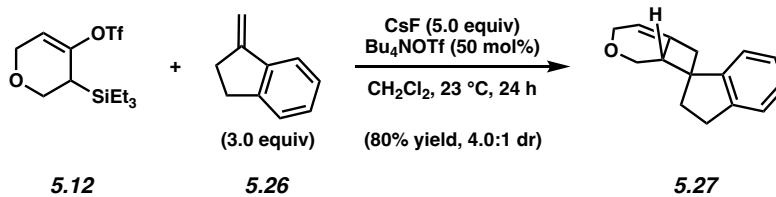
5.10.2.6 Scope of [2+2] Cycloadditions with (Het)aryl-Substituted Alkenes

General Procedure 5.4 for the scope of [2+2] cycloadditions with (het)aryl-substituted alkenes



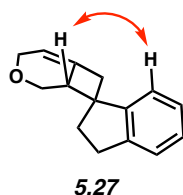
Cycloadducts 5.44 or **5.45**. To a stirred solution of silyl triflate **5.12** (52.0 mg, 0.15 mmol, 1.0 equiv), trapping partners **5.42** or **5.43** (0.45 mmol, 3.0 equiv), and Bu_4NOTf (29.4 mg, 0.08 mmol, 0.5 equiv) in CH_2Cl_2 (1.5 mL, 0.1 M) was added CsF (114 mg, 0.75 mmol, 5.0 equiv). The vial was then sealed with a Teflon-lined cap and stirred at >900 RPM for 24 h at 23 °C. The mixture was then filtered through a pad of silica (monster pipette, ~2 cm silica) eluting with EtOAc (10 mL). The eluate was concentrated under reduced pressure then purified by silica chromatography to provide cycloadducts **5.44** or **5.45**.

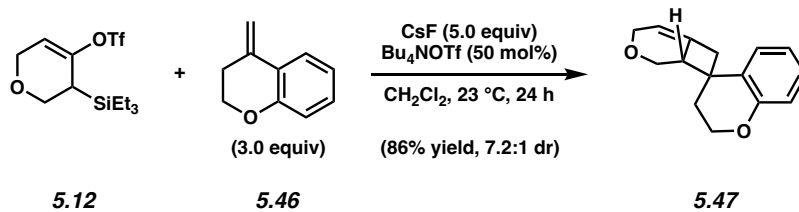
Any modification of the conditions shown in the general procedures above are specified in the following schemes.



Cycloadduct 5.27. Followed General Procedure 5.5. Purification by preparative thin layer chromatography (9:1 hexanes:EtOAc) afforded cycloadduct **5.27** (80% combined yield, average of two experiments) as a colorless oil. The dr, as determined by ^1H NMR analysis of each crude reaction mixture, was 4.0:1. An analytical sample was obtained by preparative thin layer chromatography (19:1 hexanes:EtOAc) to provide major diastereomer **5.27**. **Cycloadduct 5.27:** R_f 0.66 (9:1 hexanes:EtOAc); ^1H NMR (600 MHz, CDCl_3): δ 7.41 (d, $J = 7.5$, 1H), 7.26 (overlapped with residual solvent peak, 1H), 7.23–7.15 (m, 2H), 5.48–5.45 (m, 1H), 4.29–4.23 (m, 1H), 4.21–4.15 (m, 1H), 3.92 (dd, $J = 10.0$, 6.4, 1H), 3.43–3.38 (m, 1H), 3.34 (app. t, $J = 9.8$, 1H), 3.11–3.05 (m, 1H), 2.87 (app. dt, $J = 15.6$, 7.9, 1H), 2.80–2.69 (m, 2H), 2.21 (app. dt, $J = 12.6$, 7.4, 1H), 2.04 (ddd, $J = 12.8$, 7.6, 5.3, 1H); ^{13}C NMR (150 MHz, CDCl_3): δ 148.4, 143.4, 135.5, 126.9, 126.7, 124.4, 122.0, 113.0, 65.5, 63.9, 52.1, 48.5, 45.4, 33.5, 30.2; IR (film) 2957, 2832, 1358, 1072, 712 cm^{-1} ; HRMS-APCI (m/z) $[\text{M} + \text{H}]^+$ calcd for $\text{C}_{15}\text{H}_{17}\text{O}^+$, 213.1274; found 213.1280.

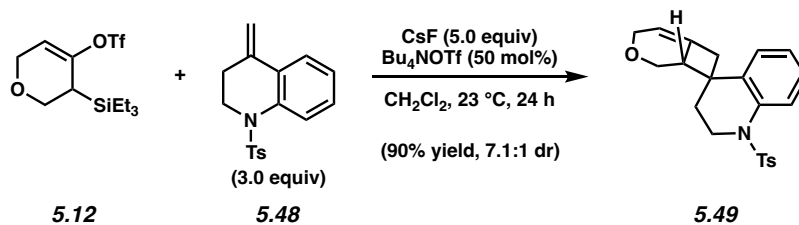
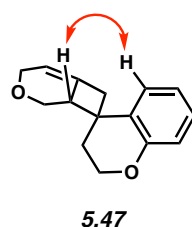
The structure of **5.27** was verified by 2D-NOESY, as the following interaction was observed:





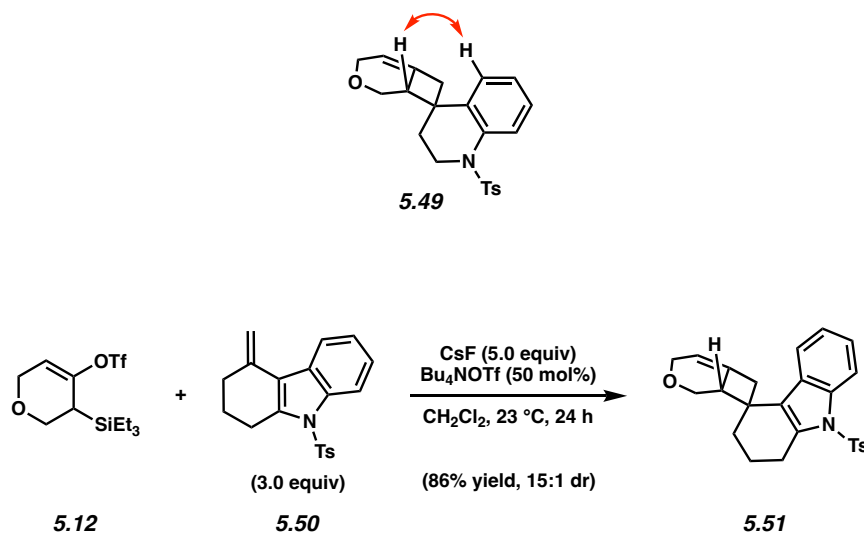
Cycloadducts 5.47. Followed General Procedure 5.5. Purification by flash column chromatography (hexanes → 12:1 hexanes:EtOAc) afforded cycloadduct **5.47** (86% combined yield, average of two experiments) as a pale yellow oil. The dr, as determined by ^1H NMR analysis of each crude reaction mixture, was 7.2:1. **Cycloadduct 5.47:** R_f 0.56 (5:1 hexanes:EtOAc); ^1H NMR (600 MHz, CDCl_3): δ 7.57 (dd, $J = 7.9, 1.3$, 1H), 7.15–7.11 (m, 1H), 7.00–6.96 (m, 1H), 6.80 (dd, $J = 8.2, 1.0$, 1H), 5.56–5.53 (m, 1H), 4.30–4.23 (m, 1H), 4.20–4.14 (m, 1H), 4.11 (ddd, $J = 11.3, 8.0, 2.7$, 1H), 4.06 (ddd, $J = 10.9, 6.3, 2.9$, 1H), 3.95 (dd, $J = 10.2, 6.6$, 1H), 3.60–3.53 (m, 1H), 3.28–3.21 (m, 2H), 2.62 (d, $J = 13.4$, 1H), 2.09 (ddd, $J = 14.0, 8.9, 2.9$, 1H), 1.97 (ddd, $J = 14.0, 6.9, 2.6$, 1H); ^{13}C NMR (150 MHz, CDCl_3): δ 154.1, 134.6, 128.2, 128.0, 127.1, 121.0, 116.9, 115.0, 65.7, 64.4, 63.5, 49.8, 48.4, 39.8, 28.9; IR (film): 3031, 2923, 1606, 1487, 1180 cm^{-1} ; HRMS-APCI (m/z) $[\text{M} + \text{H}]^+$ calcd for $\text{C}_{15}\text{H}_{17}\text{O}_2^+$, 229.1223; found 229.1222.

The structure of **5.47** was verified by 2D-NOESY, as the following interaction was observed:



Cycloadduct 5.49. Followed General Procedure 5.5. Purification by flash chromatography (19:1 hexanes:EtOAc → 4:1 hexanes:EtOAc) afforded cycloadduct **5.49** (90% combined yield, average of two experiments) as a colorless solid. The dr, as determined by ¹H NMR analysis of each crude reaction mixture, was 7.1:1. **Cycloadduct 5.49:** Mp: 56 °C; R_f 0.31 (4:1 hexanes:EtOAc); ¹H NMR (600 MHz, CDCl₃): δ 7.82–7.77 (m, 1H), 7.59–7.55 (m, 1H), 7.46–7.42 (m, 2H), 7.24–7.21 (m, 2H), 7.19 (d, *J* = 8.2, 2H), 5.48–5.44 (m, 1H), 4.22–4.15 (m, 1H), 4.10–4.04 (m, 1H), 3.90 (ddd, *J* = 13.8, 5.9, 3.4, 1H), 3.59 (ddd, *J* = 13.5, 10.1, 2.9, 1H), 3.52 (dd, *J* = 10.2, 6.6, 1H), 3.45–3.39 (m, 1H), 2.97–2.93 (m, 1H), 2.90 (app. t, *J* = 9.7, 1H), 2.40–2.36 (m, 4H), 1.58 (ddd, *J* = 13.7, 5.9, 2.9, 1H), 1.51 (ddd, *J* = 13.6, 10.1, 3.2, 1H); ¹³C NMR (150 MHz, CDCl₃): δ 143.7, 136.9, 136.0, 135.0, 134.1, 129.5, 127.1, 126.99, 126.98, 125.5, 124.5, 115.0, 65.4, 63.0, 50.0, 48.9, 44.5, 41.1, 26.9, 21.5; IR (film) 2957, 2888, 1358, 1162, 1072 cm⁻¹; HRMS-APCI (*m/z*) [M+H]⁺ calcd for C₂₂H₂₄NO₃S⁺, 382.1471; found 382.1455.

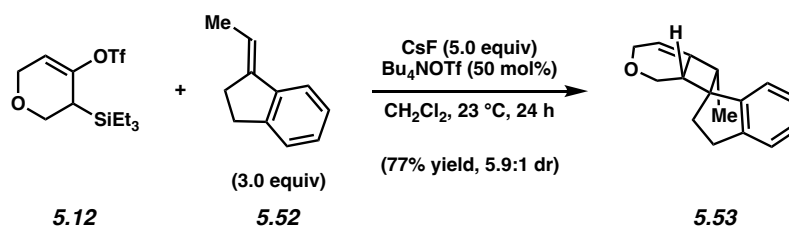
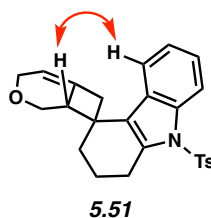
The structure of **5.49** was verified by 2D-NOESY, as the following interaction was observed:



Cycloadduct 5.51. Followed General Procedure 5.5. Purification by flash column chromatography (9:1 hexanes:EtOAc → 4:1 hexanes:EtOAc) afforded cycloadduct **5.51** (86% combined yield,

average of two experiments) as a white solid. The dr, as determined by ^1H NMR analysis of each crude reaction mixture, was 15:1. **Cycloadduct 5.51**: Mp: 67–70 °C; R_f 0.20 (5:1 hexanes:EtOAc); ^1H NMR (600 MHz, C_6D_6): δ 8.58 (d, $J = 8.6$, 1H), 7.65 (d, $J = 8.1$, 1H), 7.63–7.59 (m, 2H), 7.20–7.14 (overlapped with residual solvent peak, 1H), 7.03 (app. t, $J = 7.9$, 1H), 6.47–6.44 (m, 2H), 5.27–5.24 (m, 1H), 4.27–4.20 (m, 1H), 4.03–3.96 (m, 1H), 3.87–3.80 (m, 1H), 3.64 (dd, $J = 10.1, 7.0$, 1H), 3.51–3.46 (m, 1H), 3.08–2.99 (m, 3H), 2.17 (d, $J = 14.6$, 1H), 1.66–1.57 (overlapped with residual water peak, 4H), 1.47–1.35 (m, 2H), 1.28–1.20 (m, 1H); ^{13}C NMR (125 MHz, CDCl_3): δ 144.7, 136.6, 136.3, 135.7, 135.5, 129.9, 128.7, 126.5, 123.7, 123.1, 122.3, 120.0, 114.9, 114.7, 65.7, 63.6, 47.3, 43.8, 41.3, 30.4, 25.3, 21.6, 21.2; IR (film): 2925, 1598, 1110, 985, 849 cm^{-1} ; HRMS-APCI (m/z) $[\text{M} + \text{H}]^+$ calcd for $\text{C}_{25}\text{H}_{26}\text{NO}_3\text{S}^+$, 420.1628; found 420.1629.

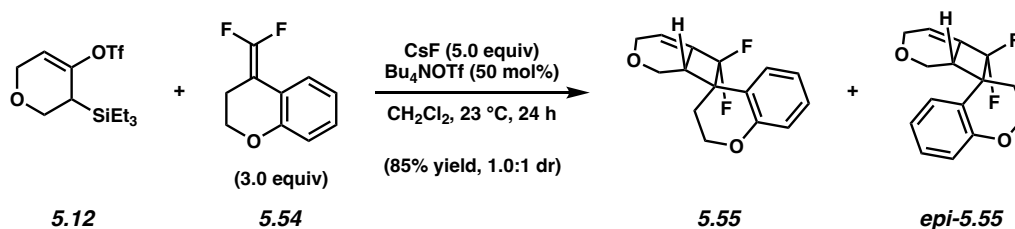
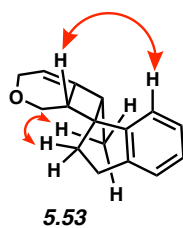
The structure of **5.51** was verified by 2D-NOESY, as the following interaction was observed:



Cycloadduct 5.53. Followed General Procedure 5.5. Purification by preparative thin layer chromatography (9:1 hexanes:EtOAc) afforded cycloadduct **5.53** (77% combined yield, average of two experiments) as a colorless oil. The dr, as determined by ^1H NMR analysis of each crude

reaction mixture, was 5.9:1. **Cycloadduct 5.53**: R_f 0.44 (9:1 hexanes:EtOAc); ^1H NMR (500 MHz, CDCl_3): δ 7.39 (d, $J = 7.5$, 1H), 7.26 (overlapped with residual solvent peak, 1H), 7.23–7.16 (m, 2H), 5.40–5.37 (m, 1H), 4.28–4.21 (m, 1H), 4.16 (app. dq, $J = 15.7$, 3.8, 1H), 3.93–3.86 (m, 1H), 3.42–3.35 (m, 1H), 3.30–3.24 (m, 2H), 2.82 (app. dt, $J = 15.5$, 7.2, 1H), 2.72 (ddd, $J = 15.5$, 7.8, 5.7, 1H), 2.09 (ddd, $J = 13.2$, 7.7, 5.7, 1H), 1.94 (ddd, $J = 13.0$, 7.8, 6.7, 1H), 1.08 (d, $J = 6.8$, 3H); ^{13}C NMR (150 MHz, CDCl_3): δ 148.4, 143.4, 141.8, 126.9, 126.7, 124.4, 122.0, 110.1, 65.4, 63.9, 54.9, 50.4, 47.6, 30.6, 27.5, 11.9; IR (film) 3018, 2957, 1216, 1098, 760 cm^{-1} . HRMS-APCI (m/z) [$\text{M} + \text{H}$] $^+$ calcd for $\text{C}_{16}\text{H}_{19}\text{O}^+$, 227.1430; found 227.1435.

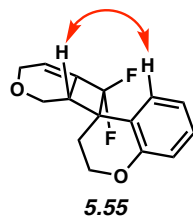
The structure of **5.53** was verified by 2D-NOESY, as the following interaction was observed:

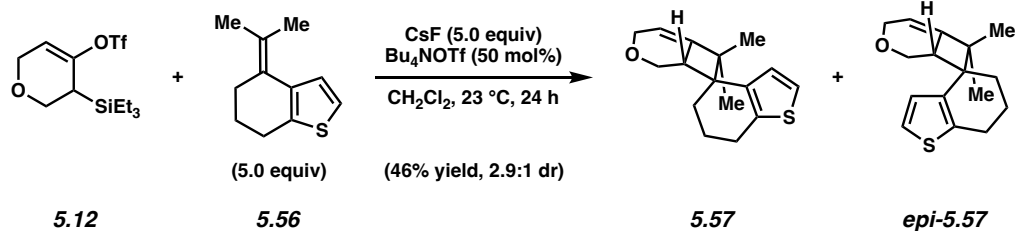


Cycloadducts 5.55 and *epi*-**5.55**. Followed General Procedure 5.5. Purification by preparative thin layer chromatography (9:1 hexanes:EtOAc) allowed for the separation of the diastereomers, affording cycloadducts **5.55** and *epi*-**5.55** (85% combined yield, average of two experiments) as colorless oils. The dr, as determined by ^1H NMR analysis of each crude reaction mixture, was 1.0:1. **Cycloadduct 5.55**: R_f 0.33 (9:1 hexanes:EtOAc); ^1H NMR (600 MHz, CDCl_3): δ 7.48 (ddd, $J = 8.0$, 3.1, 1.7, 1H), 7.22 (ddd, $J = 8.6$, 7.2, 1.6, 1H), 6.99 (ddd, $J = 8.2$, 7.1, 1.2, 1H), 6.87 (dd,

$J = 8.2, 1.0, 1\text{H}$), 6.22–6.19 (m, 1H), 4.41–4.34 (m, 1H), 4.32 (app. dt, $J = 11.2, 3.5, 1\text{H}$), 4.26–4.19 (m, 1H), 4.11–4.06 (m, 1H), 4.07–4.04 (m, 1H), 3.54–3.48 (m, 1H), 3.21 (app. t, $J = 9.73, 1\text{H}$), 2.18–2.12 (m, 1H), 1.94–1.86 (m, 1H); ^{13}C NMR (150 MHz, CDCl_3): δ 155.1, 134.53 (dd, $J = 25.3, 21.5$), 129.6 (d, $J = 4.2$), 129.2, 121.4 (d, $J = 3.1$), 121.1 (dd, $J = 299.7, 276.8$), 120.4, 118.3, 117.2, 64.9, 63.9 (d, $J = 3.1$), 63.6 (d, $J = 1.8$), 50.4 (dd, $J = 22.9, 18.0$), 41.9 (d, $J = 14.3$), 24.8; ^{19}F NMR (565 MHz, CDCl_3): δ -107.44 (d, $J = 201.7$), -108.92 (d, $J = 201.7$); IR (film) 2970, 1490, 1253, 1100, 757 cm^{-1} . HRMS-APCI (m/z) $[\text{M} + \text{H}]^+$ calcd for $\text{C}_{15}\text{H}_{15}\text{F}_2\text{O}_2^+$, 265.10346; found 265.1046. **Cycloadduct epi-5.55**: R_f 0.38 (9:1 hexanes:EtOAc); ^1H NMR (600 MHz, CDCl_3): δ 7.33 (ddd, $J = 7.9, 4.0, 1.5, 1\text{H}$), 7.17 (ddd, $J = 8.6, 7.2, 1.6, 1\text{H}$), 6.86 (ddd, $J = 8.0, 7.2, 1.2, 1\text{H}$), 6.82 (dd, $J = 8.2, 1.0, 1\text{H}$), 6.22–6.18 (m, 1H), 4.44–4.33 (m, 2H), 4.23–4.16 (m, 1H), 3.95–3.89 (m, 1H), 3.89–3.83 (m, 1H), 2.92–2.84 (m, 2H), 2.36 (ddd, $J = 14.1, 12.3, 3.8, 1\text{H}$), 2.20–2.13 (m, 1H). ^{13}C NMR (150 MHz, CDCl_3): δ 154.3, 135.5 (dd, $J = 27.2, 20.7$), 128.9, 128.1 (d, $J = 5.1$), 120.2 (dd, $J = 300.3, 272.5$), 119.8, 119.3 (d, $J = 3.5$), 117.50 (d, $J = 2.9$), 117.45, 64.6 (d, $J = 1.3$), 64.0 (d, $J = 2.3$), 63.2, 53.5 (dd, $J = 25.3, 19.3$), 46.6 (dd, $J = 12.2, 1.6$), 29.3 (d, $J = 8.4$ Hz); ^{19}F NMR (565 MHz, CDCl_3): δ -103.10 (d, $J = 208.6$ Hz), -107.27 (dd, $J = 208.5, 3.9$ Hz); IR (film) 2967, 1490, 1225, 1051, 758 cm^{-1} ; HRMS-APCI (m/z) $[\text{M} + \text{H}]^+$ calcd for $\text{C}_{15}\text{H}_{15}\text{F}_2\text{O}_2^+$, 265.10346; found 265.1045.

The structure of **5.55** was verified by 2D-NOESY, as the following interaction was observed:

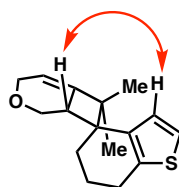




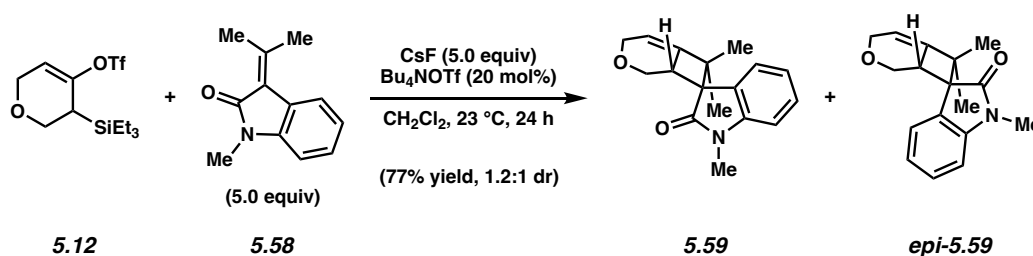
Cycloadducts 5.57 and *epi-5.57*. Followed a modified General Procedure 5.5 by altering the amount of trapping partner **5.56** (134 mg, 0.75 mmol, 5.0 equiv). Purification by preparative thin layer chromatography (9:1 hexanes:Et₂O, eluted 2x) allowed for a separation of the diastereomers, affording cycloadduct **5.57** as a yellow oil and cycloadduct *epi-5.57* as a colorless oil (46% combined yield, average of two experiments). The dr, as determined by ¹H NMR analysis of each crude reaction mixture, was 2.9:1. **Cycloadduct 5.57**: *R_f* 0.53 (9:1 hexanes:Et₂O); ¹H NMR (500 MHz, CDCl₃): δ 7.15 (d, *J* = 5.4, 1H), 7.06 (d, *J* = 5.2, 1H), 5.41–5.38 (m, 1H), 4.23 (app. dt, *J* = 15.7, 2.6, 1H), 4.15 (ddd, *J* = 15.7, 3.7, 2.6, 1H), 3.88 (dd, *J* = 10.0, 6.8, 1H), 3.61–3.54 (m, 1H), 3.27 (app. t, *J* = 10.0, 1H), 2.84–2.77 (m, 1H), 2.74–2.61 (m, 1H), 2.11 (ddd, *J* = 13.3, 4.7, 2.2 1H), 1.95–1.87 (m, 1H), 1.81–1.70 (m, 1H), 1.41–1.33 (m, 1H), 1.20 (s, 3H), 1.16 (s, 3H); ¹³C NMR (125 MHz, CDCl₃): δ 145.6, 137.9, 137.7, 128.4, 120.6, 110.9, 65.6, 63.6, 54.5, 46.6, 46.4, 27.4, 25.3, 25.2, 21.8, 21.1; IR (film): 2927, 1364, 1218, 1098, 689 cm⁻¹; HRMS-APCI (*m/z*) [*M* + H]⁺ calcd for C₁₆H₂₁OS⁺, 261.1308; found 261.1313. **Cycloadduct epi-5.57**: *R_f* 0.59 (9:1 hexanes:Et₂O); ¹H NMR (500 MHz, CDCl₃): δ 7.29–7.23 (overlapped with residual solvent peak, 1H), 7.00 (d, *J* = 5.3, 1H), 5.38–5.35 (m, 1H), 4.23–4.18 (m, 2H), 3.72 (dd, *J* = 10.5, 7.2, 1H), 3.31–3.25 (m, 1H), 3.21–3.14 (m, 1H), 2.75–2.68 (m, 2H), 2.04–1.97 (m, 1H), 1.87–1.79 (m, 1H), 1.78–1.64 (m, 2H), 1.37 (s, 3H), 0.98 (s, 3H); ¹³C NMR (125 MHz, CDCl₃): δ 145.9, 138.1, 135.7, 128.5, 119.7, 109.2, 65.0, 63.3, 52.1, 49.2, 47.6, 32.8, 25.7, 24.2, 22.1, 21.7; IR (film): 2928, 1463,

1099, 877, 692 cm^{-1} ; HRMS-APCI (m/z) $[\text{M} + \text{H}]^+$ calcd for $\text{C}_{16}\text{H}_{21}\text{OS}^+$, 261.1308; found 261.1313.

The structure of **5.57** was verified by 2D-NOESY, as the following interaction was observed:



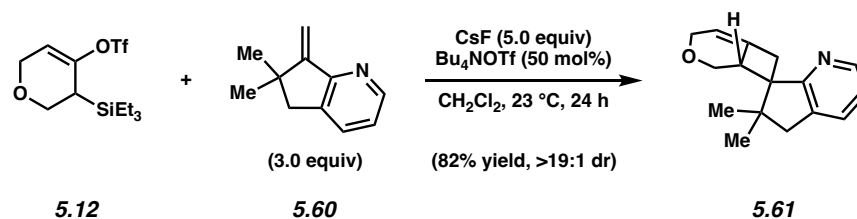
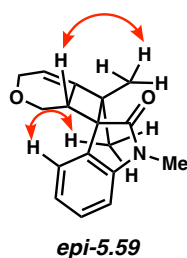
5.57



Cycloadducts 5.59 and **epi-5.59**. Followed a modified General Procedure 5.5 by altering the amount of trapping partner **5.58** (141 mg, 0.75 mmol, 5.0 equiv) and Bu_4NOTf (11.7 mg, 0.03 mmol, 0.2 equiv). Purification by flash column chromatography (8:1:1 hexanes: CH_2Cl_2 : Et_2O \rightarrow 4:1:1 hexanes: CH_2Cl_2 : Et_2O) afforded cycloadducts **5.59** and **epi-5.59** as a mixture of diastereomers (77% combined yield, average of two experiments). The dr, as determined by ^1H NMR analysis of each crude reaction mixture, was 1.2:1. Analytical samples were obtained by preparative thin layer chromatography (2:1:1 hexanes: CH_2Cl_2 : Et_2O , 2x elution) to provide cycloadduct **5.59** as a waxy clear solid and cycloadduct **epi-5.59** as a colorless oil. **Cycloadduct 5.59**: Mp: 124–126 $^\circ\text{C}$; R_f 0.56 (2:1:1 hexanes: CH_2Cl_2 : Et_2O); ^1H NMR (600 MHz, CDCl_3): δ 7.42 (dd, $J = 7.5, 0.6$, 1H), 7.28 (ddd, $J = 8.0, 7.7, 1.2$, 1H), 7.06 (ddd, $J = 8.2, 7.5, 0.8$, 1H), 6.78 (d, $J = 7.7$, 1H), 5.46–5.43 (m, 1H), 4.33–4.25 (m, 2H), 3.86–3.80 (m, 1H), 3.74–3.68 (m, 2H), 3.14 (s,

3H), 1.43 (s, 3H), 1.19 (s, 3H); ^{13}C NMR (150 MHz, CDCl_3): δ 176.0, 144.1, 142.7, 128.2, 127.9, 124.9, 121.8, 111.1, 107.7, 65.6, 62.1, 56.4, 55.0, 43.3, 25.8, 25.3, 21.2; IR (film): 2971, 1738, 1375, 1085, 755 cm^{-1} ; HRMS-APCI (m/z) $[\text{M} + \text{H}]^+$ calcd for $\text{C}_{17}\text{H}_{20}\text{NO}_2^+$, 270.1489; found 270.1489. **Cycloadduct epi-5.59**: R_f 0.63 (2:1:1 hexanes: CH_2Cl_2 : Et_2O); ^1H NMR (500 MHz, CDCl_3): δ 7.40–7.37 (m, 1H), 7.28–7.24 (overlapped with residual solvent peak, 1H), 7.03 (ddd, $J = 8.1, 7.6, 1.0, 1\text{H}$), 6.82–6.79 (m, 1H), 5.48 (ddd, $J = 6.0, 2.5, 0.6, 1\text{H}$), 4.32–4.20 (m, 2H), 3.93–3.86 (m, 1H), 3.72–3.67 (m, 1H), 3.39 (dd, $J = 11.1, 8.9, 1\text{H}$), 3.17 (s, 3H), 1.60 (s, 3H), 0.99 (s, 3H); ^{13}C NMR (125 MHz, CDCl_3): δ 175.0, 144.9, 144.0, 127.8, 127.0, 125.9, 121.2, 110.1, 108.1, 65.0, 62.3, 55.23, 55.16, 42.6, 26.3, 23.6, 22.4; IR (film): 2958, 1703, 1469, 1047, 746 cm^{-1} ; HRMS-APCI (m/z) $[\text{M} + \text{H}]^+$ calcd for $\text{C}_{17}\text{H}_{20}\text{NO}_2^+$, 270.1489; found 270.1489.

The structure of *epi-5.59* was verified by 2D-NOESY, as the following interaction was observed:



Cycloadduct 5.61. Followed General Procedure 5.5. Purification by flash column chromatography (12:1 hexanes: EtOAc \rightarrow 5:1 hexanes: EtOAc) afforded cycloadduct **5.61** (82% yield, average of two experiments) as a white solid. The dr, as determined by ^1H NMR analysis of each crude reaction mixture, was >19:1. Crystals suitable for X-ray diffraction studies were obtained by

solvent evaporation (cyclohexane and **5.61** were filtered through a 0.22 μm filter prior to crystallization): **5.61** (5.0 mg) in a 1-dram vial was dissolved in boiling cyclohexane (1.0 mL). The vial was then placed on the bench with the cap loosely sealed, and the solution was allowed to cool to 23 $^{\circ}\text{C}$ and sit over 3 d. After this point, the cyclohexane had evaporated, leaving behind crystals of **5.61**. **Cycloadduct 5.61**: Mp: 118–119 $^{\circ}\text{C}$; R_f 0.29 (5:1 hexanes:EtOAc); ^1H NMR (600 MHz, CDCl_3): δ 8.42–8.38 (m, 1H), 7.45–7.40 (m, 1H), 7.03 (dd, $J = 7.4, 5.1$, 1H), 5.34–5.28 (m, 1H), 4.34–4.28 (m, 1H), 4.24–4.15 (m, 2H), 4.04 (dd, $J = 9.8, 6.1$, 1H), 3.63 (app. t, $J = 9.9$, 1H), 3.15–3.09 (m, 1H), 2.69 (d, $J = 15.2$, 1H), 2.67–2.60 (m, 1H), 2.44 (d, $J = 15.1$, 1H), 1.38 (s, 3H), 0.87 (s, 3H); ^{13}C NMR (150 MHz, CDCl_3): δ 168.9, 147.6, 136.5, 134.0, 132.3, 121.4, 111.5, 66.2, 65.2, 58.5, 44.9, 44.3, 44.0, 39.8, 25.9, 23.3; IR (film): 2960, 1579, 1419, 1057, 790 cm^{-1} ; HRMS-APCI (m/z) $[\text{M} + \text{H}]^+$ calcd for $\text{C}_{16}\text{H}_{20}\text{NO}^+$, 242.1539; found 242.1539.

Crystal structure analysis for **5.61**

Diffraction intensities were collected at 100 K on a Bruker Smart ApexII CCD diffractometer with $\text{CuK}\alpha$ radiation, 1.54178 \AA . Absorption corrections were applied by SADABS.¹⁰⁴ All calculations were performed by the SHELXL-2014 packages.¹⁰⁵ Deposition Number 2323505 contains the supplementary crystallographic data for this paper. These data are provided free of charge by the joint Cambridge Crystallographic Data Centre and Fachinformationszentrum Karlsruhe Access Structures service www.ccdc.cam.ac.uk/structures.

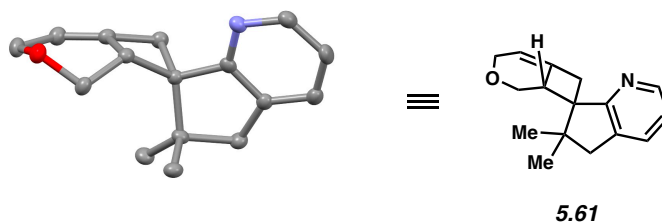


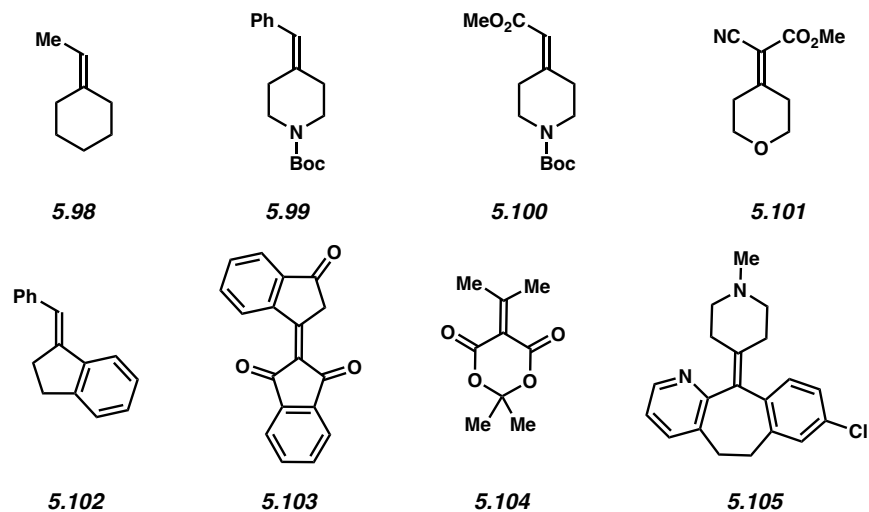
Figure 5.10. ORTEP representation of X-ray crystallographic structure **5.61**. (CCDC Registry # 2323505).

Table 5.6. Crystal data and structure refinement for compound **5.61**.

Identification code	cu_garg2302s_a
Empirical formula	C16 H19 N O
Formula weight	241.32
Temperature	100(2) K
Wavelength	1.54178 Å
Crystal system	Orthorhombic
Space group	P2 ₁ 2 ₁ 2 ₁
Unit cell dimensions	a = 6.0725(3) Å α = 90° b = 12.8665(6) Å β = 90° c = 16.4285(8) Å γ = 90°
Volume	1283.59(11) Å ³
Z	4
Density (calculated)	1.249 Mg/m ³
Absorption coefficient	0.601 mm ⁻¹
F(000)	520
Crystal size	0.22 x 0.04 x 0.04 mm ³
Theta range for data collection	4.365 to 69.709°
Index ranges	-6 ≤ h ≤ 7, -15 ≤ k ≤ 15, -19 ≤ l ≤ 19
Reflections collected	7472
Independent reflections	2326 [R(int) = 0.0460]
Completeness to theta = 67.679°	99.1%
Absorption correction	Semi-empirical from equivalents
Max. and min. transmission	0.75 and 0.65
Refinement method	Full-matrix least-squares on F ²
Data / restraints / parameters	2326 / 0 / 165
Goodness-of-fit on F ²	1.117
Final R indices [I > 2σ(I)]	R1 = 0.0382, wR2 = 0.0977
R indices (all data)	R1 = 0.0435, wR2 = 0.1020

Absolute structure parameter	0.0(2)
Extinction coefficient	n/a
Largest diff. peak and hole	0.357 and $-0.178 \text{ e.}\text{\AA}^{-3}$

A. Unsuccessful trapping partners



B. Low yielding trapping partners

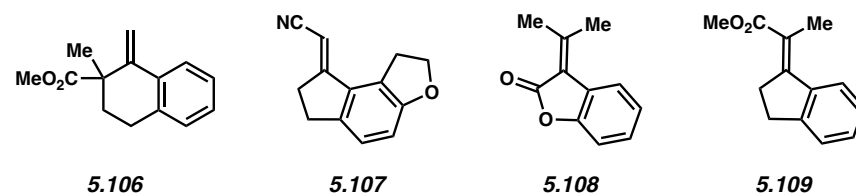
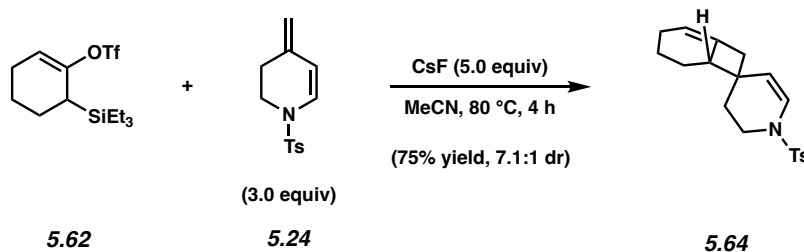


Figure 5.11. Unsuccessful and low yielding trapping partners evaluated during scope studies.

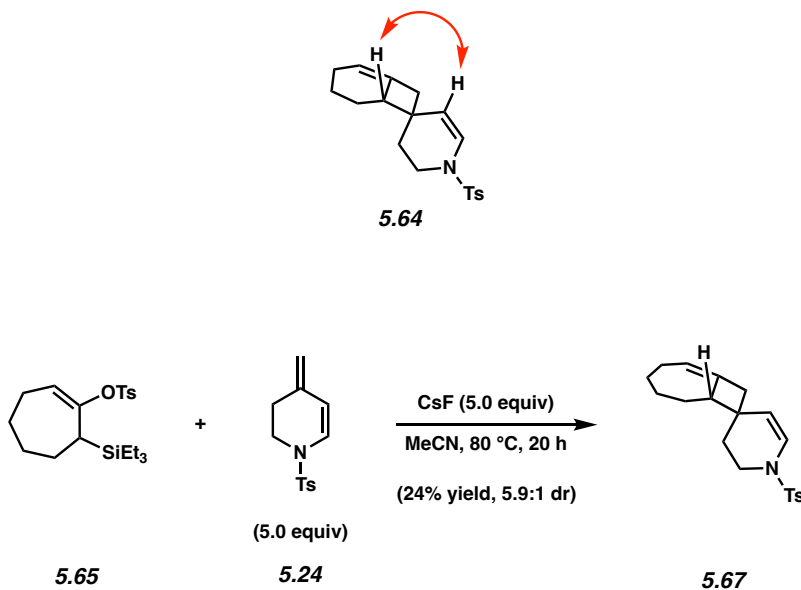
5.10.2.7 [2+2] Cycloadditions of 1,2-Cyclohexadiene (5.63) and 1,2-Cycloheptadiene (5.66)



Cycloadduct 5.64. On 0.1 mmol scale, followed a modified General Procedure 5.1 by using silyl triflate **5.62** (34.4 mg, 0.100 mmol, 1.0 equiv), three equivalents of dienamine **5.24** (74.8 mg, 0.300

mmol, 3.0 equiv), and a reaction temperature of 80 °C. Purification by preparative thin layer chromatography (5:1 hexanes:EtOAc) afforded cycloadduct **5.64** (75% yield, average of two experiments) as a colorless oil. The dr, as determined by ¹H NMR analysis of each crude reaction mixture, was 7.1:1. **Cycloadduct 5.64**: *R_f* 0.58 (5:1 hexanes:EtOAc); ¹H NMR (500 MHz, C₆D₆): δ 7.65–7.61 (m, 2H), 6.74 (d, *J* = 8.2, 1H), 6.72–6.68 (m, 2H), 5.18–5.12 (m, 1H), 4.70 (d, *J* = 8.3, 1H), 3.29 (ddd, *J* = 12.1, 7.3, 3.2, 1H), 3.06 (ddd, *J* = 12.1, 9.0, 2.6, 1H), 2.45–2.39 (m, 1H), 2.39–2.34 (m, 1H), 1.93–1.83 (m, 1H), 1.83–1.70 (m, 5H), 1.51–1.44 (m, 1H), 1.41–1.31 (m, 1H), 1.19–1.09 (m, 3H), 0.72–0.62 (m, 1H); ¹³C NMR (125 MHz, CDCl₃): δ 143.6, 136.8, 135.0, 129.7, 127.0, 123.5, 117.3, 115.4, 50.8, 45.5, 42.1, 37.6, 26.9, 24.9, 21.6, 21.3, 21.0; IR (film) 2930, 1637, 1351, 1168, 940 cm⁻¹; HRMS-ESI (*m/z*) [M + H]⁺ calcd for C₁₉H₂₄NO₂S⁺, 330.1522; found 330.1522.

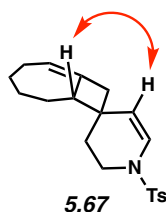
The structure of **5.64** was verified by 2D-NOESY, as the following interaction was observed:



Cycloadduct 5.67. On 0.1 mmol scale, followed a modified General Procedure 5.1 by using silyl tosylate **5.67** (40.2 mg, 0.106 mmol, 1.0 equiv), a reaction temperature of 80 °C, and a reaction time of 20 h. Purification by preparative thin layer chromatography (4:1 hexanes:EtOAc) afforded

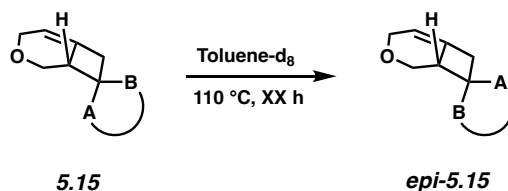
cycloadduct **5.67** (24% yield, average of two experiments) as a colorless oil. The dr, as determined by ^1H NMR analysis of each crude reaction mixture, was 5.9:1. **Cycloadduct 5.67**: R_f 0.70 (3:1 hexanes:EtOAc); ^1H NMR (600 MHz, CDCl_3): δ 7.66–7.63 (m, 2H), 7.31–7.28 (m, 2H), 6.54 (d, $J = 8.2$, 1H), 5.40–5.36 (m, 1H), 4.98 (d, $J = 8.3$, 1H), 3.51 (ddd, $J = 12.1, 6.7, 3.3$, 1H), 3.10 (ddd, $J = 12.3, 9.5, 2.8$, 1H), 2.76–2.69 (m, 1H), 2.56–2.50 (m, 1H), 2.42 (s, 3H), 2.13–2.05 (m, 1H), 2.05–1.99 (m, 1H), 2.00–1.92 (m, 1H), 1.92–1.86 (m, 1H), 1.83–1.76 (m, 1H), 1.67 (ddd, $J = 13.2, 9.5, 2.9$, 1H), 1.53–1.50 (overlapped with residual water peak, 1H), 1.47–1.41 (m, 1H), 1.30–1.23 (m, 2H), 1.16–1.08 (m, 1H); ^{13}C NMR (150 MHz, CDCl_3): δ 143.6, 141.1, 135.1, 129.7, 127.1, 123.5, 122.7, 117.8, 54.1, 43.4, 41.6, 34.4, 29.6, 29.3, 29.1, 28.2, 27.4, 21.6; IR (film) 2922, 1598, 1361, 1168, 952 cm^{-1} ; HRMS-ESI (m/z) $[\text{M} + \text{H}]^+$ calcd for $\text{C}_{20}\text{H}_{26}\text{NO}_2\text{S}^+$, 344.1679; found 344.1683.

The structure of **5.67** was verified by 2D-NOESY, as the following interaction was observed:



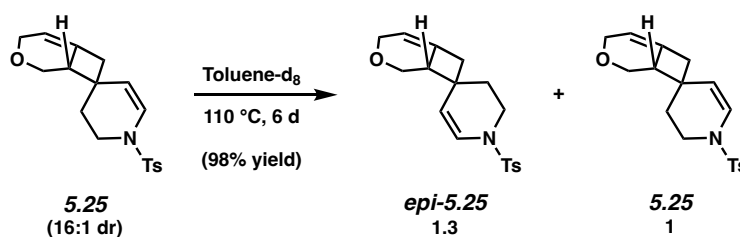
5.10.2.8 Thermal Isomerizations of [2+2] Cycloadducts

General Procedure 5.6 for the thermal isomerizations of [2+2] cycloadducts

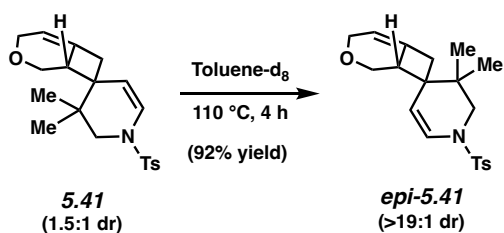


Isomers epi-5.15. A 1-dram vial was charged with cycloadducts **5.15** (0.055 mmol, 1.0 equiv), 1,3,5-trimethoxybenzene (3.1 mg, 0.02 mmol, 0.33 equiv), and toluene- d_8 (0.75 mL, 0.07 M). The

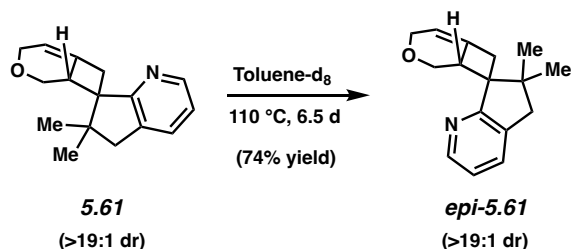
solution was then transferred to an oven dried 5 mm NMR tube. Subsequently, the tube was sealed with an NMR cap and placed in a preheated oil bath at 110 °C. After the indicated reaction time, the tube was taken out of the bath and cooled to 23 °C. Residual oil was removed from the exterior of the NMR tube and the sample was analyzed directly by ^1H NMR spectroscopy.



Isomers *epi-5.25* and 5.25. Followed General Procedure 5.6 where reaction was performed for 6 d. Isomers *epi-5.25* and **5.25** were obtained in a 98% combined yield and 1.3:1 dr by ^1H NMR analysis of the crude reaction mixture. An analytical sample was obtained by preparative thin layer chromatography (3:1 Hexanes:EtOAc) to afford a mixture of diastereomers *epi-5.25* and **5.25** as a yellow oil. **Isomer 5.25:** See Section 5.10.2.5 Scope of [2+2] Cycloadditions with Dienamines for characterization details; **Isomer *epi-5.25*** (characterized from an inseparable mixture of **5.25** and *epi-5.25*): ^1H NMR (500 MHz, CDCl_3 , *epi-5.25*): 7.62–7.60 (m, 2H), 7.31 (d, $J = 7.9$, 2H), 6.62(d, $J = 8.15$, 1H), 5.42–5.37 (m, 1H), 5.03 (d, $J = 8.29$, 1H), 4.20–4.10 (m, 1H), 4.09–4.01 (m, 1H), 3.63–3.55 (m, 1H), 3.44–3.39 (m, 1H), 2.96 (app. t, $J = 10.2$, 1H), 2.87–2.80 (m, 1H), 2.80–2.73 (m, 1H), 2.68–2.61 (m, 1H), 2.47–2.40 (m, 4H), 1.87–1.80 (m, 1H), 1.79–1.72 (m, 1H). ^{13}C NMR (125 MHz, CDCl_3 , **5.25** and *epi-5.25*): δ 143.9, 143.8, 134.9, 134.5, 134.4, 133.4, 129.8, 129.7, 127.1, 127.0, 124.9, 123.9, 116.2, 114.0, 113.9, 111.0, 65.4, 65.23, 65.35, 64.4, 62.8, 51.3, 48.9, 46.2, 44.3, 42.04, 41.99, 39.0, 38.0, 34.7, 26.8, 21.6.



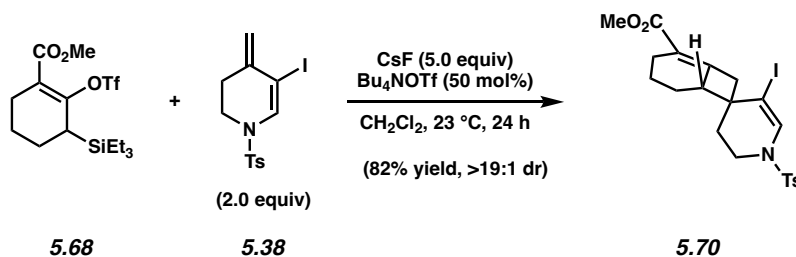
Isomer *epi-5.41*. Followed General Procedure 5.6 where reaction was performed for 4 h. Isomer *epi-5.41* was obtained in a 92% yield and >19:1 dr by ^1H NMR analysis of the crude reaction mixture. An analytical sample was obtained by preparative thin layer chromatography (3:1 Hexanes:EtOAc) to afford Isomer *epi-5.41* as a yellow oil. **Isomer *epi-5.41*:** See Section 5.10.2.5 Scope of [2+2] Cycloadditions with Dienamines for characterization details.



Isomer *epi-5.61*. Followed General Procedure 5.6 where reaction was performed for 6.5 d. Isomer *epi-5.61* was obtained in a 74% yield and >19:1 dr by ^1H NMR analysis of the crude reaction mixture. An analytical sample was obtained by preparative thin layer chromatography (2:1 hexanes:EtOAc) to afford isomer *epi-5.61* as a white solid. **Isomer *epi-5.61*:** Mp: 80–82 °C; R_f 0.42 (2:1 hexanes:EtOAc); ^1H NMR (500 MHz, CDCl_3): δ 8.42–8.38 (m, 1H), 7.43–7.39 (m, 1H), 7.02 (dd, $J = 7.5, 5.3$, 1H), 5.58–5.54 (m, 1H), 4.28–4.19 (m, 1H), 4.19–4.12 (m, 1H), 3.50–3.44 (m, 1H), 3.44–3.38 (m, 1H), 3.07–3.01 (m, 1H), 2.97–2.91 (m, 1H), 2.77 (app. t, $J = 9.5$, 1H), 2.60 (d, $J = 15.6$ 1H), 2.55 (d, $J = 15.3$, 1H), 1.26 (s, 3H), 0.85 (s, 3H); ^{13}C NMR (125 MHz, CDCl_3):

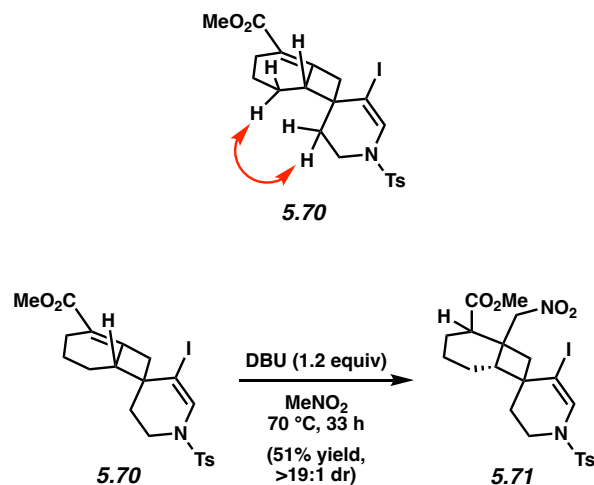
δ 166.4, 147.4, 135.4, 133.8, 132.2, 121.5, 112.9, 65.7, 63.6, 58.3, 45.2, 43.6, 43.5, 36.4, 24.1, 23.9; IR (film): 2955, 1593, 1419, 1049, 784 cm^{-1} ; HRMS-APCI (m/z) $[\text{M} + \text{H}]^+$ calcd for $\text{C}_{16}\text{H}_{20}\text{NO}^+$, 242.1539; found 242.1540.

5.10.2.9 Elaborations of [2+2] Cycloadducts



Cycloadduct 5.70. On 0.57 mmol scale, followed a modified General Procedure 5.3 by using silyl triflate **5.68** (230 mg, 0.571 mmol, 1.0 equiv) and two equivalents of trapping partner **5.38** (429 mg, 1.14 mmol, 2.0 equiv). Purification by flash column chromatography (hexanes \rightarrow 3:2 hexanes:EtOAc) afforded cycloadduct **5.70** (240 mg, 82% combined yield), as a white solid. The dr, as determined by ^1H NMR analysis of the crude reaction mixture, was $>19:1$. **Cycloadduct 5.70:** Mp: decomposes at 135°C ; R_f 0.48 (3:1 hexanes:EtOAc); ^1H NMR (600 MHz, CDCl_3): δ 7.64 (d, $J = 8.1$, 2H), 7.33 (d, $J = 8.1$, 2H), 7.17 (s, 1H), 3.67 (s, 3H), 3.38–3.30 (m, 2H), 3.25 (ddd, $J = 15.6, 4.6, 3.0$, 1H), 3.18–3.11 (m, 1H), 2.52 (d, $J = 15.6$, 1H), 2.44 (s, 3H), 2.32–2.25 (m, 1H), 2.23–2.14 (m, 1H), 1.91–1.85 (m, 2H), 1.69–1.64 (m, 1H), 1.52–1.42 (m, 2H), 1.00–0.92 (m, 1H); ^{13}C NMR (150 MHz, CDCl_3): 167.4, 153.4, 144.4, 134.7, 131.5, 130.1, 127.2, 120.5, 90.0, 52.4, 51.2, 48.0, 43.0, 41.9, 28.1, 24.4, 21.7, 21.3, 20.7; IR (film): 2935, 1710, 1610, 1435, 1168 cm^{-1} ; HRMS-APCI (m/z) $[\text{M} + \text{H}]^+$ calcd for $\text{C}_{21}\text{H}_{25}\text{INO}_4\text{S}^+$, 514.0544; found 514.0527.

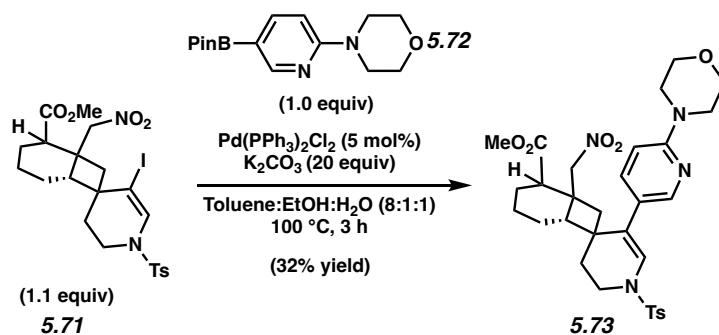
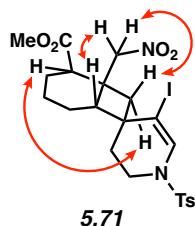
The structure of **5.70** was verified by 2D-NOESY, as the following interactions were observed:



Compound 5.71. A 1-dram vial was charged with a magnetic stir bar, cycloadduct **5.70** (31.5 mg, 61.4 μmol , 1.0 equiv), DBU (11.0 μL , 73.6 μmol , 1.2 equiv), and MeNO_2 (0.66 mL, 0.092 M). The sealed vial was heated to 70 $^\circ\text{C}$ and stirred at this temperature for 33 h. After this time, the reaction mixture was cooled to 23 $^\circ\text{C}$, diluted with EtOAc (2 mL), and washed with H_2O (0.5 mL). The organic layer was then dried over Na_2SO_4 and concentrated under reduced pressure. Purification of the crude material by preparative thin layer chromatography (3:1 hexanes:EtOAc) afforded compound **5.71** (17.8 mg, 51% yield) as a colorless oil. The dr, as determined by ^1H NMR analysis of the crude reaction mixture, was >19:1. **Compound 5.71:** R_f 0.22 (3:1 hexanes:EtOAc); ^1H NMR (600 MHz, CDCl_3): δ 7.66–7.63 (m, 2H), 7.36–7.33 (m, 2H), 7.13 (s, 1H), 4.63 (d, $J = 13.3$, 1H), 4.58 (d, $J = 12.9$, 1H), 3.62 (s, 3H), 3.47 (ddd, $J = 12.3$, 7.3, 3.3, 1H), 3.23 (ddd, $J = 12.2$, 9.6, 2.8, 1H), 2.82–2.76 (m, 2H), 2.50 (d, $J = 13.8$, 1H), 2.45 (s, 3H), 2.21 (ddd, $J = 14.1$, 9.5, 3.3, 1H), 2.08 (ddd, $J = 13.8$, 7.3, 2.7, 1H), 2.05 (d, $J = 14.1$, 1H), 1.87–1.81 (m, 1H), 1.60–1.51 (m, 2H), 1.48–1.42 (m, 1H), 1.42–1.37 (m, 2H); ^{13}C NMR (150 MHz, CDCl_3): δ 173.3, 144.4, 134.3, 131.4, 130.1, 127.1, 93.2, 79.0, 51.8, 47.4, 46.8, 44.1, 41.3, 40.6, 35.9, 31.5, 21.9, 21.6,

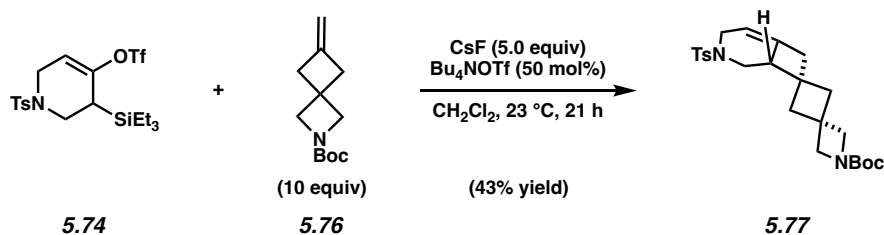
20.2, 19.2; IR (film): 2949, 1732, 1910, 1551, 1435, 1362 cm^{-1} ; HRMS-APCI (m/z) $[\text{M} + \text{H}]^+$ calcd for $\text{C}_{22}\text{H}_{28}\text{IN}_2\text{O}_6\text{S}^+$, 575.0707; found 575.0689.

The structure of **5.71** was verified by 2D-NOESY, as the following interactions were observed:



Compound 5.73. A 10 mL round bottom flask was charged with a magnetic stir bar, vinyl iodide **5.71** (37.0 mg, 64.4 μmol , 1.1 equiv), boronic ester **5.72** (15.0 μL , 58.6 μmol , 1.0 equiv), $\text{Pd}(\text{PPh}_3)_2\text{Cl}_2$ (2.1 mg, 2.93 μmol , 0.05 equiv), a mixture of 8:1 toluene:EtOH (1.2 mL, 0.04M), and an aqueous saturated solution of K_2CO_3 (135 μL). The flask was then equipped with a reflux condenser and the reaction was heated to 100 °C and stirred at this temperature for 3 h. After this time, the solution was cooled to 23 °C and Na_2SO_4 was added. The contents were then diluted with EtOAc (5 mL) and filtered through a pad of silica, eluting with EtOAc (6 mL). The eluate was then concentrated under reduced pressure. The crude material was then purified by preparative thin layer chromatography (1:1 hexanes:EtOAc) to provide **5.73** (11.3 mg, 32% yield) as a

colorless oil. **Compound 5.73**: R_f 0.21 (3:1 hexanes:EtOAc); $^1\text{H NMR}$ (500 MHz, CDCl_3): δ 7.88–7.83 (m, 1H), 7.63 (d, $J = 7.8$, 2H), 7.33 (d, $J = 7.9$, 2H), 7.27–7.20 (overlapped with residual solvent peak, 1H), 6.62 (d, $J = 8.6$, 1H), 6.44 (s, 1H), 4.10 (d, $J = 12.6$, 1H), 3.88–3.81 (m, 5H), 3.67–3.61 (m, 1H), 3.59 (s, 3H), 3.53 (t, $J = 5.0$, 4H), 3.19–3.08 (m, 1H), 2.85 (dd, $J = 12.6$, 4.8, 1H), 2.48–2.41 (m, 4H), 2.35 (d, $J = 13.6$, 1H), 2.15–2.05 (m, 2H), 2.03 (d, $J = 13.5$, 1H), 1.88–1.76 (m, 1H), 1.58–1.52 (overlapped with residual water peak, 1H), 1.50–1.42 (m, 2H), 1.40–1.31 (m, 2H); $^{13}\text{C NMR}$ (125 MHz, CDCl_3): δ 173.4, 158.8, 149.1, 144.1, 139.7, 134.2, 129.9, 127.1, 124.3, 124.1, 123.4, 106.1, 79.4, 66.7, 51.7, 46.7, 45.6, 42.4, 41.8, 40.4, 37.9, 36.2, 31.8, 22.0, 21.6, 20.4, 19.2; IR (film): 2952, 1732, 1599, 1550, 1492 cm^{-1} ; HRMS-APCI (m/z) $[\text{M} + \text{H}]^+$ calcd for $\text{C}_{31}\text{H}_{39}\text{N}_4\text{O}_7\text{S}^+$, 611.2534; found 611.2512.

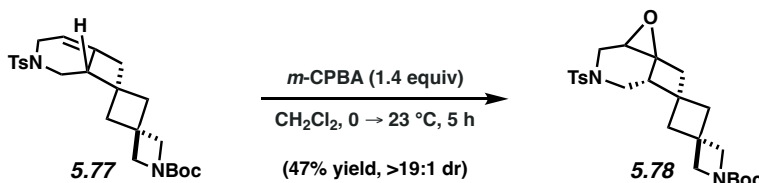


Cycloadduct 5.77. On 0.10 mmol scale, followed a modified General Procedure 5.4 by using silyl triflate **5.74** (49.6 mg, 0.10 mmol, 1.0 equiv), 10 equivalents of trapping partner **5.76** (215 mg, 1.03 mmol, 10 equiv), and a reaction time of 21 h. Purification by flash column chromatography (hexanes \rightarrow 1:1 hexanes:EtOAc \rightarrow EtOAc) afforded cycloadduct **5.77** as a mixture with a small amount of an allene dimer impurity. Subsequent repurification by preparative thin layer chromatography (1:1 hexanes:Et₂O) afforded cycloadduct **5.77** (19.0 mg, 43% yield) as a clear oil.

Cycloadduct 5.77: R_f 0.44 (2:1 hexanes:EtOAc); $^1\text{H NMR}$ (600 MHz, CDCl_3): δ 7.67–7.64 (m,

2H), 7.33–7.29 (m, 2H), 5.24–5.21 (m, 1H), 4.09–4.03 (m, 1H), 3.90 (dd, $J = 10.8, 6.7$, 1H), 3.87–3.80 (m, 3H), 3.76 (d, $J = 8.7$, 1H), 3.20–3.13 (m, 1H), 2.93–2.86 (m, 1H), 2.84–2.78 (m, 1H), 2.46 (d, $J = 13.5$, 1H), 2.43 (s, 3H), 2.23–2.11 (m, 3H), 2.08 (d, $J = 12.0$, 1H), 1.89 (dd, $J = 12.1, 2.6$, 1H), 1.42 (s, 9H); ^{13}C NMR (150 MHz, CDCl_3): δ 156.2, 143.4, 135.6, 134.5, 129.7, 127.4, 110.7, 79.4, 47.3, 44.8, 44.4, 44.0, 43.6, 39.3, 39.1, 33.4, 28.4, 21.5; IR (film): 2921, 1698, 1456, 1366, 1091 cm^{-1} ; HRMS-APCI (m/z) $[\text{M} + \text{H}]^+$ calcd for $\text{C}_{24}\text{H}_{33}\text{N}_2\text{O}_4\text{S}^+$, 445.2156; found 445.2154.

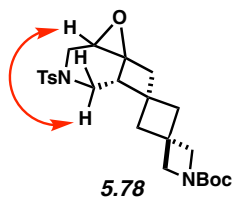
Note: 5.77 was obtained as a mixture of rotamers. These data represent empirically observed chemical shifts from the ^1H and ^{13}C -NMR spectra.



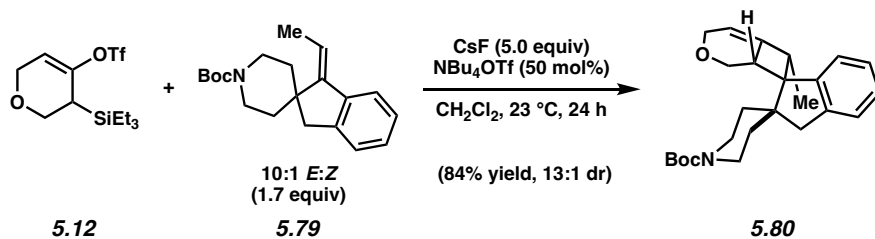
Compound 5.78. An oven-dried 1-dram vial was charged with a magnetic stir bar, cycloadduct **5.77** (4.5 mg, 0.010 mmol, 1.0 equiv), and CH_2Cl_2 (0.10 mL, 0.10 M). The vial was cooled to 0 $^\circ\text{C}$. Subsequently, *m*-CPBA (77 wt%, 3.2 mg, 0.014 mmol, 1.4 equiv) was added to the solution in one portion, and the reaction stirred at 0 $^\circ\text{C}$ for 4 h. The vial was then warmed to 23 $^\circ\text{C}$ and stirred for 45 min. After this time, the reaction was quenched with saturated aqueous solutions of sodium thiosulfate (0.5 mL) and sodium bicarbonate (0.5 mL). The mixture was then extracted with CH_2Cl_2 (2 x 3 mL), and the combined organic layers were washed with saturated sodium bicarbonate (2 x 1 mL), dried over sodium sulfate, filtered, and concentrated under reduced pressure. Purification of the crude mixture by preparative thin layer chromatography (1:1

hexanes:EtOAc) afforded epoxide **5.78** (2.2 mg, 47% yield) as a colorless oil. The dr, as determined by ^1H NMR analysis of the crude reaction mixture, was >19:1. **Compound 5.78**: R_f 0.54 (1:1 hexanes:EtOAc); ^1H NMR (600 MHz, CDCl_3): δ 7.66–7.62 (m, 2H), 7.32 (d, $J = 8.0$, 2H), 3.90 (s, 2H), 3.86 (d, $J = 8.8$, 1H), 3.81 (d, $J = 8.8$, 1H), 3.47–3.25 (m, 2H), 3.22–3.19 (m, 1H), 3.14 (dd, $J = 12.7$, 7.5, 1H), 2.84–2.72 (m, 1H), 2.62 (d, $J = 12.3$, 1H), 2.56 (app. t, $J = 6.8$, 1H), 2.47–2.41 (m, 4H), 2.28–2.23 (m, 2H), 2.21 (dd, $J = 11.9$, 3.5, 1H), 2.05–1.99 (m, 1H), 1.43 (s, 9H); ^{13}C NMR (150 MHz, CDCl_3): δ 156.2, 143.7, 134.2, 129.8, 127.5, 79.5, 55.4, 52.4, 46.5, 44.8, 43.2, 42.6, 42.1, 39.8, 33.8, 33.6, 28.4, 21.6; IR (film): 2971, 1738, 1478, 1164, 1090 cm^{-1} ; HRMS-APCI (m/z) $[\text{M} + \text{H}]^+$ calcd for $\text{C}_{24}\text{H}_{33}\text{N}_2\text{O}_5\text{S}^+$, 461.2105; found 461.2105.

The structure of **5.78** was verified by 2D-NOESY, as the following interaction was observed:

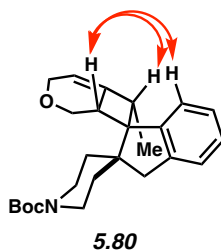


Note: 5.78 was obtained as a mixture of rotamers. These data represent empirically observed chemical shifts from the ^1H and ^{13}C -NMR spectra.

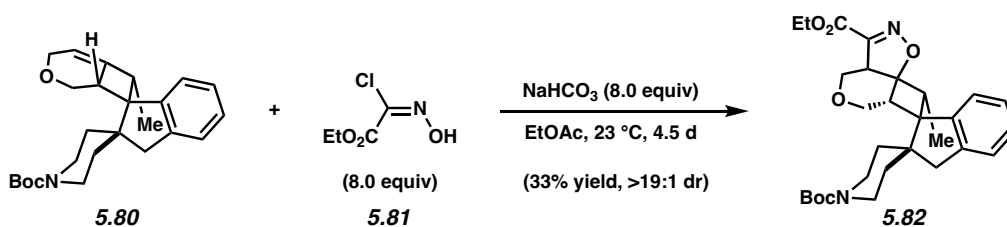


Cycloadduct 5.80. On 0.22 mmol scale, followed a modified General Procedure 5.4 by altering amount of trapping partner **5.79** (113 mg, 0.361 mmol, 1.7 equiv). Purification by flash column chromatography (hexanes → 19:1 hexanes:EtOAc → 2:1 hexanes:EtOAc) afforded cycloadduct **5.80** (72.1 mg, 84% yield) as a foamy white solid. The dr, as determined by ^1H NMR analysis of the crude reaction mixture, was 13:1. The 13:1 ratio reflects the ratio of the major diastereomer (13) to the sum of all minor diastereomers (1). **Cycloadduct 5.80:** Mp: 69–71 °C; R_f 0.52 (5:1 hexanes:EtOAc); ^1H NMR (500 MHz, CDCl_3): δ 7.33 (d, $J = 7.6$, 1H), 7.25–7.21 (overlapped with residual solvent peak, 1H), 7.20–7.12 (m, 2H), 5.26–5.22 (m, 1H), 4.36–4.28 (m, 1H), 4.28–4.19 (m, 1H), 4.12–3.70 (m, 4H), 3.69–3.61 (m, 1H), 3.21–3.12 (m, 1H), 3.04 (d, $J = 15.1$, 1H), 2.95–2.69 (m, 3H), 2.16 (br s, 2H), 1.47 (br s, 9H), 1.34 (d, $J = 7.2$, 3H), 1.23–1.13 (m, 1H), 1.11–1.01 (m, 1H); ^{13}C NMR (125 MHz, CDCl_3): δ 155.0, 151.4, 142.9, 139.5, 127.0, 126.4, 125.0, 121.5, 107.2, 79.5, 66.1, 65.0, 63.5, 56.7, 49.0, 43.6, 41.1, 39.1, 31.4, 28.5, 15.2; IR (film): 2971, 1690, 1365, 1164, 753 cm^{-1} ; HRMS-APCI (m/z) $[\text{M} + \text{H}]^+$ calcd for $\text{C}_{25}\text{H}_{34}\text{NO}_3^+$, 396.2533; found 396.2532.

The structure of **5.80** was verified by 2D-NOESY, as the following interactions were observed:

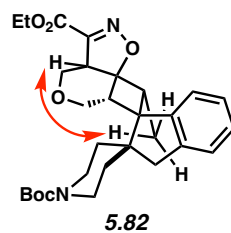


Note: 5.80 was obtained as a mixture of rotamers. These data represent empirically observed chemical shifts from the ^1H and ^{13}C -NMR spectra.



Cycloadduct 5.82. An oven-dried 1-dram vial was charged with a magnetic stir bar, cycloadduct **5.80** (20.0 mg, 0.051 mmol, 1.0 equiv), oxime **5.81** (15.3 mg, 0.101 mmol, 2.0 equiv), sodium bicarbonate (34.0 mg, 0.405 mmol, 8.0 equiv), and EtOAc (0.20 mL, 0.12 M). The heterogenous solution was then stirred at >900 RPM and 23 °C. Every 10–14 h, additional oxime **5.81** (7.6 mg, 0.050 mmol, 1.0 equiv) was added to the reaction mixture with a total reaction time of 4.5 d (total oxime **5.81** used in reaction – 66.0 mg, 0.404 mmol, 8.0 equiv). After this time, the reaction was filtered over a pad of celite eluting with EtOAc (5 mL) and concentrated under reduced pressure to afford a colorless oil. Subsequent purification by preparative thin layer chromatography (2:1 hexanes:EtOAc) afforded cycloadduct **5.82** (8.6 mg, 33% yield) as a clear oil. The dr, as determined by ¹H NMR analysis of the crude reaction mixture, was >19:1. **Cycloadduct 5.82:** *R_f* 0.56 (2:1 hexanes:EtOAc); ¹H NMR (600 MHz, CDCl₃): δ 7.33 (d, *J* = 7.6, 1H), 7.28–7.23 (overlapping with residual solvent peak, 1H), 7.20–7.14 (m, 2H), 4.45–4.31 (m, 3H), 4.26 (d, *J* = 13.8, 1H), 4.13–3.81 (m, 3H), 3.64–3.57 (m, 1H), 3.15–3.08 (m, 2H), 3.02 (d, *J* = 15.6, 1H), 2.97–2.76 (m, 4H), 2.32 (ddd, *J* = 13.8, 12.9, 4.9, 1H), 1.93–1.82 (m, 1H), 1.81–1.70 (m, 1H), 1.64–1.60 (m, 1H), 1.47 (s, 9H), 1.39 (t, *J* = 7.1, 3H), 1.23 (d, *J* = 7.5, 3H); ¹³C NMR (125 MHz, CDCl₃): δ 160.5, 155.1, 152.5, 151.7, 139.3, 127.2, 126.7, 125.0, 121.5, 85.9, 79.5, 65.7, 65.1, 62.3, 55.7, 53.9, 50.1, 43.0, 40.5, 38.2, 31.8, 28.5, 14.1, 12.6; IR (film): 2972, 1745, 1688, 1165, 737 cm⁻¹; HRMS-APCI (*m/z*) [M + H]⁺ calcd for C₂₉H₃₉N₂O₆⁺, 511.2803; found 511.2796.

The structure of **5.82** was verified by 2D-NOESY, as the following interaction was observed:



*Note: **5.82** was obtained as a mixture of rotamers. These data represent empirically observed chemical shifts from the ¹H and ¹³C-NMR spectra*

5.11 Spectra Relevant to Chapter Five:

Access to Complex Scaffolds Through [2+2] Cycloadditions of Strained Cyclic Allenes

Matthew S. McVeigh,[†] Jacob P. Sorrentino,[†] Allison T. Hands, and Neil K. Garg

J. Am. Chem. Soc. **2024**, *In Press*. doi.org/10.1021/jacs.4c03369

Purified product, ¹H NMR

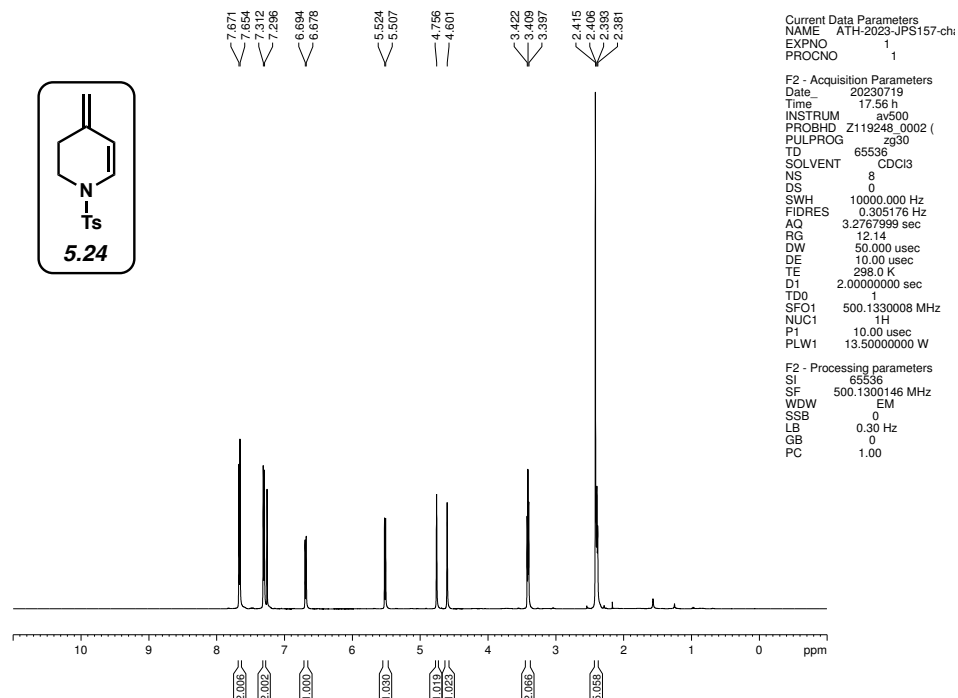


Figure 5.12. ¹H NMR (500 MHz, CDCl₃) of compound 5.24.

Purified product, ¹³C NMR

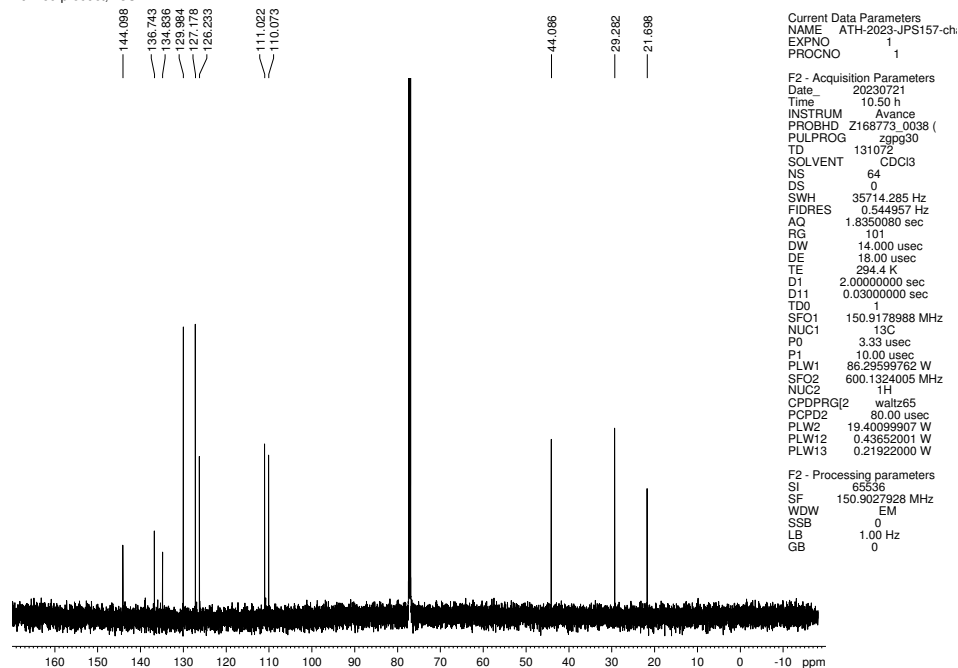


Figure 5.13. ¹³C NMR (150 MHz, CDCl₃) of compound 5.24.

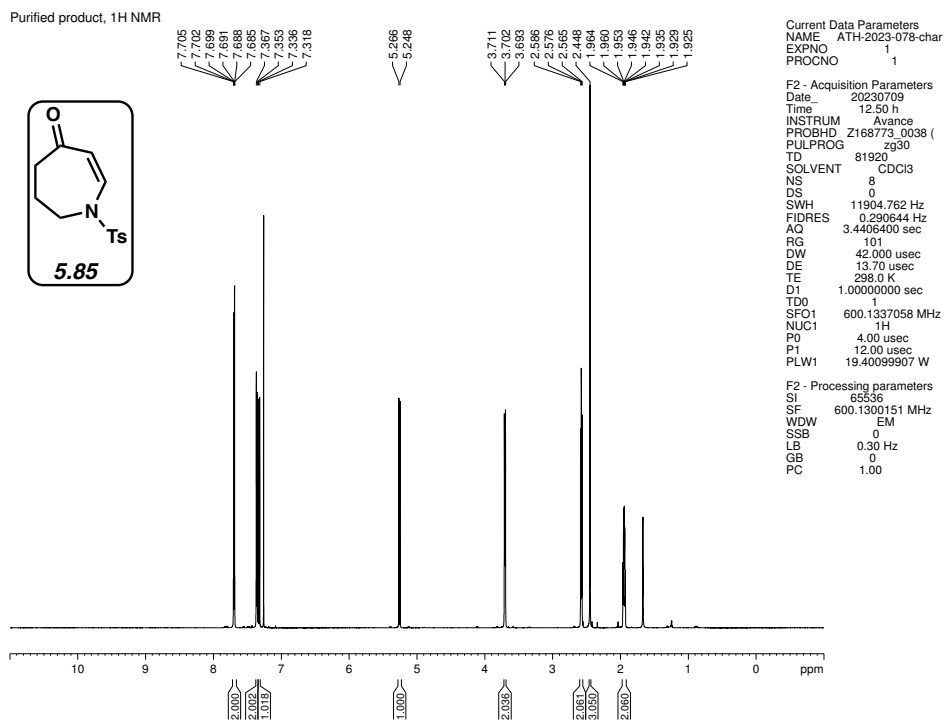


Figure 5.14. ¹H NMR (600 MHz, CDCl₃) of compound 5.85.

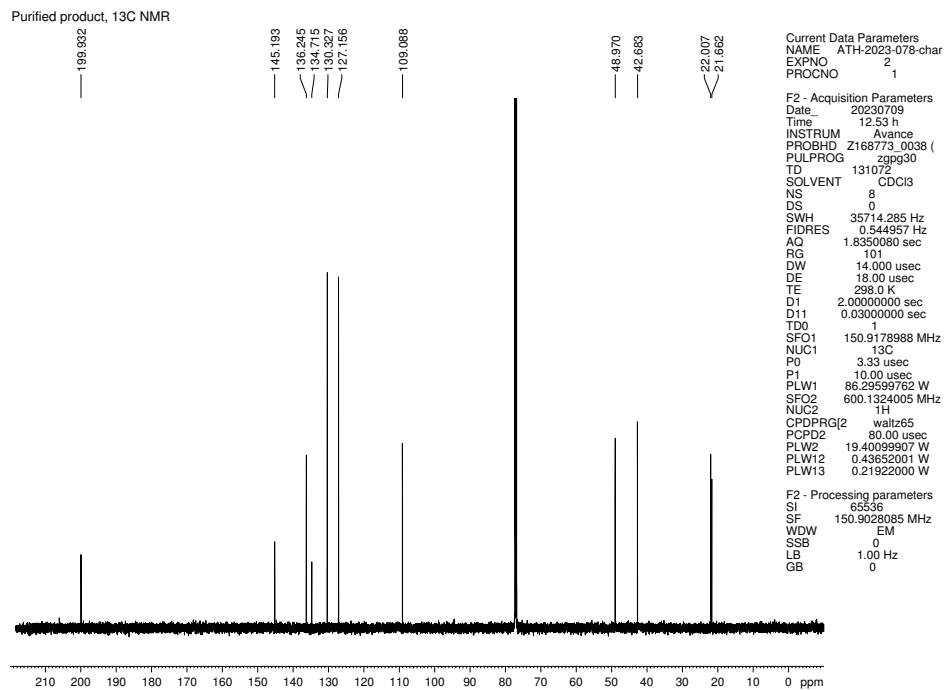


Figure 5.15. ¹³C NMR (150 MHz, CDCl₃) of compound 5.85.

Purified product, ¹H NMR

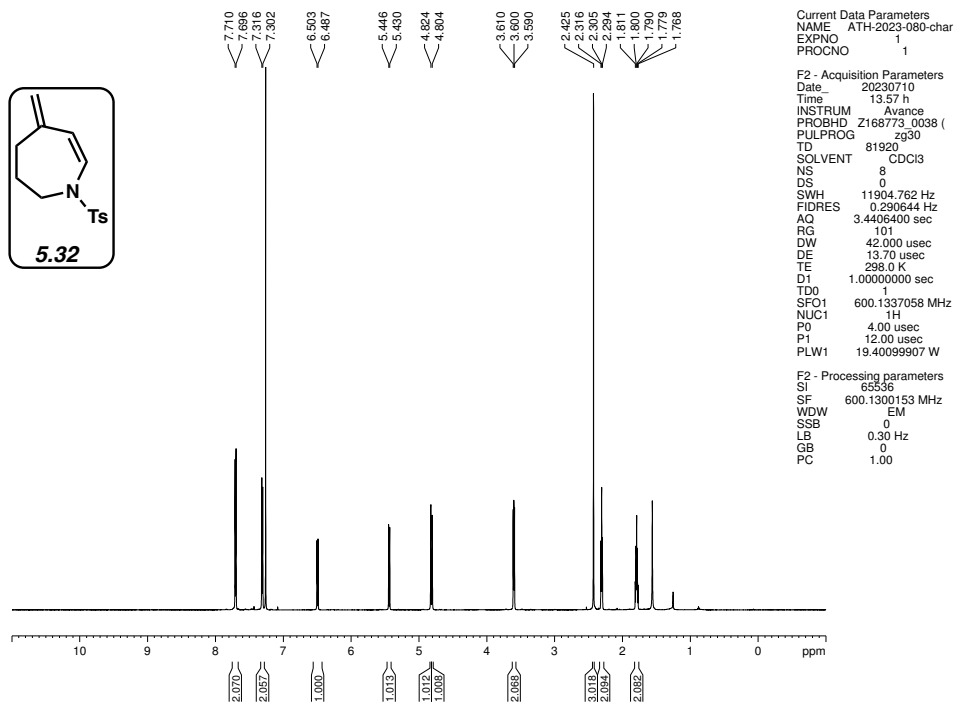


Figure 5.16. ¹H NMR (600 MHz, CDCl₃) of compound 5.32.

Purified product, ¹³C NMR

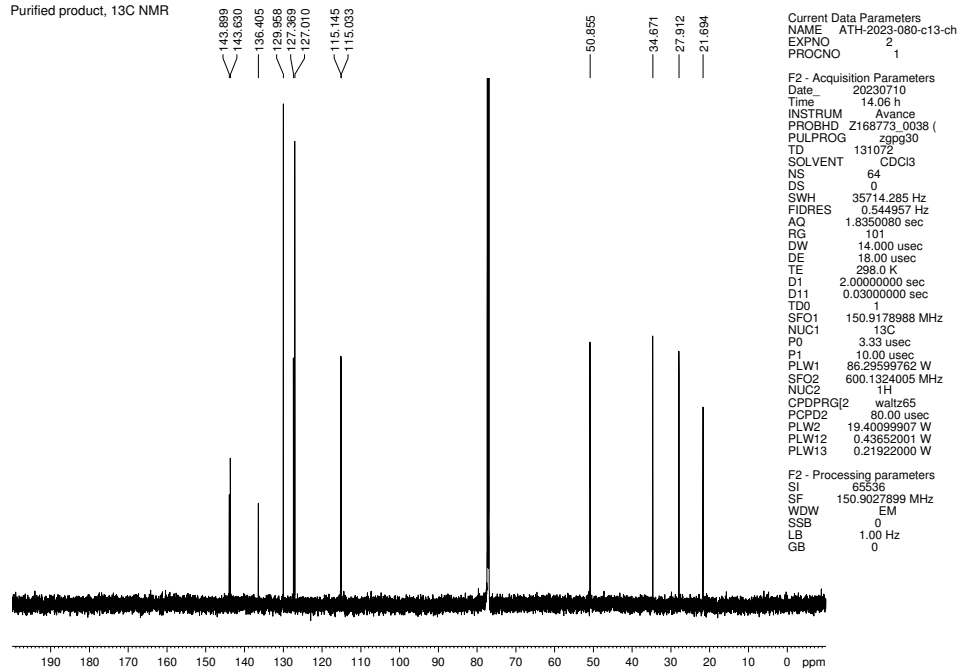


Figure 5.17. ¹³C NMR (150 MHz, CDCl₃) of compound 5.32.

Purified product, ¹H NMR

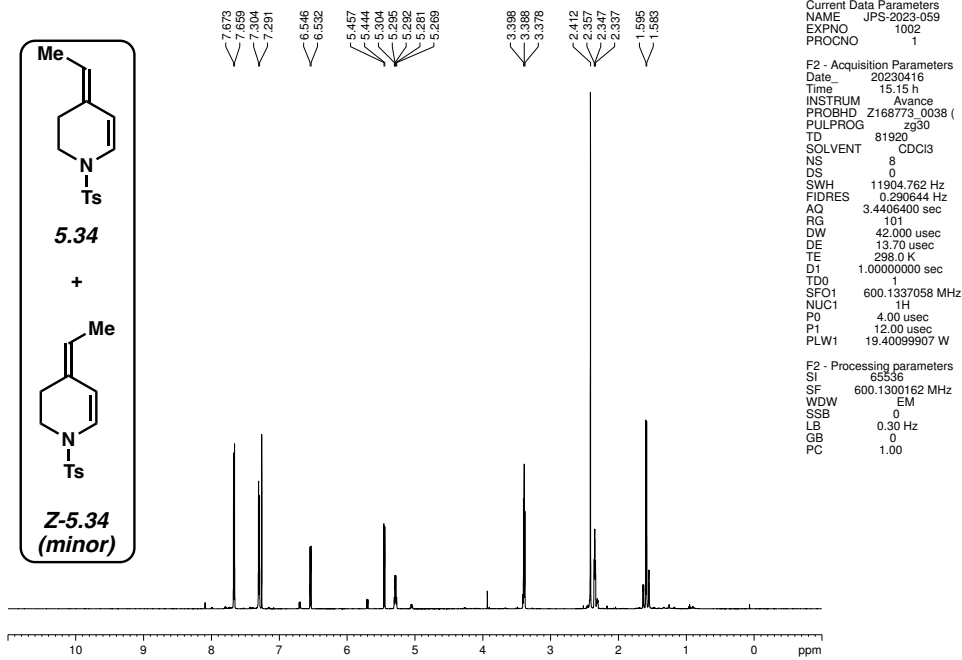


Figure 5.18. ¹H NMR (600 MHz, CDCl₃) of compound 5.34.

Purified product, ¹³C NMR

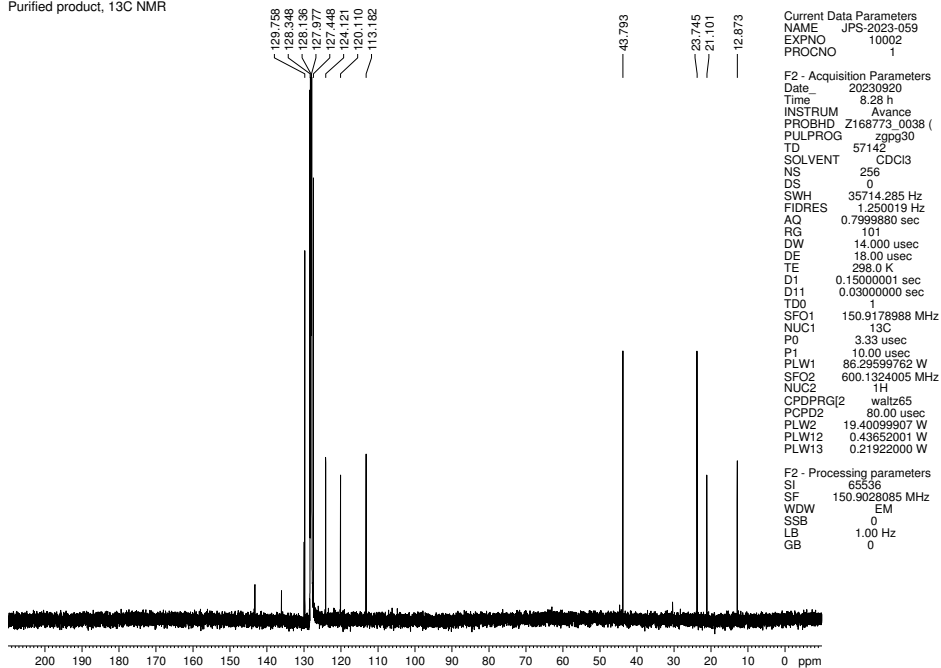
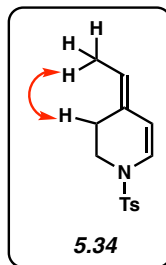


Figure 5.19. ¹³C NMR (150 MHz, CDCl₃) of compound 5.34.



Purified product, NOESY

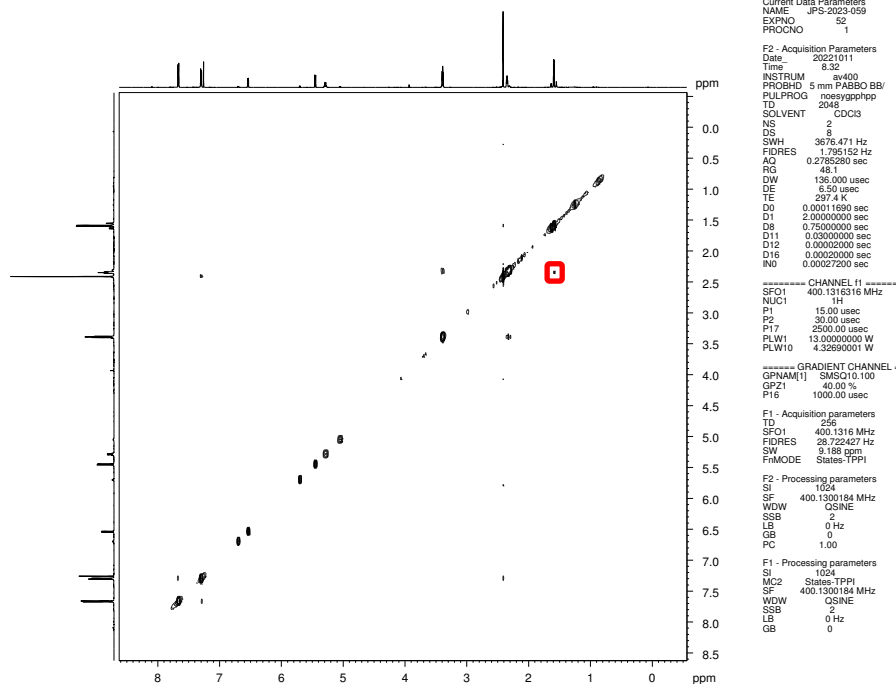


Figure 5.20. NOESY (400 MHz, CDCl₃) of compound **5.34**.

Purified product, ¹H NMR

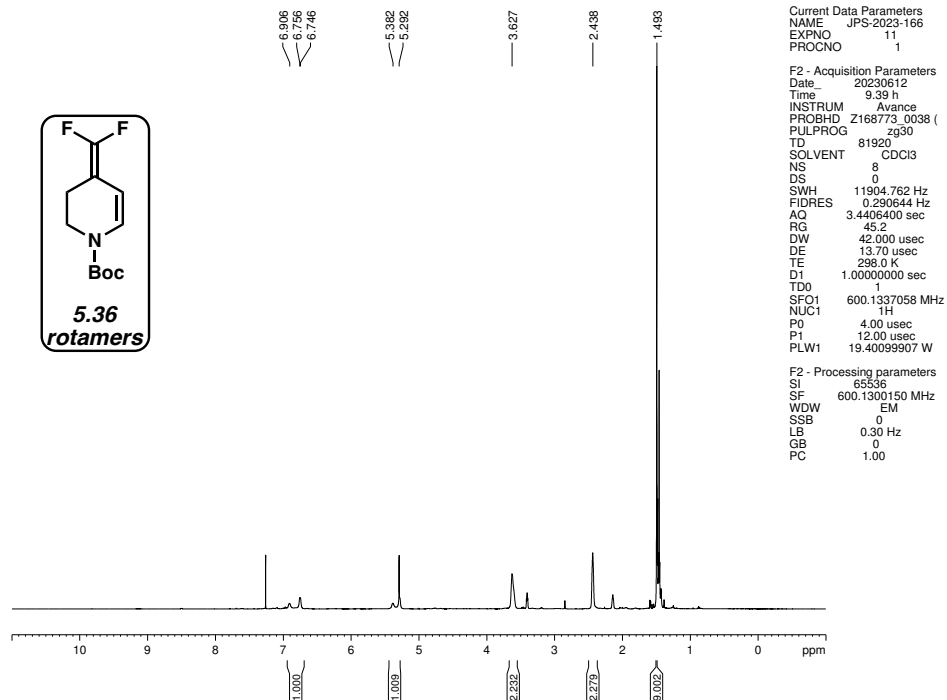


Figure 5.21. ¹H NMR (600 MHz, CDCl₃) of compound 5.36.

Purified product, ¹³C NMR

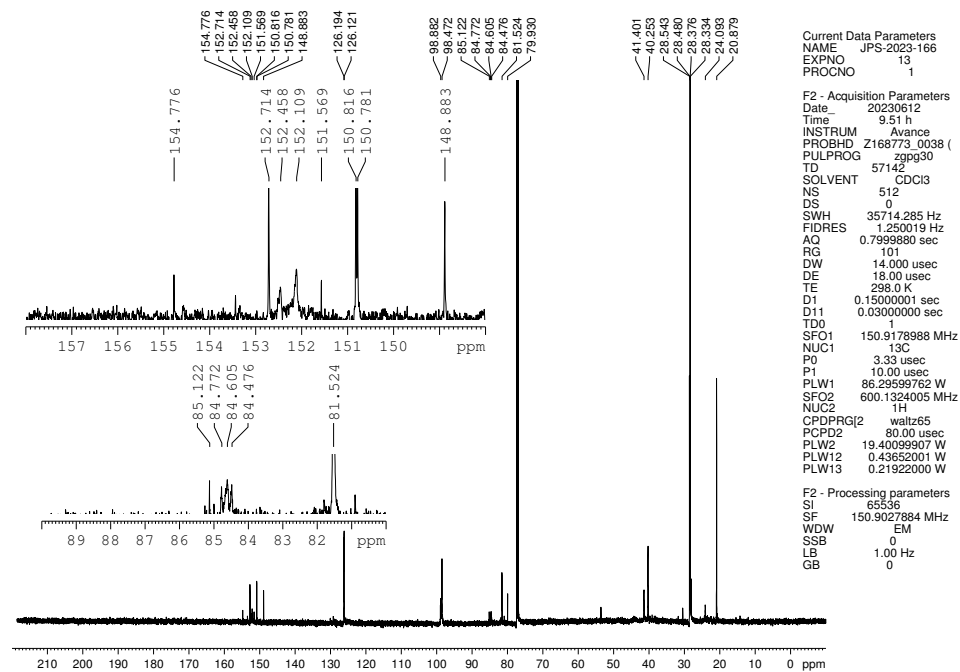
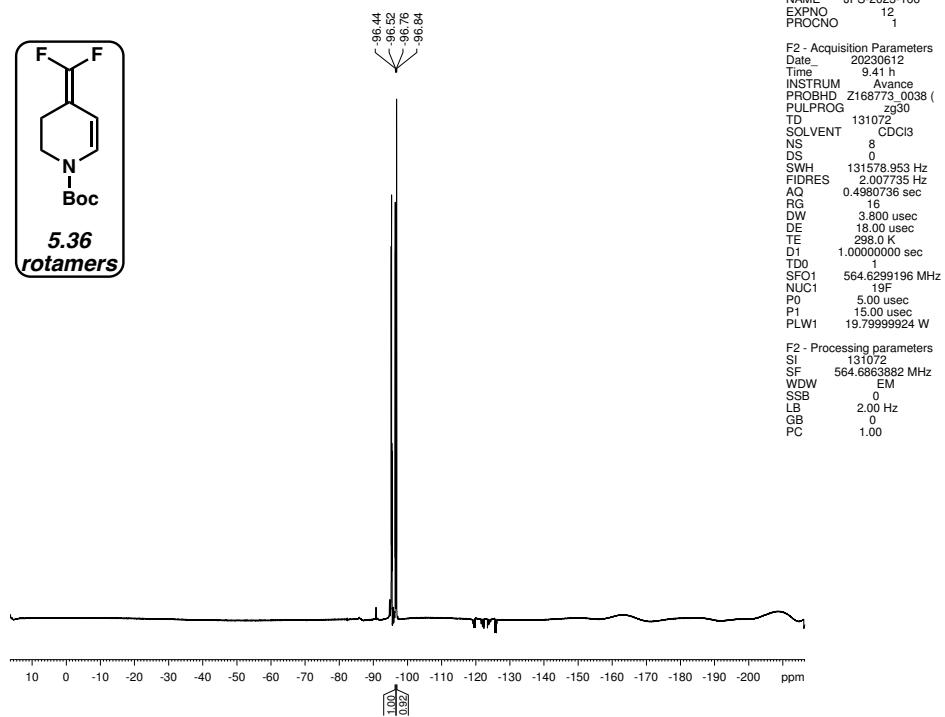
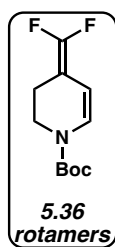


Figure 5.22. ¹³C NMR (150 MHz, CDCl₃) of compound 5.36.

Purified product, ^{19}F NMR



Current Data Parameters
NAME JPS-2023-166
EXPNO 12
PROCNO 1

F2 - Acquisition Parameters
Date_ 20230612
Time 9.41 h
INSTRUM Avance
PROBHD Z168773_0038 (PULPROG zg30)
TD 131072
SOLVENT CDCl3
NS 8
DS 0
SWH 131578.953 Hz
FIDRES 2.007735 Hz
AQ 0.4980736 sec
RG 16
DW 3.800 usec
DE 18.00 usec
TE 298.0 K
D1 1.00000000 sec
TDO 1
SFO1 564.6299196 MHz
NUC1 19F
P0 5.00 usec
P1 15.00 usec
PLW1 19.79999924 W

F2 - Processing parameters
SI 131072
SF 564.6863882 MHz
WDW EM
SSB 0
LB 2.00 Hz
GB 0
PC 1.00

Figure 5.23. ^{19}F NMR (565 MHz, CDCl_3) of compound **5.36**.

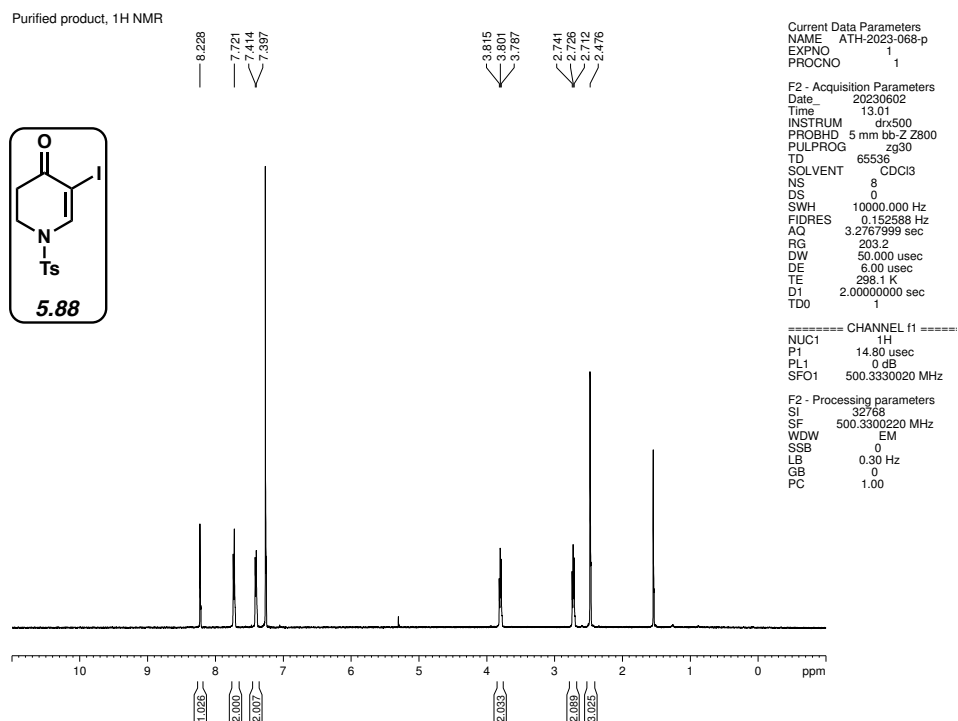


Figure 5.24. ¹H NMR (500 MHz, CDCl₃) of compound 5.88.

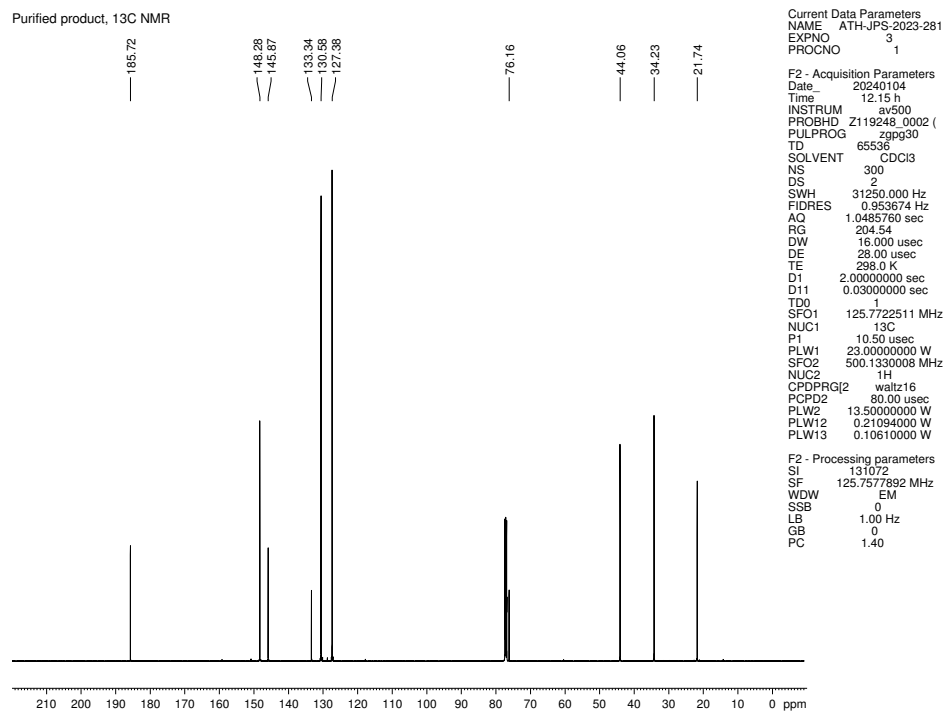


Figure 5.25. ¹³C NMR (125 MHz, CDCl₃) of compound 5.88.

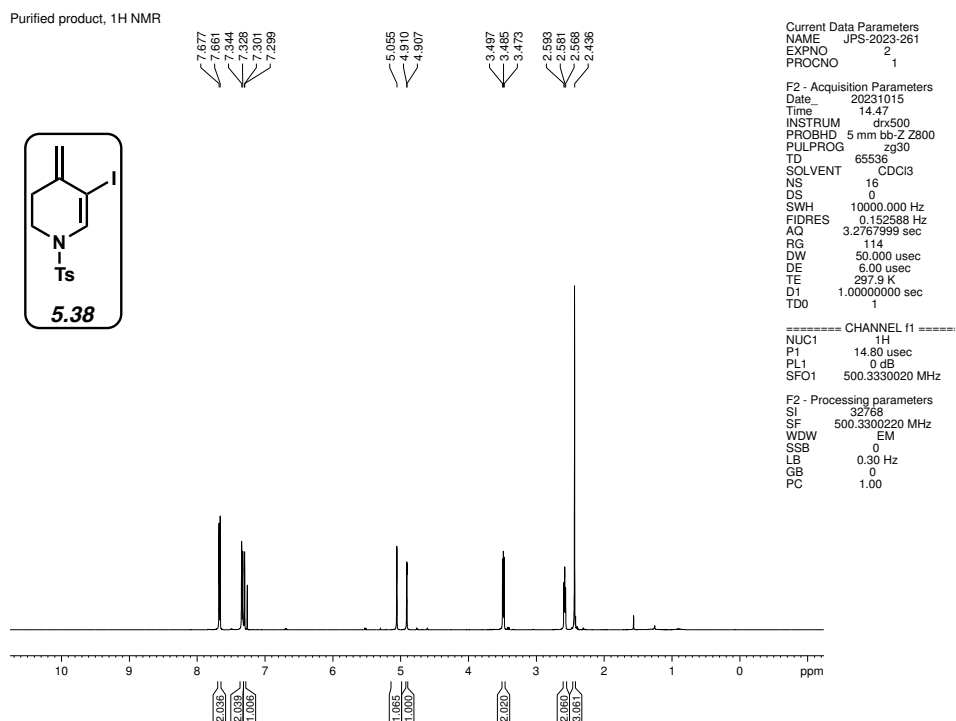


Figure 5.26. ¹H NMR (500 MHz, CDCl₃) of compound 5.38.

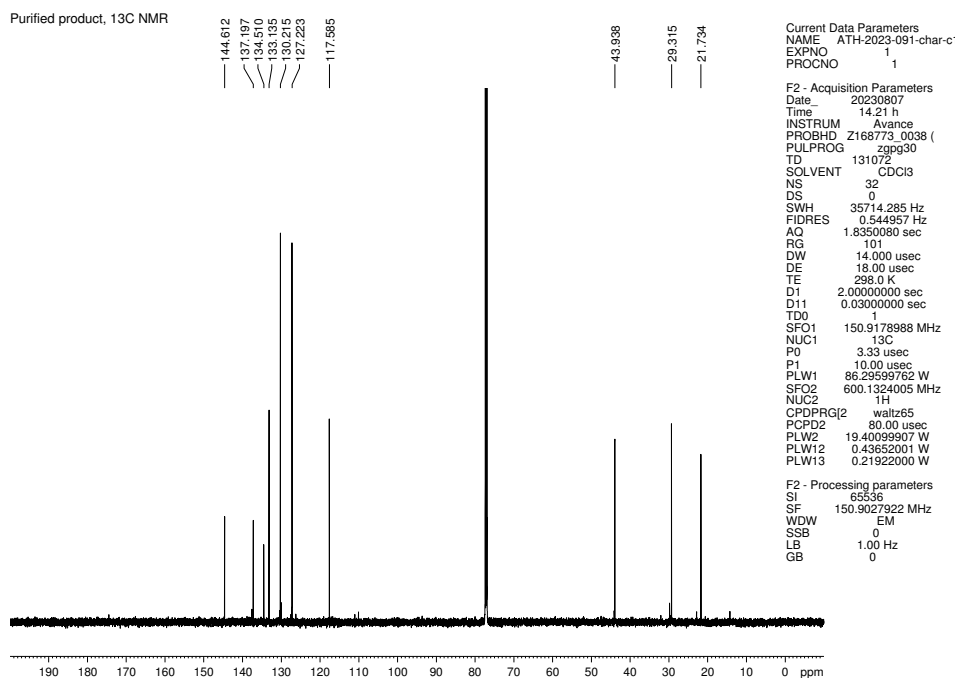


Figure 5.27. ¹³C NMR (150 MHz, CDCl₃) of compound 5.38.

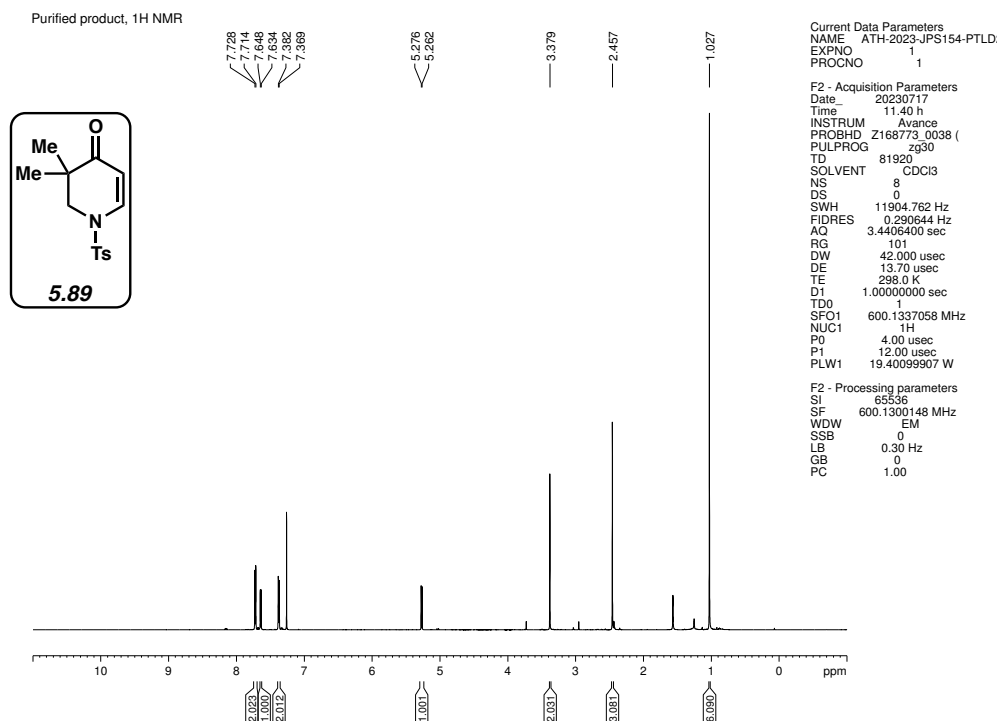


Figure 5.28. ¹H NMR (600 MHz, CDCl₃) of compound 5.89.

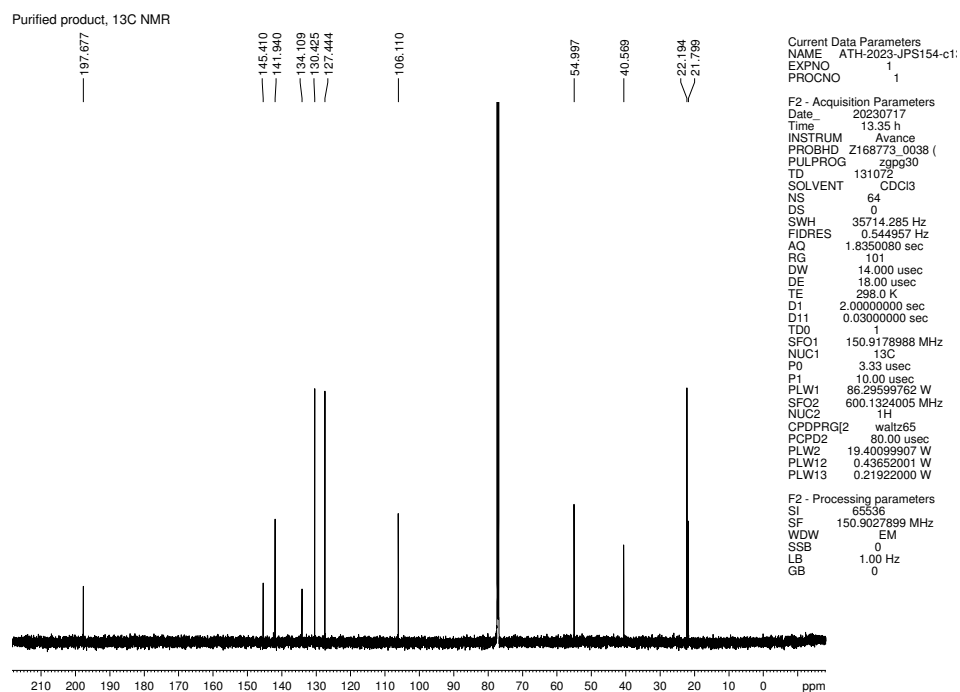


Figure 5.29. ¹³C NMR (150 MHz, CDCl₃) of compound 5.89.

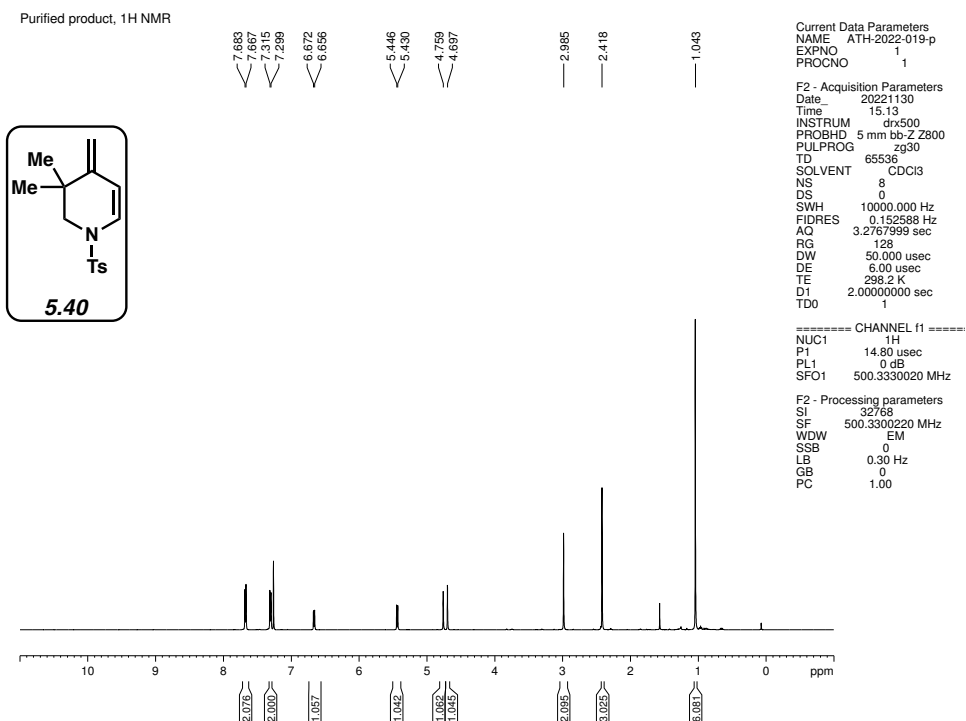


Figure 5.30. ^1H NMR (500 MHz, CDCl_3) of compound 5.40.

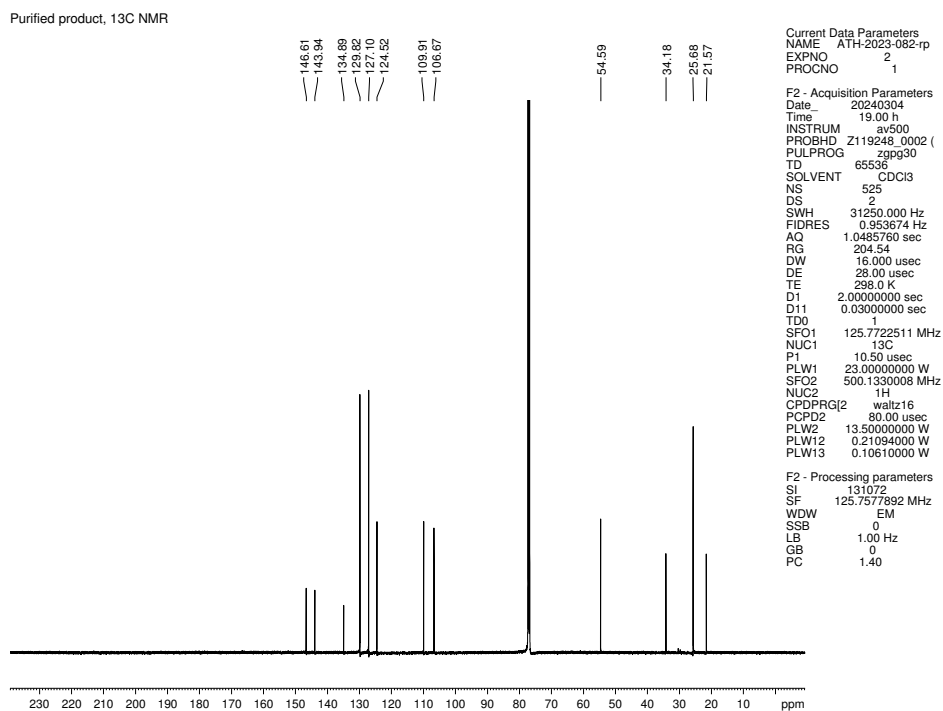


Figure 5.31. ^{13}C NMR (125 MHz, CDCl_3) of compound 5.40.

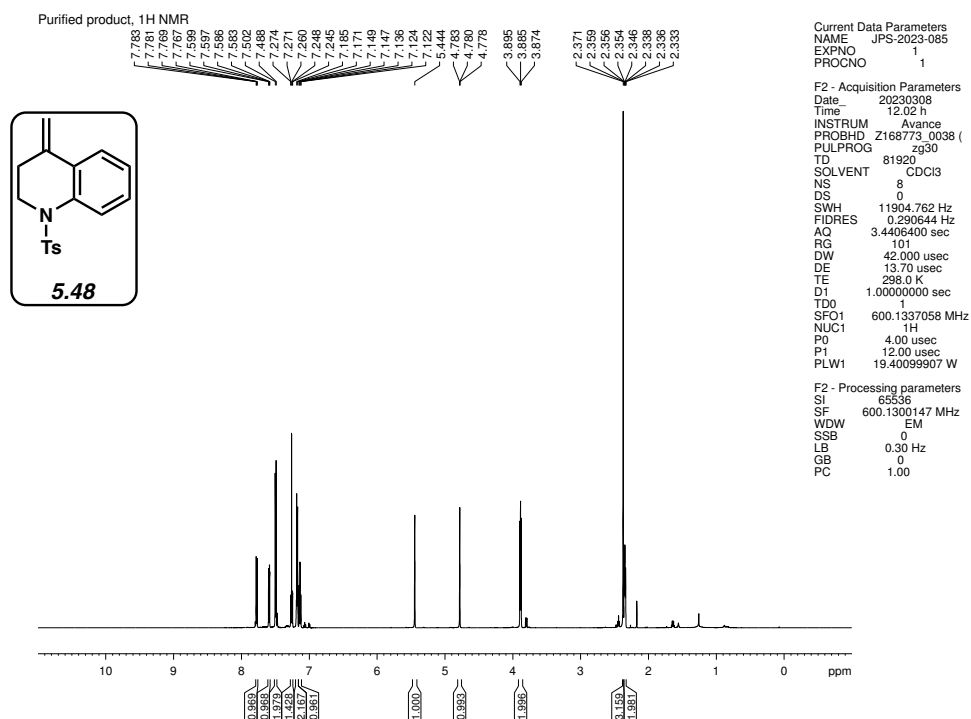


Figure 5.32. ¹H NMR (600 MHz, CDCl₃) of compound 5.48.

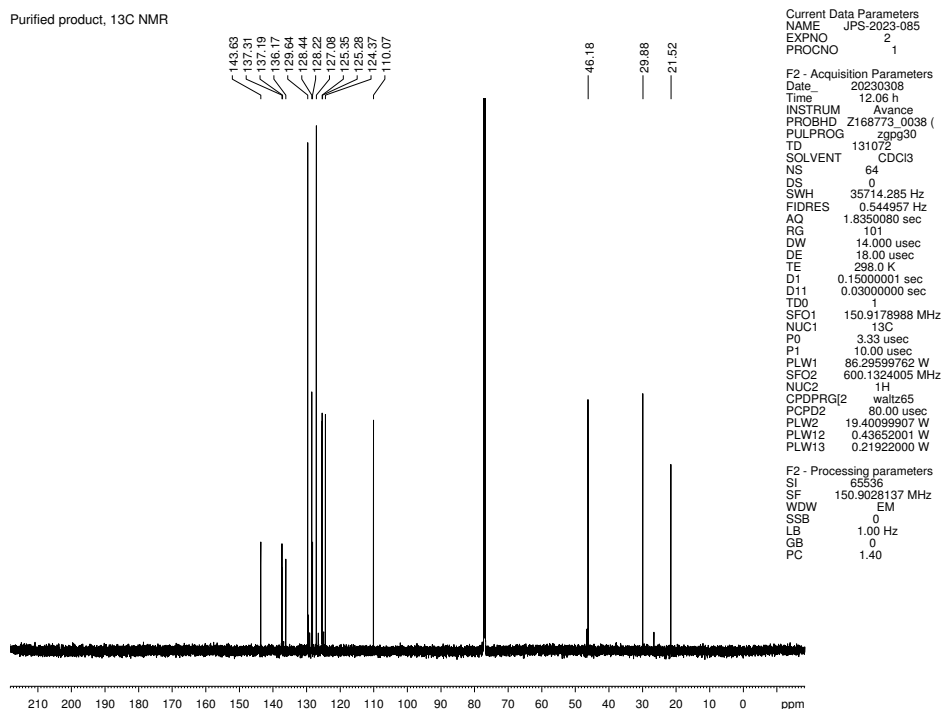


Figure 5.33. ¹³C NMR (150 MHz, CDCl₃) of compound 5.48.

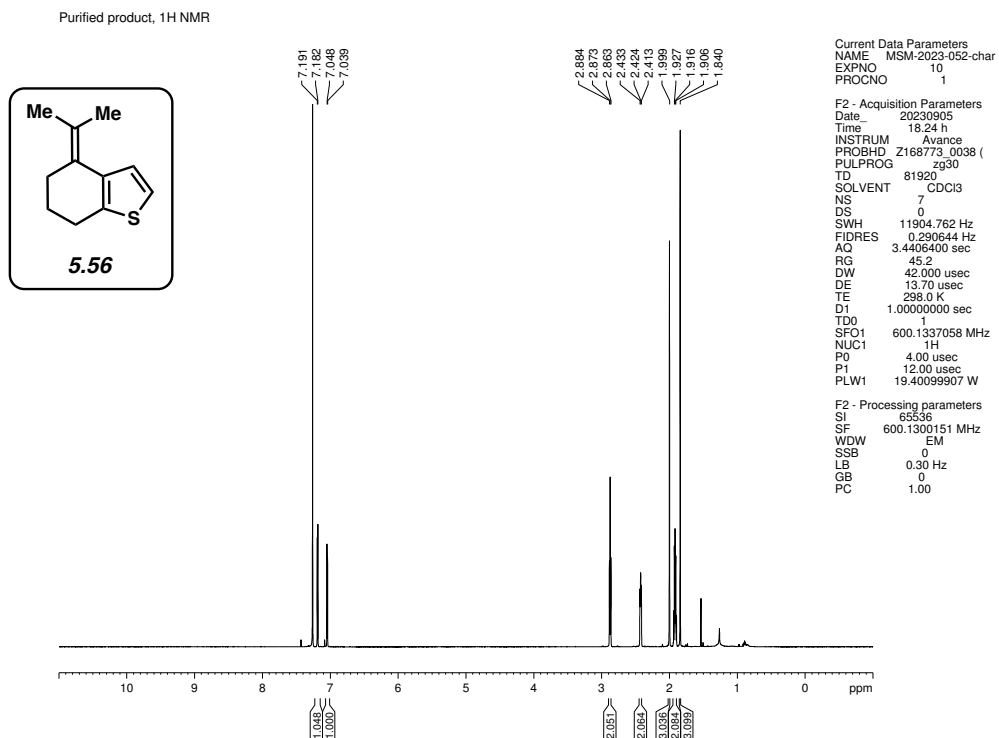


Figure 5.34. ¹H NMR (600 MHz, CDCl₃) of compound 5.56.

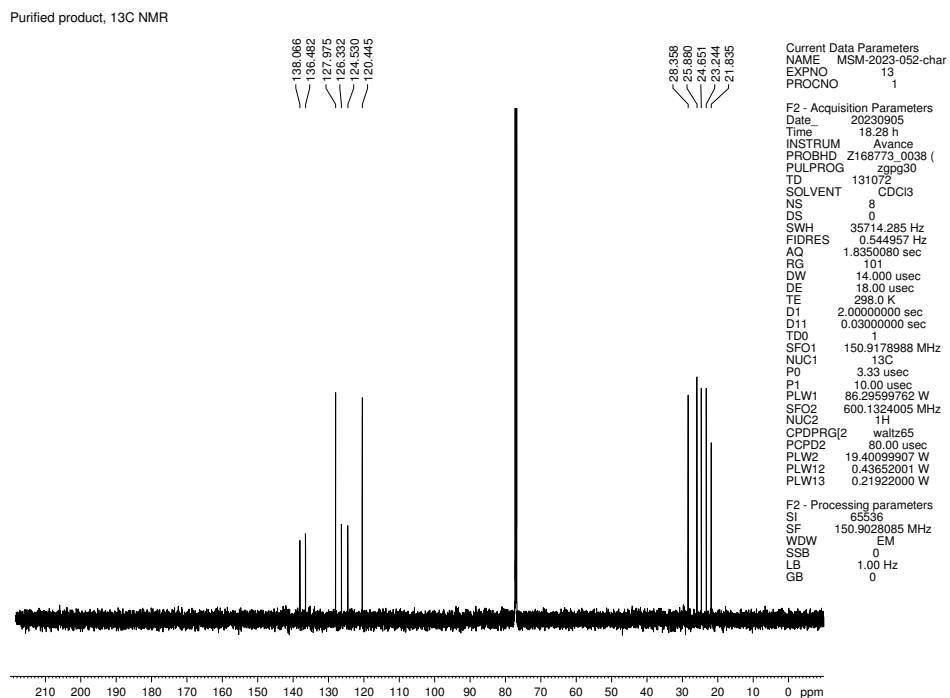


Figure 5.35. ¹³C NMR (150 MHz, CDCl₃) of compound 5.56.

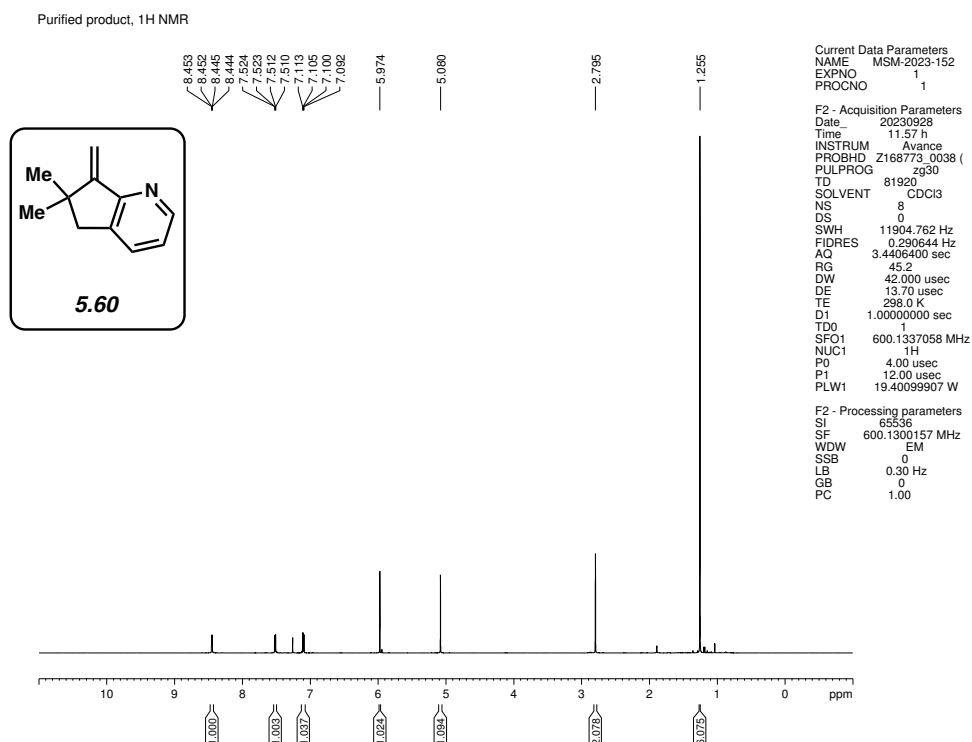


Figure 5.36. ¹H NMR (600 MHz, CDCl₃) of compound 5.60.

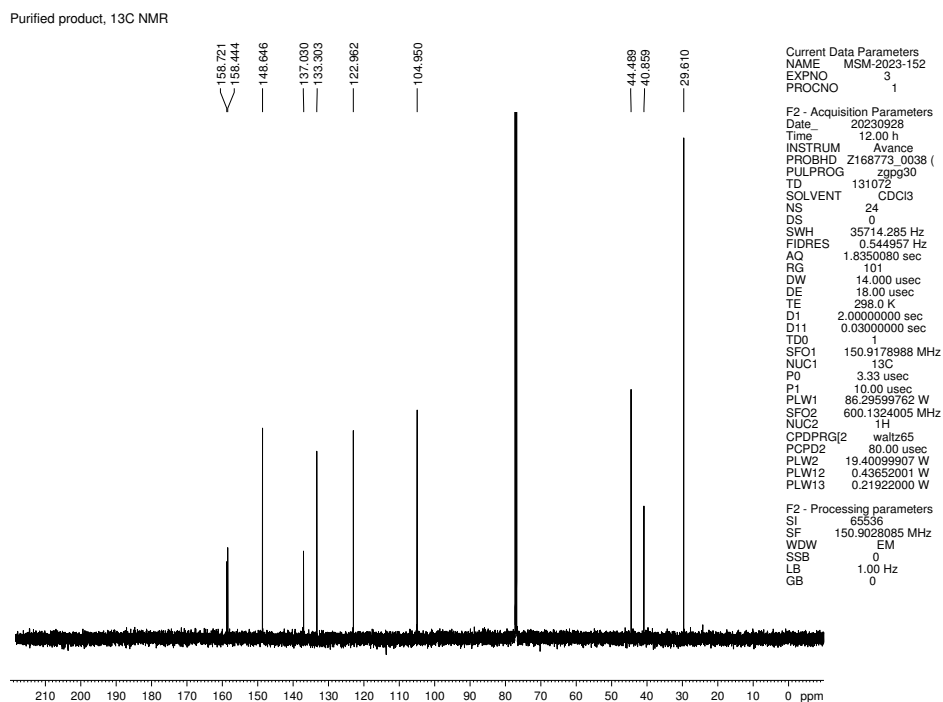


Figure 5.37. ¹³C NMR (150 MHz, CDCl₃) of compound 5.60.

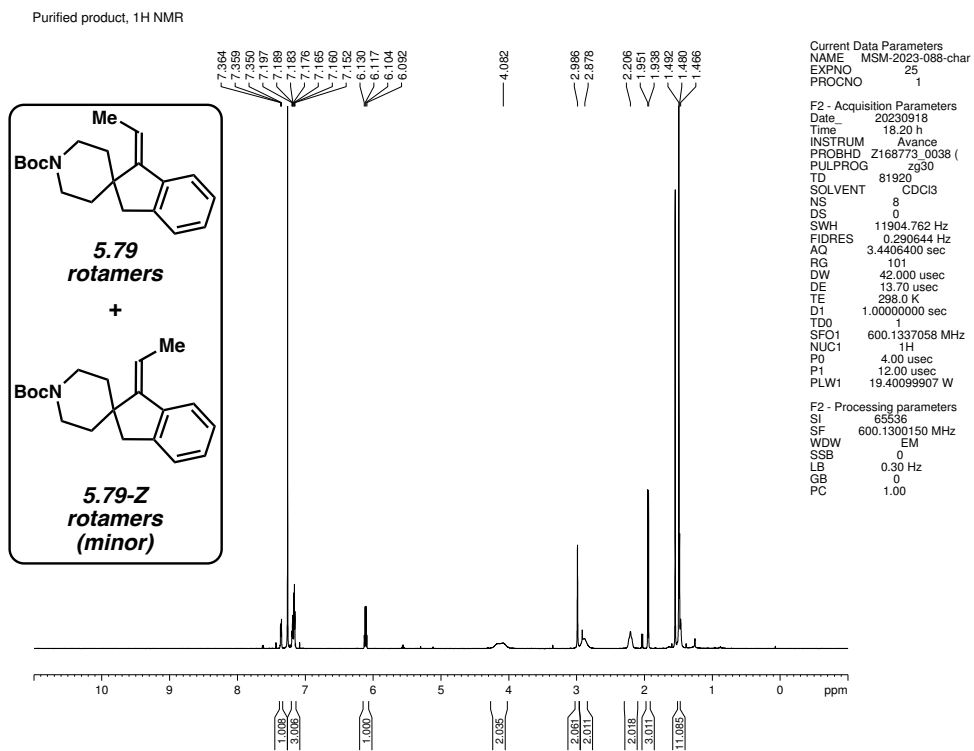


Figure 5.38. ¹H NMR (600 MHz, CDCl₃) of compound 5.79.

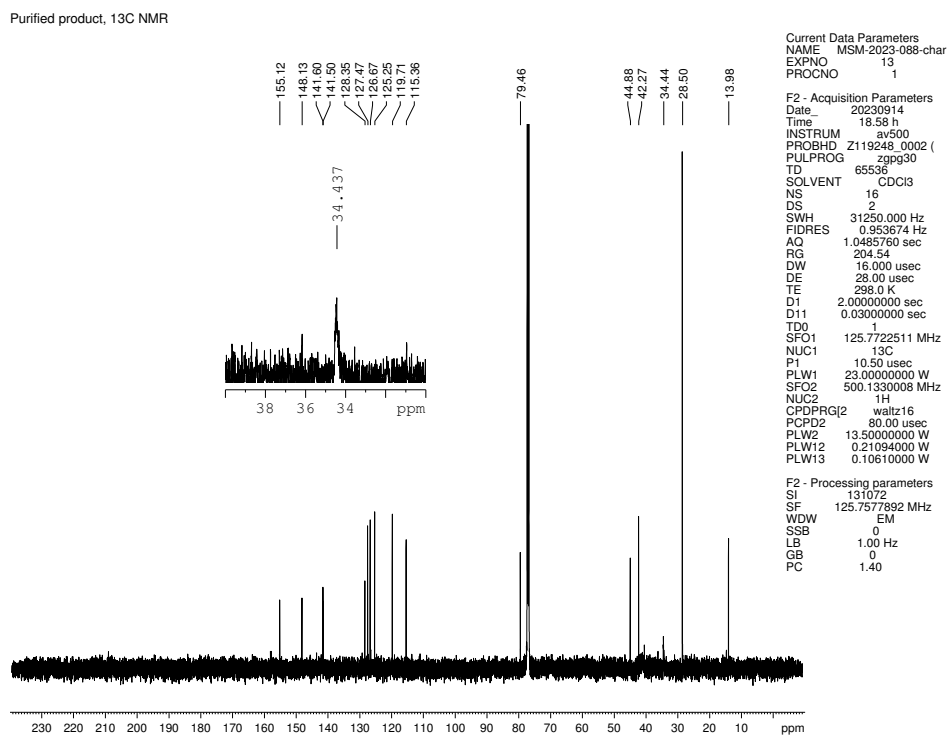
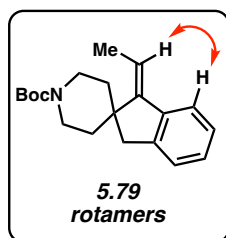


Figure 5.39. ¹³C NMR (150 MHz, CDCl₃) of compound 5.79.



Purified product, NOESY

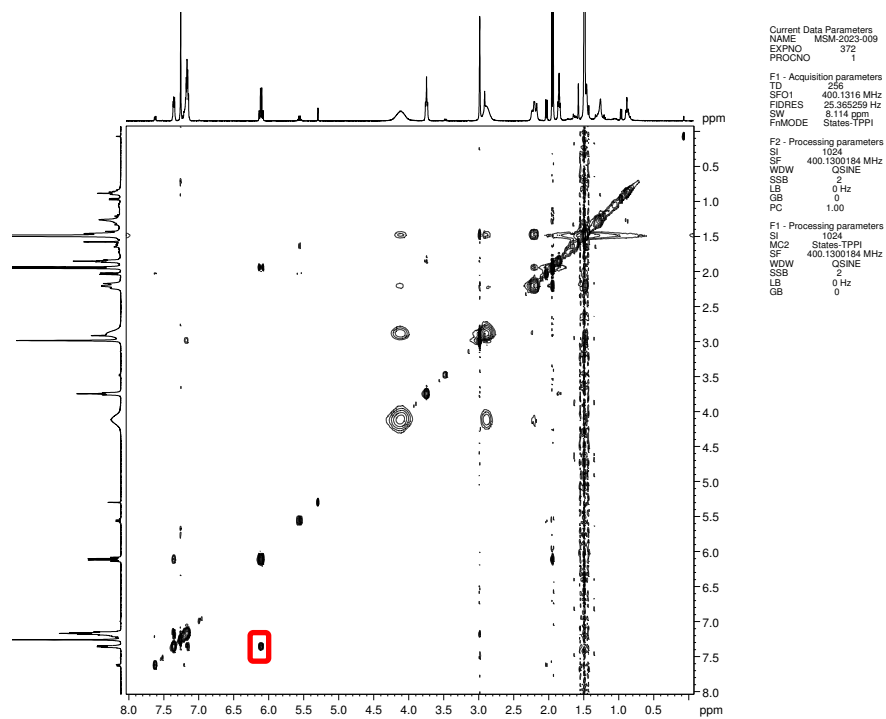


Figure 5.40. NOESY (400 MHz, CDCl_3) of compound **5.79**.

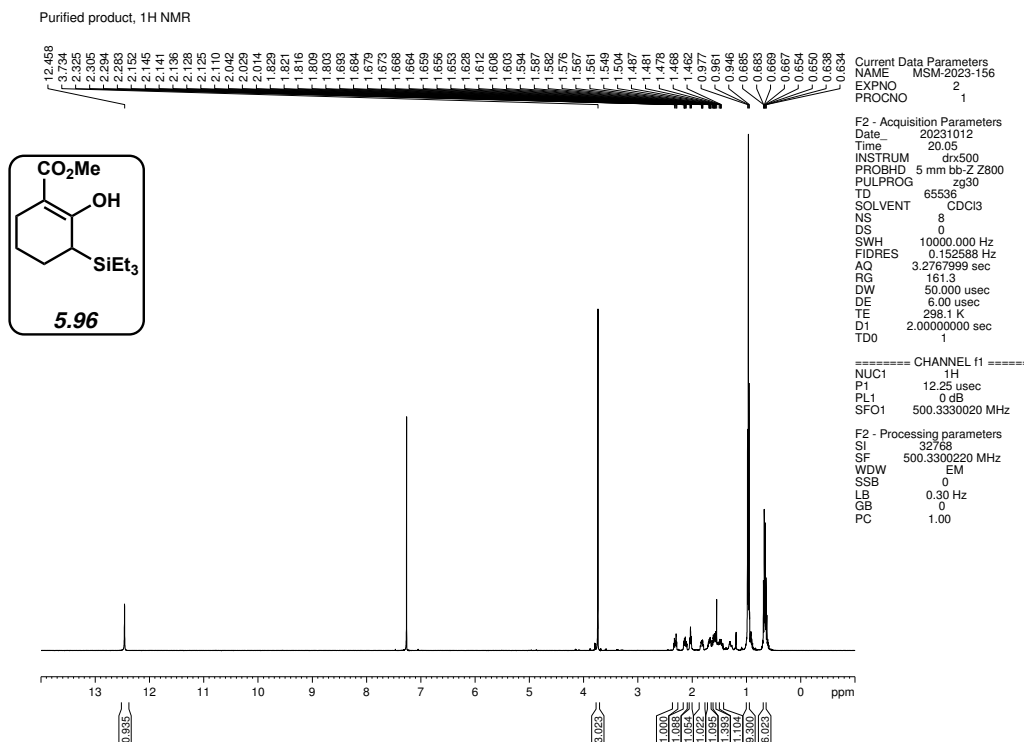


Figure 5.41. ^1H NMR (500 MHz, CDCl_3) of compound 5.96.

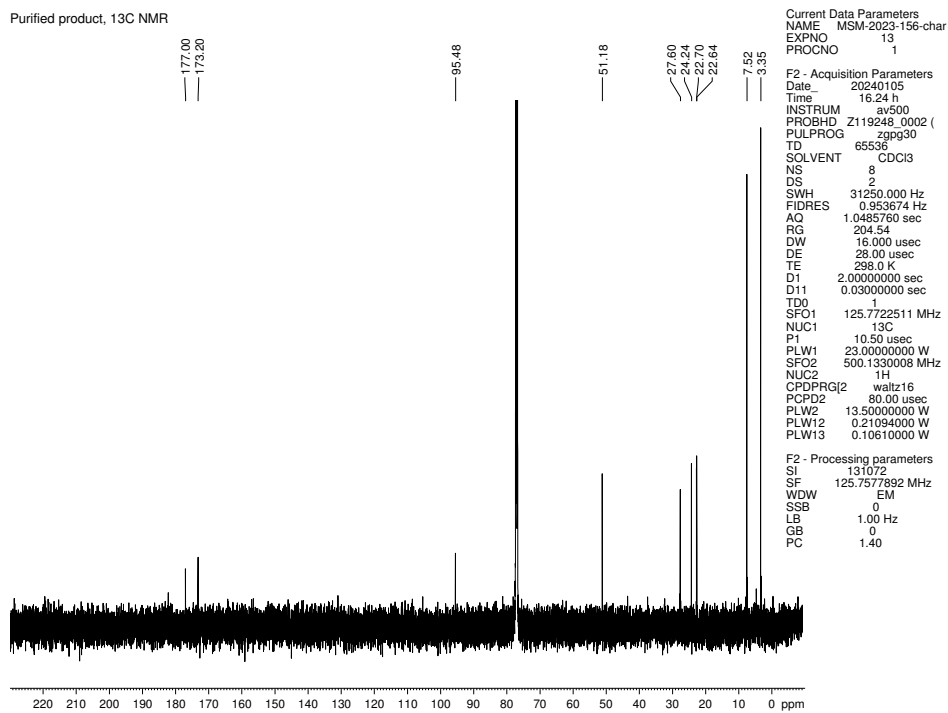


Figure 5.42. ^{13}C NMR (125 MHz, CDCl_3) of compound 5.96.

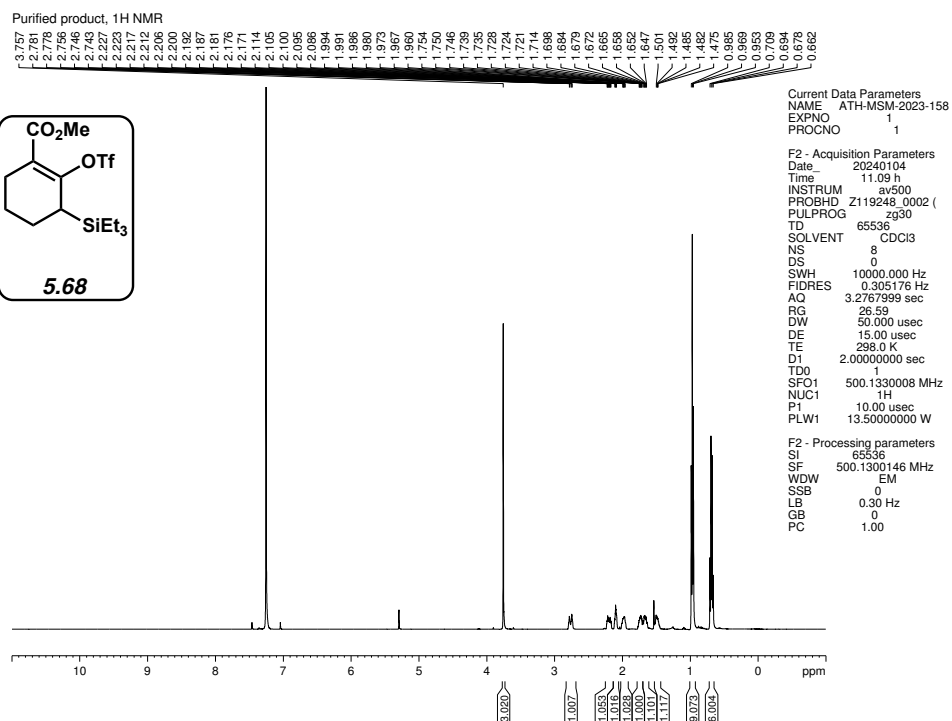


Figure 5.43. ¹H NMR (500 MHz, CDCl₃) of compound 5.68.

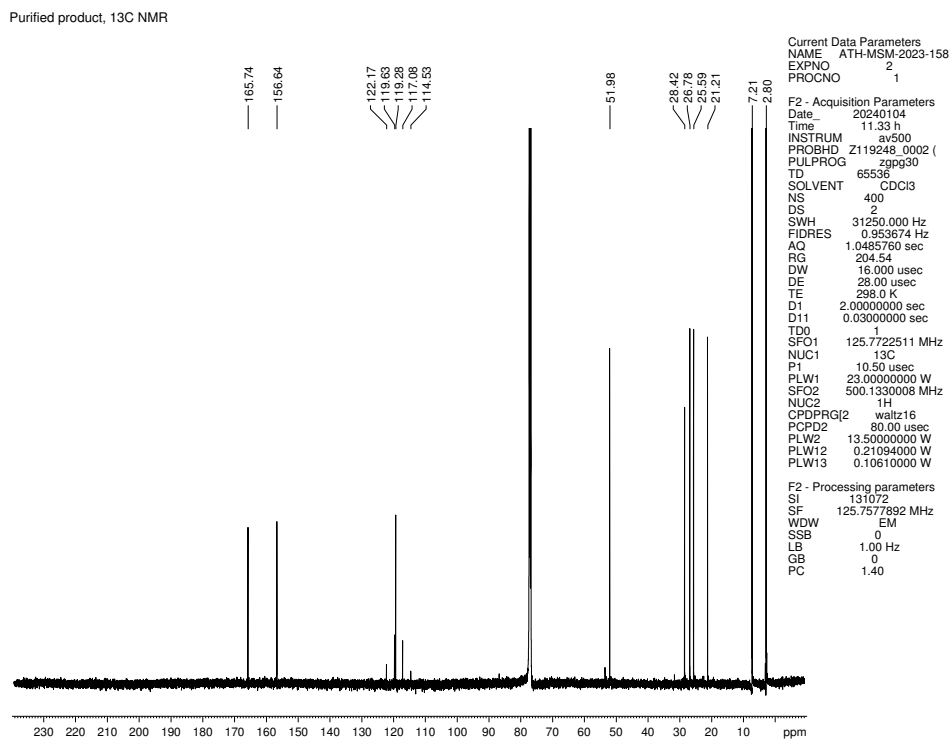


Figure 5.44. ¹³C NMR (125 MHz, CDCl₃) of compound 5.68.

Purified product, ^{19}F NMR

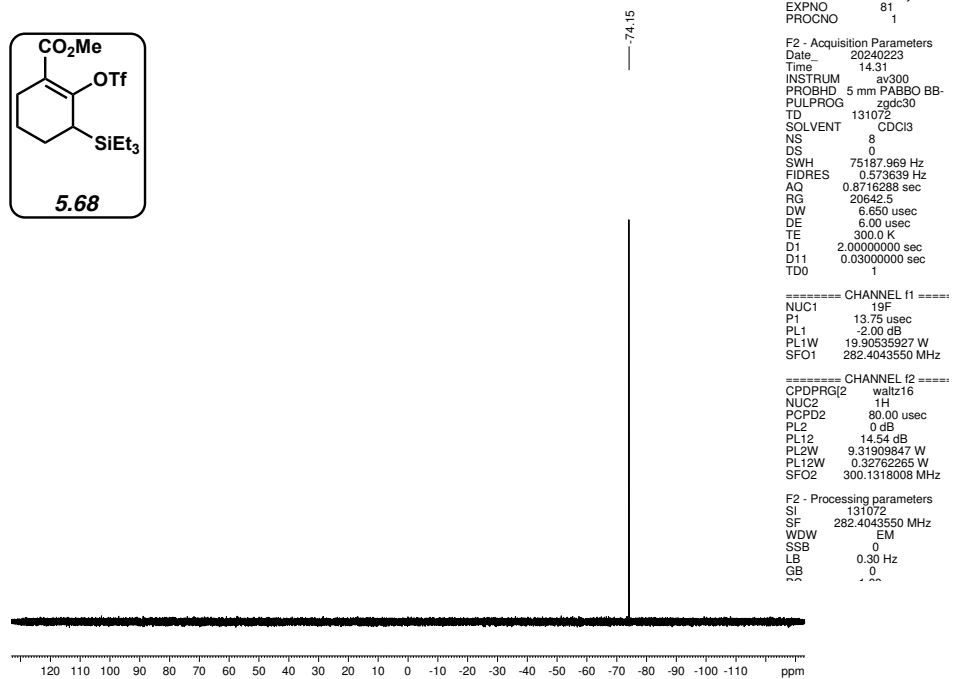
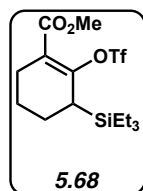


Figure 5.45. ^{19}F NMR (282 MHz, CDCl_3) of compound 5.68.

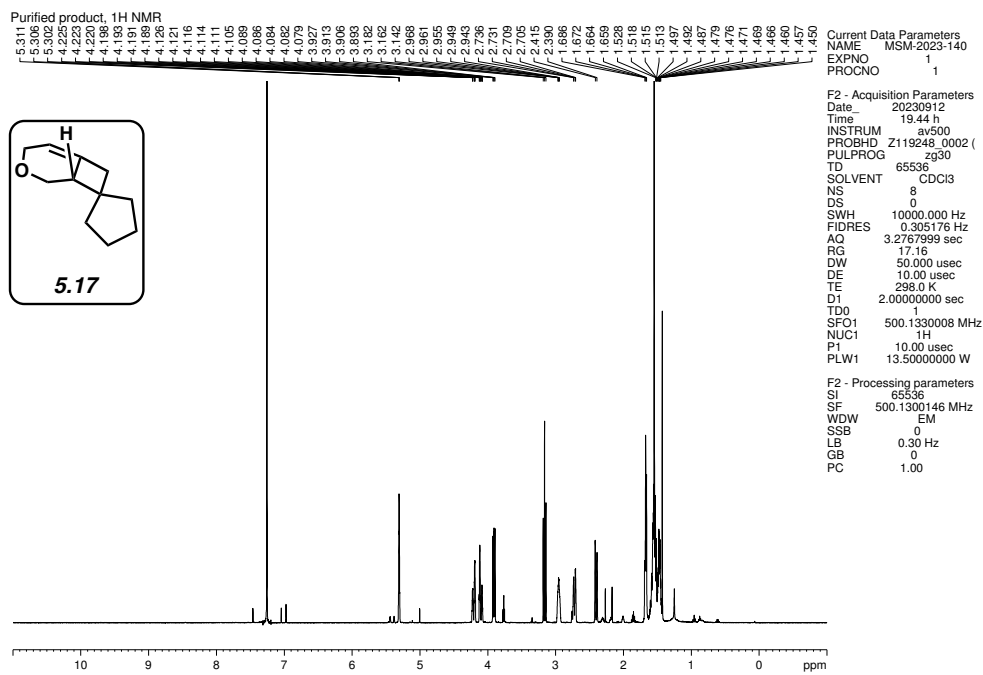


Figure 5.46. ¹H NMR (500 MHz, CDCl₃) of compound 5.17.

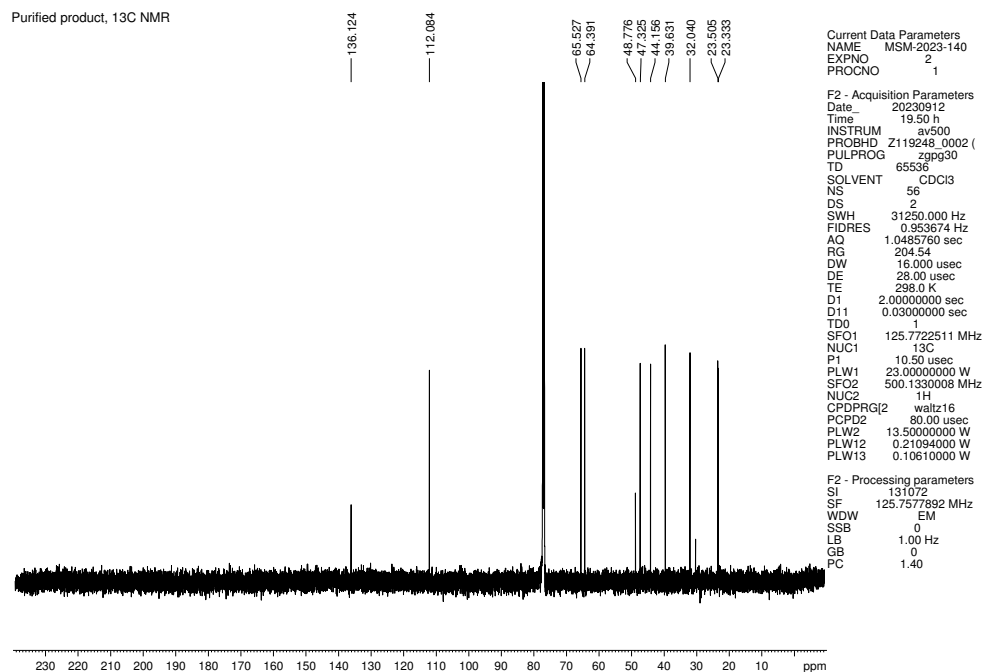
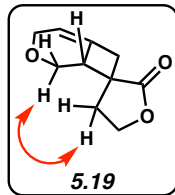


Figure 5.47. ¹³C NMR (125 MHz, CDCl₃) of compound 5.17.



Purified product, NOESY

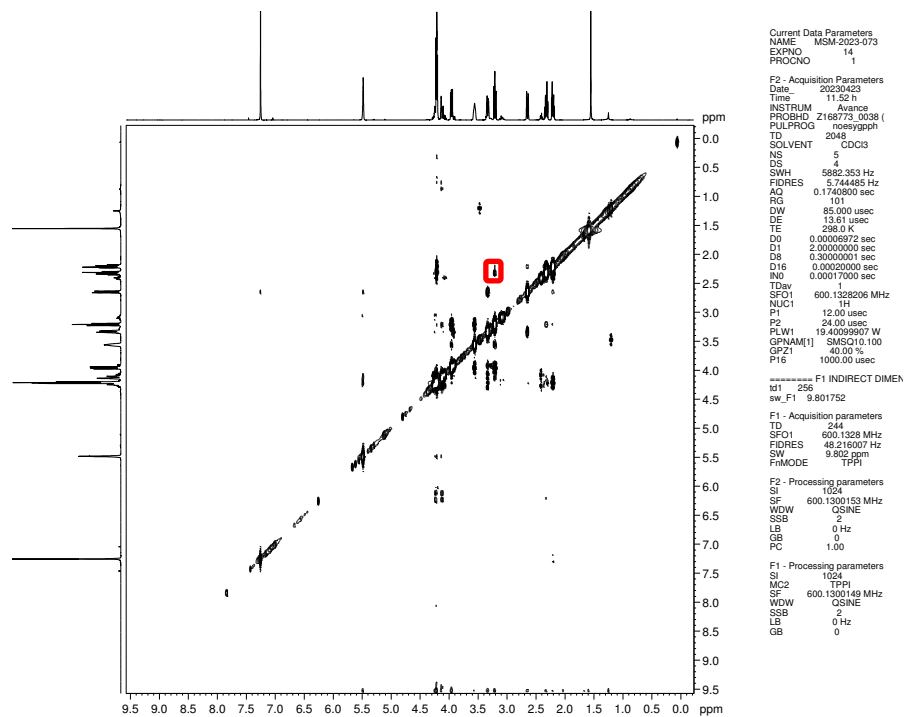


Figure 5.50. NOESY (600 MHz, CDCl₃) of compound **5.19**.

Purified product, ¹H NMR

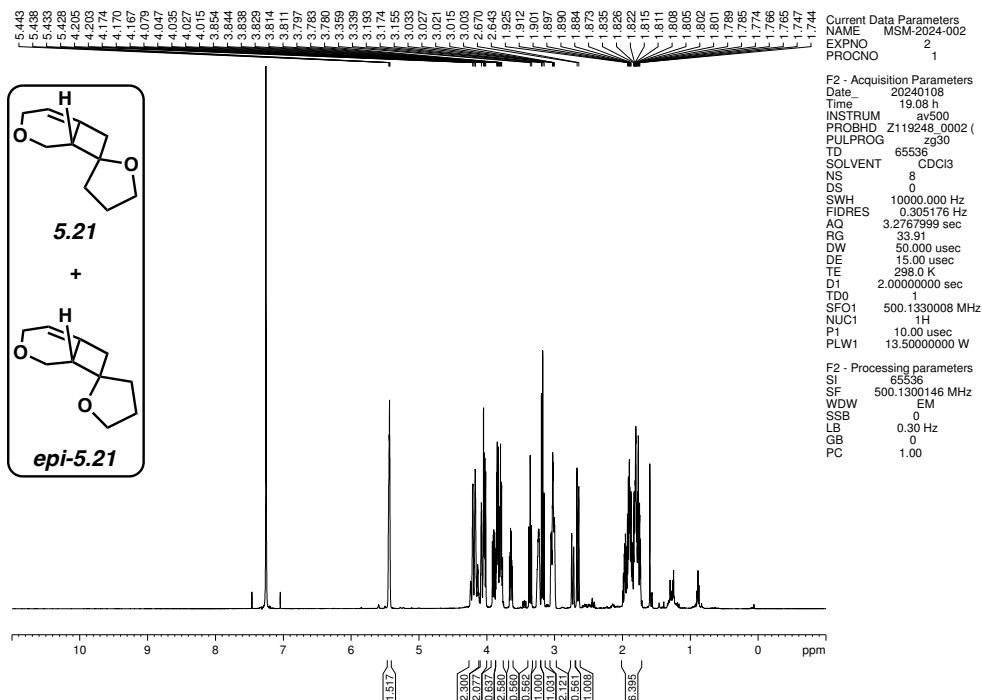


Figure 5.51. ¹H NMR (500 MHz, CDCl₃) of compounds **5.21** and *epi-5.21*.

Purified product, ¹³C NMR

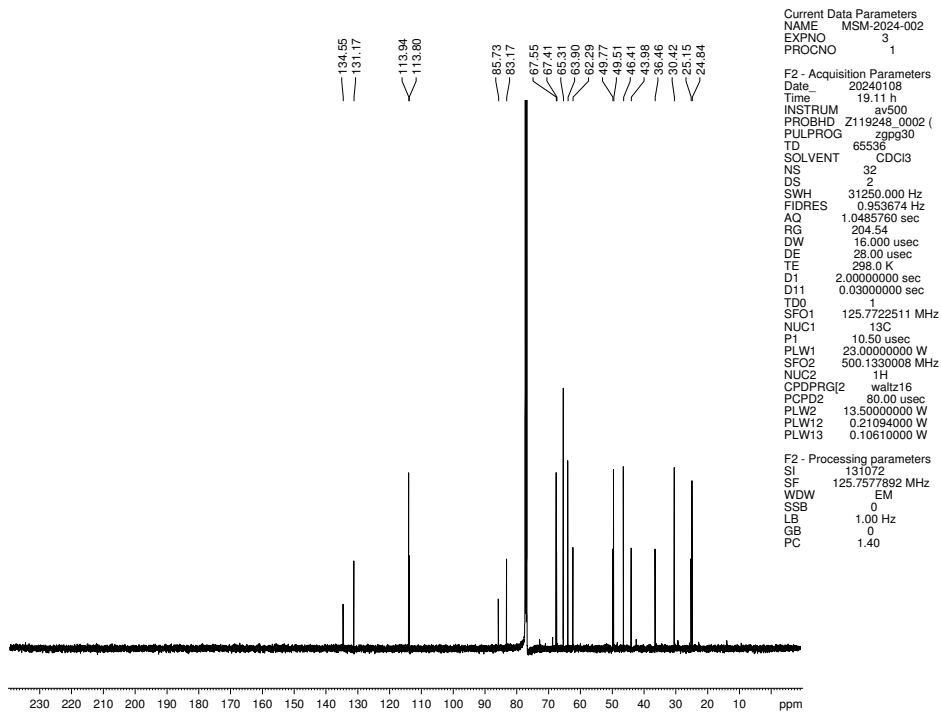


Figure 5.52. ¹³C NMR (125 MHz, CDCl₃) of compounds **5.21** and *epi-5.21*.

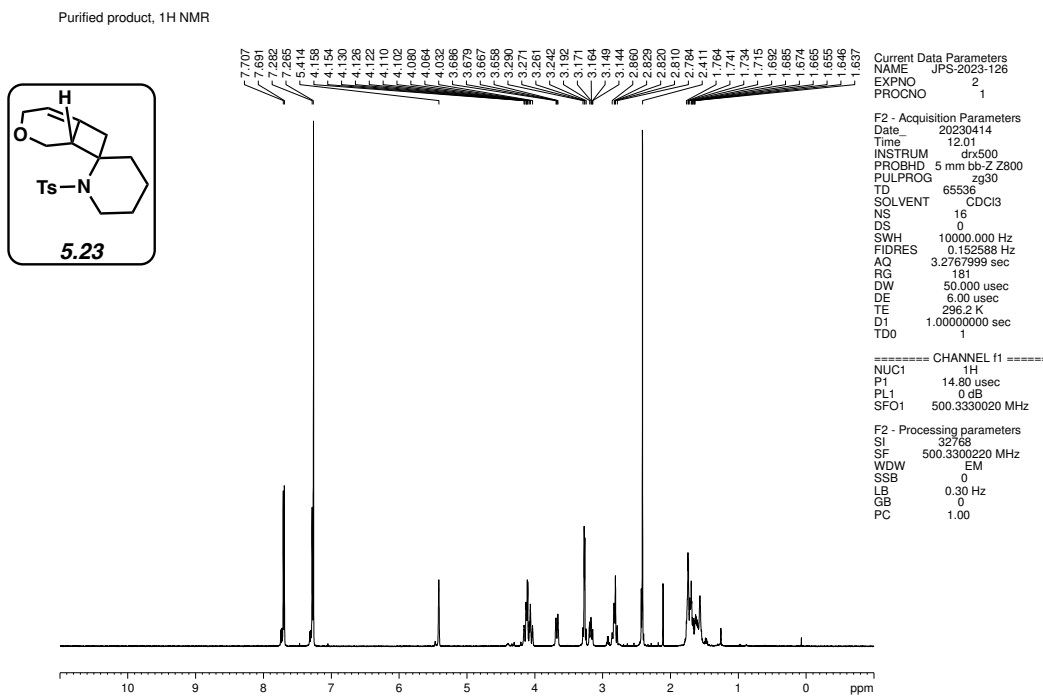


Figure 5.55. ¹H NMR (500 MHz, CDCl₃) of compound 5.23.

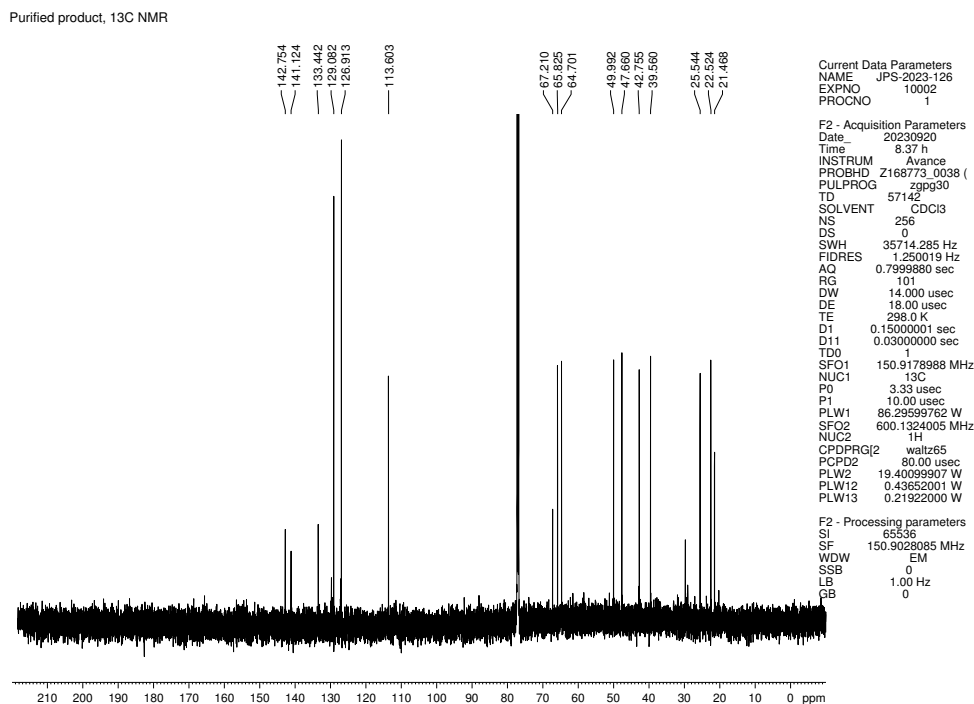


Figure 5.56. ¹³C NMR (150 MHz, CDCl₃) of compound 5.23.

Purified product, ¹H NMR

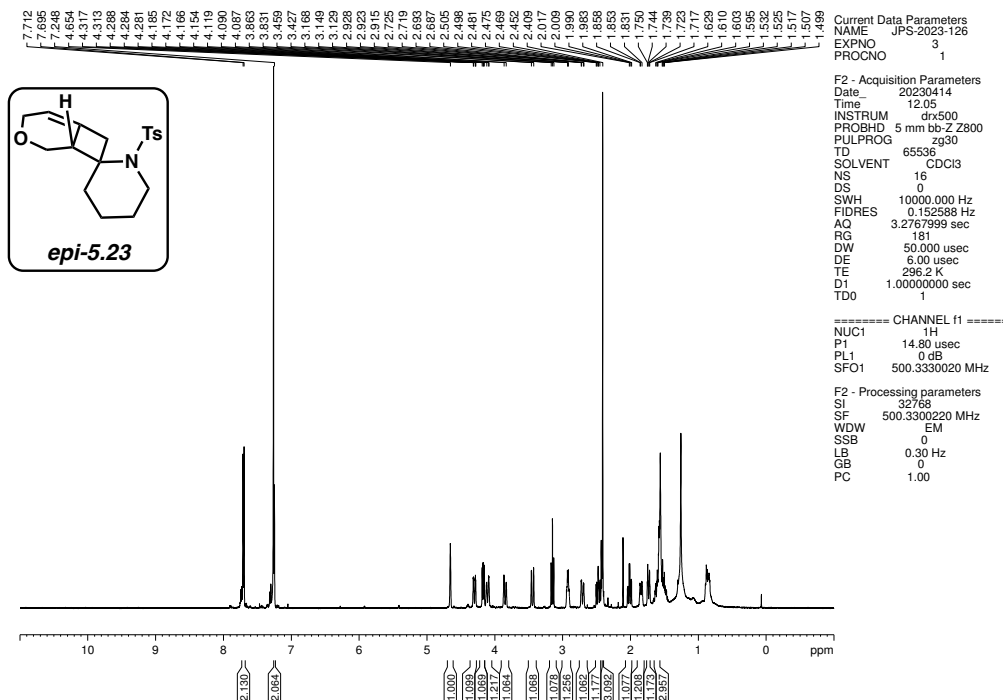


Figure 5.57. ¹H NMR (500 MHz, CDCl₃) of compound *epi*-5.23.

Purified product, ¹³C NMR

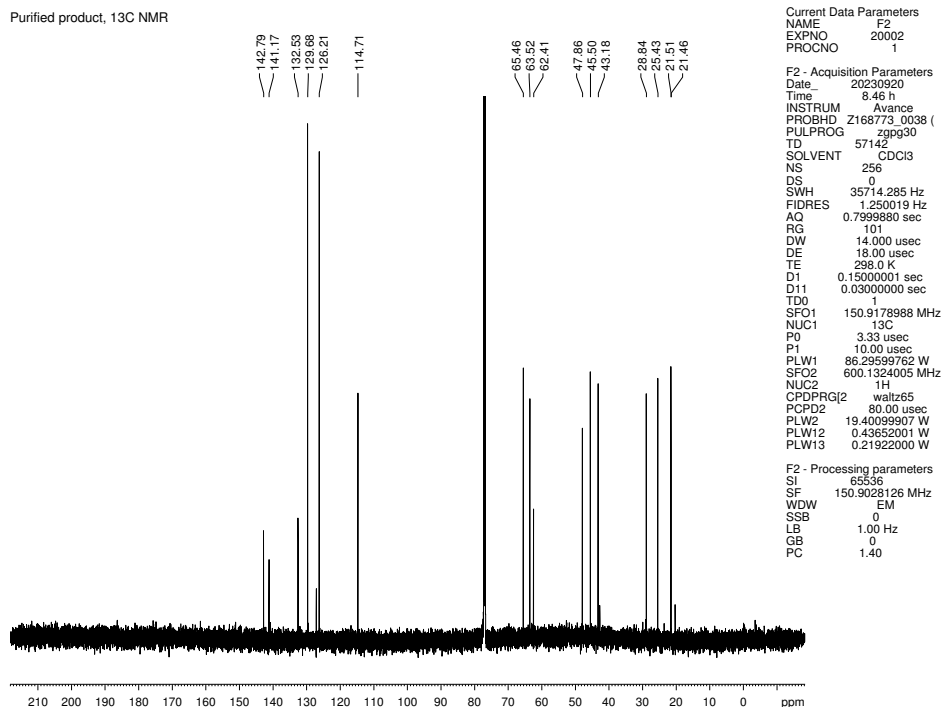


Figure 5.58. ¹³C NMR (150 MHz, CDCl₃) of compound *epi*-5.23.

Purified product, NOESY

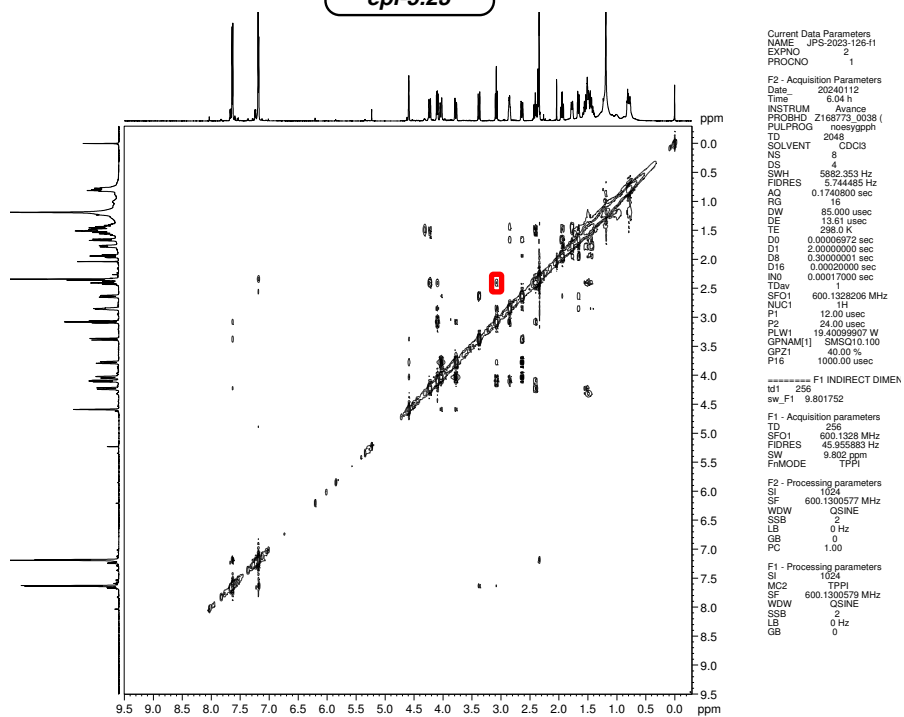
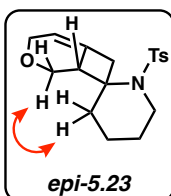


Figure 5.59. NOESY (600 MHz, CDCl₃) of compound *epi-5.23*.

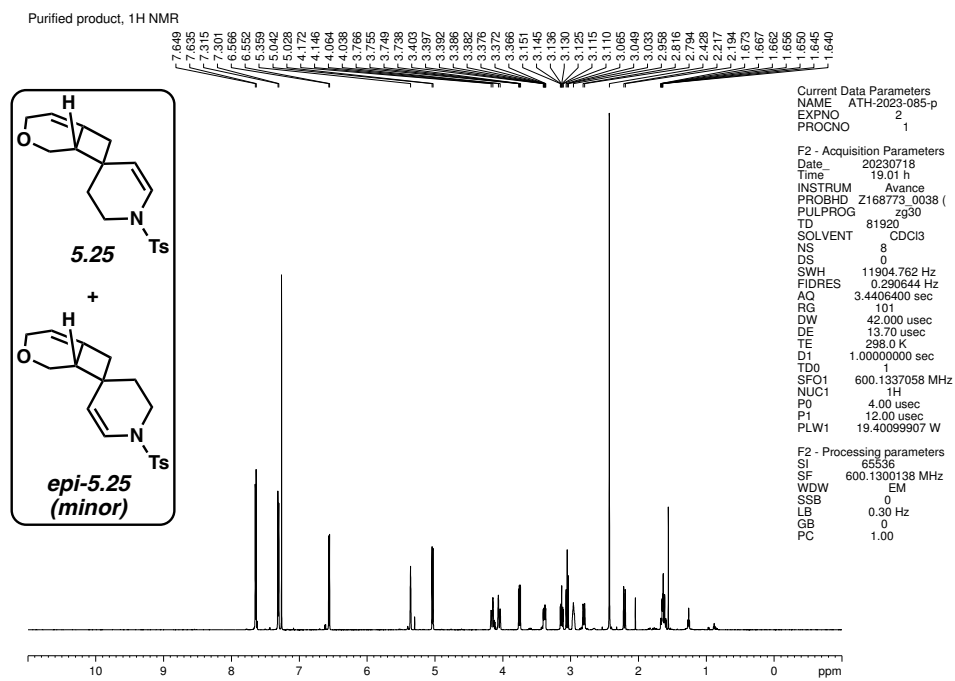


Figure 5.60. ¹H NMR (600 MHz, CDCl₃) of compound 5.25.

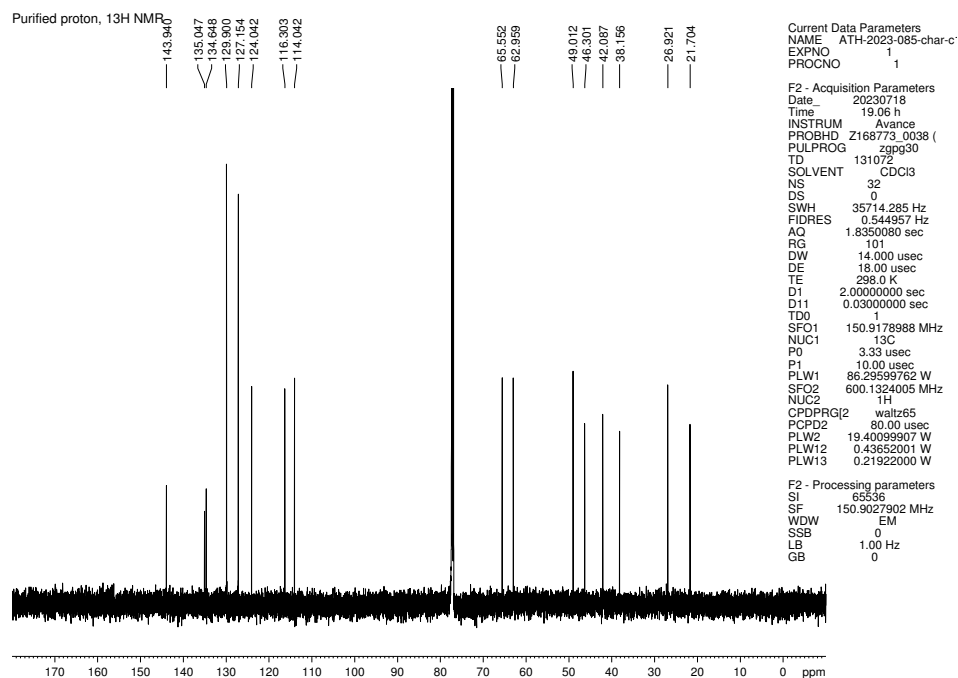
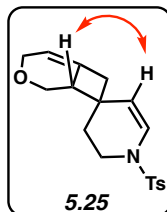


Figure 5.61. ¹³C NMR (150 MHz, CDCl₃) of compound 5.25.



Purified product, NOESY

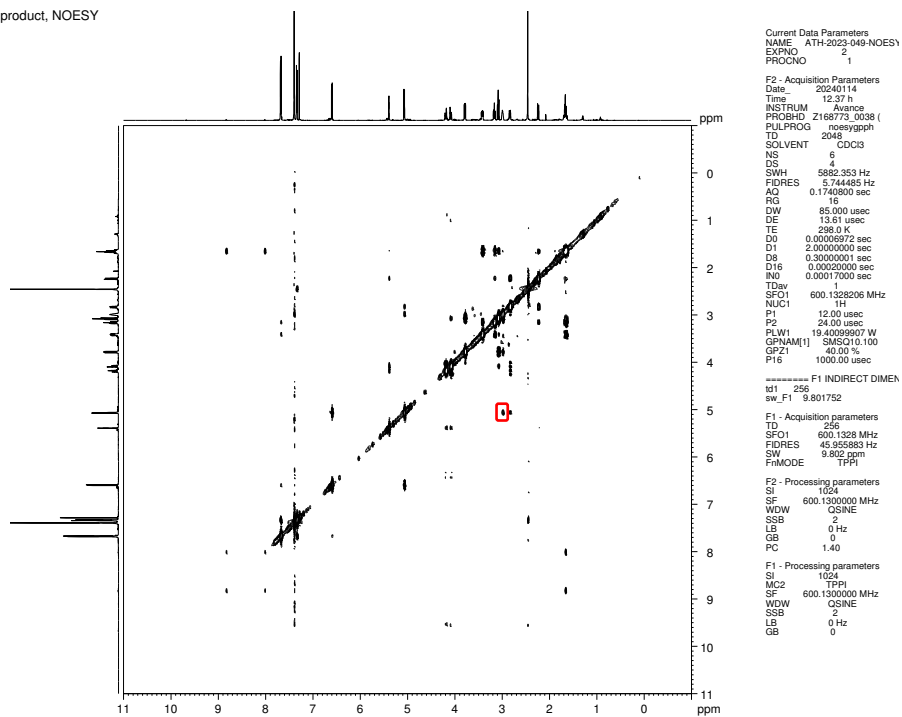


Figure 5.62. NOESY (600 MHz, CDCl₃) of compound **5.25**.

Purified product, ¹H NMR

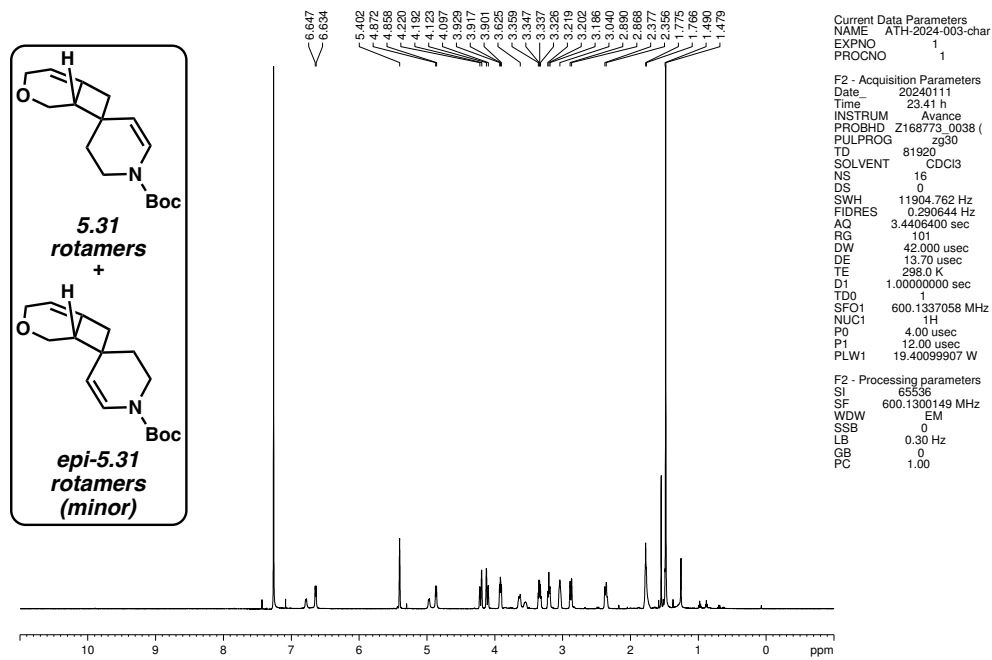


Figure 5.63. ¹H NMR (600 MHz, CDCl₃) of compound 5.31.

Purified product, ¹³C NMR

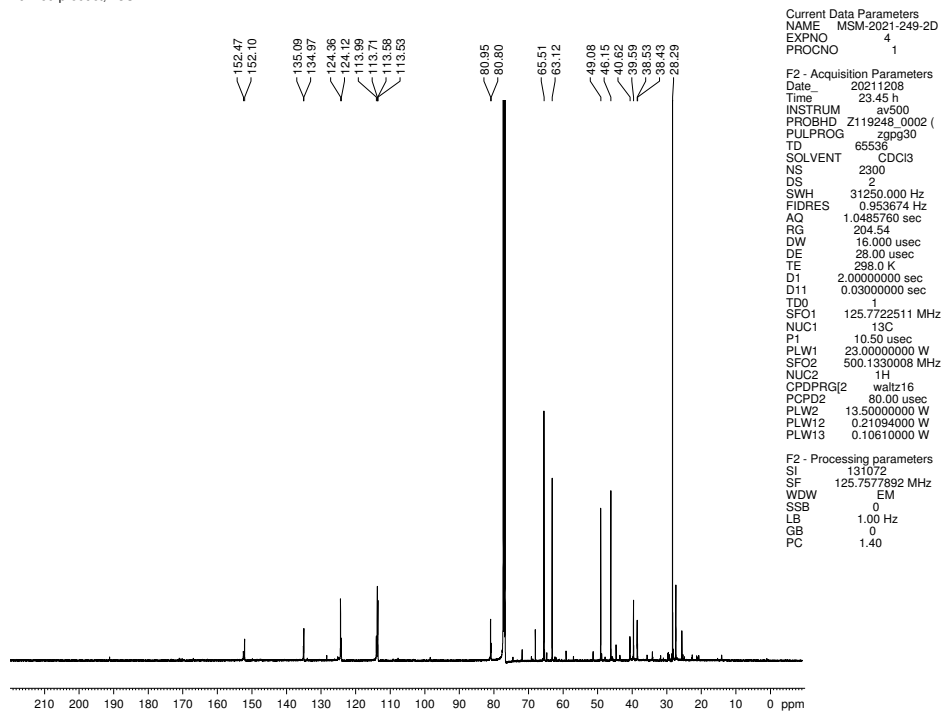


Figure 5.64. ¹³C NMR (125 MHz, CDCl₃) of compound 5.31.

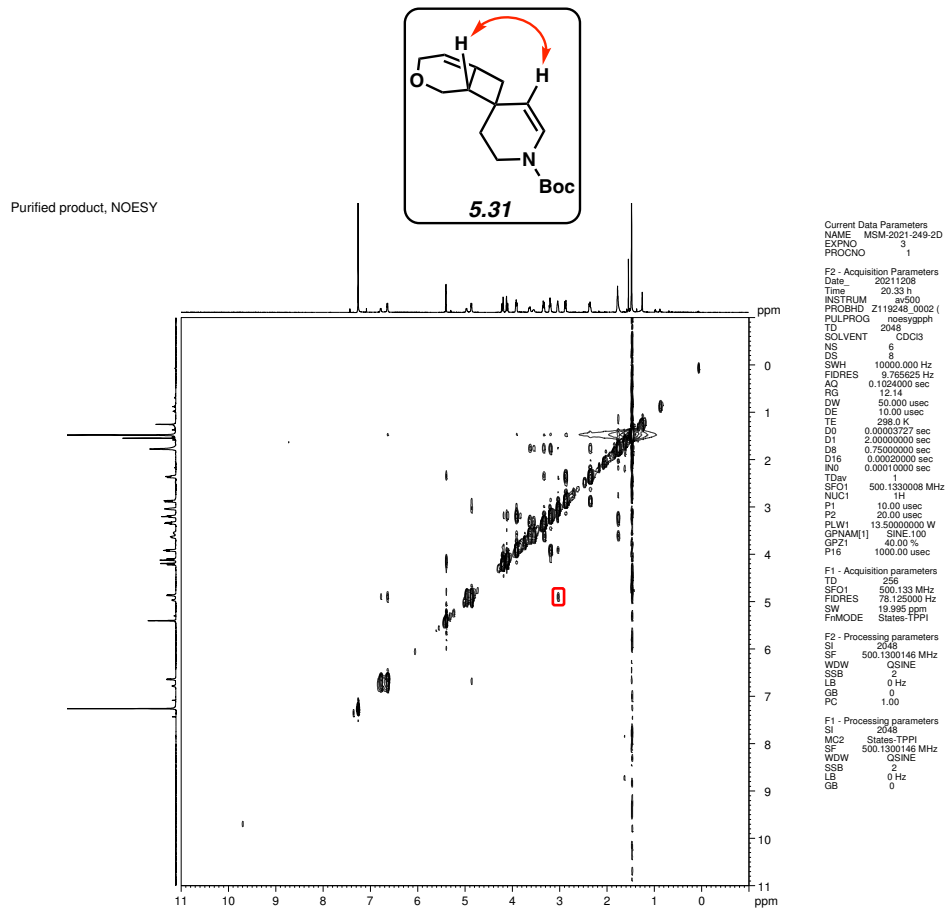


Figure 5.65. NOESY (500 MHz, CDCl_3) of compound **5.31**.

Purified product, ¹H NMR

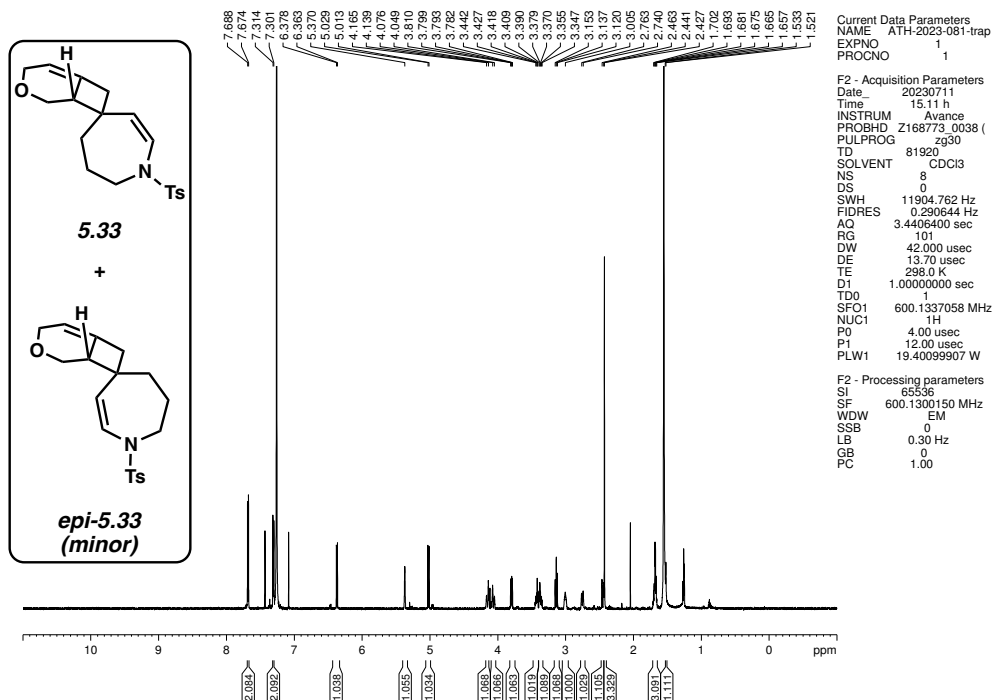


Figure 5.66. ¹H NMR (600 MHz, CDCl₃) of compound 5.33.

Purified product, ¹³C NMR

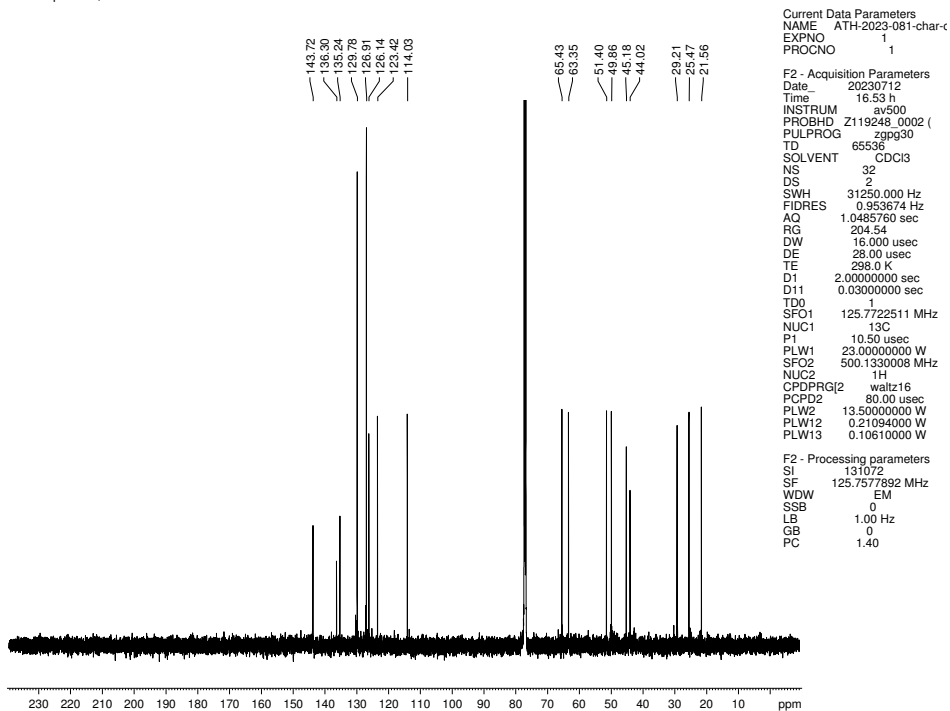


Figure 5.67. ¹³C NMR (125 MHz, CDCl₃) of compound 5.33.

Purified product, NOESY

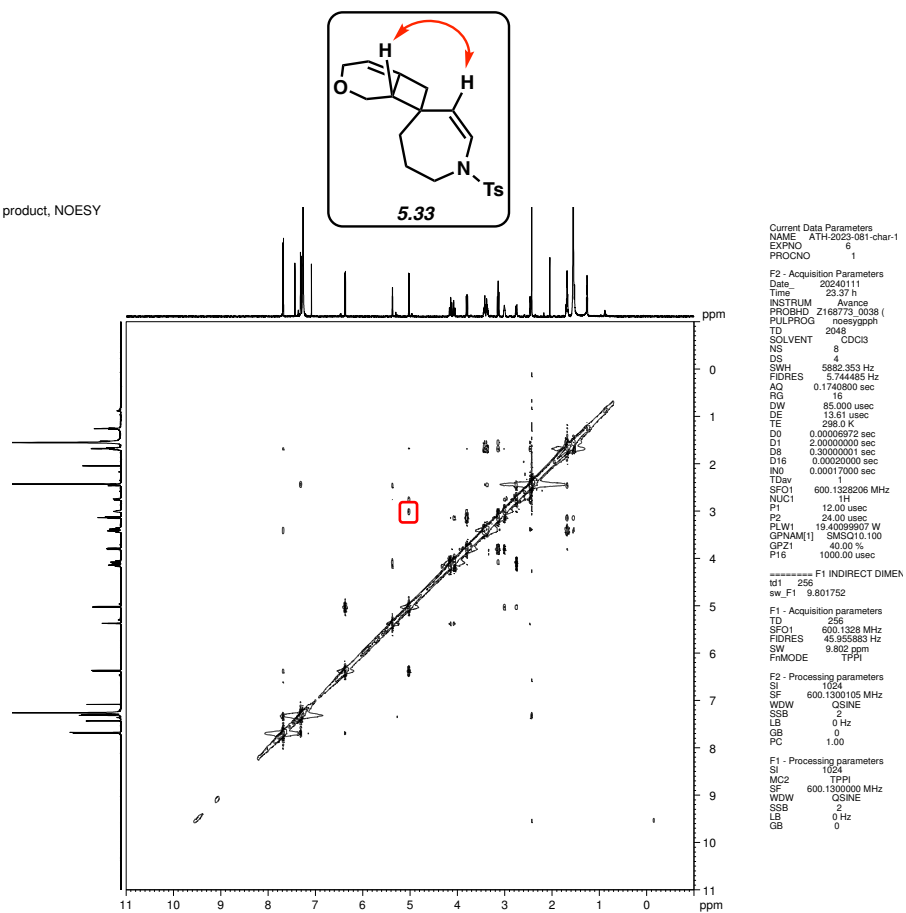


Figure 5.68. NOESY (600 MHz, CDCl₃) of compound 5.33.

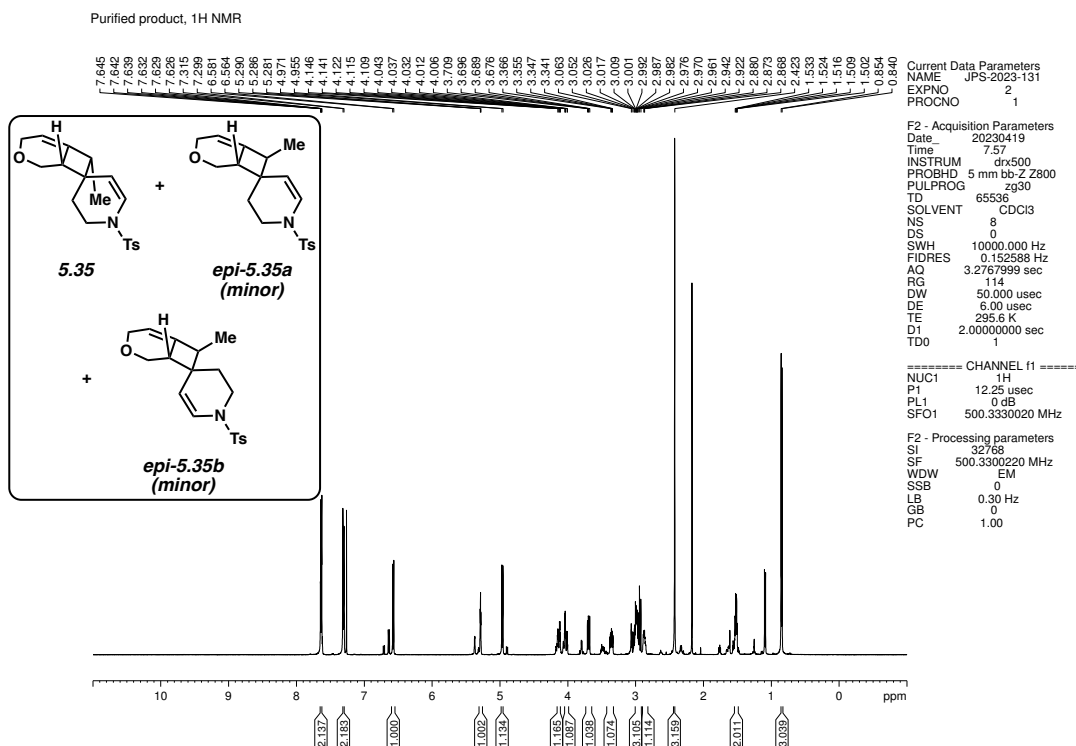


Figure 5.69. ¹H NMR (500 MHz, CDCl₃) of compound 5.35.

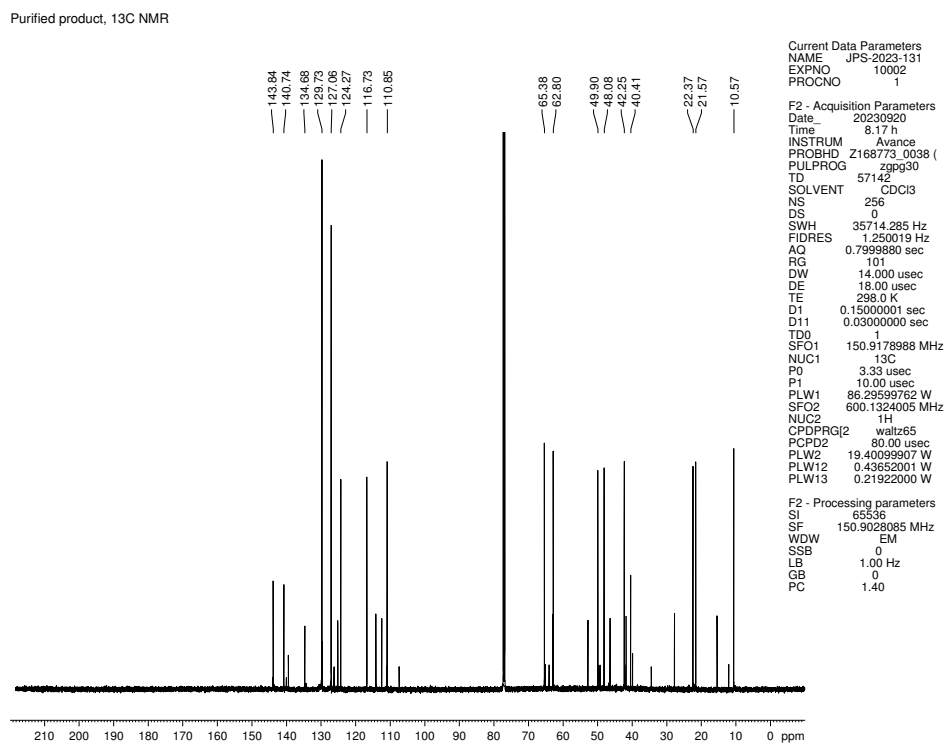


Figure 5.70. ¹³C NMR (150 MHz, CDCl₃) of compound 5.35.

Purified product, NOESY

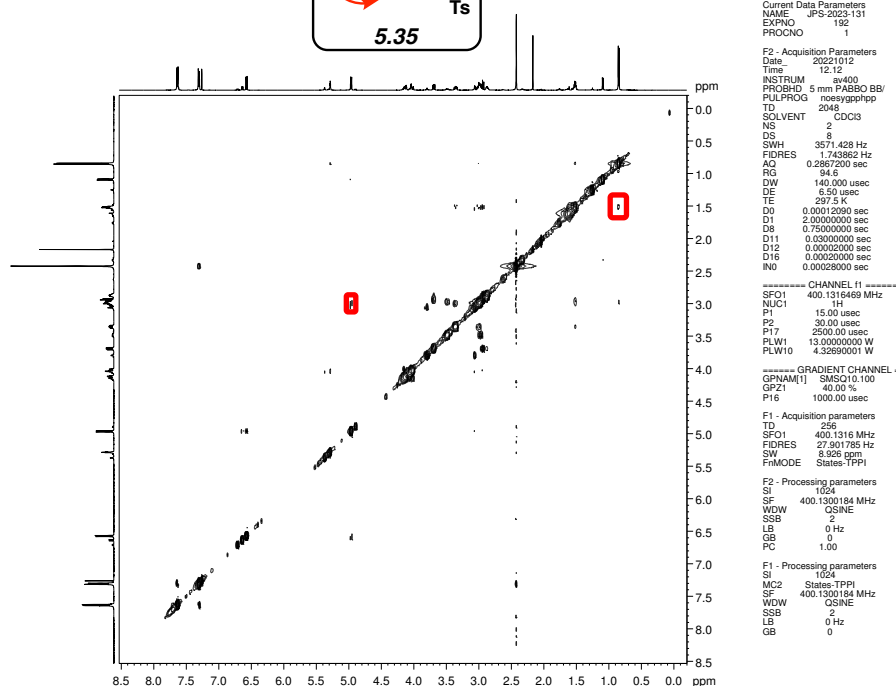
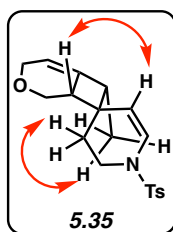


Figure 5.71. NOESY (400 MHz, CDCl₃) of compound 5.35.

Purified product, 1H NMR

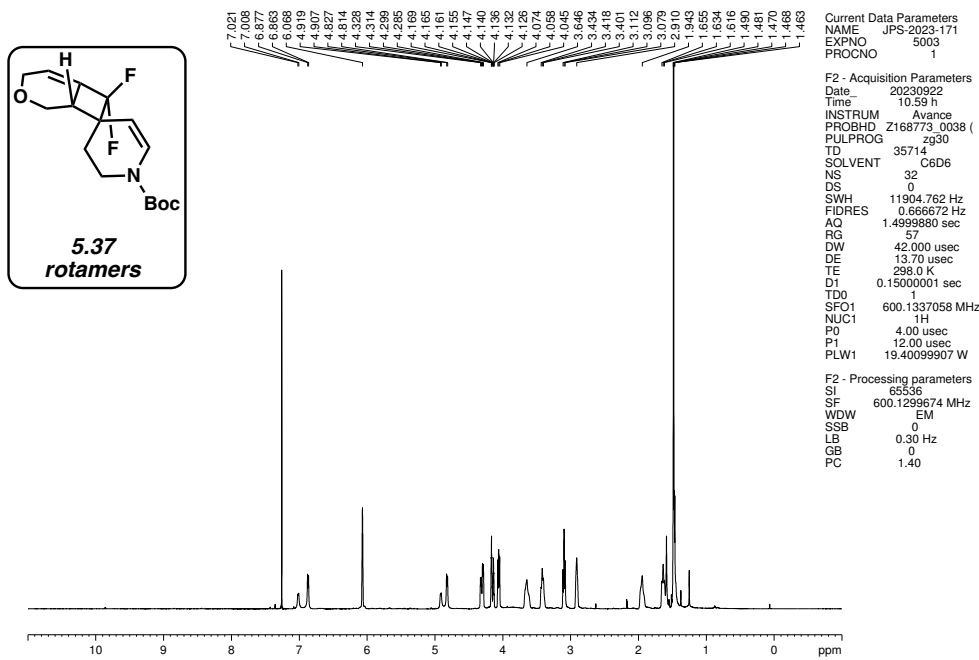


Figure 5.72. ¹H NMR (600 MHz, CDCl₃) of compound 5.37.

Purified product, 13C NMR

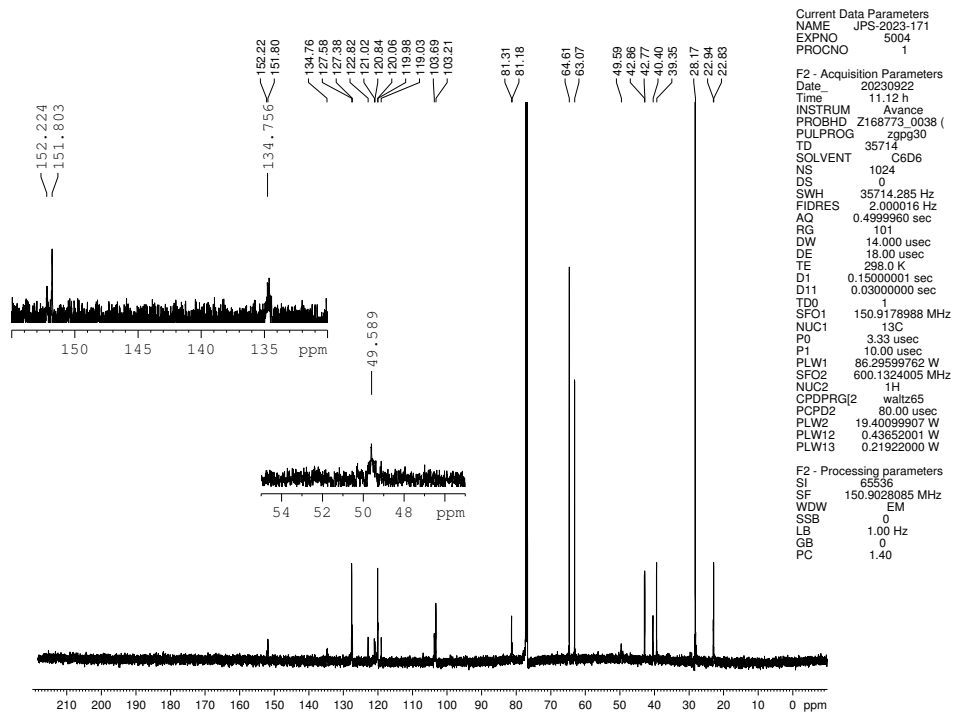
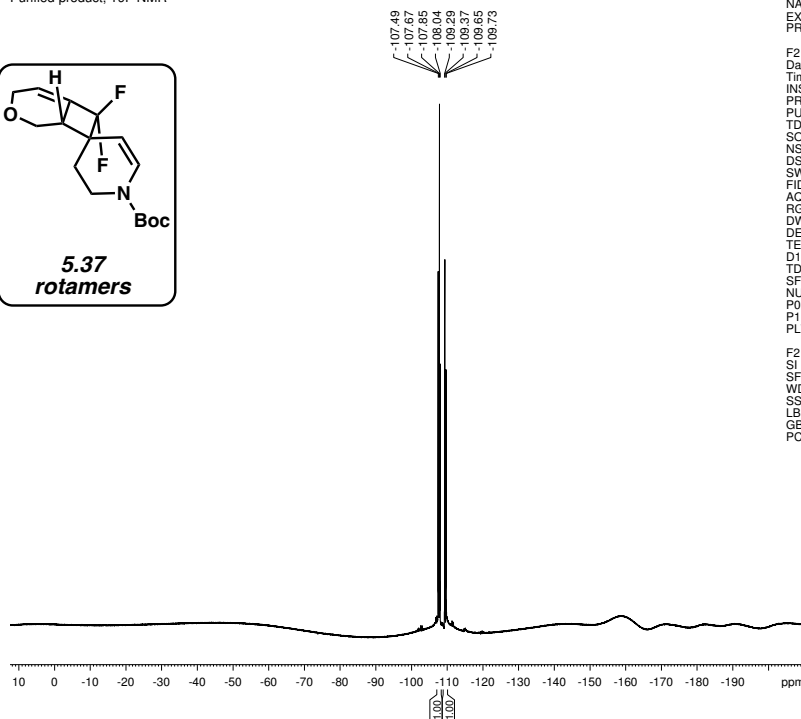
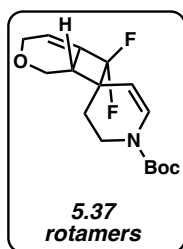


Figure 5.73. ¹³C NMR (150 MHz, CDCl₃) of compound 5.37.

Purified product, ^{19}F NMR



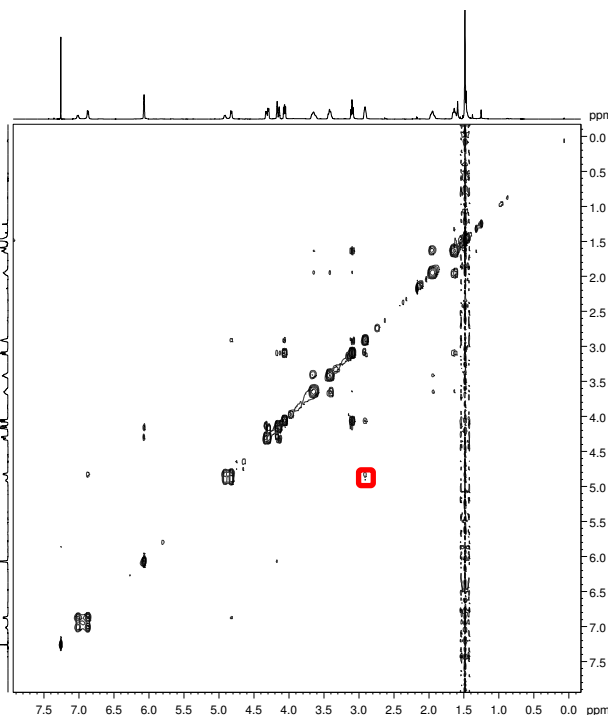
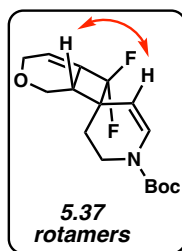
Current Data Parameters
NAME JPS-2023-171
EXPNO 5005
PROCNO 1

F2 - Acquisition Parameters
Date_ 20230922
Time 11.14 h
INSTRUM Avance
PROBHD Z168773_0038 (PULPROG zg30
TD 131072
SOLVENT C6D6
NS 32
DS 0
SWH 131578.953 Hz
FIDRES 2.007735 Hz
AQ 0.4980736 sec
RG 16
DW 3.800 usec
DE 18.00 usec
TE 298.0 K
D1 1.00000000 sec
TD0 1
SFO1 564.6299196 MHz
NUC1 ^{19}F
P0 5.00 usec
P1 15.00 usec
PLW1 19.79999924 W

F2 - Processing parameters
SI 131072
SF 564.6863882 MHz
WDW EM
SSB 0
LB 2.00 Hz
GB 0
PC 1.00

Figure 5.74. ^{19}F NMR (565 MHz, CDCl_3) of compound 5.37.

Purified product, NOESY



Current Data Parameters
NAME JPS-2023-171
EXPNO 52
PROCNO 1

F2 - Acquisition Parameters
Date_ 20230614
Time 8.53
INSTRUM av400
PROBHD 5 mm PABBO BB/PULPROG noesypphpc
TD 2048
SOLVENT CDCl_3
NS 2
DS 8
SWH 3246.753 Hz
FIDRES 1.585329 Hz
AQ 0.3153920 sec
RG 83.63
DW 154.000 usec
DE 6.50 usec
TE 297.3 K
D0 0.00013490 sec
D1 2.00000000 sec
D8 0.75000000 sec
D11 0.03000000 sec
D12 0.00020000 sec
D16 0.00020000 sec
IN0 0.00030800 sec

----- CHANNEL f1 -----
SFO1 400.1315726 MHz
NUC1 ^1H
P1 15.00 usec
P2 30.00 usec
P17 2500.00 usec
PLW1 13.00000000 W
PLW10 4.32890001 W

----- GRADIENT CHANNEL -----
GPRAM[1] SMSQ10.100
GFZ1 40.00 %
P16 1000.00 usec

F1 - Acquisition parameters
TD 256
SFO1 400.1316 MHz
FIDRES 25.365259 Hz
SW 8.114 gpm
FhMODE States-TPPI

F2 - Processing parameters
SI 1024
SF 400.1300184 MHz
WDW 2
SSB 2
LB 0 Hz
GB 0
PC 1.00

F1 - Processing parameters
SI 1024
MC2 States-TPPI
SF 400.1300184 MHz
WDW 2
SSB 2
LB 0 Hz
GB 0

Figure 5.75. NOESY (400 MHz, CDCl_3) of compound 5.37.

Purified product, ¹H NMR

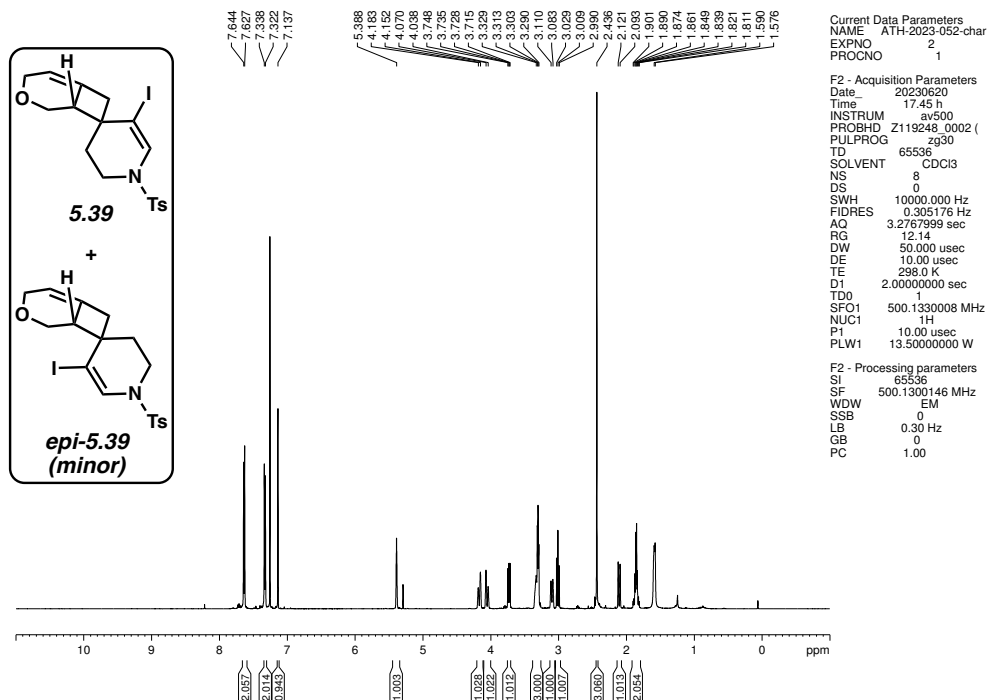


Figure 5.76. ¹H NMR (500 MHz, CDCl₃) of compound 5.39.

Purified product, ¹³C NMR

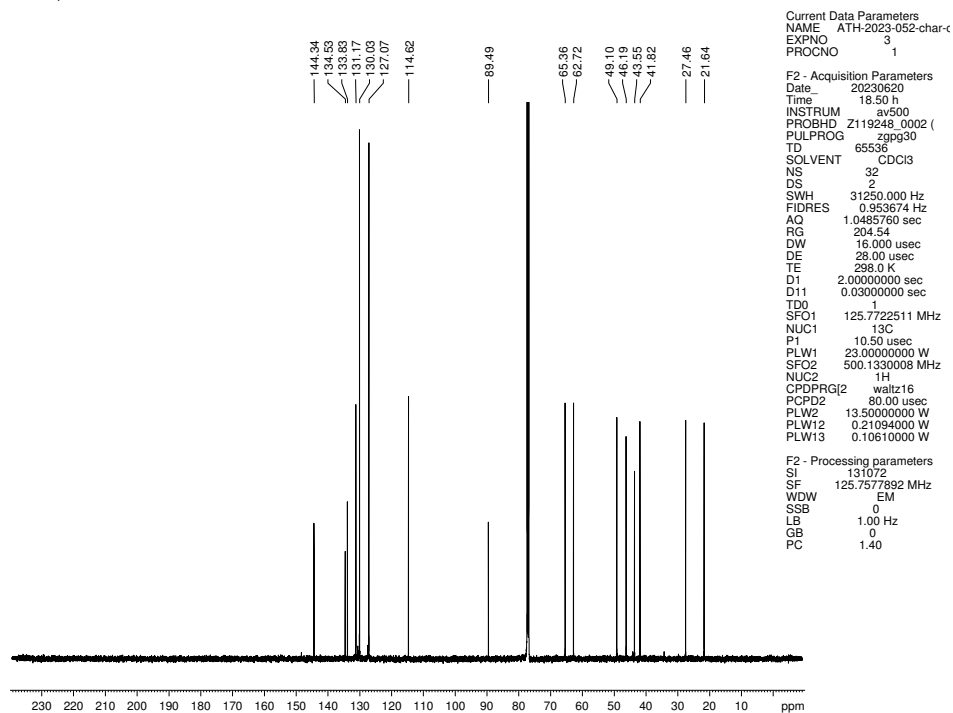


Figure 5.77. ¹³C NMR (125 MHz, CDCl₃) of compound 5.39.

Purified product, NOESY

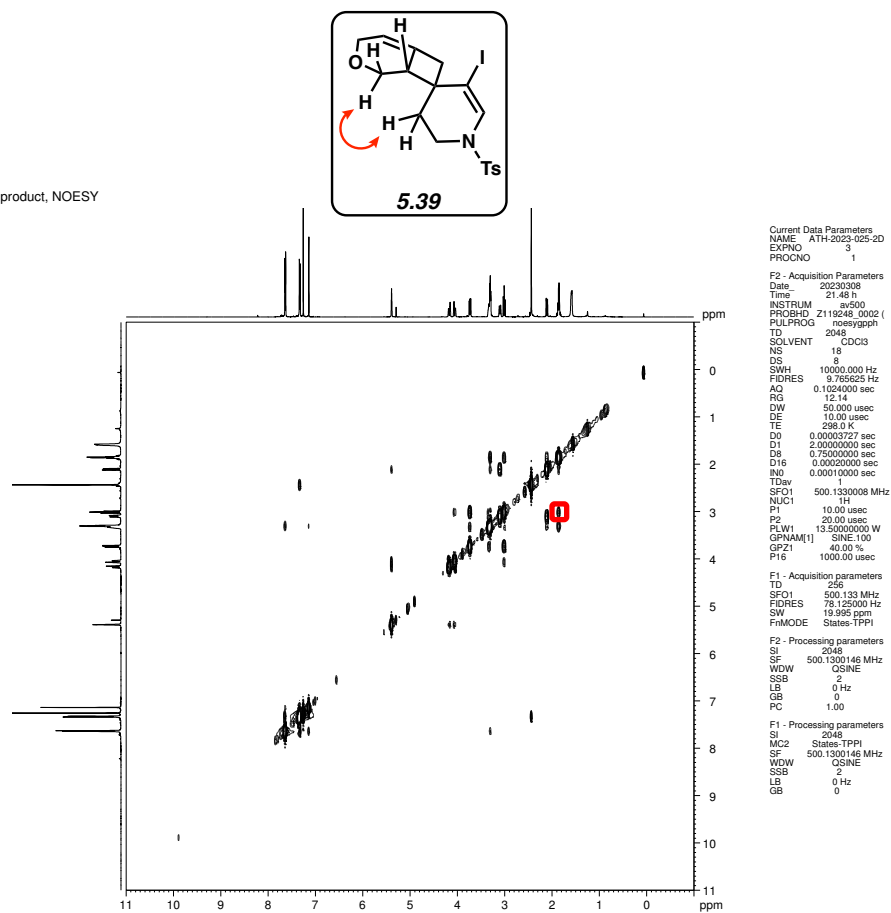
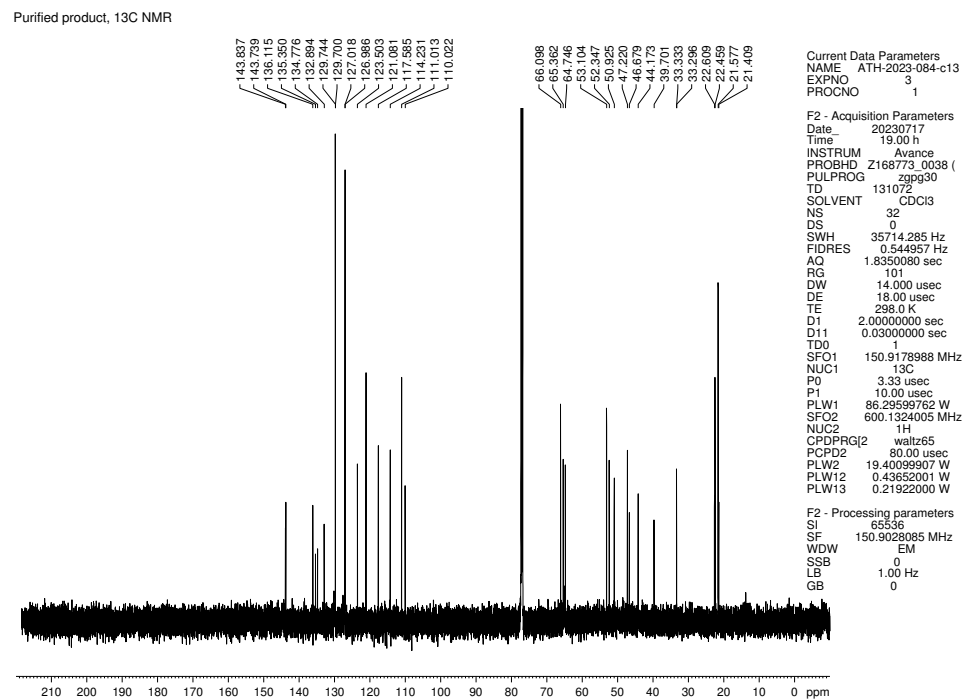
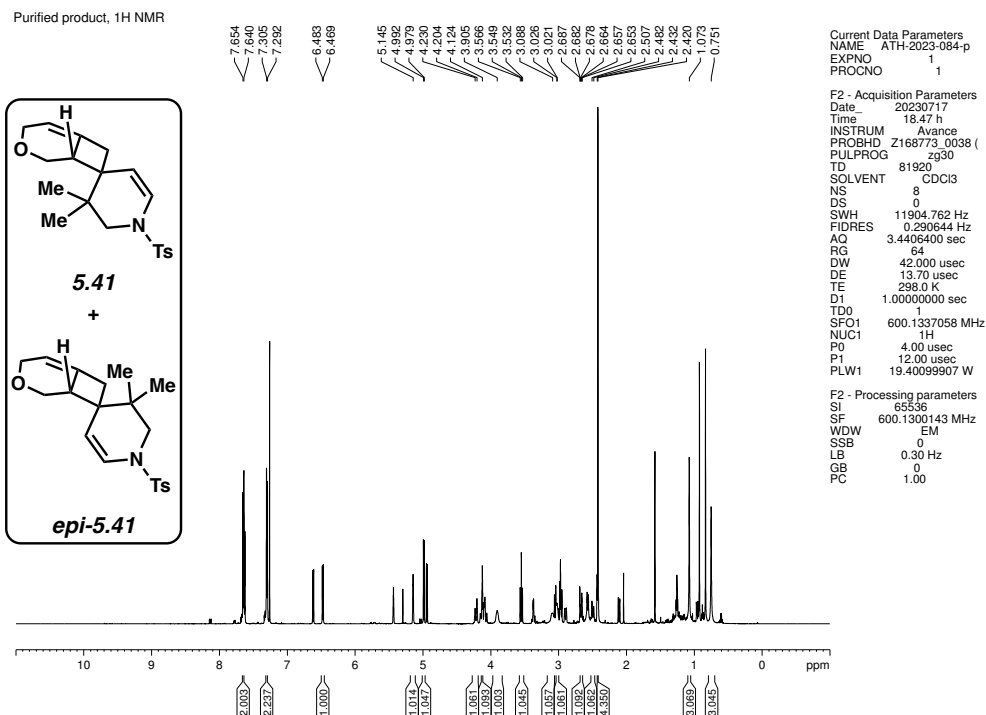


Figure 5.78. NOESY (500 MHz, CDCl₃) of compound 5.39.



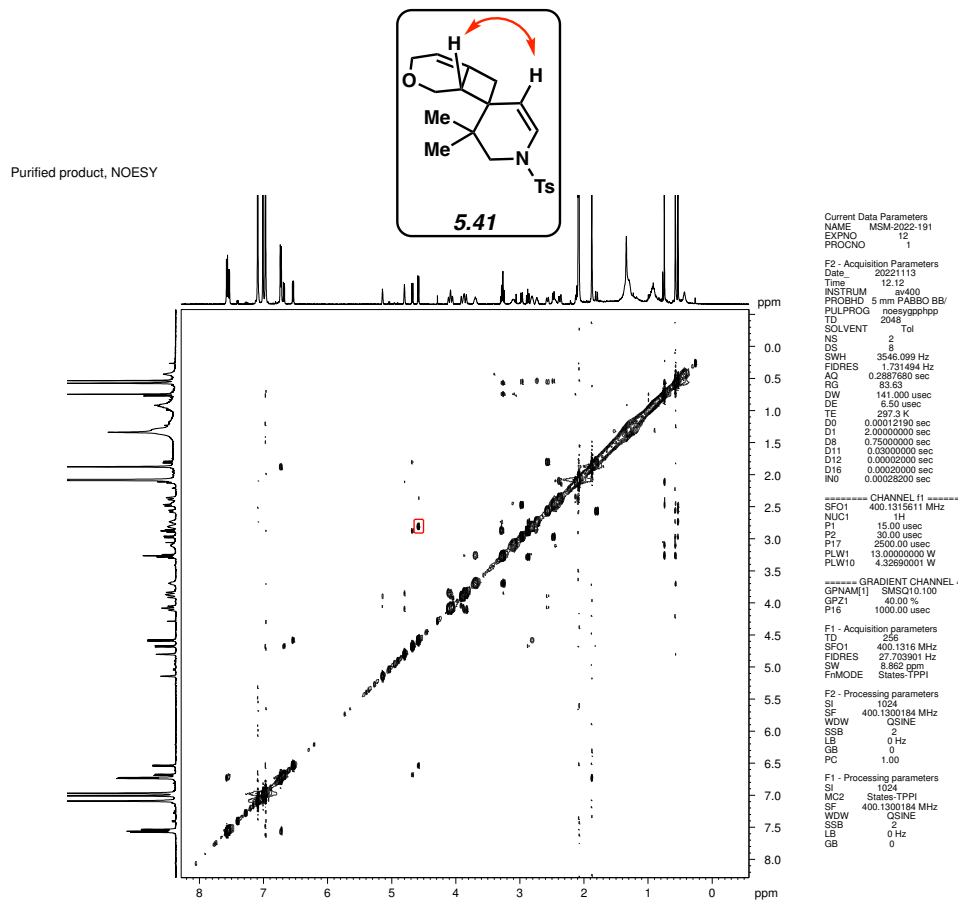


Figure 5.81. NOESY (400 MHz, toluene-d8) of compound **5.41**.

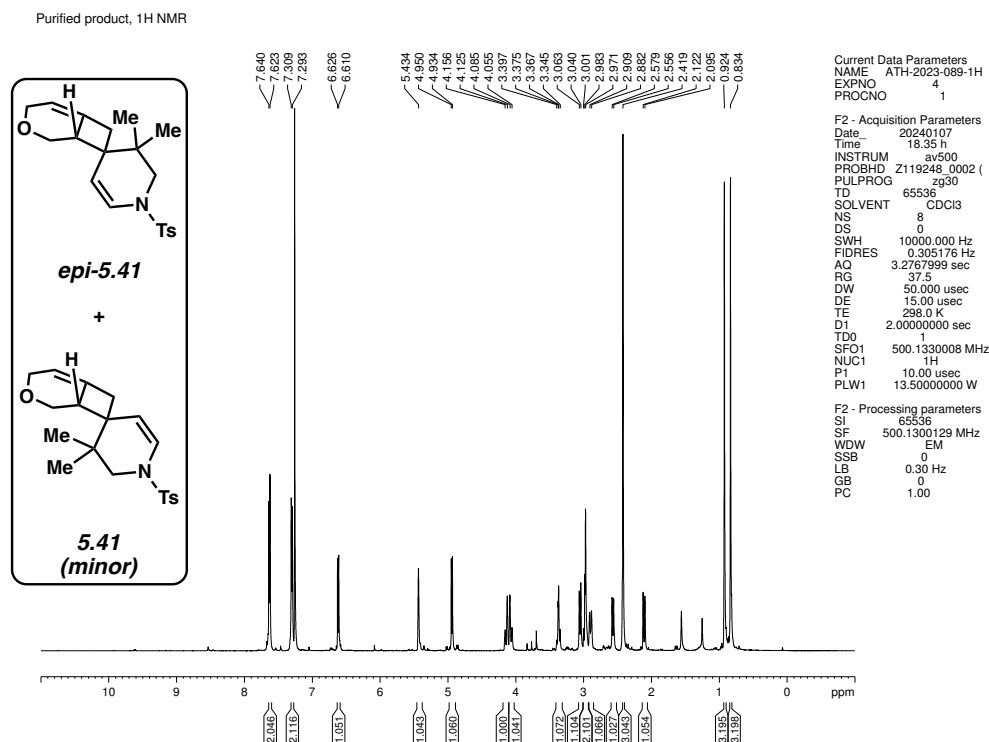


Figure 5.82. ¹H NMR (500 MHz, CDCl₃) of compound *epi*-5.41.

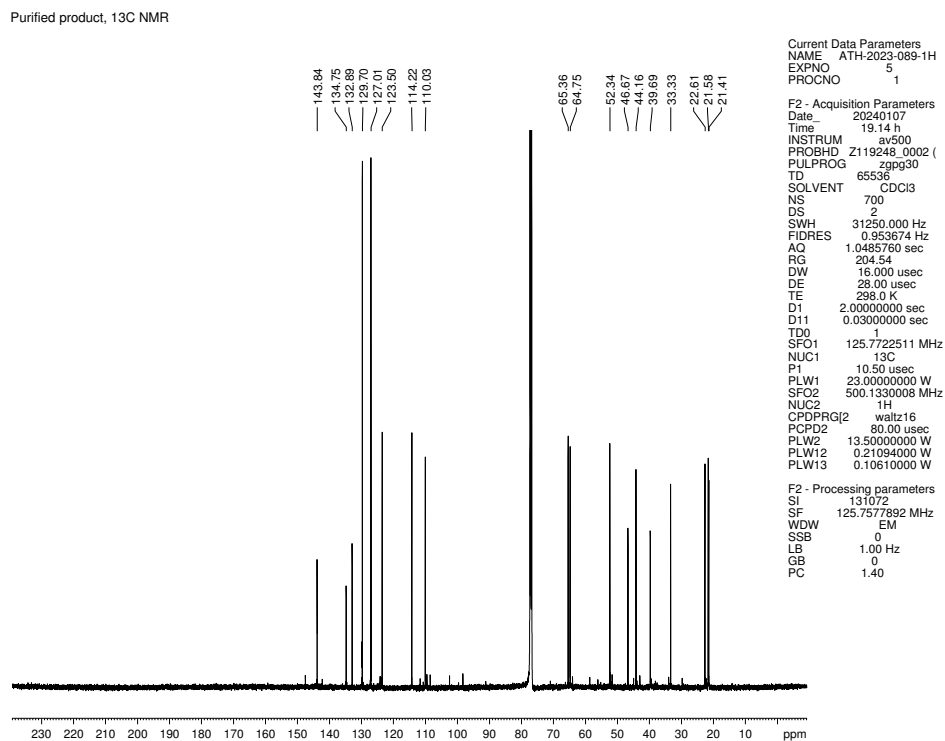


Figure 5.83. ¹³C NMR (125 MHz, CDCl₃) of compound *epi*-5.41.

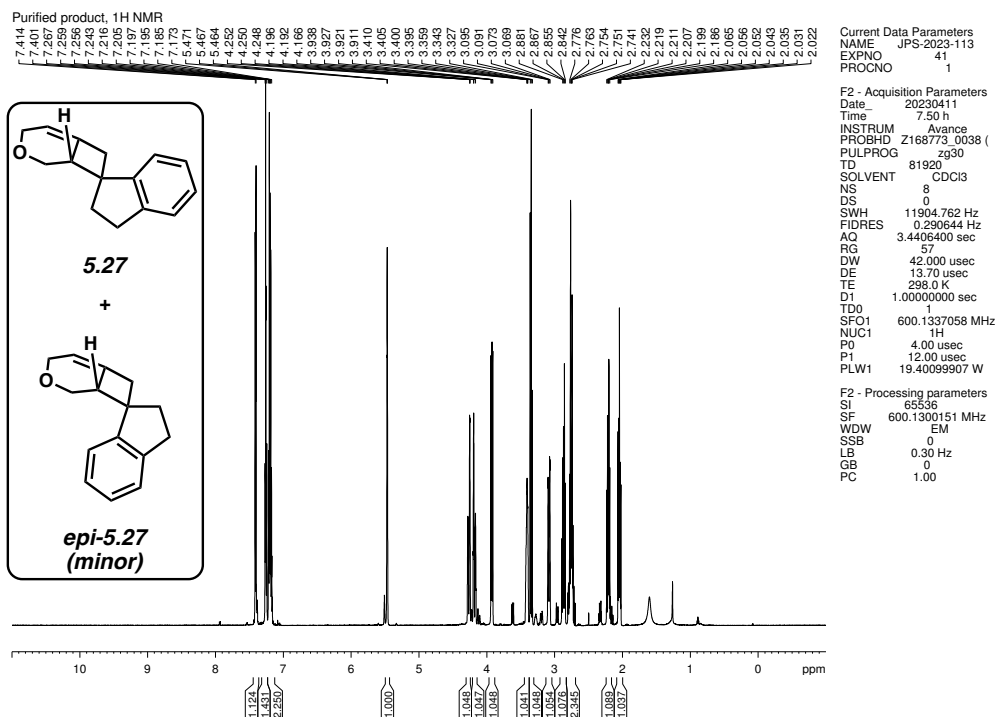


Figure 5.84. ¹H NMR (600 MHz, CDCl₃) of compound 5.27.

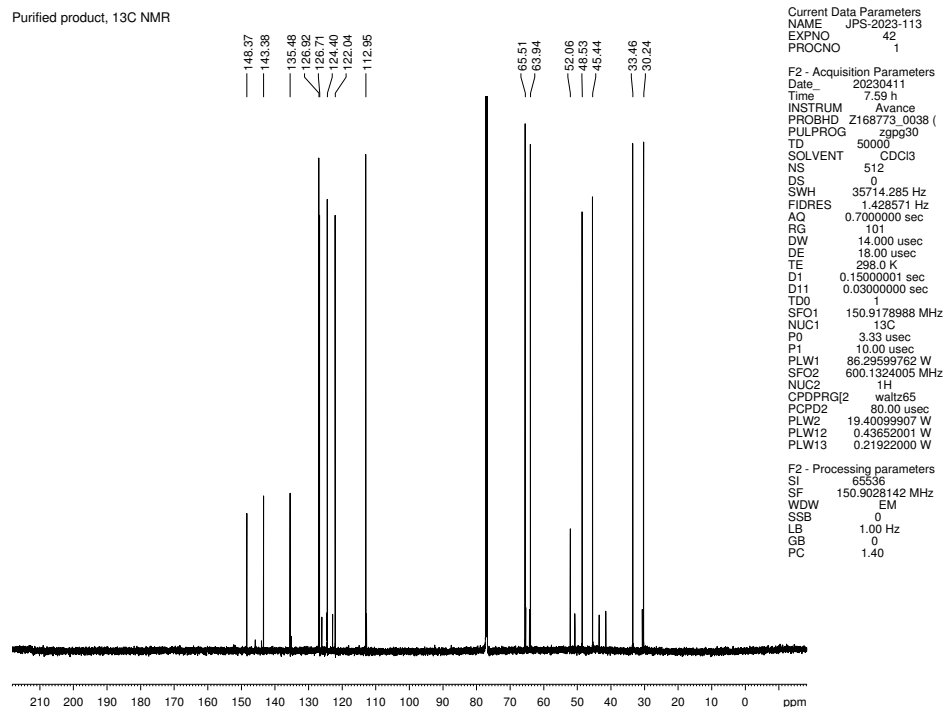


Figure 5.85. ¹³C NMR (150 MHz, CDCl₃) of compound 5.27.

Purified product, NOESY

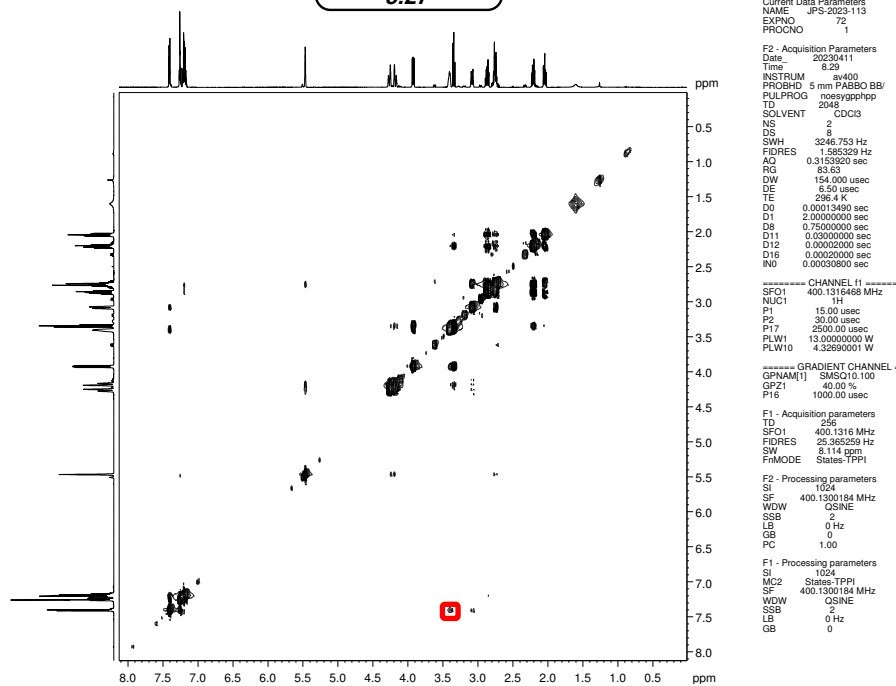
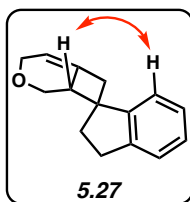


Figure 5.86. NOESY (400 MHz, CDCl_3) of compound 5.27.

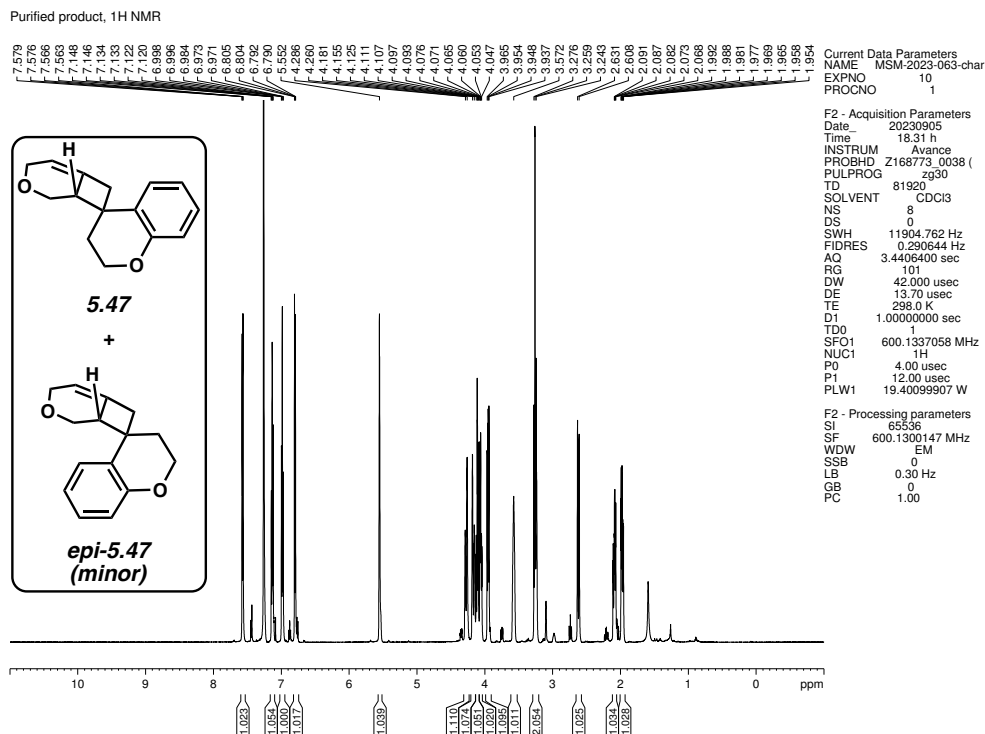


Figure 5.87. ¹H NMR (600 MHz, CDCl₃) of compound 5.47.

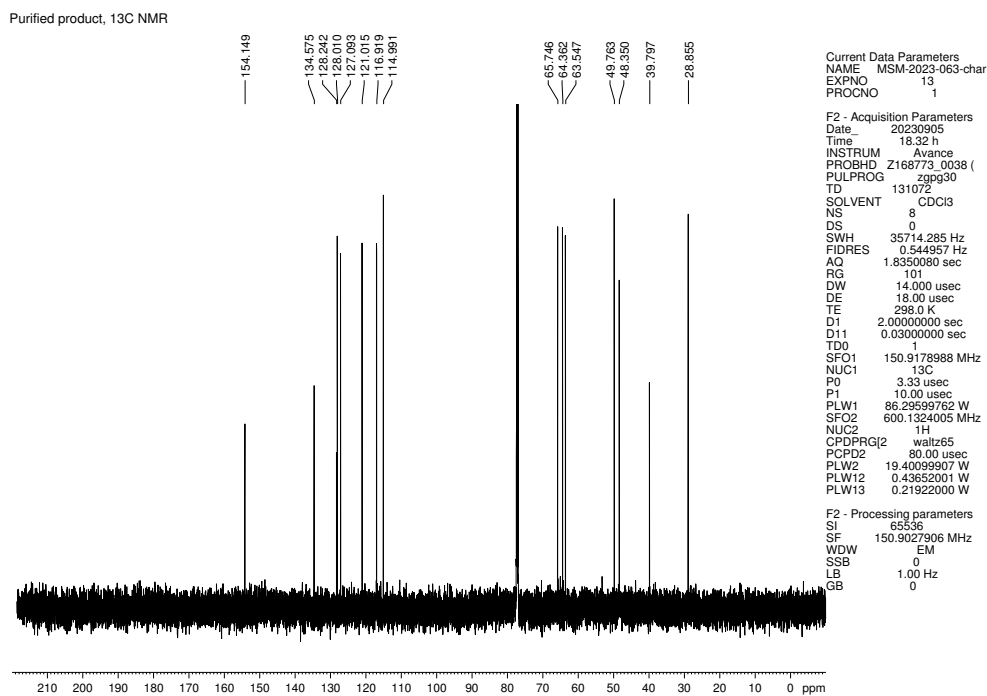


Figure 5.88. ¹³C NMR (150 MHz, CDCl₃) of compound 5.47.

Purified product, NOESY

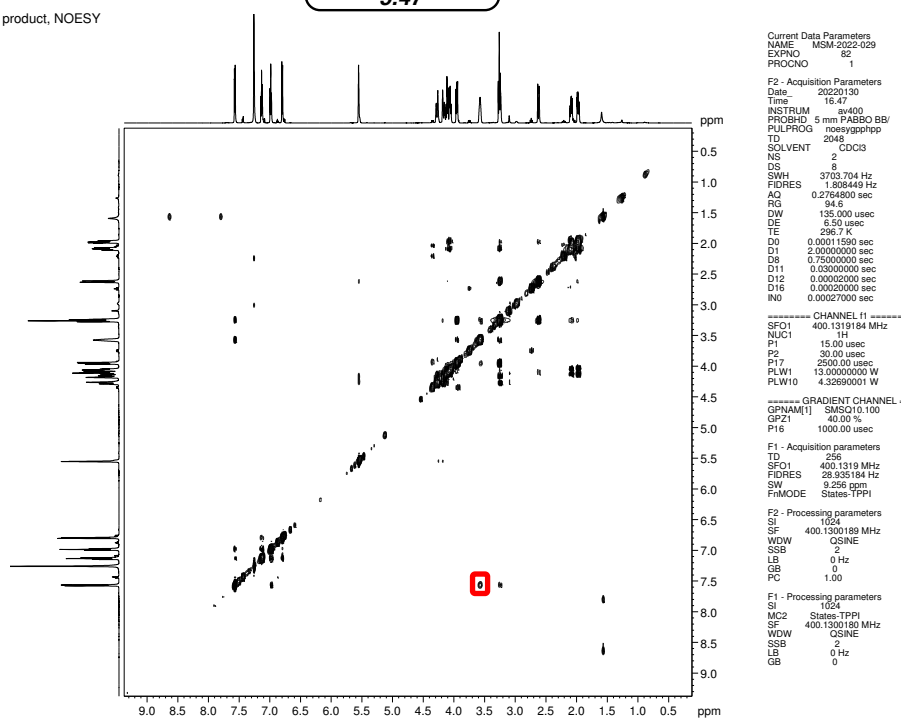
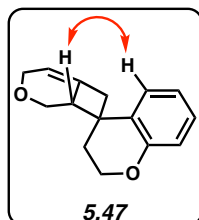


Figure 5.89. NOESY (400 MHz, CDCl₃) of compound 5.47.

Purified product, ¹H NMR

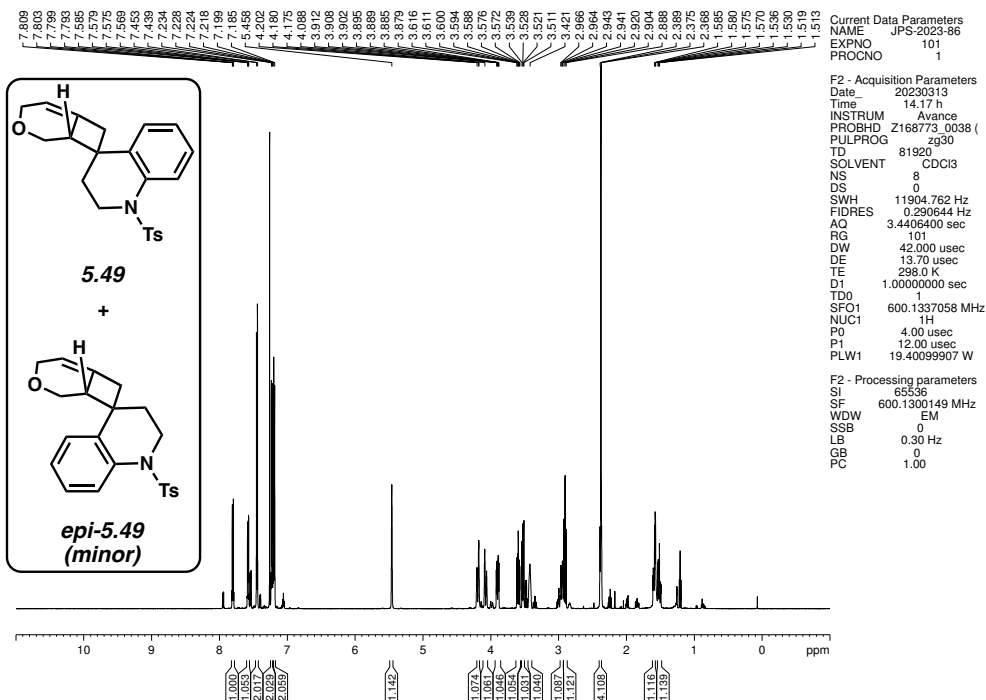


Figure 5.90. ¹H NMR (600 MHz, CDCl₃) of compound 5.49.

Purified product, ¹³C NMR

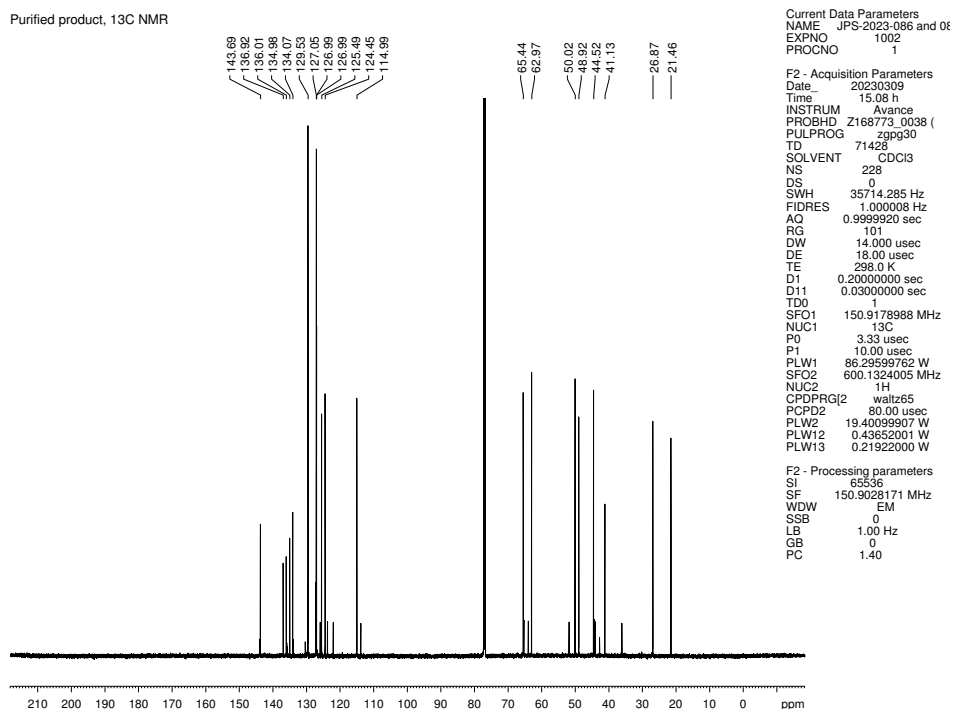


Figure 5.91. ¹³C NMR (150 MHz, CDCl₃) of compound 5.49.

Purified product, NOESY

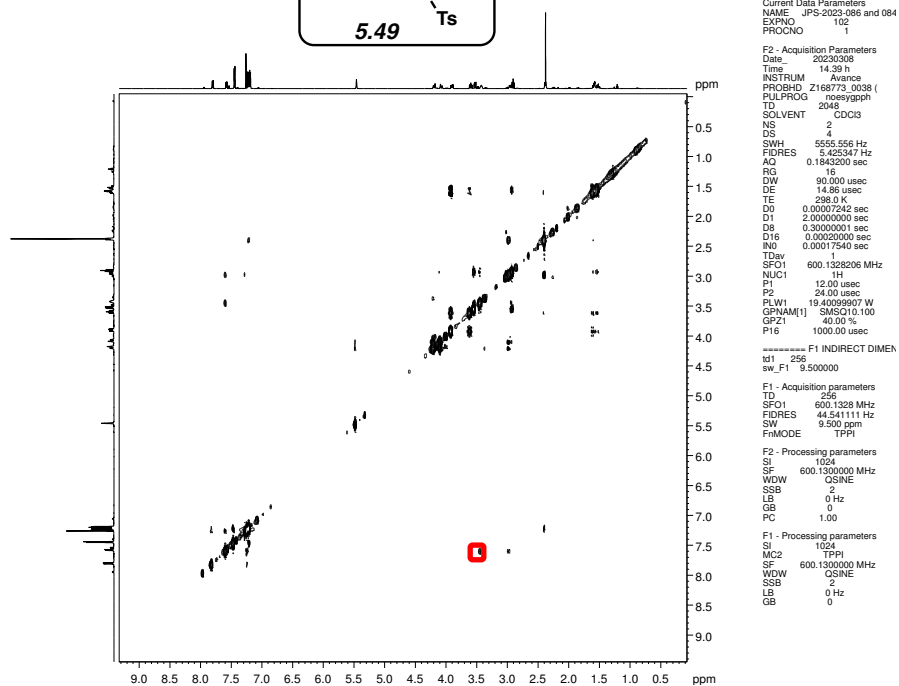
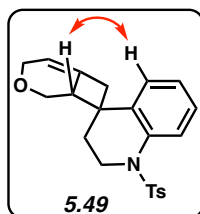


Figure 5.92. NOESY (600 MHz, CDCl₃) of compound 5.49.

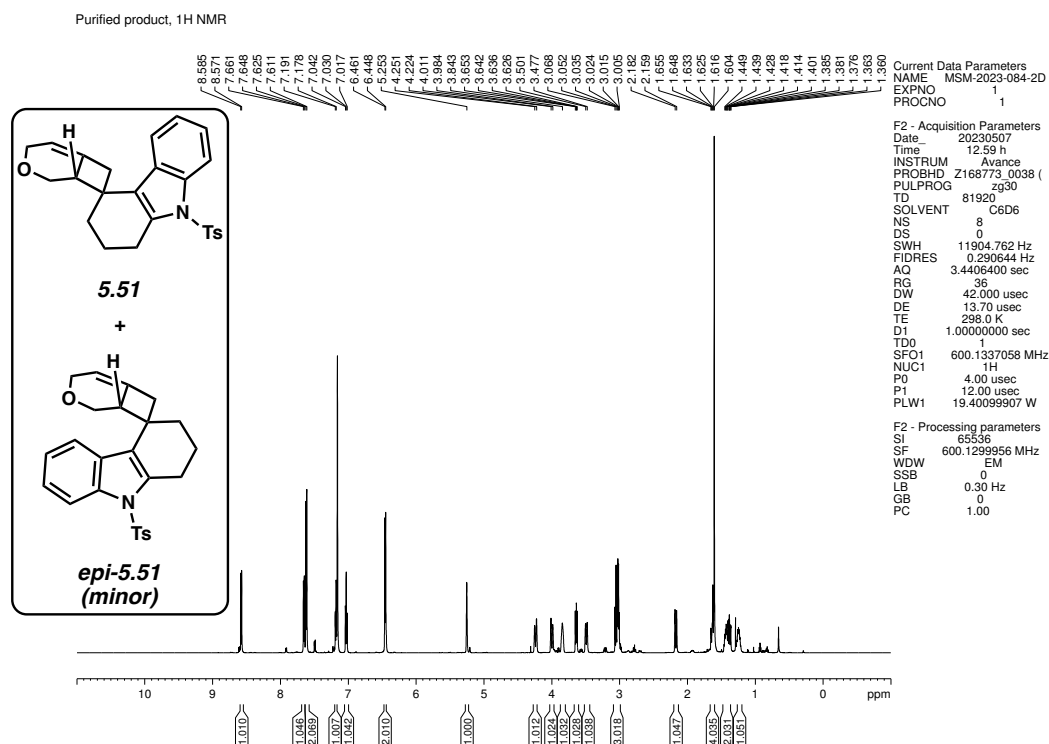


Figure 5.93. ^1H NMR (600 MHz, C_6D_6) of compound **5.51**.

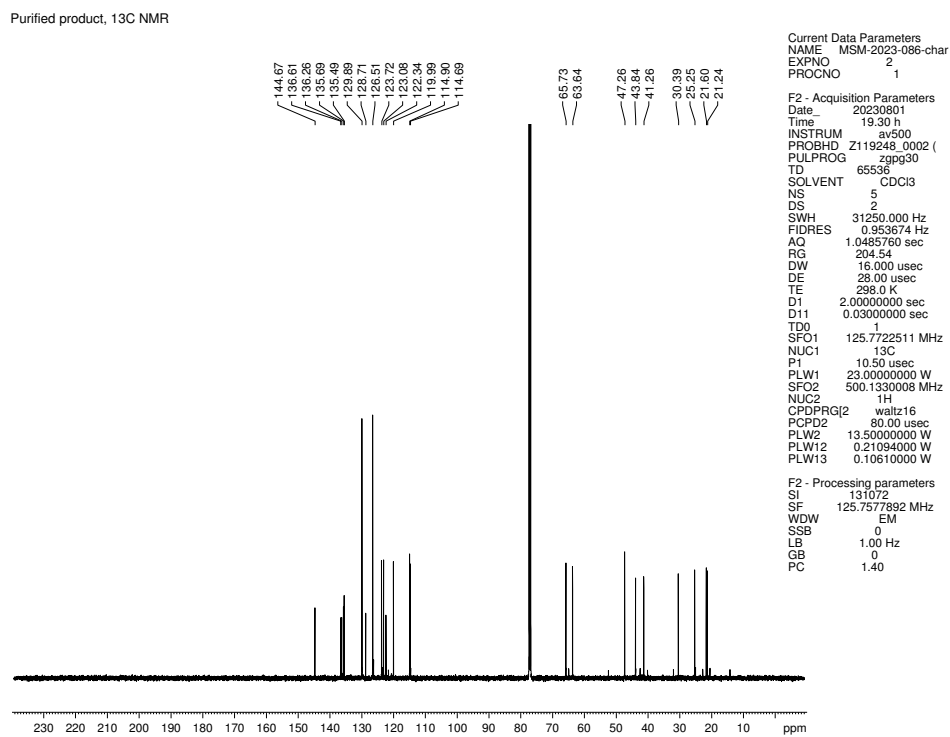


Figure 5.94. ^{13}C NMR (125 MHz, CDCl_3) of compound **5.51**.

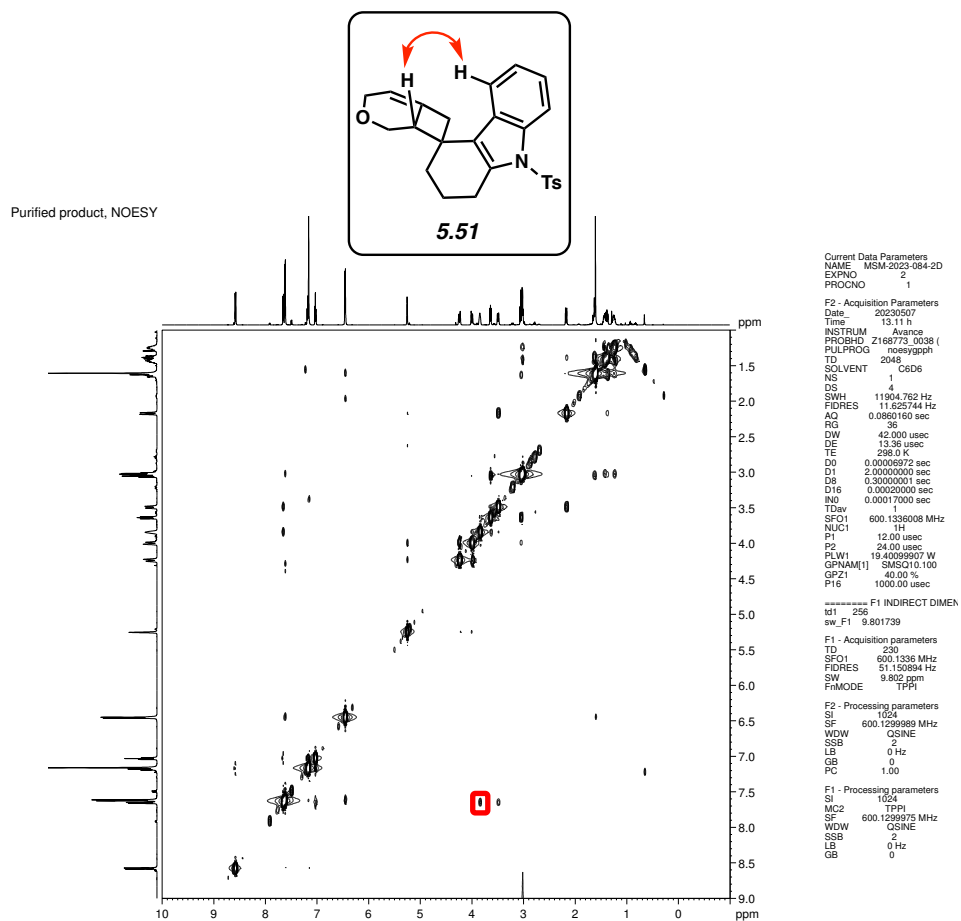


Figure 5.95. NOESY (600 MHz, C₆D₆) of compound **5.51**.

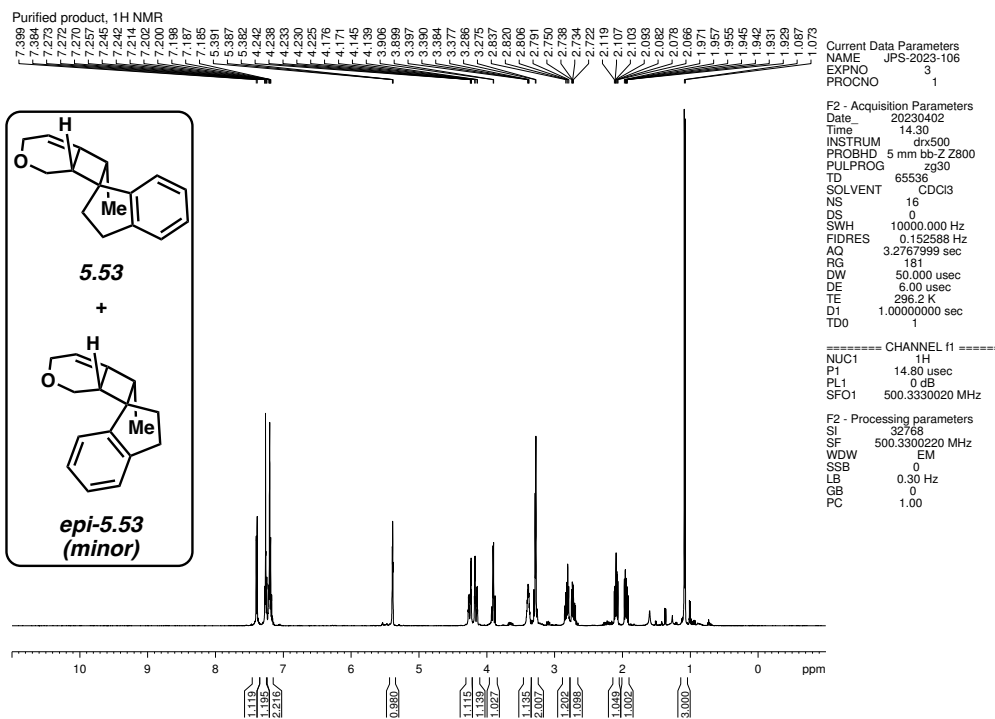


Figure 5.96. ¹H NMR (500 MHz, CDCl₃) of compound 5.53.

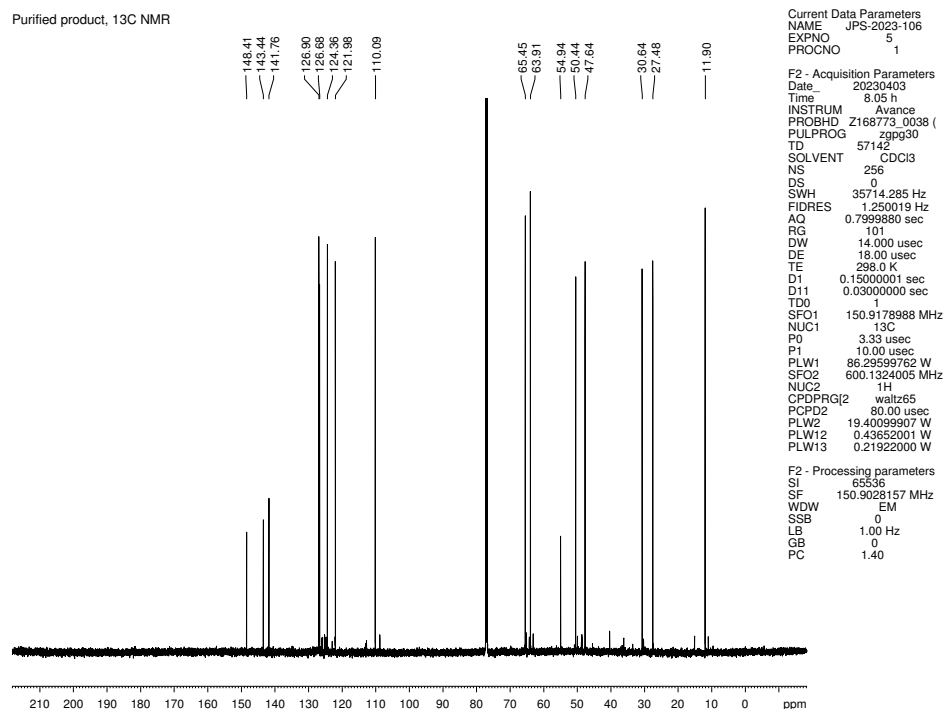


Figure 5.97. ¹³C NMR (150 MHz, CDCl₃) of compound 5.53.

Purified product, NOESY

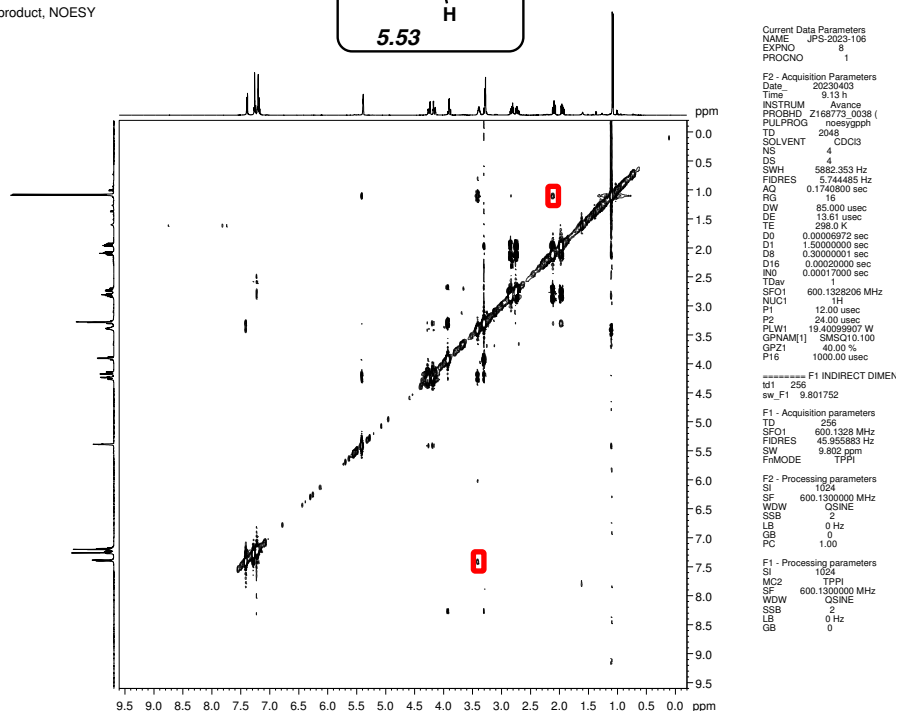
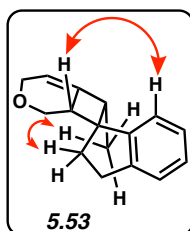


Figure 5.98. NOESY (600 MHz, CDCl₃) of compound 5.53.

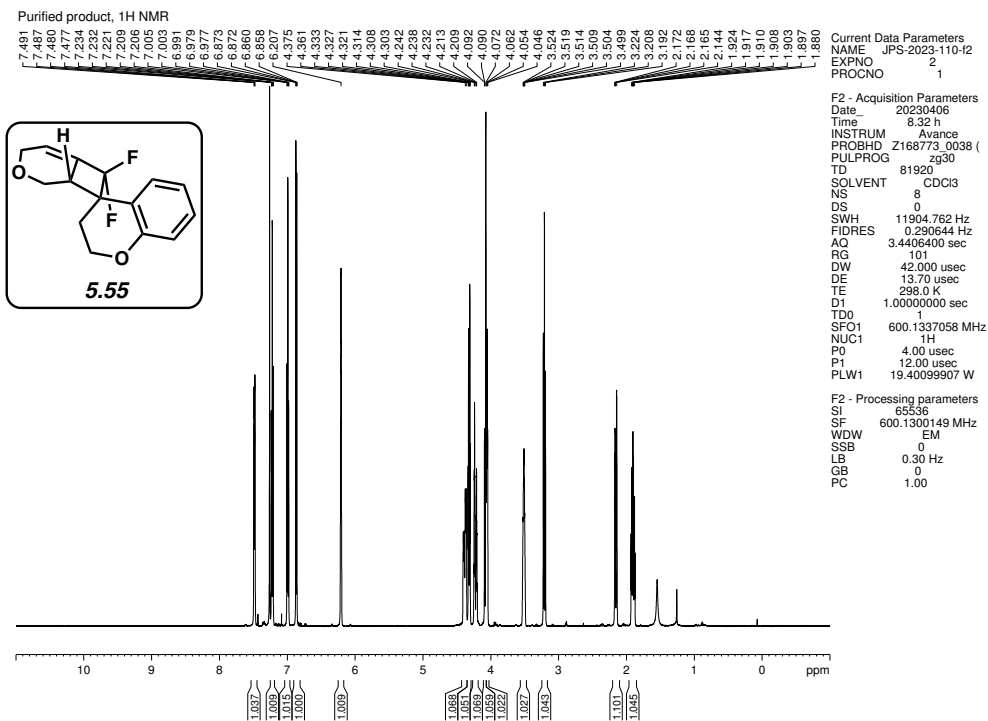


Figure 5.99. ¹H NMR (600 MHz, CDCl₃) of compound 5.55.

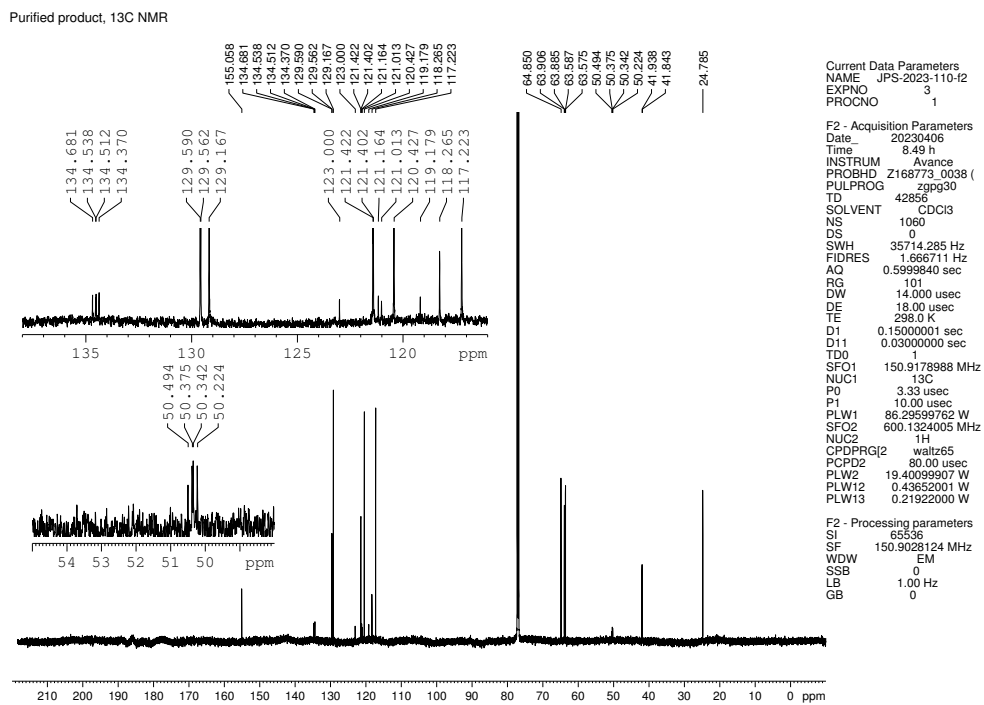
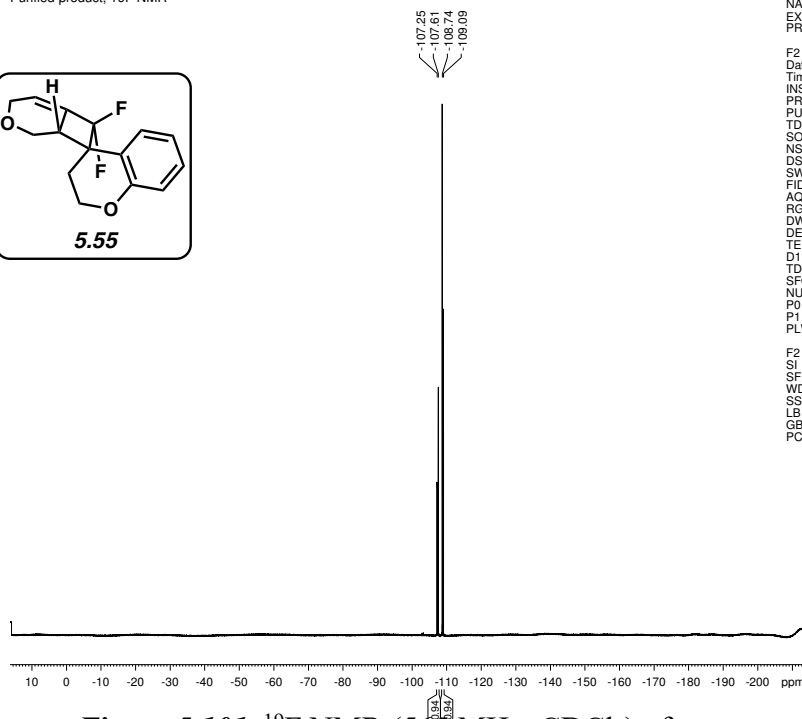
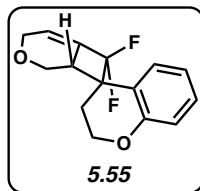


Figure 5.100. ¹³C NMR (150 MHz, CDCl₃) of compound 5.55.

Purified product, ^{19}F NMR



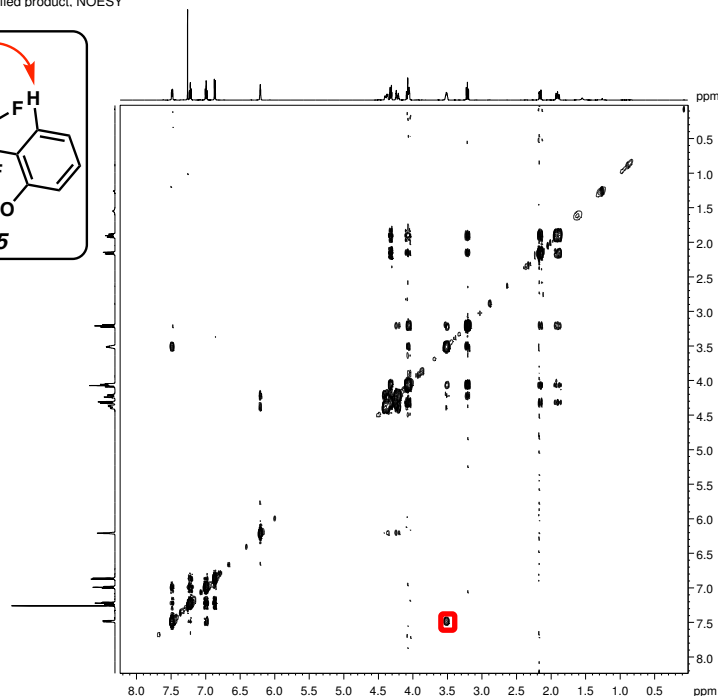
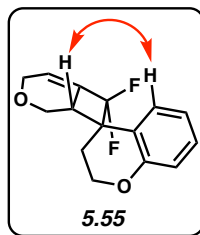
Current Data Parameters
NAME F2
EXPNO 4
PROCNO 1

F2 - Acquisition Parameters
Date_ 20230406
Time 8.51 h
INSTRUM Avance
PROBHD Z168773_0038 (PULPROG zg30
TD 131072
SOLVENT CDCl3
NS 8
DS 0
SWH 131578.953 Hz
FIDRES 2.007735 Hz
AQ 0.4980736 sec
RG 16
DW 3.800 usec
DE 18.00 usec
TE 298.0 K
D1 1.00000000 sec
TD0 1
SFO1 564.6299196 MHz
NUC1 ^{19}F
FO 5.00 usec
P1 15.00 usec
PLW1 19.79999924 W

F2 - Processing parameters
SI 131072
SF 564.6863882 MHz
WDW EM
SSB 0
LB 2.00 Hz
GB 0
PC 1.00

Figure 5.101. ^{19}F NMR (565 MHz, CDCl_3) of compound 5.55.

Purified product, NOESY



Current Data Parameters
NAME F2
EXPNO 42
PROCNO 1

F2 - Acquisition Parameters
Date_ 20230406
Time 11.25
INSTRUM av400
PROBHD 5 mm PABBO BB
PULPROG noesypphpp
TD 2048
SOLVENT 2 CDCl3
NS 8
DS 8
SWH 3289.474 Hz
FIDRES 1.698188 Hz
AQ 0.3112960 sec
RG 67.78
DW 152.000 usec
DE 6.50 usec
TE 297.0 K
D0 0.00015290 sec
D1 2.00000000 sec
D8 0.75000000 sec
D11 0.03000000 sec
D12 0.00020000 sec
D16 0.00020000 sec
RG 0.00029400 sec

----- CHANNEL f1 -----
SFO1 400.1316698 MHz
NUC1 ^1H
P1 15.00 usec
P2 30.00 usec
P17 2500.00 usec
PLW1 13.00000000 W
PLW10 4.32690001 W

----- GRADIENT CHANNEL -----
GPNAM(f1) SACSQ10.100
GPZ1 40.00 %
P16 1000.00 usec

F1 - Acquisition parameters
TD 256
SFO1 400.1317 MHz
FIDRES 23.698013 Hz
SW 8.221 ppm
FMODE States-TPPI

F2 - Processing parameters
SI 1024
SF 400.1300184 MHz
WDW CSINE
SSB 2
LB 0 Hz
GB 0
PC 1.00

F1 - Processing parameters
SI 1024
MC2 States-TPPI
SF 400.1300184 MHz
WDW CSINE
SSB 2
LB 0 Hz
GB 0

Figure 5.102. NOESY (400 MHz, CDCl_3) of compound 5.55.

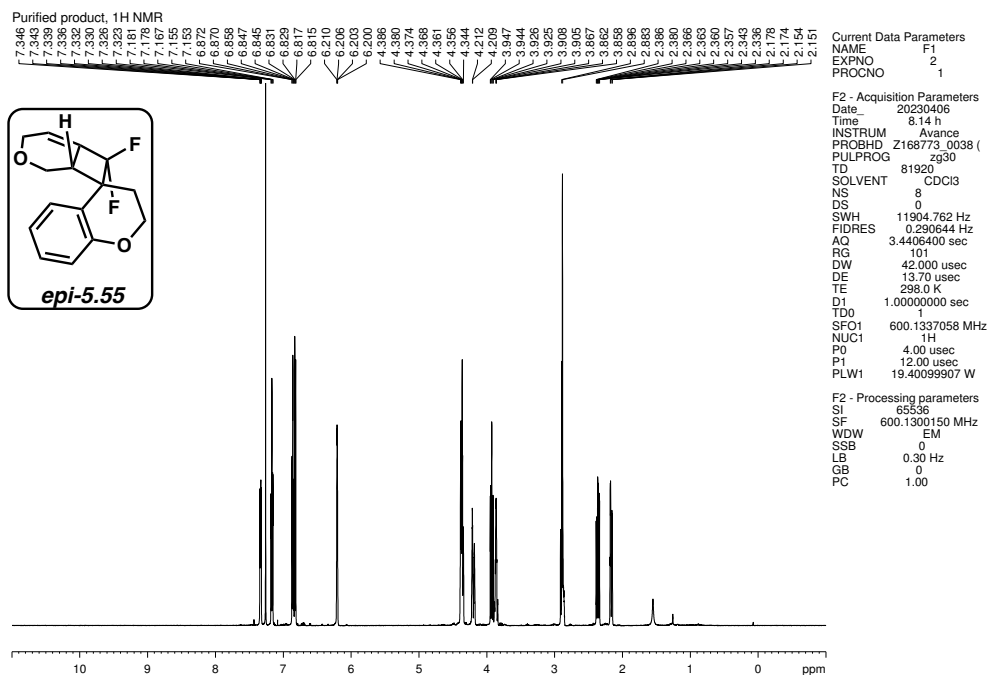


Figure 5.103. ¹H NMR (600 MHz, CDCl₃) of compound *epi-5.55*.

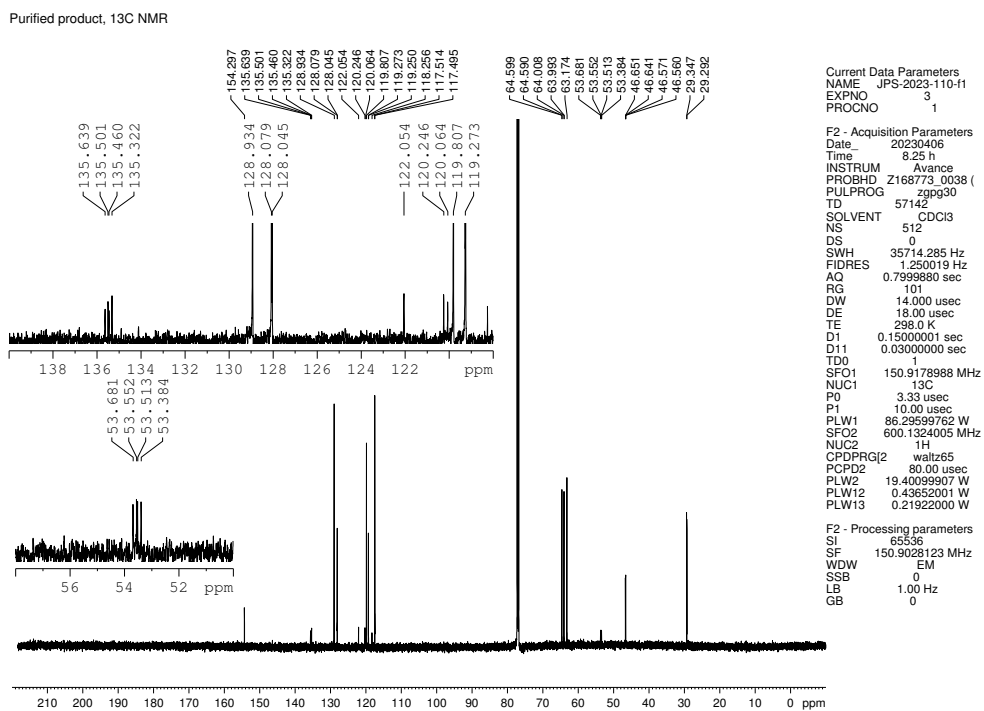


Figure 5.104. ¹³C NMR (150 MHz, CDCl₃) of compound *epi-5.55*.

Purified product, ^{19}F NMR

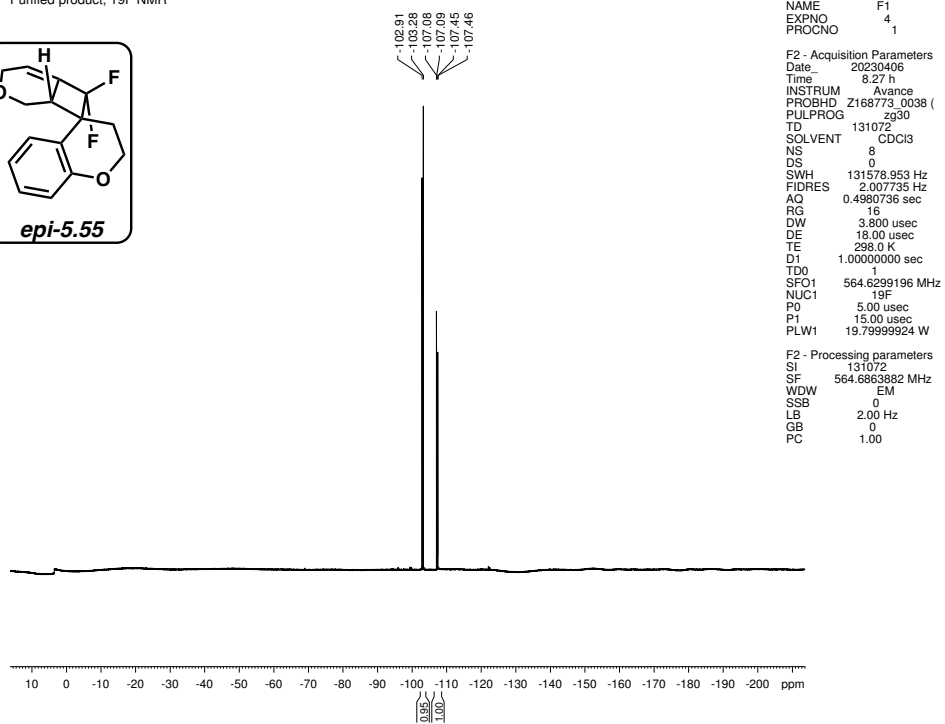
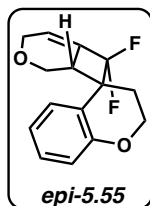


Figure 5.105. ^{19}F NMR (565 MHz, CDCl_3) of compound *epi-5.55*.

Purified product, ¹H NMR

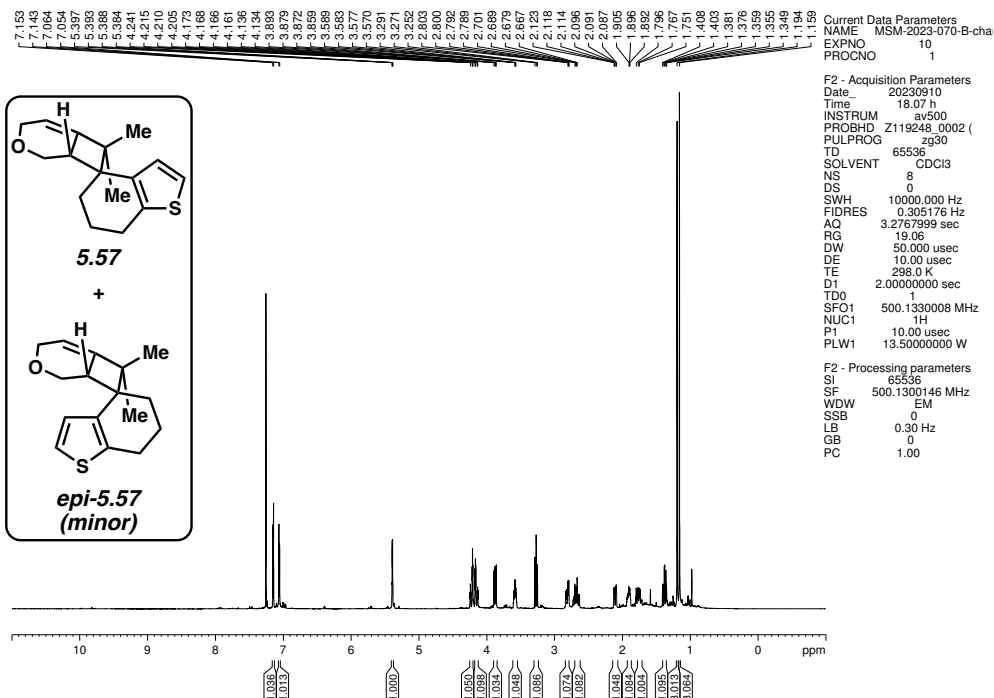


Figure 5.106. ¹H NMR (500 MHz, CDCl₃) of compound 5.57.

Purified product, ¹³C NMR

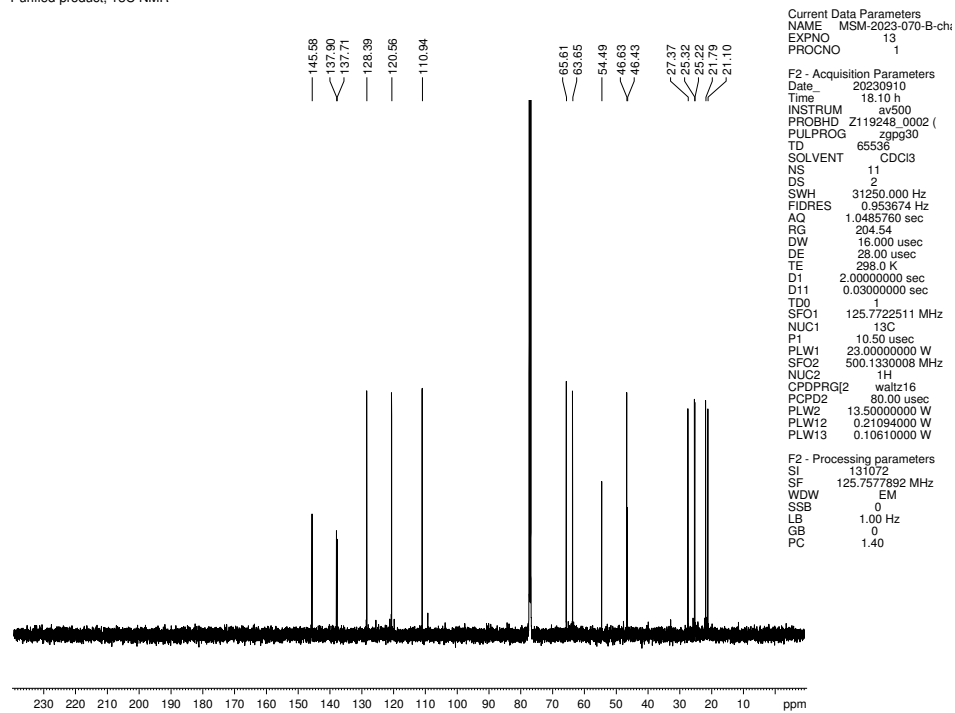


Figure 5.107. ¹³C NMR (150 MHz, CDCl₃) of compound 5.57.

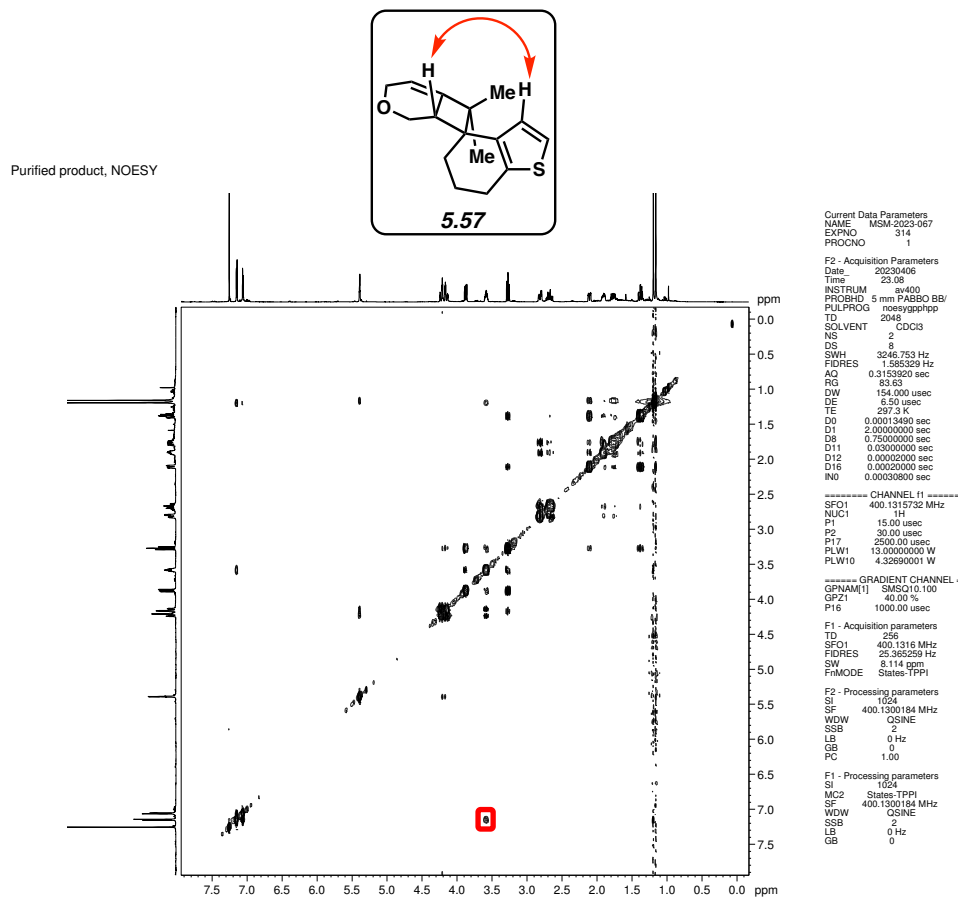


Figure 5.108. NOESY (400 MHz, CDCl₃) of compound **5.57**.

Purified product, ¹H NMR

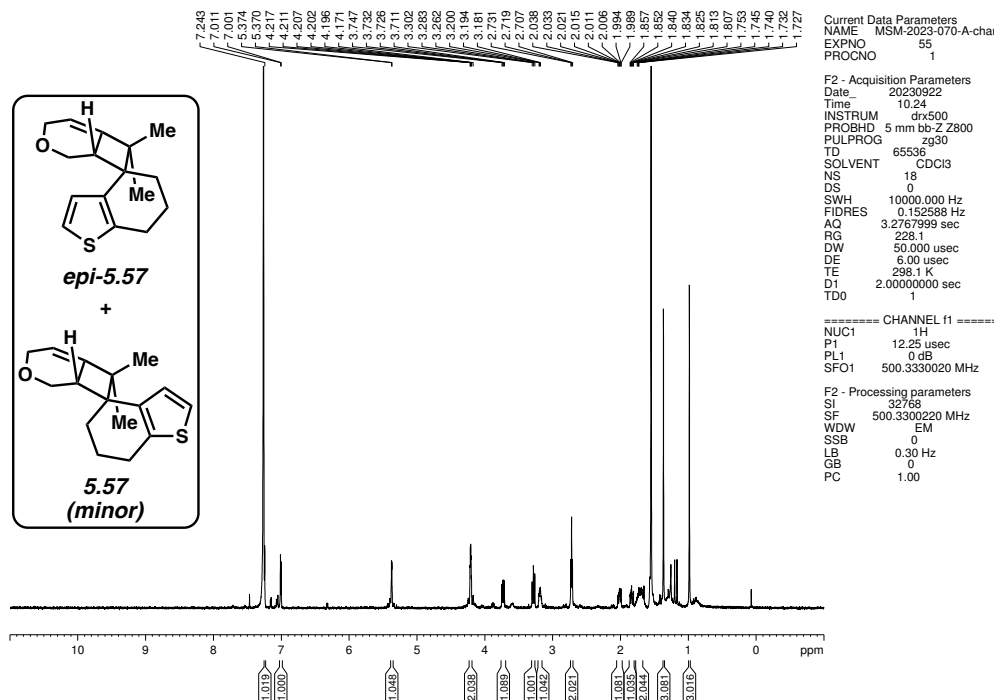


Figure 5.109. ¹H NMR (500 MHz, CDCl₃) of compound *epi*-5.57.

Purified product, ¹³C NMR

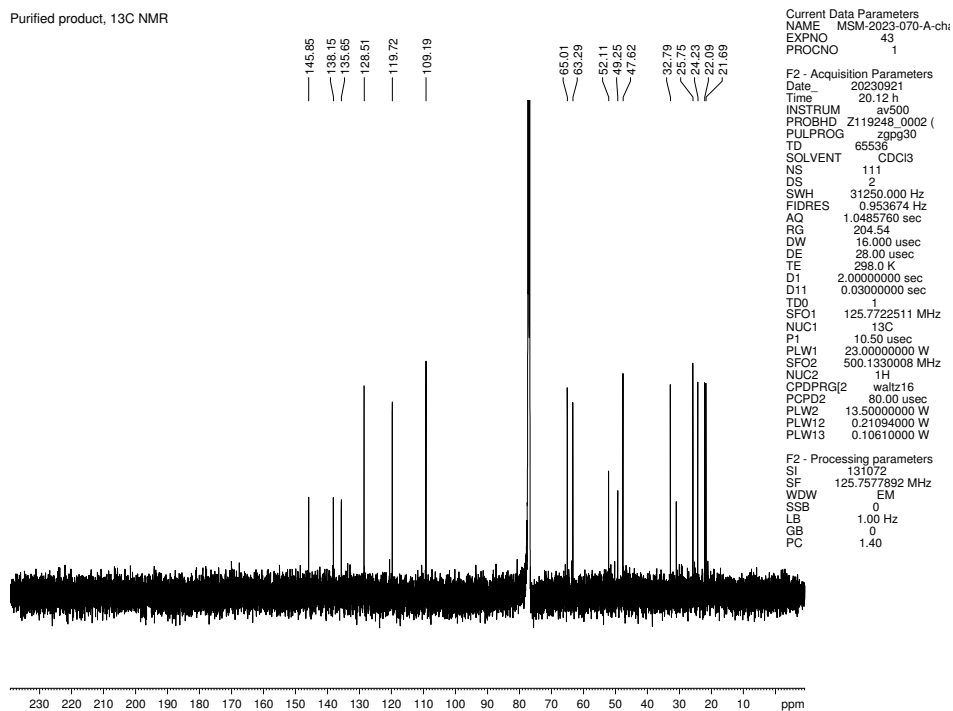


Figure 5.110. ¹³C NMR (125 MHz, CDCl₃) of compound *epi*-5.57.

Purified product, ¹H NMR

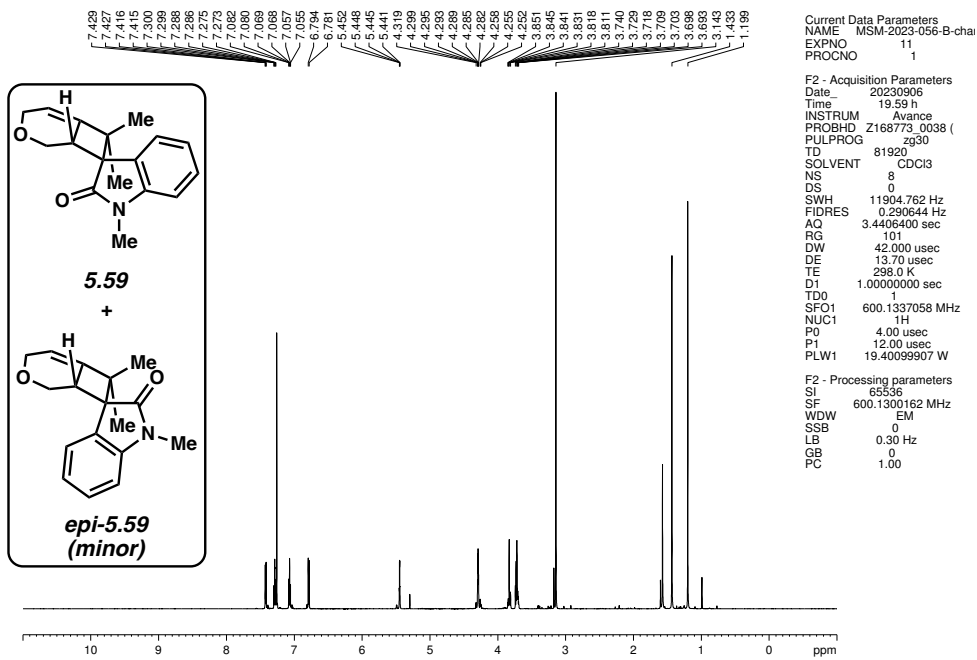


Figure 5.111. ¹H NMR (600 MHz, CDCl₃) of compound 5.59.

Purified product, ¹³C NMR

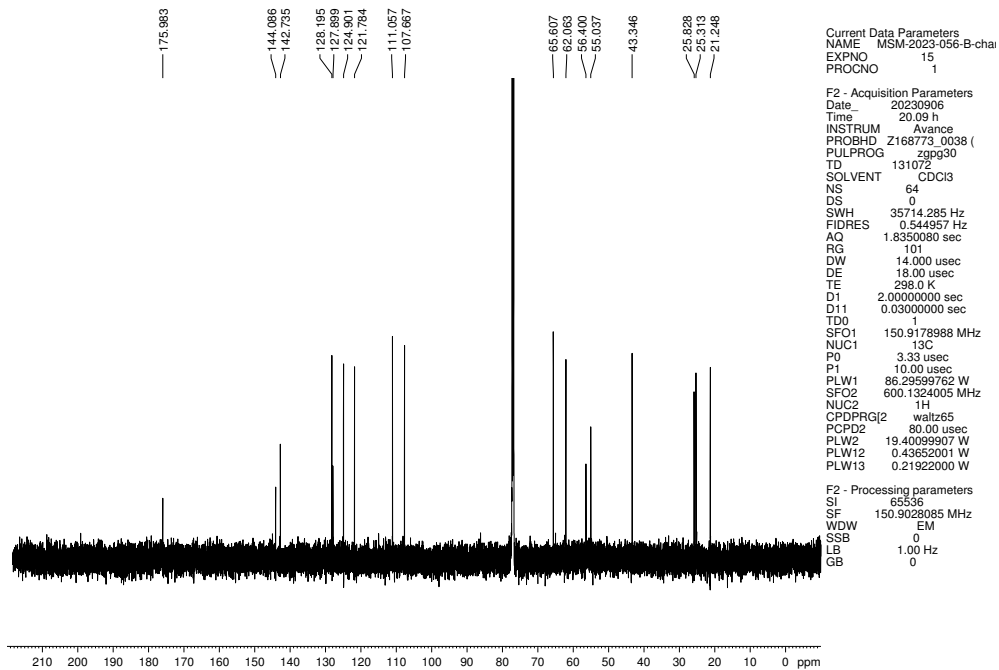
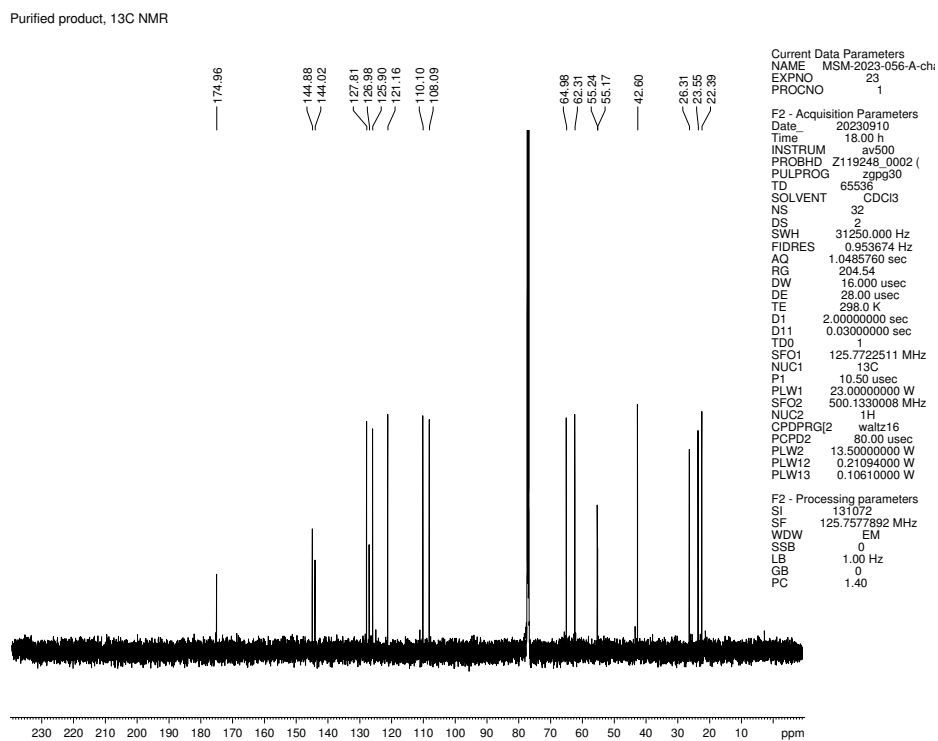
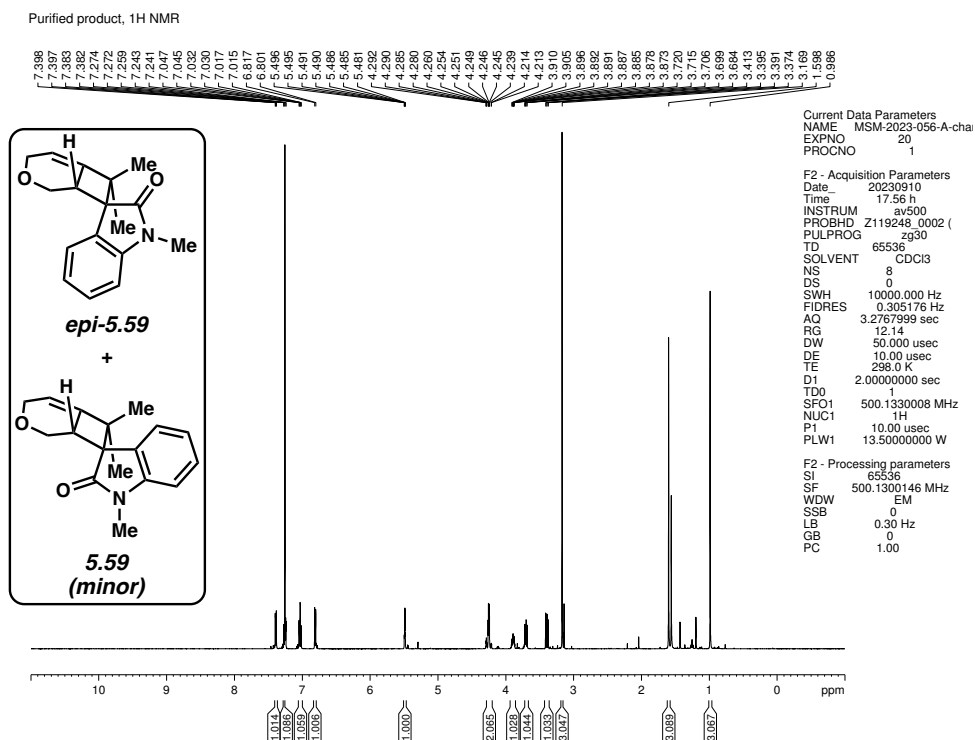


Figure 5.112. ¹³C NMR (150 MHz, CDCl₃) of compound 5.59.



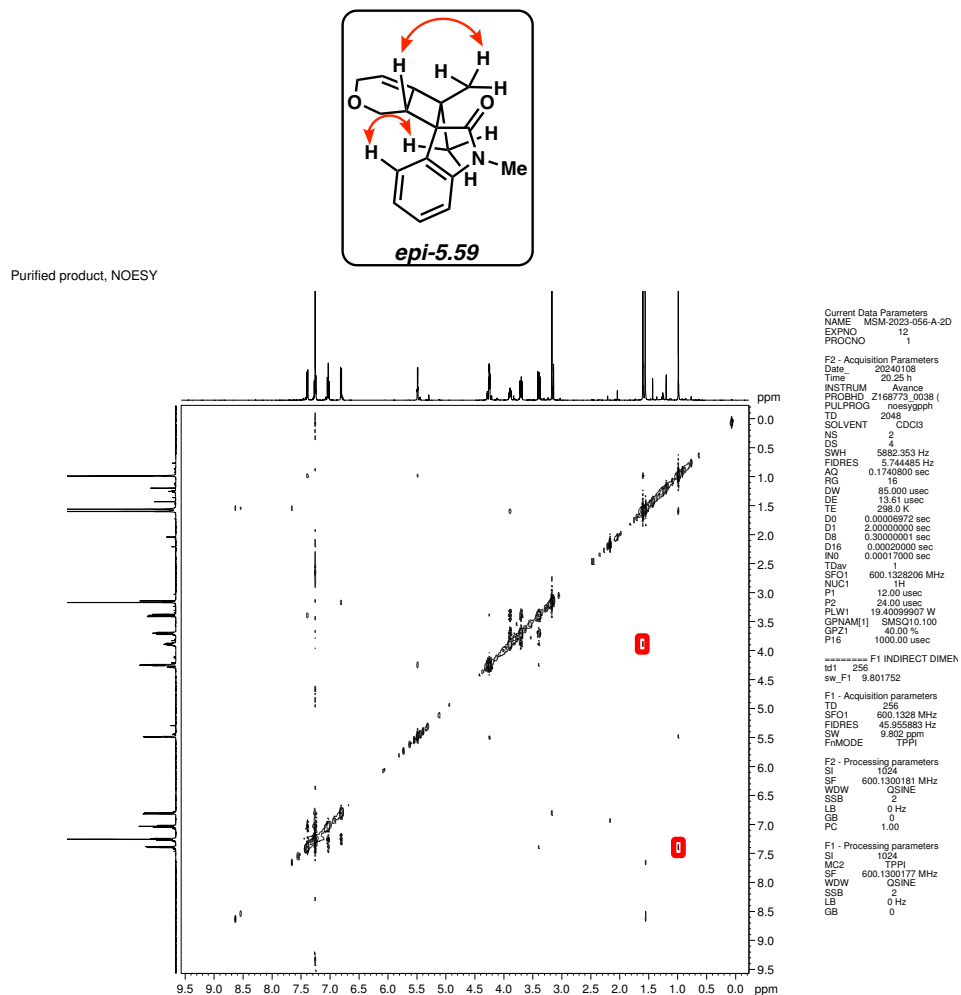


Figure 5.115. NOESY (600 MHz, CDCl₃) of compound *epi-5.59*.

Purified product, ¹H NMR

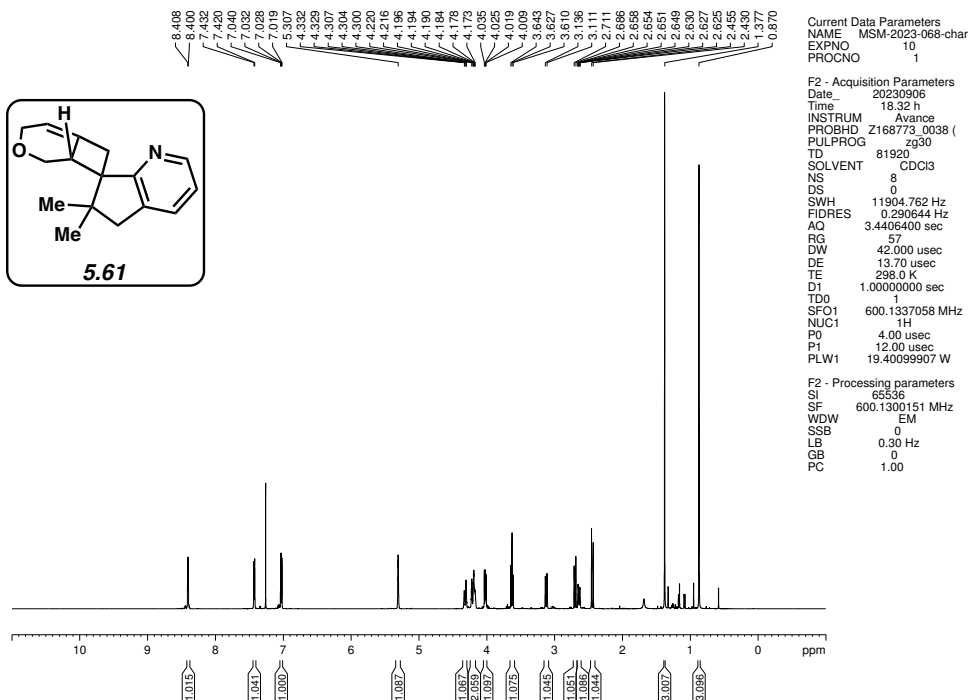


Figure 5.116. ¹H NMR (600 MHz, CDCl₃) of compound 5.61.

Purified product, ¹³C NMR

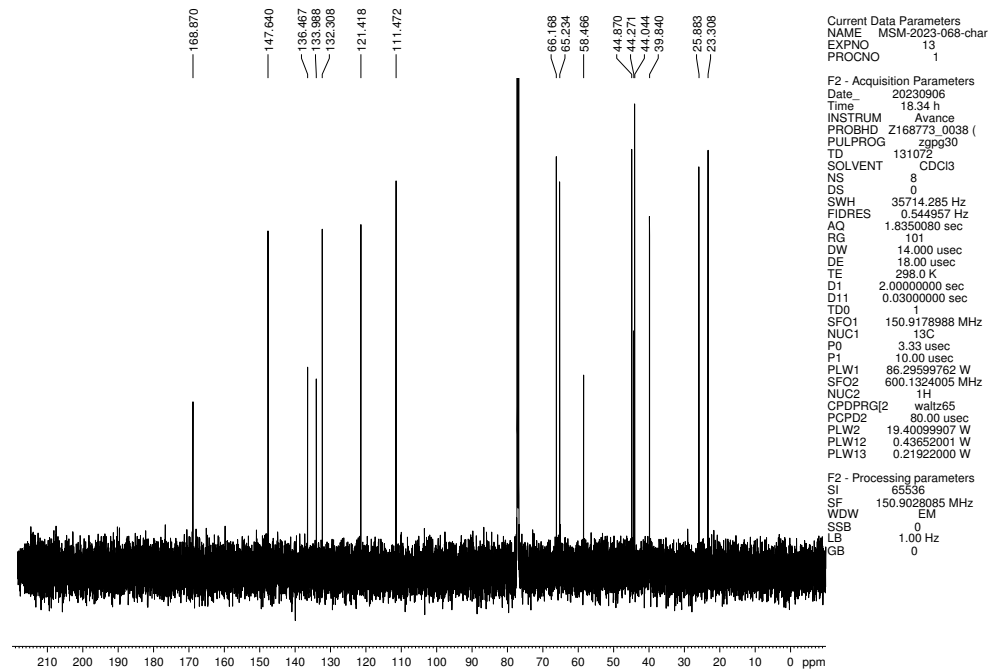
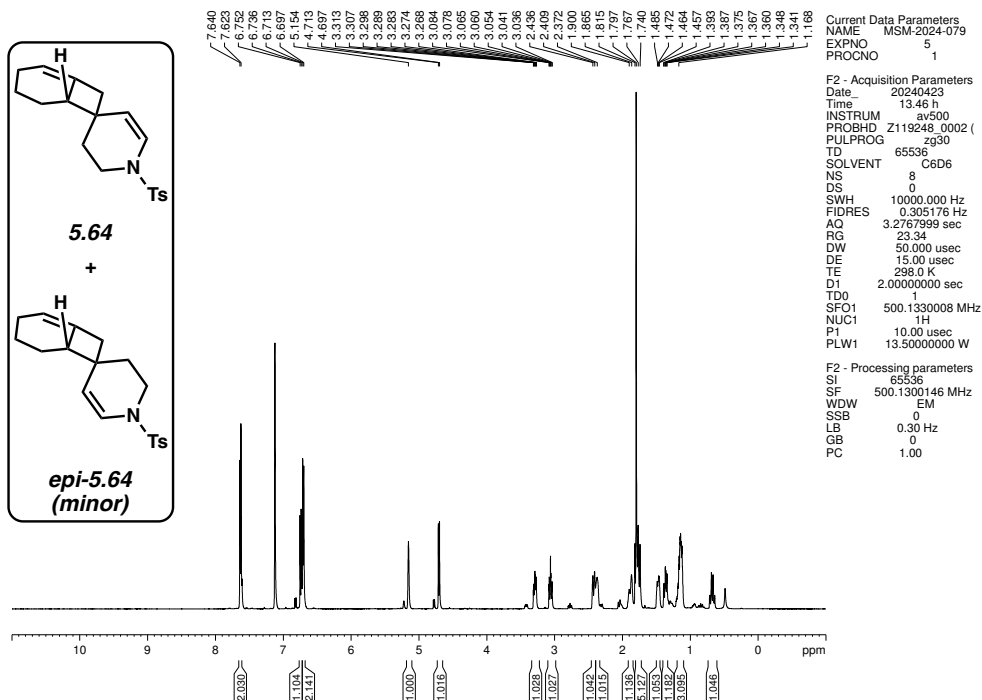
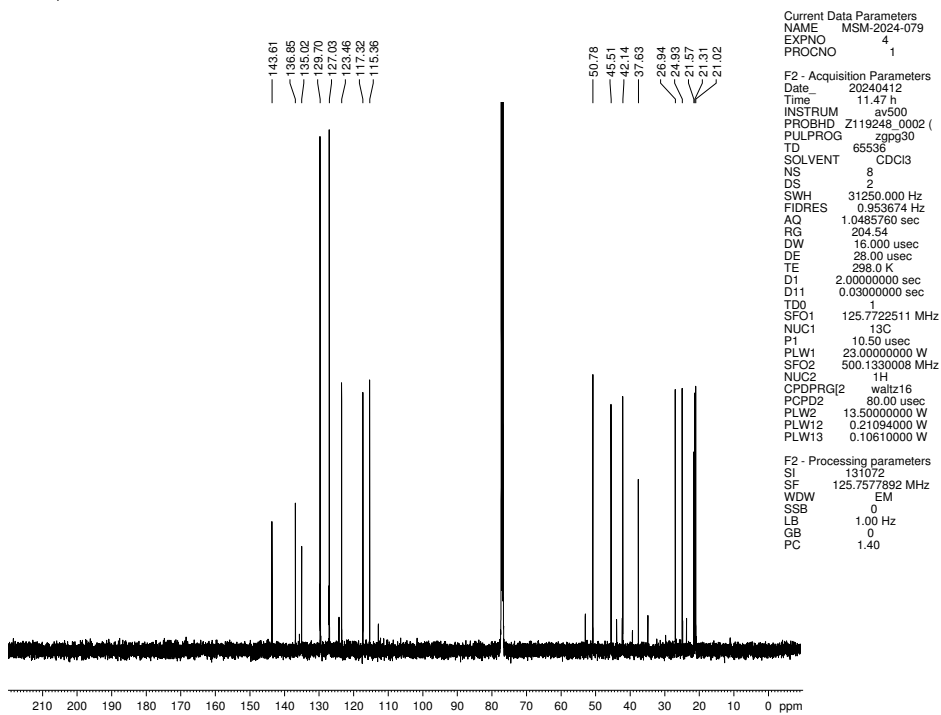


Figure 5.117. ¹³C NMR (150 MHz, CDCl₃) of compound 5.61.

Purified product, ¹H NMR



Purified product, ¹³C NMR



Purified product, NOESY

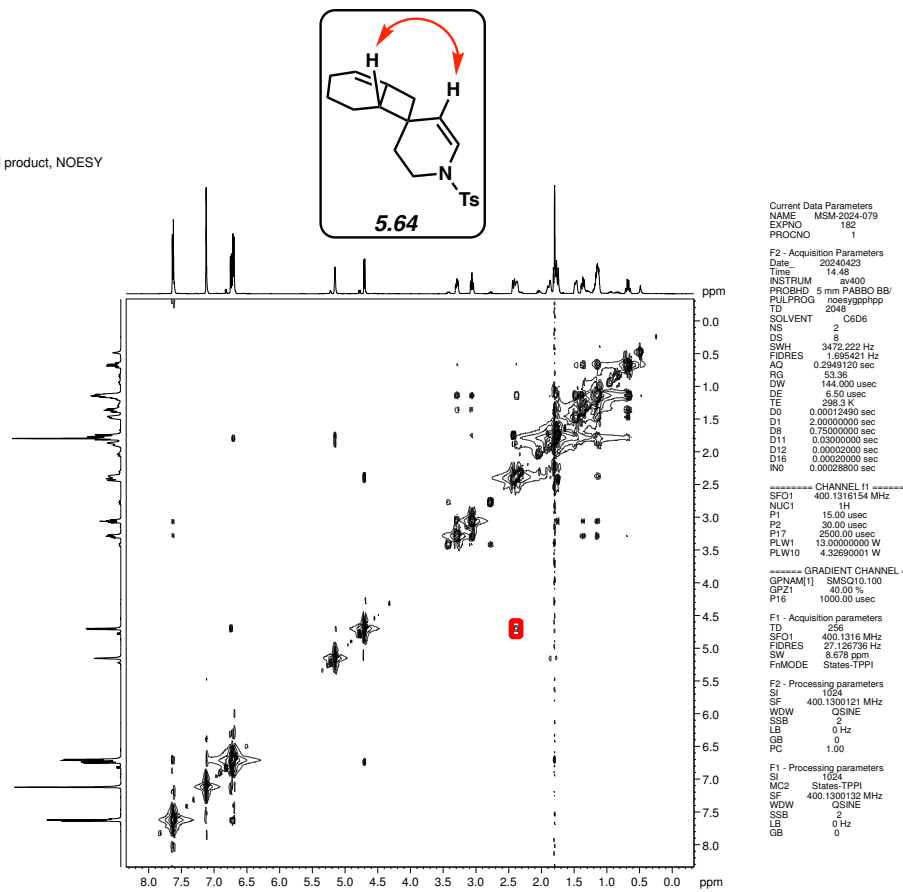


Figure 5.120. NOESY (400 MHz, CDCl₃) of compound 5.64.

Purified product, ¹H NMR

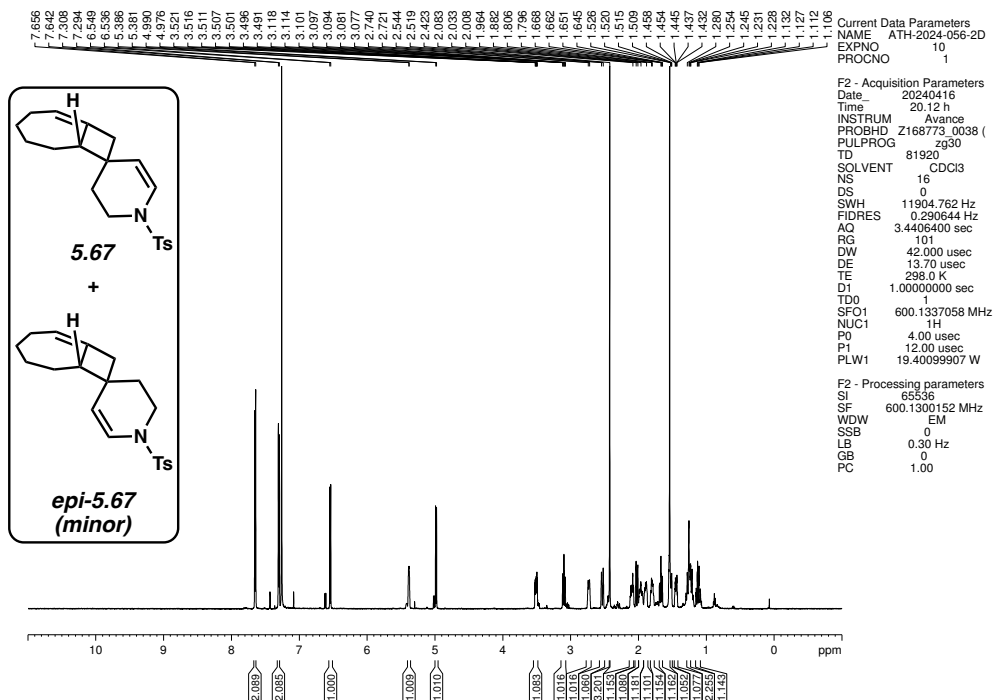


Figure 5.121. ¹H NMR (600 MHz, CDCl₃) of compound 5.67.

Purified product, ¹³C NMR

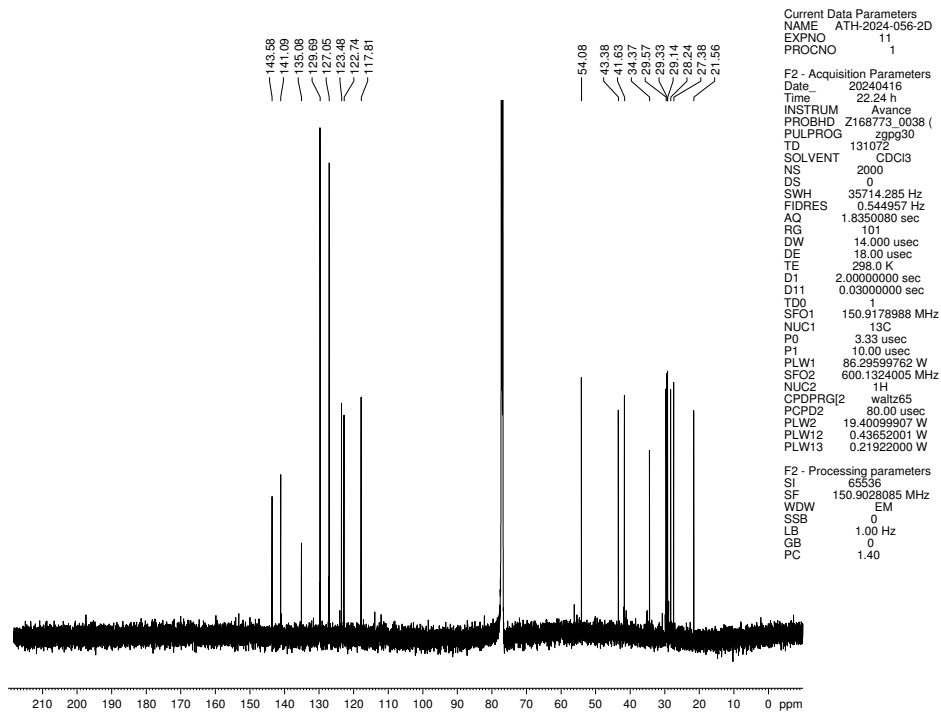


Figure 5.122. ¹³C NMR (150 MHz, CDCl₃) of compound 5.67.

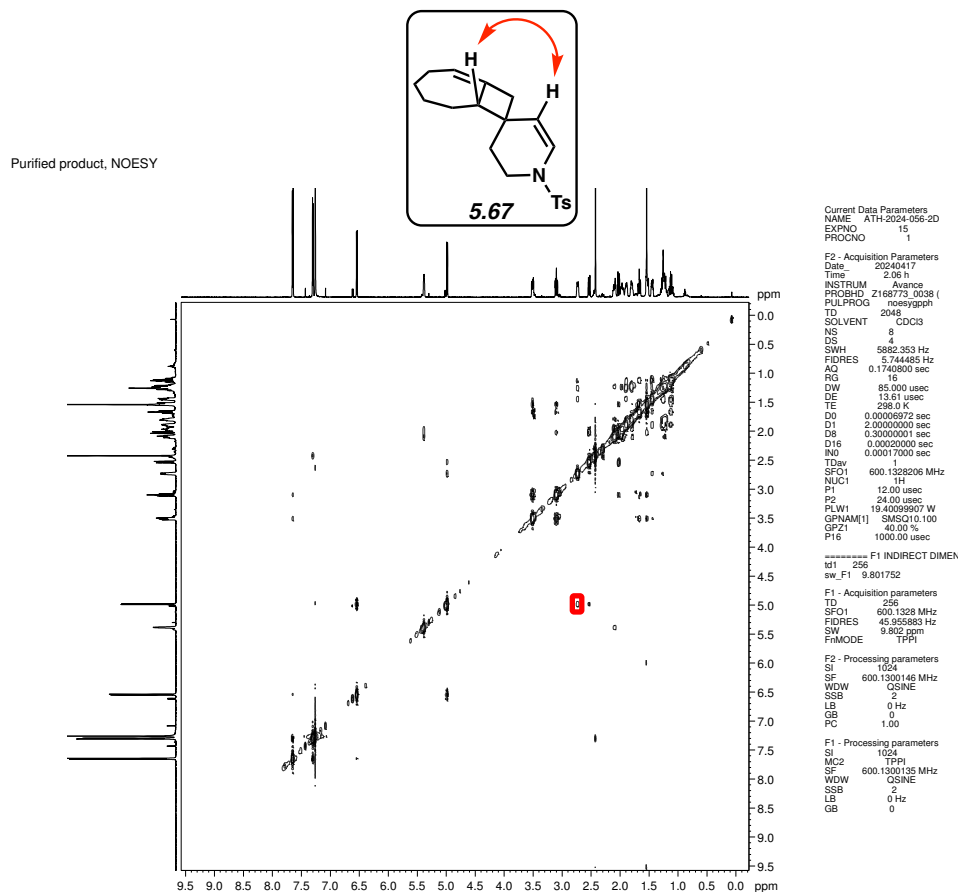


Figure 5.123. NOESY (600 MHz, CDCl₃) of compound 5.67.

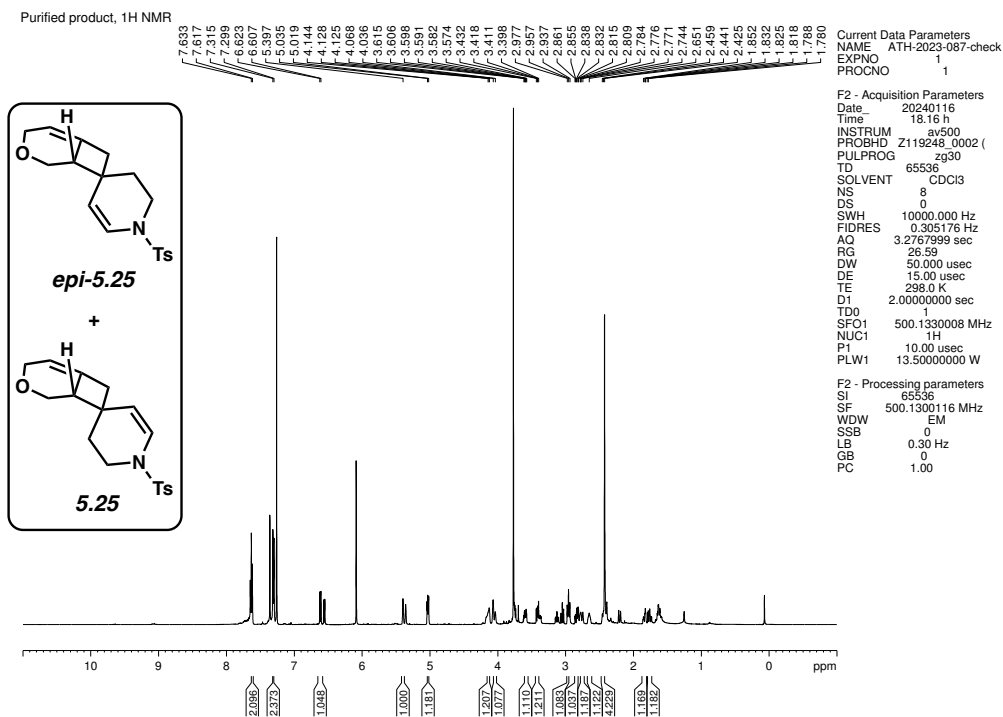


Figure 5.124. ¹H NMR (500 MHz, CDCl₃) of compounds *epi*-5.25 and 5.25.

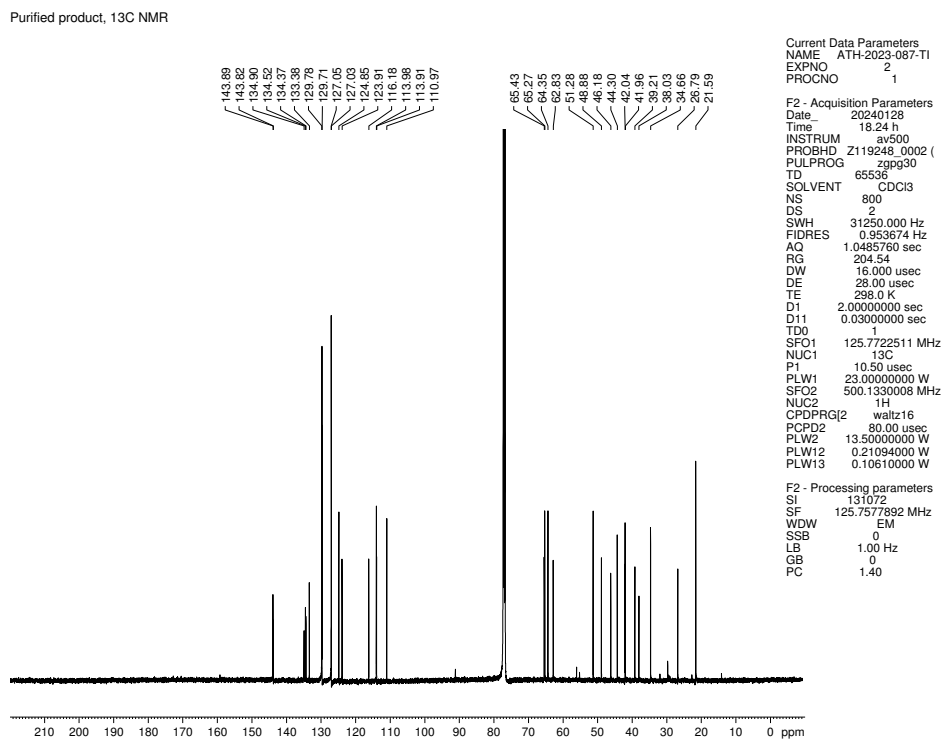


Figure 5.125. ¹³C NMR (125 MHz, CDCl₃) of compounds *epi*-5.25 and 5.25.

Purified product, ¹H NMR

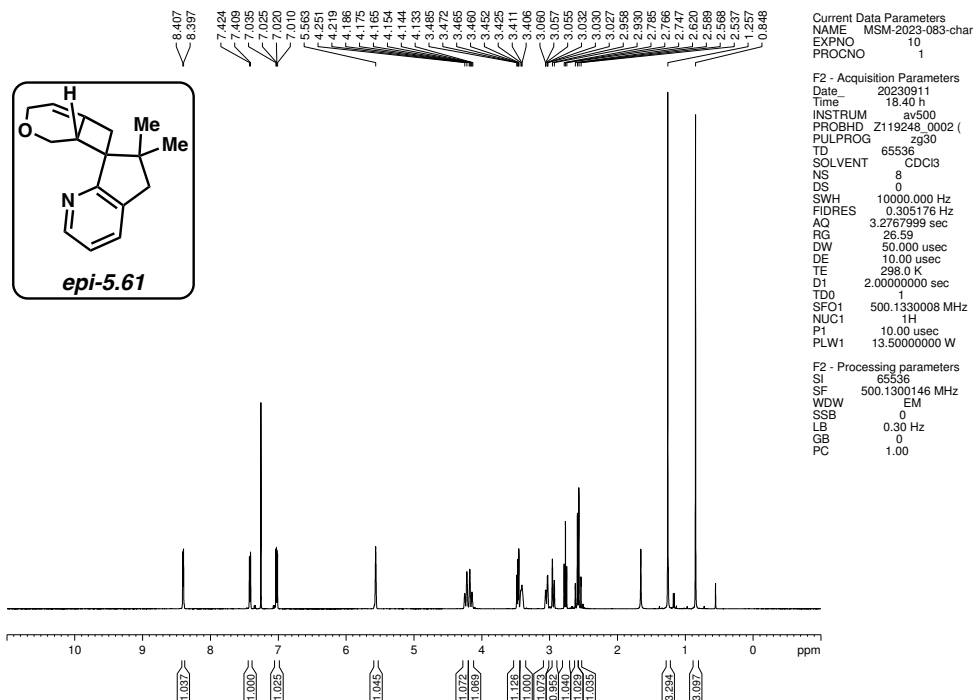


Figure 5.126. ¹H NMR (500 MHz, CDCl₃) of compound *epi-5.61*.

Purified product, ¹³C NMR

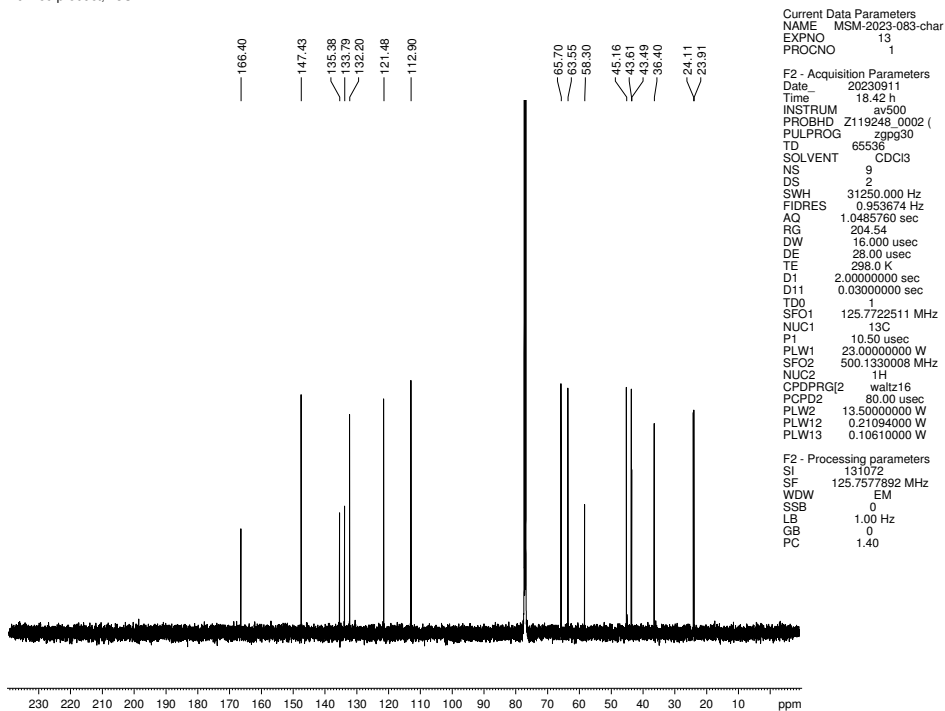


Figure 5.127. ¹³C NMR (125 MHz, CDCl₃) of compound *epi-5.61*.

Purified product, ¹H NMR

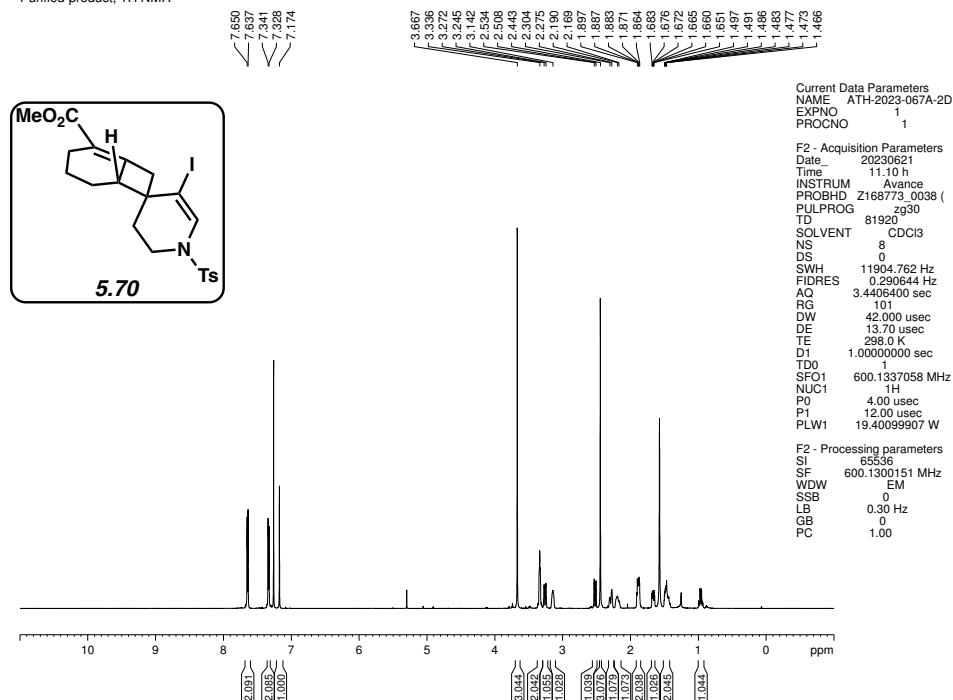


Figure 5.128. ¹H NMR (600 MHz, CDCl₃) of compound 5.70.

Purified product, ¹³C NMR

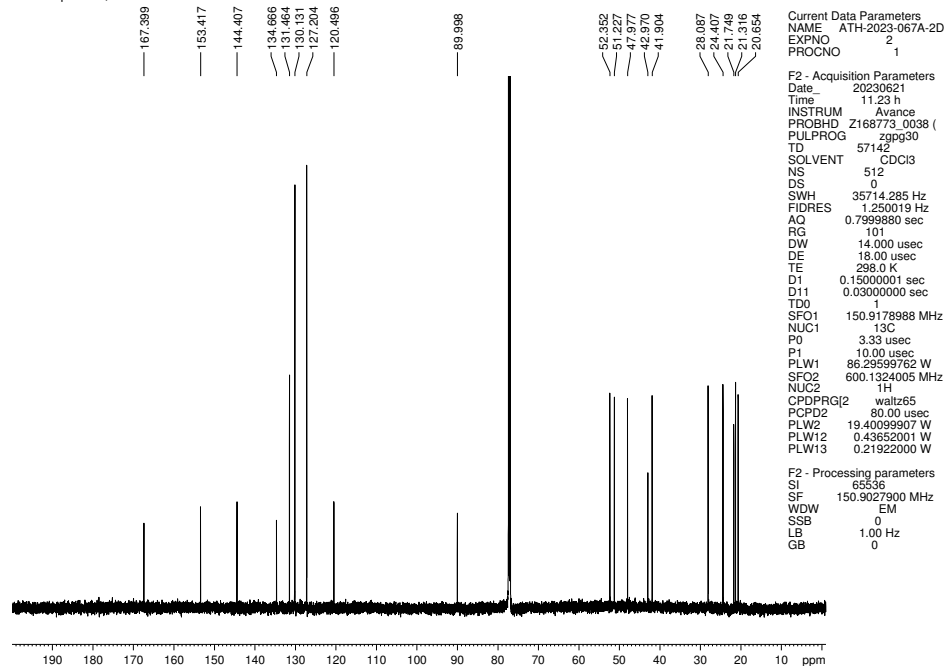
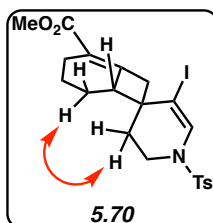


Figure 5.129. ¹³C NMR (150 MHz, CDCl₃) of compound 5.70.



Purified Product, NOESY

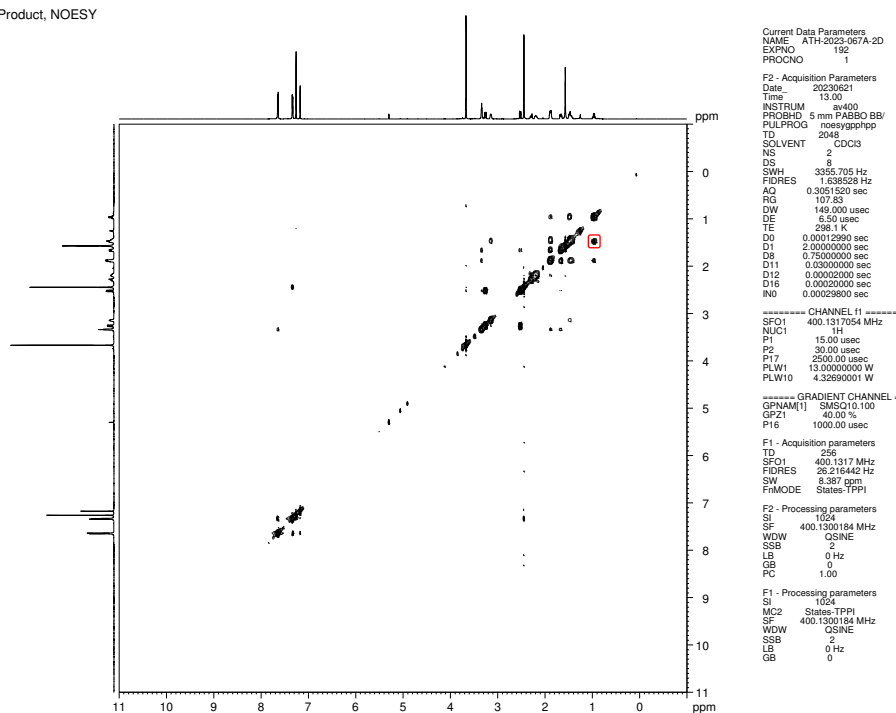


Figure 5.130. NOESY (400 MHz, CDCl₃) of compound 5.70.

Purified product, ¹H NMR

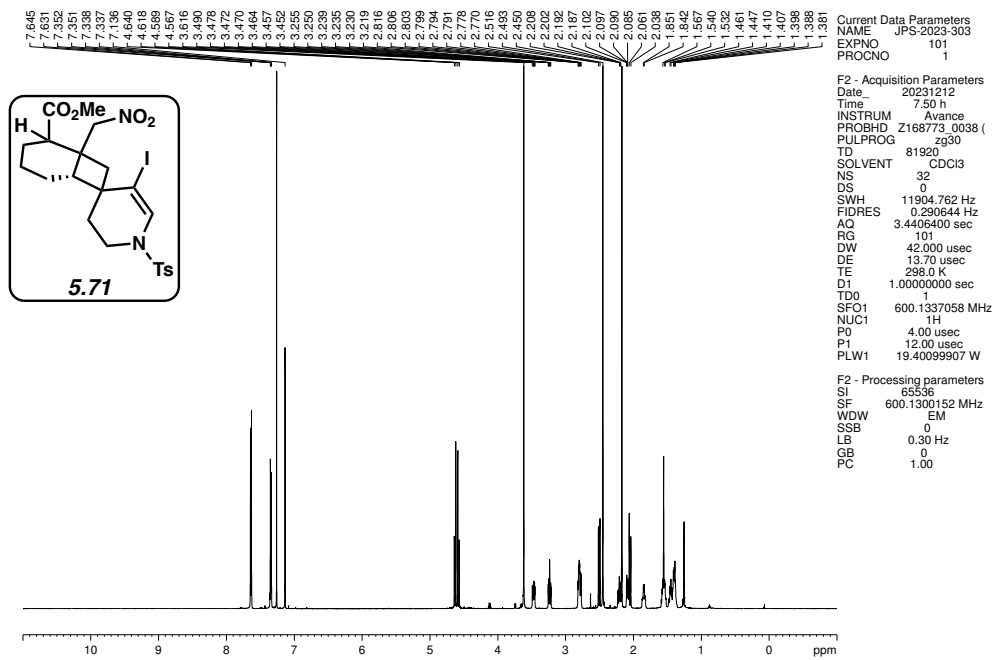


Figure 5.131. ¹H NMR (600 MHz, CDCl₃) of compound 5.71.

Purified product, ¹³C NMR

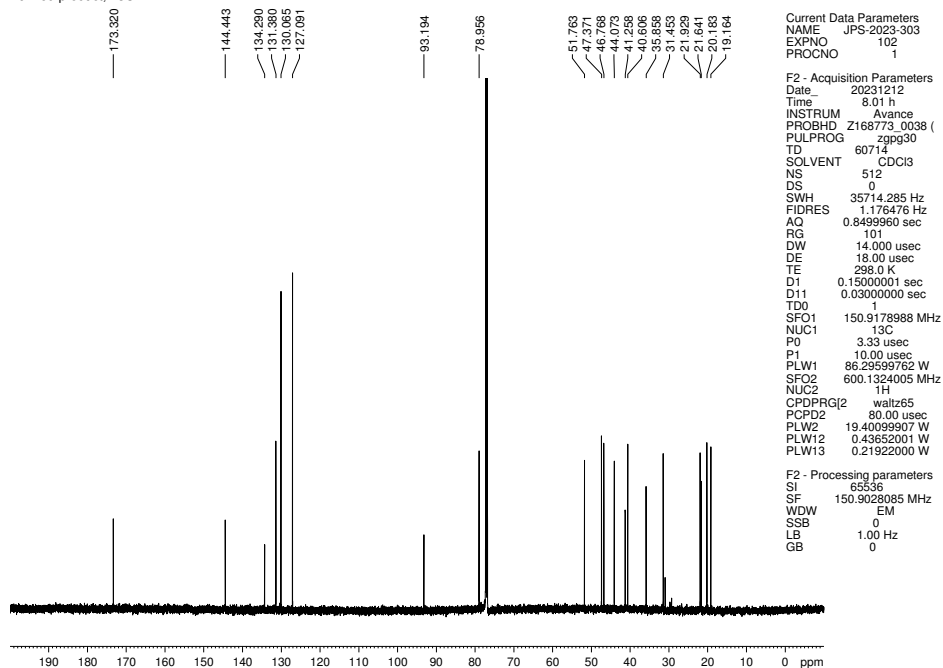
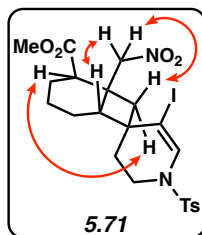


Figure 5.132. ¹³C NMR (150 MHz, CDCl₃) of compound 5.71.



Purified product, NOESY

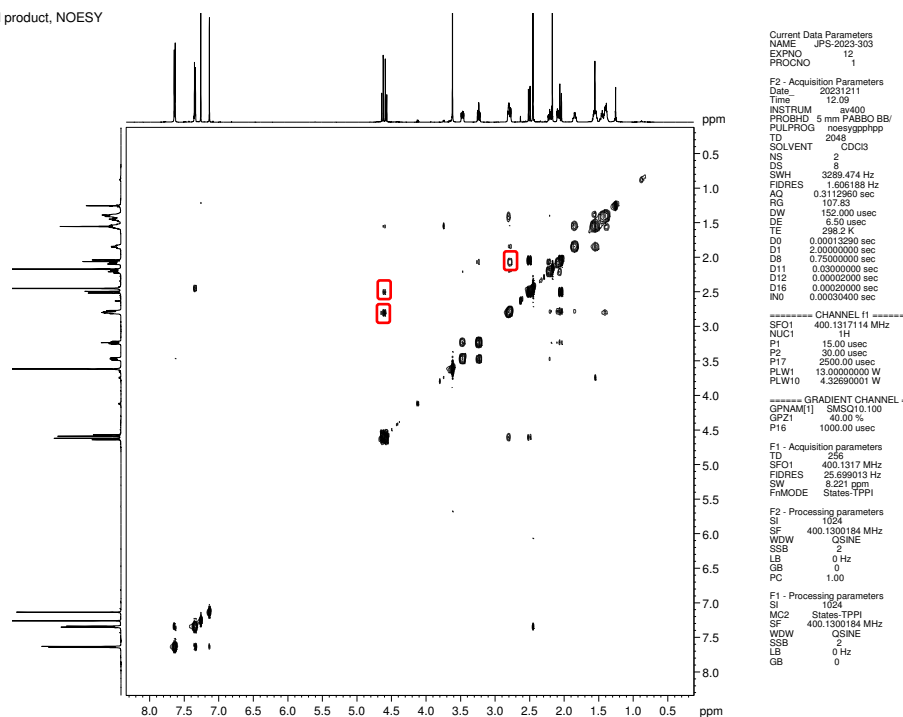


Figure 5.133. NOESY (400 MHz, CDCl_3) of compound 5.71.

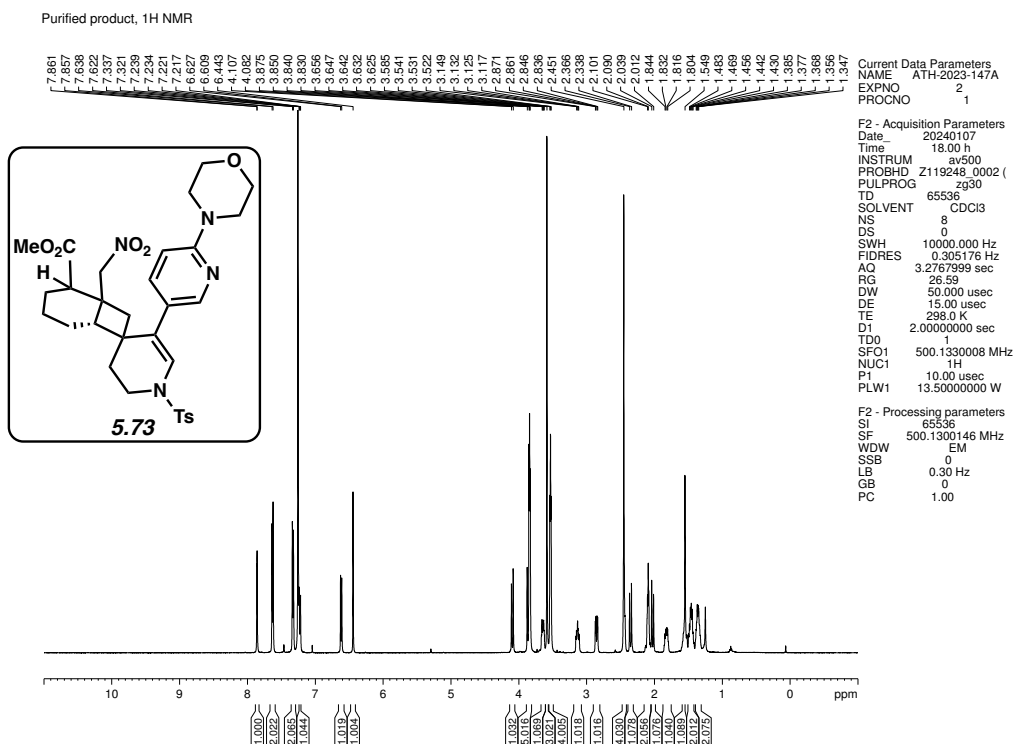


Figure 5.134. ^1H NMR (500 MHz, CDCl_3) of compound 5.73.

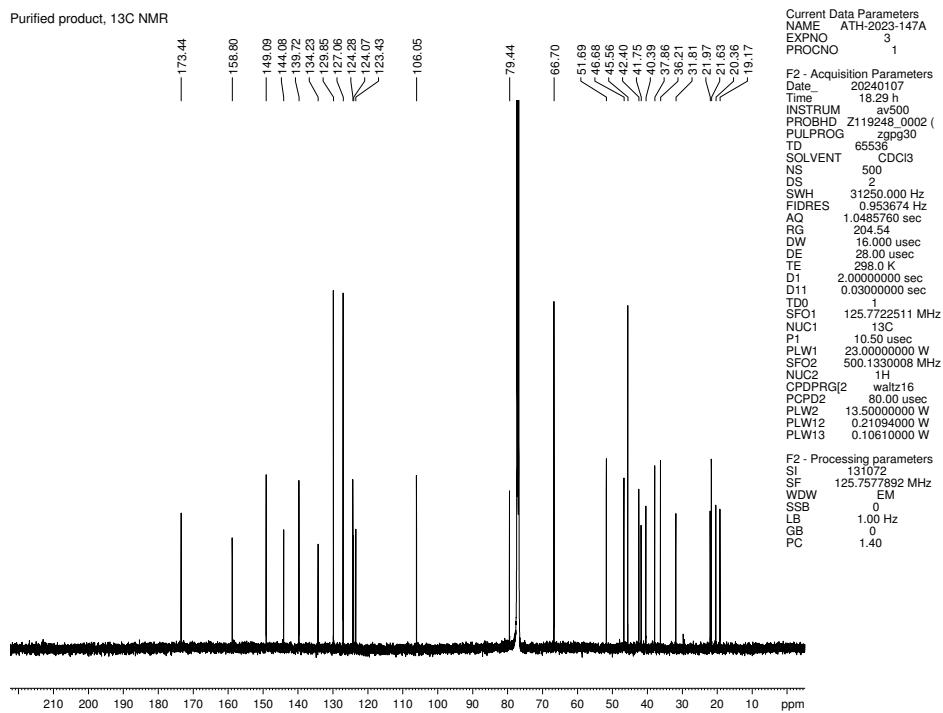


Figure 5.135. ^{13}C NMR (125 MHz, CDCl_3) of compound 5.73.

Purified product, ¹H NMR

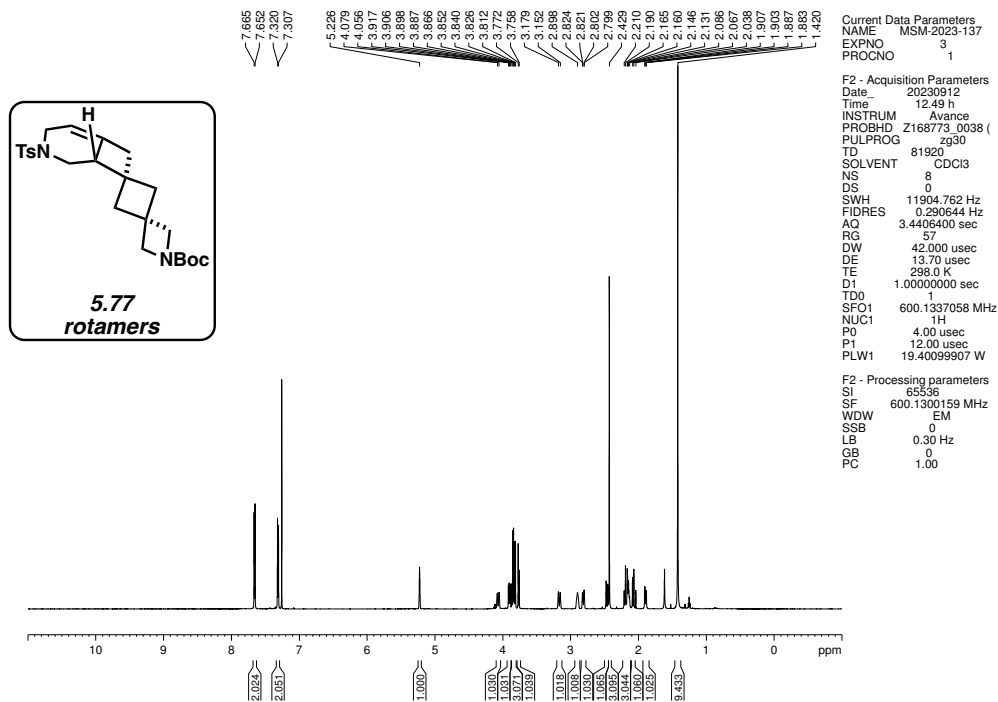


Figure 5.136. ¹H NMR (600 MHz, CDCl₃) of compound 5.77.

Purified product, ¹³C NMR

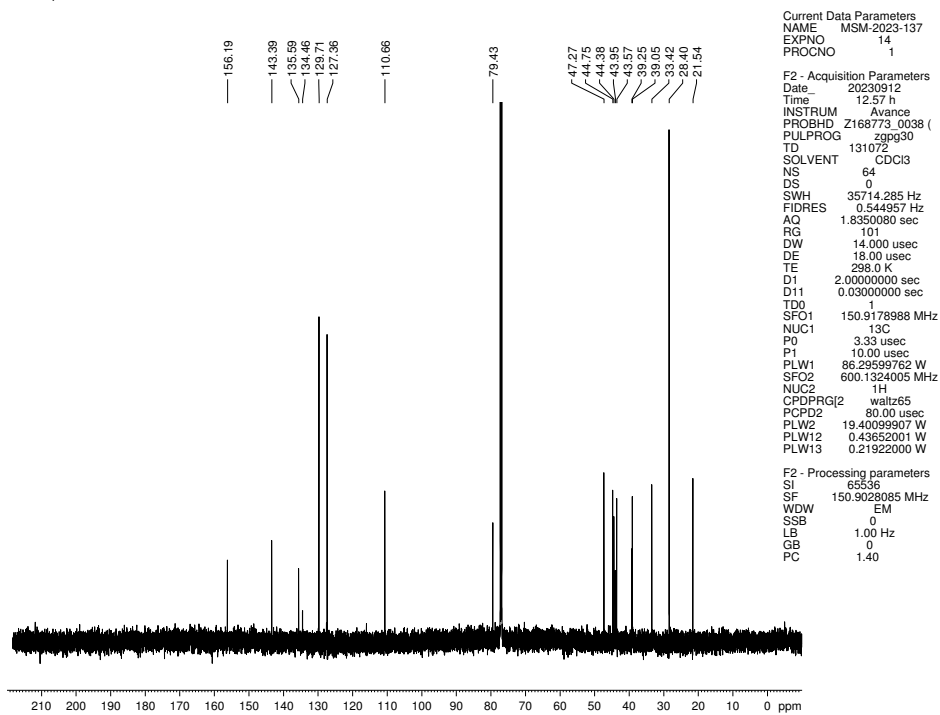


Figure 5.137. ¹³C NMR (150 MHz, CDCl₃) of compound 5.77.

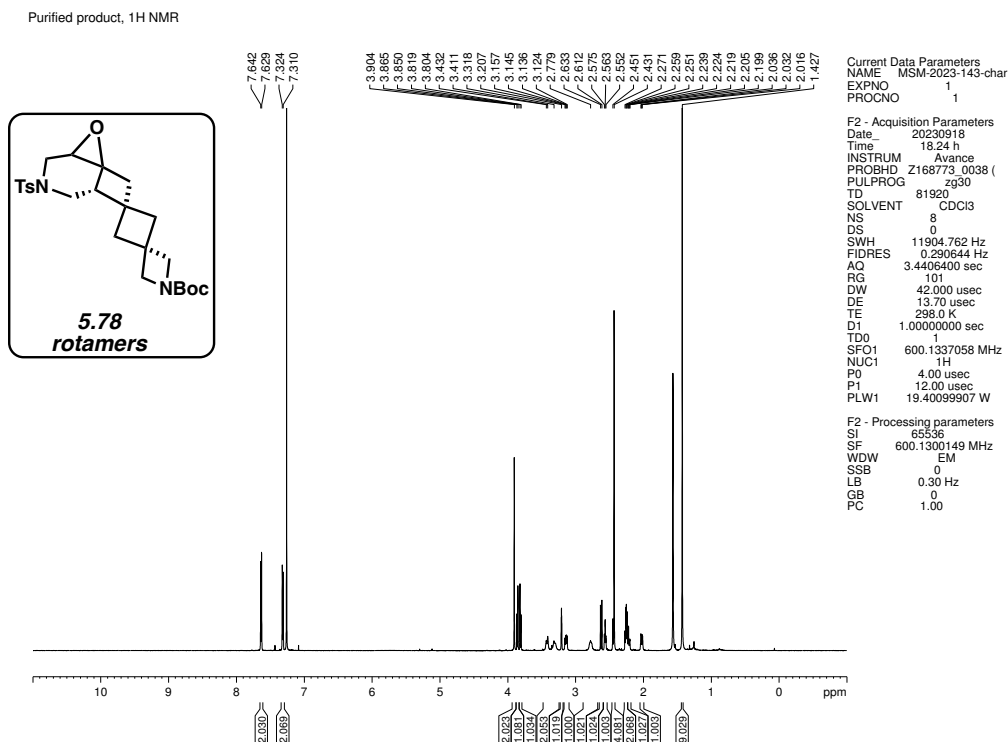


Figure 5.138. ^1H NMR (600 MHz, CDCl_3) of compound **5.78**.

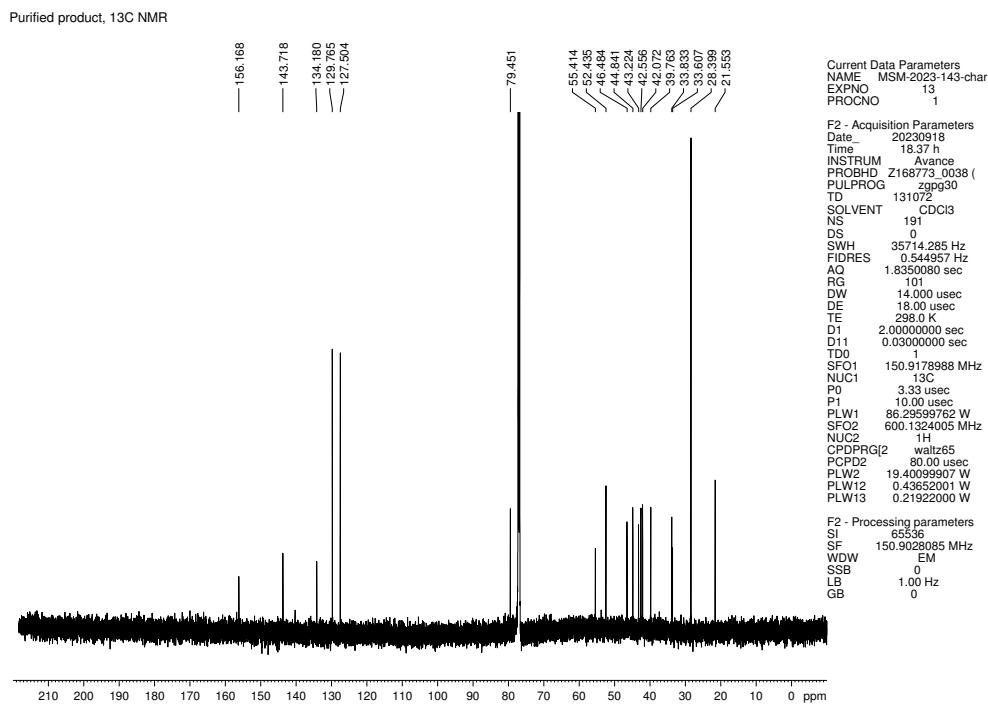


Figure 5.139. ^{13}C NMR (150 MHz, CDCl_3) of compound **5.78**.

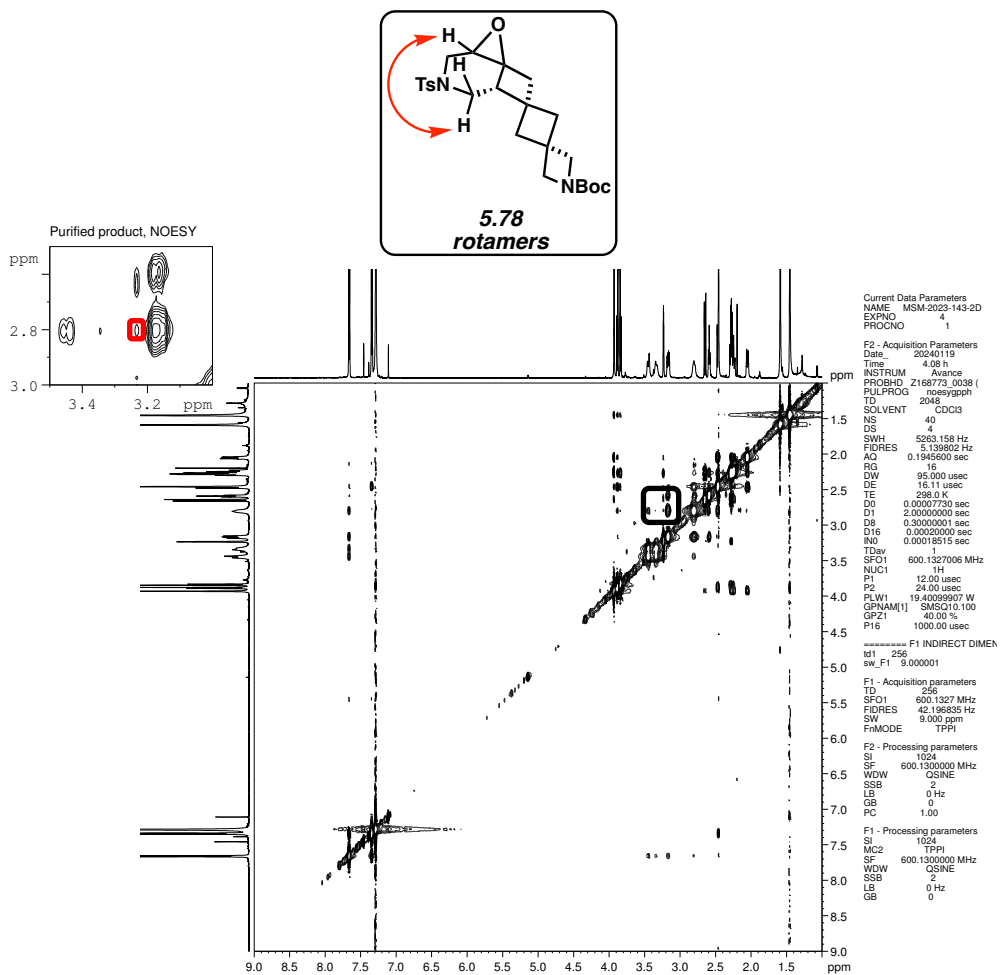


Figure 5.140. NOESY (600 MHz, CDCl_3) of compound **5.78**.

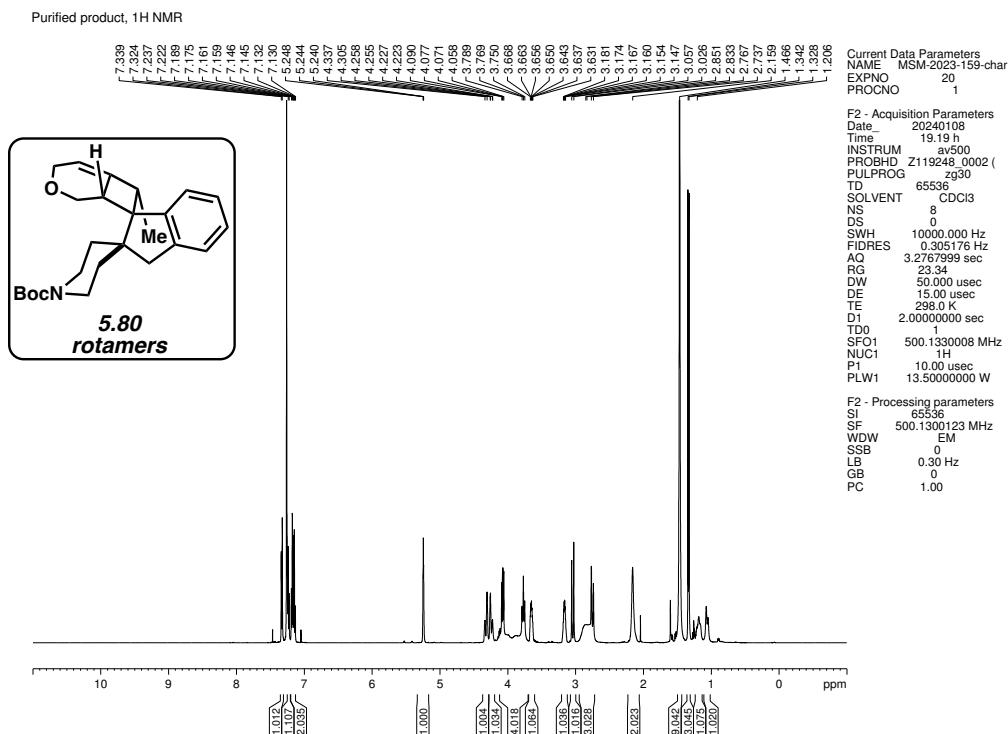


Figure 5.141. ^1H NMR (500 MHz, CDCl_3) of compound 5.80.

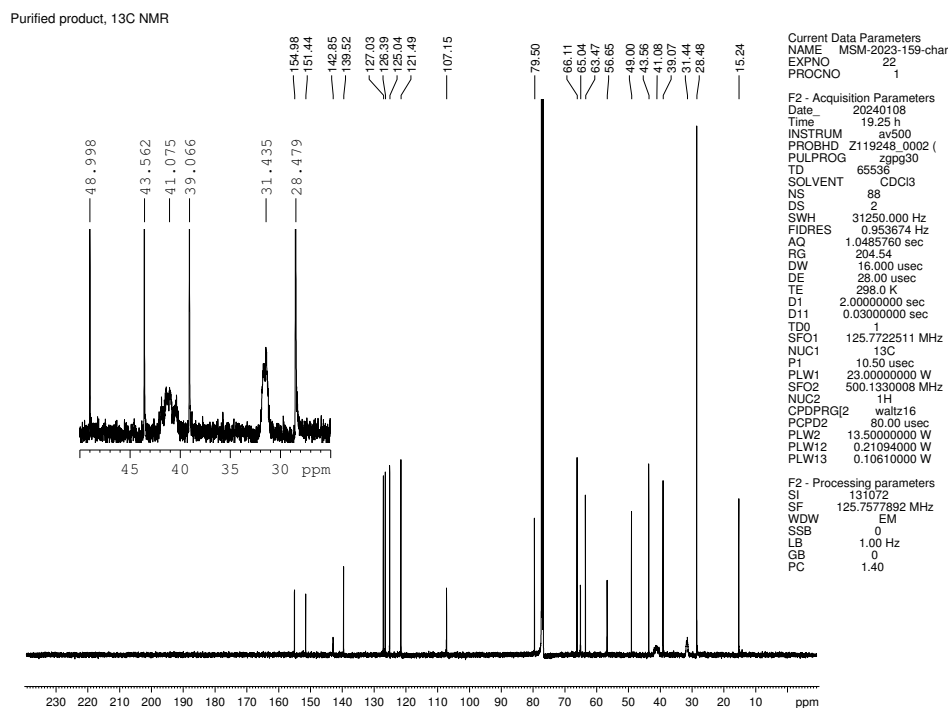


Figure 5.142. ^{13}C NMR (125 MHz, CDCl_3) of compound 5.80.

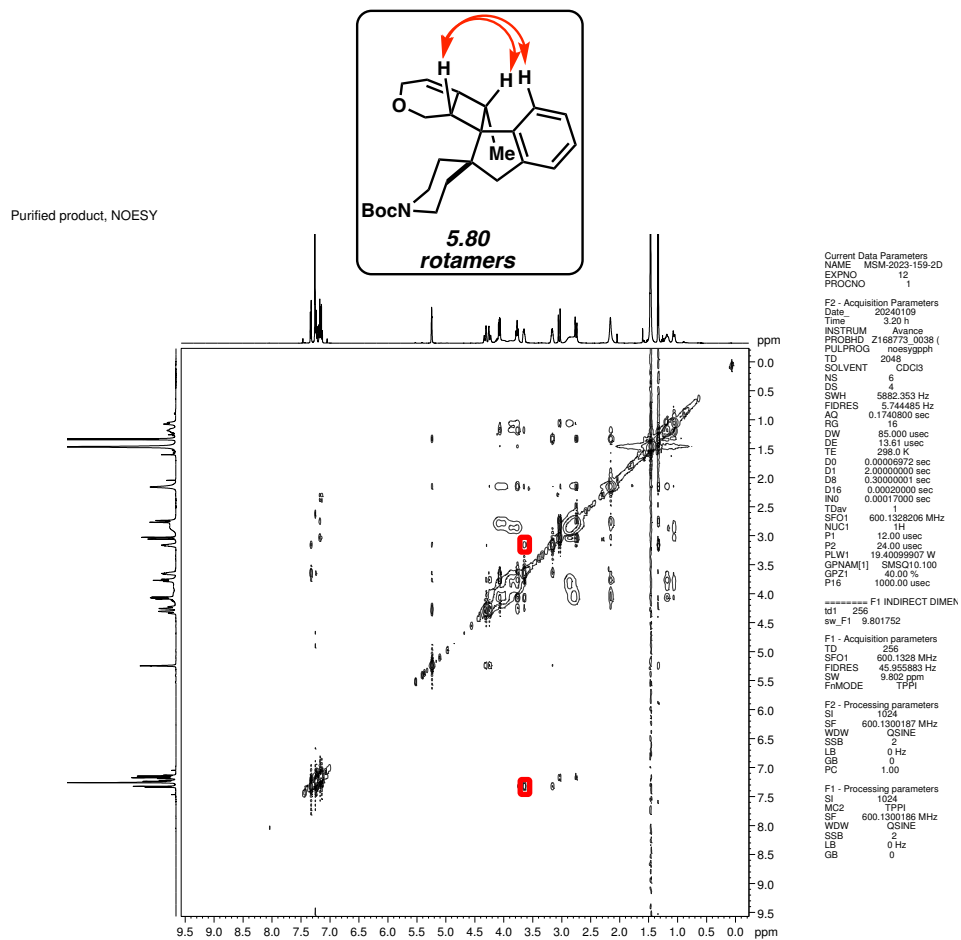


Figure 5.143. NOESY (600 MHz, CDCl₃) of compound **5.80**.

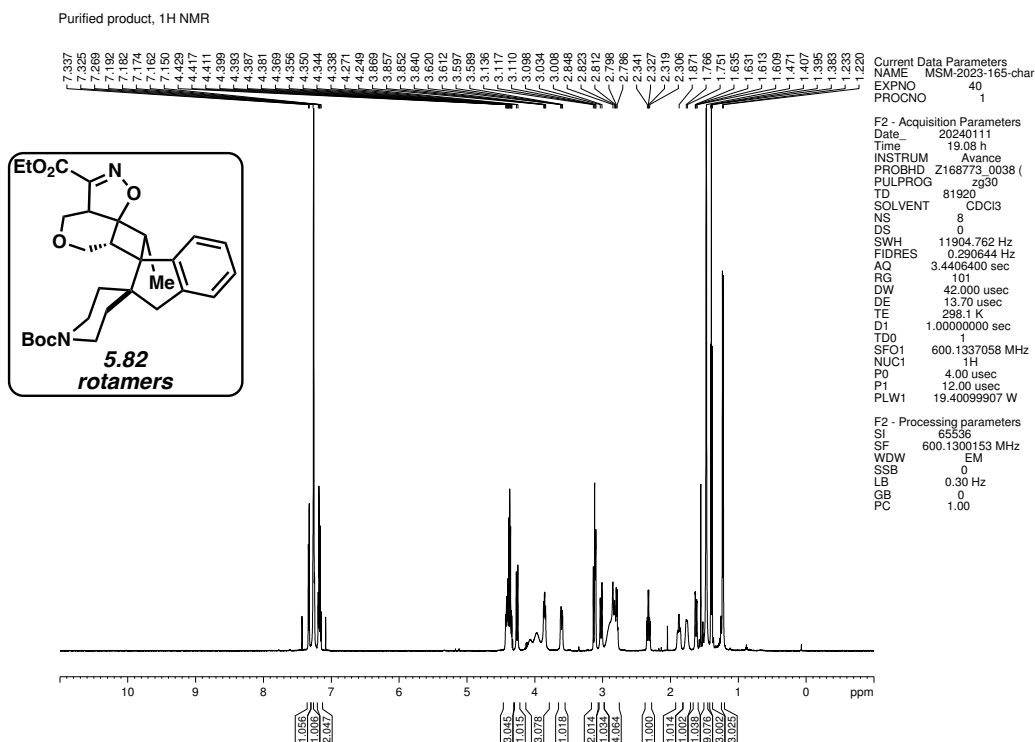


Figure 5.144. ¹H NMR (600 MHz, CDCl₃) of compound 5.82.

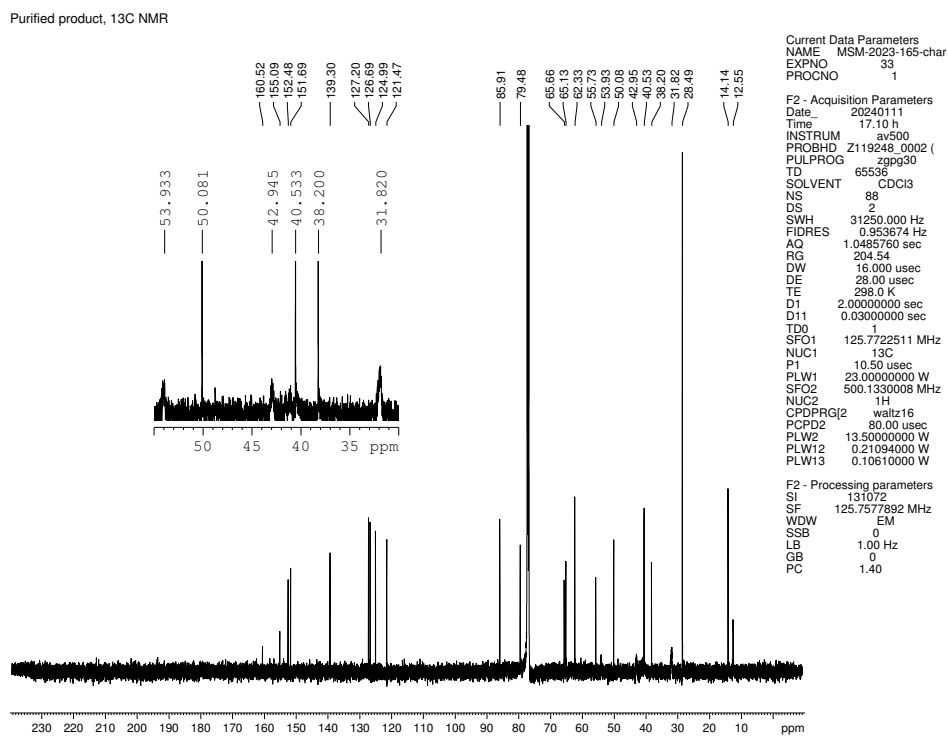


Figure 5.145. ¹³C NMR (125 MHz, CDCl₃) of compound 5.82.

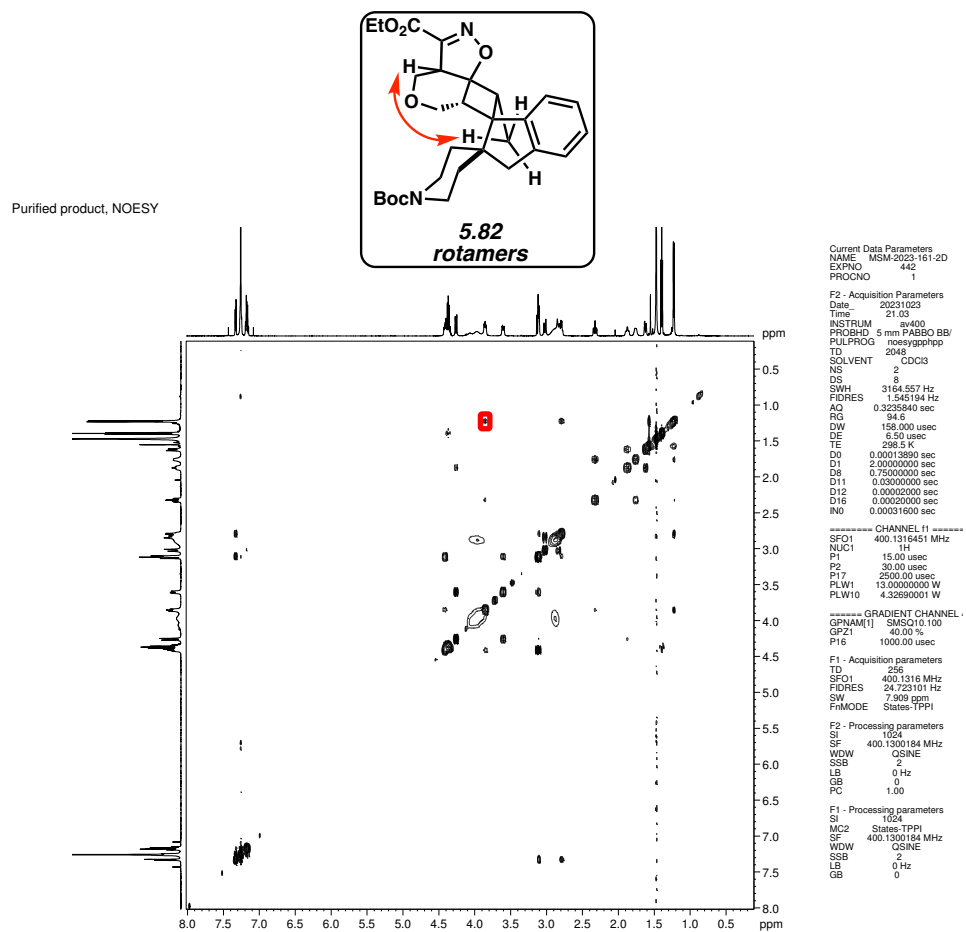


Figure 5.146. NOESY (400 MHz, CDCl₃) of compound 5.82.

5.12 Computational Section

5.12.1 Computational Methods

Conformational searches were performed in Spartan '20 V1.1.4¹⁰⁶ using Molecular Mechanics.

Conformers were then optimized in Spartan '20 V1.1.4 using DFT (B3LYP/6-31G*).^{107,74}

5.12.2 Calculated Energies for Thermal Isomerization Products

Table 5.7. Computed energies of thermal isomerization products at 25 °C using DFT (B3LYP/6-31G(d)). All units are in Hartrees.

STRUCTURE	E	ZPE	H	S·T	G
5.25	-1377.03122	0.34597	-1376.66616	0.06261	-1376.72905
<i>epi-5.25</i>	-1377.03182	0.34602	-1376.66673	0.06261	-1376.72952
5.41	-1455.64919	0.39948	-1455.22801	0.06857	-1455.29566
<i>epi-5.41</i>	-1455.65503	0.39918	-1455.23410	0.06857	-1455.30173
5.61	-751.056906	0.30369	-750.738150	0.06559	-750.792224
<i>epi-5.61</i>	-751.060092	0.30279	-750.742131	0.05367	-750.796459

5.12.3 Cartesian Coordinates and Energies of Optimized Structures

Compound **5.25**:

C	-2.599320	2.458494	-3.005626
C	-3.330434	3.768171	-2.816761
O	-2.694804	4.666391	-1.911667
C	-2.143275	4.051269	-0.743593
C	-1.004522	3.139711	-1.196613
C	-1.487623	2.244033	-2.309342
C	-0.629720	1.087493	-1.857562
C	-0.958184	0.031604	1.273214
N	0.309391	0.361082	1.947910
C	1.199899	1.210338	1.263506
C	0.855743	1.890346	0.159866
C	-0.512258	1.828762	-0.454690
C	-1.506885	1.282248	0.581356
H	-0.136121	3.747561	-1.484894
S	0.947209	-0.791035	3.021316
H	-3.053522	1.711809	-3.655322

H	-3.413251	4.321374	-3.760753
H	-4.362388	3.557441	-2.479063
H	-2.916709	3.481305	-0.206896
H	-1.816705	4.876374	-0.104144
H	-1.068234	0.082060	-1.855538
H	0.343243	1.043969	-2.362094
H	-1.654962	-0.334782	2.028669
H	-0.793776	-0.766564	0.532761
H	2.171803	1.308272	1.732092
H	1.596265	2.546613	-0.290137
H	-1.703556	2.044796	1.344088
H	-2.464564	1.029997	0.111995
O	2.125929	-0.170413	3.626113
O	-0.187329	-1.260185	3.816711
C	1.504880	-2.160794	2.005406
C	2.346233	-4.250239	0.340160
C	0.634958	-3.218013	1.733021
C	2.792059	-2.134376	1.461537
C	3.200871	-3.176876	0.634464
C	1.063063	-4.253436	0.902758
H	-0.352234	-3.233779	2.182318
H	3.465699	-1.318463	1.700637
H	4.203788	-3.160616	0.214488
H	0.389378	-5.080727	0.693901
C	2.813940	-5.388738	-0.534333
H	3.422576	-6.099607	0.039649
H	1.970528	-5.944457	-0.955791
H	3.432921	-5.028412	-1.363118

Compound *epi*-5.25:

C	1.429066	-0.495213	-4.488094
C	0.900754	0.919266	-4.576068
O	0.986702	1.650198	-3.357910
C	0.642831	0.902041	-2.187585
C	1.689581	-0.192969	-2.013234
C	1.859827	-0.942007	-3.312346
C	2.098297	-2.260319	-2.614212
C	1.368206	-1.323963	1.189991
N	0.029868	-1.935137	1.216885
C	-0.626405	-2.126243	-0.013237
C	-0.015217	-1.976432	-1.197755
C	1.438246	-1.609625	-1.332528
C	2.151331	-1.878256	-0.003175
H	2.630940	0.237960	-1.643184
H	1.351882	-1.122201	-5.375130
H	-0.148377	0.884509	-4.925078

H	1.458751	1.514571	-5.309924
H	-0.362148	0.463802	-2.281049
H	0.625581	1.629667	-1.370393
H	3.162320	-2.471196	-2.443303
H	1.622002	-3.158691	-3.021609
H	1.280168	-0.228974	1.108483
H	1.865182	-1.563642	2.131350
H	-1.654047	-2.456751	0.078066
H	-0.588455	-2.176346	-2.098595
H	3.155030	-1.436942	-0.005526
H	2.270173	-2.961207	0.127501
S	-0.892767	-1.774788	2.630991
O	-2.101896	-2.570137	2.415929
O	0.028746	-2.032857	3.737416
C	-1.373528	-0.049162	2.716614
C	-2.090844	2.657845	2.780050
C	-0.563972	0.862753	3.396736
C	-2.539965	0.371713	2.071197
C	-2.888043	1.718579	2.107676
C	-0.929115	2.208125	3.421145
H	0.324655	0.518811	3.915412
H	-3.172099	-0.352020	1.567755
H	-3.798152	2.046652	1.611353
H	-0.302671	2.919056	3.954190
C	-2.496112	4.111398	2.834305
H	-3.282477	4.272145	3.583381
H	-1.651366	4.753507	3.101811
H	-2.892484	4.452480	1.871696

Compound 5.41:

C	-0.507773	0.068826	-4.480496
C	-1.500208	-0.673017	-5.347454
O	-1.979626	-1.887132	-4.774348
C	-2.271887	-1.814651	-3.376303
C	-0.936441	-1.599601	-2.659466
C	-0.223249	-0.426391	-3.280504
C	0.408348	-0.008049	-1.977260
C	-1.158230	0.249997	0.900964
N	-0.664497	-0.870047	1.714178
C	0.049406	-1.870759	1.033424
C	0.068756	-1.948417	-0.303755
C	-0.618047	-0.970140	-1.225284
C	-1.762201	-0.244659	-0.437736
H	-0.360380	-2.529713	-2.758507
C	1.218252	0.436464	3.306968
C	1.127071	1.830532	3.311504

C	2.295290	2.587175	3.247898
C	3.554864	1.974858	3.173870
C	3.616805	0.574311	3.181114
C	2.460162	-0.199455	3.247140
C	4.811009	2.806569	3.074201
S	-0.277686	-0.554275	3.338149
O	-1.360457	0.287722	3.846989
O	0.054684	-1.850257	3.931007
C	-2.328797	1.010408	-1.135930
C	-2.925845	-1.214301	-0.138132
H	-0.120100	1.017981	-4.847777
H	-1.054796	-0.965106	-6.306782
H	-2.349585	-0.004195	-5.581730
H	-2.984260	-1.001602	-3.181495
H	-2.753649	-2.763918	-3.125905
H	0.391836	1.055279	-1.715952
H	1.437062	-0.368121	-1.856031
H	-1.921750	0.769973	1.482753
H	-0.338848	0.956557	0.694841
H	0.522665	-2.605284	1.673952
H	0.614338	-2.772818	-0.755947
H	0.155923	2.307511	3.390676
H	2.227638	3.672373	3.263949
H	4.585064	0.081384	3.143260
H	2.517847	-1.282204	3.278086
H	5.693984	2.237770	3.381217
H	4.748812	3.703197	3.700148
H	4.978776	3.142673	2.042419
H	-2.764810	0.780165	-2.111108
H	-3.121760	1.447128	-0.517282
H	-1.568080	1.782898	-1.285795
H	-3.629230	-0.753386	0.564667
H	-2.574360	-2.148342	0.306036
H	-3.482036	-1.455912	-1.048431

Compound *epi*-5.41:

C	4.105274	1.126937	-1.511607
C	3.370322	1.728167	-2.689526
O	2.126258	1.100382	-2.982730
C	1.341521	0.766274	-1.833385
C	2.098633	-0.300977	-1.049508
C	3.525871	0.137633	-0.838703
C	3.614160	-0.523721	0.514840
C	-0.212867	-1.453727	1.181593
N	-0.479617	-0.298058	2.049826
C	0.381891	0.804631	1.913463

C	1.532486	0.735308	1.230673
C	2.028450	-0.506045	0.530708
C	1.300647	-1.760885	1.107021
H	2.036050	-1.263079	-1.570025
C	-2.963726	0.464710	1.032460
C	-2.949770	1.804123	0.630817
C	-3.596328	2.165655	-0.546795
C	-4.260505	1.212266	-1.335485
C	-4.263247	-0.120521	-0.906690
C	-3.619244	-0.502897	0.270360
C	-4.963168	1.626821	-2.605857
S	-2.090236	-0.024110	2.520486
O	-2.610273	-1.328045	2.931947
O	-2.054881	1.126526	3.424295
C	1.843032	-2.072735	2.517660
C	1.457302	-3.015426	0.227595
H	5.049256	1.581764	-1.215453
H	3.957444	1.649409	-3.613334
H	3.215392	2.807233	-2.501407
H	0.379408	0.423311	-2.226427
H	1.162216	1.652732	-1.207132
H	4.002970	-1.547853	0.459382
H	4.128719	0.005206	1.324080
H	-0.751731	-2.310686	1.591390
H	-0.593831	-1.256276	0.166690
H	0.072799	1.687319	2.460186
H	2.165297	1.618338	1.213144
H	-2.459129	2.550577	1.246264
H	-3.591961	3.207731	-0.857771
H	-4.781090	-0.871831	-1.497559
H	-3.640482	-1.533067	0.609323
H	-5.784471	2.322468	-2.393769
H	-4.276708	2.139367	-3.290473
H	-5.382383	0.764403	-3.132405
H	1.791561	-1.198806	3.171137
H	2.886510	-2.402795	2.466639
H	1.262055	-2.877188	2.982984
H	2.511315	-3.233462	0.024176
H	1.036790	-3.887571	0.741364
H	0.942017	-2.919531	-0.734459

Compound **5.61**:

C	1.149142	1.403730	0.238361
C	0.675448	-1.201878	-0.311497
C	0.129565	0.174943	0.221613
C	1.240544	-1.864453	0.990030

C	0.330109	-1.343286	2.072818
C	-0.843664	1.089862	-0.626725
C	0.309685	2.035303	-0.842692
C	0.460596	2.801804	-1.918194
C	-1.499582	0.808432	-1.980811
O	-1.804003	2.077856	-2.565236
C	-0.663871	2.853165	-2.926675
H	-1.599704	1.494028	0.058124
C	-0.328145	-0.191470	1.617780
C	0.067878	-1.790186	3.361904
C	-0.843659	-1.057617	4.131125
C	-1.438664	0.078341	3.580563
N	-1.190524	0.523651	2.337024
C	1.741962	-1.106093	-1.410388
C	-0.493587	-2.081869	-0.811089
H	2.202822	1.207665	0.016878
H	1.087576	1.935594	1.195180
H	2.275924	-1.537881	1.169424
H	1.261504	-2.958583	0.919104
H	1.381682	3.332425	-2.154805
H	-0.832947	0.239892	-2.646700
H	-2.455083	0.280953	-1.908865
H	-0.280386	2.523966	-3.910934
H	-1.042085	3.874651	-3.060364
H	0.547795	-2.679439	3.764802
H	-1.091701	-1.363498	5.143286
H	-2.150018	0.661505	4.162925
H	2.650279	-0.604760	-1.061460
H	2.030346	-2.109874	-1.745371
H	1.374301	-0.556750	-2.283710
H	-0.138229	-3.100770	-1.007678
H	-0.926301	-1.704408	-1.740577
H	-1.295006	-2.144949	-0.067170

Compound *epi*-**5.61**:

C	-1.743001	0.410275	-0.826871
C	-0.855405	-0.278096	1.660979
C	-0.559339	0.086405	0.159847
C	0.426061	-1.057773	2.104098
C	0.908298	-1.699307	0.829151
C	0.043456	1.518525	-0.202957
C	-0.886132	1.518178	-1.389179
C	-0.593728	2.066811	-2.562839
C	1.466561	1.808311	-0.674958
O	1.409986	2.998792	-1.469190
C	0.683249	2.865603	-2.687783

H	-0.247343	2.254656	0.555014
C	0.330815	-1.060355	-0.278315
C	1.770972	-2.764972	0.605702
C	2.014324	-3.139456	-0.720360
C	1.381413	-2.440114	-1.749511
N	0.543723	-1.410420	-1.548918
C	-2.063186	-1.238424	1.715334
C	-1.134471	0.918366	2.577261
H	-2.044234	-0.392758	-1.506452
H	-2.626352	0.779565	-0.289499
H	1.184338	-0.364827	2.499191
H	0.214784	-1.780265	2.902006
H	-1.170089	1.884778	-3.468375
H	1.863467	0.968240	-1.261822
H	2.165016	2.033144	0.137253
H	1.320479	2.394132	-3.458884
H	0.490753	3.894035	-3.019491
H	2.238696	-3.298479	1.430321
H	2.676543	-3.968069	-0.954070
H	1.549609	-2.722120	-2.787519
H	-2.984084	-0.738231	1.396542
H	-1.918634	-2.114506	1.072819
H	-2.219141	-1.596144	2.740218
H	-1.364110	0.569930	3.591710
H	-0.275922	1.594597	2.649686
H	-1.997374	1.499972	2.229858

5.13 Notes and References

- (1) Lovering, F.; Bikker, J.; Humblet, C. Escape from flatland: Increasing saturation as an approach to improving clinical success. *J. Med. Chem.* **2009**, *52*, 6752–6756.
- (2) Lovering, F. Escape from flatland 2: Complexity and promiscuity. *Med. Chem. Commun.* **2013**, *4*, 515–519.
- (3) van der Kolk, M. R.; Janssen, M. A. C. H.; Rutjes, F. P. J. T.; Blanco-Ania, D. Cyclobutanes in small-molecule drug candidates. *ChemMedChem* **2022**, *17*, e202200020.

- (4) Li, J.; Gao, K.; Bian, M.; Ding, H. Recent advances in the total synthesis of cyclobutane-containing natural products. *Org. Chem. Front.* **2020**, *7*, 136–154.
- (5) Hui, C.; Liu, Y.; Jiang, M.; Wu, P. Cyclobutane-containing scaffolds in bioactive small molecules. *Trends Chem.* **2022**, *4*, 677–681.
- (6) Carreira, E. M.; Fessard, T. C. Four-membered ring-containing spirocycles: Synthetic strategies and opportunities. *Chem. Rev.* **2014**, *114*, 8257–8322.
- (7) Singh, J.; Bisacchi, G. S.; Ahmad, S.; Godfrey, J. D.; Kissick, T. P.; Mitt, T.; Kocy, O.; Vu, T.; Papaioannou, C. G.; Wong, M. K.; Heikes, J. E.; Zahler, R.; Mueller, R. H. A practical asymmetric synthesis of the antiviral agent Lobucavir, BMS-180194. *Org. Proc. Res. Dev.* **1998**, *2*, 393–399.
- (8) Hopkins, B.; Ma, B.; Marx, I.; Schulz, J.; Vandever, G.; Prince, R.; Nevalainen, M.; Chen, T.; Yousaf, Z.; Himmelbauer, M.; Pattaropong, V.; Jones, J.; Lin, E.; Gonzalez-Lopez de Turiso, F.; Purgett, T.; Capacci, A.; Sciabola, S. Pyrazolo[1,5-A]pyrazine derivatives as BTK inhibitors. WO 2022104079, May 05, 2022.
- (9) Sharma, R.; Nikas, S. P.; Paronis, C. A.; Wood, J. T.; Halikhedkar, A.; Guo, J. J.; Thakur, G. A.; Kulkarni, S.; Benchama, O.; Raghav, J. G.; Gifford, R. S.; Järbe, T. U. C.; Bergman, J.; Makriyannis, A. Controlled-deactivation cannabinergic ligands. *J. Med. Chem.* **2013**, *56*, 10142–10157.

- (10) Reisman, S. E.; Ready, J. M.; Weiss, M. M.; Hasuoka, A.; Hirata, M.; Tamaki, K.; Ovaska, T. V.; Smith, C. J.; Wood, J. L. Evolution of a synthetic strategy: Total synthesis of (±)-welwitindolinone A isonitrile. *J. Am. Chem. Soc.* **2008**, *130*, 2087–2100.
- (11) Baran, P. S.; Richter, J. M. Enantioselective total syntheses of welwitindolinone A and fischerindoles I and G. *J. Am. Chem. Soc.* **2005**, *127*, 15394–15396.
- (12) Misiek, M.; Williams, J.; Schmich, K.; Hüttel, W.; Merfort, I.; Salomon, C. E.; Aldrich, C. C.; Hoffmeister, D. Structure and cytotoxicity of arnamial and related fungal sesquiterpene aryl esters. *J. Nat. Prod.* **2009**, *72*, 1888–1891.
- (13) Zhou, M.; Li, X.-R.; Tang, J.-W.; Liu, Y.; Li, X.-N.; Wu, B.; Qin, H.-B.; Du, X.; Li, L.-M.; Wang, W.-G.; Pu, J.-X.; Sun, H.-D. Scopariusicides, novel unsymmetrical cyclobutanes: Structural elucidation and concise synthesis by a combination of intermolecular [2 + 2] cycloaddition and C–H functionalization. *Org. Lett.* **2015**, *17*, 6062–6065.
- (14) Namyslo, J. C.; Kaufmann, D. E. The application of cyclobutane derivatives in organic synthesis. *Chem. Rev.* **2003**, *103*, 1485–1538.
- (15) Secci, F.; Frongia, A.; Piras, P. P. Stereocontrolled synthesis and functionalization of cyclobutanes and cyclobutanones. *Molecules* **2013**, *18*, 15541–15572.

- (16) Eckart-Frank, I. K.; Wilkerson-Hill, S. M. Palladium-catalyzed trans-selective synthesis of spirocyclic cyclobutanes using α,α -dialkylcrotyl- and allylhydrazones. *J. Am. Chem. Soc.* **2023**, *145*, 18591–18597.
- (17) Scholz, S. O.; Kidd, J. B.; Capaldo, L.; Fikweert, N. E.; Littlefield, R. M.; Yoon, T. P. Construction of complex cyclobutane building blocks by photosensitized [2 + 2] cycloaddition of vinyl boronate esters. *Org. Lett.* **2021**, *23*, 3496–3501.
- (18) Sherbrook, E. M.; Jung, H.; Cho, D.; Baik, M.-H.; Yoon, T. P. Brønsted acid catalysis of photosensitized cycloadditions. *Chem. Sci.* **2020**, *11*, 856–861.
- (19) Conner, M. L.; Brown, M. K. Synthesis of 1,3-substituted cyclobutanes by allenolate-alkene [2+2] cycloaddition. *J. Org. Chem.* **2016**, *81*, 8050–8060.
- (20) Liu, Y.; Ni, D.; Brown, M. K. Boronic ester enabled [2 + 2]-cycloadditions by temporary coordination: Synthesis of artochamin J and piperarborenine B. *J. Am. Chem. Soc.* **2022**, *144*, 18790–18796.
- (21) Liu, Y.; Brown, M. K. Photosensitized [2 + 2]-cycloadditions of dioxaborole: Reactivity enabled by boron ring constraint strategy. *J. Am. Chem. Soc.* **2023**, *145*, 25061–25067.
- (22) Poplata, S.; Tröster, A.; Zou, Y.-Q.; Bach, T. Recent advances in the synthesis of cyclobutanes by olefin [2 + 2] photocycloaddition reactions. *Chem. Rev.* **2016**, *116*, 9748–9815.

- (23) Sarkar, D.; Bera, N.; Ghosh, S. [2 + 2] Photochemical cycloaddition in organic synthesis. *Eur. J. Org. Chem.* **2020**, *2020*, 1310–1326.
- (24) For a recent example of an intermolecular selective photochemical [2+2] cycloaddition, see: Jiang, Y.; Wang, C.; Rogers, C. R.; Kodaimati, M. S.; Weiss E. A. Regio- and diastereoselective intermolecular [2+2] cycloadditions photocatalysed by quantum dots. *Nat. Chem.* **2019**, *11*, 1034–1040.
- (25) Roberts, J. D.; Simmons, H. E.; Carlsmith, L. A.; Vaughn, C. W. Rearrangement in the reaction of chlorobenzene-1-C14 with potassium amide. *J. Am. Chem. Soc.* **1953**, *75*, 3290–3291.
- (26) Tadross, P. M.; Stoltz, B. M. A comprehensive history of arynes in natural product total synthesis. *Chem. Rev.* **2012**, *112*, 3550–3577.
- (27) Gampe, C. M.; Carreira, E. M. Arynes and cyclohexyne in natural product synthesis. *Angew. Chem., Int. Ed.* **2012**, *51*, 3766–3778.
- (28) Wenk, H. H.; Winkler, M.; Sander, W. One century of aryne chemistry. *Angew. Chem., Int. Ed.* **2003**, *42*, 502–528.
- (29) Goetz, A. E.; Garg, N. K.; Enabling the use of heterocyclic arynes in chemical synthesis. *J. Org. Chem.* **2014**, *79*, 846–851.

- (30) Nakamura, Y.; Yoshida, S.; Hosya, T. Recent advances in synthetic heteraryne chemistry. *Heterocycles* **2019**, *98*, 1623–1677.
- (31) Anthony, S. M.; Wonilowicz, L. G.; McVeigh, M. S.; Garg, N. K. Leveraging fleeting strained intermediates to access complex scaffolds. *JACS Au* **2021**, *1*, 897–912.
- (32) Scardiglia, F.; Roberts, J. D. Evidence for cyclohexyne as an intermediate in the coupling of phenyllithium with 1-chlorocyclohexene. *Tetrahedron* **1957**, *1*, 343–344.
- (33) Tlais, S. F.; Danheiser, R. L. *N*-Tosyl-3-azacyclohexyne. Synthesis and chemistry of a strained cyclic ynamide. *J. Am. Chem. Soc.* **2014**, *136*, 15489–15492.
- (34) Medina, J. M.; McMahon, T. C.; Jiménez-Oseés, G.; Houk, K. N.; Garg, N. K. Cycloadditions of cyclohexynes and cyclopentyne. *J. Am. Chem. Soc.* **2014**, *136*, 14706–14709.
- (35) For a comprehensive review on the different modes of reactivity of strained intermediates, including [2+2] cycloadditions, see: Shi, J.; Li, L.; Li, Y. *o*-Silylaryl triflates: A journey of Kobayashi aryne precursors. *Chem. Rev.* **2021**, *121*, 3892–4044.
- (36) Liebman, J. F.; Greenberg, A. A survey of strained organic molecules. *Chem. Rev.* **1976**, *76*, 311–365.
- (37) Moser, W. R. The Reactions of gem-Dihalocyclopropanes with Organometallic Reagents. Ph. D. Thesis. Massachusetts Institute of Technology, Cambridge, MA, 1964.

- (38) Moore, W. R.; Moser, W. R. The reaction of 6,6-dibromobicyclo[3.1.0]hexane with methylolithium. Efficient trapping of 1,2-cyclohexadiene by styrene. *J. Org. Chem.* **1970**, *35*, 908–912.
- (39) Wittig, G.; Fritze, P. On the Intermediate Occurrence of 1,2-Cyclohexadiene. *Angew. Chem., Int. Ed.* **1966**, *5*, 846.
- (40) Angus, R. O., Jr.; Schmidt, M. W.; Johnson, R. P. Small-ring cyclic cumulenes: Theoretical studies of the structure and barrier to inversion of cyclic allenes. *J. Am. Chem. Soc.* **1985**, *107*, 532–537.
- (41) Daoust, K. J.; Hernandez, S. M.; Konrad, K. M.; Mackie, I. D.; Winstanley, J.; Johnson, R. P. Strain estimates for small-ring cyclic allenes and butatrienes. *J. Org. Chem.* **2006**, *71*, 5708–5714.
- (42) Nendel, M.; Tolbert, L. M.; Herring, L. E.; Islam, M. N.; Houk, K. N. Strained allenes as dienophiles in the Diels–Alder reaction: An experimental and computational study. *J. Org. Chem.* **1999**, *64*, 976–983.
- (43) Quintana, I.; Peña, D.; Pérez, D.; Guitián, E. Generation and reactivity of 1,2-cyclohexadiene under mild reaction conditions. *Eur. J. Org. Chem.* **2009**, *2009*, 5519–5524.

- (44) Lofstrand, V. A.; West, F. G. Efficient trapping of 1,2-cyclohexadienes with 1,3-dipoles. *Chem. Eur. J.* **2016**, *22*, 10763–10767.
- (45) Barber, J. S.; Styduhar, E. D.; Pham, H. V.; McMahon, T. C.; Houk, K. N.; Garg, N. K. Nitronc cycloadditions of 1,2-cyclohexadiene. *J. Am. Chem. Soc.* **2016**, *138*, 2512–2515.
- (46) Inoue, K.; Nakura, R.; Okano, K.; Mori, A. One-pot synthesis of silylated enol triflates from silyl enol ethers for cyclohexynes and 1,2-cyclohexadienes. *Eur. J. Org. Chem.* **2018**, *2018*, 3343–3347.
- (47) Hioki, Y.; Mori, A.; Okano, K. Steric effects on deprotonative generation of cyclohexynes and 1,2-cyclohexadienes from cyclohexenyl triflates by magnesium amides. *Tetrahedron* **2020**, *76*, 131112.
- (48) Xu, Q.; Hoye, T. R. A distinct mode of strain-driven cyclic allene reactivity: Group migration to the central allene carbon atom. *J. Am. Chem. Soc.* **2023**, *145*, 9867–9875.
- (49) Miyasaka, T. Cycloaddition reaction using highly strained 6-membered allenes. *J. Syn. Org. Chem. Jpn.*, **2024**, *82*, 63–64.
- (50) Lofstrand, V. A.; McIntosh, K. C.; Almeahadi, Y. A.; West, F. G. Strain-activated Diels–Alder trapping of 1,2-cyclohexadienes: Intramolecular capture by pendent furans. *Org. Lett.* **2019**, *21*, 6231–6234.

- (51) Almehmadi, Y. A.; West, F. G. A mild method for the generation and interception of 1,2-cycloheptadienes with 1,3-dipoles. *Org. Lett.* **2020**, *22*, 6091–6095.
- (52) Wang, B.; Constantin, M.-G.; Singh, S.; Zhou, Y.; Davis, R. L.; West, F. G. Generation and trapping of electron-deficient 1,2-cyclohexadienes. Unexpected hetero-Diels–Alder reactivity. *Org. Biomol. Chem.* **2021**, *19*, 399–405.
- (53) Jankovic, C. L.; West, F. G. 2 + 2 Trapping of acyloxy-1,2-cyclohexadienes with styrenes and electron-deficient olefins. *Org. Lett.* **2022**, *24*, 9497–9501.
- (54) Jankovic, C. L.; McIntosh, K. C.; Lofstrand, V. A.; West, F. G. Stereoselective intramolecular [2+2] trapping of 1,2-cyclohexadienes: A route to rigid, angularly fused tricyclic scaffolds. *Chem. Eur. J.* **2023**, *29*, e202301668.
- (55) Westphal, M. V.; Hudson, L.; Mason, J. W.; Pradeilles, J. A.; Zécéri, F. J.; Briner, K.; Schreiber, S. L. Water-compatible cycloadditions of oligonucleotide-conjugated strained allenes for DNA-encoded library synthesis. *J. Am. Chem. Soc.* **2020**, *142*, 7776–7782.
- (56) Barber, J. S.; Yamano, M. M.; Ramirez, M.; Darzi, E. R.; Knapp, R. R.; Liu, F.; Houk, K. N.; Garg, N. K. Diels–Alder cycloadditions of strained azacyclic allenes. *Nat. Chem.* **2018**, *10*, 953–960.

- (57) Yamano, M. M.; Knapp, R. R.; Ngamnithiporn, A.; Ramirez, M.; Houk, K. N.; Stoltz, B. M.; Garg, N. K. Cycloadditions of oxacyclic allenes and a catalytic asymmetric entryway to enantiomeriched cyclic allenes. *Angew. Chem., Int. Ed.* **2019**, *58*, 5653–5657.
- (58) Chari, J. V.; Ippoliti, F. M.; Garg, N. K. Concise approach to cyclohexyne and 1,2-cyclohexadiene precursors. *J. Org. Chem.* **2019**, *84*, 3652–3655.
- (59) McVeigh, M. S.; Kelleghan, A. V.; Yamano, M. M.; Knapp, R. R.; Garg, N. K. Silyl tosylate precursors to cyclohexynes, 1,2-cyclohexadienes, and 1,2-cycloheptadiene. *Org. Lett.* **2020**, *22*, 4500–4504.
- (60) Yamano, M. M.; Kelleghan, A. V.; Shao, Q.; Giroud, M.; Simmons, B. J.; Li, B.; Chen, S.; Houk, K. N.; Garg, N. K. Interception fleeting cyclic allenes with asymmetric nickel catalysis. *Nature* **2020**, *586*, 242–247.
- (61) Ramirez, M.; Svatunek, D.; Liu, F.; Garg, N. K.; Houk, K. N. Origins of *endo* selectivity in Diels–Alder reactions of cyclic allene dienophiles. *Angew. Chem., Int. Ed.* **2021**, *60*, 14989–14997.
- (62) Kelleghan, A. V.; Witkowski, D. C.; McVeigh, M. S.; Garg, N. K. Palladium-catalyzed annulations of strained cyclic allenes. *J. Am. Chem. Soc.* **2021**, *143*, 9338–9342.
- (63) McVeigh, M. S.; Garg, N. K. Interception of 1,2-cyclohexadiene with TEMPO radical. *Tetrahedron Lett.* **2021**, *87*, 153539–153543.

- (64) Witkowski, D. C.; McVeigh, M. S.; Scherer G. M.; Anthony, S. M.; Garg, N. K. Catalyst-controlled annulation of strained cyclic allenes with π -allylpalladium complexes. *J. Am. Chem. Soc.* **2023**, *145*, 10491–10496.
- (65) Mehta, M. M.; Gonzalez, J. A. M.; Bachman, J. L.; Garg, N. K. Cyclic allene approach to the manzamine alkaloid keramaphidin B. *Org. Lett.* **2023**, *25*, 5553–5557.
- (66) Kelleghan, A. V.; Tena-Meza, A.; Garg, N. K. Generation and reactivity of unsymmetrical strained heterocyclic allenes. *Nat. Synth.* **2023**, In Press, DOI: <https://doi.org/10.1038/s44160-023-00432-1>
- (67) Roberts, C. C. Strained allenes for heterocyclic difunctionalization. *Nat. Synth.* **2024**, In Press, DOI: <https://doi.org/10.1038/s44160-023-00455-8>.
- (68) Ippoliti, F. M.; Adamson, N. J.; Wonilowicz, L. G.; Nasrallah, D. J.; Darzi, E. R.; Donaldson, J. S.; Garg, N. K. Total synthesis of lissodendoric acid A via stereospecific trapping of a strained cyclic allene. *Science* **2023**, *379*, 261–265.
- (69) Christl, M. Cyclic allenes up to seven-membered rings. *Modern Allene Chemistry*; Krause, N., Kashmi, S. A. K., Eds.; Wiley-VCH: Weinheim, 2004; pp 243–357.
- (70) Bottini, A. T.; Hilton, L. L.; Plott, J. Relative reactivities of 1,2-cyclohexadiene with conjugated dienes and styrene. *Tetrahedron* **1975**, *31*, 1997–2001.

- (71) Harnos, S.; Tivakornpannarai, S.; Waali, E. E. The addition of 1,2-cyclohexadiene to substituted styrenes. *Tetrahedron Lett.* **1986**, *27*, 3701–3704.
- (72) Christl, M.; Schreck, M. 7-Arylbicyclo[4.2.0]oct-1-ene – Synthese durch [2 + 2]-cycloadditionen von 1,2-cyclohexadien sowie 1-methyl-1,2-cyclohexadien und thermische äquilibrierung der *exo/endo*-isomeren. *Chem. Ber.* **1987**, *120*, 915–920.
- (73) Elliot, R. L.; Takle, A. K.; Tyler J. W.; White, J. Cycloadditions of cephalosporins. A general synthesis of novel 2,3-fused cyclobutane and cyclobutene cephems. *J. Org. Chem.* **1993**, *58*, 6954–6955.
- (74) Kelleghan, A. V.; Bulger, A. S.; Witkowski, D. C.; Garg, N. K. Strain-promoted reactions of 1,2,3-cyclohexatriene and its derivatives. *Nature* **2023**, *618*, 748–754.
- (75) Peterson, E. A.; Overman, L. E. Contiguous stereogenic quaternary carbons: A daunting challenge in natural product synthesis. *Proc. Natl. Acad. Sci. U. S. A.* **2004**, *101*, 11943–11948.
- (76) Caille, S.; Cui, S.; Faul, M. M.; Mennen, S. M.; Tedrow, J. S.; Walker, S. D. Molecular complexity as a driver for chemical process innovation in the pharmaceutical industry. *J. Org. Chem.* **2019**, *84*, 4583–4603.

- (77) Cyclic allene cycloadducts typically contain a high degree of saturation, as well an additional stereocenter when compared to analogous products of other strained intermediates, such as **5.7a–5.7d**.
- (78) Hiesinger, K.; Dar'in, D.; Proschak, E.; Krasavin, M. Spirocyclic scaffolds in medicinal chemistry. *J. Med. Chem.* **2021**, *64*, 150–183.
- (79) Oxacyclic allene **5.13** was chosen for this study due to a number of factors, such as the ready availability of its precursor, **5.12**, the ease of heterocyclic allene generation at ambient temperatures, and that its use results in heterocyclic products.
- (80) The variation in observed diastereoselectivities is not presently understood but will be the subject of further investigation.
- (81) Enamines and hetaryl-substituted alkenes have rarely been studied in reactions with strained cyclic allenes and therefore presented an opportunity for discovery. Furthermore, styrenyl substrates, such as **5.26** and heterocyclic variants, are readily accessible.
- (82) We postulate that reactions proceed by a stepwise mechanism, analogous to what has been proposed for the trapping of 1,2-cyclohexadiene with styrenes (ref 69). The observed regioselectivity is consistent with a mechanism involving: a) initial C–C bond formation between the central carbon of the cyclic allene and terminal position of the alkene trapping partner, leading to a stabilized diradical intermediate and b) radical recombination to form

the cyclobutyl ring. Although further studies are ongoing, kinetic isotope effect (KIE) experiments at natural abundance are consistent with this hypothesis.

- (83) These conditions proved more efficient, as they enabled the use of fewer equivalents of trapping partners and led to their improved solubility in some instances; see Section 5.10.2.4 for reaction optimization details.
- (84) Carpino, L. A.; Sau, A. C. Convenient source of ‘naked’ fluoride: Tetra-*n*-butylammonium chloride and potassium fluoride dihydrate. *J. Chem. Soc., Chem. Commun.* **1979**, 514–515.
- (85) Feng, M.; Tang, B.; Wang, N.; Xu, H.-X.; Jiang, X. Ligand controlled regiodivergent C1 insertion on arynes for construction of phenanthridinone and acridone alkaloids. *Angew. Chem., Int. Ed.* **2015**, *54*, 14960–14964.
- (86) The observed stereospecificity may indicate that the relative rate of the second C–C bond formation is faster than a s-bond rotation. However, we cannot rule out s-bond rotation occurring rapidly, with the distribution of products correlating with the kinetic barriers for each cyclization pathway.
- (87) The reaction is thought to proceed via a stepwise mechanism (see footnote 82). The presence of the *gem*-dimethyl group is thought to raise the kinetic barrier for formation of the second C–C bond (i.e., C6–C4’ forming bond of **5.41**), leading to a less selective reaction when compared to the formation of **5.25**.

- (88) Algi, F.; Özen, R.; Balci, M. The first generation and trapping of a five-membered ring allene: 2-dehydro-3a,4,5,6,6a-pentahydropentalene. *Tetrahedron Lett.* **2002**, *43*, 3129–3131.
- (89) Ceylan, M.; Yalçın, S.; Seçen, H.; Sütbeyaz, Y.; Balci, M. Evidence for the formation of a new five-membered ring cyclic allene: generation of 1-cyclopenta-1,2-dien-1-ylbenzene. *J. Chem. Research (S)* **2003**, 21–23.
- (90) Similar regioselectivity in [2+2] cycloadditions of substituted cyclic allenes was observed by West; see ref. 53
- (91) Of note, 2.0 equivalents of trapping partner **5.38** and 1.7 equivalents of trapping partner **5.79** were used in their respective transformations, highlighting that large excesses of trapping partner are not strictly required for this methodology.
- (92) Yu, X.; Seo, S.-Y.; Marks, T. J. Effective, selective hydroalkoxylation/cyclization of alkynyl and allenyl alcohols mediated by lanthanide catalysts. *J. Am. Chem. Soc.* **2007**, *129*, 7244–7245.
- (93) Kumar, P.; Zainul, O.; Laughlin, S. T. Inexpensive multigram-scale synthesis of cyclic enamines and 3-*N* spirocyclopropyl systems. *Org. Biomol. Chem.* **2018**, *16*, 652–656.

- (94) Radovan, S.; Pizzuti, M.-G.; Boersma, A. J.; Minnaard, A. J.; Feringa, B. L. Catalytic enantioselective conjugate addition of dialkylzinc reagents to *N*-substituted-2,3-dehydro-4-piperidones. *Chem. Commun.* **2005**, 1711–1713.
- (95) Ma, Y.; Lv, J.; Liu, C.; Yao, X.; Yan, G.; Yu, W.; Ye, J. Electrochemical [4+2] annulation-rearrangement-aromatization of styrenes: Synthesis of naphthalene derivatives. *Angew. Chem., Int. Ed.* **2019**, *58*, 6756–6760.
- (96) Longshaw, A. I.; Thomas, E. J. Synthesis of 5-acyl-4-methylene-1,2,3,4-tetrahydropyridines. *ARKIVOC* **2021**, *6*, 69–85.
- (97) Thullen, S. M.; Rubush, D. M.; Rovis, T. A photochemical two-step formal [5+2] cycloaddition: A condensation-ring-expansion approach to substituted azepanes. *Synlett* **2017**, *28*, 2755–2758.
- (98) Piotrowski, A. M.; Malpass, D. B.; Boleslawski, M. P.; Eisch, J. J. Organometallic compounds of Group III. Part 43. Alkylenation with geminal dialuminoalkane reagents: The synthesis of olefins from ketones. *J. Org. Chem.* **1988**, *53*, 2829–2835.
- (99) Khan, A.; Silva Jr., L. F.; Rabnawaz, M. Iodine(III)-promoted ring expansion reactions: A metal-free approach toward seven-membered heterocyclic rings. *Asian J. Org. Chem.* **2021**, *10*, 2549–2552.

- (100) Justik, M.; Koser, G. Application of [hydroxy(tosyloxy)iodo]benzene in the Wittig-ring expansion sequence for the synthesis of β -benzocycloalkenones from α -benzocycloalkenones. *Molecules* **2005**, *10*, 217–225.
- (101) Liu, H.; Ge, L.; Wang, D.-X.; Chen, N.; Feng, C. Photoredox-coupled F-nucleophilic addition: Allylation of gem-difluoroalkenes. *Angew. Chem., Int. Ed.* **2019**, *58*, 3918–3922.
- (102) Harrowven, D. C.; Stenning, K. J.; Whiting, S. W.; Thompson, T.; Walton, R. CH activation and CH₂ double activation of indolines by radical translocation: Understanding the chemistry of the indoliny radical. *Org. Biomol. Chem.* **2011**, *9*, 4882–4885.
- (103) Huang, C.; Zhang, Z.; Zhang, Y.; Yang, W.; Sun, W. Dimethyl substituted constrained cyclopyridine imine nickel complex and intermediate, preparation process and application thereof. CN106478740, March 4, 2017.
- (104) Sheldrick, G. M. (1996). *SADABS*. University of Göttingen, Germany.
- (105) Sheldrick, G. M. Crystal structure refinement with SHELXL. *Acta Cryst. C* **2015**, *71*, 3–8.
- (106) Spartan'20 Wavefunction, Inc., Irvine, CA.
- (107) Becke, A. D. Density-functional thermochemistry. III. The role of exact exchange. *J. Chem. Phys.* **98**, 5648 (1993).

CHAPTER SIX

Silyl Tosylate Precursors to Cyclohexyne, 1,2-Cyclohexadiene, and 1,2-Cycloheptadiene

Matthew S. McVeigh, Andrew V. Kelleghan, Michael M. Yamano,

Rachel R. Knapp, and Neil K. Garg

Org. Lett. **2020**, *22*, 4500–4504.

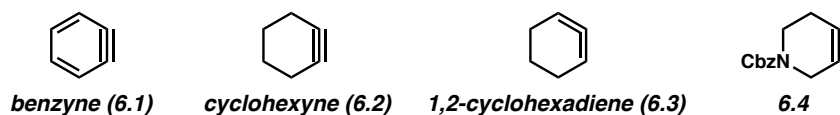
6.1 Abstract

Transient strained cyclic intermediates have become valuable intermediates in modern synthetic chemistry. Although silyl triflate precursors to strained intermediates are most often employed, the instability of some silyl triflates warrants the development of alternative precursors. We report the syntheses of silyl tosylate precursors to cyclohexyne, 1,2-cyclohexadiene, and 1,2-cycloheptadiene. The resultant strained intermediates undergo trapping in situ to give cycloaddition products. Additionally, the results of competition experiments between silyl triflates and silyl tosylates are reported.

6.2 Introduction

The chemistry of transient strained cyclic intermediates has been a popular topic of study for over a century.¹ Early efforts in the field established the existence of benzyne (**6.1**),² cyclohexyne (**6.2**),³ and 1,2-cyclohexadiene (**6.3**)⁴ through pioneering studies conducted by Roberts and Wittig in the 1950s and 1960s (Figure 6.1). Since their discovery, these species, along with their heterocyclic derivatives (e.g., **6.4**) have been employed in a host of synthetic applications spanning natural product synthesis,^{1c,1d,1i,5} heterocycle construction,^{1e,1g,1h,6} and materials chemistry,^{1e,7} as exemplified by the syntheses of **6.5–6.7**.

Key Strained Intermediates:



Applications:

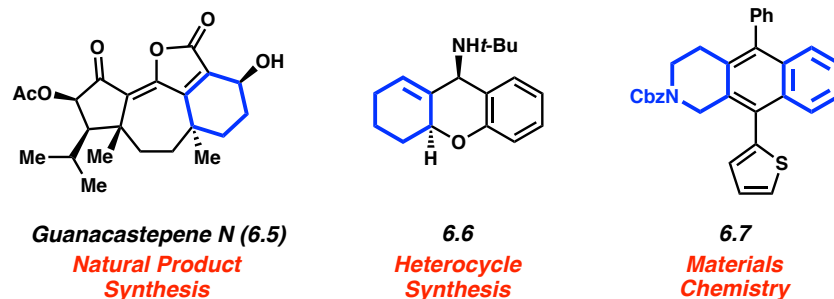


Figure 6.1. Strained cyclic intermediates and selected synthetic applications.

Many of the advanced synthetic applications of strained cyclic intermediates have been enabled by the use of silyl triflates as precursors. Initially developed by Kobayashi as precursors to benzyne (**6.1**),⁸ silyl triflates have since become the most commonly employed precursors for accessing arynes, nonaromatic cyclic alkynes, and cyclic allenes.^{1,9,10} However, we have encountered difficulties in preparing certain functionalized strained cyclic allene and alkyne precursors due to the instability of the corresponding silyl triflates. This instability can be attributed to the ease of triflate dissociation and cation formation in related systems.^{11,12}

With the aim of circumventing silyl triflate instability and accessing a wider range of strained intermediates under Kobayashi-type conditions, we sought to develop new precursors to cyclic alkynes and allenes (i.e., **6.2** and **6.3**, Figure 6.2). As mentioned above, the most common means to access **6.2** and **6.3** is via the corresponding silyl triflates (e.g., **6.8** and **6.10**, respectively) using fluoride-induced elimination. Encouraged by the success of silyl tosylates as aryne precursors,¹³ we sought to develop silyl tosylate cyclic alkyne and allene precursors **6.9** and **6.11**, respectively.¹⁴ We hypothesized that the diminished leaving group ability of a tosylate

anion relative to a triflate¹⁵ could alleviate difficulties associated with vinyl triflate instability, while retaining sufficient reactivity to form the desired strained intermediates.¹³ These alternative precursors could also allow for new synthetic methods that leverage the differences in reactivity between tosylates and triflates.¹⁶ Furthermore, we hoped that silyl tosylates **6.9** and **6.11** would be crystalline,¹⁷ in contrast to silyl triflates which are often oils. This characteristic could facilitate their purification and use in process chemistry. Herein, we describe the preparation, validation, and synthetic application of the desired silyl tosylates as strained intermediate precursors.

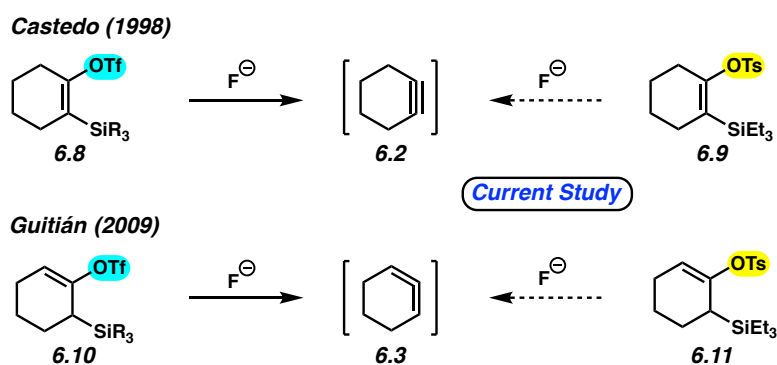


Figure 6.2. Silyl triflate (previous) and silyl tosylate (current) precursors to **6.2** and **6.3**.

6.3 Synthesis of Silyl Tosylate Precursors to Cyclohexyne and 1,2-Cyclohexadiene

Our first objective was to develop synthetic routes to the requisite silyl tosylates, which led to the preparation of **6.9** and **6.11** as shown in Figure 6.3. Following literature procedures,¹⁸ cyclohexanone (**6.12**) was converted to silyl ketone **6.14** in good yield through a sequence involving silyl enol ether formation (**6.12**→**6.13**) and allylic deprotonation/retro-Brook rearrangement (**6.13**→**6.14**). From common intermediate **6.14**, deprotonation under either thermodynamic or kinetic control, followed by quenching with *p*-toluenesulfonic anhydride, generated silyl tosylates **6.9** and **6.11**, respectively. Gratifyingly, both alkyne precursor **6.9** and allene precursor **6.11** were obtained as crystalline solids and could be prepared on gram-scale.

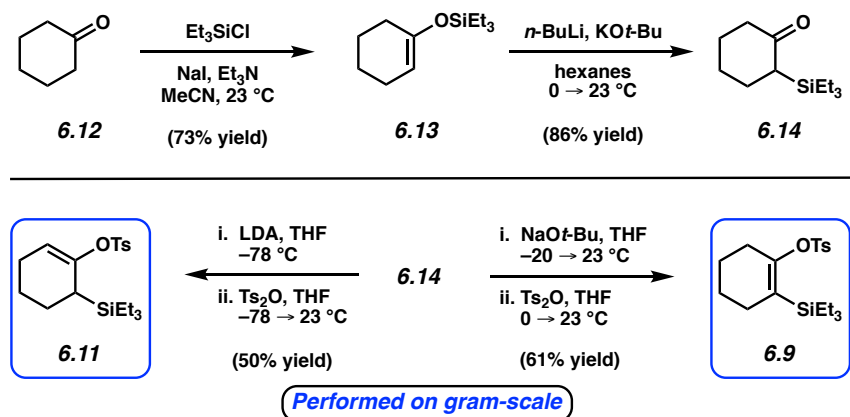


Figure 6.3. Syntheses of silyl tosylates **6.9** and **6.11**.

6.4 Comparing Silyl Tosylates and Silyl Triflates as Precursors to Cyclohexyne

As shown in Table 6.1, we found that silyl tosylate **6.9** serves as a viable precursor to generate cyclohexyne (**6.2**) with in situ trapping. It should be noted that our initial attempts to generate **6.2** from **6.9** using CsF (based on literature conditions for the corresponding trimethylsilyl triflate^{6b}) led to the recovery of unreacted **6.9**. However, the use of the more soluble fluoride source tetrabutylammonium fluoride (TBAF) proved fruitful and enabled the generation of **6.2** in situ. Trapping with diene **6.16** furnished oxabicyclo **6.17** via a (4+2) cycloaddition (entry 1). Similarly, the use of nitrene **6.18** as the trapping agent gave rise to isoxazolidine **6.19** by way of a (3+2) cycloaddition (entry 2). In both cases, yields were comparable to those observed using a silyl triflate precursor.^{6b,18b} Lastly, nucleophilic trapping of **6.2** with imidazole (**6.20**) proved successful, generating vinyl imidazole **6.21** in moderate yield.¹⁹ These trapping experiments demonstrate that silyl tosylate **6.9** serves as an effective precursor to **6.2**, rendering **6.9** a useful intermediate for the synthesis of heterocyclic products.

Table 6.1. Silyl tosylate **6.9** as a precursor to cyclohexyne (**6.2**).

Entry	Trapping Agent	Product	Yield ^a (Lit. yield from 6.8) ^b
1			76% (78%)
2			69% (61%)
3			53% (81%)

General conditions: silyl tosylate **6.9** (1.0 equiv, 0.14 mmol), trapping agent (1.5–3.0 equiv), TBAF (5.0 equiv), and THF (0.07 M) heated in a sealed vial under an atmosphere of N₂.

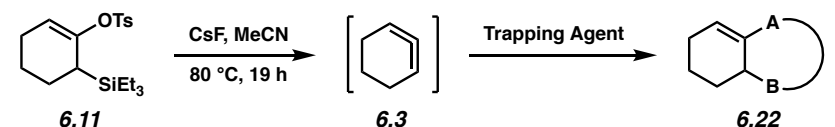
^aIsolated yields. ^bLiterature isolated yields under comparable reaction conditions when using **6.8**

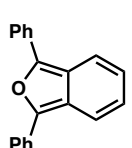
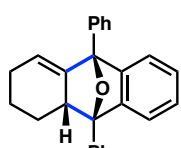
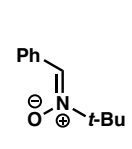
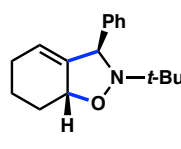
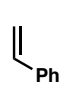
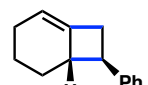
6.5 Comparing Silyl Tosylates and Silyl Triflates as Precursors to 1,2-Cyclohexadiene

We also investigated silyl tosylate **6.11** as a precursor to strained cyclic allene **6.3** (Table 6.2). In contrast to our observations in reactions of alkyne precursor **6.9**, CsF could be utilized to induce strained intermediate formation from silyl tosylate **6.11** under the same conditions reported in the literature for the corresponding silyl triflate **6.10** (R = Et).^{6a} We were delighted to find that silyl tosylate **6.11** could be employed in (4+2), (3+2), and (2+2) cycloadditions to deliver **6.23**, **6.24**, and **6.26**, respectively (entries 1–3). In all cases, yields and diastereomeric ratios were consistent with those reported in the literature for reactions employing silyl triflate

6.10 (R = Et).^{6a,18b,20} The synthesis of isoxazolidine **6.24** was also carried out on mmol-scale to demonstrate scalability.

Table 6.2. Silyl tosylate **6.11** as a precursor to 1,2-cyclohexadiene (**6.3**).



Entry	Trapping Agent	Product	Yield ^a (Lit. Yield from 6.10) ^b d.r. ^c (Lit. d.r.)
1			78% (83%) 2.7:1 (2.4:1)
2			80% (88%) 9.3:1 (8.9:1) 78%, 9.0:1 d.r. on mmol-scale
3			91% ^d (76%) ^e 2.0:1 (2.2:1)

General conditions: silyl tosylate **6.11** (1.0 equiv, 0.14 mmol), trapping agent (1.0–5.0 equiv), CsF (5.0 equiv), and MeCN (0.1 M) heated in a sealed vial under an atmosphere of N₂. ^aIsolated yields. ^bLiterature isolated yields and diastereomeric ratios under comparable reaction conditions when using **6.10** (R = Et). ^cDiastereomeric ratios determined by ¹H NMR analysis of the crude reaction mixture. ^dYield determined by ¹H NMR analysis using an external standard. ^eCyclic allene generated from 6,6-dibromobicyclo[3.1.0]hexane.

6.6 Preparation of a Precursor to 1,2-Cycloheptadiene and its Subsequent Trapping

Having established silyl tosylates as effective substitutes for silyl triflates, we sought to extend this alternative method of strained intermediate generation to address a particular shortcoming in silyl triflate chemistry. As mentioned earlier, silyl triflates can sometimes be unstable due to their pronounced leaving group ability.^{11,12} We have observed this type of

instability when attempting to synthesize a silyl triflate precursor to 1,2-cycloheptadiene (**6.29**) (Figure 6.4).²¹ Alternatively, silyl tosylate **6.28**, accessible in three steps from **6.27** (see section 6.9.2.4 for details), could be obtained as a crystalline solid. Treatment of **6.28** with isobenzofuran **6.16** under standard conditions for cyclic allene generation and trapping afforded oxabicyclo **6.30** in excellent yield via the intermediacy of cyclic allene **6.29**. This example demonstrates that silyl tosylates can be used to expand the scope of strained intermediates accessible under mild fluoride-based conditions.²²

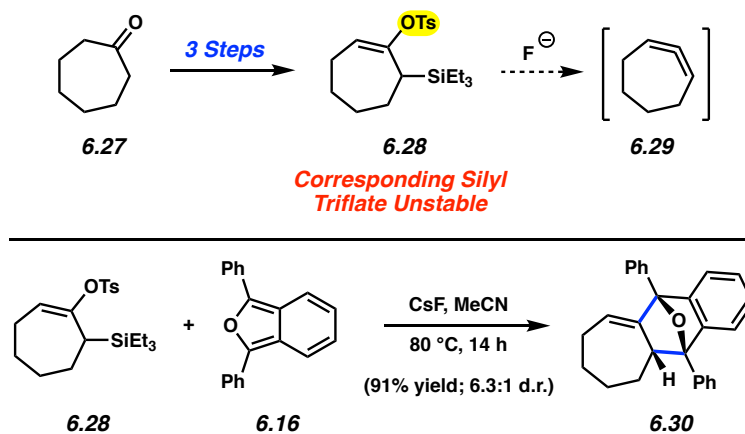


Figure 6.4. Silyl tosylate **6.28** to access 1,2-cycloheptadiene (**6.29**).

6.7 Competition Experiments Between Silyl Triflates and Silyl Tosylates

Finally, two key experiments were performed to compare the relative reactivity of our silyl tosylates to the corresponding silyl triflates (Figure 6.5). In the first, equimolar amounts of silyl triflate **6.8a** and silyl tosylate **6.9**, both precursors to cyclohexyne (**6.2**), were treated with nitrene **6.18** under CsF-based reaction conditions. We observed that silyl triflate **6.8a** reacted selectively over silyl tosylate **6.9** to generate cycloadduct **6.19**. Silyl tosylate **6.9** did not react under these conditions. An analogous competition experiment was performed using silyl triflate **6.10a** and silyl tosylate **6.11**, both of which serve as precursors to 1,2-cyclohexadiene (**6.3**). This led to the efficient formation of **6.24** and the nearly quantitative retention of silyl tosylate **6.11**.

The preferential reactivity of the silyl triflate in both cases can be rationalized based on the relative leaving group abilities of the triflate and tosylate anions.¹⁵ This observed selectivity should prove useful in synthetic applications, analogous to prior studies in which multiple strained intermediates have been generated sequentially to synthesize complex polycyclic products.⁷

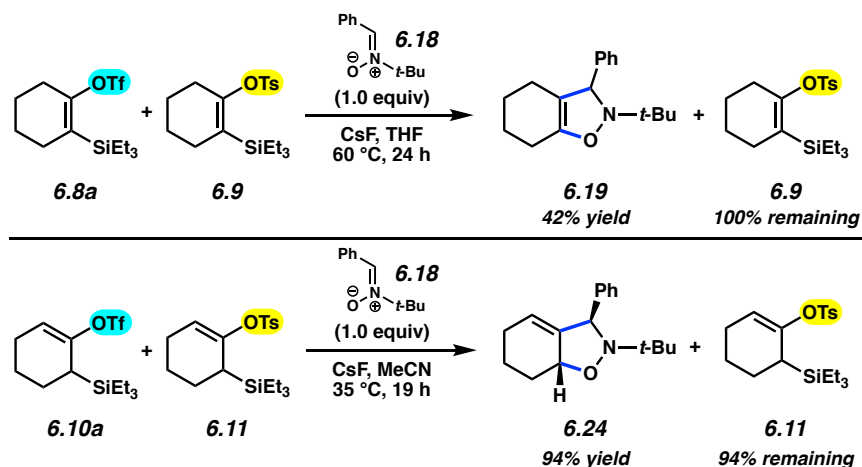


Figure 6.5. Competition experiments between silyl triflate and silyl tosylate strained intermediate precursors. Yields determined by ¹H NMR analysis with external standard.

6.8 Conclusion

In summary, we have developed scalable syntheses of silyl tosylate precursors to the transient strained intermediates cyclohexyne (**6.2**), 1,2-cyclohexadiene (**6.3**), and 1,2-cycloheptadiene (**6.29**). Our synthetic routes to these precursors generate crystalline silyl tosylates, an attribute that could prove useful to process chemists. The silyl tosylate strained intermediate precursors not only replicate the chemistry attained using silyl triflates, but also can allow access to strained intermediates inaccessible using known silyl triflate chemistry, as exemplified by silyl tosylate **6.28**. Furthermore, competition experiments demonstrate that silyl triflate precursors to **6.2** and **6.3** react chemoselectively in the presence of their silyl tosylate counterparts. This selectivity should prove useful in synthetic design. Collectively, these studies

demonstrate the synthetic utility of silyl tosylates as precursors to transient strained intermediates.

6.9 Experimental Section

6.9.1 Materials and Methods

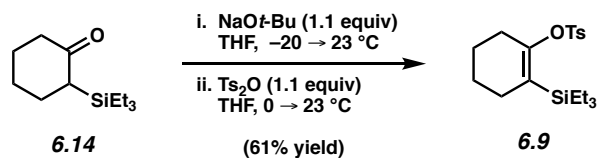
Unless stated otherwise, reactions were conducted in flame-dried glassware under an atmosphere of nitrogen using anhydrous solvents (passed through activated alumina columns). All commercially obtained reagents were used as received unless otherwise specified. Imidazole (**6.20**), *p*-toluenesulfonic anhydride (Ts₂O), *n*-butyllithium (*n*-BuLi), tetrabutylammonium fluoride (TBAF), and potassium *tert*-butoxide (KO*t*-Bu) were obtained from Sigma-Aldrich. Sodium *tert*-butoxide (NaO*t*-Bu), 1,3-diphenylisobenzofuran (**6.16**), *N-tert*-butyl- α -phenylnitrene (**6.18**), and 1,3,5-trimethoxybenzene were obtained from Alfa Aesar. Styrene (**6.25**) was obtained from Fisher Scientific and filtered through basic alumina prior to use. Cesium fluoride (CsF) was obtained from Strem Chemicals. Diisopropylamine was obtained from Acros Organics and distilled over CaH₂ prior to use. Reaction temperatures were controlled using an IKAmag temperature modulator, and reactions were performed at room temperature (approximately 23 °C) unless otherwise stated. Thin-layer chromatography (TLC) was conducted with EMD gel 60 F254 pre-coated plates (0.25 mm for analytical chromatography and 0.50 mm for preparative chromatography) and visualized using a combination of UV, anisaldehyde, and potassium permanganate staining techniques. Silicycle Siliaflash P60 (particle size 0.040–0.063 mm) was used for flash column chromatography. ¹H NMR spectra were recorded on Bruker spectrometers (500 and 600 MHz) and are reported relative to residual solvent signals. Data for ¹H NMR spectra are reported as follows: chemical shift (δ ppm), multiplicity, coupling constant (Hz), integration. Data for ¹³C NMR are reported in terms of chemical shift (at 125 MHz). IR

spectra were recorded on a Perkin-Elmer UATR Two FT-IR spectrometer and are reported in terms of absorption frequency (cm^{-1}). DART-MS spectra were collected on a Thermo Exactive Plus Orbitrap (Thermo Scientific) equipped with an ID-CUBE ion source and a Vapor Interface (IonSense Inc.). Both the source and MSD were controlled by Excalibur software v. 3.0. The analyte was spotted onto OpenSpot sampling cards (IonSense Inc.) using CH_2Cl_2 as the solvent. Ionization was accomplished using UHP He plasma with no additional ionization agents. The mass calibration was carried out using Pierce LTQ Velos ESI (+) and (-) Ion calibration solutions (Thermo Fisher Scientific).

*Note: The syntheses of silyl triflates **6.8a** and **6.10a**,^{18b} silyl ketone **6.14**,^{18b} and silyl enol ether **6.31**²³ have been published, and spectral data match those previously reported.*

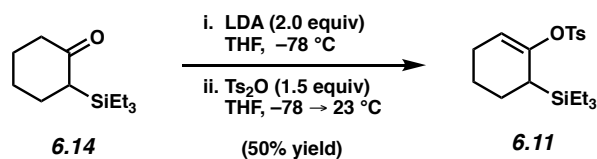
6.9.2 Experimental Procedures

6.9.2.1 Syntheses of Silyl Tosylates **6.9** and **6.11**



Silyl Tosylate 6.9. To a stirring suspension of sodium *tert*-butoxide (498 mg, 5.18 mmol, 1.1 equiv) in THF (5 mL) at $-20\text{ }^{\circ}\text{C}$ was added silyl ketone **6.14** (1.00 g, 4.71 mmol, 1.0 equiv) in THF (5 mL) via cannula addition over 5 min. The resulting dark orange-red solution was then warmed to $0\text{ }^{\circ}\text{C}$ and stirred for 1 h. Next, the ice bath was removed, and the solution was stirred at $23\text{ }^{\circ}\text{C}$ for 30 min, then recooled to $0\text{ }^{\circ}\text{C}$. *p*-Toluenesulfonic anhydride (1.69 g, 5.18 mmol, 1.1 equiv) in THF (7.0 mL) was then added over 7 min. The cooling bath was removed, and the off-

white, heterogeneous solution was stirred at 23 °C for 5 h before being quenched with sat. aqueous NaHCO₃ (20 mL). The layers were separated and the aqueous layer was extracted with diethyl ether (3 x 20 mL). The organic layers were combined, washed sequentially with deionized H₂O (1 x 20 mL) and brine (1 x 20 mL), dried with Na₂SO₄, and concentrated under reduced pressure. The crude reaction mixture was purified via column chromatography (3:97 Et₂O:hexanes) to provide silyl tosylate **6.9** (1.06 g, 61% yield) as a white, crystalline solid. Silyl tosylate **6.9**: R_f 0.55 (9:1 hexanes:EtOAc); ¹H NMR (500 MHz, CDCl₃): δ 7.82–7.79 (m, 2H), 7.34–7.30 (m, 2H), 2.44 (s, 3H), 2.23–2.20 (m, 2H), 2.11–2.06 (m, 2H), 1.64–1.58 (m, 2H), 1.53–1.47 (m, 2H), 0.88 (t, *J* = 8.1, 9H), 0.61 (q, *J* = 7.5, 6H); ¹³C NMR (125 MHz, CDCl₃): δ 154.5, 144.4, 135.8, 129.6, 127.6, 121.9, 28.8, 28.2, 23.0, 22.1, 21.7, 7.5, 3.1; IR (film): 2950, 2875, 1642, 1368, 1191 cm⁻¹; HRMS–APCI (*m/z*) [M + H]⁺ calcd for C₁₉H₃₁O₃SSi⁺, 367.1755; found 367.1754.

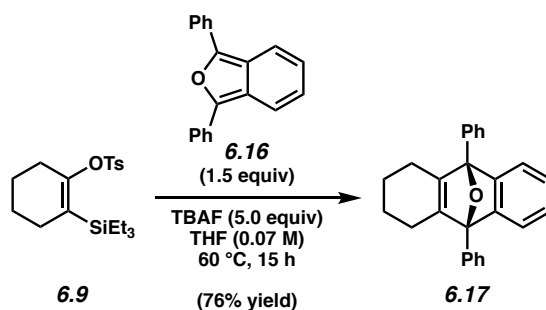


Silyl Tosylate 6.11. To a stirring solution of diisopropylamine (1.41 mL, 9.88 mmol, 2.1 equiv) in THF (14 mL) at –78 °C was added *n*-butyllithium (2.50 M in hexanes, 3.78 mL, 9.44 mmol, 2.0 equiv) dropwise over 3 min. After stirring for 20 min, the reaction was warmed to 23 °C and stirred for 10 min, before recooling the reaction to –78 °C. Next, silyl ketone **6.14** (1.00 g, 4.72 mmol, 1.0 equiv) in THF (14 mL) was added dropwise via cannula addition over 10 min. The resulting pale-yellow solution was stirred for 1 h. Then, a solution of *p*-toluenesulfonic anhydride (2.31 g, 7.08 mmol, 1.5 equiv) in THF (18 mL) was added dropwise via cannula addition over 6 min. The cooling bath was allowed to melt, gradually warming the reaction to 23 °C over 18 h, at which point it was quenched with sat. aqueous NaHCO₃ (40 mL). The layers

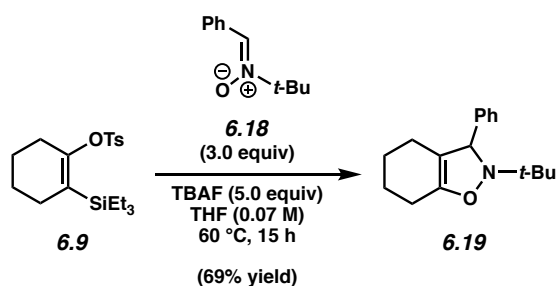
were separated and the aqueous layer was extracted with diethyl ether (3 x 40 mL). The combined organic layers were then dried over Na₂SO₄, filtered, and concentrated under reduced pressure to provide a yellow oil. The crude oil was passed through a silica plug (3:97 Et₂O:hexanes), and the eluate was concentrated to give a pale-yellow oil. This oil was dissolved in refluxing hexanes and cooled gradually to -78 °C over 4 h to induce crystallization. The crystals were filtered off, washed with cold hexanes, and the mother liquor was concentrated to give a clear oil. This oil was subjected to the same crystallization procedure, and both crops of crystals were combined to afford silyl tosylate **6.11** (860 mg, 50% yield) as a white, crystalline solid. Silyl tosylate **6.11**: R_f 0.57 (1:1 hexanes:benzene); ¹H NMR (500 MHz, CDCl₃): δ 7.78 (d, *J* = 8.1, 2H), 7.32 (d, *J* = 8.1, 2H), 5.19–5.16 (m, 1H), 2.45 (s, 3H), 2.01–1.90 (m, 2H), 1.82–1.74 (m, 2H), 1.62–1.56 (m, 1H), 1.53–1.45 (m, 1H), 1.36–1.27 (m, 1H), 0.92 (t, *J* = 7.9, 9H), 0.60 (q, *J* = 8.2, 6H); ¹³C NMR (125 MHz, CDCl₃): δ 151.4, 144.7, 133.5, 129.4, 128.5, 114.3, 25.5, 25.3, 24.1, 21.8, 21.7, 7.5, 3.0; IR (film): 2954, 2877, 1370, 1179, 1191 cm⁻¹; HRMS–APCI (*m/z*) [M + H]⁺ calcd for C₁₉H₃₁O₃SSi⁺, 367.1755; found 367.1758.

6.9.2.2 Cyclohexyne Trapping Experiments

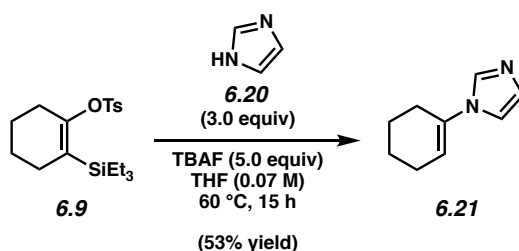
Representative Procedure 6.1 (Table 6.1, entry 1 is used as an example).



Cycloadduct 6.17. To a stirred solution of silyl tosylate **6.9** (49.6 mg, 135 μmol , 1.0 equiv), and 1,3-diphenylisobenzofuran (**6.16**) (54.9 mg, 203 μmol , 1.5 equiv) in THF (1.35 mL, 0.07 M) was added TBAF (1.0 M in THF, 677 μL , 677 μmol , 5.0 equiv). The reaction vessel was purged with N_2 , sealed with a teflon cap, and placed in a preheated, 60 $^\circ\text{C}$ aluminum heating block. After stirring for 15 h, the reaction was cooled to 23 $^\circ\text{C}$. The resultant yellow solution was filtered through a plug of silica gel (EtOAc eluent, 10 mL) and concentrated under reduced pressure to afford a crude yellow solid. Purification by preparative thin layer chromatography (3:2 benzene:hexanes) provided cycloadduct **6.17** (36.2 mg, 76% yield, average of two experiments) as a pale-yellow solid. Cycloadduct **6.17**: Spectral data match those previously reported.^{18b}



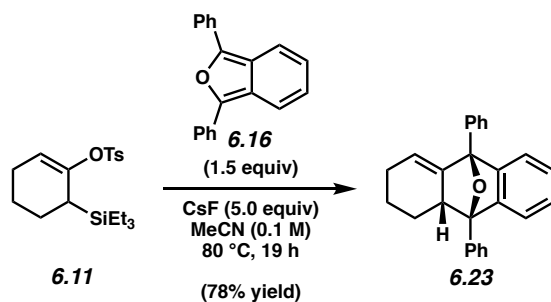
Cycloadduct 6.19. Followed Representative Procedure 6.1. Purification by preparative thin layer chromatography (9:1 Hexanes:EtOAc) provided cycloadduct **6.19** (24.2 mg, 69% yield, average of two experiments) as a white solid. Cycloadduct **6.19**: Spectral data match those previously reported.^{6b}



Imidazole adduct 6.21. Followed Representative Procedure 6.1. Purification by preparative thin layer chromatography (EtOAc) provided cycloadduct **6.21** (10.7 mg, 53% yield, average of two experiments) as an off-white solid. Imidazole adduct **6.21**: Spectral data match those previously reported.^{6b}

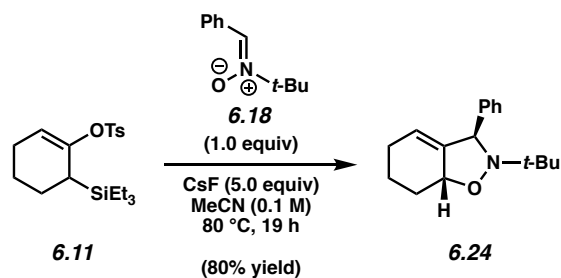
6.9.2.3 1,2-Cyclohexadiene Trapping Experiments

Representative Procedure 6.2 (Table 6.2, entry 1 is used as an example).

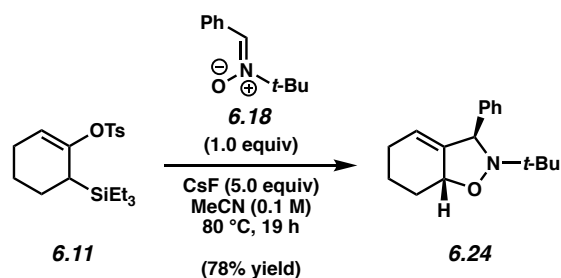


Cycloadduct 6.23. To a stirred solution of silyl tosylate **6.11** (49.7 mg, 136 μ mol, 1.0 equiv) and 1,3-diphenylisobenzofuran (**6.16**) (55.5 mg, 205 μ mol, 1.5 equiv) in MeCN (1.40 mL, 0.1 M) was added CsF (100 mg, 0.68 mmol, 5.0 equiv). The reaction vessel was purged with N₂, sealed with a teflon cap and teflon tape, and placed in a preheated, 80 °C aluminum heating block. The reaction was allowed to stir at this temperature for 19 h. After cooling to 23 °C, the yellow, heterogenous solution was filtered through a plug of silica gel (EtOAc eluent, 10 mL) and concentrated under reduced pressure to afford a crude yellow solid. Purification by preparative thin layer chromatography (2:1 hexanes:CH₂Cl₂ with 2% acetone) provided cycloadduct **6.23** as a pale-yellow solid (36.9 mg, 78% yield, 2.7:1 d.r. by ¹H NMR analysis of the crude material, average of two experiments). Cycloadduct **6.23**: Spectral data match those previously reported.^{18b}

Any modification of the conditions shown in the representative procedure above are specified in the following scheme

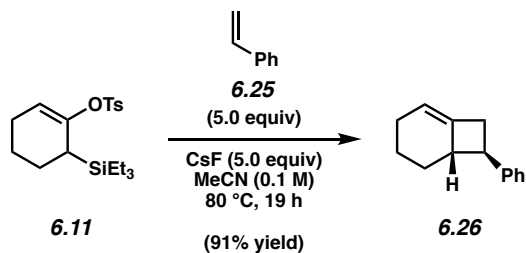


Cycloadduct 6.24. Followed Representative Procedure 6.2. Purification by preparative thin layer chromatography (1:1 hexanes:benzene) provided cycloadduct **6.24** as a white solid (30.2 mg, 80% yield, 9.3:1 d.r. by ¹H NMR analysis of the crude material, average of two experiments). Cycloadduct **6.24**: Spectral data match those previously reported.^{6a}



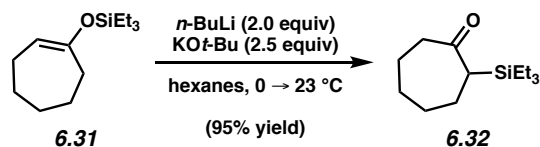
Cycloadduct 6.24 (mmol scale). To a stirred solution of silyl tosylate **6.11** (367 mg, 1.00 mmol, 1.0 equiv) and *N-tert-butyl- α -phenylnitronium* salt (**6.18**) (181 mg, 1.02 mmol, 1.0 equiv) in MeCN (10.0 mL, 0.1 M) was added CsF (761 mg, 5.01 mmol, 5.0 equiv). The reaction vessel was purged with N₂, sealed with a teflon cap and teflon tape, and placed in a preheated, 80 °C aluminum heating block. The reaction was allowed to stir at this temperature for 19 h. After cooling to 23 °C, the white, heterogenous solution was filtered through a plug of silica gel (EtOAc eluent, 30 mL) and concentrated under reduced pressure to afford a crude off-white solid. Purification by flash chromatography (4:1 to 1:1 hexanes:benzene) provided cycloadduct

6.24 as a white solid (200.2 mg, 78% yield, 9.0:1 d.r.). Cycloadduct **6.24**: Spectral data match those previously reported.^{6a}



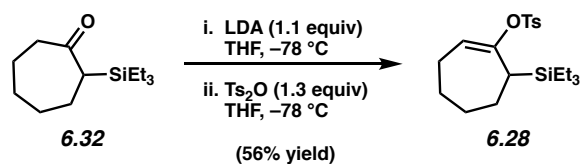
Cycloadduct 6.26. Followed a modified Representative Procedure 6.2 by adding 1,3,5-trimethoxybenzene as an external standard to the crude residue obtained by filtration of the reaction mixture. ¹H NMR analysis of this crude mixture showed cycloadduct **6.26** (91% yield, 2.0:1 d.r., average of two experiments). The volatility of **6.26** hampered isolation attempts. Cycloadduct **6.26**: Spectral data match those previously reported.²⁰

6.9.2.4 Synthesis of Silyl Tosylate 6.28



Silyl ketone 6.32. To a heterogeneous solution of potassium *tert*-butoxide (186 mg, 1.66 mmol, 2.5 equiv) in hexanes (1.3 mL) at 0 °C was added *n*-butyllithium (2.36 M in hexanes, 0.561 mL, 1.32 mmol, 2.0 equiv) dropwise over 2 min. The solution was removed from the ice bath and stirred at 23 °C for an additional 20 min. A solution of silyl enol ether **6.31** (150 mg, 0.662 mmol, 1.0 equiv) in hexanes (1.3 mL) was then added dropwise over 5 min and stirred at 23 °C. After stirring for 2 h, deionized H₂O (5.0 mL) was added to the reaction, and the aqueous layer was extracted with diethyl ether (3 x 5 mL). The combined organic layers were dried over

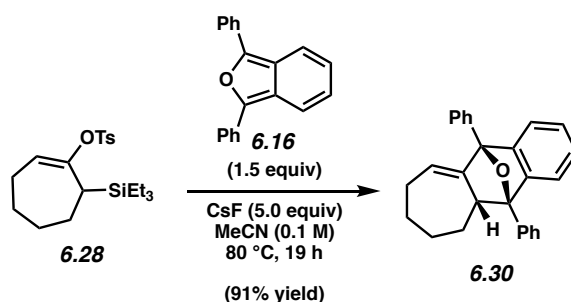
Na₂SO₄, filtered, and concentrated under reduced pressure. The resulting crude oil was purified by flash chromatography (1.5:98.5 EtOAc:hexanes) to afford silyl ketone **6.32** (142 mg, 95% yield) as a clear, colorless oil. Silyl ketone **6.32**: R_f 0.36 (99:1 benzene:Et₂O); ¹H NMR (500 MHz, CDCl₃): δ 2.63–2.56 (m, 1H), 2.37 (dd, *J* = 11.9, 4.9, 1H), 2.33–2.27 (m, 1H), 2.03–1.95 (m, 1H), 1.93–1.82 (m, 3H), 1.72–1.61 (m, 1H), 1.46–1.29 (m, 2H), 1.18–1.07 (m, 1H), 0.94 (t, *J* = 8.0, 9H), 0.60 (q, *J* = 7.5, 6H); ¹³C NMR (125 MHz, CDCl₃): δ 215.9, 47.6, 43.6, 31.1, 30.5, 25.9, 25.7, 7.3, 2.4; IR (film): 2880, 1670, 1417, 1208, 879 cm⁻¹; HRMS-APCI (*m/z*) [M + H]⁺ calcd for C₁₃H₂₇OSi⁺, 227.1826; found 227.1826.



Silyl tosylate 6.28. To a solution of diisopropylamine (0.110 mL, 0.762 mmol, 1.15 equiv) in THF (0.5 mL) at -78 °C was added *n*-butyllithium (2.36 M in hexanes, 0.309 mL, 0.729 mmol, 1.1 equiv) dropwise over 2 min. The solution was stirred for 30 min at -78 °C, then warmed to 23 °C over 15 min before being cooled to -78 °C. Silyl ketone **6.32** (150 mg, 0.662 mmol, 1.0 equiv) in THF (0.5 mL) was added dropwise over 5 min and stirred for 1 h at -78 °C. Next, *p*-toluenesulfonic anhydride (281 mg, 0.861 mmol, 1.3 equiv) in THF (2.0 mL) was added dropwise over 5 min and allowed to stir at -78 °C. After stirring for 1 h, sat. aqueous NaHCO₃ (3.0 mL) was added to the reaction, and the stirring solution was warmed to 23 °C. The aqueous layer was then extracted with diethyl ether (3 x 3 mL), and the combined organic layers were dried over Na₂SO₄, filtered, and concentrated under reduced pressure. The resulting crude solid was dissolved and passed through a plug of silica gel (2:1 hexanes:benzene eluent, 100 mL). The

eluate was concentrated and divided into three equal portions. Each portion was purified by preparative thin layer chromatography (7:3 benzene:hexanes), and the individual portions were recombined to afford silyl tosylate **6.28** (141 mg, 56% yield) as a white solid. Silyl tosylate **6.28**: M.p. 39.9–40.8 °C; R_f 0.79 (99:1 benzene:Et₂O); ¹H NMR (500 MHz, CDCl₃): δ 7.82–7.79 (m, 2H), 7.35–7.31 (m, 2H), 5.22 (dd, $J = 9.2, 4.4$, 1H), 2.45 (s, 3H), 2.10 (t, $J = 5.7$, 1H), 2.07–2.00 (m, 1H), 1.94–1.87 (m, 1H), 1.83–1.76 (m, 1H), 1.75–1.65 (m, 2H), 1.55–1.49 (m, 1H), 1.49–1.41 (m, 1H), 1.37–1.28 (m, 1H), 0.94 (t, $J = 8.1$, 9H), 0.63 (q, $J = 7.7$, 6H); ¹³C NMR (125 MHz, CDCl₃): δ 154.3, 144.6, 133.6, 129.5, 128.5, 118.4, 33.0, 28.2, 27.6, 26.0, 23.9, 21.7, 7.5, 3.6; IR (film): 2929, 2876, 1368, 1177, 994 cm⁻¹; HRMS-APCI (m/z) [M + H]⁺ calcd for C₂₀H₃₃O₃SSi⁺, 381.1914; found 381.1907.

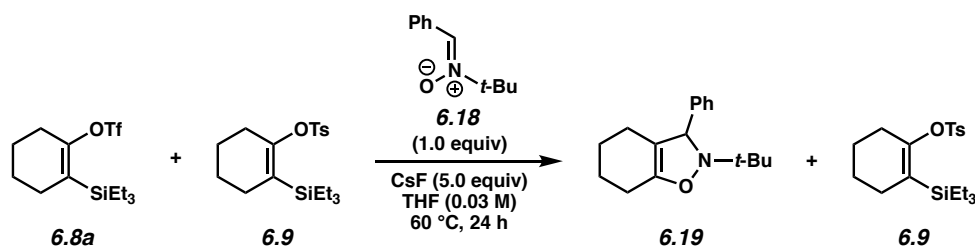
6.9.2.5 1,2-Cycloheptadiene Trapping Experiment



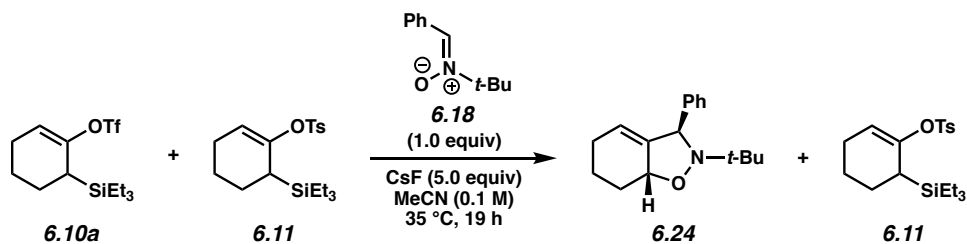
Cycloadduct 6.30. To a stirred solution of silyl tosylate **6.28** (19.8 mg, 52.0 μmol, 1.0 equiv) and 1,3-diphenylisobenzofuran (**6.16**) (21.1 mg, 78.0 μmol, 1.5 equiv) in MeCN (0.52 mL, 0.1 M) was added CsF (39.5 mg, 260 μmol, 5.0 equiv). The reaction vessel was purged with N₂, sealed with a teflon cap and teflon tape, and placed in a preheated, 80 °C aluminum heating block. The reaction was allowed to stir at this temperature for 14 h. After cooling to 23 °C, the yellow, heterogeneous solution was filtered through a plug of silica gel (EtOAc eluent, 10 mL)

and concentrated under reduced pressure to afford a crude yellow solid. Purification by preparative thin layer chromatography (2:1 hexanes:CH₂Cl₂ with 2% acetone) provided cycloadduct **6.30** (17.3 mg, 91% yield, 6.3:1 d.r. by ¹H NMR analysis of the crude material). Cycloadduct **6.30**: Spectral data match those previously reported.²²

6.9.2.6 Silyl Tosylate and Silyl Triflate Competition Experiments



Alkyne precursor competition experiment. To a stirred solution of silyl triflate **6.8a** (25.0 mg, 72.6 μ mol, 1.0 equiv), silyl tosylate **6.9** (26.6 mg, 72.6 μ mol, 1.0 equiv), and *N*-*tert*-butyl- α -phenylnitronium ion (**6.18**) (12.9 mg, 72.6 μ mol, 1.0 equiv) in THF (2.4 mL, 0.03 M) was added CsF (55.1 mg, 363 μ mol, 5.0 equiv). The reaction vessel was purged with N₂, sealed with a teflon cap, and placed in a preheated, 60 °C aluminum heating block. The reaction was allowed to stir at this temperature for 24 h. After cooling to 23 °C, the solution was filtered through a plug of silica gel (EtOAc eluent, 10 mL) and concentrated under reduced pressure to afford the crude reaction mixture. 1,3,5-trimethoxybenzene was added as an external standard. ¹H NMR analysis of the crude reaction mixture showed cycloadduct **6.19** (42% yield) and silyl tosylate **6.9** (100% remaining).



Allene precursor competition experiment. To a stirred solution of silyl triflate **6.10a** (25.0 mg, 72.6 μmol , 1.0 equiv), silyl tosylate **6.11** (26.6 mg, 72.6 μmol , 1.0 equiv), and *N*-*tert*-butyl- α -phenylnitrone (**6.18**) (12.9 mg, 72.6 μmol , 1.0 equiv) in MeCN (0.73 mL, 0.1 M) was added CsF (55.1 mg, 363 μmol , 5.0 equiv). The reaction vessel was purged with N_2 , sealed with a teflon cap, and placed in a preheated, 35 °C aluminum heating block. The reaction was allowed to stir at this temperature for 19 h. After cooling to 23 °C, the solution was filtered through a plug of silica gel (EtOAc eluent, 10 mL) and concentrated under reduced pressure to afford the crude reaction mixture. 1,3,5-trimethoxybenzene was added as an external standard. ^1H NMR analysis of the crude reaction mixture showed cycloadduct **6.24** (94% yield, 12.2:1 d.r.) and silyl tosylate **6.11** (94% remaining).

6.10 Spectra Relevant to Chapter Six:

Silyl Tosylate Precursors to Cyclohexyne, 1,2-Cyclohexadiene, and 1,2-Cycloheptadiene

Matthew S. McVeigh, Andrew V. Kelleghan, Michael M. Yamano, Rachel R. Knapp, and Neil K. Garg.

Org. Lett. **2020**, *22*, 4500–4504.

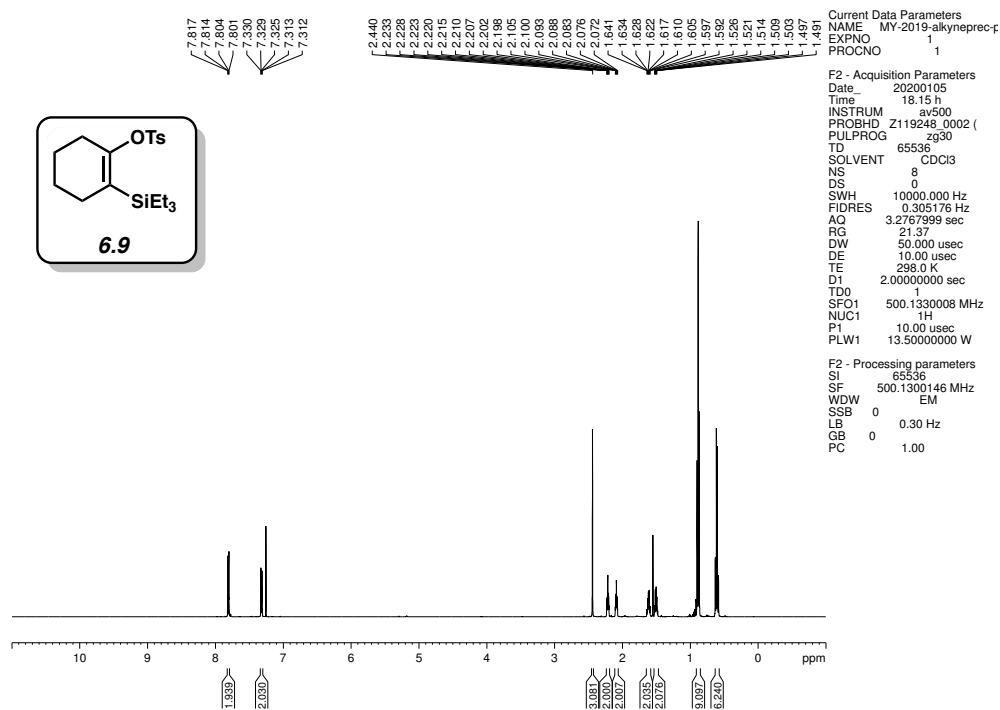


Figure 6.6. ¹H NMR (500 MHz, CDCl₃) of compound 6.9.

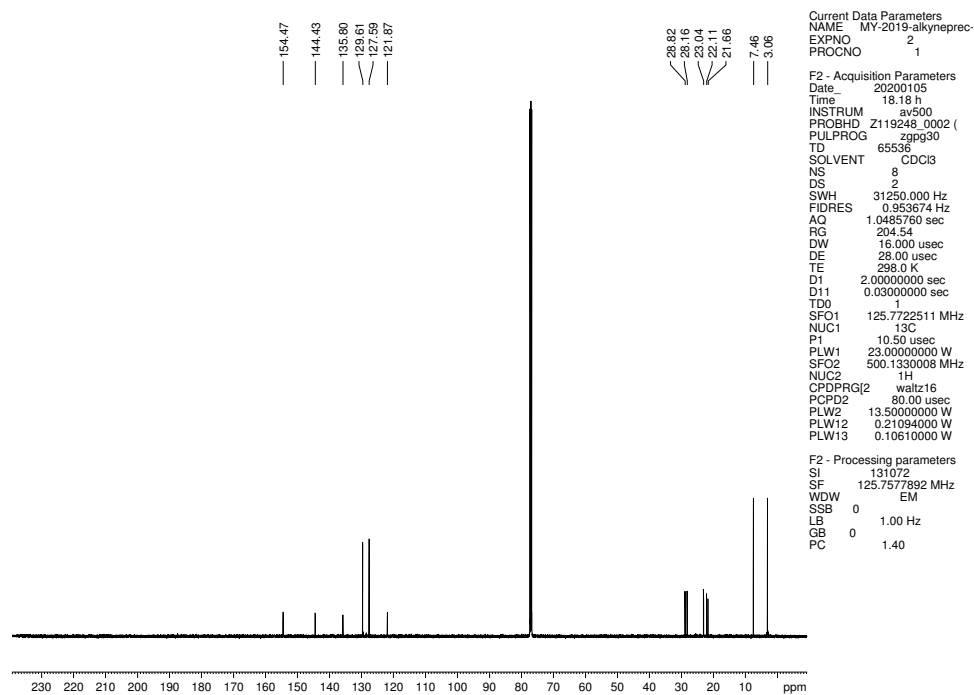


Figure 6.7. ¹³C NMR (125 MHz, CDCl₃) of compound 6.9.

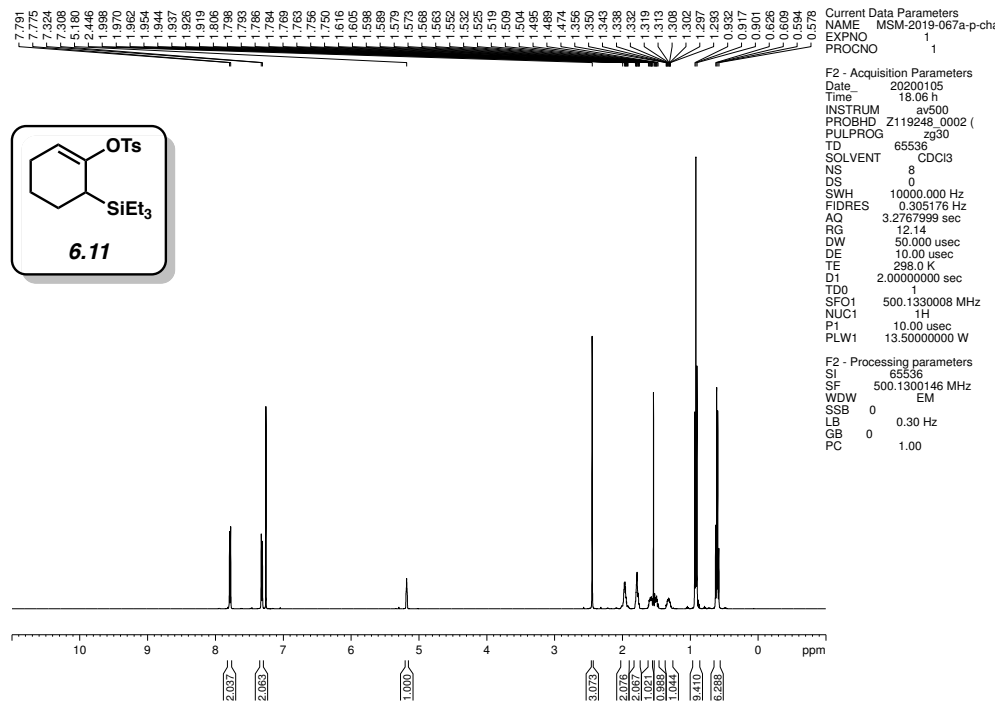


Figure 6.8. ^1H NMR (500 MHz, CDCl_3) of compound 6.11.

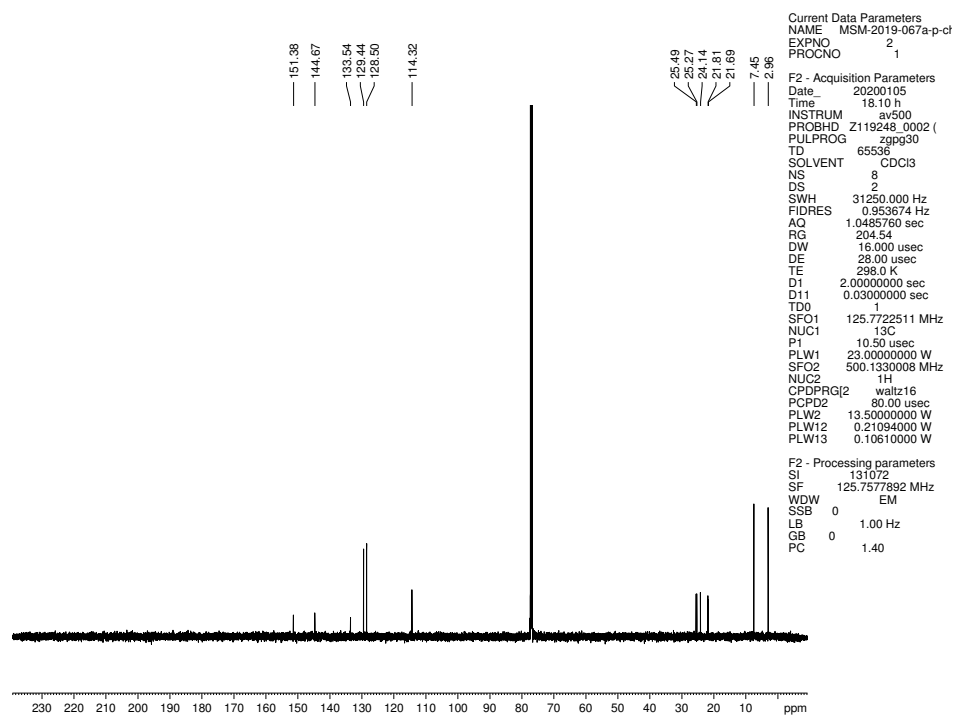
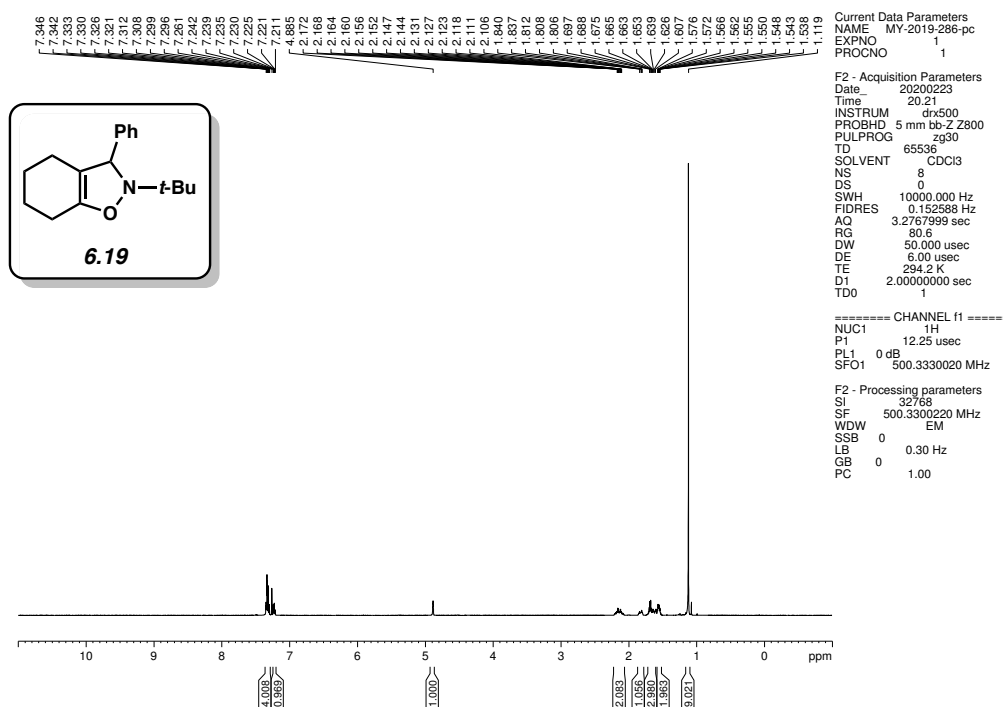
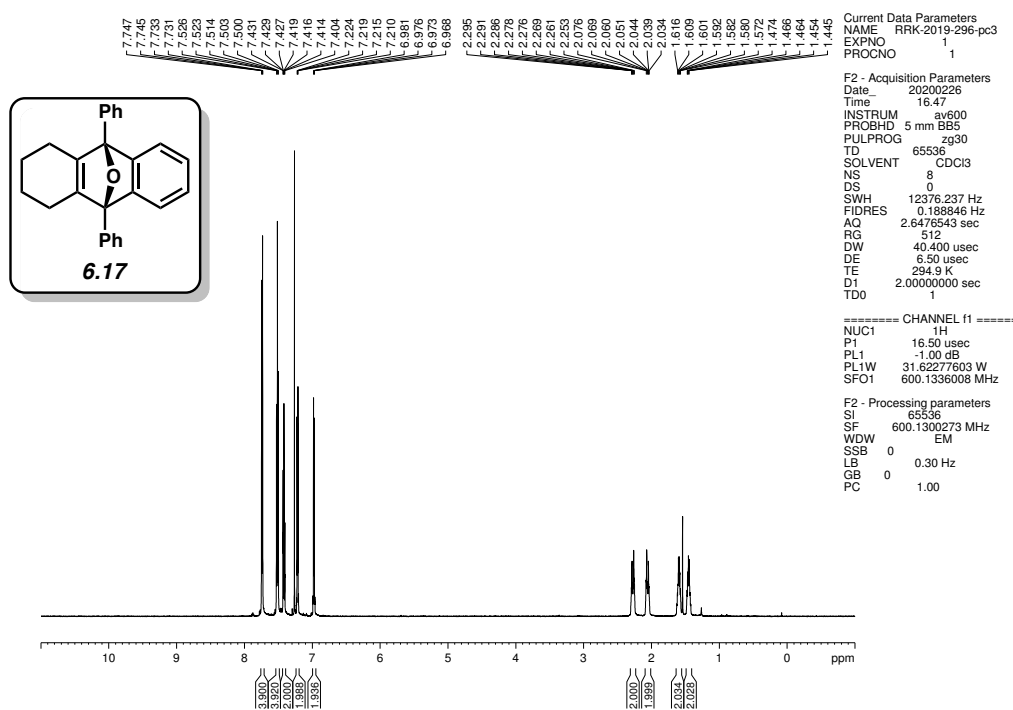


Figure 6.9. ^{13}C NMR (125 MHz, CDCl_3) of compound 6.11.



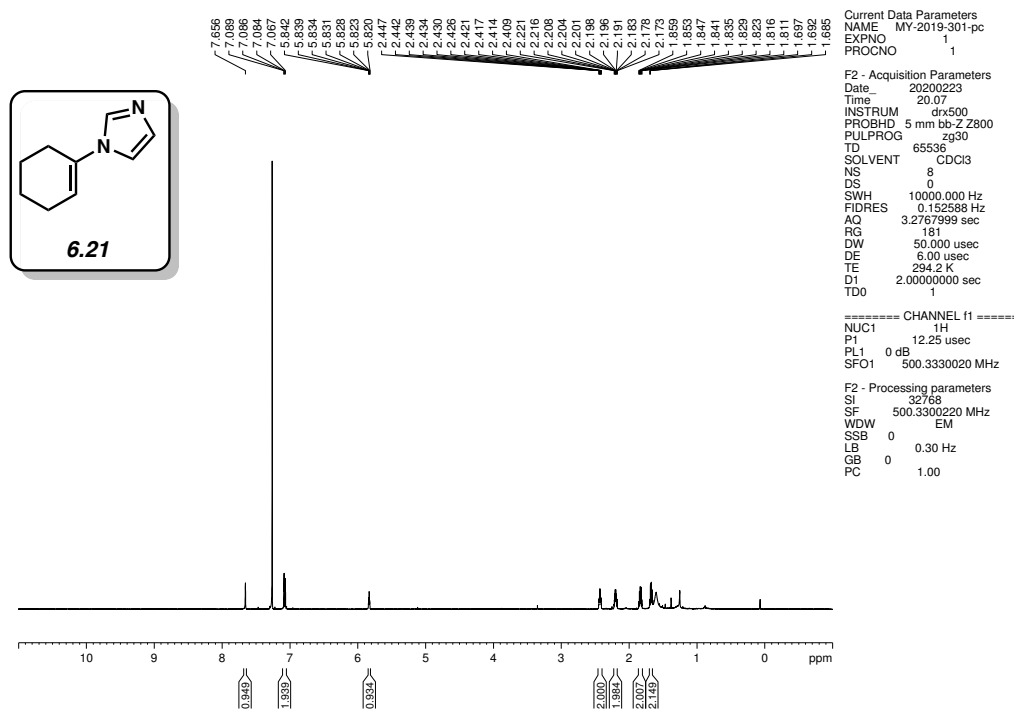


Figure 6.12. ^1H NMR (500 MHz, CDCl_3) of compound 6.21.

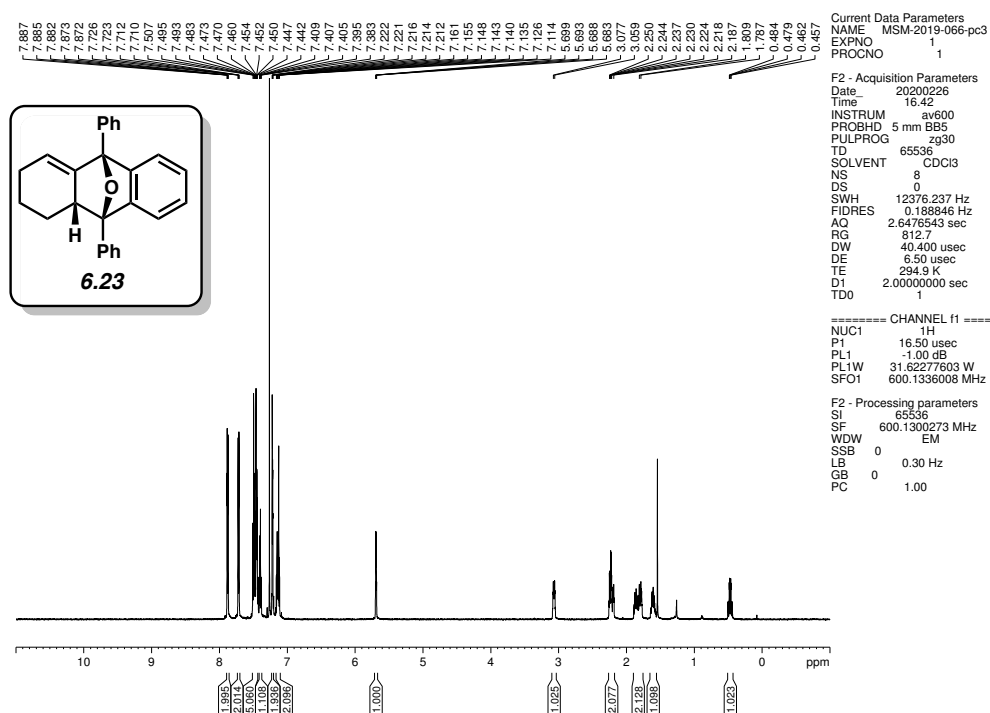


Figure 6.13. ^1H NMR (600 MHz, CDCl_3) of compound 6.23.

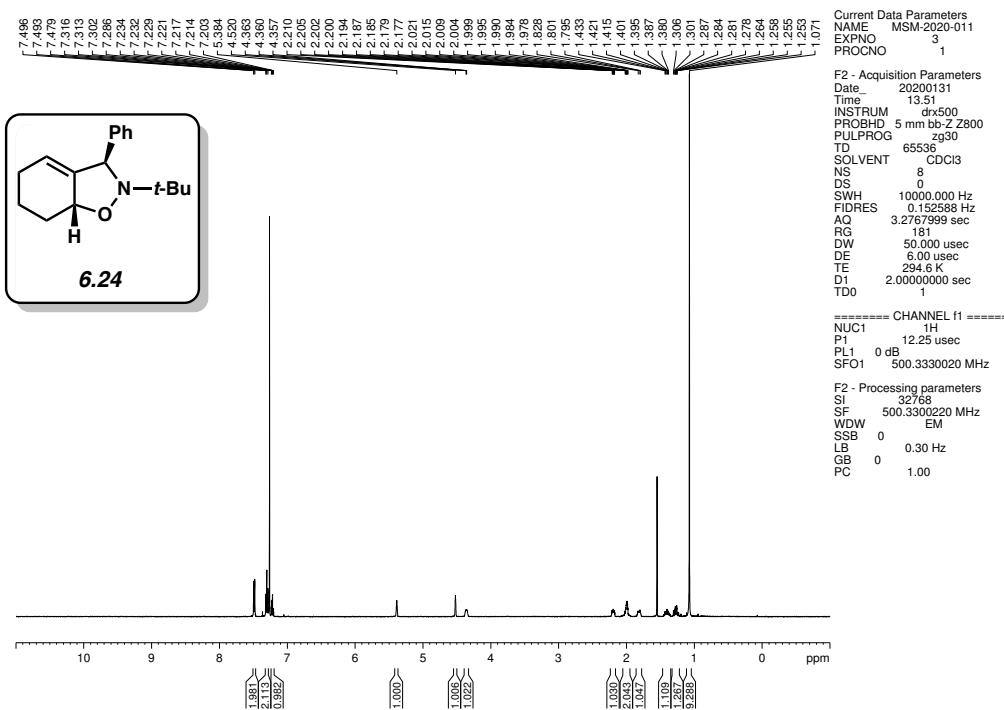


Figure 6.14. ^1H NMR (500 MHz, CDCl_3) of compound 6.24.

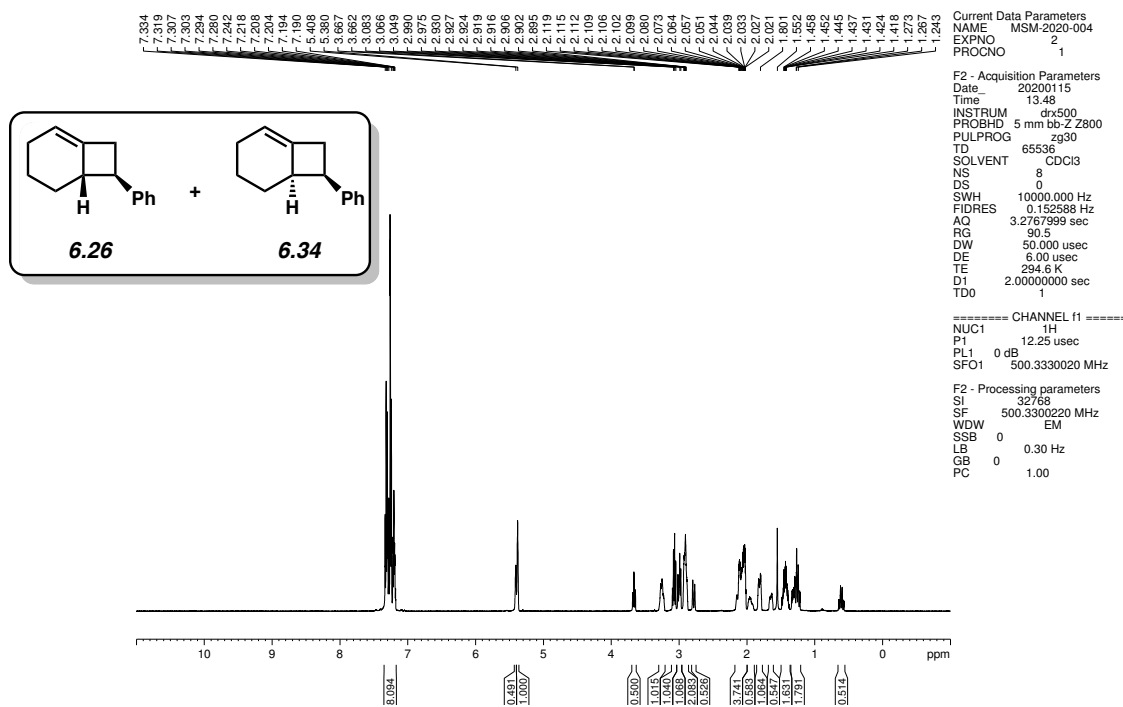


Figure 6.15. ^1H NMR (500 MHz, CDCl_3) of compounds 6.26 and 6.34.

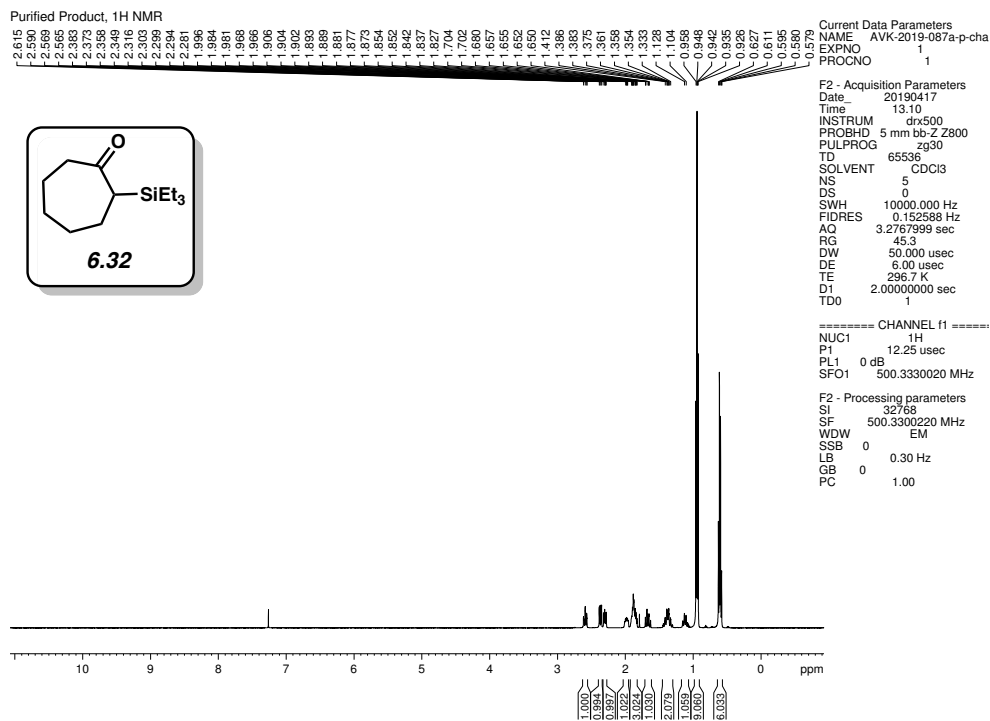


Figure 6.16. ¹H NMR (500 MHz, CDCl₃) of compounds **6.32**.

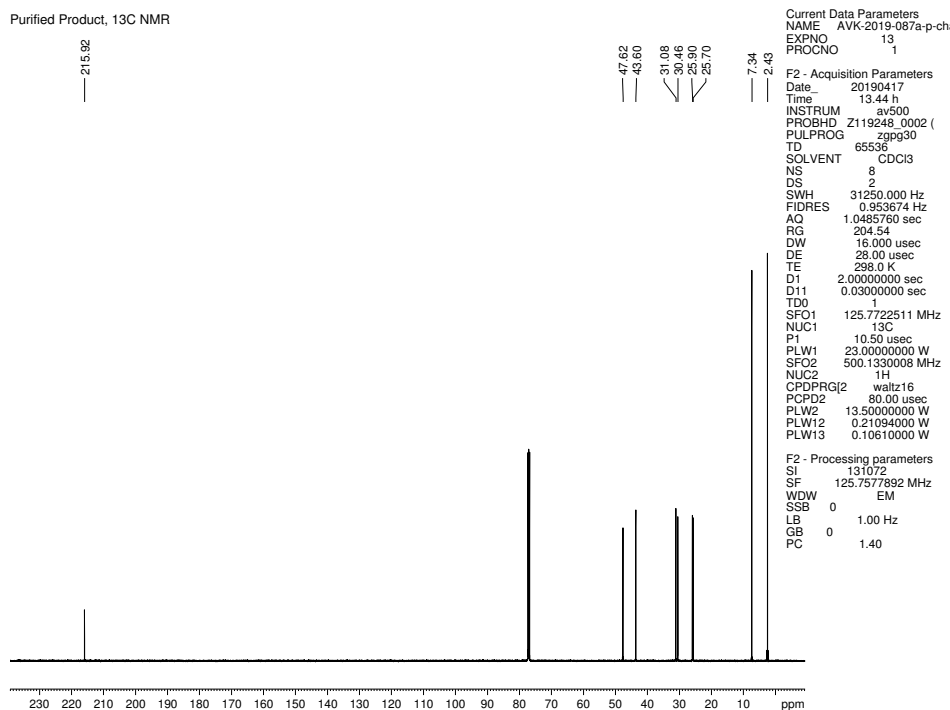


Figure 6.17. ¹³C NMR (125 MHz, CDCl₃) of compound **6.32**.

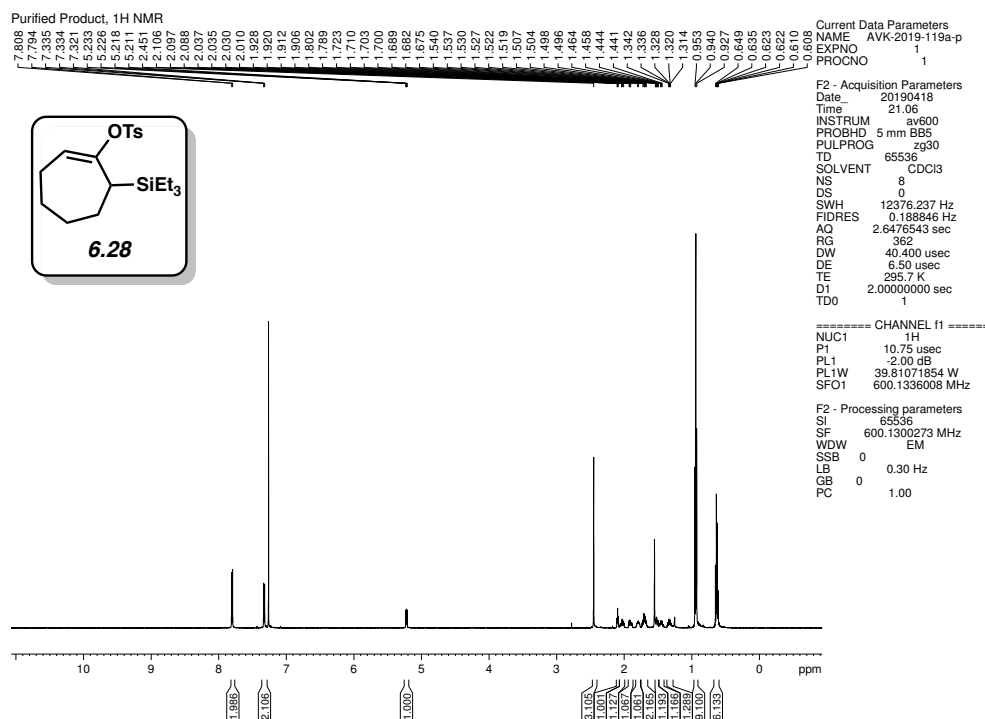


Figure 6.18. ¹H NMR (600 MHz, CDCl₃) of compounds 6.28.

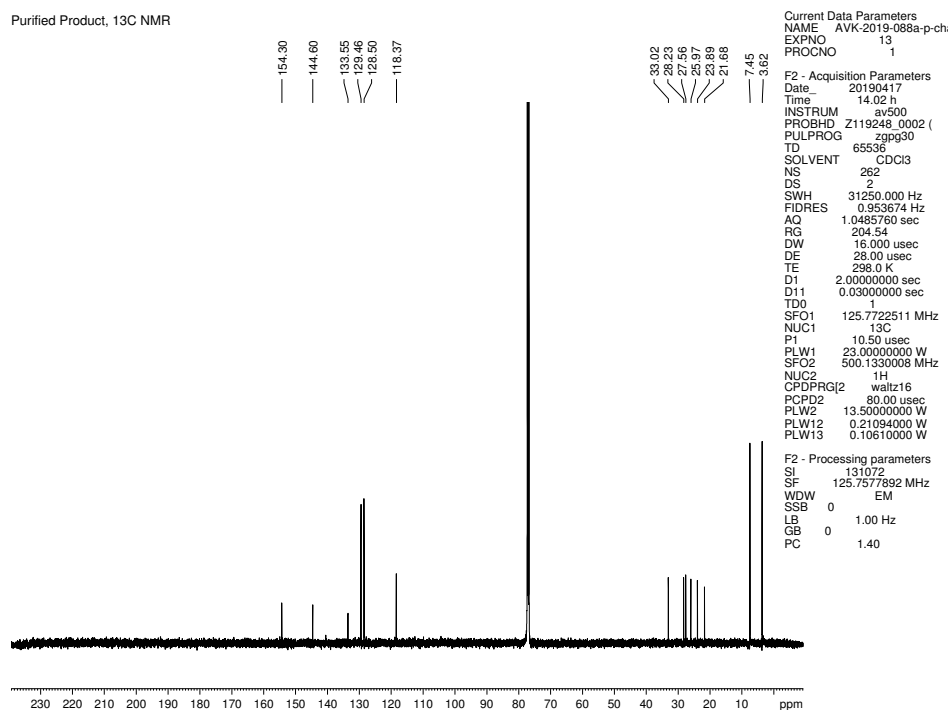


Figure 6.19. ¹³C NMR (125 MHz, CDCl₃) of compound 6.28.

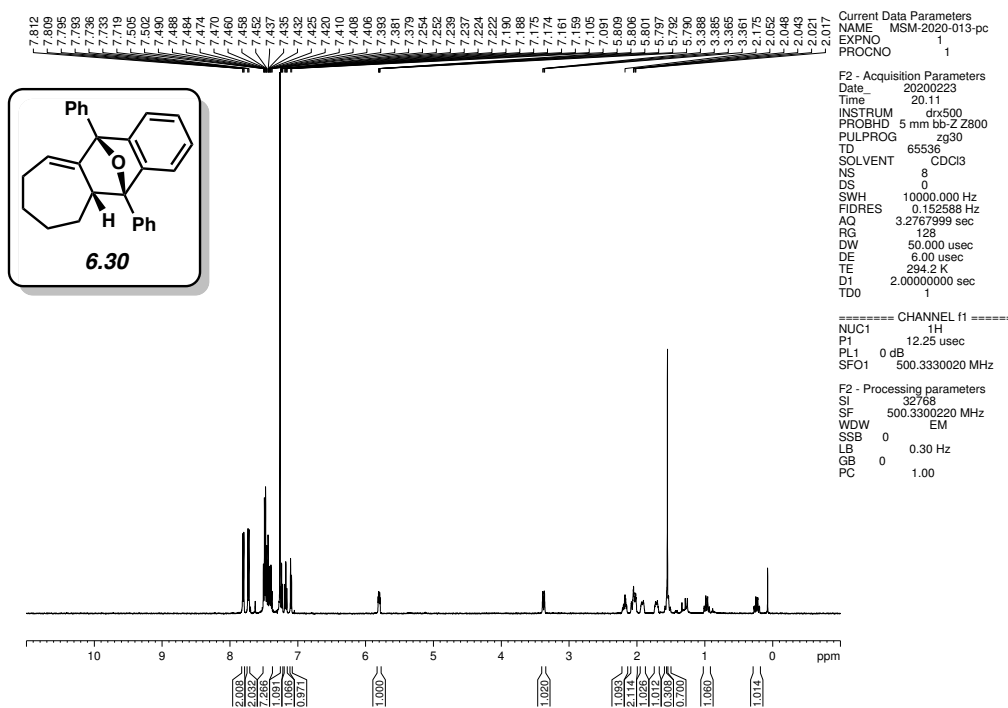


Figure 6.20. ^1H NMR (500 MHz, CDCl_3) of compounds **6.30**.

6.11 Notes and References

- (1) For reviews of transient strained cyclic intermediates, see: (a) Wenk, H. H.; Winkler, M.; Sander, W. One century of aryne chemistry. *Angew. Chem., Int. Ed.* **2003**, *42*, 502–528. (b) Bronner, S. M.; Goetz, A. E.; Garg, N. K. Understanding and modulating indolyne regioselectivities. *Synlett* **2011**, *18*, 2599–2604. (c) Tadross, P. M.; Stoltz, B. M. A comprehensive history of arynes in natural product total synthesis. *Chem. Rev.* **2012**, *112*, 3550–3577. (d) Gampe, C. M.; Carreira, E. M. Arynes and cyclohexyne in natural product synthesis. *Angew. Chem., Int. Ed.* **2012**, *51*, 3766–3778. (e) Dubrovskiy, A. V.; Markina, N. A.; Larock, R. C. Use of benzyne for the synthesis of heterocycles. *Org. Biomol. Chem.* **2013**, *11*, 191–218. (f) Hoffmann, R. W.; Suzuki, K. A “hot, energized” benzyne. *Angew. Chem., Int. Ed.* **2013**, *52*, 2655–2656. (g) Goetz, A. E.; Garg, N. K. Enabling the use of heterocyclic arynes in chemical synthesis. *J. Org. Chem.* **2014**, *79*, 846–851. (h) Yoshida, S.; Hosoya, T. The renaissance and bright future of synthetic aryne chemistry. *Chem. Lett.* **2015**, *44*, 1450–1460. (i) Takikawa, H.; Nishii, A.; Sakai, T.; Suzuki, K. Aryne-based strategy in the total synthesis of naturally occurring polycyclic compounds. *Chem. Soc. Rev.* **2018**, *47*, 8030–8056. (j) Dhokale, R. A.; Mhaske, S. B. Transition-metal-catalyzed reactions involving arynes. *Synthesis* **2018**, *50*, 1–16.
- (2) (a) Wittig, G. Phenyl-lithium, der Schlüssel zu einer neuen Chemie metallorganischer Verbindungen. *Naturwissenschaften* **1942**, *30*, 696–703. (b) Roberts, J. D.; Simmons, H. E.; Carlsmith, L. A.; Vaughan, C. W. Rearrangement in the reaction of chlorobenzene-1- C^{14} with potassium amide. *J. Am. Chem. Soc.* **1953**, *75*, 3290–3291.

- (3) Scardiglia, F.; Roberts, J. D. Evidence for cyclohexyne as an intermediate in the coupling of phenyllithium with 1-chlorocyclohexene. *Tetrahedron* **1957**, *1*, 343–344.
- (4) Wittig, G.; Fritze, P. On the intermediate occurrence of 1,2-cyclohexadiene. *Angew. Chem., Int. Ed.* **1966**, *5*, 846.
- (5) (a) Gampe, C. M.; Carreira, E. M. Total syntheses of guanacastepenes N and O. *Angew. Chem., Int. Ed.* **2011**, *50*, 2962–2965. (b) Kou, K. G. M.; Pflueger, J. J.; Kiho, T.; Morrill, L. C.; Fisher, E. L.; Clagg, K.; Lebold, T. P.; Kisunzu, J. K.; Sarpong, R. A benzyne insertion approach to hetisine-type diterpenoid alkaloids: synthesis of cossonidine (davisine). *J. Am. Chem. Soc.* **2018**, *140*, 8105–8109. (c) Goetz, A. E.; Silberstein, A. L.; Corsello, M. A.; Garg, N. K. Concise enantiospecific total synthesis of tubingensin A. *J. Am. Chem. Soc.* **2014**, *136*, 3036–3039. (d) Neog, K.; Borah, A.; Gogoi, P. Palladium(II)-catalyzed C–H bond activation/C–C and C–O bond formation reaction cascade: Direct synthesis of coumestans. *J. Org. Chem.* **2016**, *81*, 11971–11977. (e) Neumeyer, M.; Kopp, J.; Brückner, R. Controlling the substitution pattern of hexasubstituted naphthalenes by aryne/siloxyfuran Diels–Alder additions: regio and stereocontrolled synthesis of arizonin C1 analogs. *Eur. J. Org. Chem.* **2017**, 2883–2915. (f) Corsello, M. A.; Kim, J.; Garg, N. K. Total synthesis of (–)-tubingensin B enabled by the strategic use of an aryne cyclization. *Nat. Chem.* **2017**, *9*, 944–949.
- (6) (a) Barber, J. S.; Styduhar, E. D.; Pham, H. V.; McMahon, T. C.; Houk, K. N.; Garg, N. K. Nitron cycloadditions of 1,2-cyclohexadiene. *J. Am. Chem. Soc.* **2016**, *138*, 2512–2515. (b) Medina, J. M.; McMahon, T. C.; Jiménez-Osés, G.; Houk, K. N.; Garg, N. K. Cycloadditions of cyclohexynes and cyclopentyne. *J. Am. Chem. Soc.* **2014**, *136*, 14706–

14709. (c) McMahon, T. C.; Medina, J. M.; Yang, Y.-F.; Simmons, B. J.; Houk, K. N.; Garg, N. K. Generation and regioselective trapping of a 3,4-piperidyne for the synthesis of functionalized heterocycles. *J. Am. Chem. Soc.* **2015**, *137*, 4082–4085. (d) Tlais, S. F.; Danheiser, R. L. *N*-Tosyl-3-azacyclohexyne. Synthesis and chemistry of a strained cyclic ynamide. *J. Am. Chem. Soc.* **2014**, *136*, 15489–15492. (e) Shah, T. K.; Medina, J. M.; Garg, N. K. Expanding the strained alkyne toolbox: generation and utility of oxygen-containing strained alkynes. *J. Am. Chem. Soc.* **2016**, *138*, 4948–4954. (f) Barber, J. S.; Yamano, M. M.; Ramirez, M.; Darzi, E. R.; Knapp, R. R.; Liu, F.; Houk, K. N.; Garg, N. K. Diels–Alder cycloadditions of strained azacyclic allenes. *Nat. Chem.* **2018**, *10*, 953–960. (g) Nendel, M.; Tolbert, L. M.; Herring, L. E.; Islam, M. N.; Houk, K. N. Strained allenes as dienophiles in the Diels–Alder reaction: an experimental and computational study. *J. Org. Chem.* **1999**, *64*, 976–983. (h) Lofstrand, V. A.; West, F. G. Efficient trapping of 1,2-cyclohexadienes with 1,3-dipoles. *Chem. Eur. J.* **2016**, *22*, 10763–10767. (i) Yamano, M. M.; Knapp, R. R.; Ngamnithiporn, A.; Ramirez, M.; Houk, K. N.; Stoltz, B. M.; Garg, N. K. Cycloadditions of oxacyclic allenes and a catalytic asymmetric entryway to enantioenriched cyclic allenes. *Angew. Chem., Int. Ed.* **2019**, *58*, 5653–5657.
- (7) (a) Darzi, E. R.; Barber, J. S.; Garg, N. K. Cyclic alkyne approach to heteroatom-containing polycyclic aromatic hydrocarbon scaffolds. *Angew. Chem., Int. Ed.* **2019**, *58*, 9419–9424. (b) Pérez, D.; Peña, D.; Guitián, E. Aryne cycloaddition reactions in the synthesis of large polycyclic aromatic compounds. *Eur. J. Org. Chem.* **2013**, 5981–6013. (c) Xiao, X.; Hoye, T. R. The domino hexadehydro-Diels–Alder reaction transforms polyynes to benzyne to naphthyne to anthracynes to tetracyne (and beyond?). *Nat. Chem.* **2018**, *10*, 838–844. (d) Suh, S.-E.; Barros, S. A.; Chenoweth, D. M. Triple aryne–

- tetrazine reaction enabling rapid access to a new class of polyaromatic heterocycles. *Chem. Sci.* **2015**, *6*, 5128–5132. (e) Mizukoshi, Y.; Mikami, K.; Uchiyama, M. Aryne polymerization enabling straightforward synthesis of elusive poly(*ortho*-arylene)s. *J. Am. Chem. Soc.* **2015**, *137*, 74–77.
- (8) Himeshima, Y.; Sonoda, T.; Kobayashi, H. Fluoride-induced 1,2-elimination of *o*-trimethylsilylphenyl triflate to benzyne under mild conditions. *Chem. Lett.* **1983**, *12*, 1211–1214.
- (9) Atanes, N.; Escudero, S.; Pérez, D.; Guitián, E.; Castedo, L. Generation of cyclohexyne and its Diels–Alder reaction with α -pyrones. *Tetrahedron Lett.* **1998**, *39*, 3039–3040.
- (10) Quintana, I.; Peña, D.; Pérez, D.; Guitián, E. Generation and reactivity of 1,2-cyclohexadiene under mild reaction conditions. *Eur. J. Org. Chem.* **2009**, 5519–5524.
- (11) For a review related to vinyl triflate dissociation, see: Stang, P. J. Vinyl triflate chemistry: Unsaturated cations and carbenes. *Acc. Chem. Res.* **1978**, *11*, 107–114.
- (12) For references related to β -silyl stabilized vinyl cations, see: (a) Siehl, H.-U.; Kaufmann, F. P. Carbon-13 NMR spectroscopic determination of the magnitude of the β -silyl stabilization effect in 1-mesitylvinyl cations. *J. Am. Chem. Soc.* **1992**, *114*, 4937–4939. (b) Müller, T.; Meyer, R.; Lennartz, D.; Siehl, H.-U. Unusually stable vinyl cations. *Angew. Chem., Int. Ed.* **2000**, *39*, 3074–3077. (c) McGibbon, G. A.; Brook, M. A.; Terlouw, J. K. Stabilization energies for α - and β -silyl substituents on vinyl cations determined using mass spectrometric techniques. *J. Chem. Soc., Chem. Commun.* **1992**, *4*, 360–362.

- (13) (a) Cunico, R. F.; Dexheimer, E. M. Generation of 1,2-dehydrobenzene from the dehalosilylation of (*o*-halophenyl)trimethylsilanes. *J. Organomet. Chem.* **1973**, *59*, 153–160. (b) Lv, C.; Wan, C.; Liu, S.; Lan, Y.; Li, Y. Aryne trifunctionalization enabled by 3-silylaryne as a 1,2-benzdiyne equivalent. *Org. Lett.* **2018**, *20*, 1919–1923.
- (14) Although silyl triflates **6.8** and **6.10** do not suffer from instability, their known reactivity provides a useful point of comparison for developing the complementary precursors **6.9** and **6.11**, respectively.
- (15) (a) Streitwieser, A., Jr.; Wilkins, C.; Kiehlmann, E. Kinetics and isotope effects in solvolyses of ethyl trifluoromethanesulfonate. *J. Am. Chem. Soc.* **1968**, *90*, 1598–1601. (b) Noyce, D. S.; Virgilio, J. A. The synthesis and solvolysis of 1-phenylethyl disubstituted phosphinates. *J. Org. Chem.* **1972**, *37*, 2643–2647.
- (16) For methods that leverage the reactivity differences between triflates and tosylates to achieve selective, sequential functionalization of arynes, see: (a) Hamura, T.; Arisawa, T.; Matsumoto, T.; Suzuki, K. Two-directional annelation: dual benzyne cycloadditions starting from bis(sulfonyloxy)diiodobenzene. *Angew. Chem., Int. Ed.* **2006**, *45*, 6842–6844. (b) Xu, H.; He, J.; Shi, J.; Tan, L.; Qiu, D.; Luo, X.; Li, Y. Domino aryne annulation via a nucleophilic-ene process. *J. Am. Chem. Soc.* **2018**, *140*, 3555–3559.
- (17) The introduction of tosyl groups is known to impart crystallinity; for examples, see: (a) Kazemi, F.; Massah, A. R.; Javaherian, M. Chemoselective and scalable preparation of alkyl tosylates under solvent-free conditions. *Tetrahedron* **2007**, *63*, 5083–5087. (b) Jiang, X.; Li, J.; Zhang, R.; Zhu, Y.; Shen, J. An improved preparation process for gemcitabine. *Org. Proc. Res. Dev.* **2008**, *12*, 888–891.

- (18) (a) Corey, E. J.; Rücker, C. The 1,3 O→C silyl rearrangement of silyl enol ether anions – synthesis of α -silyl ketones. *Tetrahedron Lett.* **1984**, *25*, 4345–4348. (b) Inoue, K.; Nakura, R.; Okano, K.; Mori, A. One-pot synthesis of silylated enol triflates from silyl enol ethers for cyclohexynes and 1,2-cyclohexadienes. *Eur. J. Org. Chem.* **2018**, 3343–3347.
- (19) The yield of **6.21** from **6.9** is lower than when using the analogous trimethylsilyl triflate (see ref 6b). This may be attributed to an empirically observed inhibitory effect of excess imidazole on the consumption of **6.9**.
- (20) Christl, M.; Schreck, M. 7-Arylbicyclo[4.2.0]oct-1-ene – Synthese durch [2 + 2]-Cycloadditionen von 1,2-Cyclohexadien sowie 1-Methyl-1,2-cyclohexadien und thermische Äquilibrierung der *exo/endo*-Isomeren. *Chem Ber.* **1987**, *120*, 915–920.
- (21) Attempts to synthesize the corresponding silyl triflate precursor to 1,2-cycloheptadiene (**6.29**) were unsuccessful due to rapid degradation of the desired vinyl triflate upon attempted purification.
- (22) For methods to access **6.29** under harsher reaction conditions, see: (a) Bottini, A. T.; Hilton, L. L. Relative reactivities of bicyclo[3.2.1]octa-2,3-diene and 1,2-cycloheptadiene with conjugated dienes and styrene. *Tetrahedron* **1975**, *31*, 2003–2006. (b) Sutbeyaz, Y.; Ceylan, M.; Secen, H. A novel synthesis of transient 1,2-cyclohexadiene and 1,2-cycloheptadiene via β -halosilanes. *J. Chem. Res. (M)* **1993**, *8*, 2189–2196.
- (23) Chen, Q.; Tanaka, S.; Fujita, T.; Chen, L.; Minato, T.; Ishikawa, Y.; Chen, M.; Asao, N.; Yamamoto, Y.; Jin, T. The synergistic effect of nanoporous AuPd alloy catalysts on

highly chemoselective 1,4-hydrosilylation of conjugated cyclic enones. *Chem. Comm.*
2014, *50*, 3344–3346.